Computational Intelligence and Neuroscience

Computational Intelligence in Internet of Things Enabled Applications

Lead Guest Editor: Yang Gu
Guest Editors: Caifa Zhou and Guobin Chen

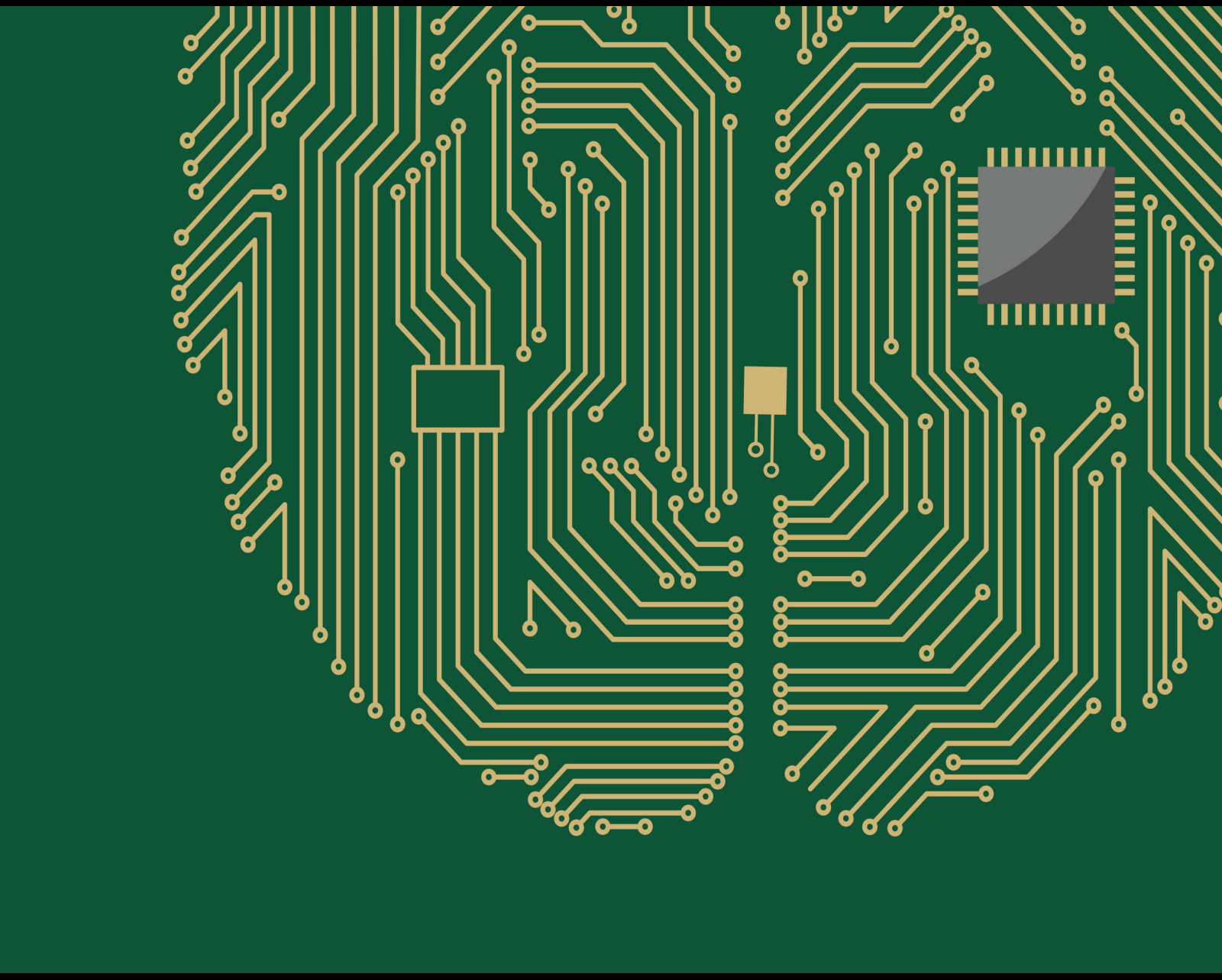

Computational Intelligence in Internet of Things Enabled Applications

Computational Intelligence and Neuroscience

Computational Intelligence in Internet of Things Enabled Applications

Lead Guest Editor: Yang Gu
Guest Editors: Caifa Zhou and Guobin Chen

Contents

Contents

Contents

Hindawi
Computational Intelligence and Neuroscience
Volume 2023, Article ID 9857932, 1 page
https://doi.org/10.1155/2023/9857932

Retraction

Retracted: The Innovation of College Students' Ideological and Political Education under the Intelligent Environment of Internet of Things

Computational Intelligence and Neuroscience

Received 19 September 2023; Accepted 19 September 2023; Published 20 September 2023

This article has been retracted by Hindawi following an investigation undertaken by the publisher [1]. This investigation has uncovered evidence of one or more of the following indicators of systematic manipulation of the publication process:

(1) Discrepancies in scope
(2) Discrepancies in the description of the research reported
(3) Discrepancies between the availability of data and the research described
(4) Inappropriate citations
(5) Incoherent, meaningless and/or irrelevant content included in the article
(6) Peer-review manipulation

The presence of these indicators undermines our confidence in the integrity of the article's content and we cannot, therefore, vouch for its reliability. Please note that this notice is intended solely to alert readers that the content of this article is unreliable. We have not investigated whether authors were aware of or involved in the systematic manipulation of the publication process.

Wiley and Hindawi regrets that the usual quality checks did not identify these issues before publication and have since put additional measures in place to safeguard research integrity.

We wish to credit our own Research Integrity and Research Publishing teams and anonymous and named external researchers and research integrity experts for contributing to this investigation.

The corresponding author, as the representative of all authors, has been given the opportunity to register their agreement or disagreement to this retraction. We have kept a record of any response received.

References

[1] X. Wang, "The Innovation of College Students' Ideological and Political Education under the Intelligent Environment of Internet of Things," *Computational Intelligence and Neuroscience*, vol. 2022, Article ID 6420262, 9 pages, 2022.

Hindawi
Computational Intelligence and Neuroscience
Volume 2023, Article ID 9825316, 1 page
https://doi.org/10.1155/2023/9825316

Retraction

Retracted: Research on Piano Performance Optimization Based on Big Data and BP Neural Network Technology

Computational Intelligence and Neuroscience

Received 19 September 2023; Accepted 19 September 2023; Published 20 September 2023

This article has been retracted by Hindawi following an investigation undertaken by the publisher [1]. This investigation has uncovered evidence of one or more of the following indicators of systematic manipulation of the publication process:

(1) Discrepancies in scope
(2) Discrepancies in the description of the research reported
(3) Discrepancies between the availability of data and the research described
(4) Inappropriate citations
(5) Incoherent, meaningless and/or irrelevant content included in the article
(6) Peer-review manipulation

The presence of these indicators undermines our confidence in the integrity of the article's content and we cannot, therefore, vouch for its reliability. Please note that this notice is intended solely to alert readers that the content of this article is unreliable. We have not investigated whether authors were aware of or involved in the systematic manipulation of the publication process.

Wiley and Hindawi regrets that the usual quality checks did not identify these issues before publication and have since put additional measures in place to safeguard research integrity.

We wish to credit our own Research Integrity and Research Publishing teams and anonymous and named external researchers and research integrity experts for contributing to this investigation.

The corresponding author, as the representative of all authors, has been given the opportunity to register their agreement or disagreement to this retraction. We have kept a record of any response received.

References

[1] X. Liu, "Research on Piano Performance Optimization Based on Big Data and BP Neural Network Technology," *Computational Intelligence and Neuroscience*, vol. 2022, Article ID 1268303, 10 pages, 2022.

Hindawi
Computational Intelligence and Neuroscience
Volume 2023, Article ID 9823751, 1 page
https://doi.org/10.1155/2023/9823751

Retraction

Retracted: The Dissemination and Evaluation of Campus Ideological and Political Public Opinion Based on Internet of Things Monitoring

Computational Intelligence and Neuroscience

Received 19 September 2023; Accepted 19 September 2023; Published 20 September 2023

This article has been retracted by Hindawi following an investigation undertaken by the publisher [1]. This investigation has uncovered evidence of one or more of the following indicators of systematic manipulation of the publication process:

(1) Discrepancies in scope
(2) Discrepancies in the description of the research reported
(3) Discrepancies between the availability of data and the research described
(4) Inappropriate citations
(5) Incoherent, meaningless and/or irrelevant content included in the article
(6) Peer-review manipulation

The presence of these indicators undermines our confidence in the integrity of the article's content and we cannot, therefore, vouch for its reliability. Please note that this notice is intended solely to alert readers that the content of this article is unreliable. We have not investigated whether authors were aware of or involved in the systematic manipulation of the publication process.

Wiley and Hindawi regrets that the usual quality checks did not identify these issues before publication and have since put additional measures in place to safeguard research integrity.

We wish to credit our own Research Integrity and Research Publishing teams and anonymous and named external researchers and research integrity experts for contributing to this investigation.

The corresponding author, as the representative of all authors, has been given the opportunity to register their agreement or disagreement to this retraction. We have kept a record of any response received.

References

[1] X. Xu and B. Sun, "The Dissemination and Evaluation of Campus Ideological and Political Public Opinion Based on Internet of Things Monitoring," *Computational Intelligence and Neuroscience*, vol. 2022, Article ID 8294613, 11 pages, 2022.

Hindawi
Computational Intelligence and Neuroscience
Volume 2023, Article ID 9813410, 1 page
https://doi.org/10.1155/2023/9813410

Retraction

Retracted: Sports Analysis and Action Optimization in Physical Education Teaching Practice Based on Internet of Things Sensor Perception

Computational Intelligence and Neuroscience

Received 19 September 2023; Accepted 19 September 2023; Published 20 September 2023

This article has been retracted by Hindawi following an investigation undertaken by the publisher [1]. This investigation has uncovered evidence of one or more of the following indicators of systematic manipulation of the publication process:

(1) Discrepancies in scope
(2) Discrepancies in the description of the research reported
(3) Discrepancies between the availability of data and the research described
(4) Inappropriate citations
(5) Incoherent, meaningless and/or irrelevant content included in the article
(6) Peer-review manipulation

The presence of these indicators undermines our confidence in the integrity of the article's content and we cannot, therefore, vouch for its reliability. Please note that this notice is intended solely to alert readers that the content of this article is unreliable. We have not investigated whether authors were aware of or involved in the systematic manipulation of the publication process.

In addition, our investigation has also shown that one or more of the following human-subject reporting requirements has not been met in this article: ethical approval by an Institutional Review Board (IRB) committee or equivalent, patient/participant consent to participate, and/or agreement to publish patient/participant details (where relevant).

Wiley and Hindawi regrets that the usual quality checks did not identify these issues before publication and have since put additional measures in place to safeguard research integrity.

We wish to credit our own Research Integrity and Research Publishing teams and anonymous and named external researchers and research integrity experts for contributing to this investigation.

The corresponding author, as the representative of all authors, has been given the opportunity to register their agreement or disagreement to this retraction. We have kept a record of any response received.

References

[1] M. Chen and J. Jiang, "Sports Analysis and Action Optimization in Physical Education Teaching Practice Based on Internet of Things Sensor Perception," *Computational Intelligence and Neuroscience*, vol. 2022, Article ID 7152953, 8 pages, 2022.

Hindawi
Computational Intelligence and Neuroscience
Volume 2022, Article ID 8340371, 15 pages
https://doi.org/10.1155/2022/8340371

Research Article

Study on the Drivers of Inclusive Green Growth in China Based on the Digital Economy Represented by the Internet of Things (IoT)

Xiaoxue Liu,[1] Shuangshuang Fan,[2] Fuzhen Cao,[1] Shengnan Peng,[2] and Hongyun Huang[3]

[1]*School of Economics, Beijing Technology and Business University, Beijing 100048, China*
[2]*School of Management, China University of Mining and Technology-Beijing, Beijing 100083, China*
[3]*Center for Economic Research, Shandong University, Jinan 250100, China*

Correspondence should be addressed to Shuangshuang Fan; amily_fan@163.com and Hongyun Huang; huanghongyun@mail.sdu.edu.cn

Received 1 June 2022; Revised 15 July 2022; Accepted 20 July 2022; Published 5 September 2022

Academic Editor: Guobin Chen

With the vigorous development of digital economy based on digital technologies such as Internet of things (IoT), big data, and artificial intelligence, new vitality has been injected into China's economic model. Inclusive green growth (IGG) supports the transformation of society towards a better quality of life and well-being, as well as environmental protection. Therefore, it is crucial to identify the main drivers of IGG. However, IGG is subject to a variety of interpretations and lacks definitional clarity. To brigade this gap, this study primarily evaluates the performance of IGG and explores the key drivers on IGG in China. Specifically, the data envelopment analysis (DEA) model is employed to calculate IGG for 281 cities in China during 2005–2020. Subsequently, we take advantage of a nest of machine learning (ML) algorithm to demonstrate the vital drivers of urban IGG, which avoids the defects of endogenous linear hypothesis of traditional econometric methods. The results indicate that digitization represented by the IoT and other digital technology is the core drivers of the urban IGG in the overall sample, accounting for about 50% among all of drivers. This finding provides new evidence supporting the "high-quality development" strategy in China, as well as shedding light on grasping the principal fulcrum to achieve the transformation towards IGG in developing economies similar to China.

1. Introduction

China has accomplished remarkable achievements after the reform and adoption of the opening-up policy, and the level of urbanization and industrialization has increased rapidly. However, the extensive pursuit of economic growth in high speed has led to a series of social and environmental problems. With the improvement in China's economy, the disharmony among different regions, the wide gap between the rich and the poor, and the deterioration of the ecological environment have become increasingly prominent, which have prevented people from sharing the benefits brought about by the growth and caused severe challenges to sustainable development, where environmental damage and damage of social equity are often ignored[1–3]. After the Rio +20 Summit in 2012, the concept of inclusive green growth (IGG) was proposed originally, which aims to combine the interests of industrialized countries with green growth and inclusive growth of developing countries. The 2015 UN Sustainable Development Goals agenda further clarified inclusive green growth (IGG) and provided ideas for China's economic development model transformation. China is entering a period of high-quality development, and coordinating the three systems of economy, society, and environment will efficiently provide a pathway for sustainable development. This precipitates a move away from pursuing economic growth speed to environmental protection, as well as reducing the gap between the rich and the poor, thus

realizing that the contemporary social members could equally share the benefits of economic growth as well as considering the interests of the future generations. This involves the coordinated ideas of efficiency and equity, and this transformation will determine the future of China's economy and the profound changes in the world economic situation.

Although China has been late to address sustainable development issues, continuous efforts are now being made in this field, especially via the central government's exploration of the growth of the inclusive and green economy [4, 5]. In 2011, in the 12th Five-Year Plan, the central government initially pointed out the vision of IGG. In 2016, the 13th Five-Year Plan further proposed the "five development concepts" of innovation, coordination, green, openness, and sharing, which identifies IGG as the main goal to achieve sustainable development. In 2017, the report of the 19th National Congress of the Communist Party of China proposed that China should shift the economy model from rapid growth to high-quality development in the future, and it is necessary to promote the innovation-driven development, regional coordination, and achievement sharing, shifting from "unbalanced distribution" to "common prosperity," accelerating the construction of ecological civilization, and changing from "high carbon growth" to "green development." It clarifies that IGG is an essential tool to achieve high-quality development in the new normal of economy period. In 2021, the 14th Five-Year Plan emphasized again to focus on unlocking the major issue of insufficient and imbalance economic development, as while as narrowing the gap between urban and rural areas, improving the level of cogovernance of society, and sharing of the wealth of nation, thus enhancing public welfare in a fair way. Additionally, the protection and governance of the ecological environment have become an extremely important planning, and it is indispensable to promote the harmonious coexistence between mankind and nature. Thus, it is quite urgent to deal with the issues such as the lack of "greening" and weak "inclusiveness" in the traditional growth mode in China. These inclusive green development concepts and strategies are compatible with each other. Therefore, the agenda for China's future is to achieve high-quality development by promoting IGG.

However, the current academic field has not formed a complete study on the method of implementation, the measurement system, and influencing factors of IGG, and its core definition has not been unified. To solve these problems, this paper tries to answer the following questions. First, what is the core concept of IGG based on China's national conditions and how to measure it in China? Second, how is the level of IGG in Chinese cities? Third, what are the main factors affecting China's IGG? Finally, what policies should Chinese government formulate to promote IGG and to contribute to the World? The purpose of addressing these issues is to reflect China's embrace of IGG.

The contribution of this study includes two aspects. First of all, it uses DEA model to measure the level of inclusive green growth efficiency (IGGE) in 281 Chinese cities from 2005 to 2020. It also reveals multiple drivers of IGG, in contrast to previous literature, which focuses on the influence of a single factor. This paper not only integrates the role of various factors, but also calculates the contribution of various factors in influencing IGG. Secondly, our work also expands the literature on the application of advanced machine learning (ML) techniques in empirical research in economics. For example, Adetunji et al. [6] explored the use of Random Forest ML technique for house price prediction. Mustafa et al. [7] trained an artificial neural network (ANN) model to recognize the pattern of the financial market and use this model to detect whether and when the market pattern has changed. Ben Jabeur et al. [8] employed a nest of ML, such as the LightGBM, CatBoost, XGBoost, Random Forest (RF), and neural network models, to predict oil prices during the COVID-19 pandemic. Richardson et al. [9] evaluated the real-time performance of popular ML algorithms in obtaining accurate nowcasts of real GDP growth for New Zealand. We advance this line of research by applying the ML technique to circumvent the multicollinearity issue in determining drivers of the urban IGG in China and providing policy suggestions, as to expand the application of ML algorithm in economics.

The remaining sections of this paper are organized as follows. Section 2 is a literature review, which combs the concept of IGG to deeply understand what IGG is and what the core concept of IGG is in China. Section 3 is the research design; we adopt the DEA model to measure the level of IGG and employ the machine learning (ML) algorithm to explore the key drivers of IGG in China. Section 4 is characteristics of IGG and plausible explanatory variables for IGG. Section 5 is determinants of IGG calculated by ML algorithm. Section 6 is conclusions and policy suggestions; we summarize the full text and propose policy suggestions, as well as pointing out the limitations of this paper.

2. Literature Review

2.1. Definition of IGG. In the 1870s, in the classic work capital, Marx considered the issues of fairness and justice and people's livelihood welfare everywhere. He believed that workers were the creators of wealth and should also be the owners of wealth. And he called on the society to pursue fairness and justice, resisting the exploitation of capital and reducing the gap between the rich and the poor. Since human society entered the 21st century, the world has experienced remarkable economic growth, especially in developing countries, where its success stories have become famous. However, inequality and the gap between the rich and the poor are still increasing, which means that the acceleration of growth has not had a subtle impact on people's social welfare [10]. Therefore, it is necessary to change from the traditional economic growth that we are familiar with to a growth that can reduce inequality and poverty, so as to achieve a growth that is beneficial to the poor. Meanwhile, the world's economic growth has increased resource scarcity and environmental issues and diverted the focus of the countries from traditional economic growth towards green growth [11]. The United Nations World Commission on Environment and

Development proposed the concept of sustainable development, where the goal is to "meet the needs of the present without compromising the ability of future generations to meet their own needs" [12]. This concept of sustainable development is not clear about how to coordinate the relationship between ecological environment and society when developing economy, so it lacks maneuverability. Inclusive green growth (IGG) is a sustainable development mode that pursues economic development, social equity, people' s welfare, achievements sharing, resources conservation, and ecological environment protection, as well as the comprehensive coordination of economy, society, and environment [13]. The term has become a buzz word for development planning and cooperation and is viewed as a means for achieving the sustainable development goals [14]. Unlike traditional growth theory, which represents "economy growth comes first," IGG is more beneficial to the inclusiveness of equilibrium and social welfare, as while as environmental protection. And it is an accepted solution to solve the poverty, unfairness, and the degradation of the environmental issues worldwide.

Table 1 lists the main definitions of the concept of IGG from literature; the ultimate goal of IGG is to achieve the coordinated and unified development of the three systems of social system, economy system, and the environmental system. And properly handling the relationship among the three systems can solve the problems of social inequity and environmental degradation in economic growth. Even though these concepts are based on different perspectives, the purpose and meaning behind them overlap, providing new ideas and contributions to global economic governance.

In the literature of sustainable development goal, scholars have continuing controversial views. Some scholars believe that economic growth will promote the inclusive in society and green development in ecology. Firstly, the economic growth of a region will empower government fiscal revenue and increase public infrastructure investment, as while as promoting technological progress and attracting foreign direct investment. On the one hand, it will benefit social care services sector—in particular early childhood education and care—as an effective target of fiscal spending for robust employment generation and gender inclusive growth [24–26]. On the other hand, it will increase the sharing of information, knowledge, and skills and thus drive employment and increase people's income [27]. Due to the "trickle-down" effect, it will provide opportunities for the poor, increase their income and welfare, promote fairness, and accomplish social inclusion. In addition, they believe that economic growth can even bring about an improvement in the natural environment and provide a higher level of sustainable development for global green growth [28]. For example, economic growth can improve labor productivity through improving health level, eliminating market failures, and improving energy and environmental efficiency through subsidies. In addition, economic growth can enable more green infrastructure or technological innovation [29, 30].

However, the emerging Amsterdam School of Governance for inclusive development argues that perpetual economic growth is incompatible with "inclusion" as a multifaceted ambition: social inclusion fails without ecological inclusion (i.e., entitlements to the ecological basis for human well-being) and relational inclusion (i.e., control over decisions that affect well-being and its basis) [31–34]. This integrated understanding means that inclusive development is a "paired" concept, whereby "inclusive" is not an adjective but implies a postgrowth transformation of "development" [35]. In recent years, scholars have proposed the "postgrowth" theory, which aims for enhancing human well-being, social justice, and environmental health by equitably and deliberately downscaling (degrowth) of overconsumption, overaccumulation, and expropriation [36, 37]. This theory advocates the growth model needs to be changed, and GDP is not the only goal of development. On the premise of economy growth, it is necessary to reduce energy consumption and protect the environment and promote members of society to enjoy the fruits of development together [38, 39].

Inclusive development and degrowth focus on the relationship among the economy, society, and environment [40]. IGG is not a new concept, which is based on the theory of inclusive development and postgrowth, emphasizing the complete harmonization of the three systems mentioned by inclusive development. Because different countries have different development policies, the definition of IGG should also be different worldwide. In the current new normal period of China's economy, the high-quality development concept of "green, coordinated and shared" has been put forward [41], which coincides with the core concept of IGG. This paper holds that IGG in China is a holistic and systematic growth model constructed by three subsystems of economy, society, and environment. In the economic subsystem, besides paying attention to the GDP growth, it also emphasizes the reduction of income gap and the coordination between different regions. In the social subsystem, attention is paid to whether social members share education and medical care and participate in employment, etc. In the environmental subsystem, attention is paid to pollutant discharge and environmental treatment, and China's IGG can be expressed as follows:

$$\mathrm{IGG} = G(\mathrm{Eco}, Soc, Env), \tag{1}$$

where Eco refers to economic growth or GDP growth. China is a developing country, and various problems must be solved to enable economic development; hence, GDP growth is still an important factor [1]. Soc refers to social equity; due to the huge differences in educational resources and capital between urban and rural areas in China, the problems of unequal opportunities and excessive income gap between urban and rural areas are more prominent [42]. Env represents environmental protection; it involves resource consumption and green technology change. Traditional high-carbon energy consumption and excessive development of heavily polluting enterprises are the main causes of environmental pollution. Assuming that the three conditions have diminishing marginal returns, the function $G(\cdot)$ represents the current IGG level.

Table 1: Definitions of IGG in literature.

Institution or authors	Definition
The United Nations Environmental Program [15]	"To Improve human well-being and social equity, while significantly reducing environmental risks and ecological scarcities"
The World Bank [16]	"In order to meet the sustainable development goal, the inclusive growth must be green, and green growth must be inclusive"
Wu and Zhou [17]	"To pursue economic growth, social equity, sharing results, resource conservation, and a good ecological environment"
The International Monetary Fund [18]	"It is a model that eliminates poverty and environmental damage while achieving economic growth to achieve sustainable development"
Bouma and Berkhout [19]; Kessler and Slingerland [20]	"To balance the relationship between growth and inclusiveness, while paying attention to the current and future growth of people's welfare"
Berkhout et al. [14]	"It is an economic growth model that takes into account the welfare of the socially poor (inclusive) and future generations (green)"
Mandle et al. [21]	"To improve human well-being through the optimization of the ecosystem and the protection and restoration of natural assets such as land, water and biodiversity"
Kumar [22]	"The core elements comprise sustainable consumption and production, equitable outcomes, and investments for environmental sustainability"
He and Du [23]	"It is a new way to attain sustainable development, aims to achieve comprehensive and coordinated economic, social, and environmental development"

2.2. Measurement of IGG. In previous study, human development index (HDI), which indicates countries combined achievements in education, health, and standard of living, has become, over time, the key reference indicator to assess countries' socioeconomic performance and is currently employed in wide-ranging areas of social sciences [43]. But the HDI's "original sin" of neglecting environmental and social sustainability issues has been discussed by researchers recently [44]. Dasgupta et al. [45] proposed the inclusive wealth index (IWI), and within this framework, economic progress is measured by growth in inclusive wealth, conceptualized by three categories of assets or capital: produced capital, human capital, and natural capital, and these aspects (among others) comprise the productive base of any country's economy [45]. The complex and interlinked problems of environment and development require simultaneous analysis of different dimensions of development processes, one of the new methodologies for this type of research is Sustainability Window analysis [46] Sustainability Window analysis is a tool for assessing the sustainability of development in all of its three dimensions simultaneously (environmental, economic, and social aspects) [47], and it is also used to analyze the level of IGG [46].

Although the concept of IGG is not unified at present, in recent years, some scholars have explored the measurement of it by using different methods. For instance, He and Du [23] took China as an example, using epsilon-based measure (EBM) model and Global Malmquist–Luenberger (GML) index to evaluate the efficiency of IGG of provinces in China, which fully considered environmental pollution and social imbalances. Albagoury [48] used the subjective weighting method to calculate the green growth and inclusive growth levels of Ethiopia to jointly reflect the inclusive green level. The Asian Development Bank [49] proposed an evaluation system including economic growth, social equity, and environmental sustainability and measured the level of IGG Asian subregion. Li et al. [50] constructed a scientific and reasonable IGG indicator system, using factor analysis supplemented by clustering method and entropy method to evaluate and cross-validate the IGG level of 37 countries and regions in the Asia-Pacific region. Narloch et al. [51] measured the IGG at the national level from five aspects: natural assets, resource efficiency and decoupling, resilience, and risks, as well as inclusiveness. Sun et al. [1] proposed a comprehensive directional distance function and slacks-based measure model to evaluate the IGG levels of 285 cities in China. However, the research scope and focus of the above literature are based on different perspectives of IGG, so they have certain limitations, such as lack of related study about the impact factor of IGG. In addition, developed countries and developing countries should have different emphasis in implementing IGG strategy and be based on specific circumstance. This paper attempts to establish a comprehensive evaluation framework based on the new era development concept of China's economy. The connotation of IGG integrates the concepts of inclusive growth and green development, aiming at pursuing an innovation-driven development model and paying attention to the coordination and unification of economic effects, social benefits, and ecological and environmental benefits.

3. Research Design

3.1. Measurement System of IGG. Referring to Sun et al. [1], we employ data envelopment analysis (DEA) model to measure urban IGG in China during the statistical period, which is one of the most important methods for efficiency estimation; it comprehensively evaluates the object from the perspectives of input and output and is more reasonable and scientific than the methods that simply consider output, such as principal component analysis and entropy weight method [23]. Previous studies have applied DEA model to evaluate efficiency, such as energy efficiency, the economic efficiency, innovation efficiency, and environmental efficiency. Tone and Tsutsui [52] proposed epsilon-based

measure (EBM) model, which not only considers the radial proportion of input frontier value and actual value, but also reflects differentiated nonradial relaxation variables among various input factors, effectively improving the accuracy and scientific nature of the results. On this basis, this paper integrates the superefficiency DEA model to measure the IGGE of sample cities in China.

Assuming that the production system has n decision making units (DMU), each DMU has three vectors, including input X, desirable output Y^g, and undesirable output Y^b, whose elements can be expressed as $x \in R^m$, $y^g \in R^s$ 1, and $y^b \in R^s$ 2; we define matrix X, Y^g, and Y^b as $X = [x_1, \ldots, x_n] \in R^{m\times n}$, $Y^g = [y_1^g, \ldots, y_n^g] \in R^s 1^{\times n}$, and $Y^b = [y_1^b, \ldots, y_n^b] \in R^s 2^{\times n}$, where $x_i > 0$, $y_i^g > 0$, and $y_i^b > 0\,(i = 1, 2, \ldots, n)$. The DEA-SBM model to evaluate efficiency is expressed as

$$\sigma = \min \frac{1 - (1/m)\sum_{i=1}^{m}\left(S_i^- / X_{i0}\right)}{1 + \left(1/\left(S_1 + S_2\right)\right)\left(\left(\sum_{r=1}^{S_i}\left(S_r^g / Y_{r0}^g\right)\right) + \sum_{r=1}^{S_2}\left(S_r^b / Y_{r0}^b\right)\right)},$$

$$s.t.\begin{cases} X_0 = X\lambda + S^-, \\ Y_0^g = Y^g\lambda - S^g, \\ Y_0^b = Y^b\lambda - S^b, \\ S^- \geq 0, S^g \geq 0, S^b \geq 0, \lambda \geq 0, \end{cases} \tag{2}$$

where s^-, s^g, s^b represent the input, desirable output, and undesirable output, respectively; and the weight vector is λ. The objective function σ is strictly monotonically decreasing with respect to s^-, s^g, and s^b. σ denotes the efficiency evaluation index. When $0 \leq \sigma \leq 1$, it means the ratio of input and output of DMU needs to be further improved. While $\sigma \geq 1$, it indicates that the DMU is in the effective status.

(1) *Inputs*: referring to Sun et al. [1], economy system runs need the labor and the capital to be involved. For this consideration, we use the total number of regional employees and private enterprises owners at the end of each year as the corresponding proxy variable.

(2) *Desirable outputs*: for developing countries, an essential prerequisite for achieve IGG goal is keeping economic growth; thus, we select GDP by urban population to represent the desired outputs of economic growth.

(3) *Undesirable outputs*: IGG emphasizes providing equal opportunities to participate in employment and equitable income distribution. Thus, the registered urban unemployment rate is selected as an undesirable output. Since China's income gap is mainly reflected in the urban-rural income gap, the urban-rural income ratio is also regarded as an undesirable output to represent income distribution. Additionally, we consider industrial sulfur dioxide, wastewater, and solid waste to represent the undesirable outputs related to environment.

3.2. Machine Learning Algorithms. Referring to Fan and Liu [53], we employ the machine learning (ML) algorithms to investigate the drivers of urban IGG in China, which include the random forest algorithm, the XGBoost algorithm, the CatBoost algorithm, and the LightGBM algorithm. Comparing to the traditional econometric model, the ML algorithm could not only overcome the multicollinearity problem among variables, but also calculate the contribution of each variable.

3.2.1. Random Forest Algorithm. Random forest (RF) regression is generated in the process of decision tree, which is based on the modeling data set sample observation and characteristic variables, respectively, through random sampling. Each time the sampling results are based on a tree [54, 55], and each tree is generated in accordance with its own attributes rules and values. The forest integrates all the rules of the decision tree and final judgment value, thus achieving the return of the random forest algorithm [56, 57]. In terms of input and output, input is an independent variable X, which is one or more definite or quantitative variables; and dependent variable Y is a quantitative variable, which is the output value and prediction effect of the model.

3.2.2. XGBoost Algorithm. XGBoost is an efficient implementation of GBDT. Different from GBDT, XGBoost adds regularization terms to the loss function [58]. And because some loss functions are difficult to compute derivatives, XGBoost uses the second-order Taylor expansion of the loss function as a fitting of the loss function. Therefore, XGBoost algorithm can better avoid the problem of overfitting. In addition, as an integrated algorithm of gradient lifting, the algorithm is highly efficient in terms of operation speed [59].

3.2.3. CatBoost Algorithm. CatBoost is a GBDT framework based on symmetric decision tree algorithm, which mainly solves the pain points of efficiently and reasonably processing classification features, processing gradient deviation and prediction deviation, and improving the accuracy and generalization ability of the algorithm [60]. CatBoost is able to build the most accurate model on a data set with minimal data preparation. In addition, it provides open-source interpretation tools and a way to quickly generate models.

3.2.4. LightGBM Algorithm. LightGBM is an efficient implementation of XGBoost. The idea is to scatter consecutive floating-point features into K discrete values and construct histogram of k width. Then the training data are iterated and the cumulative statistics of each discrete value in the histogram are calculated. In feature selection, we only need to find the optimal segmentation point according to the discrete value of the histogram. The leaf-wise strategy with depth limitation saves a lot of time and space [61].

4. Characteristics of IGG and Plausible Explanatory Variables for IGG

In this section, we mainly report the spatial dynamic evolution characteristics of the urban IGG in China in 4.1, which is calculated by DEA model in Section 3.1. Then, ten plausible explanatory variables for urban IGG which will be selected by combing the existing literature introduced in Section 4.2.

4.1. Spatiotemporal Dynamic Evolution of IGG. From Figure 1, we can see that the geographical distribution of IGGE in Chinese cities is uneven. Cities with high-level IGGE are mainly located in the southeast coastal areas and major municipalities directly under the central government, such as Beijing, Tianjin, Shanghai, and Chongqing. Simultaneously, Jiangsu and Zhejiang are most superior in China. These regions are endowed with superior resources, inherent location, infrastructure, and human capital and take the lead in economic growth, which are the foundation for priority IGGE. And IGGE in Heilongjiang and Inner Mongolia has been significantly improved. However, the urban IGGE level in the central region is relatively mediocre. The IGGE level in the western region is low, especially in Xinjiang, Xizang, Ningxia, Qinghai, Gansu, and Yunnan. This implies that, for developing countries similar to China, economic growth is still a prerequisite for improving IGGE [62].

4.2. Plausible Explanatory Variables for IGG. This section will introduce a series of explanatory variables, and the selection of these variables is based on the existing literature. Furthermore, we will elaborate the proxy variables and selection process of these variables. Next, we will draw the thermodynamic diagram of the correlation coefficient between each explanatory variable in Figure 2 as well as their statistical description in Table 2.

4.2.1. Economic Development. The impact of economic development on IGG is debatable. In Kuznets hypothesis [62], economic growth exceeding a certain threshold will reduce the level of inequality. However, inequality continued to rise in both developing and OECD countries [63]. In terms of environmental impact, Grossman and Krueger [64] proposed the Environmental Kuznets Curve theory, which supposed an inverted U-shaped relationship between income level and environmental degradation. Thus, we employ GDP per capita (pgdp) to reflect the urban economic growth and explore its impact on urban IGG.

4.2.2. Financial Development. Referring to [65], better functioning financial systems foster economic growth and poverty alleviation; moreover, a more equitable distribution of economic opportunities enhances overall economic development. According to Ahmed et al. [66], financial development promotes green economic growth, as it enables industries to access advanced types of machinery that are environmentally friendly and slow down environmental degradation to a certain extent. In addition, the interaction between financial development and technological innovation is conducive to the sustainable and stable development of green growth [67]. Thus, financial development (fd) may play an important role in accomplishing IGG. This paper selects the ratio of the balance of deposits and loans to the GDP of the region to represent the financial development level of the cities.

4.2.3. Digitization. Digitization brings new growth impetus to the economy [68]. Digitization and the development of smart systems connected to IOT can benefit the three essential elements of the food-water-energy nexus, bring sustainable food production, have access to clean and safe potable water, and accelerate the generation and consumption of green energy so as to catalyze the transition towards sustainable manufacturing practices and enhance citizens' health well-being [69]. Thus, we use the urban Internet penetration rate (inter) as a proxy variable for digitization.

4.2.4. Foreign Direct Investment. Previous studies have confirmed the positive impact of foreign direct investment (fdi) on the host country, such as introducing more advanced technology and knowledge, promoting regional employment and so on [27]. Foreign direct investment is especially well suited to effecting cross-border adoption transfer and translating it into broad-based growth, not least by upgrading human capital [27]. Studies have shown that FDI is beneficial to the promotion of inclusive green total factor productivity (IGTFP) mainly through traditional total factor productivity. Simultaneously, the inflow of FDI promotes the economic growth, thus accelerating IGTFP. It should be noted that the aggravation of environmental pollution in the FDI process is an important factor hindering the IGTFP. We choose the actual utilization amount of FDI in the city to take the right number to represent its development level.

4.2.5. Government Intervention. Previous studies have shown that government spending contributes to equity in educational opportunities and poverty eradication [70]. Furthermore, the government's expenditure on infrastructure promotes employment and economic growth through investment [71]. The education level per capita, the level of infrastructure, and the change of economic system all promote IGG of cities. In addition, agricultural financial subsidies can alleviate farmers' poverty [72]. Therefore, we use the ratio of urban fiscal expenditure to regional GDP as the proxy variable of government intervention (gove) and explore its relationship with IGGE.

4.2.6. Urbanization Process. In recent decades, China's urbanization process has made breakthrough progress, reaching about 58% in 2016, higher than the average of the world and Asia [73]. Then, rapid urbanization accompanied by extensive planning will lead to high house prices,

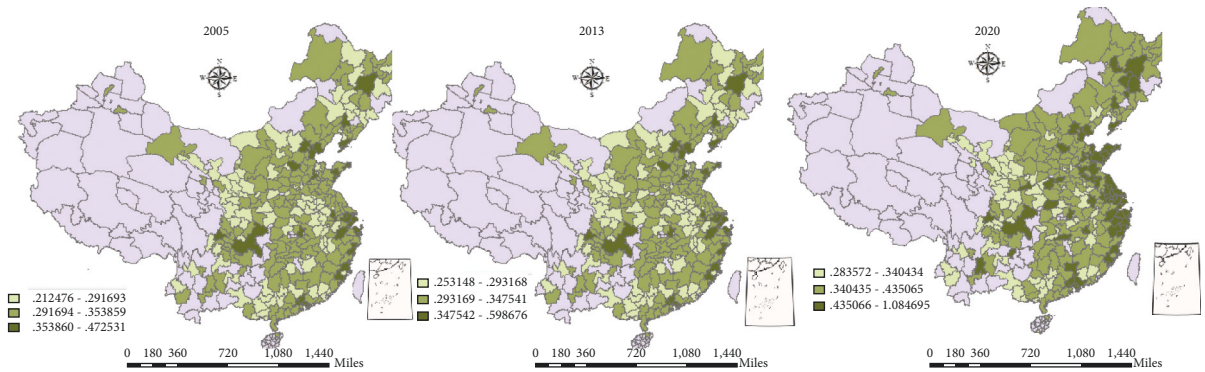

Figure 1: The spatiotemporal dynamic evolution trend of IGGE in China during 2005–2020.

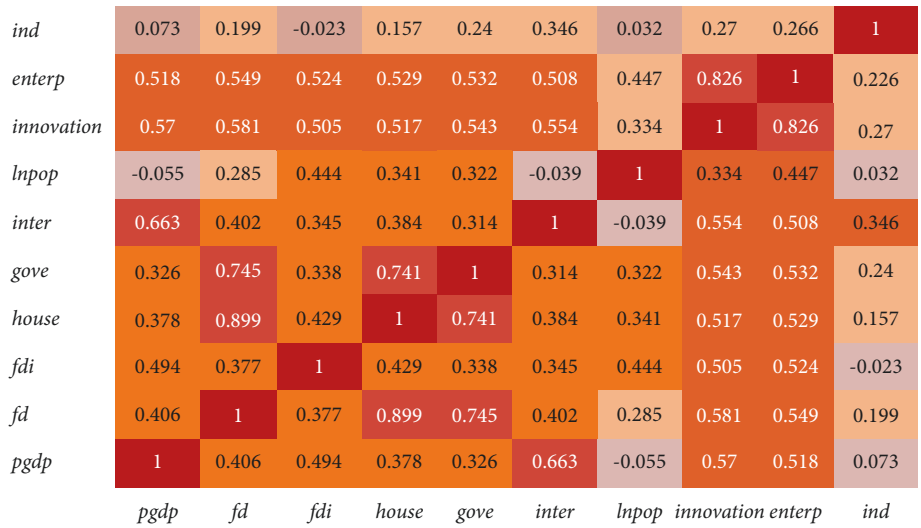

Figure 2: The thermodynamic diagram among independent variables.

Table 2: Descriptive statistical results of variables.

Variable	Obs.	Mean	Std. dev.	Min	Max
IGE	4 496	0.374	0.0669	0.237	1.029
Pgdp	4 496	53706	34539	6457	467749
Fd	4 496	3.650	8.806	0.00917	98.29
Fdi	4 496	4.329	0.852	0.477	6.489
Gove	4 496	0.335	0.640	0.00241	1.871
inter	4 496	0.227	0.153	0.00347	0.870
lnpop	4 496	2.558	0.298	1.305	3.533
house	4 496	0.235	0.501	6.45e-02	1.289
innovation	4 496	6.147	13.67	0.0250	166.6
enterp	4 496	68.36	98.87	1.030	951.7
ind	4 496	0.724	0.582	0.114	1.168

increased unemployment, and increased social inequality [74], causing misallocation of land resources, which may hinder the improving of IGG. According to Sun and Huang [75], the relationship between urbanization and emission efficiency is inverted U-shaped. This means that there may also be a nonlinear relationship between urbanization and inclusive economic growth. Therefore, we use the ratio of urban house investment to GDP (house) to represent the urbanization process.

4.2.7. Entrepreneurship. Existing research has proved positive connection between entrepreneurship [76] (especially female entrepreneurship) and inclusive growth, which may provide more employment opportunities for society. Additionally, green entrepreneurship can guide entrepreneurs to be fully aware of the prospects of environmentally friendly technologies and products and then push environmentally friendly innovation. Green entrepreneurship acts as a catalyst to accelerate environmental regulation effects and sustainable growth [77]. Thus, the number of newly established private enterprises in cities is the proxy variable of entrepreneurship (enterp). Next, we further study its relationship with IGG.

4.2.8. Innovation. Previous studies have verified the link between innovation, growth, and the environment. For instance, Ghisetti and Quatraro proposed that innovation can improve the efficiency of resource use, thereby reducing energy consumption and pollutant emissions per unit of output [67]. Furthermore, green innovation can give rise to green industries and create new market demand [78]. Some studies show that there is a complex nonlinear relationship between innovation and green development due to the

multiple factors [79], which supports the viewpoint of ecological modernization theory. It is worth noting that innovation can have a significant impact on IGG from three dimensions of economic greening, ecological greening, and social greening [80]. Based on this, we choose the number of patent invention applications in each city as the agent variable of innovation (innovation).

4.2.9. Urban Size. From the relationship between population size and environment, if all other factors remain unchanged, population size and growth increase pressure on urban land cover and CO_2 emissions. However, when considering the indirect effects of population size and growth on income and technology, it may offset or even reverse population environmental pressure [81]. Therefore, we choose the logarithm of urban population to represent the size of the city and study its impact on urban IGG in China.

4.2.10. Industrial Structure. For developing countries, the upgrading of industrial structure will promote the productive employment of the second and third industries, so as to narrow the gap between urban and rural areas. For instance, Moshi [82] took African countries as research objects and proved this conclusion. Therefore, we calculate the proportion of the added value of the secondary industry and the tertiary industry in GDP as the proxy variable of the industrial structure (ind).

4.3. Descriptive Statistics of Explanatory Variables. The data used in this study are mainly from China Urban Statistical Yearbook, China Rural Yearbook, and government official statistical website. To ensure the reliability of the data, we checked the data and deleted the cities with serious data deficiency. The final research sample was 281 prefecture level cities and cities above prefecture level cities in China from 2005 to 2020.

It is not difficult to see from Figure 2 that the correlation coefficient of some variables exceeds 0.75, indicating a strong positive correlation between the two variables. For this kind of variables, in the traditional econometric model, due to the linear hypothesis, the strong positive correlation has the problem of multicollinearity, which will lead to the inaccuracy of the regression results. Then, the true influence of an explanatory variable on the explained variable may be masked, while the ML algorithm used in this paper effectively overcomes this defect.

5. Determinants of IGG

In this section, we focus on exploring the determinants of IGG in China. We mainly use a series of ML algorithms for calculation; the process is stated in Section 5.1. And we reveal the determinants of IGG in China calculated by ML method in Section 5.2, followed by Section 5.3 which introduces robustness test to verify the robustness of the results of ML algorithm.

5.1. Machine Learning Algorithm Modeling. The process of determining the driving factors of IGGE by ML method includes data preprocessing, model construction, model prediction, and analysis. The specific steps are shown in Appendix. What we need to pay attention to is that it is quite necessary to set the hyperparameters based on the characteristics of each ML algorithm. Hyperparameters are parameters used to control the behavior of algorithms when building ML models. These parameters cannot be obtained from routine training. We need to assign values to the models before training them. In this paper, we use grid search technology to select the superparameters of the model. It builds a model for each arrangement of all given superparameter values specified in the grid and evaluates and selects the best model. Then, the explained variables and explanatory variables are regressed. The parameter settings of each model are shown in Table 3.

5.2. Determinants of Inclusive Green Growth. We input the test set into each model for calculation. The comparison between the predicted results of ML and the actual results is shown in Figure 3. A significant advantage of ML algorithm is that it can automatically calculate the important percentage of the contribution of different drivers to IGGE. Meanwhile, these ML methods do not assume that there is a linear relationship between ten explanatory variables and IGGE. However, the results of different models are different, as shown in Figure 4. Among the determinants calculated by RF algorithm, the digitization contribution weight is the largest, more than 46.33%; XGBoost's results show that the digitization contributes the most, accounting for about 50%. Among the results of CatBoost algorithm, economic growth and digitization rank the top two, accounting for about 27.35% and 17.11%, respectively. Finally, in the results of LightGBM algorithm, the contributions of economic growth and city size are in the forefront, accounting for about 24.60% and 17.52%, respectively. Therefore, it is essential to determine the optimal model and obtain the results according to the optimal model. The performance evaluation of each model is shown in Table 4.

Table 4 reveals the performance of the different ML algorithms. From goodness of fit R^2, we can see that the goodness of fit of XGBoost algorithm is 0.972, which is closest to 1 and the largest among all ML models. By comparing MAE and MAPE, we can see that the MAE value of test set and test set of XGBoost algorithm is 0.189, which is the smallest among all algorithms. For MAPE, XGBoost algorithm also has the smallest value, which shows that the ML model based on XGBoost algorithm is the best model for the study of IGGE determinants in this paper. Furthermore, the comparison between the prediction results of different algorithms presented in Figure 3 and the real value also verifies that the prediction value of XGBoost is closest to the real value. Therefore, next, we mainly analyze the operation results based on XGBoost model.

Based on the above selection process of the optimal ML model, we mainly focus on Figure 4(b), which is the calculation result of the ML model established based on the XGBoost algorithm.

Table 3: Machine learning model parameter setting.

Parameter	Random forest	XGBoost	CatBoost	LightGBM
Training time (s)	4.803	5.13	4.22	3.89
Data segmentation	0.7	0.7	0.7	0.7
Minimum node splitting	2	—	—	—
Minimum leaf node	1	—	—	—
Maximum depth of tree	10	12	10	10
Maximum leaf nodes	50	—	—	—
Decision trees number	100	—	—	—
Base learner number	—	100	—	100
Learning rate	—	0.1	0.1	0.1
L2 regular term	—	1	1	1
Number of iterations	—	—	100	—
Sample sign sampling rate (%)	—	100	—	100
Tree feature sampling rate (%)	—	100	—	100
Data shuffle	Yes	Yes	Yes	Yes

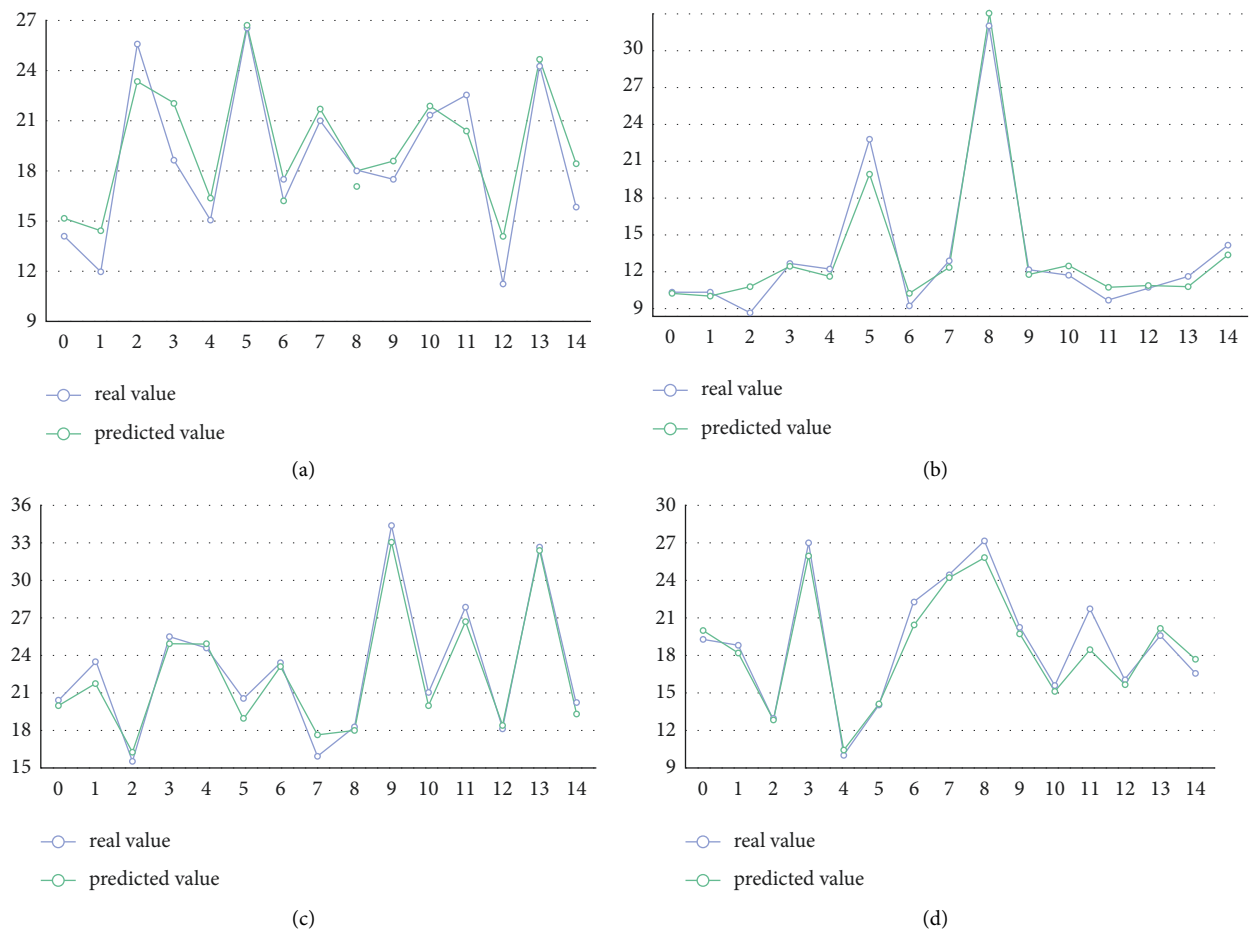

Figure 3: The comparison of ML predicted value and real value. (a) RFBoost. (b) XGBoost. (c) CatBoost. (d) LightGBM.

This figure shows that, among the 10 explanatory variables we select for IGGE, the digitization contributes the most, accounting for about 50%. It shows that, for the sample cities in the statistical period, digitization is the main engine of urban IGGE, which is consistent with the previous research conclusions [68, 69]. On one aspect, the digital economy represented by IOT will bring about new business model with high added value and low pollution to the economy. On the other aspects, poor families and individuals may get more educational and training resources from digital platform, which will enhance their capacity to acquire higher payment in labor market, thus promoting the social equity.

The contribution of innovation on IGGE ranked second, accounting for about 15.18%. The possible reason is that innovation can promote the productivity of enterprises,

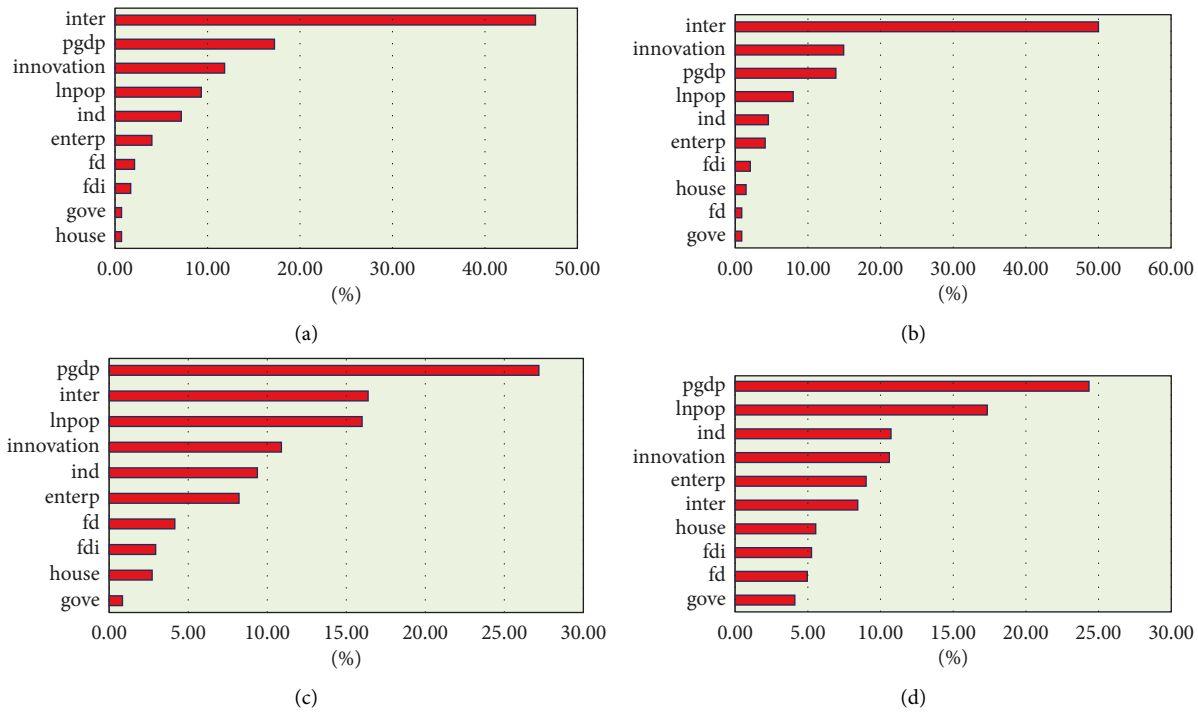

Figure 4: The contribution for determinants of IGGE. (a) The result from RF algorithm. (b) The result from XGBoost algorithm. (c) The result from CatBoost algorithm. (d) The result from LightGBM algorithm.

Table 4: Machine learning model performance measurement.

Algorithm	Dataset	RMSE	MAE	MAPE	R^2
RF	Training set	2.411	1.861	9.874	0.816
	Testing set	2.935	2.183	11.462	0.713
XGBoost	Training set	0.283	**0.192**	**1.018**	**0.983**
	Testing set	**0.291**	**0.189**	**1.012**	**0.972**
CatBoost	Training set	1.43	1.072	5.717	0.931
	Testing set	1.387	1.026	5.555	0.944
LightGBM	Training set	1.286	0.904	4.833	0.947
	Testing set	1.25	0.882	4.792	0.95

especially SMEs, so as to give full play to personal potential and provide more employment opportunities. In addition, innovation leads to new technologies and inventions, so as to benefit more members of society. Additionally, the process of innovation will bring about more high-tech production and service, which may be friendly to the environment, as well as reducing the energy consuming and pollution.

Followed by economic growth, which contributes about 14.61%. On the one hand, its role cannot be underestimated. On the other hand, for developing countries such as China, compared with digitization and innovation, the contribution of economic growth to IGGE is slightly smaller, which may be related to the fact that IGGE is the coordinated development of economy, society, and environment. The digitization can solve the role of information asymmetry and reduce transaction costs, and innovation provides technical support for economic transformation and green development. Both are conducive to the coordination of economy, society, and environment.

Next is the urban size, which contributes about 8.82%. This also verifies that large cities may play an economic agglomeration effect and contribute to IGGE. It is worth noting that regional population growth may increase the pressure of CO_2 emissions, while it may also promote innovation and income. Therefore, there is a complex nonlinear relationship between urban size and IGG.

Followed by the industrial structure and entrepreneurship, whose contribution are about 4.43%, respectively, industrialization can narrow the income gap and benefit the poor to a certain extent, but its role is limited.

Followed by foreign direct investment and the process of urbanization, which contribute 1.90% and 1.22%, respectively, there is the financial development, whose contribution is about 1.15%. The proportion of government intervention is the least, whose contribution is about 0.92%. It shows that, in current China, the government has not played its due role in promoting fair opportunities and narrowing the gap between the rich and the poor.

Table 5: Regress results of econometric model.

	(1)	(2)	(3)	(4)
	IGGE	IGGE	IGGE	IGGE
fd	0.10255***	−0.00268	−0.00510	−0.01047
	(0.02058)	(0.03357)	(0.03307)	(0.03655)
house	−0.66550*	−0.10662	0.07403	0.18944
	(0.35987)	(0.71390)	(0.71890)	(0.71512)
fdi	0.36708***	−0.19696	−0.16819	0.03019
	(0.12049)	(0.14908)	(0.12084)	(0.13818)
inter	6.41212***	6.28739***	2.38029***	3.64882***
	(0.72481)	(0.88386)	(0.74432)	(0.78199)
gove	−0.21927	0.11191	0.02886	0.00788
	(0.18355)	(0.13443)	(0.13956)	(0.14145)
innovation	0.01254	0.01155	0.03034	0.04056
	(0.01051)	(0.02187)	(0.02649)	(0.02939)
lnpop	−5.35827***	−8.64793***	−13.55774***	−6.19101***
	(0.33908)	(3.30041)	(3.26264)	(0.96659)
enterp	0.00860***	0.00553***	0.00299**	0.00409**
	(0.00145)	(0.00154)	(0.00147)	(0.00160)
ind	1.85708***	2.18074***	0.71279***	1.15808***
	(0.14347)	(0.27736)	(0.26190)	(0.28270)
pgdp	0.00005***	0.00002***	0.00000	0.00001***
	(0.00000)	(0.00001)	(0.00000)	(0.00000)
N	4496.00000	4496.00000	4496.00000	4496.00000
R^2	0.52351	0.38342	0.47507	0.4621
City fixed	Yes	No	Yes	No
Year fixed	Yes	Yes	No	No

Note: ***, **, and * denote significance at the 1%, 5%, and 10% level, respectively. Robust standard errors in parentheses are clustered by city-level.

5.3. Robust Test. In order to further verify that the conclusion obtained by XGBoost algorithm is robust and reliable, we further introduce the traditional econometric model to regress and compare the calculation results with ML model. In the setting of regression model, the independent variable is an explanatory variable, and the dependent variable is IGGE which is measured by DEA model. Table 5 reports the regression results and R^2 of the econometric model. Among them, the regression result of the first column is the regression result of controlling the urban individual and time fixed effects at the same time by ordinary least squares (OLS); the second column is the regression result that controls the time fixed effect; the third column is the regression result of controlling the fixed effect of urban individuals. The last column is the random effect model estimation.

According to R^2 of the four econometric models in Table 5, we can see that, under the model of controlling the fixed effect of urban individuals and time effect at the same time, R^2 of the regress result is 0.5235, which is the best result. Therefore, we focus on comparing the results of this column with the calculation results of ML under the previous XGBoost algorithm to judge whether the results of ML model are robust.

It can be seen from Table 5 that, among all the drivers of IGGE, the variables with positive coefficient at the 1% significance level are digitization, industrial structure, financial development, foreign direct investment, entrepreneurship, and economic growth. It is suggested that these factors have the most significant positive driving effect on urban IGGE. However, the coefficient of urban size is negative, indicating that urban size (population size) significantly inhibits IGGE in Chinese cities. The coefficient of the process of urbanization is negative at the significance level of 10%, indicating that their importance in influencing IGGE in cities is lower than the previous factors. The coefficient of innovation and government intervention is positive, but not significant. The result shows that digitization is the most important engine of IGG. At this point, the econometric model is consistent with the XGBoost model, while there are obvious deviations in the contributions of other influencing factors. However, the econometric model of R^2 is only 0.5235, which is far lower than the goodness of fit of ML algorithm 0.998. The possible reason for the difference is that the econometric model assumes the linear relationship between independent variables and dependent variables, while the ML model calculates the nonlinear relationship, so the latter is more consistent with the real situation and more robust and superior than the traditional method.

6. Conclusion and Policy Suggestion

6.1. Conclusion. As the world's largest emerging economy, China's increasing income inequality and environmental pollution are not conducive to the realization of the goal of sustainable development. Thus, it is urgent to change the growth model to IGG, as well as to identify the main engines of IGG to formulate relevant policies. In this context, the super efficiency DEA model is employed to measure the

IGGE of 281 prefecture level cities in China from 2005 to 2020. Furthermore, we introduce a nest of ML algorithms to calculate the drivers of urban IGGE, which can overcome the problem of linear relationship assumption in traditional econometric models. Through the performance evaluation of each ML model, we recognize that the calculation result of XGBoost algorithm is most ideal.

The calculation results based on this algorithm reveal that, among all the drivers of urban IGG, digitization is the most critical, and its contribution weight reaches about 50% among all the drivers. Followed by innovation and economic growth, which explain 15.18% and 14.61% of IGG, respectively, the total contribution of other factors is about 20%. Furthermore, we have tested the robustness of the ML model by traditional econometric model, which still proves the importance of digitization for the realization of urban IGGE and the excellent performance of ML algorithm.

6.2. Policy Suggestions. Based on the importance ranking of determinant of IGGE in Chinese cities calculated by XGBoost algorithm and the results of heterogeneity analysis, we provide the following policy suggestions.

First of all, in order to give full play to the role of digitization in promoting urban IGGE, the government needs to focus on promoting the digital infrastructure construction in remote and rural areas and enhancing people's ability to use digital technology, so as to narrow China's digital divide and increase residents' income. And the government needs to actively guide traditional industries to embrace digital technology, accelerate industrial transformation, and improve total factor productivity of enterprises through digital dividends, so as to improve the inclusiveness and greening of the city.

Then, in the process of rapid urbanization, urban management authorities should not only pay attention to urban per capita GDP and other economic growth indicators, but also carefully plan the sources of driving urban economic growth, which means that the authorities should promote economic growth driven by innovation, including encouraging enterprises to invent new technologies, protecting personal inventions and patents, and spurring the transformation of the innovative achievements of scientific research institutions into the source of improving urban IGGE.

Finally, in view of the role of population agglomeration in IGGE, the policy of balanced development of urban population scale needs to be further improved, which means cities with sparse population need to develop industries based on local regional characteristics, carry out supporting infrastructure construction, and issue policies for dividend talents to flow into the region, so as to promote urban population agglomeration and enhance urban IGGE. In addition, we should encourage the cross-regional flow of talents in cities and share the human capital of excellent cities with less developed cities, so as to realize the trickle-down effect between cities.

6.3. Limitations of This Paper. Limited by the scope of our research, this paper inevitably has the following limitations.

Firstly, because there is no consistent view on the concept and measurement of IGG in the academic field, this study is only based on the existing literature to measure IGGE of Chinese cities. Future research needs to try a variety of different methods, build a more complex comprehensive index system to measure IGG, expand the range of data samples, such as research based on international IGG and IGG in the Asia Pacific region, and enrich academic contributions.

Secondly, due to the availability of data, this study only combs ten drivers of IGG according to the existing literature. Then, there may be some other potential factors in reality, but they are not taken into account. Therefore, future research will further explore the impact and contribution of other factors in order to find more drivers of IGG.

Finally, although the machine learning method has good accuracy and performance in measuring IGG of Chinese cities, the potential "black box" problem makes us unable to further explore the intermediary mechanism and spatial spillover effect of influence. Therefore, in the future, we will try to cooperate with the most cutting-edge machine learning methods and spatial econometric models to deeply explore the spatial effect, as well as the mechanism of these factors driving IGG.

Appendix

The step of machine learning algorithm is as follows:

Step one: data preprocessing.

In order to improve the accuracy of ML algorithm, it is an indispensable step to standardize the sample data. The calculation of data standardization is as follows:

$$\varphi = \frac{y - y_{\min}}{y_{\max} - y_{\min}}. \tag{A.1}$$

Among them, the standardized data is represented by ϕ; and y denotes the data before normalization; $y_{\max}$ and $y_{\min}$ mean the maximal and the least data, respectively. Moreover, the data set is divided into training set and test set according to the ratio of 7 to 3.

Step two: model building.

Firstly, the initial parameters of various ML algorithms are predicted. Furthermore, the results are evaluated according to the correlation coefficient between the predicted value and the actual value. Additionally, the optimal parameters of models are obtained, and the training set is used to train the model to obtain the optimal model.

Step three: prediction and analysis.

The data of the test set is input into different ML models, and the results are obtained through calculation. We compare the actual value and predicted value of each variable, and then we infer the computational performance of each model and determine the optimal model.

Model evaluation method.

To evaluate the performance of the ML model, we calculate the goodness of fit (R^2), mean square deviation (RMSE), mean absolute error (MAE), and mean absolute percentage error (MAPE). Among these indicators, R^2 denotes the comparison between the real value and the predicted value. The closer it is to 1, the better, while the lower the simulation error represented by other indicators, the better. The calculation formulae of each index are as follows:

$$R_2 = \frac{\left(\sum_{i=1}^{n}\left(yo_t - \overline{y}o\right) * \left(ym_t - \overline{y}m\right)\right)^2}{\sum_{t=1}^{n}\left(yo_t - \overline{y}o\right)^2 * \sum_{t=1}^{n}\left(ym_t - \overline{y}m\right)^2},$$

$$\mathrm{RMSE} = \sqrt{\frac{1}{n}\sum_{t=1}^{n}\left(yo_t - ym_t\right)^2},$$

$$\mathrm{MAE} = \frac{1}{n}\sum_{i=1}^{n}\left|\left(yo_t - ym_t\right)\right|,$$

$$\mathrm{MAPE} = \sum_{t=1}^{n}\left|\frac{yo_t - ym_t}{yo_t}\right| * \left(\frac{100}{n}\right), \tag{A.2}$$

where n means the number of data; ym is the predicted result; yo is the real value; $\overline{y}m$ and $\overline{y}$ 0 denote the mean value of the predictive result and real result, respectively.

Data Availability

All data included in this study area are available upon request to the corresponding author.

Conflicts of Interest

The authors declare that they have no conflicts of interest regarding the publication of this study.

Authors' Contributions

Xiaoxue Liu performed methodology, writing (original draft, review, and editing), conceptualization, visualization, and funding acquisition; Shuangshuang Fan performed writing (original draft), supervision, and software; Fuzhen Cao performed revising, proofreading, and editing; Shengnan Peng made proofreading and editing; Hongyun Huang revised and edited the study.

Acknowledgments

This research was funded by the major project of the National Social Science Fund of China (21&ZD151) and Key Project of the National Social Science Fund of China (21ATJ007).

References

[1] Y. H. Sun, W. W. Ding, Z. Y. Yang, G. C. Yang, and J. T. Du, "Measuring China's regional inclusive green growth," *Science of the Total Environment*, vol. 713, Article ID 136367, 2020.

[2] K. Hanewald, R. Jia, and Z. N. Liu, "Why is inequality higher among the old? Evidence from China," *China Economic Review*, vol. 66, Article ID 101592, 2021.

[3] C. Ma, Z. Song, and Q. Q. Zong, "Urban-rural inequality of opportunity in health care: evidence from China," *International Journal of Environmental Research and Public Health*, vol. 18, no. 15, pp. 7792–92, 2021.

[4] K. Y. Gu, F. Dong, H. Sun, and Y. Zhou, "How economic policy uncertainty processes impact on inclusive green growth in emerging industrialized countries: a case study of China," *Journal of Cleaner Production*, vol. 322, Article ID 128963, 2021.

[5] W. Pan, W. L. Pan, C. Hu et al., "Assessing the green economy in China: an improved framework," *Journal of Cleaner Production*, vol. 209, pp. 680–691, 2019.

[6] A. B. Adetunji, O. N. Akande, F. A. Ajala, O. Oyewo, Y. F. Akande, and G. Oluwadara, "House price prediction using Random Forest machine learning technique," *Procedia Computer Science*, vol. 199, pp. 806–813, 2022.

[7] A. A. Mustafa, C. Y. Lin, and M. Kakinaka, "Detecting market pattern changes: a machine learning approach," *Finance Research Letters*, vol. 47, Article ID 102621, 2022.

[8] S. Ben Jabeur, R. Khalfaoui, and W. Ben Arfi, "The effect of green energy, global environmental indexes, and stock markets in predicting oil price crashes: evidence from explainable machine learning," *Journal of Environmental Management*, vol. 298, Article ID 113511, 2021.

[9] A. Richardson, T. van Florenstein Mulder, and T. Vehbi, "Nowcasting GDP using machine-learning algorithms: a real-time assessment," *International Journal of Forecasting*, vol. 37, no. 2, pp. 941–948, 2021.

[10] M. Kamah, J. S. Riti, and P. Bin, "Inclusive growth and environmental sustainability: the role of institutional quality in sub-Saharan Africa," *Environmental Science and Pollution Research*, vol. 28, no. 26, Article ID 34885, 2021.

[11] D. Khan and R. Ulucak, "How do environmental technologies affect green growth? Evidence from BRICS economies," *Science of the Total Environment*, vol. 712, Article ID 136504, 2020.

[12] World Commission on Environment and Development (WCED), *Our Common Future*, Oxford University Press, Oxford, UK, 1987.

[13] Y. Wu and X. Zhou, "Research on the efficiency of China's fiscal expenditure structure under the goal of inclusive green growth," *Sustainability*, vol. 13, no. 17, pp. 9725–10129, 2021.

[14] E. Berkhout, J. Bouma, N. Terzidis, and M. Voors, "Supporting local institutions for inclusive green growth: developing an evidence gap map," *NJAS - Wageningen Journal of Life Sciences*, vol. 84, no. 1, pp. 51–71, 2018.

[15] U. Unep, *Towards a green Economy: Pathways to Sustainable Development and Poverty Eradication*, UNEP, Nairobi, Kenya, 2011.

[16] World Bank, *Inclusive green Growth: The Pathway to Sustainable Development*, World Bank, Washington, DC, USA, 2012.

[17] W. L. Wu and X. L. Zhou, "The construction and application of China's inclusive green growth performance evaluation system," *Chinese Management Science*, vol. 27, no. 9, pp. 183–194, 2019.

[18] S. Spratt, S. Griffith-Jones, and J. A. Ocampo, *Mobilizing Investment for Inclusive green Growth in Low-Income Countries*, International Zusammenarbeit(GIZ)GmbH, Frankfurt, 2013, https://www.greenfinanceplatform.org/research/mobilising-investment-inclusive-green-growth-low-income-countries.

[19] J. Bouma and E. Berkhout, *Inclusive green Growth*, PBL Netherlands Environmental Assessment Agency, The Hague, Netherlands, 2015.

[20] J. J. Kessler and S. Slingerland, "Study on Public Private Partnerships for Contribution to Inclusive green Growth," http://trinomics.eu/wp-content/uploads/2015/05/Final-Report_PPPs-and-IGG.pdf 2557, PBL Netherlands Environmental Assessment Agency, The Hague, Netherlands, 2015, http://trinomics.eu/wp-content/uploads/2015/05/Final-Report_PPPs-and-IGG.pdf 2557.

[21] L. A. Mandle, Z. Y. Ouyang, J. E. Salzman, and G. C. Daily, *Green Growth that Works (Natural Capital Policy and Finance Mechanisms from Around the World)*, pp. 17–27, Springer, Berlin/Heidelberg, Germany, 2019.

[22] P. Kumar, "Innovative tools and new metrics for inclusive green economy," *Current Opinion in Environmental Sustainability*, vol. 24, pp. 47–51, 2017.

[23] Q. He and J. T. Du, "The impact of urban land misallocation on inclusive green growth efficiency: evidence from China," *Environmental Science and Pollution Research*, vol. 29, no. 3, pp. 3575–3586, 2021.

[24] R. P. Pradhan, M. B. Arvin, N. R. Norman, and S. K. Bele, "Economic growth and the development of telecommunications infrastructure in the G-20 countries: a panel-VAR approach," *Telecommunications Policy*, vol. 38, no. 7, pp. 634–649, 2014.

[25] M. Nair, R. P. Pradhan, and M. B. Arvin, "Endogenous dynamics between R&D, ICT and economic growth: empirical evidence from the OECD countries," *Technology in Society*, vol. 62, Article ID 101315, 2020.

[26] K. Kim, İ. İlkkaracan, and T. Kaya, "Public investment in care services in Turkey: promoting employment & gender inclusive growth," *Journal of Policy Modeling*, vol. 41, no. 6, pp. 1210–1229, 2019.

[27] I. K. Ofori and S. A. Asongu, "ICT diffusion, foreign direct investment and inclusive growth in sub-Saharan Africa," *Telematics and Informatics*, vol. 65, Article ID 101718, 2021.

[28] A. A. Aşıcı, "Economic growth and its impact on environment: a panel data analysis," *Ecological Indicators*, vol. 24, pp. 324–333, 2013.

[29] D. Acemoglu, P. Aghion, L. Bursztyn, and D. Hémous, "The environment and directed technical change," *The American Economic Review*, vol. 102, no. 1, pp. 131–166, 2012.

[30] R. V. D. Ploeg and C. Withagen, "Green growth, green paradox and the global economic cisis," *Environmental Innovation and Societal Transitions*, vol. 6, pp. 116–119, 2013.

[31] J. Gupta, N. R. M. Pouw, and M. A. F. Ros-Tonen, "Towards an elaborated theory of inclusive development," *European Journal of Development Research*, vol. 27, no. 4, pp. 541–559, 2015.

[32] J. Gupta and C. Vegelin, "Sustainable development goals and inclusive development," *Int. Environ. Agreements*, vol. 16, no. 3, pp. 433–448, 2016.

[33] J. Gupta and N. Pouw, "Towards a transdisciplinary conceptualization of inclusive development," *Current Opinion in Environmental Sustainability*, vol. 24, pp. 96–103, 2017.

[34] J. Gupta and L. Lebel, "Editorial access and allocation in earth system governance," *Int. Environ. Agreements*, vol. 20, no. 2, pp. 197–201, 2020.

[35] C. F. Rammelt and J. Gupta, "Inclusive is not an adjective, it transforms development: a post-growth interpretation of inclusive development," *Environmental Science & Policy*, vol. 124, pp. 144–155, 2021.

[36] G. Kallis, *Degrowth (The Economy: Key Ideas)*, Agenda Publishing, California, USA, 2018.

[37] M. Sandberg, K. Klockars, and K. Wilen, "Green growth or degrowth? Assessing the normative justifications for environmental sustainability and economic growth through critical social theory," *Journal of Cleaner Production*, vol. 206, pp. 133–141, 2019.

[38] S. Hankammer, R. Kleer, L. Mühl, and J. Euler, "Principles for organizations approaching sustainable degrowth: framework development and application to four B Corps," *Journal of Cleaner Production*, vol. 300, Article ID 126818, 2021.

[39] T. S. Smith, M. Baranowski, and B. Schmid, "Intentional degrowth and its unintended consequences: uneven journeys towards post-growth transformations," *Ecological Economics*, vol. 190, Article ID 107215, 2021.

[40] J. Gupta, M. Bavinck, M. Ros-Tonen et al., "COVID-19, poverty and inclusive development," *World Development*, vol. 145, Article ID 105527, 2021.

[41] S. H. Wang, B. B. Lu, and K. B. Yin, "Financial development, productivity, and high-quality development of the marine economy," *Marine Policy*, vol. 130, Article ID 104553, 2021.

[42] R. Molero-Simarro, "Inequality in China revisited. The effect of functional distribution of income on urban top incomes, the urban-rural gap and the Gini index, 1978–2015," *China Economic Review*, vol. 42, pp. 101–117, 2017.

[43] I. Permanyer and J. Smits, "Inequality in human development across the Globe," *Population and Development Review*, vol. 46, no. 3, pp. 583–601, 2020.

[44] M. Biggeri and V. Mauro, "Towards a more 'sustainable' human development index: integrating the environment and freedom," *Ecological Indicators*, vol. 91, pp. 220–231, 2018.

[45] P. Dasgupta, S. Managi, and P. Kumar, "The inclusive wealth index and sustainable development goals," *Sustainability Science*, vol. 17, no. 3, pp. 899–903, 2021.

[46] J. Luukkanen, J. Kaivo-oja, N. Vähäkari et al., "Green economic development in Lao PDR: a sustainability window analysis of green growth productivity and the efficiency gap," *Journal of Cleaner Production*, vol. 211, pp. 818–829, 2019.

[47] A. Saunders and J. Luukkanen, "Sustainable development in Cuba assessed with sustainability window and doughnut economy approaches," *The International Journal of Sustainable Development and World Ecology*, vol. 29, no. 2, pp. 176–186, 2021.

[48] S. Albagoury, *Inclusive green Growth in Africa: Ethiopia Case Study*, Institute of African Research and Studies, Cairo University, Cairo, Egypt, 2016.

[49] S. Jha, C. S. Sandhu, and W. Radtasiri, *Inclusive green Growth index: A New Benchmark for Quality Growth*, Asian Development Bank, Manila, Philippines, 2018.

[50] M. Li, Y. F. Zhang, Z. Y. Fan, and H. Chen, "Evaluation and research on the level of inclusive green growth in Asia-Pacific region," *Sustainability*, vol. 13, no. 13, pp. 7482–8169, 2021.
[51] U. Narloch, T. Kozluk, and A. Lloyd, *Measuring Inclusive green Growth at the Country Level*, United Nations Environment Programme, Nairobi, Kenya, 2016.
[52] K. Tone and M. Tsutsui, "An epsilon-based measure of efficiency in DEA–A third pole of technical efficiency," *European Journal of Operational Research*, vol. 207, no. 3, pp. 1554–1563, 2010.
[53] S. S. Fan and X. X. Liu, "Evaluation the performance of inclusive growth based on BP Neural Network and machine learning approach," *Computational Intelligence and Neuroscience*, vol. 2022, Article ID 9491748, 2022.
[54] M. S. Ozigis, J. D. Kaduk, C. H. Jarvis, P. da Conceição Bispo, and H. Balzter, "Detection of oil pollution impacts on vegetation using multifrequency SAR, multispectral images with fuzzy forest and random forest methods," *Environmental Pollution*, vol. 256, Article ID 113360, 2020.
[55] J. A. Kamińska, "The use of random forests in modelling short-term air pollution effects based on traffic and meteorological conditions: a case study in Wrocław," *Journal of Environmental Management*, vol. 217, no. 9, pp. 164–174, 2018.
[56] P. Ładyżyński, K. Żbikowski, and P. Gawrysiak, "Direct marketing campaigns in retail banking with the use of deep learning and random forests," *Expert Systems with Applications*, vol. 134, pp. 28–35, 2019.
[57] C. M. Yeşilkanat, "Spatio-temporal estimation of the daily cases of COVID-19 in worldwide using random forest machine learning algorithm," *Chaos, Solitons & Fractals*, vol. 140, no. 45, 210 pages, Article ID 110210, 2020.
[58] B. Sun, T. Sun, and P. Jiao, "Spatio-temporal segmented traffic flow prediction with ANPRS data based on improved XGBoost," *Journal of Advanced Transportation*, vol. 2021, no. 1, 24 pages, Article ID 5559562, 2021.
[59] H. T. Zheng, J. B. Yuan, and L. Chen, "Short-term load forecasting using EMD-LSTM neural networks with a XGboost algorithm for feature importance evaluation," *Energies*, vol. 10, no. 8, pp. 1168–68, 2017.
[60] G. He, C. Zhou, T. Luo et al., "Online optimization of fluid catalytic cracking process via a Hybrid model based on simplified structure-oriented lumping and case-based reasoning," *Industrial & Engineering Chemistry Research*, vol. 60, no. 1, pp. 412–424, 2021.
[61] L. Li, Y. Lin, D. Yu, Z. Liu, Y. Gao, and J. Qiao, "A multi-organ fusion and LightGBM based radiomics algorithm for high-risk esophageal varices prediction in cirrhotic patients," *IEEE Access*, vol. 9, no. 18, Article ID 15041, 2021.
[62] S. Kuznets, "Economy growth and income inequality," *The American Economic Review*, vol. 45, no. 36, pp. 1–28, 1955.
[63] B. Keeley, *What's happening to income inequality? In income inequality: the gap Between Rich and Poor*, pp. 31–40, OECD Publishing, Pari, France, 2015.
[64] G. M. Grossman and A. B. Krueger, *Environmental impacts of a north American free trade agreement*, National Bureau of Economic Research, Cambridge, MA, USA, 1991.
[65] World Bank, *Financial development and inclusive growth: Attaining shared and sustainable prosperity in Egypt*, vol. 3, pp. 765–791, Washington, DC, USA, 2003.
[66] F. Ahmed, S. Kousar, A. Pervaiz, and A. Shabbir, "Do institutional quality and financial development affect sustainable economic growth? Evidence from South Asian countries," *Borsa Istanbul Review*, vol. 22, no. 1, pp. 189–196, 2022.
[67] C. Ghisetti and F. Quatraro, "Green technologies and environmental productivity: a cross-sectoral analysis of direct and indirect effects in Italian regions," *Ecological Economics*, vol. 132, pp. 1–13, 2017.
[68] X. Zhang, G. Wan, G. G. Zhang, and Z. Y. He, "Digital economy, financial inclusion, and inclusive growth," *Economic Research Journal*, vol. 17, no. 8, pp. 71–86, 2019.
[69] M. E. Mondejar, R. Avtar, H. L. B. Diaz et al., "Digitalization to achieve sustainable development goals: steps towards a smart green planet," *Science of the Total Environment*, vol. 794, Article ID 148539, 2021.
[70] J. Nkurunziza, *Human capital development in Rwanda: effects of education, Social Protection and Rural Development Policies*, PhD Thesis, 2015, http://DSPACE.LIBRARY.UU.NL/BITSTREAM/HANDLE/1874/325242/NKURUNZIZA.PDF?SEQUENCE=1&ISALLOWED=Y.
[71] W. Ouattara, "Public expenditure contribution to pro-poor growth in Cote D' Ivoire: a micro simulated general equilibrium approach," *Modern Economy*, vol. 03, no. 03, pp. 330–337, 2012.
[72] W. O. Olatomide and A. O. Omowumi, "Policy interventions and public expenditure reform for pro-poor agricultural development in Nigeria," *African Journal of Agricultural Research*, vol. 9, no. 4, pp. 487–500, 2014.
[73] W. Liu, J. Y. Zhan, F. Zhao, X. Wei, and F. Zhang, "Exploring the coupling relationship between urbanization and energy eco-efficiency: a case study of 281 prefecture-level cities in China," *Sustainable Cities and Society*, vol. 64, no. 64, Article ID 102563, 2021.
[74] I. Sulemana, E. Nketiah-Amponsah, E. A. Codjoe, and J. A. N. Andoh, "Urbanization and income inequality in sub-saharan africa," *Sustainable Cities and Society*, vol. 48, no. 6, Article ID 101544, 2019.
[75] W. Sun and C. Huang, "How does urbanization affect carbon emission efficiency? Evidence from China," *Journal of Cleaner Production*, vol. 272, Article ID 122828, 2020.
[76] F. M. Ajide, T. T. Osinubi, and J. T. Dada, "Economic globalization, entrepreneurship, and inclusive growth in Africa," *Journal of Economic Integration*, vol. 36, no. 4, pp. 689–717, 2021.
[77] J. Zeng and J. Ren, "How does green entrepreneurship affect environmental improvement? Empirical findings from 293 enterprises," *The International Entrepreneurship and Management Journal*, vol. 18, no. 1, pp. 409–434, 2022.
[78] Y. Fernández Fernández, M. Fernández López, and B. Olmedillas Blanco, "Innovation for sustainability: the impact of R&D spending on CO2 emissions," *Journal of Cleaner Production*, vol. 172, pp. 3459–3467, 2018.
[79] S. J. Wang, J. Y. Zeng, and X. P. Liu, "Examining the multiple impacts of technological progress on CO2 emissions in China: a panel quantile regression approach," *Renewable and Sustainable Energy Reviews*, vol. 103, pp. 140–150, 2019.
[80] S. L. Hu, G. Zeng, X. Z. Cao, H. X. Yuan, and B. Chen, "Does technological innovation promote green development? A case study of the Yangtze River Economic Belt in China," *International Journal of Environmental Research and Public Health*, vol. 18, no. 11, p. 6111, Article ID 6111, 2021.
[81] H. Weber and J. D. Sciubba, "The effect of population growth on the environment: evidence from European regions," *European Journal of Population*, vol. 35, no. 2, pp. 379–402, 2019.
[82] H. Moshi, "Sustainable and inclusive growth in Africa: industrialization a must," *African Journal of Economic Review*, vol. 2, no. 2, pp. 19–38, 2014.

Hindawi
Computational Intelligence and Neuroscience
Volume 2022, Article ID 5766448, 6 pages
https://doi.org/10.1155/2022/5766448

Research Article

Direct Radiation Model of Louver Shading in Office Building Shade Based on Network Optimization Method

Dasi He,[1] **Chang Jianguo**,[2] **and Han Xing**[3]

[1]*School of Energy and Environment, Zhongyuan University of Technology, Zhengzhou 450007, China*
[2]*Henan Academy of Building Sciences Co., Ltd, Zhengzhou 450053, China*
[3]*PCI Technology Group, Guangzhou 510653, China*

Correspondence should be addressed to Dasi He; heds@zut.edu.cn

Received 6 May 2022; Revised 30 May 2022; Accepted 7 June 2022; Published 5 August 2022

Academic Editor: Yang Gu

In view of the current situation of excessively rapid growth of building energy consumption, a control strategy of external shading louvers based on comprehensive energy consumption is proposed to deeply tap the potential of building energy saving. First, the architectural design software Ecotect is used to establish a simulation model of a shading building in Zhengzhou and import it into the lighting analysis software Daysim and the energy consumption simulation software Energyplus to simulate the annual lighting energy consumption and air-conditioning at 11 kinds of blind angles (15~165°). For heating energy consumption, take the blind angle corresponding to the minimum comprehensive energy consumption as the opening angle of the dynamic blinds and analyze the comprehensive energy consumption for the whole year under dynamic sunshading. The results show that, compared with the conventional control strategy, the optimized control strategy based on comprehensive energy consumption can greatly improve the building's energy-saving rate.

1. Introduction

At present, building energy consumption accounts for about 40.6% of the total energy consumption. With the aggravation of environmental degradation and energy shortage, building energy conservation has attracted more and more attention [1]. The application of shading facilities can control the heat entering the room and reduce the energy consumption of air-conditioning; However, it will inevitably affect the overall indoor illumination and increase lighting energy consumption [2]. Studies have shown that most people spend more than 90% of their time in buildings or cars, so building energy conservation is the top priority in the field of energy conservation. On the premise of meeting the human body's requirements for indoor illumination, improving building energy conservation has become the focus of building design and operation.

In recent years, many scholars have studied the subject of external louver shading. Based on the original sunshade model, Huo et al. established the sunshade correction model of external louver considering the installation spacing and analyzed the influence of installation spacing on the backscattering transmittance of the sunshade model under different louver shading parameters. The results show that under different louver inclination and effective incidence angle, the difference between the two models is obvious, and the proportion of the total transmittance and the amount of backlight of the two models increases with the increase of the reflectivity of the louver surface [3]. Zhang and Wang found that China's energy-saving field mostly focused on the application of energy-saving materials and the improvement of equipment efficiency, but did not consider energy-saving optimization from the design direction [4]. Bunning and Crawford found that different shading angles have a significant impact on energy consumption by studying the impact of shading angles on energy consumption, but the consideration is relatively simple [5]. Liu et al. studied the impact of automatic louver and automatic dimming lighting system on lighting energy consumption and found that the energy-saving rate of north and east lighting can reach 65%,

with great energy-saving potential, but did not conduct a comprehensive analysis in combination with the energy consumption of air-conditioning and heating [6].

Taking the office buildings in Zhengzhou as the research object, this paper simulates and calculates the annual lighting energy consumption and air-conditioning and heating energy consumption under 11 kinds of louver inclination angles (15~165°). The comprehensive energy consumption of rooms in different directions is compared and analyzed, and the control strategy of external sunshade louvers to maximize the energy-saving potential of buildings is explored.

2. Theoretical Basis

The thermal simulation method of external sunshade louvers is mainly divided into three stages: input of simulation calculation conditions, solution based on CFD, and analysis of thermal simulation results of sunshade louver.

Among them, the input stage of simulation conditions first needs to select the simulation environment, build a 3D model, set simulation parameters, and determine the simulated sunshade louver thermal environment. CFD calculation method has the advantages of simple and easy operation and high accuracy. It can calculate the corresponding value quickly and accurately. Therefore, the energy consumption value after the control of external sunshade louver is calculated according to CFD. The CFD calculation program is shown in Figure 1.

According to the calculation program in Figure 1, the thermal simulation results of external sunshade louvers are obtained, and the building model is established on this basis.

3. Project Overview

The test site of this paper is a three storey office building in Zhengzhou. The north-south room size of the office building is $6 \times 4 \times 3.3$ m and window size is 4×1.92 m. The size of the east-west room is $4 \times 6 \times 3.3$ m and window size is 2.75×1.92 m. The window sill is 0.8 m high and the window wall ratio is 0.4. Louvers are set outside the windows in all directions for shading.

4. Technical Design

4.1. Building Model. The building model is a three storey office building located in Zhengzhou. As shown in Figure 2, the middle rooms in each direction are taken as the research object to eliminate the influence of the ground, wall, and roof. The parameter settings meet the requirements of GB 50189–2015 design standard for energy efficiency of public buildings [7] and GB 50033–2013 design standard for daylighting of buildings [8].

4.2. Description of Simulated Working Conditions. In this paper, the meteorological parameters of Zhengzhou typical meteorological year (CSWD) are selected for simulation calculation, with louver inclination and lighting control type as variables and other parameters as constants.

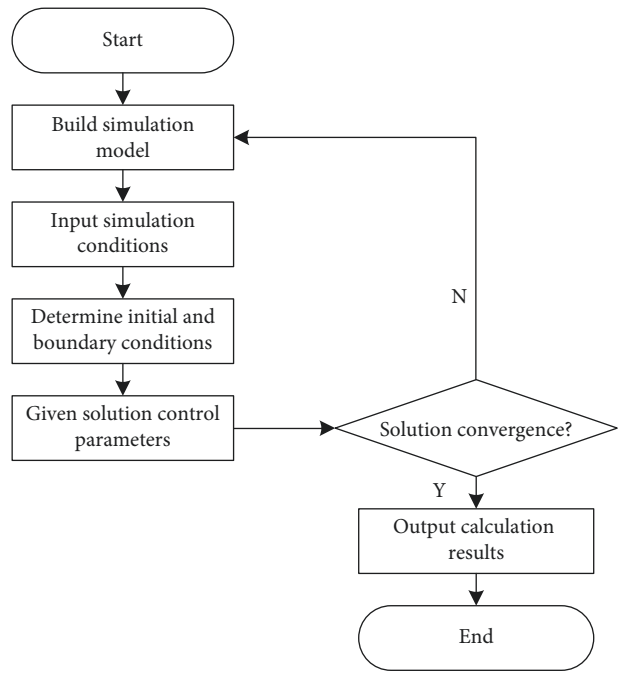

Figure 1: CFD calculation program.

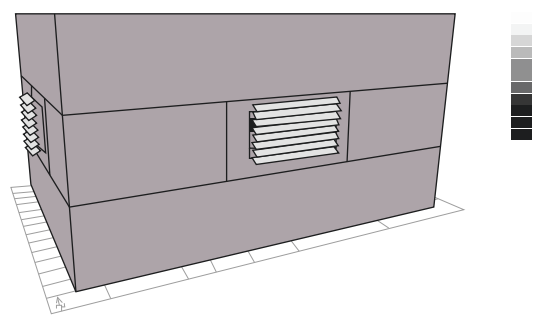

Figure 2: Schematic diagram of building model.

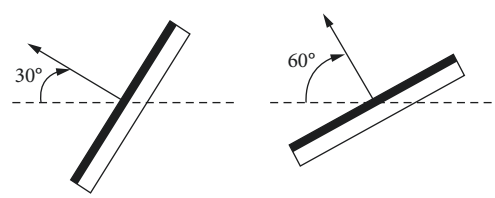

Figure 3: Schematic diagram of louver inclination.

The ideal air-conditioning system is adopted for the model. The opening time of the air-conditioner is 8 : 00–18 : 00 on working days, the infiltration air volume is 3 times/h, the indoor design temperature in summer is 26°C, the indoor design temperature in winter is 18°C, the personnel density is 0.1 person/m^2, the lighting power density is 9 W/m^2, and the electrical power density is 15 W/m^2. Set the daylighting reference plane 0.75 m from the ground, and the design illuminance is 300 LX according to the requirements of GB 50034–2013 standard for lighting design of buildings [9]. When the natural daylighting illuminance is insufficient, the lighting system is turned on for the supplement.

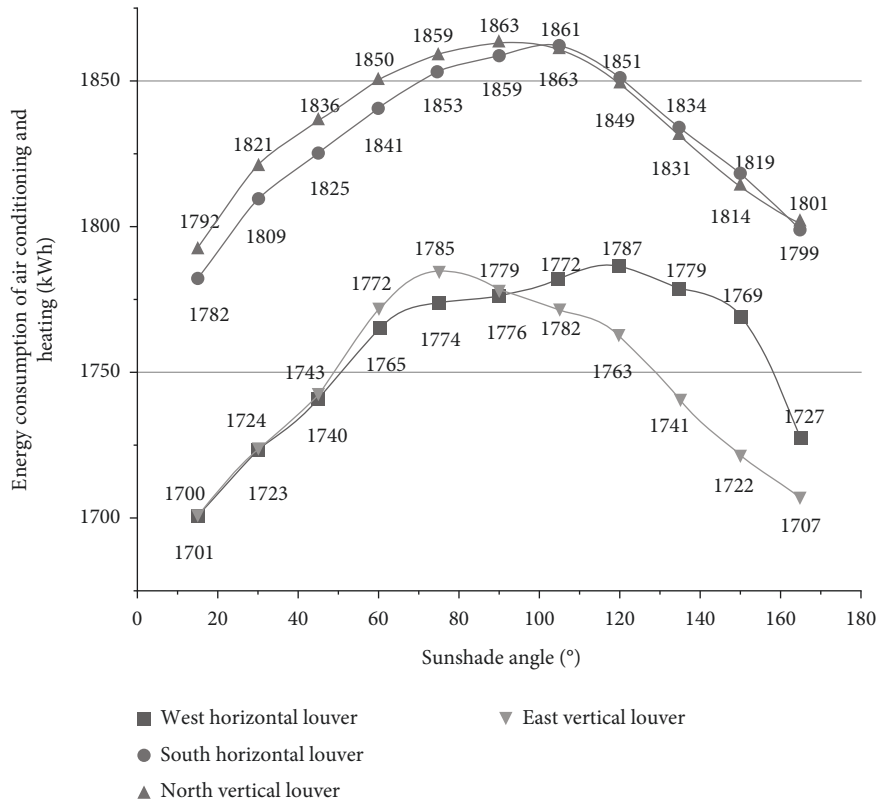

Figure 4: Distribution of energy consumption for air-conditioning and heating in various directions throughout the year.

Figure 3 shows the schematic diagram of louver inclination angle with horizontal louver shading side view or vertical louver shading top view.

According to Figure 3, the inclination angle of the louver is defined as the angle between the external normal of the window and the external normal of the louver. Horizontal shading measures shall be taken for rooms facing west and south and vertical shading measures shall be taken for rooms facing east and north. In this way, the control of external sunshade shutters based on network optimization is realized.

5. Experimental Analysis

Considering that the louver inclination angles is generally between 0° and 180°, in order to better verify the effectiveness of the proposed control strategy of external sunshade shutter based on comprehensive energy consumption, 11 kinds of louver inclination angles (15~165°) in the middle are selected as the test objects at an interval of 15°, and the simulation results are output and analyzed.

5.1. Energy Consumption Analysis of Air Conditioning and Heating. The building model is imported into Energy Plus to simulate the annual hourly air-conditioning and heating energy consumption. Figure 4 shows the distribution law of annual air-conditioning and heating energy consumption of rooms facing each direction under 11 kinds of louver inclination angles (15~165°).

From Figure 4, it is easy to know the change law of air-conditioning and heating energy consumption and the best fixed inclination angle of each room under each shading angle. The shading control mode is changed to dynamic shading based on blocking solar radiation, and then the simulation calculation is carried out. The air-conditioning and heating energy consumption of each room under dynamic shading is 1649 kWh in the west, 1737 kWh in the south, 1753 kWh in the north, and 1654 kWh in the east.

It is easy to know from Table 1 that compared with the best fixed louver shading, dynamic shading has excellent performance in energy saving. The energy-saving rate of air-conditioning and heating in each room has increased by 37.8% in the west, 34.6% in the south, 30.2% in the north, and 35.3% in the east.

5.2. Analysis of Lighting Energy Consumption. Figure 5 is the annual illumination energy consumption in rooms with different orientations distribution diagram with Daysim output under 11 louver angles (15~165°).

From Figure 5, it is easy to know the change law of lighting energy consumption towards the room under each shading angle. On the whole, with the increase of shading angle in four directions, it shows a downward trend first and then upward trend. When the west direction is 100°, the minimum energy consumption is 469 kwh, when the south direction is 105°, the minimum energy consumption is 387 kwh, when the north direction is 90°, the minimum

Table 1: Lighting energy consumption.

Control type	Manual switch (kW)	Manual switch + photoelectric dimming (kW)
Westward	482.5	404.2
Southward	479.6	390.1
Northward	486.0	392.2
Eastward	487.1	405.4

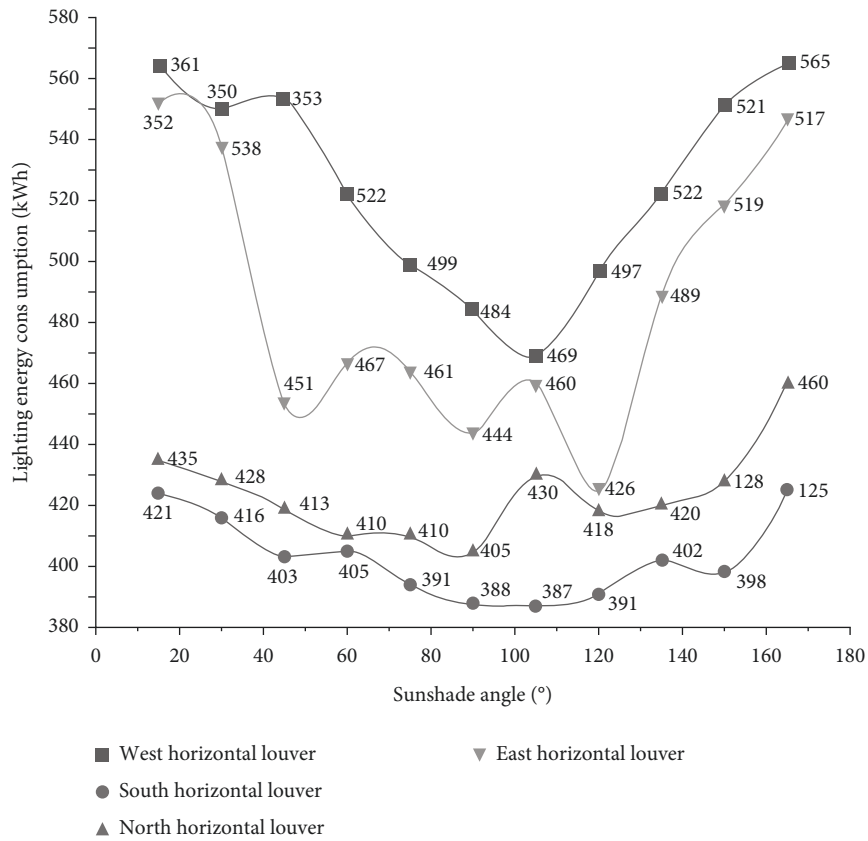

Figure 5: Distribution of annual lighting energy consumption in various directions.

energy consumption is 405 kwh, and at 120° to the east, the minimum energy consumption is 426 kwh.

Change the sunshade control mode to dynamic sunshade based on blocking solar radiation, and then conduct simulation calculation to obtain the lighting energy consumption of each facing room combined with two different lighting control systems under dynamic sunshade. The results are shown in Table 1.

It is easy to know from Table 1 that taking the manual switch control alone as the reference, adopting the photoelectric sensor dimming control can further tap the lighting energy-saving potential and increase the lighting energy-saving rate of each room by 16.2% in the west, 18.7% in the south, 19.3% in the north, and 16.8% in the east. This technology is easy to realize by controlling the electric lamp through the dimming mapping level [10].

5.3. Comprehensive Energy Consumption Analysis. Without sunshade measures, the comprehensive energy consumption of each room is 2317.5 kWh in the west, 2391.6 kWh in the south, 2407.0 kWh in the north, and 2321.1 kWh in the east. Taking no sunshade as a reference, when adopting the best fixed louver sunshade corresponding to the lowest comprehensive energy consumption, the energy-saving rate of buildings in each direction is 5.8% in the west, 5.4% in the south, 5.4% in the north, and 5.7% in the east. Taking the louver inclination corresponding to the minimum hourly comprehensive energy consumption of the whole year as the dynamic louver opening angle for simulation calculation, the annual comprehensive energy consumption is obtained.

In order to make it easy to distinguish, the dynamic shading control strategy based on blocking solar radiation is called conventional control strategy, and the control strategy of taking the louver inclination corresponding to the minimum hourly comprehensive energy consumption throughout the year as the dynamic louver opening angle is called optimal control strategy. Figure 6 shows the effect of building energy conservation under different control strategies for each facing room.

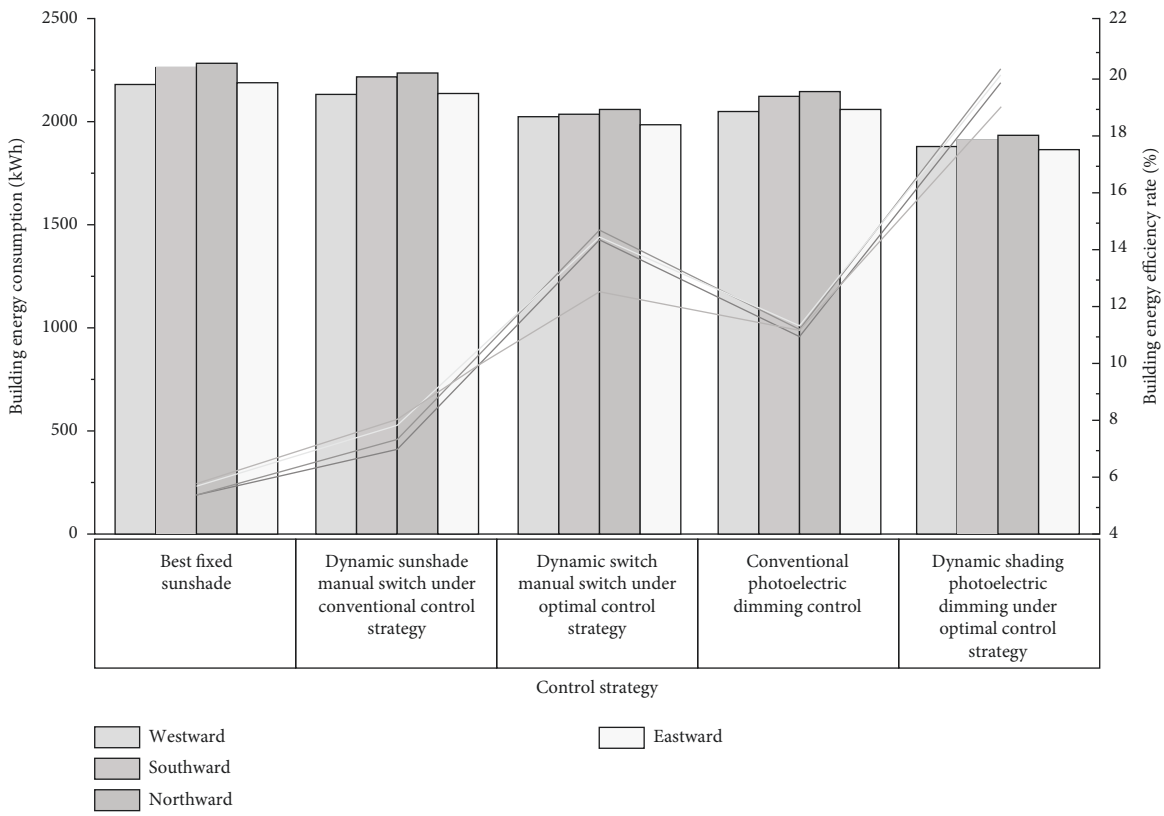

Figure 6: Energy saving effect diagram of each orientation under different control strategies.

It is easy to know from Figure 6 that compared with the conventional control strategy, the optimized control strategy can greatly improve the building energy-saving rate. Among them, when the lighting system is controlled by manual switch alone, the energy-saving rate of buildings facing rooms can be increased by 56.2% in the west, 101.5% in the south, 105.4% in the north, and 85.6% in the east. When the lighting system adopts manual switch + photoelectric sensor dimming control, the energy-saving rate of buildings facing rooms can be increased by 65.9% in the west, 82.8% in the south, 81.4% in the north, and 77.3% in the east.

It can also be seen from Figure 6 that when the lighting system adopts manual switch + photoelectric sensor dimming control, the building energy-saving potential can be further tapped. Under the conventional control strategy, compared with the manual switch control of the lighting system alone, the energy-saving rate of rooms in each direction can be further improved by 42.1% in the west, 51.1% in the south, 55.8% in the north, and 45.4% in the east. Under the optimized control strategy, compared with the lighting system adopting manual switch control alone, the energy-saving rate of rooms in each direction can be further improved by 51.0% in the west, 37.2% in the south, 37.7% in the north, and 38.9% in the east.

In this paper, the dynamic louver inclination schedule of each direction is obtained by using the above simulation results. The method is as follows: during working hours, in the air-conditioning and heating season, the louver inclination corresponding to the minimum comprehensive energy consumption is taken as the dynamic louver opening angle. In the transition season, the louver angle corresponding to the minimum lighting energy consumption is taken as the dynamic louver opening angle. During non-working hours, air-conditioning, heating, and transition seasons should be conducive to heat dissipation, heat preservation, and ventilation respectively. Therefore, the louver inclination when the louver is vertical, parallel, and perpendicular to the outer window is taken as the dynamic louver opening angle. Figure 7 shows the dynamic louver inclination schedule of north facing room in winter solstice under the control of dynamic shading and photoelectric dimming lighting system under the optimal control strategy.

Based on the above simulation results, when the lighting system is controlled by manual switch alone, the energy-saving rate of rooms in each direction can be increased by 56.2% in the west, 101.5% in the south, 105.4% in the north, and 85.6% in the east. When the lighting system adopts manual switch + photoelectric sensor dimming control, the energy-saving rate of buildings facing rooms can be increased by 65.9% in the west, 82.8% in the south, 81.4% in the north, and 77.3% in the east. After adopting the optimized control strategy in this paper, compared with the lighting system adopting manual switch control alone, the energy-saving rate of rooms in each direction can be further improved by 51.0% in the west, 37.2% in the south, 37.7% in the north, and 38.9% in the east.

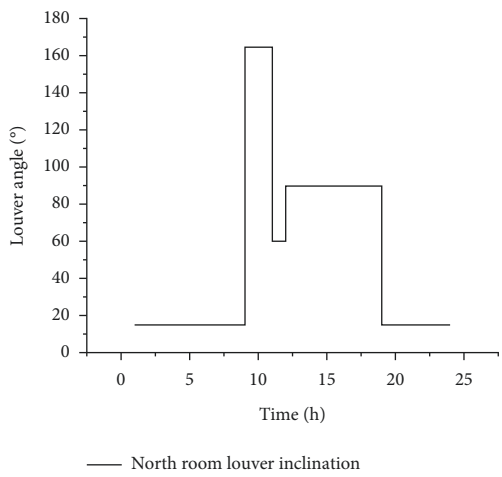

Figure 7: Dynamic louver inclination schedule.

6. Conclusion

This paper simulates, analyzes, and compares the energy consumption of air-conditioning, heating, and lighting in the typical working period of office space in cold areas of China and explores the control strategy of external sunshade louver to maximize the building energy-saving potential. The simulation analysis shows that the optimal control strategy based on comprehensive energy consumption proposed in this paper can greatly improve the building energy efficiency, and the control strategy has important reference significance for new building design. When the lighting system adopts manual switch + photoelectric sensor dimming control, the building energy-saving potential can be further tapped. This conclusion has certain reference significance for the establishment of energy-saving system.

Data Availability

The data used to support this study are available from the corresponding author upon request.

Conflicts of Interest

The authors declare that they have no conflicts of interest in the study.

References

[1] K. Lai, W. Wang, and H. Giles, "Solar shading performance of window with constant and dynamic shading function in different climate zones," *Solar Energy*, vol. 147, no. March, pp. 113–125, 2017.

[2] Z. Li, X. Pan, and Q. Zhao, "The influence of summer shading on building cooling and lighting energy consumption," *Journal of Tongji University: Natural Science Edition*, vol. 42, no. 2, pp. 305–309, 2014.

[3] H. M. Huo, W. Xu, A. G. Li, and S. Zhang, "Revision and analysis of reverse direct radiation model for horizontal external Venetian blind shading," *Building Science*, vol. 37, no. 6, pp. 1–9, 2021.

[4] H. Zhang and L. Wang, "Analysis of the influence of building energy efficiency design factors," *Building Energy Efficiency*, vol. 000, no. 001, pp. 45–49, 2016.

[5] M. E. Bunning and R. H. Crawford, "Directionally selective shading control in maritime sub-tropical and temperate climates: l," *Building and Environment*, vol. 104, no. aug, pp. 275–285, 2016.

[6] W. Liu, K. T. Chau, C. H. T. Lee, C. Jiang, W. Han, and W. H. Lam, "A wireless dimmable lighting system using variable-power variable-frequency control," *IEEE Transactions on Industrial Electronics*, vol. 67, no. 10, pp. 8392–8404, 2020.

[7] X. Wei, L. Jinqiu, B. Yang, Y. Juan, and L. Borong, "Energy planning of daxing international airport and and energy efficiency design of its terminals," *Building Energy Efficiency*, vol. 47, no. 10, pp. 8–14, 2019.

[8] L. Quan, Y. He, and Z. T. Qiu, "Study on daylighting design standard for residential living rooms," *Building Science*, vol. 35, no. 8, pp. 171–177, 2019.

[9] L. Ye, "Discussion on lighting design of sports venues," *Building Electricity*, vol. 39, no. 9, pp. 109–118, 2020.

[10] J. Xiong and A. Tzempelikos, "Model-based shading and lighting controls considering visual comfort and energy use," *Solar Energy*, vol. 134, no. sep, pp. 416–428, 2016.

Hindawi
Computational Intelligence and Neuroscience
Volume 2022, Article ID 4953721, 9 pages
https://doi.org/10.1155/2022/4953721

Research Article

College Smart Classroom Attendance Management System Based on Internet of Things

Mingtao Zhao, Gang Zhao, and Meihong Qu

Architectural Engineering School, Qingdao Huanghai University, Qingdao, Shandong 266427, China

Correspondence should be addressed to Mingtao Zhao; zhaomt@qdhhc.edu.cn

Received 19 March 2022; Revised 29 April 2022; Accepted 18 May 2022; Published 5 July 2022

Academic Editor: Guobin Chen

Since entering the information age, educational informatization reform has become the inevitable trend of the development of colleges and universities. The traditional education management methods, especially the classroom attendance methods, not only need to rely on a large number of manpower for data collection and analysis but also cannot dynamically monitor students' attendance and low efficiency. The development of Internet of things technology provides technical support for the informatization reform of education management in colleges and universities and makes the classroom attendance management in colleges and universities have a new development direction. In this study, a college smart classroom attendance management system based on RFID technology and face recognition technology is constructed under the architecture of the Internet of things, and the corresponding simulation experiments are carried out. The experimental results show that the smart classroom attendance management system based on RFID technology can accurately identify the absence and substitution of students and has the advantages of fast response and low cost. However, its recognition is easily affected by obstructions, which requires students to place identification cards uniformly. The smart classroom attendance management system based on face recognition technology can accurately record and identify the situation of students entering and leaving the classroom and identify the situations of being late and leaving early, absenteeism, and substitute classes. The experimental results are basically consistent with the sample results, and the error rate is low. However, the system is easily affected by environmental light, students' sitting posture, expression, and other factors, so it cannot be recognized. Generally speaking, both can meet the needs of classroom attendance in colleges and universities and have high accuracy and efficiency.

1. Introduction

The development of information technology and Internet of things technology has promoted the pace of educational informatization reform. The informatization development of educational management has also become one of the focuses of attention and research in colleges and universities. The development of college education management methods and mechanisms needs to measure the effectiveness and rationality of daily teaching through real and scientific data, in which student classroom attendance is an important part of college education management [1]. Classroom attendance includes student attendance and teacher attendance. It can not only reflect students' learning behavior but also reflect the authenticity and effectiveness of teachers' teaching classroom and provide important basic data information for teaching reform. The collection of classroom attendance data is closely related to the classroom attendance technology and methods. The traditional classroom attendance method is mainly manual attendance. Such attendance methods not only can dynamically grasp the attendance status of students, but also is prone to errors and omissions. It also needs to repeatedly test the attendance information, which consumes a lot of manpower and materials [2]. At the same time, manual attendance records are generally recorded, sorted, and kept by teachers, so it is not easy for students to understand their attendance. Therefore, the traditional classroom attendance method can meet neither the needs of students and teachers nor the requirements of the development of information technology in colleges and universities [3].

The development of Internet of things technology provides a new development direction for colleges and

universities to build information-based classroom attendance system and mechanism. Many colleges and universities are also constantly trying new technologies in the process of building smart classrooms. Therefore, this study proposes the research on a college smart classroom attendance management system based on the Internet of things, constructs the classroom attendance management system based on RFID technology and face recognition technology, and carries out the corresponding simulation test. This study is mainly divided into three parts: the first part expounds on the development of classroom attendance technology in colleges and universities; the second part is to build a classroom attendance management system based on RFID technology and face recognition technology under the framework of the Internet of things; the third part is the test and result analysis of classroom attendance management system based on RFID technology and face recognition technology.

Under the architecture of Internet of things, this study constructs an attendance management system of intelligent classroom in colleges and universities based on RFID technology and face recognition technology and carries out the corresponding simulation experiments. Research and innovation contributions are as follows: (1) The intelligent classroom attendance management system based on RFID technology can accurately identify the absence and substitution of students. It has the advantages of fast response and low cost. (2) The intelligent classroom attendance management system based on face recognition technology can accurately record and identify the situation of students entering and leaving the classroom and identify the situation of being late and leaving early, absenteeism, and substitute classes. The experimental results are basically consistent with the sample results, and the error rate is low. The research provides technical support for the development of Internet of things technology and the reform of educational management informatization in colleges and universities and makes the classroom attendance management in colleges and universities have a new development direction.

2. Development of Classroom Attendance Technology in Colleges and Universities

The development of college attendance technology is closely related to the development of information technology and Internet technology. Before the wide application of information technology and Internet technology, classroom attendance was mainly based on traditional manual attendance; that is, the arrival of paper signs was used to record the attendance of students and teachers in class, and then the relevant personnel carried out data statistics and analysis after class [4]. Teachers will also conduct random roll calls and multiple roll calls in class according to the actual situation to monitor students' classroom attendance. To a certain extent, this attendance method restricts the occurrence of students' behaviors such as being late, leaving early, and absenteeism and improves the management of students. In addition, the teaching method of colleges and universities is different from that of middle schools. There is no fixed class. Manual attendance can help teachers know and understand students, shorten the distance between students and teachers, and improve the communication between teachers and students [5]. However, with the expansion of the scale of colleges and universities and the increase of the number of students, the way of manual attendance will take up a lot of time, and the accuracy and efficiency of attendance will be reduced. At the same time, the way of manual attendance cannot realize the timely feedback and dynamic tracking of relevant data, and the head teacher cannot timely understand and master the situation of students' classroom attendance [6].

With the development and application of computer technology, classroom attendance also began to enter the information age. Electronic communication technology and computer technology provide technical support for the informatization of classroom attendance. Some scholars propose to combine campus magnetic card or IC card with computer technology to collect and store campus card and student information through the attendance equipment that can be read, so as to be applied to the attendance system [7]. Other scholars have combined RFID technology to design a system that can carry out attendance and recording simply, quickly, and automatically, which improves the accuracy, efficiency, and timeliness of attendance technology [8]. As campus cards and other cards are forged, fraudulently used, and embezzled, which reduces the accuracy and authenticity of attendance data, someone developed biometric attendance technology based on computer technology and biological science and technology [9]. Biometric attendance technology is composed of computer technology, optics, acoustics, biosensors, statistical principles, and other discipline technologies. It mainly verifies personal identity through the inherent behavior and physiological characteristics of human body. The common ones are fingerprint recognition, iris recognition, and so on [10, 11].

With the development of mobile Internet technology and equipment, the smart campus and smart classroom have become important development models of colleges and universities and put forward higher requirements for attendance technology and methods of colleges and universities [12]. On the basis of big data, Internet of things, and other information technologies, college classroom attendance combines intelligent mobile devices to build a new generation of classroom attendance system [13]. Some scholars have built an intelligent classroom attendance system with Internet of things technology as the core and verified its good system stability through experiments [14]. On the basis of mobile Internet, other scholars have realized the active and random data collection of classroom attendance information by using intelligent mobile terminal equipment, bluetooth, QR code, app, etc., which can feed back and track the information data in real time [15]. However, such attendance methods must be used in an environment that can connect to the network, and it is also unable to identify the substitute class. Therefore, some scholars proposed to integrate radio frequency identification technology into the classroom attendance system and constructed RFID-based automatic identification campus

attendance technology, which can carry out real-time senseless data collection [16]. Other scholars have built a classroom attendance system based on face recognition technology, which improves the uniqueness and exclusivity of attendance and reduces the number of clock outs while ensuring the accuracy of classroom attendance [17]. However, face recognition technology needs to build a corresponding database. As in the early stage of the development of this technology, the technology has certain limitations, high management cost, and easy to be affected by environmental factors [18]. With the deepening of education informatization reform in colleges and universities, colleges and universities are constantly innovating and practicing the classroom attendance system according to their own actual situation and needs and are also constantly adjusting and improving the education management mechanism, so as to provide more convenient, fast, and reliable information services for teachers and students [19].

3. College Smart Classroom Attendance Management System Based on Internet of Things

The classroom attendance management system is based on Internet of things technology. The Zige system is convenient for teachers to collect and manage students' attendance information and improve the accuracy of Zige's 3G sensor network, which not only saves students' time and attendance but also improves students' attendance and management. With the continuous development of Internet, Internet of things, and information technology, colleges and universities have been exploring and studying efficient and convenient smart classroom attendance methods that can analyze classroom attendance data in the practice of building smart classroom, so as to provide multidimensional and diversified decision support for the development of smart classroom in colleges and universities [20]. At the same time, we also need to take into account the actual needs of smart classroom in colleges and universities, the software and hardware conditions required by attendance methods, technical feasibility, and economic feasibility. Therefore, the classroom attendance management system based on RFID technology and the classroom attendance management system based on face recognition technology have become the choice of many colleges and universities. As the core content of face recognition, feature extraction and comparison recognition are to use computer technology to locate the location of biological key points. After geometric and optical corrections, the feature key points that can be compared are extracted and compared with the facial texture code of the face database. Finally, the automatic processing technology of individual identification is carried out.

3.1. Construction of College Classroom Attendance Management System Based on RFID Technology. The traditional classroom attendance card swiping method in colleges and universities can neither control the number of students in the classroom and the situation of students being late and leaving early in real time nor identify problems such as one person with multiple cards. The classroom attendance management system based on RFID technology can realize the way of real-time and efficient roll call and information attendance and master the attendance of the classroom in real time. As shown in Figure 1, it is the overall block diagram of the classroom attendance management system based on RFID technology.

RFID technology can realize indoor real-time positioning in a large range of coverage without contact and has the advantages of high visibility, convenience, and low cost. For indoor positioning based on RFID technology, the basic coordinates need to be selected according to the specific situation of the classroom, and the corresponding calculation is carried out through the coordinates. Considering that there will be a multipath effect in positioning through the distance between the electronic tag and the receiver, which will affect the accuracy of positioning coordinates, this study uses the strength of the relative received signal for indoor positioning, and its calculation is shown in the following formula:

$$PL(d) = pl(d_0) - 10n\lg\left(\frac{d}{d_0}\right) - X_0. \tag{1}$$

In the formula, the distance between the electronic tag and the reader is expressed as d, the reference distance is expressed as d_0, the environmental parameter is expressed as n, the signal strength at the distance d between the electronic tag and the reader is expressed as $PL(d)$, and the signal strength at the reference distance is expressed as $pl(d_0)$.

The coordinate position of the label to be tested is set as (x, y) and the position of the reader-writer as (X_i, Y_i). When the position is known, the distance between the label to be tested and the i reader-writer is shown in the following formula:

$$d_i = \sqrt{(x_i - x)^2 + (y_i - y)^2}. \tag{2}$$

If there is an intersection A in the effective area of two readers and writers, and there is also an intersection outside the area, then the A point is reasonable. The average value of all solutions is calculated to obtain the final solution of each label, as shown in the following formulas:

$$X = \sum_{i=1}^{I} \frac{X_i}{I}, \tag{3}$$

$$Y = \sum_{i=1}^{I} \frac{Y_i}{I}. \tag{4}$$

The label value obtained according to the formula is (X, Y), which is converted into the reference coordinates of the setting area to obtain the specific position of the label seat.

Friis path loss model realizes positioning through Frith transmission formula in a free propagation model, as shown in the following formula:

$$P_r = P_t \cdot G_r \cdot G_t \cdot L_{\text{path}}. \tag{5}$$

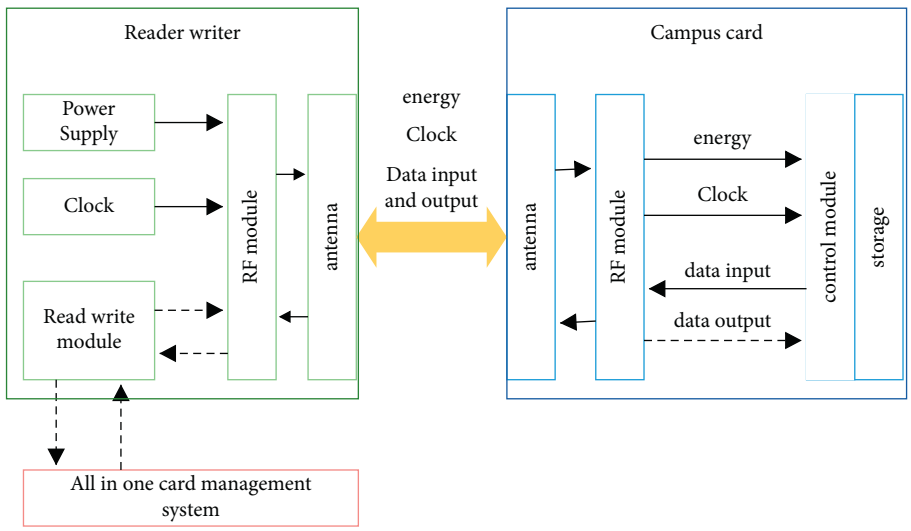

Figure 1: Overall block diagram of classroom attendance management system based on RFID technology.

The model power received by the passive tag is expressed as P_r, the transmission power of the reader is expressed as P_t, the radiation radius of its corresponding reading and writing area is expressed as R, the antenna gain of the reader is expressed as G_r, the antenna gain of the tag is expressed as G_t, and the path loss is expressed as L_{path}. The expression is shown as follows:

$$L_{\text{path}} = \left(\frac{\lambda}{4\pi R}\right)^2. \tag{6}$$

Combining formulas (5) and (6)

$$P_r = P_t \cdot G_r \cdot G_t \cdot \left(\frac{\lambda}{4\pi R}\right)^2. \tag{7}$$

The logarithm of formula (7) is obtained as follows:

$$P_r = P_t + G_r + G_t + 20\lg\left(\frac{\lambda}{4\pi R}\right). \tag{8}$$

Due to the amplitude fading caused by human interference or obstruction in the indoor environment, the reception power of passive tags is reduced, resulting in the problem of missing reading. Therefore, formula (8) is modified as follows:

$$P_r' = P_t + G_r + G_t - 20\lg\left(\frac{4\pi R}{\lambda}\right) - |X_\sigma|. \tag{9}$$

The Gaussian white noise is expressed as X_σ, its standard deviation is expressed as σ, and the actual received power of the tag is expressed as P_r'.

Each seat in the classroom represents the corresponding target area. In principle, each target area corresponds to only one electronic label. When multiple electronic labels appear on the same seat, students may brush on behalf of others. As shown in Figure 2, it is the effect diagram of antiproxy brushing of college classroom attendance management system based on RFID technology.

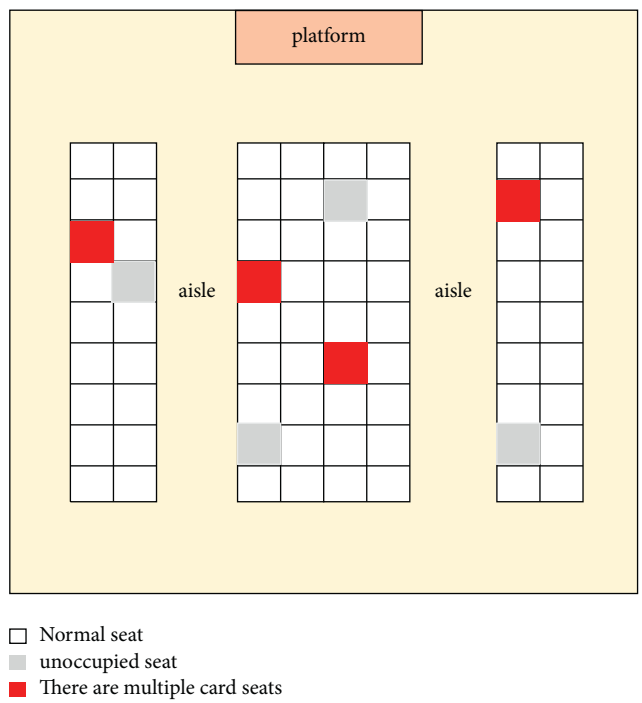

Figure 2: Effect drawing of antiproxy brushing of college classroom attendance management system based on RFID technology.

The traditional attendance management is time consuming, laborious, and inefficient, and the information is not timely, which cannot meet the management requirements of modern colleges and universities. Therefore, it is necessary to adopt the student attendance management system based on the campus network to automatically collect student attendance information through RFID (radio frequency identification) technology. To avoid that teachers' roll call takes up classroom teaching time and improve teaching efficiency, the convenience of students' leave and the efficiency of management approval is improved through online

leave and approval. Students, teachers, and teaching management departments share attendance information through the campus network to increase the transparency of information and improve the management quality of management departments. The attendance management system will automatically calculate the number and position of electronic tags according to the RFID antenna in the classroom, so as to obtain the precise position of each electronic tag in the classroom and identify normal seats, empty seats, and proxy brushing seats with multiple cards. However, if students put the card in their schoolbag or pocket, it may affect the accuracy of measurement. In actual use, students will be required to place the card in a certain position on the desktop to reduce missing reading.

3.2. Construction of College Classroom Attendance Management System Based on Face Recognition Technology. With the development of Internet of things technology, face recognition technology is widely used in the smart campus of colleges and universities. Face recognition technology combined with wireless network technology can realize classroom attendance check-in, detect students' late and early leave, absenteeism, substitute class, etc., and effectively and accurately record students' access to the classroom. The face recognition technology in this study is based on the Harr feature to detect the face; that is, the integral graph method is used to calculate many matrix features contained in the detection window. Let the sum of the luminance values of the rectangular area composed of the image starting point and point $i(x, y)$ be expressed as $s(x, y)$, and it will be saved in the memory as an integral value. When the vertical and horizontal coordinates of the image to be calculated exceed the sum of the lighting degrees of all pixels of point $i(x, y)$, it can be calculated as long as it traverses all points of the original image once, as shown in the following formula:

$$s(x, y) = s(x-1, y) + s(x, y-1) - s(x-1, y-1) + i(x, y). \tag{10}$$

In order to reduce the interference and recognition influence on the classroom attendance system and improve the recognition efficiency and accuracy, it is necessary to preprocess the image. By calculating the weighted average of the red specific gravity, green specific gravity, and blue specific gravity of the color image, the transformation of the image gray scale is completed. The calculation formula is shown as follows:

$$\text{gray} = 0.299 * R + 0.587 * G + 0.144 * B. \tag{11}$$

Then, the image is histogram equalized and its new pixel value is calculated, as shown in the following formula:

$$s_k = \sum_{j=0}^{k} \frac{n_j}{n}, \tag{12}$$

where $k = 0, 1, 2, \ldots, L-1$, the total number of image pixels is expressed as n, the number of pixels of the current gray level is expressed as n_j, and the total number of possible gray levels of the image is expressed as L.

Because the gray scale of LBP operator has good robustness and is not affected by lighting conditions, it has a fast computing speed and can analyze images in a complex real-time environment. Therefore, the university classroom attendance management system based on face recognition technology in this study is based on the LBP method for image feature extraction. LBP is initially set in the 3×3 pixel field, and the gray values of nine pixels in the field are extracted. The central pixel is selected as the threshold and the gray value is compared with the other eight adjacent pixels. When the central pixel is lower than the gray value of the adjacent pixel, the adjacent pixel is recorded as 1; otherwise, it is 0. The calculation formula of LBP value of the central pixel of the neighborhood is shown as follows:

$$LBP(x_c, y_c) = \sum_{p=0}^{p-1} 2^p s(i_p - i_c). \tag{13}$$

In the formula, the central pixel of the neighborhood is expressed as (x_c, y_c), its pixel value is expressed as i_c, other pixel values in the field are expressed as i_p, and the symbolic function is expressed as s.

In order to enable LBP to better extract texture features from large-scale images, the LBP operator is improved to a circular LBP operator; that is, it is assumed that it contains eight sampling points in the 5×5 neighborhood, and the coordinate value calculation formulas of each sampling point are shown as follows:

$$x_p = x_c + R\cos\left(\frac{2\pi p}{p}\right), \tag{14}$$

$$y_p = y_c + R\sin\left(\frac{2\pi p}{p}\right), \tag{15}$$

where the center point of the neighborhood is expressed as (x_c, y_c) and a sampling point is expressed as (x_p, y_p).

When the university smart classroom attendance management system performs face recognition through LBPH algorithm, it needs to initialize parameters first and then LBP coding; that is, $(x, y)_n$ is set as the corresponding pixel offset coordinate in the n field, and its calculation formula is shown as follows:

$$\begin{cases} x_n = -\text{radius} \times \sin\left(2.0 \times \pi \times \dfrac{n}{\text{neighbors}}\right), \\ y_n = -\text{radius} \times \cos\left(2.0 \times \pi \times \dfrac{n}{\text{neighbors}}\right). \end{cases} \tag{16}$$

The n field gray value of all pixel coordinates is calculated through bilinear difference, and the coded value is calculated according to the following formula:

$$lbp(x, y)_n = \begin{cases} 1 \ldots (\text{gray}(x, y)_n \le \text{gray}(x, y)), \\ 0 \ldots (\text{gray}(x, y)_n > \text{gray}(x, y)). \end{cases} \tag{17}$$

The calculation formula of LBP coding value of all pixels contained in each submodule is shown as follows:

$$lbp(x, y) = \sum_{n=0}^{\text{neighbors}-1} lbp(x, y)_n \times 2^n. \quad (18)$$

The histogram is calculated. The calculation formula of the width and height of each grid in the image is shown as follows:

$$\begin{cases} w\_\text{grad} = LBP_i \cdot \text{cols/gridx}, \\ h\_\text{grad} = LBP_i \cdot \text{rows/gridx}. \end{cases} \quad (19)$$

The similarity between two histograms is calculated by the card method, as shown in the following formula:

$$d(H_1, H_2) = \frac{(H_1 - H_2)^2}{H_1 + H_2}. \quad (20)$$

4. Test and Results of College Smart Classroom Attendance Management System Based on Internet of Things

4.1. Test and Results of College Classroom Attendance Management System Based on RFID Technology. The traditional manual attendance check-in or manual attendance check-in is widely used in colleges and universities. This method occupies a lot of time for teachers and is inefficient. RFID technology is used to collect student data, C/S architecture is used, and c# programming language is used to develop a card reader attendance management system. The student information is stored into the card reader database so that teachers can easily grasp the students' class situation. The system can greatly reduce the time spent on attendance, reduce the burden of teachers, and effectively improve the attendance rate of students. Before testing the college classroom attendance management system based on RFID technology, we need to understand the influence relationship between the number of readers and positioning performance. The simulation results are shown in Figure 3. As can be seen from the CDF distribution curve in the figure, when the number of readers is three, half of the probability of positioning error is not higher than 3.1 m; when the number of readers increases to four, half of the probability of positioning error is not higher than 2.35 m, and 80% of the probability is not higher than 3.2 m; when the number of readers increases to five, half of the probability of positioning error is no more than 2.2 m, and 80% of the probability is no more than 2.8 m.

Figure 4 shows the relationship between the number of readers and positioning accuracy in the Friis loss model. It can be seen from the data in the figure that when the number of readers is three, the probability of positioning error not exceeding 1.13 m is 50%, and the probability of not exceeding 1.2 m is 80%; after adding a reader, the probability of positioning error not higher than 0.89 m is 50%, and the probability of not higher than 0.94 m is 80%; when increasing to five readers, the probability of positioning error not higher than 0.84 m is half, and the probability of lower than 0.91 m is 80%.

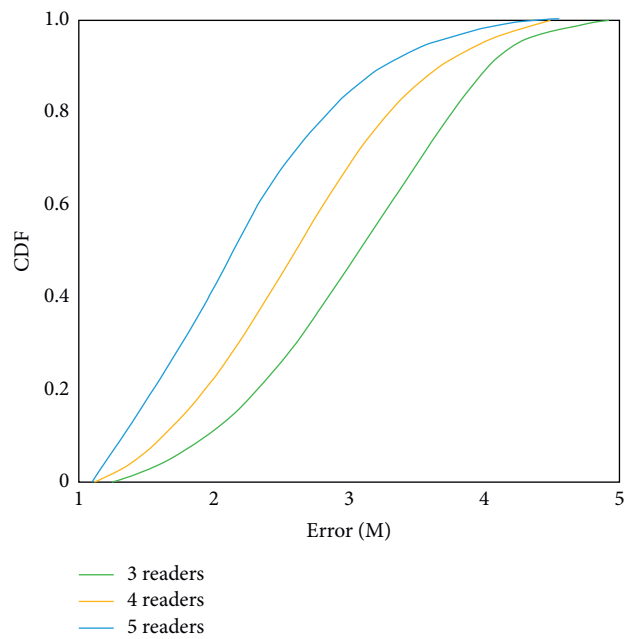

Figure 3: The influence of the number of readers in the system on the positioning accuracy.

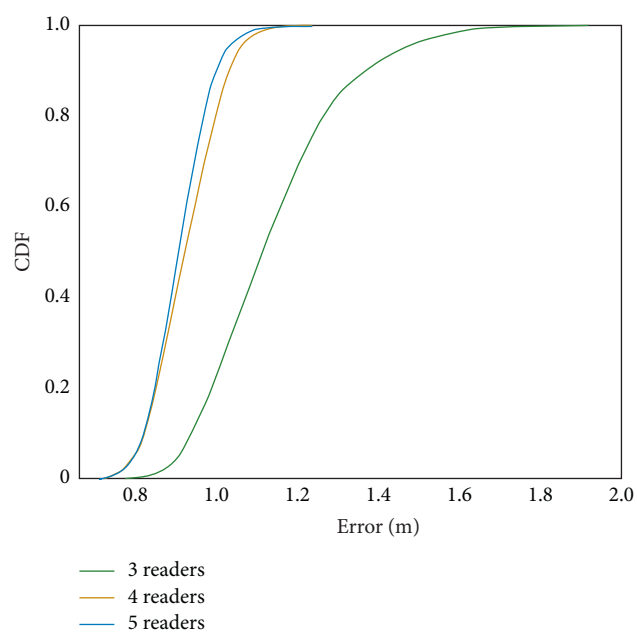

Figure 4: Effect of the number of readers in Friis loss model on positioning accuracy.

To sum up, when the number of readers increases from three to four, the error decreases greatly, and the accuracy of system positioning is significantly improved. When it is increased from four to five, the decline of system error decreases, and the impact on accuracy is very small. Therefore, the increase of the number of readers will improve the positioning accuracy of the system, and the

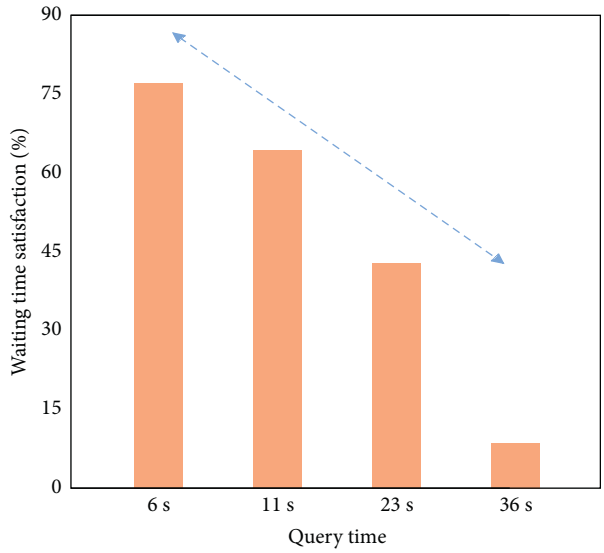

Figure 5: University classroom attendance management system based on RFID technology queries the research results of user waiting time.

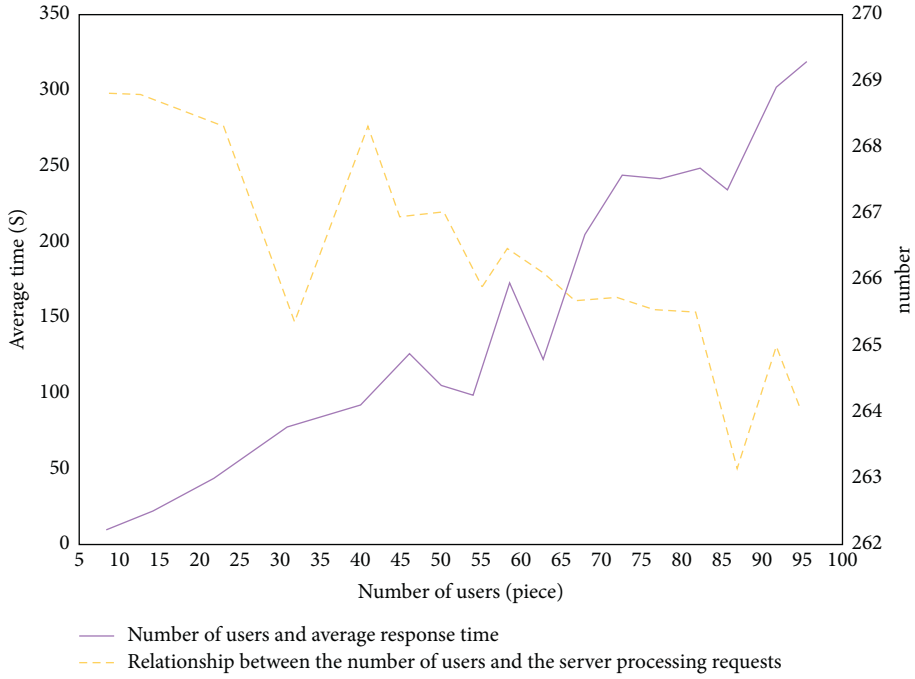

Figure 6: RFID-based campus attendance management system's user number and response time relationship and server request relationship diagram.

accuracy will increase with the increase of the number of readers. However, when the number of readers increases to a certain number, its further increase has little impact on the positioning accuracy of the system. Considering the actual situation, the number of readers is four, which is relatively appropriate.

As shown in Figure 5, the research results of user waiting time are queried by the university classroom attendance management system based on RFID technology. It can be seen from the data in the figure that 76% of users are satisfied that the time required for access query is 6 s; when the access query time increased to 11 s, the proportion of satisfied users decreased to 63%; when the access query time increased to 23 s, 41% of users were satisfied; only 5% of users said they could accept 36 s of query time. During the simulation experiment, the amount of database information of the system is relatively small and the number of users participating in the simulation test is limited. Therefore, the average query time is maintained at 5 s, which can basically meet the needs of all users. However, in a practical application, the number of users and database information will continue to increase, which will also increase the burden on the system operation. In case of slow operation, it is necessary to further optimize the system.

	IO	T1	T1	T1	T1	T1	T1	T1	T1	T1	T1	T11	fraction	explain
1	in	1	1	1	1	1	1	1	1	1	0	0	76	Leave early
2	in	1	1	1	1	1	1	1	1	1	1	1	100	
3	in	0	0	0	0	0	0	0	0	0	0	0	0	Instead of class
4	in	1	1	1	1	1	1	1	1	1	1	1	100	
5	in	1	1	1	0	1	1	1	1	1	1	1	88	late
6	in	0	1	1	1	1	1	1	1	1	1	1	88	late
7	in	1	1	1	1	1	1	1	1	0	0	0	65	Leave early
8	in	1	1	1	1	1	1	1	1	1	1	1	100	
9	in	1	1	1	0	1	1	0	1	1	1	1	78	Leave early
10	in	1	1	1	1	0	1	1	1	1	1	1	88	Instead of class
11	on	1	1	1	1	1	1	1	1	1	1	1	100	
12	in	0	0	0	0	0	0	0	0	0	0	0	0	Absenteeism

Figure 7: Test results of college classroom attendance management system based on face recognition technology.

As shown in Figure 6, it is the relationship between the university classroom attendance management system based on RFID technology, response time, and server request. It can be seen from the figure that the increase in the number of login users will prolong the system response time. When the number of users increases to 100, the system response time is 30 times that of 20 users. The number of requests that the server can handle per unit time decreases with the increase of the number of users. When the number increases to 100, the number of requests processed by the server decreases by 14 compared with the initial number.

4.2. Test and Results of College Classroom Attendance Management System Based on Face Recognition Technology. The classroom attendance test results of college classroom attendance management system based on face recognition technology are shown in Figures 7 and 8; 1 in the figure indicates that the recognition of the student in the classroom is successful, and 0 indicates that the recognition is unsuccessful. It can be seen that the university classroom attendance management system based on face recognition technology can realize independent classroom attendance and identify the access of students in the classroom, such as leaving early, absenteeism, and substitute classes. Because the face recognition technology will be affected by the lighting conditions of the surrounding environment, students' sitting posture, expression, and other factors, although some students attend class on time, the system still shows that the recognition fails. On the whole, the test results of college classroom attendance management system based on face recognition technology are basically consistent with the sample results and can meet the expected requirements.

To sum up, both the university classroom attendance management system based on face recognition technology and the university classroom attendance management system based on RFID technology can basically meet the needs of classroom attendance with high accuracy. However, due to the limitations of technology and environment, both of them have some disadvantages. The college classroom attendance management system based on RFID technology cannot meet the needs of college students of different majors to log in to the system at the same time, and the running time will slow down with the increase of the number. The university classroom attendance management system based on face recognition technology has certain requirements for the environment of classroom attendance. Therefore, both of them need to be further optimized and improved.

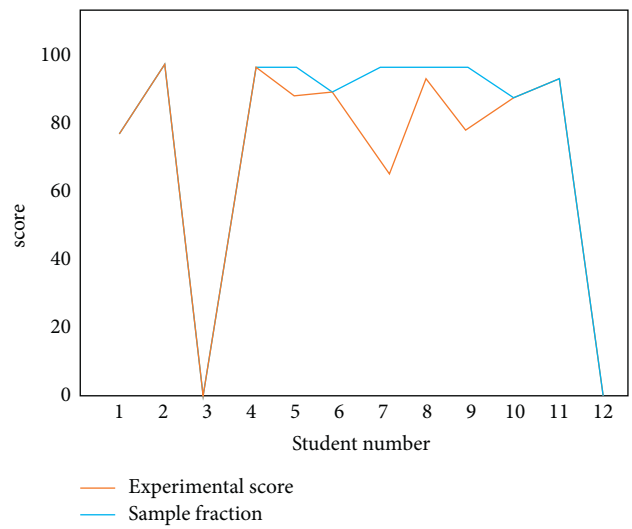

Figure 8: Comparison of attendance score and sample score in system experiment.

5. Conclusion

This study presents the research of college intelligent classroom attendance management system based on the framework of Internet of things. Under the framework of Internet of things, this study constructs a classroom attendance management system based on RFID technology

and face recognition technology. The experimental results show that the intelligent classroom attendance management system based on RFID technology can accurately identify students' absence and substitution. It has the advantages of fast response speed and low cost. The intelligent classroom attendance management system based on face recognition technology can accurately record and identify the situation of students entering and leaving the classroom and identify the situation of being late and leaving early, absenteeism, and substitute classes. The experimental results are basically consistent with the sample results, and the error rate is low. This study provides technical support for the development of Internet of things technology and the informatization reform of educational management in colleges and universities and makes the classroom attendance management in colleges and universities have a new development direction. The experimental results are basically consistent with the sample results. However, it is easily affected by ambient light, students' sitting posture, and expression and cannot be recognized. These two kinds of college classroom attendance management systems can meet the basic needs of colleges and universities, but there are still some technical limitations, which need to be further optimized and debugged.

Data Availability

The data used to support the findings of this study are available from the corresponding author upon request.

Conflicts of Interest

The authors declare that they have no conflicts of interest.

References

[1] J. Hu, "On the application of Internet of things in the construction of smart campus in Colleges and universities," *Smart city*, vol. 5, no. 18, pp. 26-27, 2019.

[2] R. Zhou and J. Ji, "How to optimize the management of science and technology funds in colleges and universities based on the policy of streamlining administration, delegating powers, improving regulation, and strengthening services," *Journal of Contemporary Educational Research*, vol. 5, no. 5, pp. 39–43, 2021.

[3] H. Yang and X. Han, "Face recognition attendance system based on real-time video processing," *IEEE Access*, vol. 8, no. 99, 2020.

[4] C. Jinbo, C. Xiangliang, F. Han-Chi, and A. Lam, "Agricultural product monitoring system supported by cloud computing," *Cluster Computing*, vol. 22, no. S4, pp. 8929–8938, 2019.

[5] P. Kowsalya, J. Pavithra, G. Sowmiya, and C. K. Shankar, "Attendance monitoring system using face detection & face recognition," *International Research Journal of Engineering and Technology (IRJET)*, vol. 6, no. 3, pp. 6629–6632, 2019.

[6] D. M. V. Salac, "PRESENT: an android-based class attendance monitoring system using face recognition technology," *International Journal of Computing Sciences Research*, vol. 2, no. 3, pp. 102–115, 2013.

[7] D Bhavana, K. K Kumar, N Kaushik et al., "Computer vision based classroom attendance management system-with speech output using LBPH algorithm," *International Journal of Speech Technology*, vol. 23, pp. 1–9, 2020.

[8] J. Song and M. Zhang, "Design and implementation of a vue.js-based college teaching system," *International Journal of Emerging Technologies in Learning*, vol. 14, no. 13, 2019.

[9] Z. Jingjing, "Exploration on the investigation and countermeasures of rural teachers' informatization teaching ability under the background of education informatization 2.0," *The Theory and Practice of Innovation and Enntrepreneurship*, vol. 3, no. 3, p. 63, 2020.

[10] R. Zhang, "Research on Key Technologies of university laboratory information management under the architecture of Internet of things," *Microcomputer Applications*, vol. 35, no. 7, p. 5, 2019.

[11] S. Kumar, R. D. Raut, and B. E. Narkhede, "A proposed collaborative framework by using artificial intelligence-internet of things (AI-IoT) in COVID-19 pandemic situation for healthcare workers," *International Journal of Healthcare Management*, vol. 13, no. 4, pp. 337–345, 2020.

[12] J. Cao and K. Wang, "Construction and practice of intelligent classroom in colleges and universities based on Internet of things," *Chinese & Foreign Entrepreneurs*, vol. 634, no. 08, p. 139, 2019.

[13] L. L. Tian, W. L. Teng, and H. H. Bian, *Research on preprocessing algorithm of two-camera face recognition attendance image based on artificial intelligence*, Springer, Cham, 2020.

[14] D. Cui and Q. Zhang, "The RFID data clustering algorithm for improving indoor network positioning based on LANDMARC technology," *Cluster Computing*, vol. 22, no. S3, pp. 5731–5738, 2019.

[15] A. Alghamdi, M. Alanezi, and F. Khan, "Design and implementation of a computer aided intelligent examination system," *International Journal of Emerging Technologies in Learning (iJET)*, vol. 15, no. 1, pp. 30–44, 2020.

[16] X. Wang, "Research on the transformation and upgrading of ideological and political education management in colleges and universities," *Journal of Contemporary Educational Research*, vol. 5, no. 3, p. 3, 2021.

[17] K. Arif, N. S. Ali, N. A. Zakaria, and M. N. Al-Mhiqani, "Attendance management system for educational sector: critical review," *International Journal of Computer Science and Mobile Computing*, vol. 7, no. 8, pp. 60–66, 2018.

[18] A. Adamu, "Attendance management system using fingerprint and iris biometric," *FUDMA Journal of Sciences*, vol. 3, pp. 427–433, 2019.

[19] F. Xu and H. Wang, "A discriminative target equation-based face recognition method for teaching attendance," *Advances in Mathematical Physics*, vol. 2021, pp. 1–11, Article ID 9165733, 2021.

[20] B. Chen, "Research on the design of intelligent classroom management system based on new technology," *Digital Technology and Application*, vol. 38, no. 10, p. 2, 2020.

Hindawi
Computational Intelligence and Neuroscience
Volume 2023, Article ID 9857932, 1 page
https://doi.org/10.1155/2023/9857932

Retraction

Retracted: The Innovation of College Students' Ideological and Political Education under the Intelligent Environment of Internet of Things

Computational Intelligence and Neuroscience

Received 19 September 2023; Accepted 19 September 2023; Published 20 September 2023

This article has been retracted by Hindawi following an investigation undertaken by the publisher [1]. This investigation has uncovered evidence of one or more of the following indicators of systematic manipulation of the publication process:

(1) Discrepancies in scope
(2) Discrepancies in the description of the research reported
(3) Discrepancies between the availability of data and the research described
(4) Inappropriate citations
(5) Incoherent, meaningless and/or irrelevant content included in the article
(6) Peer-review manipulation

The presence of these indicators undermines our confidence in the integrity of the article's content and we cannot, therefore, vouch for its reliability. Please note that this notice is intended solely to alert readers that the content of this article is unreliable. We have not investigated whether authors were aware of or involved in the systematic manipulation of the publication process.

Wiley and Hindawi regrets that the usual quality checks did not identify these issues before publication and have since put additional measures in place to safeguard research integrity.

We wish to credit our own Research Integrity and Research Publishing teams and anonymous and named external researchers and research integrity experts for contributing to this investigation.

The corresponding author, as the representative of all authors, has been given the opportunity to register their agreement or disagreement to this retraction. We have kept a record of any response received.

References

[1] X. Wang, "The Innovation of College Students' Ideological and Political Education under the Intelligent Environment of Internet of Things," *Computational Intelligence and Neuroscience*, vol. 2022, Article ID 6420262, 9 pages, 2022.

Hindawi
Computational Intelligence and Neuroscience
Volume 2022, Article ID 6420262, 9 pages
https://doi.org/10.1155/2022/6420262

Research Article

The Innovation of College Students' Ideological and Political Education under the Intelligent Environment of Internet of Things

Xia Wang

College of Maxism, Qingdao HuangHai University, Qingdao, Shandong 266427, China

Correspondence should be addressed to Xia Wang; wangx@qdhhc.edu.cn

Received 14 March 2022; Revised 29 April 2022; Accepted 18 May 2022; Published 30 June 2022

Academic Editor: Guobin Chen

With the development of the times and the continuous improvement of the requirements for college students' political literacy and identity, the informatization reform and educational innovation of college students' ideological and political education have become the focus and difficulty of teaching reform. The ideological and political education in most domestic colleges and universities still focuses on the elaboration of theoretical knowledge, ignoring the importance of social practice. Therefore, this paper puts forward the research on the innovation of college students' ideological and political education in the intelligent environment of the Internet of things, constructs the college ideological and political education training cloud system through the Internet of Things technology and AR technology, and promotes the realization of the purpose of college students' participation in social practice. The experimental results show that the college ideological and political education training cloud system based on AR and Internet of Things technology can improve the interaction and participation of ideological and political courses, stimulate students' interest and enthusiasm, deepen students' understanding of the content of ideological and political education, and better understand the importance of ideological and political education. At the same time, the system is also the exploration and practice of teaching innovation of ideological and political education in the intelligent environment of Internet of Things. It is a new attempt of ideological and political education reform in colleges and universities.

1. Introduction

Ideological and political education is not only the core embodiment of political socialization, but also the bearer of the transmission of values and beliefs of the political system [1]. The attitude of social members toward the political system will be affected by ideological and political education to a great extent. Since entering the new era, college students can be exposed to different values and information transmission in the Internet environment, and their value judgment is easy to be affected [2]. With the continuous development and evolution of the domestic and international situation, college students need to further strengthen their political literacy and identity, so as to meet the challenges of higher requirements. In recent years, colleges and universities have been strengthening and improving students' ideological and political education [3]. With the development of the times, they have continuously improved educational contents and means and achieved certain results [4]. However, there are still some problems in the ideological and political education in domestic colleges and universities, such as boring, obscure, abstract, and difficult to understand, which makes it difficult for college students to have personal experience [5]. At the same time, in terms of educational means, it still focuses on theoretical teaching, ignoring the importance of practical teaching, and the single teaching means and methods are also difficult to meet the needs of college students [6]. Therefore, how to innovate ideological and political education in colleges and universities under the background of the new era has become the research hotspot and focus of college education [7]. The theoretical content of ideological and political education in colleges and universities should not only focus on the interpretation of theoretical knowledge and theoretical system in ideological and political teaching materials [8] but also should fully tap the ideological and political education resources contained in

various courses, connect ideological and political education with general courses and professional courses in colleges and universities, and explain the ideological and political theoretical knowledge from different angles. In addition, education needs the unity of knowledge and practice [9]. The ideological and political education of college students should carry out social practice on the basis of learning theoretical knowledge and expand the ways of ideological and political education in different ways.

This paper puts forward the research on the innovation of college students' ideological and political education in the intelligent environment of Internet of things and constructs the practical training cloud system of college ideological and political education combined with AR technology and Internet of things technology. This paper is mainly divided into three parts. The first part expounds the communication means of ideological and political education; The second part is the construction of college ideological and political education and training cloud system based on AR and Internet of things technology. The third part is the application effect analysis of college ideological and political education and training cloud system based on AR and Internet of things technology. The research provides technical support for the improvement of the ideological and political education system in colleges and universities and widens the realization ways of ideological and political education in colleges and universities.

2. Communication Means of Ideological and Political Education

Ideological and political education plays an important role in any country. Different countries realize the purpose of ideological and political education through different means of communication based on their own cultural background and combined with practical needs [10]. Most foreign ideological and political education combines civic education, moral and legal education, religious education, and history education [11]. For example, the United States pays more attention to creating a moral and cultural atmosphere in the dissemination of ideological and political education, that is, cultivating students' virtues and consolidating the core values of the school through communication means such as teaching building banners, classroom decoration, school newspapers and magazines, blackboard newspaper, and so on [12]. At the same time, the United States continues to explore how to achieve the purpose and effect of civic education through the Internet platform. The United Kingdom focuses on the combination of mass media and academic circles to realize the civic education of teenagers, that is, teenagers acquire civic knowledge through the Internet, civic moral education, television, radio columns, and other channels [13]. Compared with Britain and the United States, Russia's means of communication in patriotism education are relatively more diversified, mainly divided into two parts: the innovative use of traditional media and the use of Internet. In the innovative use of traditional media, Russia will specially set up patriotic TV channels, film patriotic themes, and publish educational books on relevant themes [14]. At the same time, Russia will also set up websites and social platforms for teenagers through the Internet, and design and develop games with patriotism as the theme. Japanese colleges and universities have divided the content of ideological and political education into five categories, namely patriotism education, outlook on life education, personality and group education, international interaction, and labor education [15]. While conducting some theoretical education of ideological and political education through mass communication, they also pay attention to the application of practical methods of ideological and political education, such as taking students on field trips to local areas [16]. To sum up, although foreign universities have different communication contents of ideological and political education, there are still many common points in their communication means and methods, which can be continuously improved and innovated with the development of the times [17]. It not only integrates the needs of local characteristic culture and contemporary culture into the traditional mass communication mode to create a good ideological and political education atmosphere for colleges and universities but also constantly discusses and learns to use modern network communication mode to strengthen the teaching effect of ideological and political education.

In China, ideological and political education is one of the compulsory courses for college students, and ideological and political education also realizes the effect of communication education in colleges and universities through two ways: intraorganizational communication and interpersonal communication. As a public medium, campus media in the organizational communication channel includes traditional media means, such as campus radio, television, and periodicals, as well as new media forms, such as campus website, mobile app, and QQ group [18], which makes the communication of ideological and political education in colleges and universities have the characteristics of high exclusivity and credibility. With the development of Internet and social media, colleges and universities explore the communication value of social network as a new means of ideological and political education from the needs of college students' emotion and will. Ideological and political educators have strengthened the interaction and communication with students through wechat, microblog, live broadcast, and other social media, and have a more comprehensive and multiangle understanding of students' state of mind [19]. At the same time, some scholars of ideological and political education pointed out that digital media means have stronger information media interaction than traditional media means and can optimize information communication tools, but at the same time, negative information is also easy to appear in the massive information and content. This requires the active use of digital media means for ideological and political education communication, while improving and perfecting the mechanism of digital communication. With the continuous development of digital media and new media means, domestic ideological and political educators should actively try to change the ideas and ways of ideological and political education, explore new communication means of ideological and political education and improve

the informatization degree of ideological and political education [20].

3. Construction of College Ideological and Political Education Training Cloud System based on AR and Internet of Things Technology

The practical training cloud system of Ideological and political education in colleges and universities based on AR and Internet technology mainly includes background management function, NFC recording function, on-site AR function, and on-site team training function. On the basis of meeting the requirements of the intelligent environment of the Internet of things and the integration of ideological and political education, it greatly reduces the cost of organizing and carrying out social practice of ideological and political education in colleges and universities.

This system consists of the information release system V1.0 of ideological and political course education and teaching resource database 0 software and a remote group construction device for ideological and political education based on ar-nfc. It is the crystallization of NFC technology, AR technology, Internet of things technology, mobile communication technology, cloud database technology, and other advanced technologies. The system can effectively solve the problems encountered in the current ideological and political education and teaching in colleges and universities, which is worthy of reference and popularization and application. As shown in Figure 1, it is the overall framework of college ideological and political education and training cloud system based on AR and Internet technology. As can be seen from the figure, the system group should be divided into two parts. The upper part is ar NFC type ideological and political education remote group construction equipment, and the lower part is an external cooperation system, which can be connected with multiple remote group construction equipment.

This paper mainly expounds the Internet of things development and access point technology based on near-field communication induction, that is, NFC induction, and virtual reality based on AR scene in the college ideological and political education training cloud system based on AR and Internet technology.

3.1. Internet of Things Development and Access Point Technology based on NFC. In addition, NFC technology provides the possibility for mobile phones to realize the work of Internet of things access system under the condition of low-power consumption, and its performance is better than infrared technology and Bluetooth technology. Therefore, the Internet of things development technology based on NFC is also combined with android app development technology to realize the function of sensing proximity and triggering of NFC card through the development of mobile app. At the same time, three triggers can be triggered by reading the on-site NFC sensing code. As shown in Figure 2, it is the flow chart of Internet of things technology based on NFC sensing.

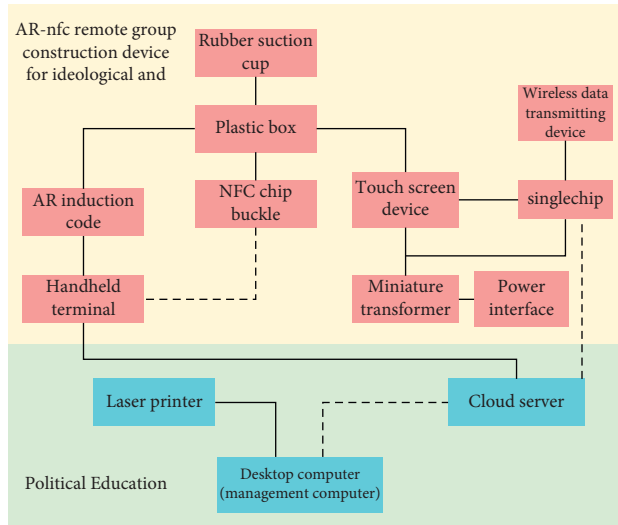

Figure 1: Overall framework of college ideological and political education training cloud system based on AR and Internet technology.

College ideological and political education training cloud system access to the Internet of things needs to be realized through NFC module. From the perspective of security defense system, the security of Internet of things can also be divided into perception layer security, network layer security, and application layer security according to the architecture of Internet of things. The design of perception layer security needs to consider the limitations of computing power, communication capacity, and storage capacity of Internet of things devices. Complex security technologies cannot be directly applied to physical devices. Network layer security is used to ensure communication security, while application layer focuses on the security of various businesses and business-support platforms. At the same time, the antenna-coupling mode of NFC module can help the system obtain power supply energy from the mobile phone. RFID chip realizes data and energy interaction with mobile phones through antenna connection. The inductance of NFC antenna coil is lant, which needs to add parallel capacitance cant and serial resistance rant during equivalence. Cant represents the capacitance loss between coils and connectors, and rant represents the resistance loss. The inductance of antenna coil is calculated as shown in formula (1):

$$L[\mathrm{nH}] = 2 \cdot l[\mathrm{cm}] \cdot \left(\ln\left(\frac{l}{D}\right) - K\right) \cdot N^{1.8}, \tag{1}$$

where the length of one coil of wire ring is expressed as l, the width of PCB wire or the diameter of coil is expressed as D, the number of coil turns is expressed as N, and $K = 1.47$ if the antenna is rectangular.

Since rant cannot directly calculate the accurate value, its estimation formula is shown in formula (2):

$$\mathrm{Rant} = 5 \cdot R_{\mathrm{DC}}, \tag{2}$$

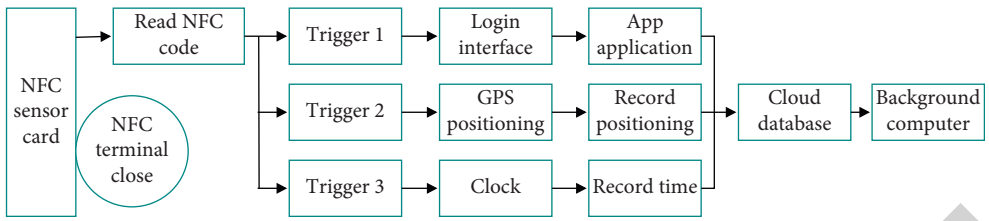

Figure 2: Flow chart of Internet of things technology based on NFC sensing.

where the DC resistance is expressed as R_{DC}.

The quality factor of the antenna can reflect the correct tuning and performance index of the antenna, and its calculation formula is shown in formula (3):

$$Q = \frac{\omega_R \cdot L_{ant}}{R_{ant}}, \quad \omega_R = 2\pi f_R. \tag{3}$$

In this paper, the pH sensor module based on OTFT is selected in the sensor module. In the module, MCU can only input the voltage value, so it needs resistance voltage division to transform the current signal and voltage signal. OTFT has poor performance in uniformity due to its large resistance value and low mobility. In order to better determine the resistance value, this paper selects diodes of the same material as OTFT as resistors for voltage division. As shown in formulas (4) and (5), it is the expression of drain current:

$$I_D = \frac{1}{2}\mu C_G \frac{W}{L}(V_{GS} - V_{th})^2, \tag{4}$$

$$I_D = \mu C_G \frac{W}{L}(V_{GS} - V_{th})V_{DS}, \tag{5}$$

where the drain current is expressed as I_D, the mobility of OTFT is expressed as μ, the capacitance per unit area of gate insulating layer is expressed as C_G, the channel width is expressed as W, the channel length is expressed as L, the threshold voltage is expressed as V_{th}, and the gate source voltage is expressed as V_{GS} and $V_{GS} = V_{in} - V_{dd}$, where V_{in} is the input voltage and V_{dd} is the supply voltage.

The circuit conduction current of pH sensor-voltage output is related to the ratio of driving OTFT aspect ratio and load aspect ratio. If the ratio is expressed as N, the relationship between voltage and input voltage under different N values is shown in Figure 3:

It can be seen from the figure that due to the poor uniformity of OTFT, there are obvious differences in the performance of different voltage output circuits based on OTFT. Therefore, it is necessary to calibrate to make the voltage output circuit have good consistency in the actual measurement. In the actual measurement process, the function of the reference voltage with respect to the output voltage can be obtained, that is, $V_{ref} = f(V_{out})$, where V_{ref} represents the reference voltage and V_{out} represents the output voltage. When the standard buffer solution of $PH = 4$ and $PH = 10$ is calibrated through the circuit, its sensitivity is shown in formula (6):

$$\text{sensitivity} = \frac{V_{ref,10} - V_{ref,4}}{10 - 4}. \tag{6}$$

The calculation formula of pH value is shown in formula (7):

$$\text{PH} = \frac{V_{ref,7} - f(V_{out})}{\text{sensitivity}} + 7. \tag{7}$$

When the Android mobile phone uses the pH sensor label for the first time, it needs to be calibrated, that is, the mobile phone will receive 25 pairs of data sent by the wireless access module and use these data to build the functional relationship between the output voltage and the input voltage. Therefore, this paper selects the Boltzmann model for fitting, and its expression is shown in formula (8):

$$y = \frac{A_1 - A_2}{1 + e^{(x - x_0)/dx}} + A_2, \tag{8}$$

where A_1, A_2, x_0, dx is the parameter.

3.2. Virtual Reality Technology based on AR Scene. Augmented reality technology, AR technology, is a derivative technology of virtual reality technology, which involves many technologies such as digital image processing, computer vision, and so on. AR technology superimposes the generated virtual information and the real scene image through the calculation of the influence position and angle of the camera, enhances the user's visual perception of the real world through the rendering of the virtual reality fusion effect, and presents the scene of parallel interaction between the virtual world and the real world on the mobile phone screen. The cloud system of ideological and political education training in colleges and universities imports the photos and other materials of real scenes into the cloud database through the background program through AR technology, and generates the corresponding ar induction code. Each ar induction code corresponds to a scene, and each scene contains multiple materials, and each material corresponds to problems in single or multiple cloud databases. In this way, the function of random extraction can be realized at the same time.

The key to the perfect and seamless integration of real scene and virtual object through AR technology is that when the relative position of camera and object in real scene changes, the corresponding registration position of virtual object will also change. The geometric model of camera imaging determines the corresponding relationship between them. In computer vision, the camera imaging process

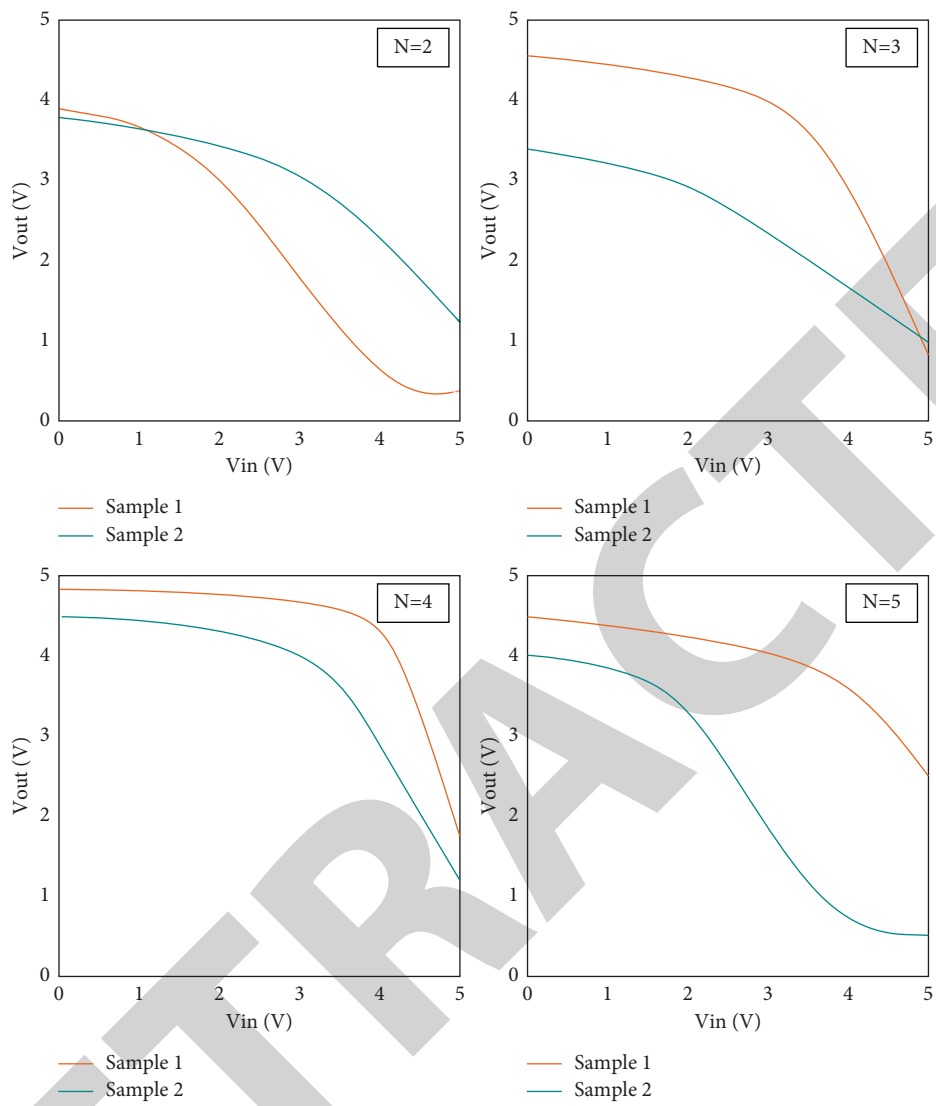

Figure 3: Relationship between voltage and input voltage under different values.

involves three very important coordinate systems, namely image coordinate system, camera coordinate system, and world coordinate system. The representation of image coordinate system is generally expressed in pixel units and physical units. Let the rectangular coordinate system be O_0uv, a coordinate in the pixel coordinate system be represented as (u, v), the corresponding physical position coordinate of the pixel in the image be represented as (x, y), and the origin O_1 of the physical coordinate system be the intersection of the camera optical axis and the plane, which is represented as (u_0, v_0) in the pixel coordinate system. The size of the unit pixel scale of a pixel in the image in the horizontal axis and vertical axis directions is expressed as k, l respectively, then the relationship between the pixel coordinates and physical coordinates is shown in formulas (9) and (10):

$$u = \frac{x}{k} + u_0, \tag{9}$$

$$v = \frac{y}{l} + v_0. \tag{10}$$

The matrix and its inverse representation are shown in formulas (11) and (12):

$$\begin{bmatrix} u \\ v \\ 1 \end{bmatrix} = \begin{bmatrix} \frac{1}{k} & 0 & u_0 \\ 0 & \frac{1}{l} & v_0 \\ 0 & 0 & 1 \end{bmatrix} \begin{bmatrix} x \\ y \\ 1 \end{bmatrix}, \tag{11}$$

$$\begin{bmatrix} x \\ y \\ 1 \end{bmatrix} = \begin{bmatrix} k & 0 & -u_0k \\ 0 & l & -v_0l \\ 0 & 0 & 1 \end{bmatrix} \begin{bmatrix} u \\ v \\ 1 \end{bmatrix}. \tag{12}$$

The homogeneous coordinates of camera coordinate system and world coordinate system are $(X_W, Y_W, Z_W, 1)$, $(X_C, Y_C, Z_C, 1)$, and the transformation relationship between them is shown in formula (13):

$$\begin{bmatrix} X_C \\ Y_C \\ Z_C \\ 1 \end{bmatrix} = \begin{bmatrix} R_{3\times3} & t_{3\times1} \\ 0^T & 1 \end{bmatrix} \begin{bmatrix} X_W \\ Y_W \\ Z_W \\ 1 \end{bmatrix}, \tag{13}$$

where $R_{3\times3} = (r_x, r_y, r_z)$ represents the orthogonal unit rotation matrix and r_x, r_y, r_z represents the rotation component on the three coordinate axes. $t_{3\times1} = \begin{bmatrix} t_x \\ t_y \\ t_z \end{bmatrix}$ is the translation vector, $0 = (0, 0, 0)^T$.

The perspective projection relationship of pinhole camera model is shown in formulas (14) and (15):

$$x = \frac{fX_C}{Z_C}, \tag{14}$$

$$y = \frac{fY_C}{Z_C}. \tag{15}$$

In the formula, the image physical coordinate of a point in space on the two-dimensional image is expressed as (x, y), and the coordinate under the camera coordinate system is expressed as (X_C, Y_C, Z_C). The relationship between the point's world coordinate (X_W, Y_W, Z_W) and its projected image pixel coordinate on the two-dimensional image plane is shown in formula (16):

$$\begin{aligned} Z_C \begin{bmatrix} u \\ v \\ 1 \end{bmatrix} &= \begin{bmatrix} \frac{1}{k} & 0 & u_0 \\ 0 & \frac{1}{l} & v_0 \\ 0 & 0 & 1 \end{bmatrix} \begin{bmatrix} f & 0 & 0 & 0 \\ 0 & f & 0 & 0 \\ 0 & 0 & 1 & 0 \end{bmatrix} \begin{bmatrix} R_{3\times3} & t_{3\times1} \\ 0^T & 1 \end{bmatrix} \begin{bmatrix} X_W \\ Y_W \\ Z_W \\ 1 \end{bmatrix}, \\ &= \begin{bmatrix} a_x & 0 & u_0 & 0 \\ 0 & a_y & v_0 & 0 \\ 0 & 0 & 1 & 0 \end{bmatrix} B \begin{bmatrix} X_W \\ Y_W \\ Z_W \\ 1 \end{bmatrix}, \\ &= KB \begin{bmatrix} X_W \\ Y_W \\ Z_W \\ 1 \end{bmatrix}, \end{aligned} \tag{16}$$

where $a_x = f/k, a_y = f/l$ and K are the internal parameter matrix of the camera, the external matrix is B, and KB is the projection matrix.

In order to make 3D virtual objects that can be superimposed into the real scene in real time, 3D registration is needed. The key problem is to clarify the relationship between different coordinate systems. Let the coordinate system of the virtual object be $X_V Y_V Z_V$, and the conversion relationship between it and the world coordinate system is shown in formula (17):

$$(X_W Y_W Z_W 1) = O(X_V Y_V Z_V 1). \tag{17}$$

Then, after the conversion between the real-world coordinate system and the camera coordinate system and the conversion between the camera coordinate system and the image coordinate system, the position of the virtual object in the two-dimensional image plane can be obtained, as shown in formula (18):

$$Z_C(u\, v\, 1) = \mathrm{OCP}(X_V Y_V Z_V 1). \tag{18}$$

4. Analysis

4.1. PH Measurement of Cloud System Sensor in College Training. As shown in Figure 4, the calibration curve and pH measurement value are obtained through the pattern search algorithm. The input voltage at the point with the largest derivative obtained by deriving the calibration curve is taken as the best measurement point, and the pH buffer solution to be measured is measured accordingly, and then the output voltage of the measured pH sensor label is marked on the curve. It can be seen from the output characteristic curve in the figure that when the output voltage reaches V_{out2} and the corresponding input voltage is V_{ref2}, the implementation of the algorithm is the solution process of the inverse function of the Boltzmann function of the output and input voltage, and then calculate the sensitivity of the pH tag. After the pH tag is put into the pH solution to be tested, repeat the process to obtain the corresponding input voltage value, and finally, obtain the pH value of the buffer solution of the pH to be tested according to the pH calculation formula.

4.2. Application Results of College Ideological and Political Education Training Cloud System based on AR and Internet of Things Technology. In order to better understand the application effect of college ideological and political education training cloud system based on AR and Internet of things technology, this paper conducted an ideological and political education training experiment for a college student. The number of participants in the experiment is 185. According to the relevant survey results, 47 students like ideological and political courses in colleges and universities, 30 students do not like ideological and political courses in colleges and universities, and the other students maintain a neutral attitude toward ideological and political courses. It can be seen that although colleges and universities take ideological and political education as a compulsory course, most college students do not pay attention to ideological and political education, and their interest and liking for the course content are not high as a whole. Figure 5 shows the survey results of the reasons why college students like and dislike ideological and political courses.

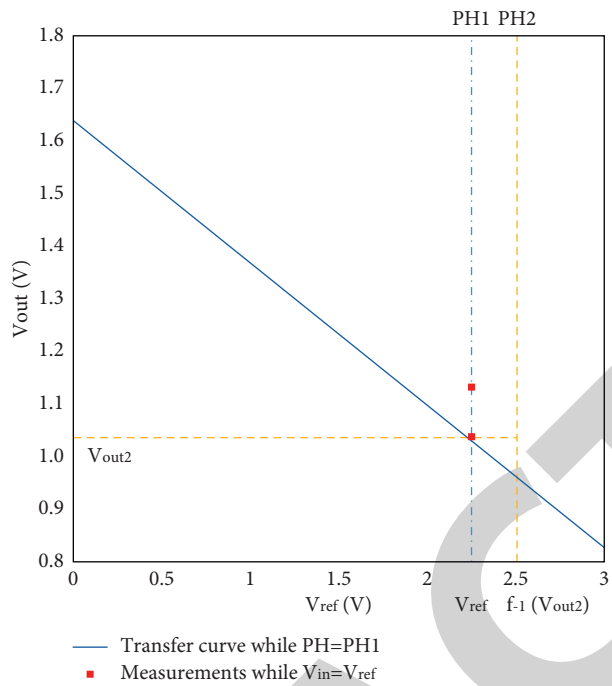

Figure 4: The calibration curve and pH measurement value are obtained by pattern search algorithm.

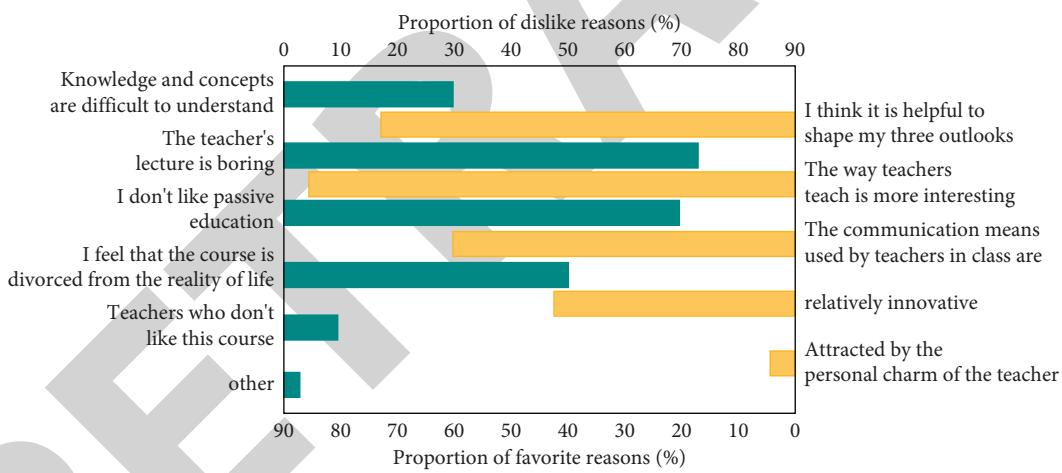

Figure 5: Investigation results of the reasons why college students like and dislike ideological and political courses.

As shown in Figure 6, it is the evaluation results of students on the current ideological and political courses and education in colleges and universities.

It can be seen from the data in the figure that 85.11% of the students who like ideological and political courses think the teaching methods of teachers are interesting, while 73.33% of the students who do not like ideological and political courses think the teaching contents of teachers are boring. In addition, 53.51% of the students pointed out that the current ideological and political education content and teaching methods are single, which does not meet the needs of college students. It can be seen that the teaching contents and methods of ideological and political education have a great impact on college students' liking for ideological and political courses. In addition, among the reasons why they do not like ideological and political courses, half of the students think that ideological and political education courses are divorced from the reality of life and are not helpful to their own life. This shows that the ideological and political education curriculum in colleges and universities is biased toward theoretical elaboration and ignores the importance of social practice, which makes the ideological and political education curriculum lack of interaction and participation.

As shown in Figures 7 and 8, it is the degree and reason why college students like the ideological and political course after participating in the ideological and political education training experiment.

It can be seen from the results in the figure that after participating in the ideological and political education

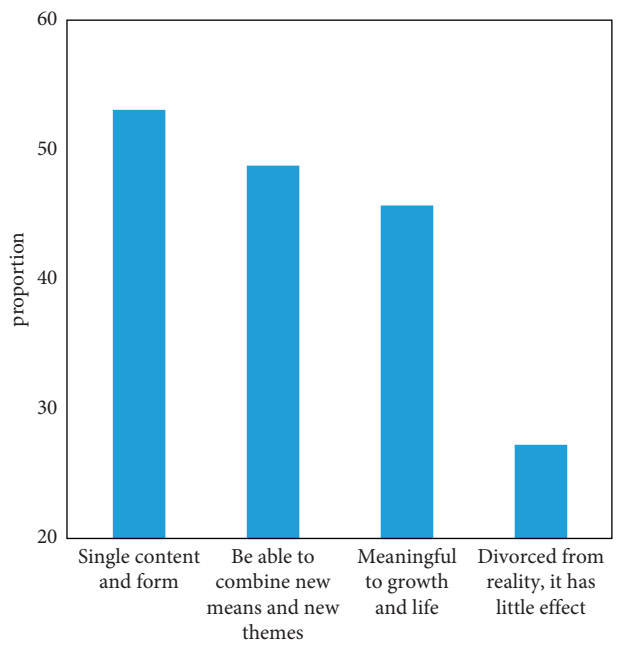

Figure 6: Students' evaluation results of ideological and political courses and education in colleges and universities.

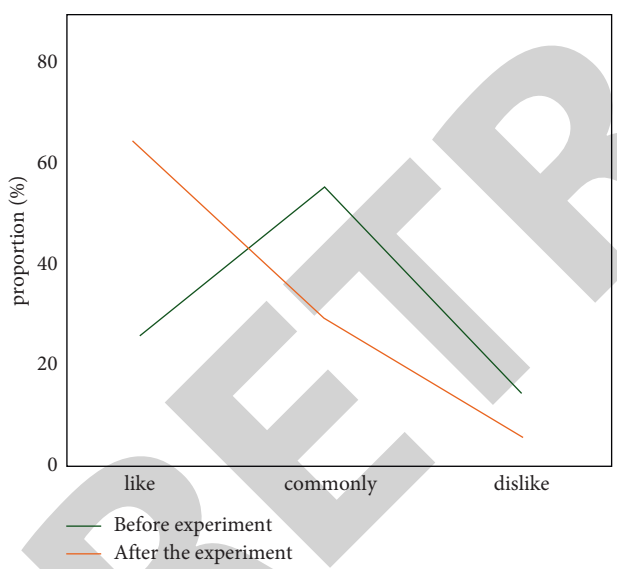

Figure 7: How much college students like the ideological and political course after participating in the ideological and political education training experiment.

training experiment, college students have greatly improved their liking for the ideological and political course, and the number of people who do not like the ideological and political course has also decreased significantly. It can be seen from the reasons that 70.3% of the students are interested in the teaching method of the ideological and political course, 51.89% of the students think that through this way, they can have a deeper understanding of the content of the ideological and political course, and 42.16% of the students think that such an ideological and political course can help shape their three outlooks and have a deeper understanding of the

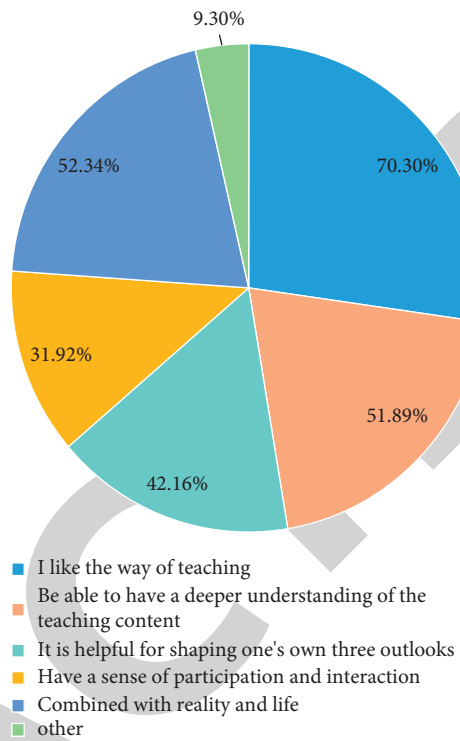

Figure 8: Reasons why college students like the ideological and political course after participating in the practical training experiment of ideological and political education.

importance of ideological and political education. In addition, 64.86% of students like the interaction and participation of ideological and political courses, which improves students' enthusiasm and sense of participation.

To sum up, the application of college ideological and political education training cloud system based on AR and Internet of things technology improves the interaction and participation of ideological and political courses, provides college students with the opportunity to participate in the courses in person, and improves students' interest and enthusiasm in ideological and political courses. The interesting teaching method is conducive to improving students' liking for ideological and political courses, so that more students can truly understand and understand the content and importance of Ideological and political courses. At the same time, the practical training cloud system of ideological and political education in colleges and universities based on AR and Internet of things technology explores and practices the innovative education model of online and offline connection, extracurricular and in class connection.

5. Conclusion

This paper puts forward the research on the innovation of college students' ideological and political education in the intelligent environment of the Internet of things and constructs the ideological and political education training cloud system through the Internet of things technology and AR technology to realize the purpose of students' participation in the practical activities of ideological and political

Hindawi
Computational Intelligence and Neuroscience
Volume 2023, Article ID 9813410, 1 page
https://doi.org/10.1155/2023/9813410

Retraction

Retracted: Sports Analysis and Action Optimization in Physical Education Teaching Practice Based on Internet of Things Sensor Perception

Computational Intelligence and Neuroscience

Received 19 September 2023; Accepted 19 September 2023; Published 20 September 2023

This article has been retracted by Hindawi following an investigation undertaken by the publisher [1]. This investigation has uncovered evidence of one or more of the following indicators of systematic manipulation of the publication process:

(1) Discrepancies in scope
(2) Discrepancies in the description of the research reported
(3) Discrepancies between the availability of data and the research described
(4) Inappropriate citations
(5) Incoherent, meaningless and/or irrelevant content included in the article
(6) Peer-review manipulation

The presence of these indicators undermines our confidence in the integrity of the article's content and we cannot, therefore, vouch for its reliability. Please note that this notice is intended solely to alert readers that the content of this article is unreliable. We have not investigated whether authors were aware of or involved in the systematic manipulation of the publication process.

In addition, our investigation has also shown that one or more of the following human-subject reporting requirements has not been met in this article: ethical approval by an Institutional Review Board (IRB) committee or equivalent, patient/participant consent to participate, and/or agreement to publish patient/participant details (where relevant).

Wiley and Hindawi regrets that the usual quality checks did not identify these issues before publication and have since put additional measures in place to safeguard research integrity.

We wish to credit our own Research Integrity and Research Publishing teams and anonymous and named external researchers and research integrity experts for contributing to this investigation.

The corresponding author, as the representative of all authors, has been given the opportunity to register their agreement or disagreement to this retraction. We have kept a record of any response received.

References

[1] M. Chen and J. Jiang, "Sports Analysis and Action Optimization in Physical Education Teaching Practice Based on Internet of Things Sensor Perception," *Computational Intelligence and Neuroscience*, vol. 2022, Article ID 7152953, 8 pages, 2022.

Hindawi
Computational Intelligence and Neuroscience
Volume 2022, Article ID 7152953, 8 pages
https://doi.org/10.1155/2022/7152953

Research Article

Sports Analysis and Action Optimization in Physical Education Teaching Practice Based on Internet of Things Sensor Perception

Mengjunguang Chen and Jingjing Jiang

Department of Physical Education, Chang'an University, Xi'an 710021, Shanxi, China

Correspondence should be addressed to Jingjing Jiang; jiangjingjing@chd.edu.cn

Received 23 February 2022; Accepted 18 April 2022; Published 30 June 2022

Academic Editor: Guobin Chen

With the progress of the Internet of things technology in recent years, all aspects of people's lives have also been affected. More and more people are immersed in the virtual world and ignore the real activities. According to the survey, nearly 50% of people in China are in subhealth, mainly modern diseases caused by long-term inactivity. Therefore, to form a good habit of physical exercise, we must start from an early age. Starting from the physical education teaching in primary and secondary schools and from the perspective of modern scientific and technological facilities, this paper discusses the practical sports analysis and action optimization of physical education teaching based on the perception of the Internet of things. Starting from the practice of Internet of things sensor sensing in physical education teaching, we have successively determined the multisensor motion acquisition system algorithm, motion pattern recognition algorithm, and motion energy consumption algorithm, which provides modern equipment for motion analysis and motion optimization in physical education teaching practice, which breaks the current situation that traditional teachers spend a lot of time and energy for students. Combining sports mode with sports energy consumption can not only analyze sports data accurately and in real time but also optimize and predict students' sports behavior in time. We hope to supervise and urge primary and secondary school students to exercise through technical means to improve the quality of primary and secondary school students' exercise and improve people's health through physical exercise.

1. Introduction

The explanation and analysis of sports behavior in traditional physical education teaching is generally the model of physical education teachers' real demonstration and students' imitation. However, physical education teaching is often a teacher who teaches multiple students at the same time, lacking enough energy and comprehensive observation [1]. Even if some students spend the same time and energy on physical exercise, their behavior is not in place or standardized, resulting in ineffective exercise and even physical damage, which is extremely unfavorable to the development and growth of teenagers [2]. With the development of science and technology, more and more types of advanced equipment are constantly introduced into the teaching classroom, such as the Trinity Interactive system between students' parents and schools, large screen computers. In physical education, some schools try to use virtual reality and other types of advanced equipment for pioneering physical education [3]. The essence of virtual reality is a wearable device, which is also a research hotspot in recent years. Wearing relevant equipment during exercise can capture relevant motion data during exercise and obtain real-time data acquisition for subsequent related processing and analysis [4]. Combined with the current situation that the physical quality of primary and middle school students in China is declining year by year, we can first collect data through the physical condition or physical condition of students and then analyze the specific situation of students and formulate corresponding and reasonable training plans. This can not only make primary and secondary school students get effective exercise but also control the energy consumed by exercise, avoid excessive consumption within a reasonable range, and effectively improve students' physical

quality to the greatest extent. Firstly, this paper analyzes three kinds of sports often carried out by primary and secondary school students, namely, jumping, walking, and running [5]. The Internet of things collects standard action data as the identification benchmark of subsequent actions. The acceleration speed of these three actions is very different. Therefore, the main principle of motion recognition is to judge which of the three motion modes is an action by calculating the motion acceleration of the current actual action. In addition, a series of motion data signals such as acceleration, signal amplitude, local tilt angle, and average acceleration in acceleration stage are also analyzed in this paper. Finally, the above motion recognition algorithm is combined with the Internet of things sensor technology for physical education practice analysis and motion optimization.

A good algorithm must need corresponding quantitative indexes, referring to the quantitative index of physical exercise, sports energy consumption. Therefore, we also take the energy consumed in the process of sports as the embodiment of the effect of physical exercise. At the same time, considering that different exercise modes consume different energy, different individuals perform the same exercise mode, and the energy consumption is also different due to individual differences [6]. Therefore, we propose three models to calculate the motion energy consumption under different conditions. Firstly, based on the principle of multiple regression linear model, we can roughly get the optimal value of the linear regression relationship between individual students' age, height, weight, gender, and energy consumption and then get the linear acceleration model according to different exercise forms. Based on the linear acceleration model, the relationship between acceleration and energy consumption is analyzed, and then a linear integral model is proposed. Finally, the students' motion energy consumption is estimated through the kinetic energy theorem. Because the above three models are based on different calculation principles and methods, although they are helpful to the quantitative evaluation of sports energy consumption of primary and middle school students, there are still some differences in the accuracy of the models. Therefore, this paper finally carries out a computer simulation test on the above work and analyzes the estimation results of the three models. Finally, it shows that the linear acceleration model is the most accurate for the calculation of sports energy consumption of primary and secondary school students.

Starting from the physical education teaching in primary and secondary schools and from the perspective of modern scientific and technological facilities, this paper discusses the practical sports analysis and action optimization of physical education teaching based on the sensor perception of the Internet of things. The research and innovation contributions include the following: (1) Starting from the practice of Internet of things sensor sensing in physical education teaching, we have successively determined the multisensor motion acquisition system algorithm, motion pattern recognition algorithm, and motion energy consumption algorithm, which provides modern equipment for motion analysis and motion optimization in physical education teaching practice, which breaks the current situation that traditional teachers spend a lot of time and energy for students. (2) It fully embodies the interdisciplinary characteristics; that is, it combines modern network technologies such as network communication, data acquisition computer system, and electronic sensor system, involving sports health and human movement. (3) The combination of motion mode and motion energy consumption can not only analyze the motion data accurately and in real time but also optimize and predict the motion behavior in time.

Starting from the physical education teaching in primary and secondary schools and from the perspective of modern scientific and technological facilities, this paper discusses the practical sports analysis and action optimization of physical education teaching based on the sensor perception of the Internet of things. This paper is divided into five parts. The first part expounds the explanation and analysis of sports behavior in traditional physical education teaching. At the same time, it analyzes the sports often carried out by primary and secondary school students. The second part analyzes the literature application of sports equipment sensors. From the perspective of modern scientific and technological facilities, the third part discusses the practical sports analysis and action optimization of physical education teaching based on the sensor perception of the Internet of things. The fourth part describes the model results. Compared with different models, the estimation result of linear acceleration model is the most accurate, which can be used for motion analysis and motion optimization in the practice of Internet of things sensing physical education teaching. Finally, the full text is summarized.

2. Related Work

In recent years, mobile devices suitable for ordinary sports lovers have been gradually listed on the market, such as Huawei smart bracelet, Nike +, Adidas MiCoach, and other mobile devices. Because these mobile devices can enable exercisers to carry and record relevant sports data during physical training, these mobile devices also belong to generalized wearable data acquisition products [7]. The emergence of these products facilitates the data collection in the training process to a certain extent. They belong to the application of sensorable technology in sports. However, such products are usually only applicable to professional sports teams or a single sports event. In the final analysis, because the algorithm of such products is relatively single, they can only collect, simulate, and analyze sports data in specific situations [8]. At the same time, the use of such products usually requires corresponding auxiliary equipment for auxiliary training, and the relevant auxiliary equipment is usually expensive [9]. For example, in the use of a common sports equipment in the market, the cost of setting up a camera alone is as high as 100000 euros. If we want to promote and use it in physical education teaching in primary and secondary schools, it is obvious that the cost exceeds the budget [10]. At the same time, this kind of equipment has a large volume and is not suitable for primary

and secondary school students to wear and use at any time. To sum up, for the application of sensorable technology in sports practice and analysis in physical education teaching, there is an urgent need for a special data acquisition system to analyze action practice and wear wearable devices for action guidance and optimization.

At present, there are many research results on motion data acquisition system at home and abroad. Sport Universal Process, a French data company, has developed a sports club data analysis system especially used to analyze football match data. The essence of the system is to compare the collected data with the standard data and analyze and generate the corresponding analysis data results through the corresponding algorithm of the software. Among them, the data acquisition source of the acquisition system is mainly the high-speed cameras installed in various places in the sports field. These high-speed cameras will record the whole process of the game and generate data analysis sources [11]. German SAP data company uses match insights data analysis system to predict football solutions and analyze various game data. The system helped Germany successfully predict and win the Hercules cup at the 2014 World Cup in Brazil. The system is also equipped with supporting mobile devices and analysis applications. Through the prediction and analysis system, the football team can obtain kinematics anytime and anywhere and formulate football plans and various competition data of rival teams [12]. Nanjing University of Technology and others have also designed relevant football sports data acquisition systems. At the same time, they have cooperated with the French laboratory PROTEE to design a sports acquisition system based on a wireless sensor network [13]. Shenyang University and others designed ZigBee's motion data acquisition system and transmission module [14].

The data characteristics of different motion modes are different, so the research on motion mode recognition is also more extensive at home and abroad. By combining the relevant principles of motion mechanics and biology, Simi company of Germany has designed a motion capture and analysis system for restoring human motion posture, and the test shows that the system has high accuracy. Tian LAN and Greg Mori designed a conditional random field object recognition model based on the hiding condition principle of maximum boundary value. The design system first compares the local features with the standard data features and then integrates the local features to form a large number of global features, which are compared with the standard data features again, so as to distinguish different sports actions. The Institute of Computing Technology of the Chinese Academy of Sciences has developed a method to extract data from the moving human body under different dynamic background structures, such as running, jumping, long jump, and javelin, so as to identify different movement modes with high accuracy. Overall, the motion system is based on three-dimensional human motion simulation and video analysis and computer-aided motion recognition, extraction, and judgment [15].

The common sports index is energy consumption. The higher the flow consumption, the more effective the sports. Therefore, the data analysis system usually carries the function of identifying the amount of energy consumed. For example, American companies BodyMedia and Sense Wear wrap the arm strap of the product sent by the data collector around the exerciser's big arm, and the exerciser drives the sensor on the arm to generate relevant fluctuations through physical movement so as to obtain the exercise data during the exercise of the exerciser and analyze these data through specific algorithms and software. We can get how much energy the exerciser consumes in the exercise process so as to judge the exercise effect. Therefore, it is necessary to promote the perceptible technology in the physical education teaching of primary and middle school students so as to analyze the quality and efficiency of physical exercise. By selecting an effective sports model and reasonable energy consumption, we can objectively analyze and evaluate the overall sports process, provide scientific sports suggestions, and formulate a reasonable sports plan so as to effectively improve the physical quality of students.

3. Method

The key point and difficulty of sports analysis and action optimization engineering in physical education practice lie in the identification of sports mode. Only by effectively identifying the collected data can it be compared, judged, and analyzed with the standard data. The data source of this paper is that the experimenter wears sensing equipment for physical exercise and collects the experimenter's sports data through the data acquisition algorithm.

Firstly, it is necessary to determine the wearing position of the data collector. The data signals generated by different body parts are different. Therefore, the wearing position of the data collector is directly related to the authenticity and effectiveness of the collected data. Through the research on the wearing position of the existing data collector in the market, it is found that the main wearing positions are waist, wrist, upper arm, lower leg, and ankle. Through the verification of specific experimental tests, we found that when the upper limb wears the data collector, such as wrist, upper arm, and other parts, because the upper limb is an auxiliary part, different sports movements need coordinated movements of the upper limb, so there is little difference between different sports movements. Therefore, in the subsequent analysis, especially when the heat consumed by the collected action is compared and analyzed, the difference comparison cannot be made. At the same time, when the upper limb of the body moves, it usually makes a circular motion with the shoulder as the reason and the arm as the radius. Even in the in situ motion, the acceleration of the circular motion is obvious. This leads to a large amount of acceleration in the collected data, which greatly interferes with the subsequent analysis process, especially the number of motion steps.

Next, we consider wearing the data collector on the experimenter's lower limbs, such as lower legs or ankles, but the effect is not ideal. When the experimenter performs strenuous exercise, such as running or jumping, the strength and support of lower limbs are more important, so the whole lower limbs will participate, resulting in the impact of knee

and ankle joints and greater friction, resulting in a large amount of irregular noise in the subsequently collected data, which cannot be separated from the real data. It is not conducive to further analysis and processing of the data collected by the data collector. At the same time, the lower leg and ankle are lower in the human body structure. During the experiment, the data collector worn on the lower leg and ankle is thrown out due to too intense leg movement, resulting in equipment damage.

This paper also considers putting the wearable device into the experimenter's pocket, but it is found that the wearable device sensor will rub a lot with the experimenter's clothes, which is not conducive to the subsequent analysis and processing of the collected data. At the same time, when wearable devices are worn on the body, it can be assumed that they are integrated and have the same acceleration. However, when the wearable device is placed in the clothing pocket, the two are separated. After the wearable device sensor is subjected to upward force, due to its different mass, it is also different from the body acceleration. Therefore, the reliability of the collected data also needs to be further reduced.

To sum up the data, the final experiment found that wearing the wearable device at the waist is the most suitable position. Firstly, the waist participates in different activities such as walking, running, and jumping, and the force and trajectory of the waist are different in different activities. Therefore, the data characteristics of the waist are the most obvious, and the data collected by the collector worn on the waist is vertical data, which changes more than the horizontal data collected by other parts. At the same time, wearing the wearable device sensor on the experimenter's waist will minimize the movement process of the experimenter. Even if it is worn for a long time, it will not affect the whole movement. Therefore, it can reflect the movement process of the experimenter to the greatest extent, and the reference value of data collection is also the greatest.

After determining the exercise mode and relevant experimental design, we will officially start the experiment. First, we randomly recruited a group of 40 primary and secondary school student volunteers, including 23 boys and 17 girls. When wearing a multisensor data collector at the waist, these experimenters carried out 5 standing long jumps, 5 5-meter run-up long jumps, 5 normal speed walks in 1 minute, 5 fast walks in 1 minute, 5 slow runs in 1 minute, and 5 fast runs in 1 minute. In order to avoid the interference of irrelevant signals, we uniformly adjusted the data sampling frequency to 50 Hz. At the same time, in order to further analyze the differences in the same exercise between different individuals, individual information such as height, weight, gender, and age was recorded at the same time. In order to ensure the accuracy of the experimental data, that is, the sports carried out by the experimenter in a good and normal state, this experiment is carried out in batches. Sufficient rest time shall be reserved between different experimental items to avoid the state after the previous exercise affecting the next exercise (see Figure 1).

After collecting the specific motion data of the experimenter through the data collector with a multisensor sensing

Figure 1: Schematic diagram of wearable devices.

function, due to the experimental environment and design reasons, the initially collected data inevitably contains a lot of noise. Therefore, the first step of data analysis is to clean the original data and wash away the invalid data. Firstly, we analyze the available digital signals collected by the data sensor, such as the acceleration generated by human motion and the gravity acceleration of the Earth. In addition, there is the acceleration generated by the sensor sliding due to the motion process, as well as the minor actions caused by the unavoidable environmental factors in the measurement process, such as the experimenter's own shaking or external forces such as wind. In order to avoid the influence of invalid data, that is, noise, we first improved the sensor for collecting data and put it firmly on the waist so as to reduce the noise caused by the sliding of the sensor. However, objective factors such as shaking of the experimenter or wind cannot be avoided, so we hope to clean the data by filtering method. First, assume that there is a column of ordered data:

$$a_1, a_2, a_3, a_{4,} \ldots, a_{n-1}, a_n. \tag{1}$$

If a window with a fixed length m (m is an odd number) is used for the data sequence, m data sequences will be taken out continuously from the original sequence at random as follows:

$$a_{i-v}, \ldots, a_{i-1}, a_i, a_{i+1}, a_{i+2}, \ldots, a_{i+v}. \tag{2}$$

Then, the median of the sequence is a_i, and the median is M_i; then, there is

$$M_i = \mathrm{Med}\{a_{i-v}, \ldots, a_{i-1}, a_i, a_{i+v}, \ldots, a_{i+v}\}. \tag{3}$$

Therefore, we call M_i the final result output value of the window crossing sequence with length m. In practical application, the size of m value directly affects the final output result. As shown in Figures 2 and 3, when the time values of the x-axis and y-axis change, the constant speed acceleration remains unchanged and is in dynamic balance. Through experiments, it is found that when the m value is 3, 5, and 13, the effect of data noise reduction is the best. Finally, we go to $m = 3$, process the data collected by the multisensor sensing data collector, and draw the motion acceleration relationship as follows (see Figures 2 and 3).

After data cleaning, it is necessary to analyze the cleaned data to identify the classification of motion modes as accurately as possible. Here, only three basic movements commonly used in physical education teaching in primary and secondary schools are studied, namely, walking,

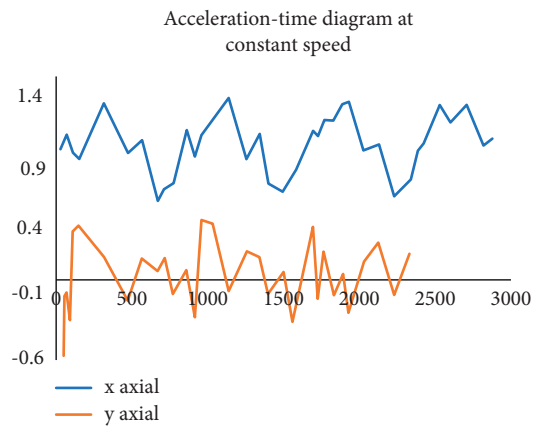

Figure 2: Acceleration-time diagram at a constant speed.

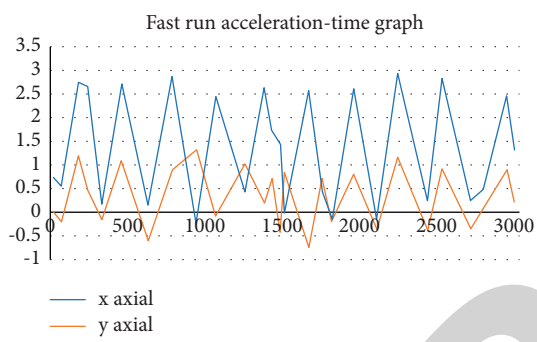

Figure 3: Fast run acceleration-time diagram at a constant speed.

running, and jumping. The specific classification of each type of movement is shown in Figure 4.

Firstly, we identify jumping movement. The biggest difference between walking and running is that the first two are periodic movements. From the specific data signals, we can also see that the overall movement changes periodically. Jumping belongs to explosive movement, and the duration is short. After the experimenter took off, the acceleration value gradually decreased under the action of gravity in the ascending stage. The horizontal acceleration is 0 from the landing to the next take-off, and the vertical acceleration is about 1 g until the next take-off. Thus, the formula for calculating the take-off resultant force acceleration of the experimenter is

$$a(t) = \sqrt{a_x^2 + a_y^2 + a_z^2}. \tag{4}$$

The left side of the equal sign represents the resultant acceleration of the experimenter, and the right side of the equation represents the motion acceleration component of the experimenter in the X, Y, and Z directions.

For walking and running, they have great similarity and only change greatly in step amplitude. The specific step frequency formula is as follows, but obviously, it is not accurate enough to distinguish the two movement modes only by step amplitude, so we still need other recognition conditions for reference:

$$\text{stride frequency} = \frac{\text{Total steps}}{\text{Duration of exercise}}. \tag{5}$$

After determining the sports mode, in order to further analyze sports and optimize related actions in physical education teaching, we introduce the research on sports energy consumption for measurement. From the biological point of view, energy consumption is positively proportional to the product of individual mass and exercise time. The specific relationship is as follows:

$$\text{energy consumption (kcal)} = \text{weight (kg)} \times \text{exercise time (min)} \times 0.179. \tag{6}$$

However, the formula only considers the role of exercise time in overall exercise and does not consider the change of exercise mode on energy consumption in finishing exercise. Therefore, in the sports analysis of physical education practice, we cannot accurately understand the real sports situation of students. Therefore, we need a more accurate energy consumption calculation formula. According to the data, the linear calculation formula between accelerometer output data and energy consumption has been summarized in the experiment, which has been widely used in academia and has a high reference value. Therefore, this paper also takes it as the calculation formula of motion energy consumption. In this formula, there is a linear relationship between accelerometer output data (AO) and energy consumption. The specific formula is as follows:

$$EE = 1.294 \times AO + 77.988. \tag{7}$$

In the linear formula, r value and p value are the basis for measuring the accuracy of the model. The value of r is called the correlation coefficient, that is, the regression coefficient in the regression equation. The greater the absolute value of r, the higher the linear correlation between the independent variable and the dependent variable. We use x_i and y_i $(i = 1, 2, 3 \ldots n)$ to represent two variables; $\overline{x}$ and $\overline{y}$, respectively, represent the average value of the two variables, so the calculation method of r value is as follows:

$$r = \frac{\delta_{xy}^2}{\delta_x \delta_y} = \frac{\sum_{i=1}^{n} (x_i - \overline{x})(y_i - \overline{y})}{\sqrt{\sum_{i=1}^{n} (x_i - \overline{x})^2} \sqrt{\sum_{i=1}^{n} (y_i - \overline{y})^2}}. \tag{8}$$

Next, we verify the accuracy of energy consumption calculation through experiments for the optimization of practical actions in physical education teaching. It is known that the normal range of body mass index of standard BMI (body mass index) is 18.5–24.99. The calculation method is as follows:

$$\text{BMI} = \frac{\text{weight (kg)}}{\text{height (m)}^2}. \tag{9}$$

After determining the approximate linear relationship of the energy consumption calculation method, we began to estimate the specific calculation model through the

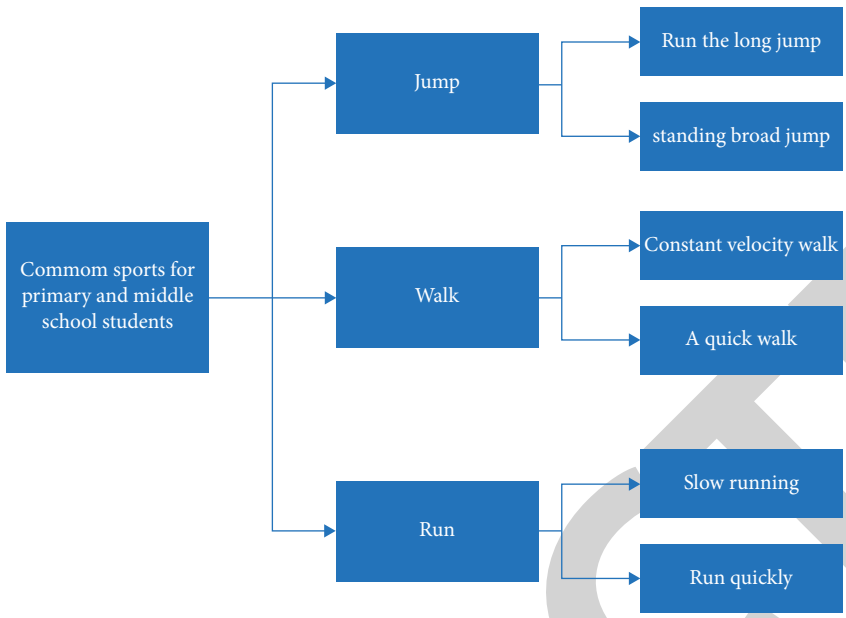

Figure 4: Classification diagram of motion modes.

principles of linear acceleration, linear integral, and kinetic energy theorem. The specific model is as follows:

$$\begin{aligned} &\text{Motion energy consumption} = \text{a} \times \text{Kinematic acceleration} + \text{b}, \\ &EE_a(t) = a_1 \times H(t) + b_1 \times V(t) + c. \end{aligned} \tag{10}$$

According to relevant experimental calculations, a_1 and b_1 have the following linear relationship:

$$\begin{aligned} a_1 &= a_1 \times weight(kg) + \beta_1 \times height(cm) \\ &\quad + \gamma_1 \times age(year) + \delta_1, \\ b_1 &= a_2 \times weight(kg) + \beta_2 \times height(cm) \\ &\quad + \gamma_2 \times age(year) + \delta_2, \\ IA &= IA_x + IA_y + IA_z, \\ EE(t) &= a_2 \times IA(t) + b_2. \end{aligned} \tag{11}$$

To sum up, according to the principle that energy consumption is linear with individual mass and motion time and based on the principles of linear acceleration, linear integral, and kinetic energy theorem, three motion energy consumption models are proposed in this paper. The model adds the differences in motion mode and individual parameters to the original energy consumption model, which makes the calculation degree of the model more accurate.

4. Result Analysis and Discussion

According to the above theoretical research results, finally, we verify our theoretical results through computer simulation, that is, the performance of data acquisition system, the accuracy of motion recognition algorithm, and the accuracy of energy model consumption.

Firstly, the performance of the data acquisition system is verified. The acquisition system is tested on 8 runways of the standard 400 m playground, and the perception of the sensor is verified through the test. During the test, the sensing central machine is located above the playground facing the podium, which is generally in the middle of the whole playground. The central sensor can be used as a signal tower to communicate the transmitting end and receiving end of the collector. One person acts as a physical education teacher, which is located on one side of the central sensor and holds a signal receiving device to receive and view students' sports data in real time. Forty students wear multisensor sensing physical education teaching equipment and move randomly in the playground. After the test, the relationship between line mileage, request, and delay is shown in Figure 5. It can be seen that the delay is short and the overall acceptance is good. In order to avoid the situation that the dead corner of the playground cannot transmit data, the experiment focuses on the corners and other places. The results show that the communication between the data collector and the hardware base station is correct.

The energy consumption calculation of the traditional Meijer algorithm and the algorithm model proposed in this paper is tested. Under the condition of the same motion

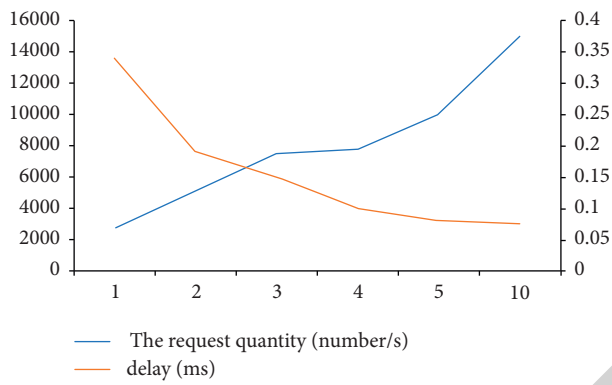

Figure 5: A large number of request environment simulation test results.

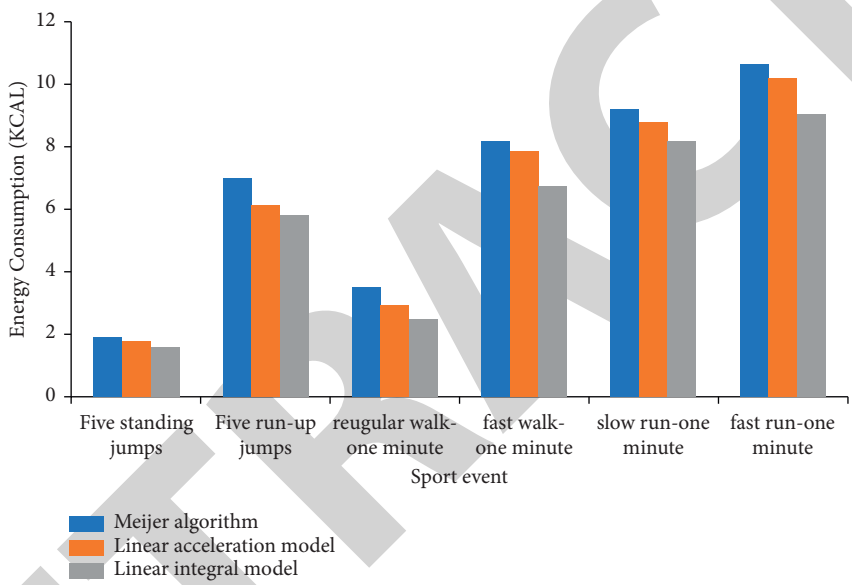

Figure 6: Comparison of average energy consumption calculated by different algorithms.

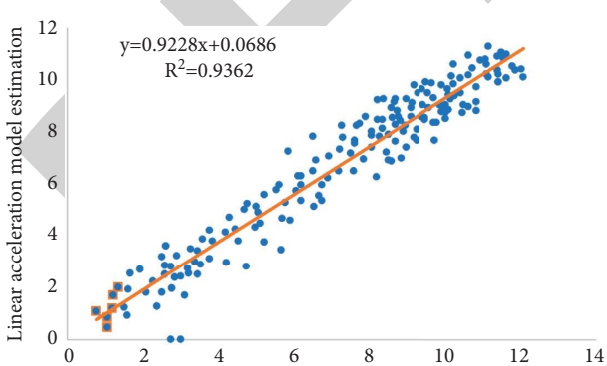

Figure 7: Schematic diagram of linear analysis of the estimated value of linear acceleration model and Meijer formula.

mode and time, it is more accurate to observe the algorithm. The specific results are shown in Figure 6.

Firstly, it can be seen from Figure 6 that the change trend of data values calculated by the three algorithms is basically the same. It can be seen that the calculation of this algorithm is basically correct, and the response is basically consistent with the energy consumption of physical exercise in physical education teaching practice. However, on the whole, the energy consumption of the three models under the same sports events is lower than that of the traditional Meijer algorithm. Through further observation, we can see that the energy consumption of the two sports modes of constant speed walking and fast running is much lower than that of other sports. According to the literature, in order to counteract the influence of gravity during walking, the human body automatically generates more acceleration in the vertical direction, resulting in the reduction of motion energy consumption in the vertical direction. To sum up, the relevant linear analysis diagram is obtained after the energy consumption of various sports indicators (Figure 7).

To sum up, the three algorithms have certain advantages. Compared with the general algorithm, the estimation result of linear acceleration model is the most accurate, which can be used for motion analysis and motion optimization in the practice of Internet of things sensing physical education teaching.

Hindawi
Computational Intelligence and Neuroscience
Volume 2022, Article ID 3310676, 10 pages
https://doi.org/10.1155/2022/3310676

Research Article

Analysis of the Intelligent Tourism Route Planning Scheme Based on the Cluster Analysis Algorithm

Na Lou

Zhengzhou College of Finance and Economics, Zhengzhou, Henan 450000, China

Correspondence should be addressed to Na Lou; lnn2020@hbzy.edu.cn

Received 25 May 2022; Accepted 9 June 2022; Published 28 June 2022

Academic Editor: Yang Gu

In view of the problems of the traditional cluster analysis algorithm such as strong dependence on the initial cluster center, the traditional k-means cluster analysis algorithm is improved and the experiment proves that the improved algorithm has a better clustering effect; in view of the problems of the traditional tourism route planning, the improved k-means cluster analysis algorithm is applied to the intelligent tourism route planning scheme design and an intelligent tourism planning scheme based on the cluster analysis algorithm is proposed; the tourists' preference metric is fully considered, and the experimental results show that the scheme has certain reasonableness and reference value.

1. Current Situation of Tourism Route Planning

1.1. The Development of the Tourism Industry. With the improvement of the economy and the increase in people's happiness, China's tourism industry has made great achievements since the reform and opening up, both at home and abroad, China's tourism industry with concept features such as tourist cities and tourist hometowns has been deeply rooted in people's hearts [1]. In 2021, under the grip of the epidemic, China still received nearly 93 million people, while the total number of travel agencies in the country was more than 40,000, an increase of 4.3% year-on-year, indicating that under the epidemic, the number of people going to travel in China with good protection against the epidemic is still incessant, which also reflects the "vitality" of China's tourism industry under the epidemic from the side. The tourism industry in China is "vibrant" under the epidemic [2].

However, according to the "Analysis of Tourism Economy in 2021 and Development Forecast in 2022" released by China Tourism Research Institute, China's national tourism economy in 2022 is still suffering from a decline; in 2021, more than 70% of China's scenic spots suffered serious losses; a large part of this is due to not planning tourist routes, not understanding the needs of tourists, and other reasons [3]. However, there are still a lot of scenic spots that profited than in previous years because such scenic spots mastered the "flow" code, cracked the epidemic under the core of tourism as it was people-oriented, and mastered the wisdom of route planning, understanding the needs of tourists, and knowing what tourists want. Therefore, in today's development situation of the new crown epidemic, constructing intelligent tourism route planning is an important part of developing tourism.

1.2. Definition and Classification. Tourism planning, in academic circles, has three definitions, which are as follows [4].

The first one is the formulation and planning of tourism development goals and programs for a specific area in the future period of time, and then the tourism development and construction of that specific area after approval and adoption by relevant government departments or government agencies. In tourism planning, it is necessary to coordinate the overall situation and provide specific implementation plans and detailed guidance programs for the tourism practice of the region [5].

The second type is a tourism work plan based on the changing factors of the market, history, and current situation of the tourism industry. Under this plan, it is necessary to

coordinate all available resources, such as urban and rural areas, so that the tourism industry in each region can develop in a coordinated and competitive way, and eventually achieve the effect of a hundred flowers [6].

The third type is an economic and technical act, i.e., intellectual resources, of which economy and technology are the primary conditions. The essence of this definition is the question of how to coordinate the relationship between the economy and the tourism industry, using the appropriate economic instruments and technical resources to determine the status and composition of the tourism industry in the national economic plan, and to propose goals for the development of the tourism industry, which, of course, is defined at the level of national economic development.

In this paper, the study is focused on regional tourism planning, i.e., it corresponds to the first definition mentioned above. Among the types of tourism route planning, there are again the following [7] as shown in Figure 1.

Firstly, according to the spatial span, it can be divided into large- and medium-scale tourism routes and small-scale tourism routes. In the large- and medium-scale tourism routes, the travel agency needs to contact the source of tourists and a series of tourist paths of tourist places in advance; secondly, the tourism route on a small scale refers to the tour route of tourist attractions and the arrangement of related tour projects to meet the tourists' psychological and physiological needs, such that tourists can feel the joy and pleasure of tourism during the journey [8]. Secondly, according to the attribute, the tourist route can be divided into peripatetic and stay-type tourist routes. The circumambulation tourism route obviously refers to the global browsing and sightseeing, experiencing the whole city or the entire tourist attractions, such as the former residence of a historical figure, and so on, and then feeling the local history and culture and life; a stay-type tourism route is obviously a very short period of short-term sightseeing behavior; this is mainly for small scenic spots, and historical and cultural heritage is not deep enough in such scenic spots [9]. For this type of scenic spot, the use of stay-type tourism route planning is a good choice; after all, the tourism team needs to consider the overall travel experience; the inclusion of stay-type tourism routes can take into account the feelings of most people and points of interest, so as to not to leave behind classic scenic spots [10].

The third is divided by functional purpose, which can be divided into sightseeing, scientific research, adventure, thematic, shopping, and leisure vacation type. Sightseeing type is obviously for sightseeing scenery, including urban scenery, scenic scenery, rural scenery, etc.; scientific research type is mainly for some professionals' who are into the research and development of some scenic spots and set up; adventure type is mainly for people seeking excitement and adventure significance in some scenic spots. Thematic type is mainly for some specific topics, or different types of scenic areas; shopping type of tourism route planning has shopping as the main body, and the entire tourist route guides will guide tourists to spend; for leisure and vacation type, the main content is leisure and vacation, catering to people who are looking to relax from the usual work pressure [11].

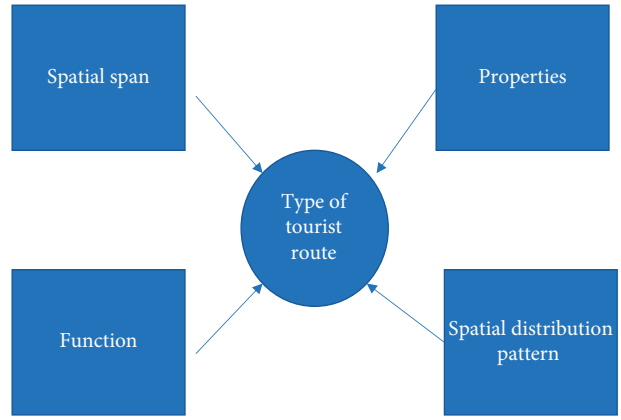

Figure 1: Classification of tourist routes.

1.3. Tourism Route Planning Research Status. After the above analysis, the economic growth trend of China's tourism industry in recent years has slowed down under the epidemic, but it is still optimistic on the whole. However, China's tourism industry still faces many challenges, and in order to solve various challenges, many research scholars based on tourism professions have put forward many insights [12]. For example, for specific regional tourism planning routes, Zhou Shengkang et al. took 26 attractions in Huang and Zhong Autonomous Prefecture as research objects and constructed a 16-indicator evaluation system for tourist attractions in four aspects: talent, system, facilities, and environment, while using qualitative and quantitative calculations to obtain the weights of each indicator, and used the hierarchical analysis method in multi-objective decision making to rationalize the data [13]. The data were calculated and analyzed using the hierarchical analysis method in multi-objective decision making, and finally the planning plan of the tourist route with the shortest travel time or the least cost was developed. In this study, the authors introduced multilevel analysis into the design of the tourism route planning scheme, which is a new inspiration for tourism-related research. Secondly, some researchers have also combined the Android system with travel route planning and proposed a personalized travel route recommendation system based on the Android system client and springboot-based back-end; based on this, the attractions in the Beijing region were used as examples, and were finally tested to achieve user login registration and personalized travel route planning recommendation functions [14].

The developing times and the deepening of artificial intelligence research have led to a deeper understanding of artificial intelligence and big data. For this reason, in response to the problems of traditional tourism route planning, such as time-consuming and poor user experience, many researchers have proposed a method to integrate tourism route planning with the ant colony algorithm in artificial intelligence. In this study, the author describes the basic principles of the ant colony algorithm and proposes improvements to the problems of the ant colony algorithm, such as the long time spent, the addition of a real-time pheromone update stage, the centralization of the search

range, etc [15]. Finally, the model is applied to the actual case design, and the improved algorithm analysis results in an optimal tourist route that meets the cost and experience [4] goals. In addition, there are also specific cities using the ant colony algorithm to design and study tourism routes [16]. For example, Yaxin Xu added the constraints of touring time and sightseeing value for Fuzhou in the way of travel merchant's problem, and established the mathematical model of touring in the shortest time, so as to realize the study of Fuzhou tourism routes based on the ant colony algorithm.

In addition to the use of the ant colony algorithm to calculate the optimal tourism planning route in the study, some researchers also use the particle swarm algorithm to carry out the shortest tourism route planning; in this planning design, the authors mainly apply the principle of the particle swarm algorithm to the city of Lhasa and find the shortest distance between major popular attractions, so as to enhance the tourist experience, reduce the cost, ensure the tourists' play time and quality, and save costs for tourism companies [17].

The advent of information technology has caused people to think about the value of data, and thus data mining and data analysis have emerged as hot topics for research. At the same time, tourism has become a way for people to relax, enjoy themselves, and broaden their horizons. Although the boom of tourism has brought economic growth, the feeling given to tourists in the planning of tourist routes is not friendly, and there are many problems about youth groups or senior groups of leisure tours but have been taken by the guide to spend [18]. One of the reasons for such problems is the lack of a "human-centered" design concept in the planning and design of tourism routes. For this reason, some scholars have proposed personalized travel route planning recommendations; in order to better exploit and make full use of the database accumulated in the tourism industry, Gong Yuan proposes the use of data mining to design the best travel route planning system, and the combination of hardware and software to achieve the best travel route planning function. In order to highlight the advantages of its route planning, it adds comparison experiments to the experimental process, and the experimental results show that the performance of the best tourism route planning system proposed by the authors is significantly better than the traditional best tourism route planning system [19].

2. The Necessity of Tourism Route Planning

China's tourism industry has also entered the stage of comprehensive development of the masses since it entered the comprehensive building of a well-off society, but at the same time China's tourism industry has entered the bottleneck period and some deep-seated contradictions have become more prominent during the epidemic, and these contradictions mainly focus on the dysfunction of the tourism industry structure, the lack of total tourism products, a single type of route, and the industry norms as they are not standardized [20].

2.1. Lack of Holistic Planning of Tourism Routes. First of all, Western countries for the planning of tourism routes have formed a specific and more standardized path design process, but China has not formed a set of more standardized design specifications. The reason for this phenomenon is that the line design involves more variables, is a more complex system design process, and the lack of training for this type of talent in China, thus leading to a gap in the market for tourism route planning designers in China [21]. Therefore, the current travel agency's tourist routes are generally undertaken by the relevant departments, and the planning staff in the design of tourist routes, due to the lack of professional knowledge, rely only on the main traffic routes and the scenic nodes as a series of points, resulting in the design of tourist routes in the program of the same without considering the essence of the tourist preferences, a characteristic key factor that should be paid attention to the dynamic changes in the market.

In addition, because the tourist route planning and design of the scenic area does not have a certain unified standard, it results in the design of the tourist route planning program in the short cycle, slow updates, the degree of homogenization, and other problems [22]. Individual units highlight the relationship between the road layout of the scenic spot, ignoring the low carrying capacity caused by the scenic spot route, and the resources have also suffered the same damage. It can be seen that the attention to the tourist route specification scheme design as a whole is a key part in achieving optimal route planning [23].

2.2. Not Deep Enough Development of the Product Type of Tourist Routes. Nowadays, most of the tourism products in the market are based on sightseeing tourism and vacation tourism, and a single type of tourism gives little space for people to choose, and the design and development of tourism routes is not deep enough. In addition, the route planning scheme is relatively rough and unrefined in design, and most of the routes are not integrated with the local humanities and history. Secondly, some of the smaller travel agencies do not have the concept of developing a variety of tourism products, making it difficult to survive the epidemic and becoming a "stepping stone" for other travel agencies [24]. Some even have thematic tourism routes that do not correspond to the actual phenomenon, which greatly affects the mood and experience of tourists. In summary, the root causes of the above problems are due to the lack of depth in the development of the product range of travel itineraries by travel agencies as shown in Figure 2.

2.3. The Design Theme of Tourism Routes Is Not Innovative and Not Compelling Enough. After decades of development of the tourism industry in China, under the guidance of the national tourism department, the characteristics of our tourism resources are actually quite distinct and the number of tourism resources of the same type is high, but the design themes of our tourism routes are not innovative and not compelling enough. The fundamental reason for this problem is that the purpose of today's tourism route design

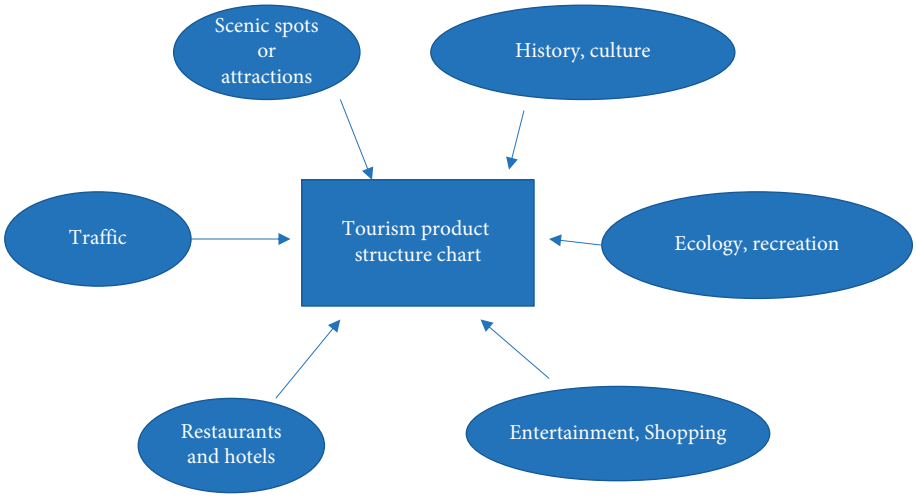

Figure 2: Structure of tourism products.

is based on "how to get people to the scenic area at the least cost," and in the eyes of most tourism route planners, "tourists arrive at the scenic area" is the same as "This equivalence is actually wrong [25]." The essence of such problems is that the designers are not aware of the "contextual design." For example, in the case of peripatetic tourism, there is a lack of "contextual design," and most of the tours are designed to allow people to walk around and see the sights while ignoring the local cultural characteristics, history, and customs. In general, the planning and design of the tourist route is not innovative, and does not consider the design concept of the core of the tourists' feelings [26].

2.4. The Combination of Design Elements Based on the Tourist Route Is Low. What does the design combination of tourist routes refer to? Is tourism just about going to a place? The answer is not at all. Travel is a way to pack up and go to another place to experience another kind of life, a trip to feel other customs and historical features. Since it is a trip, it inevitably includes food, clothing, housing, transportation, the distance from the place of residence to the scenic spot, the time of the tour, etc [27]. This paper believes that tourism should be the combination of all the above route design elements and the reasonable allocation of resources of all parties; the rationality of tourism route planning also depends on this. However, China's travel agencies in the design of route planning lack of a reasonable configuration of these elements and in the combination of elements of focus on the poor. For example, for Zhuhai–Macau, a two-day tour, the travel agency designed the route mainly as a shopping tour, and focused almost all the time on shopping, and ignored the local attractions of Zhuhai and Macau [28]. Excessive shopping will inevitably lead to dissatisfaction; although the theme is a shopping tour, other attractions and sightseeing time must be involved; otherwise, it will only cause tourists' dissatisfaction with the tour, thus reducing the sense of experience, and losing the original intention to travel is relaxation and happiness [29].

To sum up, through the analysis of relevant literature, coupled with the arrival of the era of artificial intelligence and big data, coupled with the overall development of tourism, there are many challenges in the development direction of tourism under the epidemic. Tourism route planning solutions are also emerging in an endless stream, whether in terms of improvement or in the application level, they are very effective. Among them, the clustering algorithm is more intuitive than the traditional algorithm. Therefore, this paper proposes the use of cluster analysis algorithms to analyze tourism route planning schemes and incorporate the concept of "wisdom" to make tourism route planning more human-like in thinking. The next paper will analyze the classification and basic principles of cluster analysis in order to select the appropriate cluster analysis algorithm to find the best tourism route planning plan.

3. Clustering Analysis Algorithm

Clustering analysis algorithm is an important research topic based on data mining. Data mining refers to the ability to mine and discover valuable, meaningful, and implicit potential knowledge or rules from a large amount of data in order to give decision support to the problems provided by users [30].

In data mining, the main algorithms are the association rule analysis algorithm, decision tree, classification pattern, clustering pattern analysis, and nowadays the widely researched neural network algorithm. Among them, the clustering analysis algorithm is a very effective unsupervised machine learning algorithm for the classification of certain [8]problems. Clustering is different from classification in that classification is a way of classifying things by type, nature, or rank, while clustering is a way of partitioning data in a dataset into different clusters or classes according to a specific criterion or rule, and making the similarity or correlation of data objects in the same class or cluster as large as possible. Essentially, data objects with the same properties are grouped in the same "group" (cluster) under a certain criterion, and those with more different properties are

placed in another group. In short, clustering itself is an unsupervised learning method that does not care about the labels of the data, but only whether the aggregated data are in the same cluster or the same category.

Cluster analysis is a rigorous mathematical process; the algorithm has been extensively studied for many years since it was proposed in 1984, and has evolved from the initial four processes to the following six basic steps as shown in Figure 3.

The first step is to determine the dataset or sample, followed by the preprocessing of the dataset or sample; the second step is the selection or transformation of features, which refers to the selection of suitable variables, and the selection of variables is related to the efficiency and correctness of the subsequent algorithm; thus, this is an important and critical step; after the selection of suitable variables, the next step is the scaling of data, the search for outliers, etc. The next step is to select a suitable clustering algorithm or to improve the clustering analysis algorithm, which will be discussed in Section 3.1; the next step is to confirm the number of classes, i.e., to evaluate and analyze the clustering results, and finally to visualize the clustering results, so as to realize the verification of the results.

3.1. Basic Methods of Data Clustering Classification. Nowadays, mainstream data-based clustering analysis algorithms can be classified into the following categories: hierarchical methods, division methods, density-based clustering methods, new methods, etc. Next, the following different types of clustering algorithms are analyzed and compared, so as to select the appropriate cluster analysis algorithm for the design of the tourism route planning scheme.

First is the hierarchical cluster analysis algorithm. The hierarchical cluster analysis algorithm is firstly "hierarchical," i.e., the dataset or sample is divided into different levels of clusters, and the clusters generated by the later layer are based on the results of the previous layer, and the hierarchical cluster analysis algorithm generally has the following two kinds: the first one is agglomerative hierarchical clustering, followed by divisive hierarchical clustering. In agglomerative hierarchical clustering, each selected object starts with a cluster, i.e., clusters, and each time the two closest clusters are merged to generate a new cluster according to certain criteria or standards, and the process is cycled until all clusters are merged into one large cluster. It should be noted that agglomerative hierarchical clustering is suitable for mixed data types, with better noise immunity and arbitrary cluster shapes, but its algorithm is slow; for divisive hierarchical clustering, also known as the top-down (i.e., top-down) hierarchical clustering analysis algorithm, and the above-mentioned hierarchical clustering algorithm, what is different from the above hierarchical clustering is that the algorithm puts all the datasets or samples into one big class, i.e., clusters, and each time divides a certain clusters into multiple clusters according to certain criteria or guidelines, and keeps looping this process until all the clusters can no longer be classified, i.e., at this time all the clusters are a single cluster as shown in Figure 4.

Next is the density-based cluster analysis algorithm. In this cluster analysis algorithm, density is mainly used instead of similarity, and the density of the distribution of data or sample objects as a starting point; the density cluster analysis algorithm is applied on this basis to select regions large enough to be connected such that clusters of various shapes can be composed in the data. One of the most classic density-based cluster analysis algorithms is the DBSCAN algorithm proposed by Ester et al. [10]. In the DBSCAN algorithm, two parameters M and μ need to be defined, where M denotes the neighborhood density threshold of the clusters and μ denotes the neighborhood radius that defines the density. The idea of the algorithm is to first discover the points with higher density, and then connect the points with similar densities according to a certain minimum threshold specified by the standard that the objects contained in the neighborhood of a given radius cannot be less, and gradually connect them together, and then generate various [11] clusters. The principle of one of the algorithm implementations is as shown in Figure 5.

As can be seen in Figure 5, the circle above the blue color represents the base cluster and its radius represents the neighborhood radius of the density μ. In this algorithm, first of all, for each data object as the center of the circle, draw a circle with the neighborhood as the radius; if a circle has as many points in it, then this number is the density value of that point. Then a suitable density threshold minpts is selected and the density threshold is used as the reference; if the points within the circle are higher than the density threshold, they are classified as high-density points; conversely, if they are lower than the density threshold, they are treated as low-density points. If two or more high-density points are both in the same circle, the two points are connected with two-way arrows. If there are low-density points within a circle with high-density points, they are also connected, eventually forming a cluster. As shown in the figure, blue points indicate high-density points, red points indicate boundary points, and anomalous points do not appear in this cluster. All the blue and yellow points are connected together to form a cluster.

Based on the above analysis, it is clear that the DBSCAN algorithm has the following characteristics:

(1) The division of cluster classes is based on the parameter μ and the cluster density threshold M value, and both the parameters are considered to be set

(2) It is sensitive to the selection of initial values, but insensitive to noise points and has certain noise immunity

(3) It is not necessary to set the number of clusters in advance

(4) The clustering effect is poor for data with uneven density, and it is only applicable to the aggregation of more concentrated data or samples

The last is the analysis of the division-based clustering analysis algorithm. Delineation clustering analysis is the

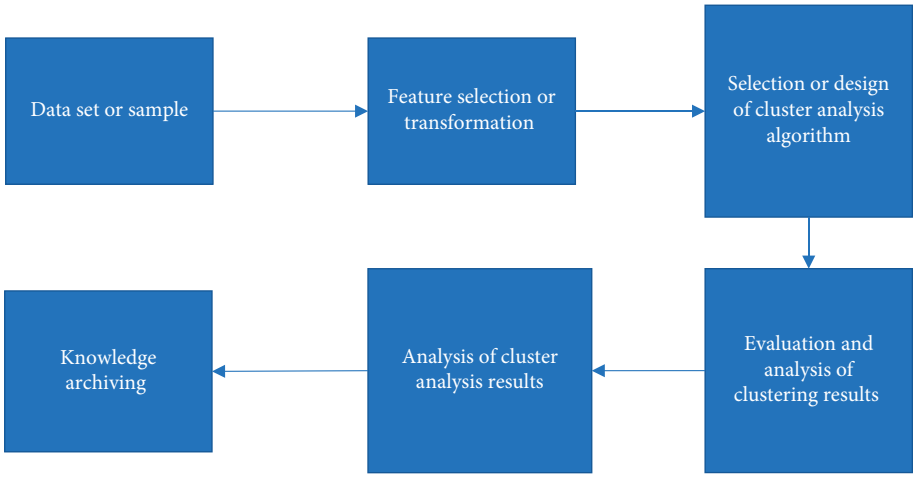

Figure 3: The process of cluster analysis.

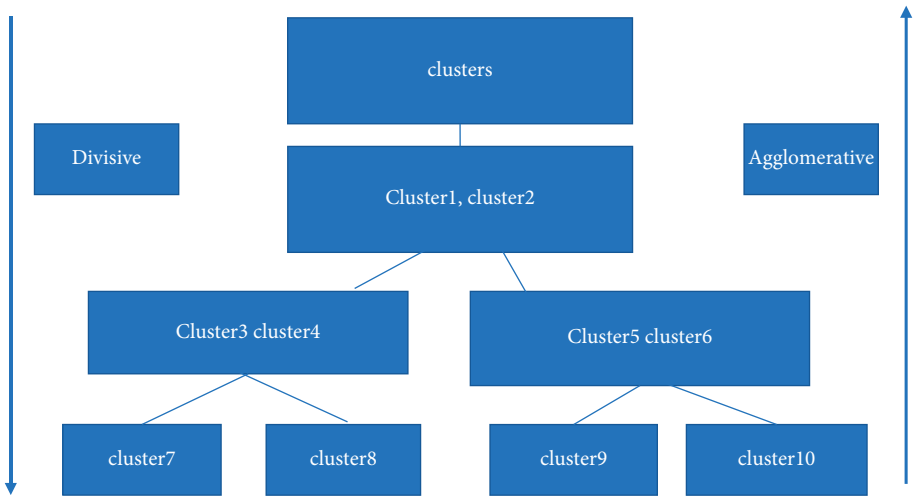

Figure 4: Comparison of agglomerative hierarchical cluster analysis and divisive hierarchical cluster analysis algorithms.

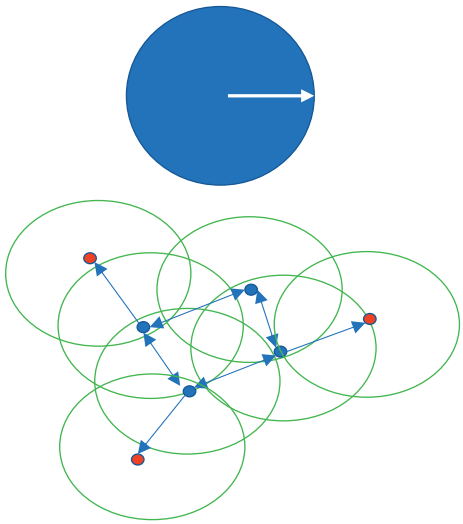

Figure 5: The basic principle of the DBSCAN algorithm.

most common and basic clustering algorithm. The basic idea of delineation clustering is to divide a dataset or sample that needs to be divided or aggregated into k [12] clusters. In the partitioned clustering analysis algorithm, the k value, i.e., the number of cluster centers or clusters, is specified in advance, and then the data or samples are initially clustered, and after repeated iterations, the final goal of "the points within the cluster are close enough and the points between the cluster and the cluster are far enough" is achieved. The clustering result is obtained when the goal of "the points within the cluster are close enough and the points between the cluster and the cluster are far enough" is reached, i.e., the optimal solution state is reached or the clustering can no longer be performed. The common divisional clustering analysis algorithms include k-means clustering algorithm, its variant k-means++ clustering algorithm, as well as bi-kmeans clustering algorithm and kernel k-means clustering algorithm. The next section focuses on the most classical k-means clustering algorithm.

3.2. k-Means Clustering Analysis Algorithm. Among the clustering analysis algorithms, the main research is mainly in distance-based clustering analysis. The typical representative of this kind of cluster analysis is the k-means algorithm. The k-means clustering analysis algorithm is a dynamic clustering algorithm, in which the initial value of k is given, and the samples or datasets to be measured are divided into k classes, and then the distance from the sample to the center of the cluster is the smallest or shortest sum of squares for the purpose of classifying the samples or datasets. In the k-means clustering algorithm, firstly, k is used as a parameter criterion as the size of the number of clusters to divide n data objects or samples into k clusters, such that the data objects or samples or points within a cluster have a high similarity (which can also be called the shortest distance) and a high dissimilarity between clusters (which can also be called a long distance beyond the set distance threshold).

The process of the classical k-means cluster analysis algorithm is as shown in Figure 6.

As can be seen from Figure 6, for the classical k-means cluster analysis algorithm, the first step is to determine the number of categories and the center of mass after preprocessing the data, and then to divide and label the clusters by calculating the Euclidean distance of the data objects or cluster centers, in which the data points are assigned to the nearest clusters; after this step is completed, the iterative process is entered, and the mean value of each cluster is recalculated for each of the previously divided cluster. After this step, the iterative process is carried out, and the mean value of each cluster is recalculated and used as the center of mass, i.e., the center of clusters. The above process is repeated for all data objects or samples until all clusters can no longer be divided, and the final result of cluster analysis is obtained.

In summary, the k-means cluster analysis algorithm has the following characteristics:

(1) Need to consider setting the k-value

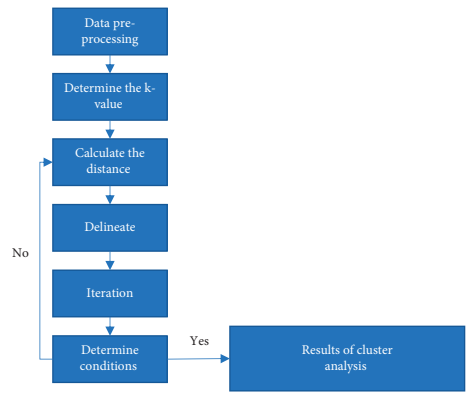

Figure 6: Classical k-means clustering analysis algorithm flow.

(2) Dependent on and sensitive to the initial center of mass (clustering center)

(3) It is more sensitive to abnormal data or samples

4. Intelligent Tourism Route Planning Scheme Design

4.1. Algorithm of Smart Tourism Route Planning. After the analysis in Section 3, three classification methods of cluster analysis algorithms are commonly used, which are density-based cluster analysis algorithm, division-based cluster analysis algorithm, and hierarchical cluster analysis algorithm. There are advantages and disadvantages in each of these three algorithms.

For the density-based cluster analysis algorithm, its advantage is that it can cluster dense datasets of any shape, but unlike the k-means cluster analysis algorithm, the density cluster analysis algorithm is not sensitive to the outliers in the dataset, and it also has the ability to find outliers while clustering. If the density of the dataset or sample is not uniform or the density of clusters between clusters differs greatly, it will lead to poorer clustering results; more importantly, for the case of a large number of datasets or sample sets, the density clustering analysis algorithm clustering process takes longer and the convergence time is slower; the adjustment parameters are mainly for the neighborhood density threshold minpts and the distance threshold μ joint. This is more complicated than the traditional k-means clustering algorithm, and different combinations of parameters have a greater impact on the final clustering results.

For the hierarchical cluster analysis algorithm, its advantage is that the definition of the prescribed similarity is easier, the selection of the distance is not difficult, and there is no need to develop the k-value and the number of clusters in advance; due to the nature of the algorithm, it itself can also discover the hierarchical relationship of the classes and the diversity of the shapes of the clusters; however, compared to the k-means cluster analysis algorithm, the complexity of the calculation is too high, and it also generates singular values, which has a great impact on the quality of the clustering. However, compared to the k-means clustering analysis algorithm, the computational complexity is

too high, and it also generates singular values, which has a great impact on the quality of clustering results, and the shape of the clusters is likely to be clustered into chains.

Therefore, through the above analysis, for the optimal route selection problem in tourism route planning, compared with the other two types of cluster analysis algorithms, the k-means cluster analysis algorithm has the advantages of simplicity, easy to understand and implement, and low time complexity, but the traditional k-means algorithm has the sensitivity to the initial value and some excessive outliers will bring great influence to the clustering results; thus, this paper decided to improve the k-means cluster analysis algorithm, and the improved cluster analysis algorithm is used to make the optimal planning of the tourist routes in a city, and to propose the design of an intelligent tourist route planning scheme.

4.2. Scheme Design and Result Analysis. For the traditional k-means cluster analysis algorithm, its biggest drawback lies in determining the k-value in advance, i.e., k points have to be selected as the center of the initial clustering beforehand, and then the clustering center can be updated iteratively on this [9]basis. Therefore, the traditional k-means clustering analysis algorithm is very dependent on the initial value, and once the initial value is not properly selected, it will lead to poor quality of the final clustering results. Therefore, in order to solve the problem that the traditional k-means clustering analysis algorithm is very dependent on the initial value, this paper proposes to find the expected value of all points of the data volume or sample after data preprocessing, and then select the largest and smallest points as the two clustering centers according to the Euclidean distance between the expected value and the points, i.e., class k and class $k-1$; then, repeat the above process until the clustering is completed as shown in Figure 7.

For the planning of smart tourism routes, this paper first constructs a dataset of m classes representing the IDs of m attractions in a city, where each ID has its own attributes, followed by finding the expected value for all the distances of the m attractions, and then calculating the Euclidean distance between the attractions according to the calculated expected value, selecting the maximum and minimum values of the Euclidean distance as k classes and $k-1$ classes; at the same time, adding the tourists' preference metric, it is then divided and iterated, and the above process is repeated continuously, in addition to averaging between satisfying tourists' preferences and distances; routes below the average will be directly excluded, forming the optimal tourist routes in turn. At last, the results of this clustering analysis are judged by the sum of the distances between the traditional k-means clustering and the improved k-means clustering analysis algorithms of this paper as shown in Figure 8.

Figure 8 shows that the sum of distances is used as the criterion for judging the clustering results, followed by the horizontal coordinate indicating the number of clusters and the vertical coordinate indicating the sum of distances, where the smaller the sum of distances, the better the clustering results. From the results in Figure 8, it can be seen

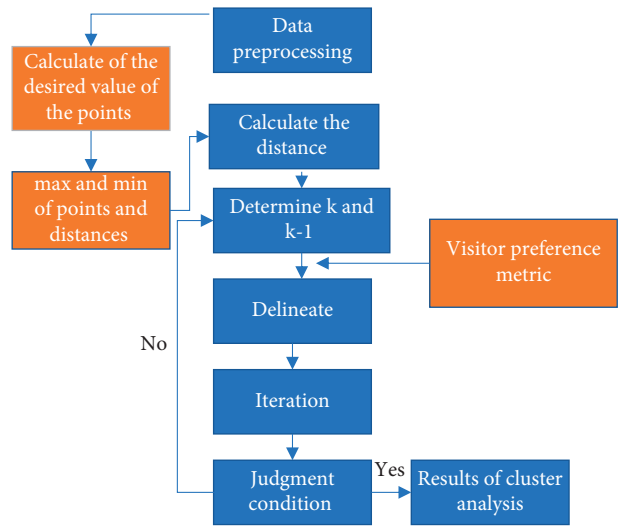

Figure 7: Improved k-means clustering analysis algorithm flow.

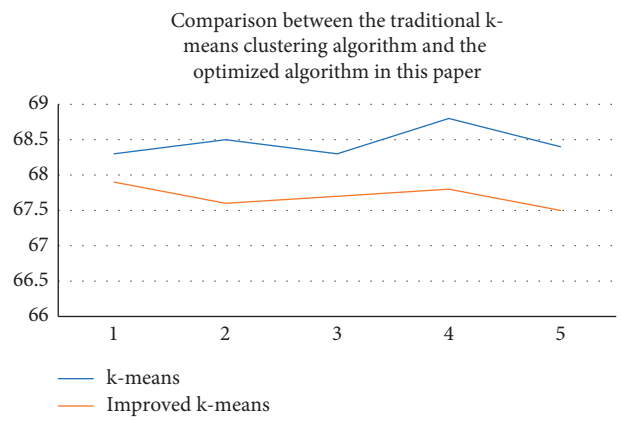

Figure 8: Comparison of the traditional k-means clustering analysis algorithm and the improved algorithm in this paper for the optimization of smart tourism road route planning.

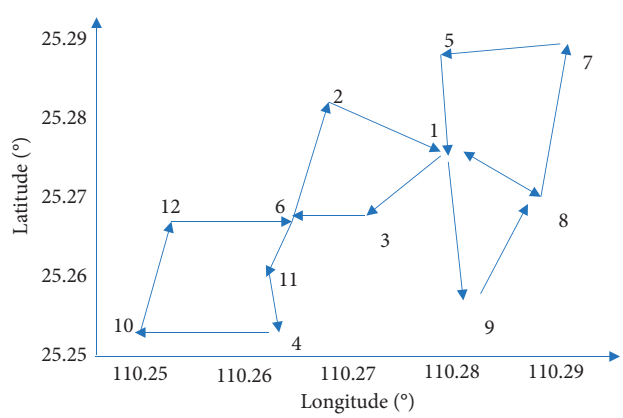

Figure 9: Intelligent tourism route planning results based on the improved k-means cluster analysis.

that the improved k-means algorithm is significantly better than the traditional k-means clustering algorithm in terms of clustering results. Finally, after adding the tourist preference

metric as a reference factor, the smart tourism route planning based on cluster analysis for a city in this paper is as shown in Figure 9.

From the experimental results in Figure 9, it can be seen that the intelligent tourism route planning for a city based on the improved k-means cluster analysis algorithm is reasonable, and the system fully takes into account the interest measure of tourists' preferences, which has a reference value for both tourism agencies and tourists.

5. Conclusion

This paper analyzed the development of the tourism industry in today's epidemic state, the problems and current situation of tourism route planning, and designed a smart tourism route planning scheme based on the cluster analysis algorithm in order to improve the rationality and achieve optimization of tourism route planning; in order to solve the problem of high dependence of the traditional k-means cluster analysis algorithm on the initial value, the improvement of the algorithm was proposed. In order to solve the problem of high dependence of the traditional k-means clustering analysis algorithm on initial values, the algorithm is improved and successfully applied to the route planning of a tourist city while introducing the tourist favorite interest metric, and the experiment verifies that the scheme achieves good results.

However, there are still some shortcomings in the design of the scheme, such as an optimal intelligent tourism route planning scheme should be complete, with strong coverage and meet the individual needs of tourists in various aspects such as clothing, food, accommodation, and transportation; this paper only aims at optimizing the route with the shortest route and considering tourists' preferences, which has some reference value, but more considerations can be added in the subsequent research to make the optimal tourism route/scheme. This paper only aims at optimizing the routes with the shortest routes and considering tourists' preferences.

Data Availability

The dataset can be accessed upon request to the author.

Conflicts of Interest

The author declares no conflicts of interest.

Acknowledgments

This work received funding from Research on the Development Path of Rural Cultural Tourism Integration in Dabie Mountain Area of Henan Province under the Strategy of Rural Revitalization (SKL—2021-1008).

References

[1] G. C. Hays, N. Atchison-Balmond, G. Cerritelli, J. O. Laloë, P. Luschi, and J. A Mortimer, "Travel routes to remote ocean targets reveal the map sense resolution for a marine migrant," *Journal of The Royal Society Interface*, vol. 19, no. 190, Article ID 20210859, 2022.

[2] H. Huang, W. Yulu, and C. Han, "Travel Route Safety Estimation Based on Conflict simulation[J]," *Accident Analysis and Prevention*, vol. 171, 2022.

[3] S. He and F. Liu, "Research on Tourism Route Recommendation Strategy Based on Convolutional Neural Network and Collaborative Filtering Algorithm," *Security and Communication Networks*, vol. 2022, Article ID 4659567, 9 pages, 2022.

[4] S. Manisha and S. Sahoo Shwetasaibal, "Puri-konark tourist circuit of odisha: coastal tourism hotspots, calamities, and resurgence," *Electrochemical Society Transactions*, vol. 107, no. 1, 2022.

[5] Q. Tang and S. Zhong, "A personalized travel route recommendation model using deep learning in scenic spots intelligent service robots," *Journal of Robotics*, vol. 2022, Article ID 3851506, 8 pages, 2022.

[6] H. Xiao and X. Ning, "Scenic tourist route planning algorithm based on mobile computing and grey entropy decision model," *Wireless Communications and Mobile Computing*, vol. 2022, Article ID 4030565, 10 pages, 2022.

[7] S. Zhu, "Multi-objective route planning problem for cycle-tourists," *Transportation Letters*, vol. 14, no. 3, pp. 298–306, 2022.

[8] J. Wang, X. Wu, and X. Ning, "Personalized original eco-tourism route recommendation based on ant colony algorithm," *Wireless Communications and Mobile Computing*, vol. 2022, Article ID 6783567, 1–9 pages, 2022.

[9] X. Zhou, J. Tian, and M. Su, "Tour-route-recommendation algorithm based on the improved AGNES spatial clustering and space-time deduction model," *ISPRS International Journal of Geo-Information*, vol. 11, no. 2, p. 118, 2022.

[10] D. M. Hoelscher, L. A Ganzar, D Salvo et al., "Effects of large-scale municipal safe routes to school infrastructure on student active travel and physical activity: design, methods, and baseline data of the safe travel environment evaluation in Texas schools (STREETS) natural experiment," *International Journal of Environmental Research and Public Health*, vol. 19, no. 3, p. 1810, 2022.

[11] W. Matthe, "Mapping the margins: national borders, transnational networks and images of coherence in interwar Italy and yugoslavia," *Contemporary European History*, vol. 31, no. 1, 2022.

[12] Z. Li, J. Cai, and M. Hu, "Design of tourism route guidance platform based on 3D visualization," *World Scientific Research Journal*, vol. 8, no. 2, 2022.

[13] X. Huang and S. Zhong, "Personalized travel route recommendation model of intelligent service robot using deep learning in big data environment," *Journal of Robotics*, vol. 2022, Article ID 7778592, 8 pages, 2022.

[14] Y. Wang, Y. Wu, and Z. Li, "Route Planning for Active Travel Considering Air Pollution exposure," *Transportation Research Part D*, vol. 103, 2022.

[15] E. Tenenboim, N. Munichor, and S. Shiftan, "Justifying Toll Payment with Biased Travel Time Estimates: Behavioral Findings and Route Choice modeling," *Transportation*, vol. 2020, 2022.

[16] B. Karolina and K. RogulaKozłowska, "Properties of particulate matter in the air of the wieliczka salt mine and related health benefits for tourists," *International Journal of Environmental Research and Public Health*, vol. 19, no. 2, 2022.

[17] E. Lee, E Hak, and K. Kim, "Exploring for route preferences of subway passengers using smart card and train log data," *Journal of Advanced Transportation*, vol. 2022, 2022.

[18] A. Palandri, "The Irish adaptation of marco polo's travels: mapping the route to Ireland," *Ériu*, vol. 69, no. 1, pp. 127–154, 2019.
[19] McP. Cameron, "Pytheas of MASSALIA'S route of travel[j]," *Phoenix*, vol. 68, no. 3, 2022.
[20] X. Zhang, L. Lauber, H. Liu, J. Shi, and M. Y. Xie, "Travel time prediction of urban public transportation based on detection of single routes," *PLoS One*, vol. 17, no. 1, Article ID e0262535, 2022.
[21] G. Zhou, F. Kurauchi, S. Ito, and R. Du, "Identifying golden routes in tourist areas based on AMP collectors," *Asian Transport Studies*, vol. 8, Article ID 100052, 2022.
[22] C. Li and W. Shao, "Design of information push system for global tourist routes in eco-scenic spots based on GIS," *International Journal of Information Technology and Management*, vol. 21, no. 1, p. 46, 2022.
[23] M. Ding and N. Balakrishnan, "Research on tourism route planning based on artificial intelligence technology," *Wireless Communications and Mobile Computing*, vol. 2021, Article ID 2227798, 1–7 pages, 2021.
[24] Y. Zhang, Z. Tang, and G. Sun, "Cross-modal travel route recommendation algorithm based on internet of things awareness," *Journal of Sensors*, vol. 2021, Article ID 5981385, 1–11 pages, 2021.
[25] M. Smith Christopher, L. Ranjit, and S. Robert, "Calculating real-world travel routes instead of straight-line distance in the community response to out-of-hospital cardiac arrest," *Resuscitation plus*, vol. 8, 2021.
[26] S. H. Cho and S. Y. Kho, "Heterogeneous Route Choice Model Incorporating Group Segmentation Based on Travel Experience," *KSCE Journal of Civil Engineering*, vol. 16, 2021.
[27] V. Vasey Thomas, J. Carroll Suzanne, and M. Daniel, "Estimating children's active school travel behaviour using the ROute observation for travelling to school (ROOTS) instrument," *Journal of Transport & Health*, vol. 23, 2021.
[28] S. de Oliveira e, A. Rodrigo, and G. Cui, "Personalized Route Recommendation through Historical Travel Behavior analysis," *GeoInformatica*, vol. 2021, 2021.
[29] Z. Wang, Y. Yu, F. Cecilia, and H. Hu, "A route optimization model based on building semantics, human factors, and user constraints to enable personalized travel in complex public facilities," *Automation in Construction*, vol. 133, Article ID 103984, 2022.
[30] Y. Liu, Y. Ji, and F. Tao, "A route analysis of metro-bikeshare users using smart card data," *Travel Behaviour and Society*, vol. 26, 2022.

Hindawi
Computational Intelligence and Neuroscience
Volume 2022, Article ID 3174530, 5 pages
https://doi.org/10.1155/2022/3174530

Research Article

5G Traffic Prediction Based on Deep Learning

Zihang Gao

Department of Information and Technology, Wenzhou Vocational College of Science and Technology, Wenzhou 325006, China

Correspondence should be addressed to Zihang Gao; gaozihang@wzvcst.edu.cn

Received 30 May 2022; Accepted 14 June 2022; Published 24 June 2022

Academic Editor: Yang Gu

The demand of wireless access users is increasing explosively. The 5G network traffic is increasing exponentially and showing a trend of diversity and heterogeneity, which makes network traffic forecasting face many challenges. By studying the actual performance of the 5G network, this paper makes an accurate prediction of the 5G network and builds a smoothed long short-term memory (SLSTM) traffic prediction model. The model updates the number of layers and hidden units according to the prediction accuracy adaptive mechanism. At the same time, in order to reduce the randomness of the 5G traffic sequence, the output feature sequence of the original time series is stabilized by the seasonal time difference method. In the experiments, the prediction results of the proposed algorithm are compared with those of the traditional algorithms. The results show that the SLSTM algorithm can effectively improve the accuracy of 5G traffic prediction. The model can be used for 5G traffic prediction for decision-making.

1. Introduction

With the rapid deployment and development of the Internet of Things (IoT), the 4G network is facing the challenge of nearly a thousand times the mobile traffic and has gradually been unable to meet the demand for massive access to the IoT. The 5G technology is developed and used to meet the explosion of mobile communication needs. The new technology revolution of rapid growth has vigorously promoted the digitization, networking, and intelligence of the economy and society [1–4]. The 5G network has the advantages of ultra-high speed, ultra-reliability, and ultra-short delay. It can be accessed anytime and anywhere, which meets the resource requirements of massive terminal access. However, it is accompanied by exponential growth of network traffic, diversity, and heterogeneity. In order to solve the huge traffic load caused by massive heterogeneous data on traditional cellular networks, 5G operators deploy a large number of low-power micro-base stations and pico-base stations on the periphery of macro-base stations to offload traffic and achieve load balancing for macro-base stations. At the same time, in order to optimize the deployment and allocation of 5G cellular network resources in large-scale cities and improve the intelligence and reliability of traffic management, it is crucial to predict traffic with high accuracy. 5G network traffic is essentially time-series data, so its prediction problem can be transformed into a time-series prediction modeling problem. Existing research mainly focuses on two categories of methods: parametric and nonparametric model methods [5–7]. The former methods mainly model and predict traffic flow based on mathematical theoretical knowledge such as statistics and probability distribution. This type of method models traffic flow through finite parameters and does not depend on the size of the dataset. Reference [8] analyzed the network traffic of many cellular base stations and distinguished the traffic into two parts, i.e., predictable and unpredictable ones, which proves that the predictable traffic has autocorrelation. Reference [9] proposed a seasonal SARIMA model, which accurately captured the seasonal characteristics of network traffic by analyzing the autocorrelation of time series, and then obtained long-term traffic forecast results. In order to verify whether the traffic of the cellular base station is affected by the number of base stations in the surrounding area, reference [10] proposed a model to predict network traffic from the perspective of time and space. The experimental results showed that the prediction accuracy of this model is significantly improved compared with the previous linear frameworks. As cellular

networks expanded in width and depth, the network traffic characteristics have long deviates from the linear prediction models described above. Although nonlinear prediction models such as the generalized multifractal wavelet model and the autoregressive conditional heteroscedasticity model can describe the nonlinear characteristics of flow [11–14], their parameter estimation and model fitting have the problem of low accuracy. In recent years, with the help of the rapid development of big data collection technology and artificial intelligence technology, deep learning has gradually become a popular direction of nonparametric prediction models and has been favored by more researchers. Early shallow learning methods such as the support vector regression (SVR) model can better solve the learning problem of small sample traffic data, but cannot rely on comparative experiments or exhaustive search to obtain model parameters of large sample traffic data, which seriously affects learning ability and generalization ability [15–17]. On the other hand, the shallow learning methods are easy to capture the temporal correlation of network traffic, but not easy to capture the spatial characteristics. The multilayer architecture makes the 5G network traffic depend on heterogeneity in the spatiotemporal dimension, and it is necessary to capture the spatiotemporal dimension features at the same time to improve the traffic prediction performance. Therefore, how to accurately predict large-scale and high-complexity 5G network traffic with the powerful learning ability of deep learning has become one of the urgent problems for operators to efficiently supervise cellular networks and improve user service quality [18–22]. Based on the convolutional neural network (CNN), literature [18] designed the XGBoost model for traffic prediction, and the experiments proved that CNN can effectively extract the spatial features of traffic. Reference [19] combined CNN and the long short-term memory network (LSTM) to form a Conv-LSTM module, which effectively reduced the prediction error by extracting the spatiotemporal correlation of traffic. Reference [20] predicted network traffic based on a hybrid deep learning model of LSTM and stacked autoencoder (SAE). For 5G traffic flow prediction methods mentioned above, more complex models are used to improve the accuracy of prediction. And the prediction effect is rarely improved by processing eigenvalues. Therefore, for the adaptive ability of 5G traffic prediction, this paper uses the method of data autocorrelation analysis to preprocess the data sequence and proposes a 5G traffic prediction model based on smooth LSTM (SLSTM). The proposed method uses the relevant data to conduct experiments and analysis. By comparing and analyzing a large number of experimental results with some existing algorithms [9–19], it is found that the proposed model has the advantages of small calculation amount and good real-time performance in 5G traffic prediction. The higher tolerance can not only effectively improve the prediction accuracy but also be simpler and more efficient than other algorithms. The model updates the number of layers and hidden units according to the prediction accuracy adaptive mechanism. At the same time, in order to reduce the randomness of the 5G traffic sequence, the output feature sequence of the original time series is stabilized by the seasonal time difference method. In the experiments, the prediction results of the proposed algorithm are compared with those of the traditional algorithm. The results show that the SLSTM algorithm can effectively improve the accuracy of 5G traffic prediction.

2. Method Description

2.1. LSTM. The LSTM network is an improvement of the recurrent neural networks (RNN) algorithm [19–21]. A cell is added to the original algorithm to increase the long-term memory function, so that the information is no longer attenuated, so as to overcome the problem of gradient disappearance in the RNN network. In the LSTM network, the added cells are usually composed of three threshold structures of forget gate, input gate, and output gate and a state vector transmission line. Among them, the state vector transmission line is responsible for long-term memory and the three thresholds are responsible for the selection of short-term memory. The forget gate determines how to retain the historical information of the memory module at the current moment. The input gate determines the transmission of input layer information to the hidden layer memory module. The output gate determines the memory and output of module information. When the information enters the LSTM network, it is judged whether it is useful or not according to the set rules, and the information that is judged to be useful is left. The rest of the information is forgotten through the forget gate. The schematic diagram of the LSTM network model is shown in Figure 1, in which the rectangular box represents the neural network layer and the circular box represents the point-by-point operation.

The forward propagation process of information in the network is described as follows:

Step 1: the forget gate is updated. The information that is allowed to pass through the cell is selected by the sigmoid neural layer. The input values h_{t-1} and x_t are input to the sigmoid function, and output a vector f_t with a value of 0~1, indicating the proportion of each part of the information passing, where 1 means all information is passed and 0 means all information is discarded. The functional relationship between the output vector f_t and the input value h_{t-1} and x_t is as follows:

$$f_t = \sigma\left(W_f \cdot \left[h_{t-1}, x_t\right] + b_f\right), \tag{1}$$

where W_f and b_f represent the weight and bias of the forget gate, respectively, and σ represents the sigmoid function.

Step 2: the cell status value is updated. This process decides what information needs to be updated and replaces the initial state value with an alternative value generated by the tanh layer.

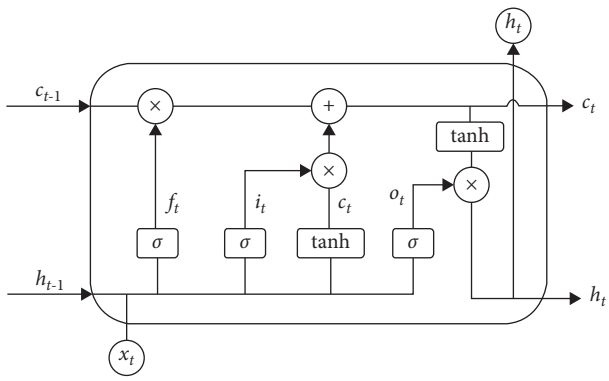

Figure 1: Basic structure of LSTM.

The intermediate vectors i_t and $\widetilde{C}_t$ are related with the input vector h_{t-1} and x_t, which are described as follows:

$$\begin{aligned} i_t &= \sigma\left(W_i \cdot \left[h_{t-1}, x_t\right] + b_i\right), \\ \widetilde{C}_t &= \tanh\left(W_C \cdot \left[h_{t-1}, x_t\right] + b_C\right). \end{aligned} \tag{2}$$

Then, the state C_{t-1} to state C_t are updated, that is, multiplying C_{t-1} by the proportion of the information passed f_t, and then discard the information according to proportion. Among them, the update equation of the state C_t is as follows:

$$C_t = f_t \cdot C_{t-1} + i_t \cdot \widetilde{C}_t. \tag{3}$$

Step 3: the output value is determined. First, the part of information to output through the sigmoid layer is determined. Then, the state vector through the tanh layer is processed, and it is multiplied with the output weight of the sigmoid layer to get the final result. The intermediate vector O_t, input vector h_{t-1} and x_t, and output value h_t are related as follows:

$$\begin{aligned} O_t &= \sigma\left(W_o \cdot \left[h_{t-1}, x_t\right] + b_O\right). \\ h_t &= O_t \times \tanh C_t, \end{aligned} \tag{4}$$

where W_o and b_O are the weight and bias of the output gate, respectively.

The LSTM network also includes a backpropagation process, starting from the current time t, calculating the error term at each time, and propagating it to the upper layer. The gradient of each weight is calculated according to the corresponding error term, and the parameters are iteratively updated by gradient descent.

2.2. SLSTM for 5G Traffic Prediction. Since 5G traffic has the characteristics of dynamic change with time, LSTM is suitable for the analysis and prediction of 5G traffic data. The 5G traffic data time series is a random time series, which usually shows nonstationary characteristics. Therefore, it is necessary to evaluate the stationarity of the original 5G traffic observation series. Here, auto correlation function (ACF) is used to obtain the estimated value.

$$\mathrm{ACF} = \frac{\sum_{t=k+1}^{n}\left[\left(X_t - \overline{X}\right)\left(X_{t-k} - \overline{X}\right)\right]}{\sum_{t=1}^{n}\left(X_t - \overline{X}\right)^2}. \tag{5}$$

The ACF chart of the estimated value is drawn to judge the state of the time series and confirm the period. When the autocorrelation function value exceeds the 95% confidence interval and there is an obvious tailing effect, the series can be judged as a nonstationary series. Otherwise, the series is a stable sequence.

When the 5G traffic sequence is a nonstationary sequence, its periodic difference $\nabla^T X_t$ can be calculated based on the original traffic sequence to obtain a stationary difference sequence $\{\nabla^T X_t, t = 1, 2, 3, \ldots\}$. Here, the stationary difference sequence is used as the output field of the sample set to reconstruct the sample set. The SLSTM is used to predict the result, and restore the result to the original 5G traffic.

Figure 2 shows the general flow of the SLSTM algorithm implementation. It can be seen that the algorithm is divided into two processes: forward propagation and backward propagation. The forward propagation is mainly the calculation of the training results of the input training samples, and the backward propagation is the reverse update of network weights and biases. The SLSTM algorithm implemented in this paper adds a data stabilization process before the forward propagation process on the basis of the above process and adds a data sequence restoration process after outputting the prediction results.

3. Experiment and Analysis

3.1. Dataset and Preprocessing. The dataset used in this experiment is from a foreign network operator. The dataset is generated in two modes: static and in-vehicle in the 5G network environment. Large bandwidth is considered to be one of the remarkable characteristics of 5G networks. This paper uses traffic bandwidth data as an indicator to measure the performance of 5G networks. The traffic downlink bandwidth data generated by file download in a static environment is used as the input data, and the CNN, gate recurrent unit (GRU), and LSTM models are selected for comparison with the model in this paper. First, the training data is preprocessed. The original dataset is multiple small files, and the data collected every 5 days during the experimental period is integrated. Then, some useless data is removed, and some data that is not in the downloading state is given up, that is, the data whose download bandwidth is 0 (this part of invalid data is considered to be interference caused by the device or the environment). Finally, the 5G network bandwidth traffic characteristics of the dataset are analyzed. The input characteristics of bandwidth prediction are determined. The bandwidth data and time data are normalized to between (0, 1), which are used as the input of the method in this paper.

3.2. Evaluation Index. In order to better evaluate and analyze the prediction results of the network model, the root mean square error (RMSE), mean absolute error (MAE), and

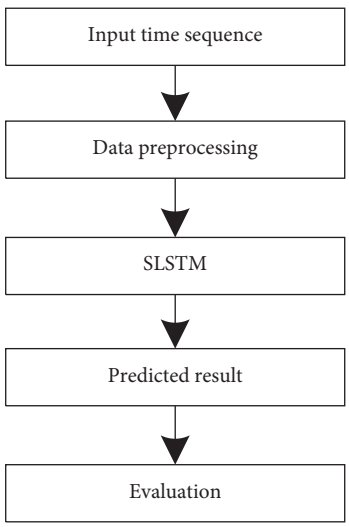

Figure 2: Prediction of 5G traffic based on SLSTM.

R-squared are used as evaluation indicators. The mathematical expressions of the evaluation formula are shown in formulas (6)–(8). The RMSE can more accurately reflect the degree of dispersion of the training model. When the value of RMSE is smaller, it indicates that the degree of aggregation of the model is higher, and the model is more accurate.

$$\mathrm{RMSE} = \sqrt{\frac{1}{n}\sum_{i=1}^{n}\left(f_i - y_i\right)^2}. \tag{6}$$

The MAE is to take the difference between the predicted result of the experiment and the actual result. And the absolute value is first used, and then the mean value is calculated. When the value of MAE is smaller, the error of the model is smaller.

$$\mathrm{MAE} = \frac{1}{n}\sum_{i=1}^{n}\left|f_i - y_i\right|. \tag{7}$$

R-squared is considered by scholars to be one of the best methods to measure linear regression. R-squared mainly converts the prediction results into the accuracy before the range of 0 to 1, which can more intuitively show the accuracy of a model. When the fit of the model is very ideal, its value will be wirelessly close to 1.

$$R^2 = 1 - \frac{\sum_{i=1}^{n}\left(y_i - f_i\right)^2}{\sum_{i=1}^{n}\left(y_i - \overline{y}\right)^2}. \tag{8}$$

3.3. Result and Discussion. For the training dataset, the LSTM, GRU, CNN, and SLSTM model proposed in this paper are used for experiments. The experimental results are shown in Table 1. The experimental results show that the training results of LSTM and GRU are close, and the difference of R-squared is only one percentage point. Compared with the method in this paper, the three types of comparison methods have gaps in performance under the three evaluation indicators. In particular, comparing the LSTM method with the improved model in this paper, the performance improvement of the method in this paper is more obvious, and the R-squared index is improved by 4%. These results prove the effectiveness of the proposed method.

Table 1: Comparison of prediction performance of different methods.

	RMSE	MAE	R-squared
Proposed	3014.2	287.3	0.83
CNN	3054.3	289.6	0.81
GRU	3096.1	295.1	0.79
LSTM	3102.5	296.8	0.78

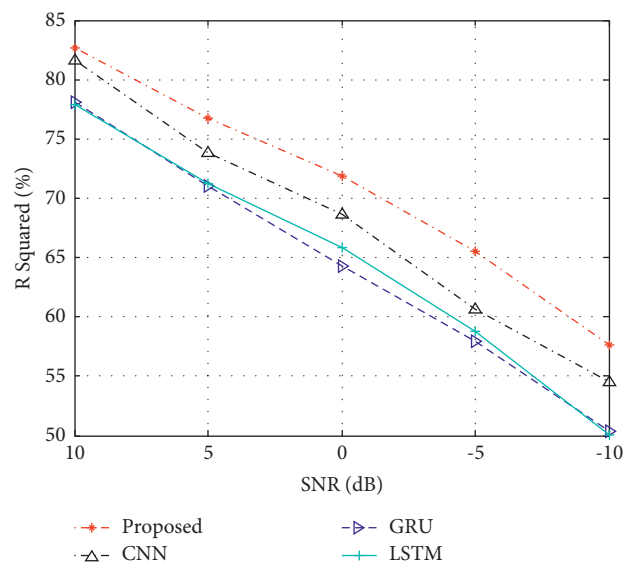

Figure 3: Prediction performance under noise corruption.

In the actual process, due to the influence of signal transmission factors, certain errors may occur in the prediction model. To this end, the experimental data is subjected to a certain degree of noise condition to reflect the volatility of flow data. On this basis, R-squared is used as the basic evaluation index to test the prediction performance trend of various methods, and the results are shown in Figure 3. It can be seen from the figure that the performance of various methods is degraded to a certain extent due to the influence of noise. In contrast, the method in this paper can maintain a more robust performance under different noise interference conditions, showing its advantages.

4. Conclusion

In the complex environment of 5G networks, high-precision traffic prediction is of great significance to the planning and scheduling of network resources and is conducive to reliable and efficient transmission of network data. In this paper, a 5G traffic prediction model based on the SLSTM is established, and the data sequence is preprocessed by the method

of data autocorrelation analysis to further improve the reliability of the model. Analysis and verification of real data show that the model can effectively predict 5G traffic. Comparing the method proposed in this paper with several existing 5G traffic prediction methods, the results show that the model in this paper has higher fitting degree, smaller error, and more accurate prediction and has certain advantages. However, there is still room for improvement in this model. For example, the factors affecting 5G traffic are not considered comprehensively. In the follow-up research, it is necessary to consider related 5G traffic factors in multiple dimensions, so as to better adapt to the actual situation of 5G use.

Data Availability

The dataset can be accessed upon request.

Conflicts of Interest

The authors declare that they have no conflicts of interest.

Acknowledgments

The authors acknowledge the Basic Scientific Research Project of Wenzhou (Grant: G2020021) and the Key Laboratory (Engineering Center) Construction Project of Wenzhou (Grant: ZD202003).

References

[1] A. Ghosh, A. Maeder, M. Baker, and D. Chandramouli, "5G evolution: a view on 5G cellular technology beyond 3GPP release 15," *IEEE Access*, vol. 7, no. 99, pp. 127639–127651, 2019.

[2] Q. Liang, T. S. Durrani, J. Liang, and X. Wang, "Enabling technologies for 5G mobile systems," *Mobile Information Systems*, vol. 2016, Article ID 1945783, 2 pages, 2016.

[3] D. Raca, J. Quinlan, and D Leahy, "Beyond throughput, the next generation: a 5G dataset with channel and context metrics," in *Proceedings of the ACM Multimedia Systems Conference (MMSys '20) ACM*, At: Istanbul, Turkey, 2020.

[4] G. Soos, D. Ficzere, and P. Varga, "Towards traffic identification and modeling for 5G application use-cases," *Electronics*, vol. 9, no. 4, p. 640, 2020.

[5] P. Chakraborty, M. Corici, and T. Magedanz, "A comparative study for Time Series Forecasting within software 5G networks," in *Proceedings of the 2020 14th International Conference on Signal Processing and Communication Systems (ICSPCS)*, 2020.

[6] S. Irina, S. Irina, and M. Anastasiya, "Forecasting 5G network multimedia traffic characteristics," in *Proceedings of the 2020 IEEE 15th International Conference on Advanced Trends in Radioelectronics, Telecommunications and Computer Engineering (TCSET)*, 2020.

[7] F. Xu, Y. Lin, J. Huang et al., "Big data driven mobile traffic understanding and forecasting: a time series approach," *IEEE Transactions on Services Computing*, vol. 9, no. 5, pp. 796–805, 2016.

[8] H. Kusdarwati and S. Handoyo, "System for prediction of non stationary time series based on the wavelet radial bases function neural network model," *International Journal of Electrical and Computer Engineering*, vol. 8, no. 4, pp. 2327–2337, 2018.

[9] R. Li, Z. Zhao, J. Zheng, C. Mei, Y. Cai, and H. Zhang, "The learning and prediction of application-level traffic data in cellular networks," *IEEE Transactions on Wireless Communications*, vol. 16, no. 6, pp. 3899–3912, 2017.

[10] L. Yang, X. Gu, and H. Shi, "A noval satellite network traffic prediction method based on GCN-GRU," in *Proceedings of the 2020 International Conference on Wireless Communications and Signal Processing (WCSP)*, 2020.

[11] Y. Lee, H. Jeon, and K. Sohn, "Predicting short-term traffic speed using a deep neural network to accommodate citywide spatio-temporal correlations," *IEEE Transactions on Intelligent Transportation Systems*, vol. 22, no. 3, pp. 1–14, 2020.

[12] C. M. Vong, I Weng-Fai, W Pak-kin, and Y Jing-yi, "Short-term prediction of air pollution in Macau using support vector machines," *Journal of Control Science and Engineering*, vol. 2012, Article ID 518032, 2 pages, 2012.

[13] Y. Liu, H. Zheng, X. Feng, and Z. Chen, "Short-term traffic flow prediction with Conv-LSTM," in *Proceedings of the 2017 9th International Conference on Wireless Communications and Signal Processing (WCSP)*, 2017.

[14] W. Jing, T Jian, X Zhiyuan et al., "Spatiotemporal modeling and prediction in cellular networks: a big data enabled deep learning approach," in *Proceedings of the 2017 - IEEE Conference on Computer Communications IEEE*, IEEE INFOCOM, Atlanta, GA, USA, 2017.

[15] P. Hewage, A. Behera, and M. Trovati, "Temporal convolutional neural (TCN) network for an effective weather forecasting using time-series data from the local weather station," *Soft Computing*, vol. 24, p. 21, 2020.

[16] T. Aldhyani, A Melfi, A Ahmed Abdullah, Y. A Mohammed, and M. B Alwi, "Intelligent hybrid model to enhance time series models for predicting network traffic," *IEEE Access*, vol. 8, p. 1, 2020.

[17] S. Guo, L Youfang, L Shijie, C Zhaoming, and W Huaiyu, "Deep spatial-temporal 3D convolutional neural networks for traffic data forecasting," *IEEE Transactions on Intelligent Transportation Systems*, vol. 20, no. 10, pp. 1–14, 2019.

[18] S. Sun and C. Zhang, "The selective random subspace predictor for traffic flow forecasting," *IEEE Transactions on Intelligent Transportation Systems*, vol. 8, no. 2, pp. 367–373, 2007.

[19] T Tchrakian, B Biswajit, and O. M Margaret, "Real-time traffic flow forecasting using spectral analysis," *Intelligent Transportation Systems IEEE Transactions on System*, vol. 15, 2012.

[20] Q. Ye, W. Y. Szeto, and S. C. Wong, "Short-term traffic speed forecasting based on data recorded at irregular intervals," *IEEE Transactions on Intelligent Transportation Systems*, vol. 13, no. 4, pp. 1727–1737, 2012.

[21] Ya Zhang, M. Lu, and H. Li, "Urban traffic flow forecast based on FastGCRNN," *Journal of Advanced Transportation*, vol. 2020, Article ID 8859538, 9 pages, 2020.

[22] W. Lu, J. Li, Y. Li, A. Sun, and J. Wang, "A CNN-LSTM-Based model to forecast stock prices," *Complexity*, vol. 2020, Article ID 6622927, 10 pages, 2020.

Hindawi
Computational Intelligence and Neuroscience
Volume 2022, Article ID 3008206, 10 pages
https://doi.org/10.1155/2022/3008206

Research Article

Research on Detection and Early Warning Mechanism of Emergency Public Health Medical Education System Based on Internet of Things Technology

Lu Fang, Caixia An, and Bin Yi

Gansu Provincial Maternity and Chlid-Care Hospital, Lanzhou 730050, China

Correspondence should be addressed to Bin Yi; hn135@wfd.edu.ug

Received 18 March 2022; Revised 25 April 2022; Accepted 18 May 2022; Published 24 June 2022

Academic Editor: Guobin Chen

Sudden public health and medical education events have tested the stability of society to a great extent. The government need to strengthen capacity building, make use of system dynamic supervision, warn public health events in advance, and minimize the impact scope and related harmfulness of events. This not only facilitates the rapid mobilization of resources by the later government but also facilitates the comprehensive and detailed deployment and arrangement of decision-makers. As we all know, the Internet of Things is used by all walks of life because of its outstanding advantages of low power consumption, low cost, and wide range. Therefore, this article takes the Internet of Things as the technical basis of the system. According to the actual demand and resource design, it includes two system functions: detection and early warning. The results show that: (1) considering the practical principle, the evaluation system interface found that the scores of font size and color style are all below 80%, which need to be optimized and adjusted; the overall interface basically meets the needs of users. (2) The throughput of the three methods is different. The CoAP-E has superior throughput. (3) With the increase in packet loss rate, the request success rate of the CoAP method decreases in a "drop" manner. The CoAP-E method in this article has the best performance. (4) When the packet loss rate is 25%, the network adaptability of this method is the strongest, and the retransmission rate is less than 18%; the CoAP method is as high as 35%. (5) When the number of concurrent requests is less than 2500, there is no obvious difference between the three methods; the optimal performance of the dynamic load balancing method is 10.1 s. (6) The system comprehensively considers various factors of five site selections. The highest comprehensive score of Final Site, 5 is 8.7, which can be used as the resettlement place of emergency rescue facilities. This article starts from the characteristics and needs of public emergencies, and the final set of the system runs well. It can quickly reflect public health emergencies and medical education events. Use the most effective system functions for risk control, and maximize the analysis, organization, and coordination of events. The follow-up optimization of system details needs to be studied.

1. Introduction

It is necessary and important to study public health care and educational events in emergencies. This process involves many rules, procedures, and methods. There are many basic theories to study this aspect, but the design and implementation of specific systems need to be comprehensively analyzed and integrated. The existing detection and early warning processing system in China have not yet defined the specific responsibilities, the functions are not perfect, and there are many detections and early warning problems. For example, the current systematic detection of public health emergencies and medical education in China is slow and complicated. In addition, the current system does not use new computer technology, the structure is old and the operation is backward, and it usually consumes a lot of funds and human resources, so it cannot respond to the demand quickly and timely. As for the early warning mechanism, first, the boundaries of authority are unclear, the responsibilities are vague, and there is no specific detail of the division problem. Second, the system's early warning mechanism design is unreasonable and unscientific, which

cannot perfectly coordinate the conflict between public and personal interests. The reserve of professional knowledge talents for early warning is insufficient, the early warning mechanism lacks corresponding laws and regulations, and there are problems with the system and mechanism. The system is assisted by GIS, load balancing, big data, and other technologies. The system designed in this article can properly reflect the situation of interest protection and power coordination when people and government encounter unexpected situations. The following documents can provide a valuable reference for the construction of emergency detection and early warning system designed in this article.

According to the need for emergency communication support in typical scenarios, an emergency communication system is constructed [1]. According to the existing emergency support communication system, a 5G + air-space integrated emergency support system is proposed [2]. In view of the application of high-speed rail, we should further improve the transportation support level of emergency materials and study the emergency support system for public health emergencies [3]. Focusing on the logistics support work carried out by emergency command organizations and executive agencies, this article studies the emergency support system of agency affairs [4]. This article systematically analyzes the emergency guarantee system of public health safety of urban water system and puts forward emergency capability, technical requirements, overall emergency strategy, and "5 + 3" emergency plan [5]. Based on the INSARAG system, a general module of emergency rescue drug support was established [6] to strengthen the construction and management of the emergency system [7]; improve the construction of emergency plans and explore the construction mode of emergency support mode of clinical medical engineering in medical rescue [8]; discuss the management level and quality of emergency materials logistics support [9]; construct and evaluate the emergency management system of general wards during novel coronavirus pneumonia [10]; and improve the strategic function of the human information system and discuss the role of hospitals in preventing and treating public health emergencies [11]. In view of public health emergencies, this article takes the epidemic situation in novel coronavirus in 2019 as an example to [12] support the emergency response mechanism of the public health safety system with "big data + grid" [13] and establish a remote intelligent prevention and control diagnosis platform based on artificial intelligence under sudden epidemic situations [14]. From the global emergencies, aiming at the oral medical and public health system, we should make differentiated protection and emergency plans at different levels [15]. To sum up, we learn from each other's strengths and selectively select valuable and advantageous research results as the theoretical basis of this article. This can effectively help us understand the problem from the essence.

2. Theoretical Basis

2.1. Internet of Things Technology. IoT [16], one of its important infrastructures is sensors. The agreed transmission protocol mainly completes the communication between people and things and effectively manages and monitors the connection between goods and people. Therefore, it is closely related to cloud computing, big data, communication, embedded hardware, and other technologies. It has more application prospects in many fields such as smart cities, artificial intelligence, and home medicine, serving human society and bringing excellent experience effects to users.

IoT is called the Internet of Things technology, which means "everything is connected to each other into a network (Internet)." Through the sensor, a large amount of data collection can be carried out effectively. This technology shows the advantages of low power consumption, low cost, wide-coverage, and a large number of connections. The most commonly used system architecture on the Internet of Things technology is the transmission system based on NB-IoT. Our platform unifies the data of all devices that can be connected to the Internet of Things.

The technical architecture represented by it combines terminal equipment, NB-IoT controller, and sensor settings into a community. It is transmitted to the base station by COAP/UDP protocol, and the operator reports the data collected by the sensor to the IoT platform, that is, the Internet of Things platform. At the same time, the platform can also use the HTTP protocol to take the enterprise server as a third-party application system, and open the interface, which is convenient for relevant professionals to manage enterprise equipment. The service performance transmitted by this architecture is extremely superior (Figure 1).

2.2. Public Health Emergencies

2.2.1. Demarcation of Event Boundaries. Emergencies [17] generally refer to sudden events in our ordinary daily life. Such events are often unexpected or unexpected. From a specific point of view, emergencies usually refer to public emergencies. Up to now, there is no clear, official, and unified definition of public emergencies. But we collect many experts and scholars of the more representative explanations and made a certain summary. We can analyze and compare the characteristics of several events, to have a deeper understanding of the boundaries of public emergencies (Table 1).

2.2.2. Public Health Emergencies. There are various public emergencies in the world, especially in health, medical treatment, and education, such as biological, chemical, major infectious diseases, campus gun battles, and other events that belong to the division scope of this event. Because of its sudden occurrence, people are caught off guard. It is easy to cause or likely to cause widespread panic. When such an incident occurs, it is important for various departments and organizations to take various measures to deal with it as quickly as possible in the shortest reflection time to minimize the loss of personnel and property to a certain extent. Specific event classification and grading are shown in Table 2.

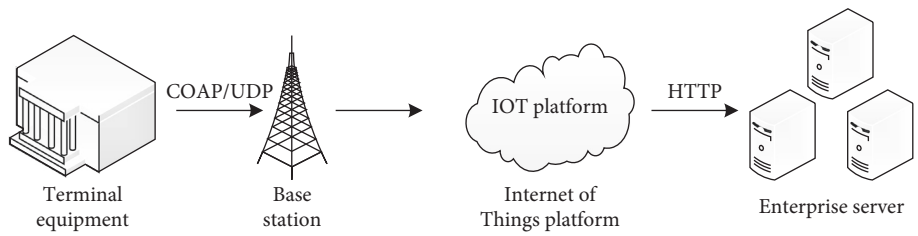

Figure 1: Internet of things transmission architecture.

Table 1: Definition of event characteristics.

Type	Characteristics of an event	Notes and remarks
Public emergencies [18]	The characteristic of being sudden, usually occurring in an explosive manner on a large scale	An emergency may be a public emergency. But it may not be included relationships [19].
An emergency	A more urgent event. Usually, the time for processing is very tight	
Hazardous events [20]	Such incidents have usually produced dangerous and serious consequences	The biggest difference between the two types of events is that crisis is a hazard that has not yet happened. It is potential, but it shows serious consequences.
Crisis event	This is a serious state and there is a potential danger	
Disaster event	Events usually caused by natural factors, which are very destructive	Disaster events can be regarded as a higher level escalation of disaster events, with higher severity and greater destructiveness. Catastrophic events may happen suddenly, but they may also be expected.
Catastrophic events [21]	Destructive, serious	

Table 2: Classification and grading of events.

Classification of events	Classification of events
A major epidemic of infectious diseases	Particularly important events are set to level I
Group diseases of unknown origin [22]	Major events are set to level II
Major food and occupational poisoning	Larger events are set to level III
Other events seriously affecting public health	General events are set to level IV

2.3. Facility Location. After the occurrence of public emergencies, to solve the problem most quickly, we need to choose the best address as the dispatching center according to the central position of the event to meet the needs of various job transfers. The aim is to shorten the distance from the event center under the condition of meeting the decision conditions. For traditional site selection, there is continuous and discrete site selection.

2.3.1. Continuous Site Selection

$$(x, x) \in R * R, \tag{1}$$

$$\min(x, y) \sum_{i \in I} w_i d_i(x, y), \tag{2}$$

$$(x, y)\sqrt{(x - a_i)^2 + (y - b_i)^2}. \tag{3}$$

2.3.2. Discrete Site Selection

$$\overline{x} = \frac{x_1 f_1 + x_2 f_2 + x_3 f_3 + \ldots x_k f_k}{k}. \tag{4}$$

Among them, a_i and b_i refer to each demand point; $w_i d_i(x, y)$ represents the weighted distance from the event center; w_i indicates that the weight corresponding to the demand point is small; i refers to the standard set.

The model established in this article is as follows:

$$\text{Min } L, \tag{5}$$

$$ST:$$

$$\sum_{j \in I} x_j \le P, \tag{6}$$

$$\sum_{j \in I} z_{ij} p_{jk} = Q_i \forall i \in I, \tag{7}$$

$$z_{ij} \le x_i \forall i \in I, j \in J, \tag{8}$$

$$L \ge \frac{\sum_{j \in J} \beta_{ik} e_{ik} M_i \mathrm{d}_{ij} z_{ij}}{Q_i} \forall i \in I, k \in K, \tag{9}$$

$$x_j, z_{ij} = \{0, 1\} \forall i \in I, j \in J. \tag{10}$$

If we need two emergency facilities, then we need to modify two functions, as shown:

$$MinL_1 + L_2, \tag{11}$$

$$L_r \geq \frac{\sum_{j\in J} \beta_{ik} e_{ik} M_i \mathrm{d}_{ij} z_{ij}}{Q_i^r} \forall i \in I, k \in K, r = 1, 2. \tag{12}$$

Using a genetic algorithm to solve the model,

(1) Coding scheme

$$Z\colon z_1 z_2 \ldots z_j. \tag{13}$$

(2) Initialization [23]: all facilities must meet the conditions, and the algebraic times at this time $t = 0$:

$$\sum_{j\in J} x_j \leq P. \tag{14}$$

(3) Fitness function: convert the target value to obtain the individual fitness value:

$$F(i) = \frac{1}{f(i)}. \tag{15}$$

(4) Select the operation: until the set special termination conditions are reached, the solution of the model is ended.

$$p_i = \frac{F(i)}{\sum_N F(i)}, \tag{16}$$

$$\sum_{i=1}^{i=N} p_i < u_i \leq \sum_{i=1}^{i=N+1} p_i, \tag{17}$$

where $i = 1, 2, \ldots, N$; j denotes the j-th alternative address; J is the number of selected facilities; z_j is 0 to indicate that it is not selected; and Q_i^2 is 1 to indicate that it is selected. A indicates that the demand point is serviced by 2 implementation points. The model in this article has P capacity constraints. $I * J$ is the nonnegative constraints; $I * J * K$ is the requirement constraints; and L represents the sum of the distances from the facility to the grid demand point.

2.4. GIS Technology. The GIS auxiliary system carries on the facility location work. It can accurately find the emergency location in urgent need of support and make a series of planning and decision according to the route.

GIS [24], geoscience information system, is a kind of spatial information system that collects, manages, and describes the natural geographic location data. It integrates visual effects and geographical analysis functions of maps, and also adds database operation. In recent years, with the development of various computer technologies, data analysis is becoming more and simpler. With the support of computer technology, it is very important for many applications. It is widely used for smart city construction, transportation system construction, Internet of Things technology, edge computing, and other technologies. Taking ArcGIS as an example, it has a wide range and rich functional modules, and can easily obtain diversified data analysis. Spatial analysis of vector data is shown in Figure 2.

Buffers can be defined as

$$P = \{x | d(x, A) \leq r\}. \tag{18}$$

The radius of curvature of Maoxi circle:

$$N = \frac{a}{\sqrt{1 - e^2 \sin^2 B}}. \tag{19}$$

2.5. Load Balancing

2.5.1. Load Information Collection. CPU information: calculate the utilization rate of the CPU and record the information activity time of each CPU.

$$\mathrm{CPU_{use}} = \frac{(\mathrm{total2} - \mathrm{total1}) - (\mathrm{idle2} - \mathrm{idle1})}{\mathrm{total2} - \mathrm{total1}} \times 100\%. \tag{20}$$

Load information [25]:

$$\mathrm{MEM_{available}} = (\mathrm{Meml_{free}} + \mathrm{Buffers} + \mathrm{cached}), \tag{21}$$

$$\mathrm{MEM_{use}} = \frac{\mathrm{MEM_{total}} - \mathrm{MEM_{available}}}{\mathrm{MEM_{total}}} \times 100\%. \tag{22}$$

2.5.2. Load Information Processing. Specific gravity coefficient of CPU of i th server node:

$$C_a = \frac{C_i}{\sum_{i=1}^{n} C_i}. \tag{23}$$

Specific gravity coefficient of memory:

$$M_a = \frac{M_i}{\sum_{i=1}^{n} M_i}. \tag{24}$$

Specific gravity coefficient of disk I/O:

$$D_a = \frac{D_i}{\sum_{i=1}^{n} D_i}. \tag{25}$$

Specific gravity coefficient of network bandwidth:

$$W_a = \frac{W_i}{\sum_{i=1}^{n} W_i}. \tag{26}$$

Finally, the initial weight value of the server node can be obtained from this formula

$$\mathrm{weight_{init}} = K_c \times C_a + K_m \times M_a + K_d \times D_a + K_w \times W_a. \tag{27}$$

2.5.3. Weight Modification. Average response time of cluster system to process network requests:

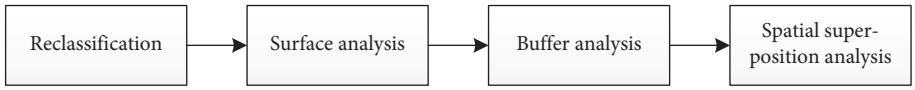

Figure 2: Spatial analysis diagram.

$$T_{\text{avg}} = \frac{\sum_{i=1}^{n} T_i}{n}. \tag{28}$$

Variance of cluster system:

$$D_t = \sum_{i=1}^{n} \frac{\left(T_i - T_{avg}\right)^2}{n}. \tag{29}$$

3. Public Health Medical Education System

3.1. Design Principle. The design of this system can effectively manage all kinds of resources and information related to public health education. Our goal is to turn the system into an efficient, convenient, and easy to operate practical tool. While monitoring and detecting public emergencies, effective intervention is carried out through an early warning mechanism. It provides a reliable basis for the decision-making of the government and leaders.

(1) Advanced and scalable: on the premise of meeting all functions, consider the update iteration problem and ensure the continuous innovation of data storage and management, which requires scalable. Maintain the advanced technology for a long time in the future and hope to keep pace with the times and ensure the upgradability of software.

(2) Practicality: always remember that the ultimate goal of the system is to serve people's needs. According to the specific actual needs, strive to achieve the humanized design. It should not only be simple and easy to operate, but also have a simple and beautiful interface. Whether it is a system upgrade or daily maintenance, it should not be too difficult, but easy to get started.

(3) Security: the information and data in the system are confidential and cannot be leaked. Therefore, there should be perfect data backup, authority management, automatic recording of access, monitoring, and other security measures.

(4) Openness: support a variety of hardware devices; adopt a standard interface; ensure that the system designed in this article can exchange and share data with other systems; and support secondary development and utilization.

(5) Overall situation and integrity: our system is special and applied to emergency handling. Therefore, we must consider the architecture design of the system and the functional design of various modules from a global, multi-faceted, and multi-angle perspective. Ensure that the design is not repeated, the functions are not messy, and there is no unnecessary intersection. This concept can better help us to design the system.

3.2. Functional Requirements. According to the actual situation, the functions of our system are as follows:

(1) emergency preparedness and construction of emergency resource database

(2) improve the early warning mechanism

(3) monitoring and testing public health education and medical emergencies

(4) emergency treatment and professional services

(5) termination and evaluation function

(6) construct a data warehouse and manage all kinds of information

(7) comprehensive inquiry platform

(8) statistical analysis of public knowledge base, case base, database, document report, and other documents as a certain reference

(9) site selection of emergency rescue facilities.

Four subsystems are planned to be designed as follows:

(1) mobile emergency system

(2) Internet of Things peripheral device system

(3) GIS monitoring system

(4) Public opinion monitoring system

3.3. System Design. Generally speaking, the emergency management system has five functional modules. Their respective system functions and responsibilities are different. Among them, command and dispatch are the highest decision-making function and the "total" processing brain is the system. The command system is the most basic and important setting in the whole system construction. It can effectively guarantee normal function. The other four functions are subfunctions, which belong to the support system. They all listen to the deployment of the "brain." Several functions coordinate and support each other (Figure 3).

3.4. Architecture Design. The architectural design of the whole system is divided into three parts. The first part is the data layer. The second part is the application of the support layer; rely on the WEB application server in this layer, including J2EE, SDE spatial data engine, and ArcIMS. The third part is the application layer, the practical application of nine functions and four subsystems is realized (Figure 4).

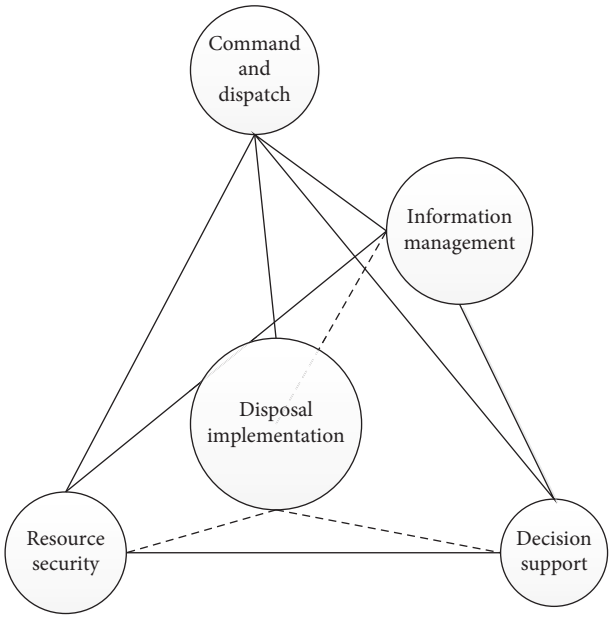

Figure 3: Emergency management diagram.

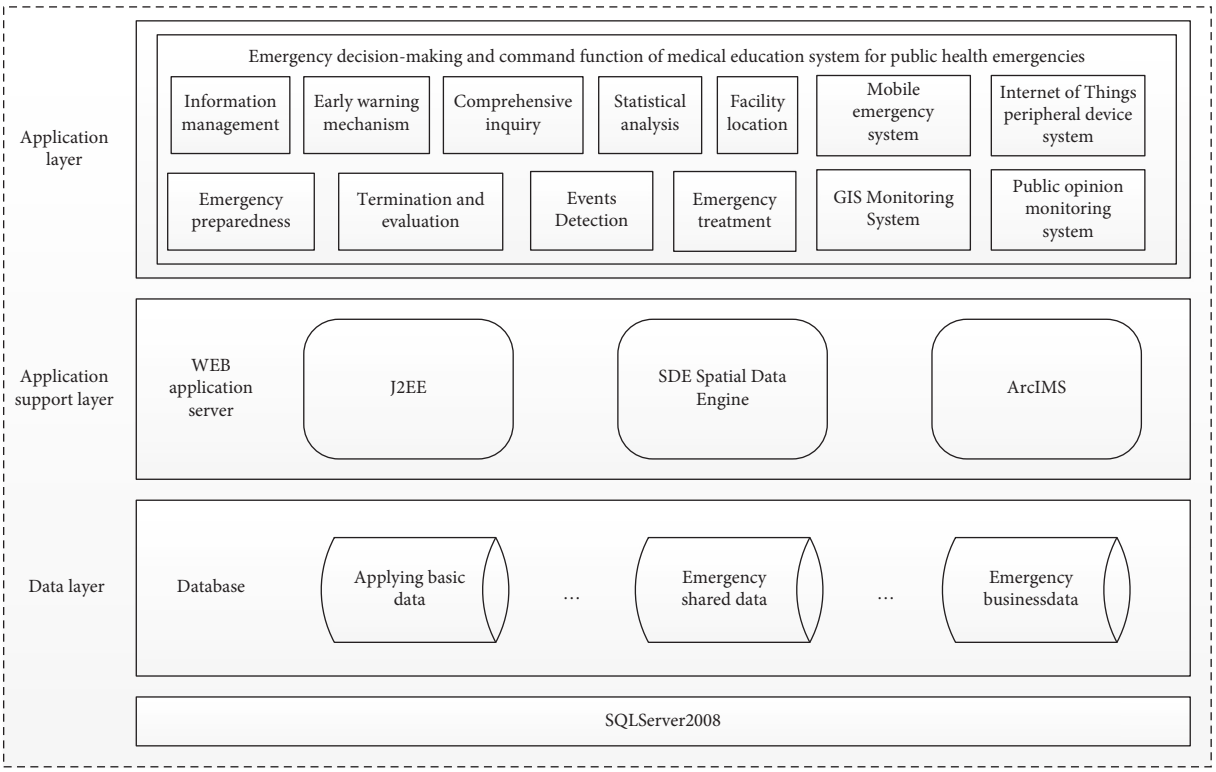

Figure 4: System logical architecture diagram.

4. Experimental Analysis

4.1. Development Environment. In this section, we will explain the software and hardware development of the system used in some of the platforms and other related equipment (Table 3).

4.2. System Test. Among the evaluation criteria of a system, the solution to the problem of increasing concurrent visits is undoubtedly a great test for the carrying capacity of the system. Once the system is enabled, if our system cannot often face the pressure of a large number of concurrent requests in a short time and the background server cannot

Table 3: Development environment of the system.

Environment	Name	Specific equipment
Software environment	System software	Microsoft Windows 2000/XP
	Database (DBMS)	IBM DB2
	Application server	IBM WebSphere
Hardware environment	Database server	The main frequency requires a dual CPU with the main frequency above 2.0 GHz; memory requirements of more than 1 GB; the hard disk requires more than 80 GB.
	Web server	The main frequency is required to be above 2.0 GHz, and the main frequency is double CPU; memory requirements of more than 1 GB; the hard disk requires more than 60 GB.
	Map server	The main frequency requires a dual CPU with the main frequency above 2.0 GHz; memory requirements of more than 1 GB; the hard disk requires more than 40 GB; the network card requires a network adapter card above 100M; the display requires VGA or super VGA display with resolution above 1024∗768; the graphics card requires a display card with more than 64M video memory.

bear the huge access pressure, then the system will crash and cannot provide normal services. Through load balancing algorithm and practical application scenarios, the request processing performance of the system is optimized and improved to be more practical, which is more in line with the requirements of this system. To better illustrate the superiority of this method, CoAP, CoCoA, and CoAP-E (i.e., the Internet of Things method introduced in this article) are used to compare the performance and verify the specific situation of scene use under the Internet of Things technology.

4.2.1. Interface Testing. For the design of a system, we consider the principle of practicality. The user interface we initially finalized needs to be evaluated for external esthetics and internal operation friendliness. To verify the fairness and accuracy of the experiment, voluntary participants were invited and divided the number into five groups. These participants often participate in public emergency rescue and are volunteers who often need to use this system. The number of people in each group for the interface test is controlled at about 10, with a total of 50 people (Figure 5).

According to the results, we observe that everyone has different preferences for the interface and has strong personal subjectivity. To better adjust the public's preferences, the adjustment of the system mainly focuses on the test items with extreme scores. If the scores of other items are determined to be above 80% (including 80%), they will be retained and judged as qualified interfaces. Finally, the parts that need to be adjusted in the system interface test are font size and color style. On the whole, although the interface test basically meets the needs of users, there are still details to be optimized.

4.2.2. Throughput Test. This is a test point to prove the superior performance of the system. We can find that with the increasing network delay, the throughput of the three methods also decreases. When the delay is 0, the throughput of the CoAP method is much less than that of other methods. On the whole, the throughput of CoAP-E in this article is obviously superior to the other two methods, which opens a big gap (Figure 6).

4.2.3. Request Success Rate. In this section, according to the change in packet loss rate, the request success rate of the three methods is compared. This test can well reflect the reliability of data transmission. We can find that with the gradual increase of packet loss rate, the request success rate under the three methods is reduced to varying degrees. Among them, the request success rate of the CoAP method shows a "drop" decline. The CoAP-E method has the best performance, followed by the CoCoA method (Figure 7).

4.2.4. Data Retransmission Rate. Reuploading data will cause a waste of resources or excessive overhead for users and clients. Therefore, the smaller the retransmission rate, the better the equipment performance of the system. The test is carried out under the change of packet loss rate. The retransmission rate of this method cannot exceed 18% at most under the packet loss rate of 25%. Under the same packet loss rate, the CoAP method has a data retransmission rate as high as 35%. It is enough to show that the network adaptability of this method is the strongest, so the retransmission rate is the lowest (Figure 8).

4.2.5. Average Response Time. When the number of concurrent requests is less than 2500, the time increase of the three methods is slow, the difference is not big, and the performance distinction is not obvious. However, when the number of concurrent requests reaches 3500, the corresponding time of the traditional method is as high as 19.5 s, and the effect is the worst. The response time of the weighted polling method is about 15.2 s, dynamic load balancing has the best performance, and the duration is 10.1 s (Figure 9).

4.2.6. Site Selection Test. The system selects five sites to evaluate six indexes: A, B, C, D, E, and F. Take a 10-point system to score. Site 4 has the lowest comprehensive score, with a score of about 6.9 points. The scores of Site 1 and Site 2 are about 8.5 points; Site 3 scored 8.1. Only the final score

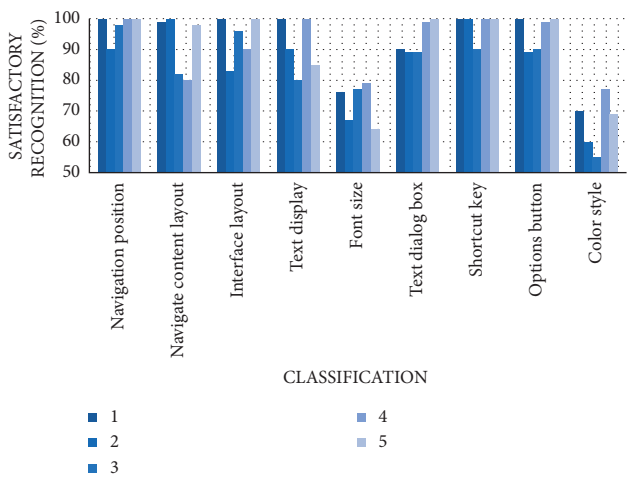

Figure 5: User interface testing.

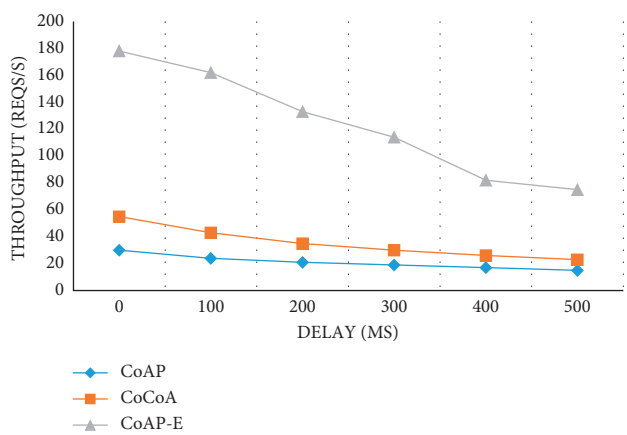

Figure 6: Throughput testing.

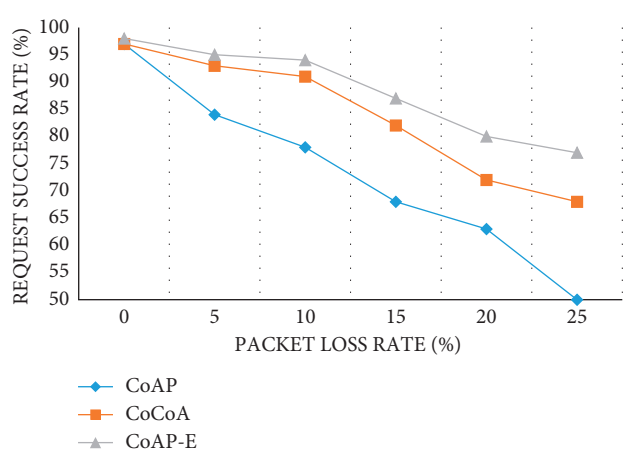

Figure 7: Request success rate.

of Site 5 is as high as 8.7 points. Considering all factors comprehensively, the fifth site should be selected as the resettlement site of emergency rescue facilities (Figure 10).

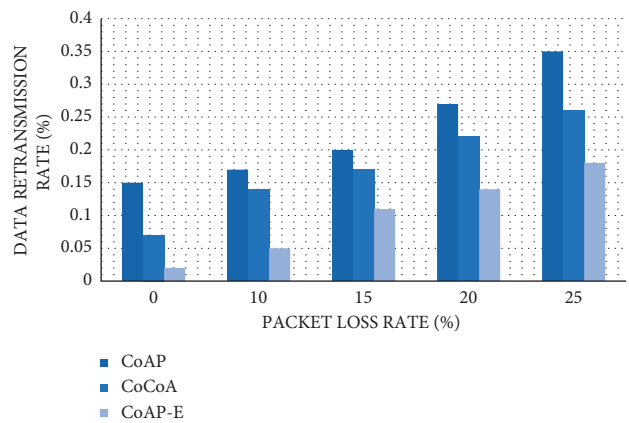

Figure 8: Data retransmission rate.

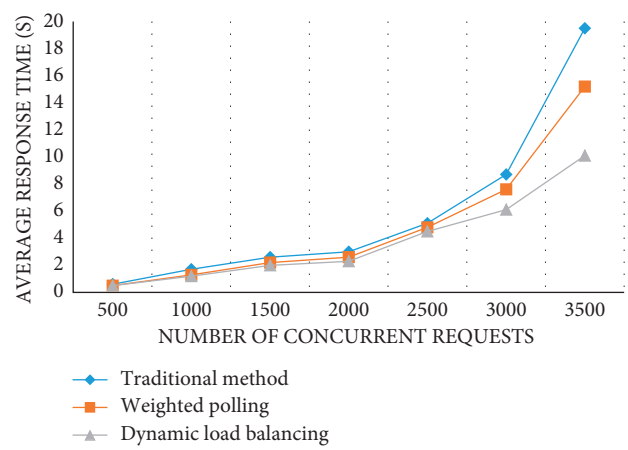

Figure 9: Average response time of the system.

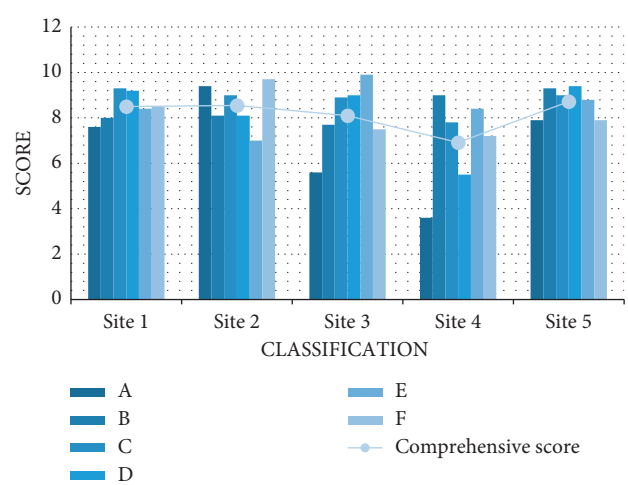

Figure 10: Location score test.

5. Conclusion

The rational application of Internet of Things technology can bring excellent performance to the basic construction of the system. According to the requirements of the system, the

functional modules are designed. Using GIS technology to quickly respond and select the address of event assistance; through load balancing technology, the concurrency optimization research of Internet of Things technology is completed. Reduce unnecessary system development expenditure and system development time as much as possible. Using computer technology to improve the processing efficiency of the system. According to the experiment and system test, the final research results of this article show that the standard system mode is used to realize the emergency detection and early warning design of public emergencies. The old architecture has been transformed, and new technologies such as the Internet of Things has been added. It mainly aims at public health emergencies and solves the problems in medical care and education. The system can accumulate and optimize the experience and methods to solve emergency incidents. The system can effectively improve the efficiency of the government and staff to deal with events, and coordinate the relevant interests of the public and the people. However, there are still many problems and deficiencies in this system, which need to be continuously optimized and improved. For example, the requirements analysis of the system should also be further excavated and studied to understand the specific relationship between problems and functions. The system needs a more humanized design, close to people's lives, and professionals only need simple training to get started. The performance optimization of the Internet of Things system needs to be tested according to the actual use to obtain more accurate and true performance. In this experiment, the selection range of some variables and parameters is narrow and the analysis is limited, and the problems with a wider range and more requirements need further study; For future research, GIS technology and Internet of Things technology should be better combined, and Internet big data should be dynamically used so that the target selection can get the optimal solution. These are the problems that must be further faced and solved in the research process.

Data Availability

The data used to support the findings of this study are available from the corresponding author upon request.

Conflicts of Interest

The authors declare that they have no conflicts of interest.

Acknowledgments

This work was supported by Gansu Provincial Maternity and Child-Care Hospital.

References

[1] S. Wang and X. Wang, "Conception of emergency communication support system construction," *Radio Engineering*, vol. 50, no. 4, p. 4, 2020.

[2] J. Zhou, J. Jia, and Z. Zhang, "Key technologies of 5G networked UAV for emergency support," *Journal of Chongqing University of Posts and Telecommunications: Natural Science Edition*, vol. 32, no. 4, p. 8, 2020.

[3] H. Ma, "Application research on incorporating high-speed railway into national emergency support system for responding to public health emergencies," *Railway Standard Design*, vol. 65, no. 5, p. 6, 2021.

[4] X. Jiang and Li Jing, "Research on emergency support system of organs affairs under major emergencies," *China Organs Logistics*, no. 5, p. 4, 2021.

[5] H. Zhang, J. Ma, and M. Li, "Construction and thinking of emergency guarantee system for public health safety of urban water system [J]," *Water Supply and Drainage*, vol. 46, no. 4, 12 pages, 2020.

[6] Y. Li, S. Liu, and W. Li, "Management and practice of international emergency rescue support drugs based on INSARAG system," *Disaster Science*, vol. 35, no. 2, 6 pages, 2020.

[7] R. Xia, "Strengthening environmental emergency management to ensure environmental safety," *China Interior Decoration World*, vol. 000, no. 009, p. 141, 2020.

[8] Z. Fan, "Discussion on the construction of emergency support mode of clinical medical engineering in medical rescue," *Electronic Journal of Clinical Medical Literature*, vol. 7, no. 26, 2 pages, 2020.

[9] X. Gong, "How to do a good job in hospital emergency materials logistics support," *Physician Online*, vol. 11, no. 33, 1 page, 2021.

[10] X. Fu, Y. Zhang, and C. Chen, "Construction of emergency management system in general wards of non-designated hospitals in novel coronavirus pneumonia," *Nursing Times*, vol. 10, no. 6, p. 6, 2021.

[11] K. Kumari, "On the strategic function of human information system in hospitals for prevention and treatment of public health emergencies [J]," *Continuing Medical Education*, vol. 35, no. 5, p. 3, 2021.

[12] Y. Chen and G. Cai, "Discussion on the education and training of medical regulators to deal with public health emergencies--Taking the epidemic situation in Novel Coronavirus in 2019 as an example," *Chinese Journal of Public Health*, vol. 37, no. 7, pp. 1011–1014, 2021.

[13] X. Zhou and H. Wu, "On the construction of public health safety system in higher vocational colleges under the new situation," *Journal of Hubei Open Vocational College*, vol. 34, no. 18, 3 pages, 2021.

[14] C. Gao, T. Yuan, and J. Cui, "Research on the design of remote intelligent prevention and control diagnosis platform for sudden epidemic," *China Medical Equipment*, vol. 35, no. 6, 4 pages, 2020.

[15] He Cai, Y. Cheng, and X. Ren, "Viewing the present situation and future development of China's oral medicine and public health system from global emergencies," *Journal of Sichuan University (Engineering Science Edition): Medical Edition*, vol. 53, no. 1, p. 6, 2022.

[16] H. Xu, "New situation of health records management in medical institutions for public health emergencies under the new situation," *Basic Medical Theory Research*, vol. 2, no. 6, pp. 51-52, 2021.

[17] K. Zeng, G. Pan, H. Nan, and C. Wu, "Discussion on emergency medical material security management in health emergencies," *China Medical Device Information*, vol. 26, no. 15, pp. 169–171, 2020.

[18] F. Tao, "Bridging the gap between public health and clinical medical education and promoting the practice of integration

of medicine and prevention," *Chinese Journal of Preventive Medicine*, vol. 54, no. 5, p. 4, 2020.

[19] H. Guo and X. Zhang, "Problems exposed by hospital information system in the process of epidemic prevention and treatment in novel coronavirus pneumonia, Wuhan and their thoughts," *Chinese Medical Education Technology*, vol. 34, no. 2, 6 pages, 2020.

[20] H. Fan, "Epidemiological characteristics of public health emergencies in Huzhu County from 2004 to 2019," *Qinghai Medical Journal*, vol. 50, no. 11, 4 pages, 2020.

[21] B. Qin, "Construction of students' psychological support system under the background of public emergencies," *Journal of Nantong Vocational University*, vol. 35, no. 2, p. 4, 2021.

[22] W. Jin and W. Pan, "Design of remote intelligent medical system based on Internet of Things technology [J]," *Microcomputer Applications*, vol. 36, no. 5, p. 4, 2020.

[23] L. Xiao, J. Liao, Y. Hong, and Z. Yan, "Design and application research of intelligent leasing system for medical equipment in hospital based on Internet of Things technology," *China Medical Equipment*, vol. 17, no. 11, pp. 120–124, 2020.

[24] C. You, Q. Gong, and Y. Huang, "Construction and practice of hospital-level medical equipment data collection and management platform based on Internet of Things technology," *China Medical Equipment*, vol. 35, no. 3, p. 4, 2020.

[25] J. Shen and P. Zhang, "Design and implementation of community medical management system based on Internet of Things," *Information and Computer*, vol. 32, no. 1, 3 pages, 2020.

Hindawi
Computational Intelligence and Neuroscience
Volume 2022, Article ID 7588303, 18 pages
https://doi.org/10.1155/2022/7588303

Research Article

An Intelligent Fusion Model with Portfolio Selection and Machine Learning for Stock Market Prediction

Dushmanta Kumar Padhi,[1] **Neelamadhab Padhy**,[1] **Akash Kumar Bhoi**,[2,3,4] **Jana Shafi**,[5] **and Seid Hassen Yesuf**[6]

[1]*School of Engineering and Technology, Department of Computer Science and Engineering, GIET University, Gunupur, India*
[2]*KIET Group of Institutions, Delhi NCR, Ghaziabad 201206, India*
[3]*Directorate of Research, Sikkim Manipal University, Gangtok 737102, Sikkim, India*
[4]*AB-Tech eResearch (ABTeR), Sambalpur, Burla 768018, India*
[5]*Department of Computer Science, College of Arts and Science, Prince Sattam Bin Abdulaziz University, Wadi Ad-Dawasir 11991, Saudi Arabia*
[6]*Department of Computer Science, College of Informatics, University of Gondar, Maraki 196, Gondar, Ethiopia*

Correspondence should be addressed to Seid Hassen Yesuf; seid.yesuf@uog.edu.et

Received 12 April 2022; Revised 17 May 2022; Accepted 26 May 2022; Published 23 June 2022

Academic Editor: Yang Gu

Developing reliable equity market models allows investors to make more informed decisions. A trading model can reduce the risks associated with investment and allow traders to choose the best-paying stocks. However, stock market analysis is complicated with batch processing techniques since stock prices are highly correlated. In recent years, advances in machine learning have given us a lot of chances to use forecasting theory and risk optimization together. The study postulates a unique two-stage framework. First, the mean-variance approach is utilized to select probable stocks (portfolio construction), thereby minimizing investment risk. Second, we present an online machine learning technique, a combination of "perceptron" and "passive-aggressive algorithm," to predict future stock price movements for the upcoming period. We have calculated the classification reports, AUC score, accuracy, and Hamming loss for the proposed framework in the real-world datasets of 20 health sector indices for four different geographical reasons for the performance evaluation. Lastly, we conduct a numerical comparison of our method's outcomes to those generated via conventional solutions by previous studies. Our aftermath reveals that learning-based ensemble strategies with portfolio selection are effective in comparison.

1. Introduction

Before the end of the twentieth century, low-frequency financial data were available for analysing and forecasting the stock market. Fewer professionals and academicians use these low-frequency data for their empirical studies, but as there are no sufficient related data available, the empirical research will not succeed [1]. Due to the rapid development of science and technology, the cost of data capture and storage has been reduced dramatically, which makes it easy to record each day's trading data related to the financial market. As a result, significant financial analysis of data has become a prominent area of research in economics and a variety of other disciplines [2].

With the recent rapid economic expansion, the quantity of financial activities has expanded, and their fluctuating trend has also become more complex. Asset prices trend forecast is a classic and fascinating issue that has piqued the interest of numerous academics from several fields. Academic and financial research subjects to understand stock market patterns and anticipate their growth and changes. Portfolio construction through competent stock selection has long been a critical endeavour for investors and fund managers. Portfolio enhancement and optimization have

emerged among the most pressing issues in modern financial studies and investment decision-making in this era [3]. Portfolio development success is highly contingent on the future performance of financial markets. Forecasts that are realistic and exact can provide substantial investment returns while mitigating risk [4]. The prevailing economic and financial theory is the efficient market hypothesis (EMH) [5]. According to this hypothesis, forecasting the valuation of capital assets is challenging. However, according to past research, equity markets and yields can be predicted [6]. Before the invention of efficient machine learning algorithms, academics generated prediction models for research using a variety of alternative and econometric approaches [7]. Traditional statistical and econometric tools require linear models and cannot anticipate or analyse financial goods until nonlinear models are turned into linear models. Many studies have proven that nonlinearities arise in financial markets and that statistical models cannot effectively control them. With the rapid rise of AI and machine learning over the last decade, an increasing number of financial professionals have begun to analyse the index value of gaugeable models, have different requirements, and experiment with diverse methodologies [8]. K-NNs [9], Bayes classifiers [10], decision trees [11], and SVMs [12] are presently widely used for classification tasks [13]. However, in practice, these solutions fail to function when data are collected over an extended period, and storage space is limited (processing data at once are impractical).

Due to the ever-growing volume of incoming data, such as stock market indices, sensor readings, and live coverage, online learning has become highly significant [14]. When it comes to online learning, a system should absorb more training data without having to retrain from the beginning. Traditional AI frameworks, such as supervised learning tasks, usually work in a batch learning mode. A training dataset is supplied beforehand to train the model to use some learning algorithm. Due to the high cost of training, this paradigm necessitates the accessibility of the full training set before the learning assignment, so the learning process is frequently conducted offline [15]. In addition to being inefficient and low in both time and space costs, batch learning approaches have the disadvantage of being unable to scale for a range of applications since models would frequently need to be retrained from scratch for new learning data. With incremental learning, a learner attempts to acquire and improve the best predictor for a model as they go along through a sequential flow of information rather than using batch classifiers. Online learning overcomes the limitations of batch learning by allowing prediction models to be updated quickly in response to current data examples. Since machine learning jobs in real-world information analytic platforms tend to involve large volumes of information arriving at high speeds, online learning techniques offer a much more flexible and effective method for handling massive data inputs. In the real world, online learning can solve problems in several different application areas, just as traditional (batch) machine learning can.

Asset prices and economic forecasts are among the most complex and challenging activities in finance. Most traders depend on technical, fundamental, and quantitative analysis for making forecasts or creating price signals. With the advent of AI in different fields, its rippling effect may also be seen in finance and price forecasting. As stock prices are updated every second, there is always a possibility of a drift in the data distribution and rendering [16]. Continual advances in computational science and data innovation are essential to the globalization of the economy [17]. While numerous methods exist for estimating the cost of financial exchange, the latter has been the focus of the investigation. We may discover many issues and constraints in coming to more critical data even though there are many methods. Because classic analytical approaches have apparent flaws in dealing with nonlinear difficulties, several machine learning algorithms are being used in stock exchange inquiries [18].

Financial backers can make sound decisions, increase productivity, and reduce possible losses using a model capable of forecasting the growth path of a stock's value. As a result, accurate forecasting and stock market research have become more complex and less favourable. We must constantly improve our deciding approaches for stock price prediction. Previously, several domestic and international researchers were dedicated to developing measurable monetary frameworks to forecast index growth. Before the advent of expert AI computations, analysts routinely used a variety of statistical approaches to create expectation models. A stock market prediction can be made with linear and nonlinear models. Most linear models are based on statistics, while most nonlinear models are based on machine learning techniques [19]. In principle, customary monetary structures and the arising automated thinking model might accomplish stock expense estimating, but the expectation sway is very astounding [20]. Observing systems with work on predicting future outcomes through model combination and inspection is advantageous for some analysts, and it also has excellent speculative value [21]. In reality, authentic data may be coordinated into monetary systems to forecast future data. For instance, assuming the stock worth check is more prominent, the model predicts that the future share price will be higher than the end-of-day price will climb. Monetary allies might choose to stay retaining the shares to obtain a higher return on investment [22]. If the asset value guesstimate is less than the day's end price, the share price will likely fall later. As a result, developing a monetary framework to recognize asset value measuring is very feasible [23]. Furthermore, if you can correctly forecast the asset price movements and price flow patterns, it has a significant incentive for governments, listed companies, and private financial backers [24].

Recently, there has been a growth in research that looks at the path or pattern of financial market changes. Presently, the examination is advancing by inspecting the interest and pattern of securities exchanges. Academics have long been interested in equity market forecasting as an appealing and challenging subject. The amount of information that is available daily continuously increases; as a result, we are confronted with new issues in handling data to extract information and estimate the impact on asset values. There is always a challenge and disagreement when determining the optimal strategy to forecast the stock market's daily return

trend. As the study aims to anticipate the future market, this study topic has a self-sabotaging behaviour that has proven to be fascinating and prevalent for stock market forecasting. Researchers can always discover industry secrets and analyse the market using their unique methods, thanks to the fast development of machine learning models, techniques, and technologies. The machine learning models can improve their prediction performance by identifying suitable feature selections. A poor feature selection reduces the model's performance and results in biased outcomes. Developing a reliable forecasting technique capable of identifying risk factors and providing favourable and unfavourable market direction is as important as appropriate feature extraction throughout the modelling procedure.

The purpose of this study was to develop an online learning framework based on machine learning that can reduce investment risk (by constructing an optimal portfolio) and make a predictive judgement regarding the direction of the selected indices. In addition, this study provides a new method for minimizing investment risk by building a framework that combines the mean-variance model for selecting stocks with minimal risk and an online learning framework for index forecasting.

This framework, in particular, has two major phases: portfolio selection and stock prediction. This study's primary contributions are summarized as follows:

(i) Compared with previous studies on portfolio development and machine learning-based forecasting strategies in general, it is always a top task to find the hidden features. So, the suggested approach has some unique combination of features generated from the raw transaction data with less effort on the human being.

(ii) The system is intended for real-world use. Therefore, we adopted a unique framework that combines the mean-variance model for portfolio development and the online learning model for financial market prediction.

(iii) Our experiment examined the performance of four different geographical reasons' health sector equities throughout volatility stress and smooth trending periods, as well as the durability of financial crises and clustering. For this objective, a large amount of data was collected over a lengthy period.

The remainder of the article can be deduced from the information provided below. Section 2 portrays the related work, Section 3 depicts the materials and techniques, and Section 4 investigates our proposed framework. Section 5 focuses on exploratory research findings and discusses the most significant discoveries made during our investigation. Last but not least, in Section 6, we discuss the conclusion section of our work and the future scope of our research.

2. Related Work

Investing proponents and professionals have long held that stock price movements are unpredictable. The phrase "efficient market hypothesis" was coined by Fama [25] and gave rise to this point of view (EMH). The nonstationary and dynamic nature of financial market data, according to Fama, makes it impossible to make predictions about the capital market [25]. According to the EMH, the market reacts immediately to new information about financial assets. As a result, it is impossible to break into the market. According to Shiller [26], the financial sector entered the 1990s when academics dominated behavioural finance. From 1989 to 2000, Shiller's [26] study found that fluctuations in the stock market were driven by investor mood. When Thaler [27] predicted that the Internet stock boom would collapse, he criticized the generally accepted EMH of accepting all financial supporters as usual and making plausible forecasts about the future.

On the other hand, behavioural finance argues that stock market movements are always based on real knowledge, according to Shiller [26]. Shiller [26] showed that short-term stock prices are unpredictable, while long-term stock market movements are predictable. Fundamental and technical variables are both important when it comes to financial market forecasting [28, 29]. The entire analysis considers how much money the company has left, how many workers there are, how the directorate makes decisions, and what the company's yearly report looks like [30]. It also takes into account things such as unnatural or catastrophic events, as well as information about politics. People look at the main things are the company's GDP, CPI, and P/E ratios [31]. Stock market forecasting can benefit from a fundamental strategy that prioritizes the long term above the immediate [32]. Specialized observers [33] use trend lines and technical indicators to forecast the securities market for specialized observers [33]. Technical analysts can make educated guesses using mathematical algorithms and previous price data [34].

Researchers now have more resources to work with as AI techniques improve and datasets become more widely available, opening up new directions for investigation. According to Marwala and Hurwitz [35], advances in AI technologies have influenced the EMH and fuelled a need to learn from the market. According to a growing corpus of studies, capital markets can be predicted to some extent, according to a growing corpus of studies [36, 37]. Consequently, investors have the chance to minimize their losses while maximizing their earnings while dealing with the stock market [38]. Recent research suggests that statistical and machine learning are two distinct approaches [39].

Statistical techniques were utilized before machine learning to analyse market trends and analyse and forecast stocks. To assess the financial market, several statistical models are employed [40–42]. Traditional statistical approaches have struggled tremendously, and machine learning approaches are beginning to develop to circumvent the drawbacks of conventional statistical methods [43]. Numerous machine learning algorithms have been used to anticipate the stock market [44–49]. Prior research has established that machine learning techniques outperform all other predicting stock market directionality [50]. Traditional models are less flexible than AI approaches [51, 52]. Several

machine learning algorithms have been investigated in the past [53, 54]. Some examples are logistic regression, SVM, K-NN, random forests, decision trees [34, 37, 40], and neural networks [37, 38]. As described in the literature, SVM and ANN are the most frequently used algorithms for stock market forecasting. A long-term financial market forecasting classification system was proposed by Milosevic et al. [55]. They say that a stock is excellent if its value improves by 10% in a fiscal year; otherwise, it is bad. Eleven fundamental ratios were recovered throughout the model-building process and are used as input features by several algorithms. They found that the random forest had an F score of 0.751 in differentiation using naive Bayes and SVM. Choudhury and Sen [56] trained a back propagation neural network and a multilayer feedforward network to forecast the stock value. A regression value of 0.996 was obtained using their proposed model.

Boonpeng and Jeatrakul [57] developed a multi-class categorization problem to determine whether a stock is a good investment. According to their findings, one-against-all neural networks beat the traditional one-against-one and classic neural network models with a 72.50% accuracy rate. According to Yang et al. [58], an effective forecasting model requires understanding the nonlinear components of stock. Multiple machine learning models for stock market direction prediction have been created, as Ballings et al. [59] noted. In addition to datasets from European businesses, they used a range of ensemble machine learning algorithms. They also used neural networks and logistic regression. Finally, using the random forest approach, they could predict the long-term fluctuations in the stock market using their dataset. According to Leung et al. [60–62], accurate forecasts of the growth of the stock worth list are essential for the creation of effective trading approaches such as financial backers that can protect against the predicted dangers of the securities exchange. Even if only a little accuracy is gained, anticipating execution is a considerable benefit. When it comes to predicting the financial markets, machine learning techniques often fall into one of two camps: predicting the stock market using solitary machine learning algorithms or employing many models. According to a number of studies, ensemble models are more accurate than solitary forecasting models. Only a few studies have looked into ensemble models [63].

Many ensemble approaches have been developed in machine learning platforms to improve predicting performance and decrease bias and variance trade-offs [64]. The most often used algorithms for machine learning-based ensemble learning include AdaBoost [65], XGBoost [66], and GBDT [67]. In Nobre and Neves [66], an XGBoost-based binary classifier is introduced. The results demonstrate that the framework may provide greater average returns. Furthermore, a stock forecasting model employing technical indicators as input features was proposed by Yun et al. [68]. According to the researchers, their XGBoost models outperformed both SVM and the ANN. Based on risk categorization, Basak et al. [25] created a methodology for forecasting whether the stock price will rise or fall. When employing random forest and XGBoost classifiers, researchers demonstrated that hybrid models perform much better with the right set of indicators as input features for a classifier. Ecer et al. [63] claim that ensemble machine learning approaches are superior to individual machine learning models in terms of performance. Multilayer perceptron, genetic algorithms, and particle swarm optimization are included in two new methods proposed by Ecer et al. [63]. A total of nine technical indicators were used to train their model and resulted in RMSEs of 0.732583 for MLP–PSO and 0.733063 for MLP–GA, respectively. According to the researchers, a combination of machine learning techniques can improve prediction accuracy.

Yang et al. [69] presented a feedforward network composed of many layers for Chinese stock market forecasting. Back propagation and Adam algorithms were used to train the model, and an ensemble was created using the bagging approach. The model's performance may be enhanced by further normalizing the dataset. Wang et al. [70] constructed a combined approach that forecasts the financial markets every week using BPNN, ARIMA, and ESM. In predicting stock market direction, they found that hybrid models beat regular individual models with an accuracy of 70.16 percent. Finally, Chenglin and colleagues [71] proposed a model for forecasting the direction of the fiscal market. According to the researchers, mixed models, which included SVM and ARIMA, outperformed standalone models. Tiwari et al. [72] proposed a hybrid model that combines the Markov model and a decision tree to forecast the BSE, India, with an accuracy of 92.1 percent. Prasad et al. [39] investigated three algorithms, XGBoost, Kalman filters, and ARIMA, as well as two datasets, the NSE and NYSE. First, they looked at how well individual algorithms could predict and how well a hybrid model they made with Kalman filters and XGBoost worked. Finally, they looked at four models and found that the ARIMA and XGBoost models did well on both datasets, but the accuracy of the Kalman filter was not consistent. Jiayu et al. [62] developed a combined LSTM and attention mechanism, called WLSTM + attention, and demonstrated that the suggested model's MSE became less than 0.05 on three independent measures. Moreover, they asserted that proper feature selection might enhance the model's forecasting accuracy.

Portfolio enhancement is the circulation of abundance among different assets, wherein two parameters, in particular, anticipated returns and risks, are vital. The ultimate goal of financial backers is usually to increase the returns and decrease the risks. Usually, as the return margin increases correspondently, the risk margin also increases. The model introduced by Markowitz [73] is popularly known as the mean-variance (MV) model, whose main objective is to solve the problems during portfolio optimization. The main parameter of this model is means and variances quantified by returns and risks, respectively, which facilitates financial supporters to strike a balance between maximizing expected return and reducing risk. After the exploration of Markowitz's mean-variance model, some researchers tried to develop a modified version of this model in different ways: (i) an optimized portfolio selection with respect to multi-period [74–76] and (ii) introducing alternate risk assessment

methods. The safety-first model [77], the mean-semi-variance model [78], the mean absolute deviation model [79], and the mean-semi-absolute deviation model [80] are all examples. (iii) Many real-world constraints, such as cardinality constraints and transaction costs, were also included in the study. [81–84]. Nonetheless, the above examinations focus harder on the improvement and extension of the mean-variance model; however, they never consider that it is essential to select high-quality assets for creating an optimal portfolio. The investment strategy process generally said that if we provide high-quality assets as input, there is a quiet assurance that we construct a reliable optimized portfolio. In the last few years, a few studies have been done to ensure that the asset selection and the portfolio determination models work together.

For an investment decision, Paiva et al. [85] develop a model. First, they use an SVM algorithm to classify assets, and then, they use the mean-variance model to make a portfolio. A hybrid model proposed by Wang et al. [86] is a combination of LSTM and Markowitz's mean-variance model for optimized model creation and asset price prediction. These investigations showed that the mix of stock forecast and portfolio determination might give another viewpoint to financial analysis. So, in our current study, we use the mean-variance model for portfolio selection and determine individual assets' contribution towards our model-building process.

Machine learning strategies have been broadly utilized for classification-related issues [13]. A couple of techniques and models are discussed in the above literature. However, instead of dealing with theoretical concepts if we deal and work with the practical environment, in the stock market the data are coming in continuously over a long duration time and the execution of current data at once each time is impossible, so these techniques are not working properly for forecasting in a real environment. As a result, online learning is becoming increasingly important in dealing with never-ending incoming data streams such as sensor data, video streaming data, and financial market indexes [14]. So, when it comes to online learning, a system should absorb extra training data without retraining from the start.

During the online learning process, the continuous data flows are coming in a sequence, and the predictive model generates a prediction level on each round of data flows. Then, according to the current data, the predictive online learning model may update the forecasting mechanism. Perceptron [87] is a basic yet effective incremental learning algorithm that has been widely researched to improve its generalization capability. Crammer et al. [88] introduced the passive-aggressive (PA) algorithm, which is faster than perceptron and sometimes shows more promise than perception. When the new sample comes in, it changes the model to ensure it does not lose too much data and that it is almost the same as the old one. The retrained model guarantees that it has a minimal loss on the current sample and is similar to the present one. A few online machine learning approaches have been developed to cope with massive streaming data. New rules may be discovered when new data arrive, while current ones may be revised or partially deleted [89]. In the training phase of traditional machine learning algorithms, each sample was considered equally valuable. However, in real-world applications, different samples should contribute to the decision boundary of participating classifiers in distinct ways [90]. Perceptron-based projection algorithm was proposed by Orabona et al. [91]; however, the number of online hypotheses is limited in this technique by projecting the data into the space encompassed by the primary online hypothesis rather than rejecting them. In ALMAp [92], the maximum margin hyperplane is estimated for a collection of linearly separable data.

Furthermore, SVMs have been updated for numerous iterative versions [93–95], which define a broad online optimization issue. For example, Laughter [96] introduced two families of image classification online developing classifiers. The created classifiers are first given training upon specific pre-labeled training data before being updated on newly recorded samples. In [97], a robust membership computation approach that works extraordinarily when confronted with noisy data was given. However, many membership generation algorithms are designed for specific data distributions or presuppose batch delivery of training samples. Because the early phases of distribution information are erroneous, transferring such approaches directly to online learning may provide additional issues. More significantly, when a fresh instance is obtained, the new decision boundary must be computed using the complete existing training set, which takes more time. As far as we know, very few articles have been written about the subject. As a result, a solid and efficient framework of incremental forecasted model based on the stock market is required for online classification. Overall, this research line has demonstrated significant promise for incremental model parameter modification and excellent understand ability of online learning systems in dynamically changing contexts. Table 1 shows the numerous research studies conducted based on batch learning techniques.

When we forecast the financial market using these methodologies, the literature mentioned above has some shortfalls, like these techniques follow the traditional batch learning techniques, which further can be improved by the help of online learning techniques. Moreover, some literature faces imbalanced classification problems when multiple indices are examined from different countries' indices. Therefore, we selected quality-based stocks using the mean-variance model instead of focusing on the randomly selected stock for the experiment. So, we have introduced a framework that can handle the situations outlined above.

3. Materials and Methods

Before discussing our framework, we have emphasized the significant methodologies and datasets that will be employed in our proposed framework. Online learning or incremental learning is a machine learning approach for sequential data in which the learner attempts to develop and demonstrate the best predictor for each new dataset. Allowing the prediction model to be modified quickly for any current data instances, online learning makes up for the weaknesses of

Table 1: Numerous research studies conducted based on batch learning techniques.

SL. No.	Authors (year)/ publisher	Dataset used	Target output	Period of forecasting	Preferred technique
1	Jiang et al. (2019) [98]	Three major US stock indices (S&P 500, Dow 30, Nasdaq)	Market direction	Short	Tree-based ensemble method + deep learning
2	Ayala et al. (2021) [99]	IBEX, DAX, and DJIA	Stock index prediction	Short span (for a particular window)	Linear regression and ANN regression model performed well among all ML models
3	Nabipour et al. (2020) [100]	Tehran Stock Exchange	Price prediction	Short term	Technical indicators + LSTM
4	Shafiq et al. (2020) [101, 102]	Chinese stock market	Index trend	Short-time period	Feature engineering-based fusion model using PCA and LSTM
5	Jothimani and Yadav (2019) [28]	Nifty Index	Asset price	Short span	CEEMDAN, ANN, SVR, EEMD, EMD
6	Zhong and Enke (2019) [44]	US SPDR S&P 500 ETF (SPY)	Daily return direction	Short term	Fusion of deep neural network and principal component analysis.
7	Ampomah et al. (2020) [50]	NYSE, Nasdaq, NSE	Daily return direction	Short term	A comparative study done using different tree-based ensemble models where extra tree performs better
8	Sun et al. (2020) [103]	Chinese stock market	Return direction of asset	Short period	AdaBoost-SVM + SMOTE
9	Yang et al. (2020) [104]	Shanghai and Shenzhen 300 Index	Market volatility forecast	Short term	SVM
10	Jiayu et al. (2020) [62]	S&P 500, DJIA, HSI	Index price	Short term	Long short memory with attention mechanism
11	Boonpeng and Jeatrakul (2016) [57]	Thailand Stock Exchange	Index price	Short term	OAA-neural network
12	Yang et al. (2019) [58]	China Stock Exchange	Market volatility	Intra-day	SVM
13	Yun et al.(2021) [68]	Apple and Yahoo	Index price	Short term	XGBoost
14	Ecer et al. (2020) [63]	Borsa Istanbul	Return direction of asset	Short term	MLP–GA, MLP–PSO
15	Wang et al. (2012) [70]	Shenzhen Integrated Index and DJIA	Index price	Weekly	BPNN, ARIMA, and ESM
16	Chenglin et al., (2020) [71]	China Stock Exchange	Trend of stock market	Short term	ARI-MA-LS-SVM
17	Tiwari et al. (2010) [72]	BSE, India	Index price	Short term	Markov model + decision tree
18	Paiva et al.(2018) [85]	IBOVESPA	Portfolio selection and stock prediction	Dailly	SVM+ mean-variance
19	Wang et al. (2020) [86]	US Stock Exchange 100 Index	Portfolio selection and stock prediction	Return per year	LSTM + mean-variance
20	Basak et al. (2018) [25]	10 Indian Stock Exchange Companies	Index price increase or decrease	Medium to long run	XGBoost + random forest

batch learning. As we all know, stock market data always come into existence sequentially and regularly. As a result, the batch learning process suffered greatly. So, we constructed two online learning algorithms for our experimental goals, which are briefly described below.

3.1. Perceptron. The perceptron algorithm is the most ancient method for online learning. The perceptron algorithm for online binary classification is described in Algorithm 1.

In general, if a specific margin can separate the data, the perceptron technique should result in a maximum of $(R/yp)^2$ errors, where the margin λ is specified as $\lambda = \min_{td\in[TD]}|xi_{td..}wg^*|$ and R is a constant such that $\forall_{td} \in [TD], xi_{td} \leq R$. The higher the margin λ, the narrower the error bound.

Numerous variations of perceptron algorithms have been presented in the literature. A straightforward modification is the normalized perceptron method, which varies only in its updating rule:

```
initialize: wg_1 = 0
For td = 1, 2, 3, 4, ..., TD do
Assume the current incoming instance xi_t, prd
ŷp_td = f_td(xi_td) = sign(wg_td.xi_td);
Receive the true class label yp_td ∈ {+1, −1};
if ŷp_td ≠ yp_td then
wg_td+1 ← wg_td + yp_1 xi_1;
    end if
end for
```

Algorithm 1: Perceptron.

$$wg_{td+1} = wg_{td} + yp_{td}\frac{xi_{td}}{\| xi_{td} \|}. \tag{1}$$

3.2. Passive-Aggressive Classifier. When a new piece of data comes in, the model is updated to ensure that the new piece of data does not get lost and that the model is close to the one already there [15, 105, 106].

This algorithm falls under the family of first-order online learning algorithms, and it works with the principle of margin-based learning [95].

Given an instance $\mathbf{xi_{tr}}$ at round tr, the passive-aggressive generates the optimization as follows:

$$\begin{gathered} WE_{tr+1} = \underset{w \in R^d}{\text{arugmin}}\, i \frac{1}{2} \| WE - WE_{tr} \|^2, \\ \text{s}\ell_1 (WE) = 0, \end{gathered} \tag{2}$$

where $\ell_1 (WE) = \max i (0, 1 - yp_{tr} WE.xi_{tr})$ is the hinge loss of the classifier. When the hinge loss is zero, i.e., $WX_{tr+1} = WX_{tr}$ when $\ell = 0$, then the classifier is passive and the classifier is treated as aggressive, and when loss is nonzero, then the algorithm is named as "passive-aggressive" (PA) [95]. So, the aim of the passive-aggressive classifier is to update the classifier WX_{tr+1} and stay close to the previous one.

In particular, PA aims to keep the updated classifier WX_{tr+1} stay close to the previous classifier ("passiveness") and make sure all incoming instances are correctly classified by updating the classifier.

It is critical to recognize a significant distinction between PA and perceptron algorithms. Perceptron updates only when a classification error occurs. However, a PA algorithm updates aggressively anytime the loss is nonzero (even if the classification is correct). Although PA algorithms have equivalent error limitations to perceptron algorithms in principle [95], they frequently outperform perceptron considerably practically.

3.3. Modern Portfolio Theory. Modern portfolio theory (MPT), sometimes referred to as mean-variance analysis, is a mathematical framework for designing an asset portfolio to maximize expected returns for a given level of risk. It is a formalization and extension of diversification in investing, which maintains that possessing a diverse portfolio of financial assets is less risky than owning only one type. Its fundamental premise is that an asset's risk and return should not be evaluated in isolation but rather in connection to contributing to the portfolio's overall risk and return. Asset price volatility is used as a proxy for risk. Economist Harry Markowitz [73] popularized MPT in a 1952 article for which he was later given the Nobel Memorial Prize in Economic Sciences, which became known as the Markowitz Prize.

As per the following multi-objective optimization formula, the mean-variance model maximizes profits and reduces risks simultaneously.

$$\begin{gathered} \min \sum_{k-1}^{N} \sum_{l-1}^{N} z_k z_l \sigma_{kl}, \\ \max \sum_{k=1}^{n} z_k \mu_k, \\ \text{s} \begin{cases} \sum_{k=j}^{N} z_1, \\ 0 \le z_k \le 1, \forall k = 1.....N, \end{cases} \end{gathered} \tag{3}$$

where σ_{kl} denotes the correlation between assets k and l, z_k and z_l denote the fraction of the original value; and μ_1 is the expected return on asset k.

3.4. Imbalanced Data Handling Techniques. Imbalanced data distribution is frequently used in machine learning and data science. It occurs when the number of observations in one class is considerably more or smaller than the number of observations in other classes. However, because machine learning algorithms maximize accuracy by decreasing mistakes [107], they ignore class distribution. In more technical words, if our dataset includes an unequal data distribution, our model is more susceptible to situations in which the minority class has very little or no recall.

3.4.1. Synthetic Minority Oversampling Technique (SMOTE). You can use synthetic minority oversampling technique (SMOTE) to deal with not evenly split up data. It tries to even things out by adding minority class examples at random through replication.

Step 1. By calculating Euclidean distances between x and each other sample in set A, we define the minority classes set A for each k-nearest neighbors of x.

Step 2. To determine the sampling rate N, an imbalanced proportion is calculated. The set A1 is constructed by randomly selecting N (i.e., $x1$, $x2$, . . ., xn) from its k closest neighbors, for each $x \in A$.

Step 3. To make a new example for each complex $x_k \in A_1$, $(k = 1, 2, 3....N)$, the following formula is used:

$$x' = x + \text{rand}(0, 1) * |x - x_k|, \tag{4}$$

where rand (0, 1) denotes a random value between 0 and 1.

SMOTE is a well-known data preparation approach for addressing the issue of class imbalance. Sun et al. [103] provide the SMOTE technique, which generates new samples by identifying the k-nearest neighbors of each minority class sample and randomly interpolating between them to achieve sample class balance before training classifiers [103]. SMOTE, one of the most often used oversampling techniques for dealing with class imbalance, provides new minority class samples to balance the training dataset, hence enhancing the model's classification performance. SMOTE creates extra minority class samples combined with the initial training set to form an equitable training set. As an illustration of how SMOTE may be used to address a class imbalance in our prediction model, the SMOTE approach can be used to batch balance the original training dataset before starting the ensemble approach.

3.5. Evaluation Matrices. To assess the efficiency of the suggested model, we used performance matrices such as accuracy, receiver operating characteristic (ROC) curve (AUC), and F score. As a result, we evaluated the framework's performance using a mixture of matrices rather than a single one. The following are the performance matrices.

$$\begin{aligned} \text{precision} &= \frac{tr_p}{tr_p + fa_p}, \\ \text{recall} &= \frac{tr_p}{tr_p + fa_n}, \\ \text{F score} &= 2\frac{\text{precision} * \text{recall}}{\text{precision} + \text{recall}}, \\ \text{accuracy} &= \frac{tr_p + t_{rn}}{tr_p + tr_n + fa_p + fa_n}, \end{aligned} \tag{5}$$

where tr_p denotes the total number of real positive values; tr_n denotes the total number of real negative values; fa_p denotes the total number of false-positives values; and fa_n denotes the total number of false-negative values.

According to Shen and Shafiq [101], the area under curve is an acceptable assessment matrix for classification issues; as the AUC value grows, so does the model's prediction ability.

3.5.1. Hamming Loss. In general, there is no magical metric that is the best for every problem. In every problem, you have different needs, and you should optimize for them. The Hamming loss is the proportion of wrong labels compared with the total number of labels. Hamming loss is calculated as the Hamming distance between actual and predicted values. Generally, the Hamming loss is related to imbalance classification problems.

3.6. Instrumentation and Systems Employed. We used the Python open-source environment and Google Colab for our scientific experiment purposes for our suggested framework. Here, we used the Scikit library to access the predefined library functions related to machine learning models and the TA-Lib library to find the technical indicators used in our experiment. The complete development procedure was run on an Intel CPU (Core-i5-1035G1, 1.19 GHz) processor, with RAM installed of 8 GB, and the OS used 64 bit Windows.

3.7. Dataset. In particular, for our innovations, five different health sector indexes have been selected from four different stock markets of four different nations, namely London, Germany, France, and America. The data on equity indexes are updated daily. In addition, each trading day's equity indexes are included in all datasets. Initially, we chose five high-quality companies from each nation based on their performance over time and asset size. When we are considering the stock market for forecasting, as we know, the nature of the dataset is random. So, if we take only one dataset for our experiment, we may not conclude that our model can also perform better on other datasets. So, for making a model as a general one we will suggest multiple datasets. The details of the stock are shown in Tables 2 and 3.

4. Proposed Framework

This study suggests a new technique to minimize the investment risk by developing a framework that is a combination of the mean-variance model for selecting minimal risk-based stock and a machine learning-based online learning model for stock forecasting. The proposed framework is shown in Figure 1. This framework, in particular, has two major phases: portfolio selection and stock prediction. So, during our framework setup, our empirical research was gone through four stages:

(1) Initial asset selection.

(2) Developing a mean-variance model for return prediction and final stock selection for an experiment.

(3) Predictive model setup.

(4) *Outcome Evaluation.* The Python programming language is used to prepare the computations, Scikit-learn is used to configure and train the online predictive model, and PyPortfolioOpt is used to implement the optimization strategies for finding the most valuable stocks for investment.

Table 2: List of stocks initially selected for an experiment with different geographic areas.

USA	London	Germany	France
DHR	AZN	AFX	CGN
JNJ	DPHL	BAYN	CVS
MDT	GSK	BRM	EWL
NVO	HIKL	MRK	MTO
UNH	SNL	SRT	TN8

Table 3: List of different geographic stocks finally selected for experiment.

Name of the stocks	DHR	NVO	UNH	DPHL	AFX	MRK	CVS	EWL	MTO	TN8
Range of the dataset	5/11/1987 to 24/11/2021	04/01/1982 to 24/11/2021	26/03/1990 to 24/11/2021	21/09/2000 to 24/11/2021	22/03/2000 to 24/11/2021	26/06/1998 to 24/11/2021	03/01/2000 to 24/11/2021	08/03/2001 to 24/11/2021	11/09/2000 to 24/11/2021	11/09/2000 to 24/11/2021

DHR- Danaher Corporation; NVO- Novo Nordisk A/S; UNH- UnitedHealth Group Incorporated; DPHL- Dechra Pharmaceuticals PLC; AFX- Alpha FX Group plc; MRK -Merck & Co., Inc.; CVS - CVS Health Corporation; EWL - iShares; MSCI Switzerland ETF; MTO -Mitie Group plc; TN8 - Thermo Fisher Scientific Inc.

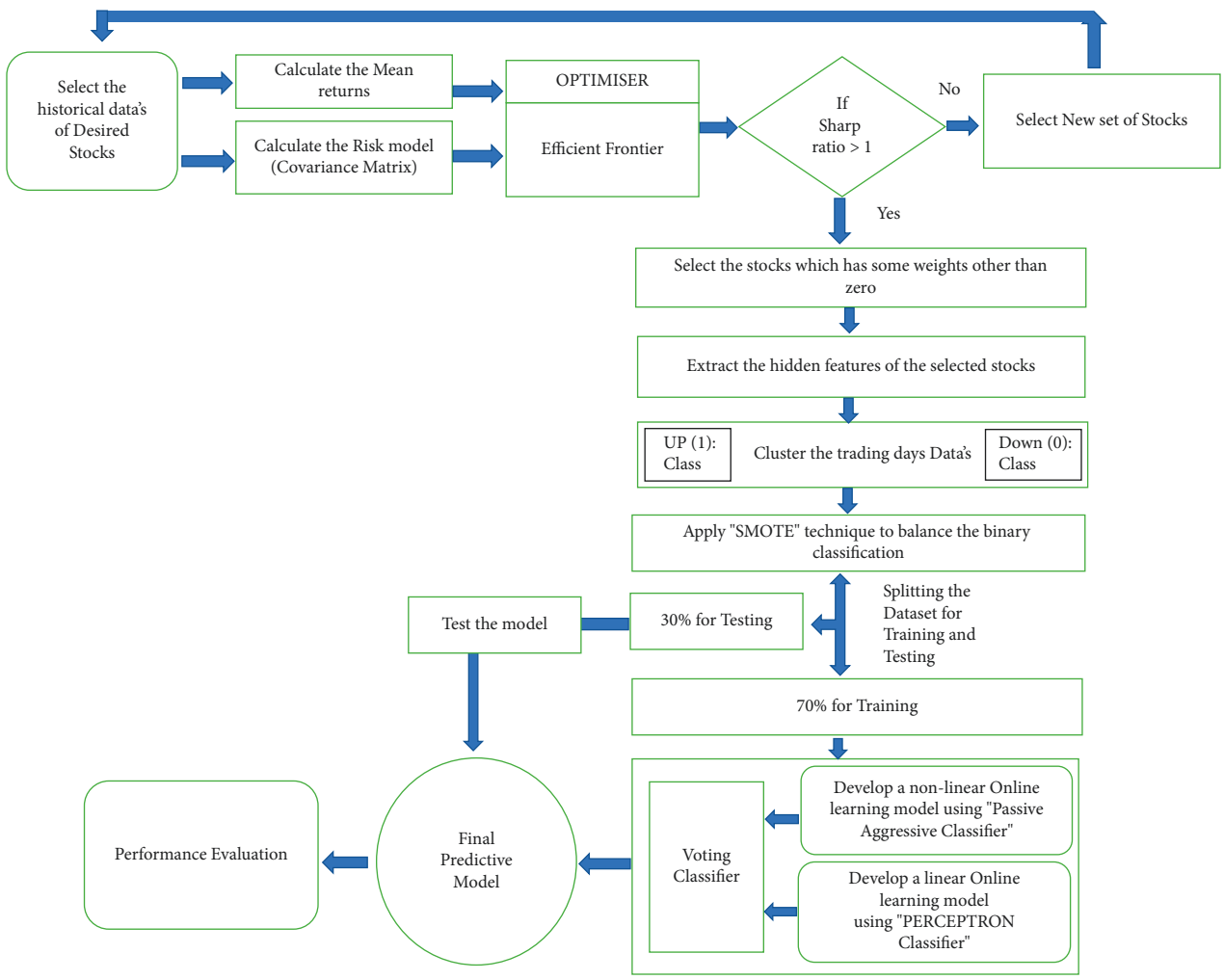

Figure 1: Proposed framework.

Initially, we selected 20 stocks for four different geographic reasons; they are enumerated in Table 2. The stock selection is based on the previous and current performances according to the market capitalization, and those stocks have been selected for their market existence for more than 20 years.

After selecting individual 20 stocks for different geographic reasons, we have to find the potential stocks that give

a minimum loss and a maximum profit for an investor. Finally, those will be taken for the final experiment. For the selection of potential stocks, we examine the current portfolio theory, sometimes referred to as the mean-variance model, which was presented by Markowitz [73].

From the selected stocks' historical datasets, we have collected for one year. We have extracted the mean return and covariance matrix of each stock according to geographic reasons from the historical price. Then, the extracted parameters, i.e., mean return and covariance matrix, are passed to the mean-variance model using the efficient Frontier optimizer. After implementing this optimization technique, we got the following potential stocks for future productivity: here, the following Tables 4–7 show the weights of each stock according to the geographic reason.

According to the modern portfolio theory, stocks with weight values other than zero are considered potential stocks. So, from the Tables 4–7, we have recorded the weights of each stock, and finally, we have to select only stocks that have weights greater than zero. To minimize the risk factor again, we have added one condition that those group stocks with a sharp ratio of more than 1 will be a great advantage for investors in choosing whether or not to purchase or sell a particular stock. Now, it is time to extract the real stocks, which will be carried out for our experiment.

After successfully selecting potential stocks, our next objective is to create an online training approach before developing an online training approach. It is crucial to find the essential features for finding the hidden truth behind our stock. Data preprocessing makes the dataset more powerful and makes sense for a machine learning model. Here, we are highlighting the steps.

4.1. Data Preprocessing. An earlier study of related topics lacked explicit instructions for picking relevant input features to predict the index's flow direction. As a result, we can confidently assert a hidden behaviour behind every technical feature. For example, according to Weng et al. [18], investors use covert behaviour to analyse the present circumstances and determine whether to purchase or sell. Ultimately, given their opinion on the indicators that evaluate the concealed performance of these input data, it is possible to anticipate the fiscal market uniquely. As a result, we used indicators in our investigation and other elements to forecast asset price movement.

The raw dataset must be preprocessed once it has been received. As part of the data preprocessing, we followed the following steps:

(1) In general, the index collected from the online site has specific preexisting attributes such as open, close, low, high, and soon. Therefore, we needed to deal with the null and missing values with the dataset in hand.

(2) We extracted eight technical indicators from the previously stated line in the second phase. In addition, our process included two additional features: the variation between the opening and closing prices of a stock on a given day, which represents both a growth and a fall in its value, as well as the difference between the high and low price, which represents the volatility of that day's stock price.

(3) As part of our response anticipated variable, we created a binary feedback variable for individual trading days, i.e., *Dn* 0 and 1. The forecasted feedback variable on the *N*th day is computed as follows:

If $\mathrm{Op}_n < \mathrm{Cl}_n$
Then
$D_{\mathrm{n}} = 1$
Else
$D_{\mathrm{n}} = 0$
End If

In this case, D_n is our forecasted variable since we used the prediction label "TREND." On the *n*th day of the index's life, Op_n is its opening price and Cl_n is its closing price. For instance, if the D_n returns a value of "1," then the fund's value will rise, but if the D_n returns a value of "0," then the fund's value will fall. Traders and researchers use the (TaLib) library to calculate technical indicators in the technical analysis [108]. We use the VIF technique to find the best set of features out of many.

Table 4: List of American stocks with their weights.

Name of the stocks	DHR	JNJ	MDT	NVO	UNH
Weights	0.04507	**0.0**	**0.0**	0.69592	0.25901

DHR- Danaher Corporation; JNJ- Johnson & Johnson; MDT- Medtronic plc; NVO- Novo Nordisk A/S; UNH- UnitedHealth Group Incorporated.

Table 5: List of United Kingdom stocks with their weights.

Name of the stocks	AZN	DPHL	GSK	HIKL	SNL
Weights	0.0	**1.0**	**0.0**	0.0	0.0

AZN- AstraZeneca PLC; DPHL- Dechra Pharmaceuticals PLC; GSK- GlaxoSmithKline plc; HIKL- Hikma Pharmaceuticals PLC; SNL - smith & nephew plc.

Table 6: List of Germany stocks with their weights.

Name of the stocks	AFX	BAYN	BRM	MRK	SRT
Weights	0.31381	0.0	0.0	0.68619	0.0

Annual volatility: 20.7%; Sharpe ratio: 2.80.

Table 7: List of France stocks with their weights.

Name of the stocks	CGN	CVS	EWL	MTO	TN8
Weights	0.0	**0.23574**	**0.36912**	0.16845	0.22668

Annual volatility: 15.6%; Sharpe ratio: 2.37.

4.2. Extracted Features

4.2.1. SAR Indicator. An indicator called the parabolic SAR is a way to see how the price of a specific thing will change over time.

4.2.2. Parabolic SAR Extended. It is an indicator designed for opsonists as it is reactive at the beginning of the trend but then remains little influenced by the movements. Although significant, that does not change the current trend. Buy signals are generated when the indicator is above 0; sell signals are generated when the indicator is below 0.

4.2.3. Aroon Indicator. The Aroon indicator determines whether a price is trending or trading inside a range. Additionally, it can show the start of a new trend its strength and assist in anticipating transitions from trading ranges to trends.

4.2.4. The Balance of Power (BOP). The balance of power (BOP) indicator measures a price trend by evaluating the strength of buy and sell signals, determining how strongly the price moves between extraordinarily high and low levels. The BOP oscillates between −1 and 1, with positive values indicating more substantial buying pressure and negative values indicating intense selling pressure. When the indicator gets closer to zero, it shows that the buyers' and sellers' strength is equating.

4.2.5. The Directional Movement Index. The DMI is a useful metric that is used to cut down on the number of false signals. It analyses both the degree and direction of a price movement. The greater the spread between the two main lines, the more influential the trend.

4.2.6. The Chaikin A/D Oscillator. The indicator examines the line of moving average convergence-divergence that shows how much money is added or taken away. A cross above the accumulation-distribution line means that people in the market are buying more shares, securities, or contracts, which is usually a good thing.

4.2.7. OBV. On balance volume (OBV) is a straightforward indicator that uses turnover and pricing to determine how much people buy and sell. There is much-buying pressure when positive volume outnumbers negative volume, and the OBV line rises.

4.2.8. True Range. It looks at the range of the day and any different from the previous day's close price.

4.2.9. COS. Vector cosine calculates the trigonometric cosine of each element in the input array.

4.2.10. Open. This is a feature that has been there for a long time. It shows the stock price at the start of every day.

4.2.11. Open-Close. Under this instance, the disparity between the entry and exit prices is clearly shown in all of the transactions that happen each day.

4.2.12. High-Low. This feature shows how volatile each trading day is. On that day, it is the gap between the top and low price points.

4.2.13. Close. At the close of the stock each day, this feature shows the stock price. Again, this is a feature that has been there before.

4.2.14. Volume. This feature shows each day's total buying and selling quantity on each trading day.

As it is a binary classification problem whether the stock goes up or down, we found different stocks from different geographic regions during the preprocessing data stage, which leads to a data imbalance problem. So to avoid this problem, we used the SMOTE technique to balance the dataset. Finally, as part of the data processing stage, we used the scaling approach to normalize the characteristics that would be fed to our model. After acquiring a balanced dataset, 75 percent of the dataset was used for training and 25 percent for testing; we divided it into these two groups. As we know, during ML model training there is a chance of overfitting, so technically, during our practical experiment, we adopted the cross-validation technique to avoid overfitting issues.

As far we discussed the demerits of offline learning models, we have implemented two online learning models that can allow the prediction model to be upgraded quickly for any current data instances. Consequently, online learning algorithms are substantially more efficient and scalable than traditional machine learning algorithms to be applied to a wide range of machine learning problems encountered in actual data analytic applications. So, we have used two online learning algorithms. One is a perception, and the other one is a passive-aggressive classifier. Instead of developing a single predictive model for forecasting, we combine the models' predictive capabilities and pass them to a voting classifier. Finally, the voting classifier merged the performances and built a highly reliable online predictive forecasting model.

5. Results and Discussion

To evaluate the suggested method's performance, we employed 10 potential indices for different geographic reasons, as reflected in Table 3. In this research, we assume that optimization techniques represented by the mean-variance model are well suited to enhancing the Sharpe ratio for building a portfolio of different geographically reason-based stocks. For selecting potential stocks, the primary performance measure that we use is the Sharpe ratio, and we calculate the weights of each index using the mean-variance optimization technique. The results are reflected in Tables 4–7. To test our online learning predictive model, we have selected different geographic stocks whose performance measures are given below according to the geographic reasons.

As shown in Table 8, our proposed model was performed on three American stock indices, likely UNH,

NVO, and DHR, whose performances and accuracy measures are shown in Table 8. The recorded results found that the UNH index has a training accuracy of 99.16, while the testing accuracy is 99.60. The recorded AUC score is 99.6041, and the Hamming loss is 0.00399. The precision value recorded about group 0 is 0.99 and to group 1 is 1.00, whereas the recall value recorded pertaining to group 0 is 1.00 and to group 1 is 0.99. Finally, the $f1$ score related to group 0 is 1.00 and about group 1 is 1.00. The NVO index has a training accuracy of 99.68, whereas the testing accuracy is 99.73. The recorded AUC score is 99.7322, and the Hamming loss is 0.002368. The precision value recorded in group 0 is 0.99 and related to group 1 is 1.00, 0, whereas the recall value recorded in group 0 is 1.00 and related to group 1 is 0.99. Finally, the $f1$ score related to group 0 is 1.00 and about group 1 is 1.00. The DHR index has a training accuracy of 99.47, while the testing accuracy is 99.36. The recorded AUC score is 99.3724, and Hamming loss is 0.00635. The precision value recorded about group 0 is 0.99 and group 1 is 1.00. In contrast, the recall value recorded about group 0 is 1.00 and on group 1 is 0.99, and finally, the $f1$ score about group 0 is 99.00 and related to group 1 is 99.00. Table 9 shows the confusion matrix.

Our proposed model was performed on four French stock indices, likely CVS.F, EWL.F, MTO.F, and TN8.F, whose performances and accuracy measures are shown in Table 10. From the recorded results, we found that the CVS.F index has a training accuracy of 99.72, whereas the testing accuracy is 99.49. The recorded AUC score is 99.50, and the Hamming loss is 0.00508. The precision value recorded pertaining to group 0 is 0.99 and to group 1 is 1.00, whereas the recall value recorded pertaining to group 0 is 1.00 and to group 1 is 0.99. Finally, the $f1$ score related to group 0 is 99.00, and pertaining to group 1 is 1.00. By looking at the table, the EWL. F index has a training accuracy of 99.87 percent, whereas the testing accuracy is 99.61 percent. The recorded AUC score is 99.60, and the Hamming loss is 0.00386. The precision value recorded pertaining to group 0 is 0.99 and pertaining to group 1 is 1.00. In contrast, the recall value recorded pertaining to group 0 is 1.00 and pertaining to group 1 is 0.99, and finally, the $f1$ score pertaining to group 0 is 1.00 and pertaining to group 1 is 1.00. The MTO.F index has a training accuracy of 99.94, whereas the testing accuracy is 99.91. The recorded AUC score is 99.91, and the Hamming loss is 0.00086. The precision value recorded pertaining to group 0 is 1.00 and pertaining to group 1 is 1.00, whereas the recall value recorded pertaining to group 0 is 1.00 and pertaining to group 1 is 1.00, and finally, the $f1$ score pertaining to group 0 is 1.00 and pertaining to group 1 is 1.00. The TN8.F index has a training accuracy of 99.81, whereas the testing accuracy is 99.84. The recorded AUC score is 99.84, and Hamming loss is 0.00151. The precision value recorded pertaining to group 0 is 1.00 and pertaining to group 1 is 1.00, whereas the recall value recorded pertaining to group 0 is 1.00 and pertaining to group 1 is 1.00. Finally, the f1 score pertaining to group 0 is 1.00 and pertaining to group 1 is 1.00. Table 11 shows the confusion matrix.

As shown in Tables 12 and 13, our proposed model was performed on two German stock indices, likely AFX.DE and MRK.DE, whose performances and accuracy measures are shown in the table. From the recorded results, we found that the CVS.F index has a training accuracy of 99.1627, while the testing accuracy is 99.1631. The recorded AUC score is 99.15, and Hamming loss is 0.00836. The precision value recorded as group 0 is 0.99 and group 1 is 1.00. In contrast, the recall value recorded related to group 0 is 1.00 and about group 1 is 0.99, and the $f1$ score related to group 0 is 99.00 and related to group 1 is 99.00. For the index MRK.DE, the training accuracy is 99.4553, while the testing accuracy is 99.4771. The recorded AUC score is 99.15, and the Hamming loss is 0.00522. The precision value recorded in group 0 is 0.99 and in group 1 is 1.00. In contrast, the recall value recorded related to group 0 is 1.00 and related to group 1 is 0.99, and finally, the $f1$ score about group 0 is 99.00 and related to group 1 is 99.00. Table 11 shows the confusion matrix.

As shown in Table 14, our proposed model was performed on one London stock index, likely DPH.L, whose performances and accuracy measures are shown in Table 14. From the recorded results, we found that the DPH.L index has a training accuracy of 98.74, whereas the testing accuracy is 98.40. The recorded AUC score is 98.44, and the Hamming loss is 0.01591. The precision value recorded pertaining to group 0 is 0.97 and pertaining to group 1 is 1.00. In contrast, the recall value recorded pertaining to group 0 is 1.00 and pertaining to group 1 is 0.97, and finally, the f1 score pertaining to group 0 is 98.00 and about group 1 is 98 .00. The forecast performances of online learning ensemble model, London indices. Table 15 shows the confusion matrix.

5.1. Performance Comparison with Past Works. Table 16 shows a relative performance level with the past works with our proposed model.

5.2. Practical Implications. Nowadays, machine learning-based systems give recommendations about certain companies to investors to have a basic notion and minimize their investing losses. By analysing vast quantities of data and developing simple, widely accessible solutions that benefit everyone, not just businesses, AI has a big impact on the exchange of currency. In contrast to humans, who appear to be overly enthusiastic about the trading of assets, AI will make reasoned, accurate, and fair speculative decisions. This strategy could be used to develop new trading strategies or to manage investment portfolios by rebalancing holdings based on trend forecasts. This will help various financial institutions collect information about share prices so they can advise their clients on how to maximize earnings and reduce losses. In addition, it pushes the research community on a new path by illustrating how online algorithms can be combined with various technical markers and the ramifications of modifying various parameters [102, 113].

Table 8: Forecast performances of the online learning ensemble model, American indices.

	Accuracy		AUC score	Hamming loss	Precision		Recall		$f1$ score	
	Train	Test			0	1	0	1	0	1
UNH	99.16	99.60	99.6041	0.00399	0.99	1.00	1.00	0.99	1.00	1.00
NVO	99.68	99.73	99.7322	0.00268	0.99	1.00	1.00	0.99	1.00	1.00
DHR	99.47	99.36	99.3724	0.00635	0.99	1.00	1.00	0.99	99.00	99.00

Table 9: Confusion matrix of American indices.

	TP	FP	TN	FN
UNH	1013	2	984	6
NVO	1300	0	1302	7
DHR	1105	1	1083	13

Table 10: Forecast performances of the online learning ensemble model, France indices.

	Accuracy		AUC score	Hamming loss	Precision		Recall		$f1$ score	
	Train	Test			0	1	0	1	0	1
CVS.F	99.72	99.49	99.50	0.00508	99.00	1.00	1.00	99.00	99.00	1.00
EWL.F	99.87	99.61	99.60	0.00386	99.00	1.00	1.00	99.00	1.00	1.00
MTO.F	99.94	99.91	99.91	0.00086	1.00	1.00	1.00	1.00	1.00	1.00
TN8.F	99.81	99.84	99.84	0.00151	1.00	1.00	1.00	1.00	1.00	1.00

Table 11: Confusion matrix of France indices.

	TP	FP	TN	FN
CVS.F	998	0	958	10
EWL.F	11013	1	1049	7
MTO.F	1162	0	1151	2
TN8.F	989	0	984	3

Table 12: Forecast performances of the online learning ensemble model, German indices.

	Accuracy		AUC score	Hamming loss	Precision		Recall		$f1$ score	
	Train	Test			0	1	0	1	0	1
AFX.DE	99.1627	99.1631	99.15	0.00836	99.00	1.00	1.00	99.00	99.00	99.00
MRK.DE	99.4553	99.4771	99.47	0.00522	99.00	1.00	1.00	99.00	99.00	99.00

Table 13: Confusion matrix of German indices.

	TP	FP	TN	FN
AFX.DE	702	2	720	10
MRK.DE	762	1	760	7

Table 14: Forecast performances of the online learning ensemble model, London indices.

	Accuracy		AUC score	Hamming loss	Precision		Recall		f1 score	
	Train	Test			0	1	0	1	0	1
DPH.L	98.74	98.40	98.44	0.01591	97.00	1.00	1.00	97.00	98.00	98.00

Table 15: Confusion matrix of London indices.

	TP	FP	TN	FN
DPH.L	748	0	736	24

Table 16: Comparison of historical stock market forecasting methods to our suggested model's performance.

Author	Output	Performance measurement (accuracy) (%)
Malagrino et al. (2018) [109]	Daily asset flow	71–78
Zho et al. (2018) [110]	Daily asset flow	66.67
Zheng et al. (2018) [107, 111]	Daily asset flow	79.4
Ren et al. (2018) [112]	Daily asset flow	89.0
Hu et al. (2018) [113]	Daily asset flow	89.0
Fischer and Krauss (2018) [114]	Daily asset flow	56
Our proposed model	Daily asset flow	**98-99**

Table 17: Average accuracy of the proposed framework of different geographic indices.

Country	America	German	France	London
Average accuracy	99.56	99.32	99.71	98.40

6. Conclusion

In this manuscript, we come up with a method that uses an ensemble-based incremental learning approach for short-term stock price forecasting that can minimize investment risk (an optimal portfolio) and make a predictive decision to find the direction of the selected stocks. Our proposed framework is composed of two models. The first model is the mean-variance model, which is used to minimize the risk assessment of individual stocks. The second model is an incremental-based ensemble model composed of two online learning algorithms, i.e., perceptron and passive-aggressive classifier. Besides the historical data of stock market closing prices, open price volume, nine indicators, and two extracted features are also inserted to boost the ensemble framework's performance. Initially, we selected 20 stocks from four different geographic countries, i.e., America, Germany, France, and London. Still, after implementing the mean-variance model, we got only 10 indices for the final experiment. Our fact-finding technique revealed that, as the stock market is always a source of data collection at regular intervals, it is always a good perspective from a researcher's point of view. Therefore, instead of using a batch learning technique, an online learning technique is used for forecasting the financial market. Our experimental bench reveals that the random selection of stock market data for forecasting is a meaningless practice for the researcher, which should be avoided with the help of different portfolio selection techniques. As a reference, our proposed framework revealed a lot. Our study found that our proposed online learning ensemble models' performance, which is depicted in Table 17, shows the average accuracy level of indices belonging to four different geographic reasons.

The study revealed that performance levels may increase when we add indicators as our input features and handle the imbalanced dataset. Therefore, instead of using a batch learning-based single predictive model for forecasting, it is always better to practice using an ensemble model based on online learning to improve forecasting performances, as shown in Table 16. However, if we look into the runtime of this framework, it takes the range of training time, i.e., 4 to 12 seconds to train the model on different datasets. As the number of folds increases, the training time also increases, as well as when the data size increases, the training time also increases.

6.1. Limitations and Future Work. However, despite the excellent prediction performance of our proposed methodology, certain limitations may be resolved in the future. First, as our current study only predicts the direction of stocks one day in advance, it will require growth in the future for long-term market direction predictions. This study was limited to four stock exchanges, but it could have been more comprehensive if it had included stock exchanges from additional countries. In conclusion, future research must also employ this dataset, as the study did not investigate additional information sources, such as fundamental and sentiment analysis [52, 105, 106, 112–114].

Data Availability

The data used to support the findings of this study are available from the first author upon request.

Conflicts of Interest

The authors declare no conflicts of interest.

Acknowledgments

Jana Shafi would like to thank the Deanship of Scientific Research, Prince Sattam bin Abdulaziz University, for supporting this work.

References

[1] G. Shivam, K. Arpan Kumar, B. Abdullah, A. A. Wassan, and K. Al, "Big data with cognitive computing," *A review for the future,International Journal of Information Management*, vol. 42, pp. 78–89, 2018, ISSN 0268-4012.

[2] C. Shousong, W. Xiaoguang, and Z. Yuanjun, "Revenue model of supply chain by internet of things technology," *IEEE Access*, vol. 7, pp. 4091–4100, 2018.

[3] T. Bodnar, S. Mazur, and Y. Okhrin, "Bayesian estimation of the global minimum variance portfolio," *European Journal of Operational Research*, vol. 256, no. 1, pp. 292–307, 2017.

[4] F. Yang, Z. Chen, J. Li, and L. Tang, "A novel hybrid stock selection method with stock prediction," *Applied Soft Computing*, vol. 80, pp. 820–831, 2019.

[5] M. Jensen, "Some anomalous evidence regarding market efficiency, J," *Finance and Economics*, vol. 6, no. 2–3, pp. 95–101, 1978.
[6] E. F. Fama, "Random walks in stock market prices," *Financial Analysts Journal*, vol. 21, no. 5, pp. 55–59, 1965.
[7] P. Yu and X. Yan, "Stock price prediction based on deep neural networks," *Neural Computing & Applications*, vol. 32, no. 6, pp. 1609–1628, 2020.
[8] F. Kunze, M. Spiwoks, K. Bizer, and T. Windels, "The usefulness of oil price forecasts-e," *Managerial and Decision Economics*, vol. 39, no. 4, pp. 427–446, 2018.
[9] B. V. Dasarathy, "Nearest-neighbor classification techniques," IEEE Computer Society Press, Los Alomitos, CA, USA, 1991.
[10] M.-L. Zhang, J. M. Peña, and V. Robles, "Feature selection for multi-label naive Bayes classification," *Information Sciences*, vol. 179, no. 19, pp. 3218–3229, 2009.
[11] B. Chandra and P. Paul Varghese, "Moving towards efficient decision tree construction," *Information Sciences*, vol. 179, no. 8, pp. 1059–1069, 2009.
[12] O. Chapelle, P. Haffner, and V. N. Vapnik, "Support vector machines for histogram-based image classification," *IEEE Transactions on Neural Networks*, vol. 10, no. 5, pp. 1055–1064, 1999.
[13] D. Fisch, B. Kühbeck, B. Sick, and S. J. Ovaska, "So near and yet so far: new insight into properties of some well-known classifier paradigms," *Information Sciences*, vol. 180, no. 18, pp. 3381–3401, 2010.
[14] A. Bouchachia, "Learning with incrementality," in *Proceedings of the 13th International Conference on Neural Information Processing*, pp. 137–146, Hong Kong, China, October 2006.
[15] S. C. H. Hoi, D. Sahoo, J. Lu, and P. Zhao, "Online learning: a comprehensive survey," *Neurocomputing*, vol. 459, pp. 249–289, 2021, ISSN 0925-2312.
[16] W. Farida Agustini, I. R. Affianti, and E. R. Putri, "Stock price prediction using geometric Brownian motion," *Journal of Physics: Conference Series*, vol. 974, Article ID 012047, 2018.
[17] K. Adam, A. Marcet, and J. P. Nicolini, "Stock market volatility and learning," *The Journal of Finance*, vol. 71, no. 1, pp. 33–82, 2016.
[18] T.-A. Dinh and Y.-K. Kwon, "An empirical study on importance of modeling parameters and trading volume-based features in daily stock trading using neural networks," *Informatics*, vol. 5, no. 3, p. 36, 2018.
[19] S. Mehdizadeh and A. K. Sales, "A comparative study of autoregressive, autoregressive moving average, gene expression programming and Bayesian networks for estimating monthly streamflow," *Water Resources Management*, vol. 32, pp. 1–22, 2018.
[20] Y. Zhang, W. Song, M. Karimi, C.-H. Chi, and A. Kudreyko, "Fractional autoregressive integrated moving average and finite-element modal: the forecast of tire vibration trend," *IEEE Access*, vol. 6, pp. 40137–40142, 2018.
[21] Q. Li, G. Cao, and W. Xu, "Relationship research between meteorological disasters and stock markets based on a multifractal detrending moving average algorithm," *International Journal of Modern Physics B*, vol. 32, Article ID 1750267, 2018.
[22] T. Petukhova, D. Ojkic, B. McEwen, R. Deardon, and Z. Poljak, "Assessment of autoregressive integrated moving average (ARIMA), generalized linear autoregressive moving average (GLARMA), and random forest (RF) time series regression models for predicting influenza a virus frequency in swine in Ontario, Canada," *PLoS One*, vol. 13, no. 6, Article ID e0198313, 2018.
[23] D. Wang and L. Zhang, "A fuzzy set-valued autoregressive moving average model and its applications," *Symmetry*, vol. 10, no. 8, p. 324, 2018.
[24] R. Rui, D. D. Wu, and T. Liu, "Forecasting stock market movement direction using sentiment analysis and support vector machine," *IEEE Systems Journal*, vol. 13, pp. 60–770, 2018.
[25] S. Basak, S. Kar, S. Saha, L. Khaidem, and S. Dey, "Predicting the direction of stock market prices using tree-based classifiers," *The North American Journal of Economics and Finance*, vol. 47, pp. 552–567, 2018.
[26] R. J. Shiller, "From efficient markets theory to behavioral finance," *The Journal of Economic Perspectives*, vol. 17, no. 1, pp. 83–104, 2003.
[27] R. H. Thaler, "The end of behavioral finance," *Financial Analysts Journal*, vol. 55, no. 6, pp. 12–17, 1999.
[28] D. Jothimani and S. S. Yadav, "Stock trading decisions using ensemble-based forecasting models: a study of the Indian stock market," *Journal of Banking and Financial Technology*, vol. 3, no. 2, pp. 113–129, 2019.
[29] I. K. Nti, A. F. Adekoya, and B. A. Weyori, "A systematic review of fundamental and technical analysis of stock market predictions," *Artificial Intelligence Review*, vol. 53, no. 4, pp. 3007–3057, 2020.
[30] P. Agarwal, S. Bajpai, A. Pathak, and R. Angira, "Stock market price trend forecasting using machine learning," *International Journal for Research in Applied Science and Engineering Technology*, vol. 5, pp. 1673–1676, 2017.
[31] M. Schmeling, "Investor sentiment and stock returns: some international evidence," *Journal of Empirical Finance*, vol. 16, no. 3, pp. 394–408, 2009.
[32] Z. Haider Khan, T. Sharmin Alin, and A. Hussain, "Price prediction of share market using artificial neural network 'ANN'," *International Journal of Computer Application*, vol. 22, no. 2, pp. 42–47, 2011.
[33] R. E. Schapire, "Explaining AdaBoost," in *Empirical Inference*, B. Schölkopf, Z. Luo, and V. Vovk, Eds., Springer. Berlin/Heidelberg, Berlin, Germany, 2019.
[34] D. K. Padhi and N. Padhy, "Prognosticate of the financial market utilizing ensemble-based conglomerate model with technical indicators," *Evolutionary Intelligence*, vol. 14, no. 2, pp. 1035–1051, 2021.
[35] T. Marwala and E. Hurwitz, "Artificial intelligence and economic theory: skynet in the market," Springer, London, UK, 2017.
[36] B. M. Henrique, V. A. Sobreiro, and H. Kimura, "Literature review: machine learning techniques applied to financial market prediction," *Expert Systems with Applications*, vol. 124, pp. 226–251, 2019.
[37] E. Chong, C. Han, and F. C. Park, "Deep learning networks for stock market analysis and prediction: methodology, data representations, and case studies," *Expert Systems with Applications*, vol. 83, pp. 187–205, 2017.
[38] C. N. Avery, J. A. Chevalier, and R. J. Zeckhauser, "The "CAPS" prediction system and stock market returns," *Review of Finance*, vol. 20, no. 4, pp. 1363–1381, 2016.
[39] V. V. Prasad, S. Gumparthi, L. Y. Venkataramana, S. Srinethe, R. M. SruthiSree, and K. Nishanthi, "Prediction of stock prices using statistical and machine learning models: a comparative analysis," *The Computer Journal*, vol. 65, 2021.

[40] E. Zong, "Forecasting daily stock market return using dimensionality reduction," *Expert Systems with Applications*, vol. 67, pp. 126–139, 2017.

[41] M. Hiransha, E. A. Gopalakrishnan, V. K. Menon, and K. P. Soman, "NSE stock market prediction using deep-learning models," *Procedia Computer Science*, vol. 132, pp. 1351–1362, 2018.

[42] S. Yauheniya, T. M. McGinnity, S. A. Coleman, and B. Ammar, "Forecasting movements of health-care stock prices based on different categories of news articles using multiple kernel learning," *Decision Support Systems*, vol. 85, pp. 74–83, 2016.

[43] B. Huang, Y. Huan, L. D. Xu, L. Zheng, and Z. Zou, "Automated trading systems statistical and machine learning methods and hardware implementation: a survey," *Enterprise Information Systems*, vol. 13, no. 1, pp. 132–144, 2018.

[44] X. Zhong and D. Enke, "Predicting the daily return direction of the stock market using hybrid machine learning algorithms," *Financ. Innov.,* vol. 5, pp. 1–20, 2019.

[45] M. Qiu, Y. Song, and F. Akagi, "Application of artificial neural network for the prediction of stock market returns: the case of the Japanese stock market," *Chaos, Solitons & Fractals*, vol. 85, pp. 1–7, 2016.

[46] K. Chourmouziadis and P. D. Chatzoglou, "An intelligent short term stock trading fuzzy system for assisting investors in portfolio management," *Expert Systems with Applications*, vol. 43, pp. 298–311, 2016.

[47] A. Arévalo, J. Niño, G. Hernández, and J. Sandoval, "High-frequency trading strategy based on deep neural networks," in *Intelligent Computing Methodologies*, D. S. Huang, K. Han, and A. Hussain, Eds., p. v9773, Springer. Berlin/Heidelberg, Berlin, Germany, 2016.

[48] P. Paik and B. Kumari, "Stock market prediction using ANN, SVM, ELM: a review," *IJETTCS*, vol. 6, pp. 88–94, 2017.

[49] D. Murekachiro, "A review of artifcial neural networks application to stock market predictions," *Network and Complex Systems*, vol. 6, p. 3002, 2016.

[50] E. K. Ampomah, Z. Qin, and G. Nyame, "Evaluation of tree-based ensemble machine learning models in predicting stock price direction of movement," *Information*, vol. 11, no. 6, p. 332, 2020.

[51] H. Basak, R. Kundu, P. K. Singh, M. Fazal, and W. Marcin, "A union of deep learning and swarm-based optimization for 3D human action recognition," *Scientific Reports*, vol. 12, p. 5494, 2022.

[52] A. Vulli, P. Naga, M. Sai, J. Shafi, and J. Choi, "Fine-tuned DenseNet-169 for breast cancer metastasis prediction using FastAI and 1-cycle policy," *Sensors*, vol. 22, p. 2988, 2022.

[53] D. Shah, H. Isah, and F. Zulkernine, "Stock market analysis: a review and taxonomy of prediction techniques," *International Journal of Financial Studies*, vol. 7, no. 2, p. 26, 2019.

[54] S. Basak, S. Kar, S. Saha, L. Khaidem, and S. R. Dey, "Predicting the direction of stock market prices using tree-based classifiers," *The North American Journal of Economics and Finance*, vol. 47, pp. 552–567, 2019.

[55] N. Milosevic, "Equity forecast: predicting long term stock price movement using machine learning," 2016, https://arxiv.org/abs/1603.00751.

[56] S. S. Choudhury and M. Sen, "Trading in Indian stock market using ANN: a decision review," *Advances in Modelling and Analysis A: General Mathematics*, vol. 54, pp. 252–262, 2017.

[57] S. Boonpeng and P. Jeatrakul, "Decision support system for investing in stock market by using OAA-neural network," in *Proceedings of the Eighth International Conference on Advanced Computational Intelligence (ICACI)*, pp. 1–6, Chiang Mai, Thailand, February 2016.

[58] R. Yang, L. Yu, Y. Zhao et al., "Big data analytics for financial Market volatility forecast based on support vector machine," *International Journal of Information Management*, vol. 50, pp. 452–462, 2019.

[59] M. Ballings, D. Van den Poel, N. Hespeels, and R. Gryp, "Evaluating multiple classifiers for stock price direction prediction," *Expert Systems with Applications*, vol. 42, no. 20, pp. 7046–7056, 2015.

[60] M. T. Leung, H. Daouk, and A.-S. Chen, "Forecasting stock indices: a comparison of classification and level estimation models," *International Journal of Forecasting*, vol. 16, no. 2, pp. 173–190, 2000.

[61] B. S. Omer, O. Murat, and D. Erdogan, "A deep neural-network based stock trading system based on evolutionary optimized technical analysis parameters," *Procedia Computer Science*, vol. 114, pp. 473–480, 2017.

[62] Q. Jiayu, W. Bin, and Z. Changjun, "Forecasting stock prices with long-short term memory neural network based on attention mechanism," *PLoS One*, vol. 15, Article ID e0227222, 2020.

[63] F. Ecer, S. Ardabili, S. S. Band, and A. Mosavi, "Training multilayer perceptron with genetic algorithms and particle swarm optimization for modeling stock price index prediction," *Entropy*, vol. 22, no. 11, p. 1239, 2020.

[64] O. Sagi and L. Rokach, "Ensemble learning: a survey, wiley interdiscip. Rev.-Data mining knowl," *Discover*, vol. 8, no. 4, Article ID e1249, 2018.

[65] X.-d. Zhang, A. Li, and R. Pan, "Stock trend prediction based on a new status box method and AdaBoost probabilistic support vector machine," *Applied Soft Computing*, vol. 49, pp. 385–398, 2016.

[66] J. Nobre and R. F. Neves, "Combining principal component analysis, discrete wavelet transform and xgboost to trade in the financial markets," *Expert Systems with Applications*, vol. 125, pp. 181–194, 2019.

[67] F. Zhou, Q. Zhang, D. Sornette, and L. Jiang, "Cascading logistic regression onto gradient boosted decision trees forforecasting and trading stock indices," *Applied Soft Computing*, vol. 84, Article ID 105747, 2019.

[68] K. K. Yun, S. W. Yoon, and D. Won, "Prediction of stock price direction using a hybrid GA-XGBoost algorithm with a three-stage feature engineering process," *Expert Systems with Applications*, vol. 186, Article ID 115716, 2021.

[69] B. Yang, G. Zi-Jia, and Y. Wenqi, "Stock market index prediction using deep neural network ensemble," in *Proceedings of the 36th Chinese Control Conference (CCC)*, pp. 3882–3887, Dalian, China, July 2017.

[70] J.-J. Wang, J.-Z. Wang, Z.-G. Zhang, and S.-P. Stock, "Stock index forecasting based on a hybrid model," *Omega*, vol. 40, no. 6, pp. 758–766, 2012.

[71] X. Chenglin, X. Weili, and J. Jijiao, "Stock price forecast based on combined model of ARI-MA-LS-SVM," *Neural Computing & Applications*, vol. 32, pp. 5379–5388, 2020.

[72] S. Tiwari, P. Rekha, and R. Vineet, "Predicting future trends in stock market by decision tree rough-set based hybrid system with hhmm," *International Journal of Electronics*, vol. 1, pp. 1578–1587, 2010.

[73] H. Markowitz, "Portfolio selection," *The Journal of Finance*, vol. 7, no. 1, pp. 77–91, 1952.

[74] R. C. Merton, "Lifetime portfolio selection under uncertainty: the continuous-time case," *The Review of Economics and Statistics*, vol. 51, no. 3, pp. 247–257, 1969.

[75] E. F. Fama, "Multiperiod consumption-investment decisions," *The American Economic Review*, vol. 60, no. 1, pp. 163–174, 1970.
[76] W. Chen, D. Li, and Y.-J. Liu, "A novel hybrid ICA-FA algorithm for multiperiod uncertain portfolio optimization model based on multiple criteria," *IEEE Transactions on Fuzzy Systems*, vol. 27, no. 5, pp. 1023–1036, 2019.
[77] A. D. Roy, "Safety first and the holding of assets," *Econometrica*, vol. 20, no. 3, pp. 431–449, 1952.
[78] H. Markowitz, *Portfolio Selection: Efficient Doversification Of Investments*, Wiley, Hoboken, NJ, USA, 1959.
[79] H. Konno and H. Yamazaki, "Mean-absolute deviation portfolio optimization model and its applications to Tokyo stock market," *Management Science*, vol. 37, no. 5, pp. 519–531, 1991.
[80] M. Speranza, "Linear programming models for portfolio optimization," *Finance*, vol. 12, pp. 107–123, 1993.
[81] W. Chen, Y. Wang, S. Lu, and M. Mehlawat, "A hybrid FA-SA algorithm for fuzzy portfolio selection with transaction costs, Ann," *Operations Research*, vol. 269, no. 1–2, pp. 129–147, 2018.
[82] W. Chen, Y. Wang, P. Gupta, and M. Mehlawat, "A novel hybrid heuristic algorithm for a new uncertain mean-variance-skewness portfolio selection model with real constraints," *Applied Intelligence*, vol. 48, no. 9, pp. 2996–3018, 2018.
[83] J. Zhou and X. Li, "Mean-semi-entropy portfolio adjusting model with transaction costs," *Journal of Digital Information Management*, vol. 2, no. 3, pp. 121–130, 2020.
[84] M. A. Akbay, C. B. Kalayci, and O. Polat, "A parallel variable neighborhood search algorithm with quadratic programming for cardinality constrained portfolio optimization," *Knowledge-Based Systems*, vol. 198, Article ID 105944, 2020.
[85] F. D. Paiva, R. T. N. Cardoso, G. P. Hanaoka, and W. M. Duarte, "Decision-making for financial trading: a fusion approach of machine learning and portfolio selection," *Expert Systems with Applications*, vol. 115, pp. 635–655, 2019.
[86] W. Wang, W. Li, N. Zhang, and K. Liu, "Portfolio formation with preselection using deep learning from long-term financial data," *Expert Systems with Applications*, vol. 143, Article ID 113042, 2020.
[87] F. Rosenblatt, "The Perceptron: a probabilistic model for information storage and organization in the brain," *Psychological Review*, vol. 65, no. 6, pp. 386–408, 1958.
[88] K. Crammer, O. Dekel, J. Keshet, S. S. Shwartz, and Y. Singer, "Online passive–aggressive algorithm," *Journal of Machine Learning Research*, vol. 7, pp. 551–585, 2006.
[89] L. Wang, H.-B. Ji, and Y. Jin, "Fuzzy Passive–Aggressive classification: a robust and efficient algorithm for online classification problems," *Information Sciences*, vol. 220, pp. 46–63, 2013.
[90] J. Xiao, C. He, X. Jiang, and D. Liu, "A dynamic classifier ensemble selection approach for noise data," *Information Sciences*, vol. 180, no. 18, pp. 3402–3421, 2010.
[91] F. Orabona, J. Keshet, and B. Caputo, "Bounded kernel-based online learning," *Journal of Machine Learning Research*, vol. 10, pp. 2643–2666, 2009.
[92] C. Gentile, "A new approximate maximal margin classification algorithm," *Journal of Machine Learning Research*, vol. 2, pp. 213–242, 2001.
[93] G. Cauwenberghs and T. Poggio, "Incremental and decremental support vector machine learning," *Advances in Neural Information Processing Systems*, vol. 13, pp. 409–415, 2000.
[94] C. P. Diehl and G. Cauwenberghs, "SVM incremental learning, adaptation and optimization," in *Proceedings of the International Joint Conference, Neural Networks*, pp. 2685–2690, Portland, OR, USA, July 2003.
[95] P. Laskov, C. Gehl, S. Kruger, and K. R. Muller, "Incremental support vector learning: analysis, implementation and applications," *Machine Learning*, vol. 7, pp. 1909–1936, 2006.
[96] E. Lughofer, "On-line evolving image classifiers and their application to surface inspection," *Image and Vision Computing*, vol. 28, no. 7, pp. 1065–1079, 2010.
[97] G. Heo and P. Gader, "Fuzzy SVM for noisy data: a robust membership calculation method," in *Proceedings of the 2009 IEEE International Conference on Fuzzy Systems*, pp. 431–436, Jeju, Korea, June 2009.
[98] M. Jiang, J. Liu, and L. Zhang, "An improved stacking framework for stock index prediction by leveraging tree-based ensemble models and deep learning algorithms," *Physica A*, 2019.
[99] J. Ayala, M. García-Torres, J. L. V. Noguera, F. Gómez-Vela, and F. Divina, "Technical analysis strategy optimization using a machine learning approach in stock market indices," *Knowledge-Based Systems*, vol. 225, Article ID 107119, 2021.
[100] M. Nabipour, P. Nayyeri, H. Jabani, A. Mosavi, and E. Salwana, "Deep learning for stock market prediction," *Entropy*, vol. 22, p. 840, 2020.
[101] J. Shen and M. O. Shafiq, "Short-term stock market price trend prediction using a comprehensive deep learning system," *J. Big Data*, vol. 7, pp. 1–33, 2020.
[102] Y. Kumar, A. Koul, R. Singla, and M. Fazal, "Artificial intelligence in disease diagnosis: a systematic literature review, synthesizing framework and future research agenda," *Journal of Ambient Intelligence and Humanized Computing*, 2022.
[103] J. Sun, H. Li, H. Fujita, B. Fu, and W. Ai, "Class-imbalanced dynamic financial distress prediction based on Adaboost-SVM ensemble combined with SMOTE and time weighting," *Information Fusion*, vol. 54, pp. 128–144, 2020.
[104] R. Yang, Yu Lin, Y. Zhao et al., "Big data analytics for financial Market volatility forecast based on support vector machine," *International Journal of Information Management*, vol. 50, pp. 452–462, 2020.
[105] D. K. Padhi, N. Padhy, A. K. Bhoi, J. Shafi, and M. F. Ijaz, "A fusion framework for forecasting financial market direction using enhanced ensemble models and technical indicators," *Mathematics*, vol. 9, p. 2646, 2021.
[106] N. Srinivasu, P. Naga, and W. Kim, "Classification of skin disease using deep learning neural networks with MobileNet V2 and LSTM," *Sensors*, vol. 21, no. 8, p. 2852, 2021.
[107] Ijaz, M. Fazal, M. Attique, and Y. Son, "Data-driven cervical cancer prediction model with outlier detection and oversampling methods," *Sensors*, vol. 20, no. 10, p. 2809, 2020.
[108] Ta-Lib, "Technical analysis library," 2021, http://www.ta-lib.org.
[109] L. Malagrino, N. Roman, and A. Monteiro, "Forecasting stock market index daily direction: a Bayesian network approach," *Expert Systems with Applications*, vol. 105, pp. 11–22, 2018.
[110] P.-Y. Zhou, K. Chan, and C. Ou, "Corporate communication network and stock price movements: insights from data mining," *IEEE Transactions on Computational Social Systems*, vol. 5, no. 2, pp. 391–402, 2018.

[111] Q. Wang, W. Xu, and H. Zheng, "Combining the wisdom of crowds and technical analysis for financial market prediction using deep random subspace ensembles," *Neurocomputing*, vol. 299, pp. 51–61, 2018.

[112] R. Ren, D. Wu, and T. Liu, "Forecasting stock market movement direction using sentiment analysis and support vector machine," *IEEE Systems Journal*, vol. 13, 2018.

[113] H. Hu, L. Tang, S. Zhang, and H. Wang, "Predicting the direction of stock markets using optimized neural networks with Google trends," *Neurocomputing*, vol. 285, 2018.

[114] T. Fischer and C. Krauss, "Deep learning with long short-term memory networks for financial market predictions," *European Journal of Operational Research*, vol. 270, no. 2, pp. 654–669, 2018.

Hindawi
Computational Intelligence and Neuroscience
Volume 2022, Article ID 5507951, 8 pages
https://doi.org/10.1155/2022/5507951

Research Article

The Application of Internet of Things Data Analysis in the Development of International Trade

Hao Qiuxia and Hou Yujie

School of International Business, Qingdao Huanghai University, Qingdao 7266000, Shandong, China

Correspondence should be addressed to Hao Qiuxia; haoqx@qdhhc.edu.cn

Received 14 March 2022; Accepted 20 May 2022; Published 20 June 2022

Academic Editor: Guobin Chen

There are some problems in the application of current data analysis methods in international economy and trade, such as low service efficiency, low data utilization, and low degree of intelligence. Based on this, this paper studies the application of the Internet of things data analysis method in international trade development and economic and industrial growth. Firstly, the Internet of things economic data analysis model (IOT-EET model) based on simulated annealing early warning algorithm is established to store and analyze the data in the whole chain of international trade. Then, combined with the analysis methods of international trade economic data over the years, it is fed back to the IOT-EET model for error calibration. Finally, relevant experiments are designed to analyze the correlation between international trade development and national economic growth. The results show that compared with the traditional method based on module data analysis, this IOT-EET model can realize the correlation matching analysis of the data involved in the development of international trade in combination with the Internet of things technology and analyze the factors affecting international trade transactions. Therefore, it has the advantages of good reliability and strong pertinence.

1. Introduction

At present, under the impact of the new generation of information and communication technology, the Internet of things is accelerating its penetration into urban management, new energy, medical treatment, manufacturing, and other fields. Especially in recent years, with the emergence of developed countries and regions in Taiwan, the relevant policies of the Internet of things have been strategically laid out. We hope to seize the opportunity in the new round of information industry development, and the Internet of things industry in Tongqiu is growing rapidly. The Internet of things has become the third wave of the world information industry after computers and the Internet. With the advent of economic globalization and the rapid development of Internet of things data analysis technology, international trade also presents great changes in data analysis methods and business processing [1]. In recent years, with the rapid development of Internet of things technology and the emergence and application of trade economic analysis methods and the IOT-EET model, international trade is also facing an important transformation of digital development [2]. Therefore, how to share trade data with high accuracy has become an important indicator to measure the accuracy of trade data [3]. On the other hand, although there are many international trade economic growth analysis models, they can not completely solve the practical problems [4]. For example, in the analysis of the development potential of international trade, most of the current analysis models belong to customized analysis models, so there will be large loopholes in the actual application process [5]. Based on this background, this paper studies the interaction degree analysis system of international trade and economic development and puts forward the Internet of things economic data analysis model (IOT-EET model) based on Internet of things data analysis, which can quantitatively analyze and characterize the internal interaction degree of international trade and data analysis.

In this paper, the application of the IOT-1 algorithm in the process of international economic growth is divided into four parts: slow economic growth and low efficiency of international trade. Section 1 introduces the research background, research route, and innovation. Section 2 objectively introduces the evaluation methods of international trade economic growth and the research status of data mining methods in international trade. In Section 3, the IOT-EET model based on simulated annealing early warning algorithm is constructed, and the high-dimensional multivariate analysis system is established by using the "Newton avige" high-dimensional equation method. Section 4 tests the data peacekeeping system of international trade and economic growth constructed in this paper, analyzes the results, and draws a conclusion.

At present, the mainstream international trade economic growth analysis model (mainly a quantitative data analysis model based on an intelligent dimension collaborative algorithm) has the disadvantages of small application scope and uncontrollable error rate. The innovation of this paper is to build a data analysis model of the correlation between international trade and economic growth through simulated annealing early warning algorithm, combined with the IOT-EET model in the field of artificial intelligence big data and Internet of things technology. On this basis, the model can not only record and store the data between international trade and economic growth in multiple regions, but we can also make full use of the characteristics of economic growth between each region and the normalization standard of existing economic models to realize intelligent analysis through the IOT-EET model. On the other hand, using Newton factor quantitative index to complete the factor reliability analysis of international trade and economic growth can effectively reduce the error analysis of trade and economic data.

This paper studies the application of the Internet of things data analysis method in the development of international trade and economic and industrial growth. The economic data analysis model of the Internet of things (IOT-EET model) based on simulated annealing early warning algorithm is established. The innovation contribution is that the model has the advantages of high precision and wide application range. Compared with the traditional research methods of international trade and economic growth based on regional unconventional data analysis, the IOT-EET model can realize high-dimensional reliability analysis and adjustment in the process of the impact of international trade on the local economy. It is helpful for the application of current data analysis methods in international economy and trade. It provides a solution reference for the problems of low service efficiency, low data utilization, and low degree of intelligence.

2. Related Work

In the process of market-oriented economic analysis of existing international trade, there are problems of low data utilization, slow economic growth, and low service efficiency. Most scholars have innovated the internal data analysis methods of international trade and economic growth and tried to solve the above problems [6]. According to the characteristics of the existing international trade system and the differentiated characteristics of economic globalization, Rocki et al. build a data analysis model based on the method of national system construction to realize the analysis and quantitative representation of the responsibilities of different countries in international trade [7]. Aiming at the low efficiency of data analysis strategy in the process of international trade and economic development, according to the macrocontrol strategy in economics, Rocki et al. put forward an international trade and economic analysis dam model based on high-latitude analysis strategy, which realizes the high accuracy analysis of trade data by combining the idea of the marginal effect of dam burst [7]. Lin et al. found that most countries have large trade deficits in the process of international trade transactions, so they proposed an international trade rationalization system based on national conditions and macroeconomic theory. The system clearly combines the Internet of things data analysis technology to realize the rationalization prediction of international trade, but it needs to know the economic data of different industries [8]. Cao and other scholars put forward an Internet of things data analysis model combining artificial intelligence technology and strategy in order to realize the high-latitude application and analysis of data analysis methods in the trade economy. The model can predict the economic demand of different industries through trade data information, but the accuracy of prediction is related to the type of input parameters [9]. In order to effectively improve the accuracy of international trade, Peng et al. realize the interconnection of economics and trade in different regions through the Internet of things technology and then realize the calibration and control of different types of databases with the help of data analysis strategy [10]. Aiming at the problem of low data utilization in the development of international trade, Hoffmann C and other scholars put forward an orthogonal decomposition matching adaptive model, which can effectively insert and guide different types of databases and realize high accuracy analysis of different trade data information [11]. Siddig and other scholars achieve high accuracy at different levels through serial interworking of various types of data [12]. In order to further study the influencing factors in the process of international trade and economic development, scholars such as Gilliland combined with the idea of the economic data analysis model of the Internet of things proposed a serial interworking method based on reliability analysis. This method can effectively improve the potential income space of international trade, but the industry needs to be limited [13]. Aiming at the problem of high cost growth of international trade, Rui Wa and other scholars adopted different types of correlation data models and proposed an ultrahigh-precision data exchange method. This method can effectively improve the high-precision data characteristics of different trade data, but it is necessary to conduct high-intensity analysis on different data analysis [14]. According to the averaging shortcomings of different international trade in development, Paroussos and other scholars put forward a collaborative innovation

method of high-value trade based on the CNN network. Experiments show that international trade can indirectly support the improvement of the local economy [15]. In order to solve the problems of the high-value analysis industry in the development of international trade, Feuerbacher A and other scholars put forward an economic growth innovation evaluation model based on the characteristics of regional development, so as to strengthen the analysis and intelligent management of the construction of international trade system [16].

Based on the above research results, we can know that the current mainstream international trade economic growth analysis model (mainly based on quantitative data evaluation and analysis model) has the disadvantage of the small scope of application [17–19]. On the other hand, in the quantitative evaluation of international trade and economic development, different types of innovative analysis methods have high-value cultivation strategies with low value and low accuracy, which leads to the improvement of the overall computational complexity and the internal analysis efficiency [20, 21]. Therefore, it is of great significance to study the application of the IOT-EET model based on the Internet of things data analysis strategy in the development of international trade.

3. Methodology

3.1. Application of IOT-EET Model Based on Simulated Annealing Early Warning Algorithm in Economic Growth Analysis. Simulated annealing early warning algorithm is a commonly used algorithm for data analysis. This method solves the calculation problems with high dimension and large amount of data by simulating the idea of how to effectively extinguish the fire source in the effective space and realizes the sampling solution of complex problems. The Internet of things economic data analysis model (IOT-EET) includes three significant features. The first is "interactivity," which guarantees and stipulates the iterative data acquisition method of economic entities. In this model, one of the representative features is to maximize the use of utility economic data. International trade also follows the decision-making principle of cost minimization and also includes economic entities such as government, trade organizations, importers, and exporters, which respond to price changes [22]. Secondly, it is "discrete," which means that it includes the discrete analysis of demand and supply. Many prices in the model are determined by both supply and demand, and the price change finally makes the market realize equilibrium [23]. Finally, it is "normalized" because the model reflects the actual trade data and the economic problems existing in the actual region, which is closer to the current situation of economic development. In addition, it also involves industrial policy, income distribution, trade policy, etc. [24]. Therefore, the IOT-EET model combined with simulated annealing early warning algorithm can well solve the problem of super precision noncorrelation between international trade and regional economic growth. The data correlation analysis process of the IOT-EET model based on simulated annealing early warning algorithm in international trade and economic growth is shown in Figure 1.

3.2. Data Analysis Process of IOT-EET Model in International Trade and Economic Growth. In the process of international trade, the economic data of different regions have different characteristics, and their correlation also has certain laws. For example, the economic data of the logistics industry in regions with large exports to the manufacturing industry will increase more significantly. Therefore, after the IOT-EET model is established. It is necessary to quantitatively discuss the economic data analysis process of the IOT-EET model in international trade and economic growth.

According to the necessary conditions of the macroeconomic model in trade economics, it is necessary to design the upper limit value, coordination strategy, and error analysis system function of the IOT-EET model. Therefore, the upper limit function $R(x)$ of economic growth, the synergy strategy function $T(x)$, and the error analysis system function $Y(x)$ are set as follows:

$$R(x) = \frac{\sum_{k=1}^{p} x_k^2 / x_{k+1}^2 / k\overline{x}_p + 1 / \sum_{p=1}^{k} k\overline{x}_p}{2},$$

$$T(x) = \frac{p!/1 + \overline{x}_p + \sqrt{x_1 + x_k + x_p / \overline{x}_{p+k-1}}}{\overline{x}_{p+k}}, \tag{1}$$

$$Y(x) = \sum_{k=1}^{p} \left(x_k - \overline{x}_p\right)^2 + \sum_{k=1}^{p} \left(x_k + \overline{x}_p\right)^2 + \frac{1}{(k+1)\overline{x}_p},$$

where x_k is the iterative international trade volume data, p is the overall number of international trade transactions, k is the number of international trade service types, and $\overline{x}_p$ is the average error data of regional quarterly trade and economic growth. After the standard characteristic analysis of the above system function, the corresponding expression is

$$R'(x) = \frac{k - \sum_{k=1}^{p} x_k^2 / x_{k+1}^2}{1 + k\sum_{k=1}^{p}\left(x + \overline{x}_p / 1 + \overline{x}_p\right)^2},$$

$$T'(x) = \sqrt{\frac{(p+1)!}{p + \overline{x}} + \frac{x_1 + x_k + x_p}{\overline{x}_{p+k-1}}}, \tag{2}$$

$$Y'(x) = \sqrt{2 + \sum_{k=1}^{p} \left(x_k + \overline{x}_p\right)^2 + \frac{1}{1 + k\sum_{k=1}^{p}\left(x + \overline{x}_p / 1 + \overline{x}_p\right)^2}}.$$

After completing the regional international trade indicators, it is necessary to retrieve the correlation matching characteristics of different types of international trade and economic growth data and realize multidimensional division according to the growth rate. After ultrahigh analysis, it is necessary to perturb and match its internal trade deficit data and input its data center group into the IOT-EET model. The simulation analysis results of the simulation data group on the analysis efficiency of international trade and economic development are shown in Figure 2 (where *A-J* is the

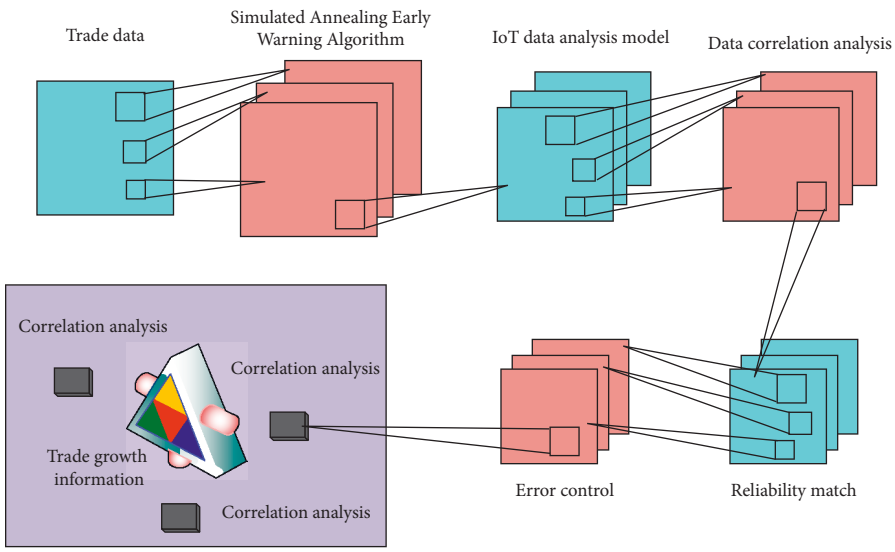

Figure 1: Operational analysis principle of IOT-EET model based on simulated annealing early warning algorithm.

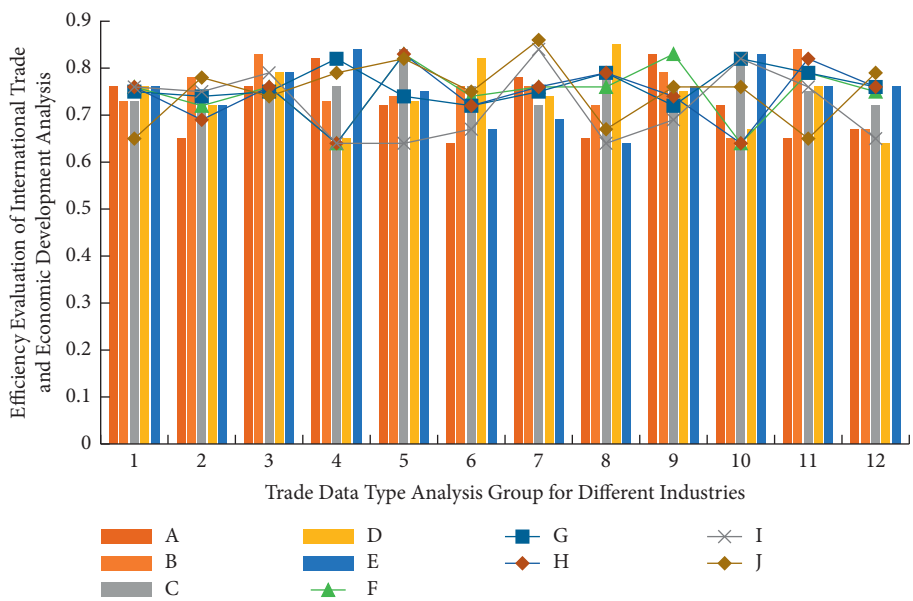

Figure 2: Simulation analysis results of the IOT-EET model on the analysis efficiency of international trade and economic development.

standard discriminant index with 10 groups of dimensions gradually increasing).

It can be seen from Figure 2 that among the 12 groups of databases, the internal relevance is quite different from the dimension of 10 indicators, but the internal data change trends are similar, both within a relatively stable change range, and the data consistency of the fourth group of databases is the highest, because after setting the operation threshold. It is also necessary to give priority to the relevant data affecting international trade and economic growth in combination with different types of matching degrees and combine them with numerical change indicators for variable weight analysis. The trade deficit tracking function $F(x)$, economic growth classification function $G(x)$, and trade error evaluation function $H(x)$ used in the vector comparison process in the above simulation analysis stage are

$$F(x) = \sqrt{1 + \frac{\sqrt{|x|^2 + m|x| + \sqrt{|x|}}}{\sqrt{k|x|} + m|x|^2 + \sqrt{k}}},$$
$$G(x) = \frac{\sqrt{m|x|^2 + m|x| + \sqrt{|x|}} + \sqrt{\sum_{k=1}^{m} 1/m|x| + k|x|^2 + \mathrm{mk}}}{3\mathrm{mk}}, \quad (3)$$
$$H(x) = \frac{\sqrt{kG^2(x) + mF(x)/kG(x) + \mathrm{mx}} + \sqrt{(1 + H(x)/\mathrm{km})}}{m},$$

where $|x|$ is the high-precision matching grade index of international trade economic data vector, m and k are the type and upper limit value of data in the process of international trade economic growth, respectively. After fuzzy analysis and processing of the above-mentioned three functions, the corresponding expression is

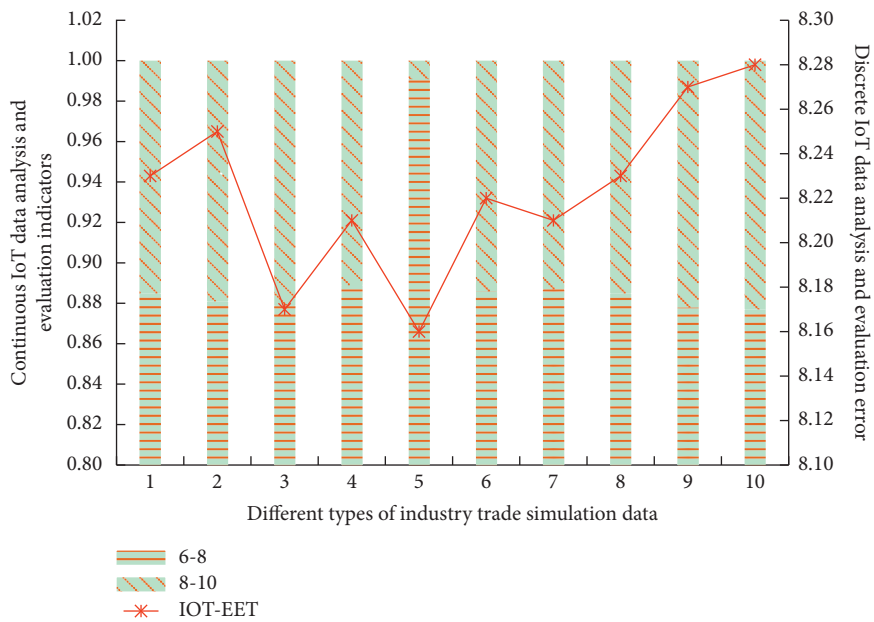

Figure 3: Economic growth simulation analysis of two types of random international trade economic data by IOT-EET model.

$$F'(x) = \frac{|x|^2 + m|x| + \sqrt{|x|}}{k|x| + m|x|^2 + k},$$

$$G'(x) = k\sqrt{\sum_{k=1}^{m} \frac{\sqrt{m|x|^2 + m|x| + \sqrt{|x|}}}{m|x| + k|x|^2 + \mathrm{mk}} + \frac{1}{\sqrt{m|x|} + k|x|^2 + \mathrm{mk}}}, \quad (4)$$

$$H'(x) = \frac{G(\mathrm{kx})}{mF(\mathrm{kx}) + kH(\mathrm{kx})} + \sum_{k=1}^{m} \frac{H'(x)}{mF(\mathrm{kx}) + kG(\mathrm{kx})}.$$

In this stage, the simulation analysis results of the IOT-EET model on the economic growth of two types of random international trade economic data are shown in Figure 3.

It can be seen from Figure 3 that under the IOT-EET model based on simulated annealing early warning algorithm, there are certain differences in international trade and economic data among different regions. Specifically, the content is inconsistent with the value of international trade and economic information stored in the cloud in terms of analysis type and standardized evaluation.

The existing computer cannot reach the level of complete ultrahigh precision in the process of matching and analyzing trade data. With the increase of simulation analysis times, the internal correlation evaluation and error analysis of different types of data groups show different trends. Different types of intersections appear under different simulation times.

3.3. Simulation Verification Process of International Trade Economic Growth Analysis Model Combined with IOT-EET Model. After adopting the trade economic data analysis model based on Internet of things technology and simulated annealing early warning algorithm, in order to further analyze the internal relationship between regional trade economy and industry development, it is also necessary to reverse verify the analysis results of its international trade differentiated data in combination with the Internet of things data verification strategy, Therefore, it is necessary to analyze a number of economic differentiation characteristic data packets within international trade. The analysis process is shown in Figure 4.

In the international trade and economic transaction data of different industries (such as manufacturing industry, household industry, and digital industry), the corresponding identification error rate and correlation evaluation results are different, because the calculation and identification of different types of similarity can be based on the difference and similarity of international trade data information, and intelligent high-precision classification is carried out through the economic data analysis model of the Internet of things. The classification simulation analysis results after correction are shown in Figure 5.

It can be seen from Figures 4 and 5 that the classification effect and coupling correlation degree of the data analysis results of local and regional international trade data under the IOT-EET model are different because the data obtained by the IOT-EET model analysis method have carried out the high-precision standardized classification of different types of data groups in the process of analysis. Therefore, when it is reflected in the final data analysis results, the corresponding differences will not change greatly.

Finally, in the prediction and analysis of international trade volume data, the trade accuracy evaluation function $C(x)$ and noncorrelation function $V(x)$ based on simulated annealing early warning algorithm are introduced, and their mathematical expressions are as follows:

$$C(x) = \sqrt{\frac{1}{\sqrt{\sum_{j=1}^{p}\left(jx_j^2 + \overline{x}^3\right)}} + \frac{1}{\sqrt{\sum_{k=1}^{p}\left(kx_k^2 - \overline{x}^2\right)}}},$$

$$V(x) = \sum_{k=1}^{p}\left(kx_k^2 - \overline{x}^2\right)^2 - \frac{1}{1 + p\overline{x}}, \quad (5)$$

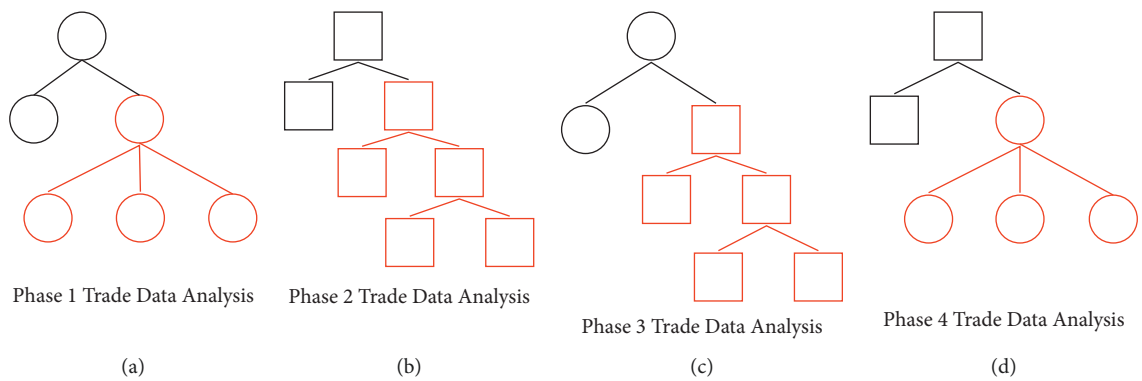

Figure 4: The process of analyzing the data package of multiple economic differentiation characteristics within international trade. (a) Phase 1 Trade data analysis. (b) Phase 1 Trade data analysis. (c) Phase 1 Trade data analysis. (d) Phase 1 Trade data analysis.

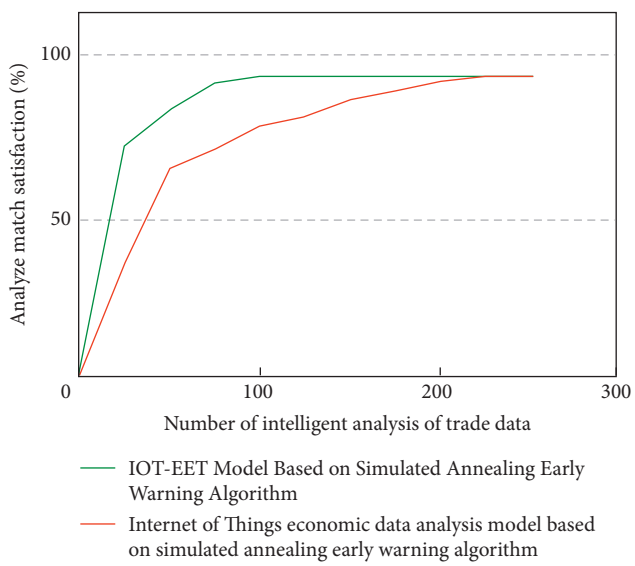

Figure 5: Classification simulation analysis results after correction of two different models.

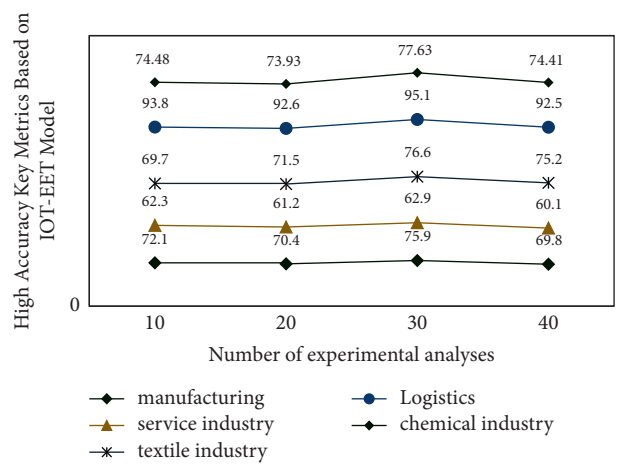

Figure 6: Preliminary experimental analysis results of 3 sets of experimental data.

where x represents the cluster samples of different trade and economic growth data groups, k and j represent different data cluster numbers, and p represents the maximum number. In the process of reducing the error of the IOT-EET model and correcting the results of the overall international trade operation and analysis function, it is necessary to normalize the sample data. The intelligent data set of trade center classification used in this process is shown in the following expression:

$$P(x) = \frac{l + \mathrm{rx}}{lx + r} + \frac{\sum_{i=1}^{m} (x-1) + \sum_{i=1}^{r} x}{m + r}. \quad (6)$$

Here, x represents different types of international trade and economic growth data sets, l and r represent different trade transaction rule factors.

4. Result Analysis and Discussion

4.1. Confirmatory Test of Correlation Analysis between International Trade and Economic Growth Based on IOT-EET Model. After constructing the international trade and economic growth evaluation system based on the IOT-EET model, in order to further verify the accuracy and error of its analysis model, this study sets different parameters to verify the data, and the internal correlation between different data groups is random. Therefore, for different types of trade data indicators, their internal relevance shows an obvious change trend. The preliminary analysis results of international trade data of different industries during the experiment are shown in Figure 6, in which the horizontal axis represents the number of experiments and the vertical axis represents the key measurement indicators of high accuracy based on the IOT-EET model.

It can be seen from Figure 6 that under the simulated annealing early warning algorithm, with the increase of the number of experiments, the analysis type data of international trade show different types of change trends, and the number of internal correlation consistent data shows a trend of decreasing first and then stable, compared with the data group without correction factor. There are more standardized correlation degree and economic growth data in the international trade data set with a correction factor, because the operation method adopted this time is the international trade economic correlation analysis model of the improved IOT-EET model combined with the simulated

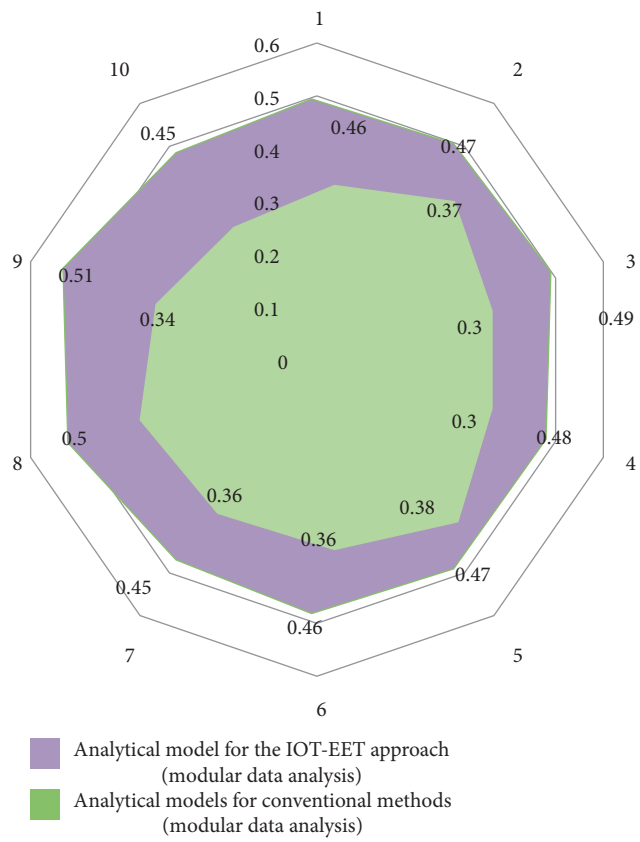

Figure 7: Analysis of the correlation error degree of the experimental results.

annealing early warning algorithm, and the threshold parameters of different numbers of data envelopment sets are set. To characterize the relevance and relevance between international trade and local economic growth.

4.2. Experimental Results and Analysis. In the process of analyzing the experimental results, this study is based on the revenue and expenditure data disclosed by all scenic spots in Beijing in recent 5 years. The experimental group adopts the IOT-EET model and the control group adopts the analysis model of the conventional method (modular data analysis). The analysis results are shown in Figure 7. In Figure 7, purple represents the analysis model of the IOT-EET method, and green represents the analysis model of the conventional method.

Through the analysis of the results in Figure 7, it can be found that under the IOT-EET model, in the process of efficient exchange of different types of international trade data, the error rate of the final result will be significantly reduced, which is due to the significant differences in the internal relevance of different types of data groups.

Compared with the traditional research methods of international trade and economic growth based on regional unconventional data analysis, the EET model of the Internet of things can realize high-dimensional reliability analysis and adjustment in the process of the impact of international trade on the local economy. This is helpful to the application of current data analysis methods in international economy and trade. It provides a reference for solving the problems of low service efficiency, low data utilization, and low degree of intelligence.

5. Conclusion

At present, there are some problems in international trade in terms of service volume and economic growth, such as low service efficiency, poor coordinated development, and slow economic growth. Compared with the problems of low data analysis dimension and poor reliability in the current mainstream international trade economic growth analysis model, this paper studies the correlation analysis system between international trade and economic industrial growth based on Computable General Equilibrium (IOT-EET) model. Firstly, the IOT-EET data analysis model based on simulated annealing early warning algorithm is established to carry out multiscale collaborative processing of different types of international trade data information to realize the intelligent classification of the data. Then, combined with the international trade economic data and local economic growth rate in previous years, it is fed back to the IOT-EET model for error analysis, Finally, relevant experiments are designed to analyze the matching and reliability of international trade and local economic growth. The results show that compared with the traditional research method of international trade and economic growth based on regional unconventional data analysis, this IOT-EET model can realize high-latitude reliability analysis and adjustment in the process of the impact of international trade on the local economy. Therefore, it has the advantages of high accuracy and wide application range. However, this study does not consider the multiple security of international trade data. Therefore, in terms of strengthening the security of international trade and regional economic growth in different regions, an in-depth dimensional analysis is needed.

Data Availability

The data used to support the findings of this study are available from the corresponding author upon request.

Conflicts of Interest

The authors declare that they have no conflicts of interest.

References

[1] N. I. Tziavos, H. Hemida, N. Metje, and C. Baniotopoulos, "Non-linear finite element analysis of grouted connections for offshore monopile wind turbines," *Ocean Engineering*, vol. 171, no. JAN.1, pp. 633–645, 2019.

[2] T. Evangelos, A. N. Antonakis, B. Ismini et al., "ProteoSign v2: a faster and evolved user-friendly online tool for statistical analyses of differential proteomics," *Nucleic Acids Research*, vol. 49, no. W1, p. W1, 2021.

[3] F. Khalid, S. R. Hasan, S. Zia, O. Hasan, F. Awwad, and M. Shafique, "MacLeR: machine learning-based runtime hardware trojan detection in resource-constrained IoT edge devices," *IEEE Transactions on Computer-Aided Design of*

Integrated Circuits and Systems, vol. 39, no. 11, pp. 3748–3761, 2020.

[4] R. B. Staszewski, Y. H. Liu, V. K. Purushothaman, and C. Bachmann, "Design and analysis of a DCO-based phase-tracking RF receiver for IoT applications," *IEEE Journal of Solid-State Circuits*, vol. 759, Article ID 143512, 2019.

[5] T. Zhang, Y. Ma, and A. Li, "Scenario analysis and assessment of China's nuclear power policy based on the Paris Agreement: a dynamic CGE model," *Energy*, vol. 228, Article ID 120541, 2021.

[6] G. Li, R. Zhang, and T. Masui, "CGE modeling with disaggregated pollution treatment sectors for assessing China's environmental tax policies," *The Science of the Total Environment*, vol. 761, Article ID 143264, 2021.

[7] J. M. P. Pintor and J. P. C. Garrinhas, "Eurocity Elvas, Badajoz and Campo Maior (EUROBEC): the socio-economic and territorial reality of a new cross-border governance structure in Portugal," *Journal of Interfaces in Arts and Culture*, vol. 4, no. 1, p. 73, 2021.

[8] V. Komarova, N. Selivanova-Fyodorova, O. Ruza, and J. Kaźmierczyk, "Modern trends in the economic differences between countries and within them: comparison of the world and the European Union," *Entrepreneurship and Sustainability Issues*, vol. 8, no. 3, pp. 110–121, 2019.

[9] Z. Cao, G. Liu, S. Zhong, H. Dai, and S. Pauliuk, "Integrating dynamic material flow analysis and computable general equilibrium models for both mass and monetary balances in prospective modeling: a case for the Chinese building sector," *Environmental Science & Technology*, vol. 53, no. 1, pp. 224–233, 2019.

[10] D. Peng, Q. Yang, H. J. Yang, H. Liu, Y. Zhu, and Y. Mu, "Analysis on the relationship between fisheries economic growth and marine environmental pollution in China's coastal regions," *The Science of the Total Environment*, vol. 713, no. Apr.15, pp. 136641.1–136641.9, 2020.

[11] C. Hoffmann, "Estimating the benefits of adaptation to extreme climate events, focusing on nonmarket damages[J]," *Ecological Economics*, vol. 164, no. OCT, pp. 106250.1–106250.20, 2019.

[12] K. Siddig, D. Stepanyan, M. Wiebelt, H. Grethe, and T. Zhu, "Climate change and agriculture in the Sudan: impact pathways beyond changes in mean rainfall and temperature," *Ecological Economics*, vol. 169, 2020.

[13] T. E. Gilliland, J. N. Sanchirico, and J. E. Taylor, "Market-driven bioeconomic general equilibrium impacts of tourism on resource-dependent local economies: a case from the western Philippines," *Journal of Environmental Management*, vol. 271, no. 4, Article ID 110968, 2020.

[14] W. A. Rui, B. Hd, G. Yong, X. Yang, and T. Xu, "Impacts of export restructuring on national economy and CO 2 emissions: a general equilibrium analysis for China," *Applied Energy*, vol. 248, pp. 64–78, 2019.

[15] L. Paroussos, K. Fragkiadakis, and P. Fragkos, "Macro-economic analysis of green growth policies: the role of finance and technical progress in Italian green growth," *Climatic Change*, vol. 160, 2020.

[16] A. Feuerbacher, S. Mcdonald, C. Dukpa, and H. Grethe, "Seasonal rural labor markets and their relevance to policy analyses in developing countries," *Food Policy*, vol. 93, 2020.

[17] H. Liu, S. E. Shladover, X. Y. Lu, and X. D. Kan, "Freeway vehicle fuel efficiency improvement via cooperative adaptive cruise control," *Journal of Intelligent Transportation Systems*, vol. 25, no. 6, pp. 574–586, 2021.

[18] I. V. Karavaeva, E. A. Ivanov, and M. Y. Lev, "Modern trends for assessing the maximum permissible indicators of economic security in Russia," *Economics and Management: Problems, Solutions*, vol. 1, no. 3, pp. 36–53, 2021.

[19] T. Dogru, E. A. Marchio, U. Bulut, and C. Suess, "Climate change: v," *Tourism Management*, vol. 72, no. JUN, pp. 292–305, 2019.

[20] V. Ramos, M. Ruiz-Pérez, and B. Alorda, "A proposal for assessing digital economy spatial readiness at tourism destinations," *Sustainability*, vol. 13, 2021.

[21] V. Matyushok, V. Krasavina, A. Berezin, and J. Sendra García, "The global economy in technological transformation conditions: a review of modern trends," *Economic Research-Ekonomska Istraživanja*, vol. 34, no. 1, pp. 1471–1497, 2021.

[22] X. Li, S. Celotto, D. Pizzol et al., "Metformin and health outcomes: An umbrella review of systematic reviews with meta-analyses," *European Journal of Clinical Investigation*, vol. 51, no. 7, Article ID e13536, 2021.

[23] H. Hu and L. Tang, "Edge intelligence for real-time data analytics in an IoT-based smart metering system," *IEEE Network*, vol. 34, no. 5, pp. 68–74, 2020.

[24] B. K. Chae, "The evolution of the Internet of Things (IoT): a computational text analysis," *Telecommunications Policy*, vol. 43, 2019.

Hindawi
Computational Intelligence and Neuroscience
Volume 2022, Article ID 1707259, 11 pages
https://doi.org/10.1155/2022/1707259

Research Article

The Application of Internet of Things in Robot Route Planning Based on Multisource Information Fusion

Yunfeng Yao,[1] Na He,[2] and Min Zhang[3]

[1]*College of Mechanical and Electrical Engineering, Jiaxing Nanhu University, Jiaxing, Zhejiang 314001, China*
[2]*Gongqing Institute of Science and Technology, Gongqingchengshi, Jiangxi 332020, China*
[3]*Dean's Office of Henan Polytechnic University, Henan Polytechnic University, Jiaozuo, Henan 454000, China*

Correspondence should be addressed to Min Zhang; zhangmin@hpu.edu.cn

Received 21 March 2022; Revised 26 April 2022; Accepted 23 May 2022; Published 17 June 2022

Academic Editor: Guobin Chen

With the advent of the Internet of Everything era, multi-information integration, and development, technology has penetrated into all aspects of life, promoting the continuous progress of social development, and people's requirements for a happy life are getting higher and higher. In this, robots play an extremely important role. It is especially important for the route planning of robots. This paper analyzes the DWA dynamic window algorithm through the verification of the global route planning algorithm, namely, the Dijkstra algorithm and the A^* algorithm; the verification of the local route planning algorithm; the application of the DWA mobile robot algorithm in the robot route planning. The three aspects of the evaluation function are described by a formula, the experimental simulation is carried out, the relationship between the evaluation function terms is obtained, and the feasibility of the algorithm is verified.

1. Introduction

With the continuous progress of the times, the continuous development of science and technology, and the continuous improvement of people's living needs, the participation of robots in life is getting higher and higher, and the practical application scenarios of robots are becoming more and more extensive. It is a very obvious trend that the application scenarios of robots have begun to shift to the service industry on a large scale and are no longer limited to industrial production. This also means that the robot industry has become one of the important industries for China's future development and will play an important role in promoting China's industrial transformation and upgrading, and the replacement of labor by robots will also be the trend of future manufacturing.

Nowadays, all kinds of robots participate in various activities in people's social life, such as mobile robot [1], rehabilitation robot [2], lower limb robot [3], experimental quantitative robot [4], distributed multirobot [5], robot-assisted surgery [6]. These versatile robots not only replace people in repetitive and intensive manual labor but also greatly increase the efficiency of manufacturing, reduce labor costs, and play an important role in social development.

The route planning technology is one of the core contents of the research in the field of robotics, and the robot must navigate according to the planned path. Different types of robots adapt to different route planning. Path planning for transportation systems [7] can reduce hazards on turn-limited routes [8]. Multimodal transport route planning [9] integrates personalized route planning methods with different decision-making strategies [10] to solve the problem of optimizing the route planning of automatic guided vehicles (AGVs) in semiconductor manufacturing plants [11]. The comprehensive three-dimensional analysis of urban environment based on network [12] describes the road for strangers in the city, which requires completely different cognitive processes and strategies from the actual walking to the destination, and can highly adapt to the degree of perceptual information available for the task [13].

With the continuous development of communications, the Internet of Things [14] realized by the latest developments in RFID, smart sensors, communication technologies,

and Internet protocols, as a belated communication worldview [15], is closely related to many fields [16]. The proposed information fusion method is applied to formation drill ability prediction [17], state of the art in robust speech processing [18], constraint fusion analysis [19], Bayesian network fault diagnosis method based on multisource information fusion [18, 20], and integrating a large number of different heterogeneous terminal systems to develop a large number of digital services [21]. Accompanying the rapid growth in the number of sensors deployed globally [22] is the discovery of services and on-demand provisioning of missing functions in an infrastructure consisting of a large number of networked, resource-constrained devices [23].

2. About the Theoretical Basis

2.1. Information Fusion

2.1.1. Advantages and Applications of Multisource Information Fusion Technology. The sensor collects multiple information and confirms different sensor systems multiple times so as to improve the reliability and detection capability of the sensor system, improve the quality and credibility of the system detection data and information, improve the system's perception of specific data and the ability of data logical reasoning, speed up the accuracy and response speed of the system, and improve the detection reliability of the system. Data fusion of data information obtained by sensors from different information sources improves the system's information decision-making and analysis capabilities, shortens the system's information response delay time, and improves the system's information detection and processing performance. Information fusion processing is an information processing behavior that imitates biological environmental conditions. At the same time, information fusion processing can also be regarded as a comprehensive optimization process of information processing and multisource collection. Its purpose is to help people make accurate decisions and accurately judge the behavior of individuals or groups by optimizing information.

The most beneficial application of multisource information fusion is in medicine. On the one hand, it directly measures human physiological and medical data through multiple medical sensor probes and then simultaneously transmits it to the upper computer operation interface of patients, family members, and even doctors and community doctors. Based on the measured physiological and physical data, a conclusion is drawn whether the body meets the health standards. The physiological data and the measured waveform image data transmitted by the doctor through the probe can effectively and in real time help the patient determine the current user's physical health status, and the patient can also directly obtain information and results about their own health assessment; on the other hand, it is important to help patients retrieve similar symptoms and medical waveform images through medical waveform images and semantic information retrieval and to fuse semantic information with the current patient's situation, so as to help patients be diagnosed and treated in a timely manner and better prevent and treat various diseases. This not only greatly saves the time of seeing a patient but also reduces the cost of seeing a patient. In addition, it has made great contributions to the timely diagnosis of the early causes of cardiovascular diseases and other diseases and the early detection of clinical signs of the disease, which can effectively reduce the mortality rate of the disease.

2.1.2. IoT Information Fusion. The Internet of Things is a new type of electronic technology or data network system developed on the basis of Internet technology. With the rapid development of the network and the progress of sensor networks, the research on the Internet of Things and its technology has become the future development direction of the Internet. This electronic technology or network system is mainly based on the coding of electronic products and uses RFID identification technology to identify and identify all physical items in the world so as to realize dynamic monitoring of physical items. Among them, digital calculation modules, data calculation, and so on will be used. In addition, purely technically speaking, the Internet of Things is an interconnected structure of things, objects, and intelligence about RFID technology, remote sensing technology, nanotechnology, and intelligent identification technology. Of course, the Internet of Things itself is also an expansion of Internet technology because the Internet of Things is mainly developed based on network technology and then controls physical objects on a larger scale. However, in the evolution and development, the Internet of Things is also a business or application, especially in today's society; in addition to technological innovation, the Internet of Things must continuously optimize its applications and develop the Internet of Things model based on user experience.

The Internet of Things information fusion technology refers to the analysis, refinement, and integration of information data obtained by sensors. The purpose of applying this technology is to obtain more accurate information data so as to provide information data for certain decision-making needs or data analysis. The key of information fusion technology is to refine the information data so as to improve the practicability of the information data. The main application field of information fusion technology is the military field, but it has gradually expanded to the civilian field and has played a huge role. According to the different levels of information and data fusion, IoT information fusion technology can be divided into three levels: data-level fusion technology, feature-level fusion technology, and decision-level fusion technology.

2.2. Robot. Since the 1950s, many countries in the world have vigorously developed the robot industry. Americans were the first to research and develop the first industrial application robot. The role of this robot is to replace people in repetitive and intensive manual labor, which greatly increases the efficiency of manufacturing and reduces labor costs. The development of robots is the result of the development of human society and science and technology. On the one hand, the development of robots has a significant impact on human society. Robots are typical representatives of high-end intelligent equipment and core assets. From a national perspective, robot technology is even an important

factor in examining a country's technological level and technological innovation capabilities. Therefore, many countries in the world have long paid special attention to the development of robots, and some countries have even raised the development of robots to the height of the national scientific and technological strategic layout and successively introduced a series of related measures to encourage and stimulate the development of the robot industry. In the layout plan of "Made in China 2025" proposed by my country in 2015, the development of robots has been raised to a national strategic perspective. Government departments have released a series of relevant measures for the development of robots. Robots have received unprecedented development opportunities. A large number of robots have gradually become a reality and have been applied to all walks of life. At the same time, the functions of robots are becoming more and more powerful and meet people's needs.

In recent years, the practical application scenarios of robots have become more and more extensive. It is a very obvious trend that the application scenarios of robots have begun to shift to the service industry on a large scale and are no longer limited to industrial production. Especially in this year's fight against the epidemic, service robots have played a huge role. Service robots have been quickly put into the fight against the epidemic. They can automatically detect the body temperature of passing people and perform disinfection and sterilization functions in public places, greatly reducing the work pressure of epidemic prevention personnel. Reflecting the superiority of service robots, it is a temperature measurement and disinfection robot.

Service robots have entered an unstoppable trend from public service places to home applications. One of the important reasons is that the aging problem in some developed countries in the world is already very serious. The reality makes the pension problem even more serious: on the one hand, because the pace of modern life has been accelerating, young people are facing huge work challenges and do not have more energy to accompany the elderly at home and take care of housework. The cost of the elderly has increased significantly. In the case of increasing aging, there will be a reality that there is no ability to take good care of the elderly and ensure a better life for the elderly. This is not only an urgent problem for a family but also an urgent problem for society.

2.2.1. Development and Research Status of Robots. Entering the 21st century, with the continuous development of the economy and society, the domestic economy is changing from a labor-intensive manufacturing method to an increasing demand for automated robots to replace manual labor. The reason for this is that the labor-intensive and extensive manufacturing pattern in the country in the past few decades was difficult to maintain due to the declining demographic dividend of the aging population. The robot industry has become one of the important industries for China's future development and will play an important role in promoting China's industrial transformation and upgrading, and the replacement of labor by robots will also be the trend of future manufacturing.

With the continuous development of robots, more and more disciplines are covered. In addition to traditional electronic information, mechanical design, sensor technology, information processing, and computers, more and more bioelectric signals, material design, nanotechnology, and so on are involved. Intelligence is also progressing. Robots are widely used in industry. In addition, the application of robots in other work environments that are difficult for humans to reach and to meet the specific requirements of people in specific situations, such as service fields and military fields, is also extremely important. The most popular robot recently is the robot dog made by Boston Dynamics Engineering Company for the military. It is used for tasks such as transporting materials in rugged mountains during wartime. It has a vision system that can be used to perform related tasks autonomously and has a certain intelligence. Different from the previous way of walking on wheels, Big Dog adopts a bionic limb design and is equipped with four legs to walk, which can climb, jump, and resist side impact.

2.2.2. Classification of Robots. Robots have gradually become a research hotspot of artificial intelligence and have developed rapidly. Robots are mainly divided into aerial drones and ground mobile robots. UAVs are widely used in logistics and distribution, fire warning, target detection, border patrol, and so on. However, due to the limited endurance of the UAV, it can only work continuously for 20–30 minutes before replacing the battery, making it unable to perform time-consuming tasks, and its load capacity is limited, thus limiting the development of UAVs. Mobile robots have large loads and can perform tasks for a long time.

With the development of science and technology and the emergence of various complex environments and complex tasks, it is difficult for a single robot to meet the requirements of more and more complex tasks, especially in the military, police departments, logistics distribution, and other industries. The task execution efficiency of a single flying robot is low, and multirobot cooperation is needed. There are three main types of multirobots: multi-UAV, multimobile robot, and heterogeneous robot system composed of UAV and mobile robots. Among them, due to the respective advantages of drones and mobile robots, the combination of drones and mobile robots makes up for the shortcomings of short battery life and limited load when drones work alone and at the same time makes up for the lack of wide vision of mobile robots. The disadvantage of not being flexible enough to exercise, combining the advantages of the two, has the advantages of time, space, and function. Heterogeneous robot systems can adapt to more and more complex task requirements and have broad application prospects in military, agriculture, industry, and service industries.

3. Route Planning

Route planning technology is one of the core contents of the research in the field of robotics, and the robot navigates according to the route planning. The route planning of the

robot can be divided into the robot moves from the starting position to the specified position; the algorithm can bypass the obstacles on the walking route during the movement of the robot, and at the same time, it can complete the specified work task in a specific position; based on the implementation of the first two problems, we try to optimize the walking route.

3.1. Classification of Planning Algorithms. The path planning of the robot is the problem of optimal path selection. Route planning algorithms can be generally classified according to different algorithm sources, whether it is a single algorithm to realize the path planning function, whether it is inspired by biology, whether it is a pure mathematical theory, and so on, as shown in Figure 1.

3.1.1. Sampling-Based Methods. The core of the sampling-based path planning algorithm is to collect the environmental information of the space through sensors and then randomly sample the points in the space that are not within the obstacle range and connect the random sample points to form a path that can connect the beginning and end states to navigate. Since the algorithm only focuses on the points in the unobstructed space and does not process the obstacle points in the state space, it saves a lot of computing time. The algorithm does not construct the obstacle space. When there are too few sampling points or the distribution is not balanced, it will cause incompleteness. For example, Voronoi can perform global or local map planning; RRT is a fast path search without collision; PRM is a method based on graph search, which has the characteristics of complete probability and is not optimal.

3.1.2. Algorithms of Mathematical Models and Multifusion Algorithms. The core idea of the algorithm of the mathematical model is to describe the motion state and constraint conditions in the form of mathematical optimization, and the representative algorithms include MILP and NLP.

The multifusion algorithm can realize the optimal solution of path planning. If a single algorithm may focus on fastness or effectiveness, the collective algorithm has better time performance and work effect than a single algorithm because it integrates multiple algorithms and integrates the advantages of multiple algorithms. A good advantage is the ability to achieve global optimization and cost minimization.

3.1.3. Algorithms Based on Biological Heuristics. Bioinspired algorithms refer to researchers who, inspired by a phenomenon in the real natural environment, propose mathematical theories with similar ideas to solve some problems. There are three common algorithms.

Neural networks are widely used in pattern classification and other problems, using neurons to approximate any nonlinear function, and neural networks also have some related applications in path planning. The aspect of supervised learning is path planning with CNN's laser and A*. The other is based on reinforcement learning. Given a planned goal, the machine can collide and update the network autonomously without the need to manually set a route.

The ant colony algorithm is a global algorithm, emphasizing the cooperation of individuals in the community. If the map is in grid format, and the ant colony algorithm is used in the grid map, the robot planning route will bring problems such as many turns and delays. The shortest path of each iteration needs to be further improved to achieve a more optimal path and real-time performance.

The genetic algorithm takes a single point in the whole space as an object and uses the probability method to search the space. Mathematically, it does not require the processing of structural objects required for function derivation and continuity; it can search the space by itself and plan the direction by itself. It has good global planning ability and strong robustness.

3.1.4. Node-Based Approach. The node-based method is the grid method, which is used in grid maps. The grid map divides the spatial environment into the form of grids, in which each grid represents the probability of possession. The type of map used in the ROS system is a grid map. In raster maps, Dijkstra's algorithm and A^* algorithm can be used as global static navigation algorithms; D^* algorithm used in dynamic environments can also work well in changing environments.

3.2. Global Route Planning Algorithm. Global path planning is to search for an optimal or approximately optimal line that meets the conditions in all state spaces according to the constraints when the robot has obtained the position information of the objects in the space. In the grid method, the size of the divided grid needs to be based on the size of the robot so that the robot can use the global search optimization algorithm for path walking when navigating. The research of this subject is global route planning based on the grid method.

3.2.1. Dijkstra Algorithm. Dijkstra's algorithm process is as follows:

(1) Initially, $S = \{v\}$, where the distance of v is 0. Z contains all vertices of the complement except v, v.

(2) Select d with the smallest distance from v in Z and add it to S.

(3) Using the newly added point d as the intermediate point, modify the distance of each vertex in Z. If the distance from point v to Z through d is shorter than the distance without d, then the d value of the vertex plus the weight is used as the new value of Z. Repeat steps 2 and 3 until the vertex set in Z is empty.

Dijkstra's algorithm is a greedy strategy. The algorithm compares and calculates from a global perspective to obtain the shortest path. Therefore, the maximum complexity of the algorithm is $O(n^2)$. When the number of nodes in a graph increases, the algorithm needs more time to calculate the weight comparison between nodes, resulting in the low

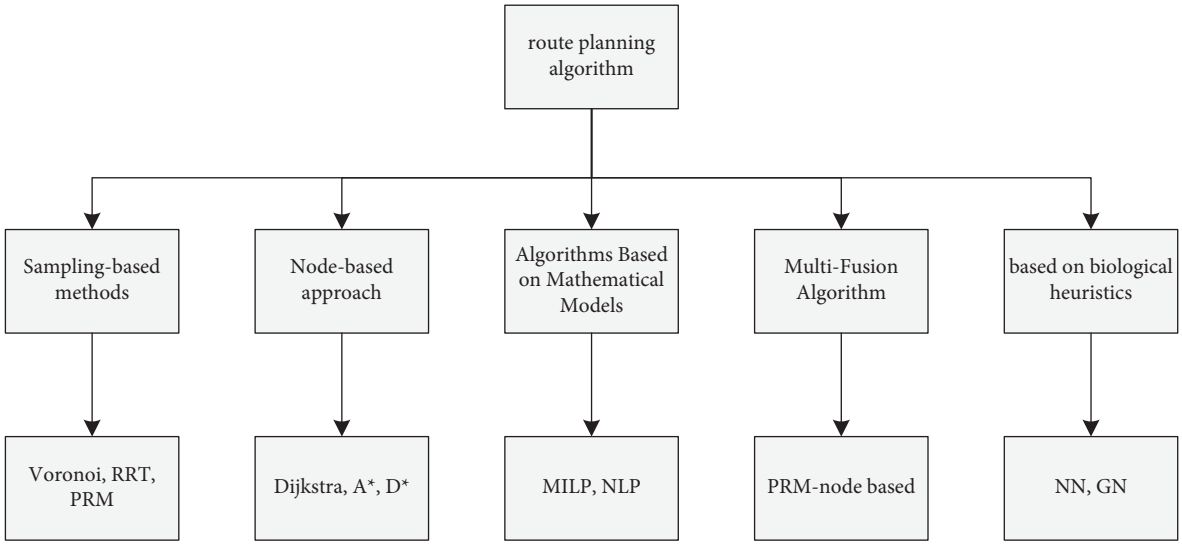

Figure 1: Route planning classification.

efficiency of the algorithm. At the same time, due to the increase in the amount of calculation, the more the data that needs to be accessed, the larger the memory space occupied, and the certain requirements for the performance of the processor can better achieve the real-time effect.

3.2.2. A^* Algorithm. The A^* algorithm is the global shortest path search algorithm. It is different from the Dijkstra algorithm's nondirectional diffusion method in the process of tracing. The A^* algorithm is to search for the path directional toward the endpoint according to a certain cost function. The difference between the A^* algorithm and the Dijkstra algorithm is also an improvement. Compared with the greedy strategy of Dijkstra's algorithm, which searches all over the space, the A^* algorithm has a directional strategy, which needs to traverse relatively fewer nodes, and the search efficiency is higher. When the A^* algorithm searches toward the endpoint, the evaluation function needs to be used to evaluate whether the route through the node to the endpoint is the optimal path. Different trajectories can be obtained according to the different evaluation functions used in the algorithm. The key evaluation function of the A^* algorithm is

$$f(n) = g(n) + h(n). \tag{1}$$

In the formula, $f(n)$ represents the total evaluation function of the current node n; $g(n)$ represents the actual cost from the starting point to the current point; $h(n)$ represents the estimated cost from the current node to the endpoint.

The value of $h(n)$ determines the performance of the algorithm. $h(n)$ often uses Euclidean distance and Manhattan distance as the value of the algorithm for two points in space. By using the Manhattan distance as the value of $h(n)$, there are two points (X_1, Y_1) and (X_2, Y_2):

$$D_{\text{Manhattan}} = |x_1 - x_2| + |y_1 - y_2|. \tag{2}$$

3.3. Local Route Planning Algorithm. In the actual environment, the robot cannot safely reach the designated position strictly according to the established path due to the inaccuracy of the actual measurement information and the change of the environment due to the accuracy of its own sensor. The global application is used in static planning, and local path planning is required in dynamic planning. In the local path planning algorithm, the robot continuously collects the position information of the surrounding obstacles through the sensor during the walking process and at the same time predicts the obstacle information on the original map in advance so as to realize the local dynamic planning and make it conform to the previous global plan. The DWA dynamic window method performs multiple sets of velocity sampling within the window range to simulate the planned path; the artificial potential field method is to construct a virtual artificial potential field in space. For a single local planning algorithm, the robot has high real-time performance and good practicability in the process of path planning. However, if there is no global reference information, the robot is prone to fall into local extreme points, causing the robot to fail to reach the target point according to the instructions. For this reason, it is necessary to match the global planning while applying the local planning algorithm so as to better ensure that the robot navigates to the specified target position normally.

3.3.1. DWA Mobile Robot Algorithm. The dynamic window method (DWA) is mainly used in indoor static environments. Local path planning is performed with the assistance of paths planned with the help of a global algorithm. Its core is to continuously collect its own robot pose and external environment information through the measurement sensor carried within a certain time interval and obtain a series of acceleration and angular velocity by sampling. Because the sampled acceleration and angular velocity are within a range

of values, it is called a window, and the sampled acceleration and angular velocity are used to numerically simulate the path that the robot will walk. Multiple paths can be obtained through numerical calculation and simulation, and then the optimal path is selected relative to the current motion control variables of the robot according to the evaluation function used as the basis for the selection of the scheme.

The DWA algorithm needs to obtain the model state expression of the robot. Therefore, a two-wheeled robot based on differential drive has no velocity in the y-axis direction. And the motion trajectory of the robot in two sampling adjacent periods can be approximately considered as a straight line. Assuming that the robot travels a small distance at an angle θt between the speed v and the x-axis during the Δt time, the movement increments Δx and Δy of the robot on the x-axis and the y-axis can be obtained:

$$\begin{aligned} \Delta x &= x + v\Delta t\ \cos(\theta t), \\ \Delta y &= y + v\Delta t\ \sin(\theta t). \end{aligned} \tag{3}$$

From the above, the mathematical expression of the moving mathematical trajectory is as follows:

$$\begin{aligned} x &= x + v\Delta t\ \cos(\theta t), \\ y &= y + v\Delta t\ \sin(\theta t), \\ \theta t &= \theta t + w\Delta t. \end{aligned} \tag{4}$$

During the sampling of the speed window, the robot body collects multiple sets of trajectory speed values. In order for the robot to safely perform path planning within the tolerance range of its own control performance, some necessary speed limits are required. During operation, the robot first performs a limited range of speed and angular velocity value changes, and the range formula is as follows:

$$V_m = \{v \in [v_{\min}, v_{\max}], w \in [w_{\min}, w_{\max}]\}. \tag{5}$$

And because the robot has different torque performance parameters when selecting the motor, the robot starts from the angle of the motor. Knowing the current speed v_c and angular speed w_c of the robot at this moment, it must also satisfy the actual speed that can be achieved:

$$\begin{aligned} V_d = \{(v, w) | v \in (v_c - \dot{v}_b\Delta t, v_c + \dot{v}_a\Delta t), \\ w \in (w_c - \dot{w}_b\Delta t, w_c + \dot{w}_a\Delta t)\}. \end{aligned} \tag{6}$$

In the formula, $\dot{v}_a$ and $\dot{w}_a$ are the maximum acceleration; $\dot{v}_b$ and $\dot{w}_b$ are the maximum deceleration.

Finally, when the robot can safely detour when it encounters obstacles during walking, the following formula for the speed needs to be satisfied within the range of the speed value:

$$V_d = \left\{(v, w) | v_c \le \sqrt{2 \cdot \mathrm{dis}(v.w) \cdot \dot{v}_b}, w_c \le \sqrt{2 \cdot \mathrm{dis}(v.w) \cdot \dot{w}_b}\right\}. \tag{7}$$

In the formula, $\mathrm{dis}(v.w)$ is the minimum distance of obstacles on the planned trajectory.

On the basis of the trajectory that meets the speed requirements, the evaluation function is used to evaluate, and the optimal trajectory is selected:

$$G(v, w) = \sigma(\alpha \mathrm{head}(v, w)) + \beta \mathrm{dis}(v, w) + \gamma \mathrm{vel}(v, w). \tag{8}$$

Among them, $\alpha \mathrm{head}(v, w)$ represents the gap between the target angle of the assessment and the end of the route; $\mathrm{dis}(v, w)$ is the minimum distance of obstacles on the planned route; $\mathrm{vel}(v, w)$ represents the speed evaluation at this moment; σ is a smooth function; and α, β, and γ are evaluation coefficients.

3.4. Mathematical Theory of Graph Optimization. Graph optimization is expressed in the form of a graph according to the relationship between points and edges. When using the optimization algorithm in SLAM, the key is to describe the nonlinear motion state estimation of the robot in the form of a graph to optimize the solution. The robot can obtain an observation data z_i of the position at the position x_i at each moment through the sensor carried by itself. For this reason, it can be expressed by a functional relationship:

$$z_i = h(x_i). \tag{9}$$

Since the data is collected by the robot's own sensor, there must be noise. For this reason, there are error terms on both sides of the above formula. The error terms of the observation equation of the robot are defined as follows:

$$e_i = z_i - h(x_i). \tag{10}$$

In the robot, the graph model obtained from the robot's pose and observation point has n edges, and the optimized objective function can be obtained:

$$\min_x \sum_{i=1}^{n} e_i(x_i, z_i)^T \Omega_i e_i(x_i, z_i), \tag{11}$$

where z_i is the observation data, x_i is the observation point, and Ω_i is the inverse of the covariance matrix.

Since the observation data z_i is the data collected by the robot at each sampling point, it can be obtained directly. Therefore, the objective function can be simplified and written in the form of the following sum:

$$\min F(x) = \sum_{i=1}^{n} e_k(x_i)^T \Omega_i e_i(x_i). \tag{12}$$

From the optimization function obtained above, since the robot has multiple edges and multiple nodes in the actual operation process, when our goal is to solve it, we only need to get one of the initial points and the iteration direction. When only one edge is considered and an increment Δx is calculated for the initial point $\tilde{x}_i$, the error term becomes $e_i(\tilde{x}_i + \Delta x)$, and the first-order Taylor expansion can be obtained:

$$\begin{aligned} e_i(\tilde{x}_i + \Delta x) &\approx e_i(\tilde{x}_i) + \frac{\mathrm{d}e_i}{\mathrm{d}x_i}\Delta x, \\ e_i(\tilde{x}_i + \Delta x) &= e_i + J_i \Delta x. \end{aligned} \tag{13}$$

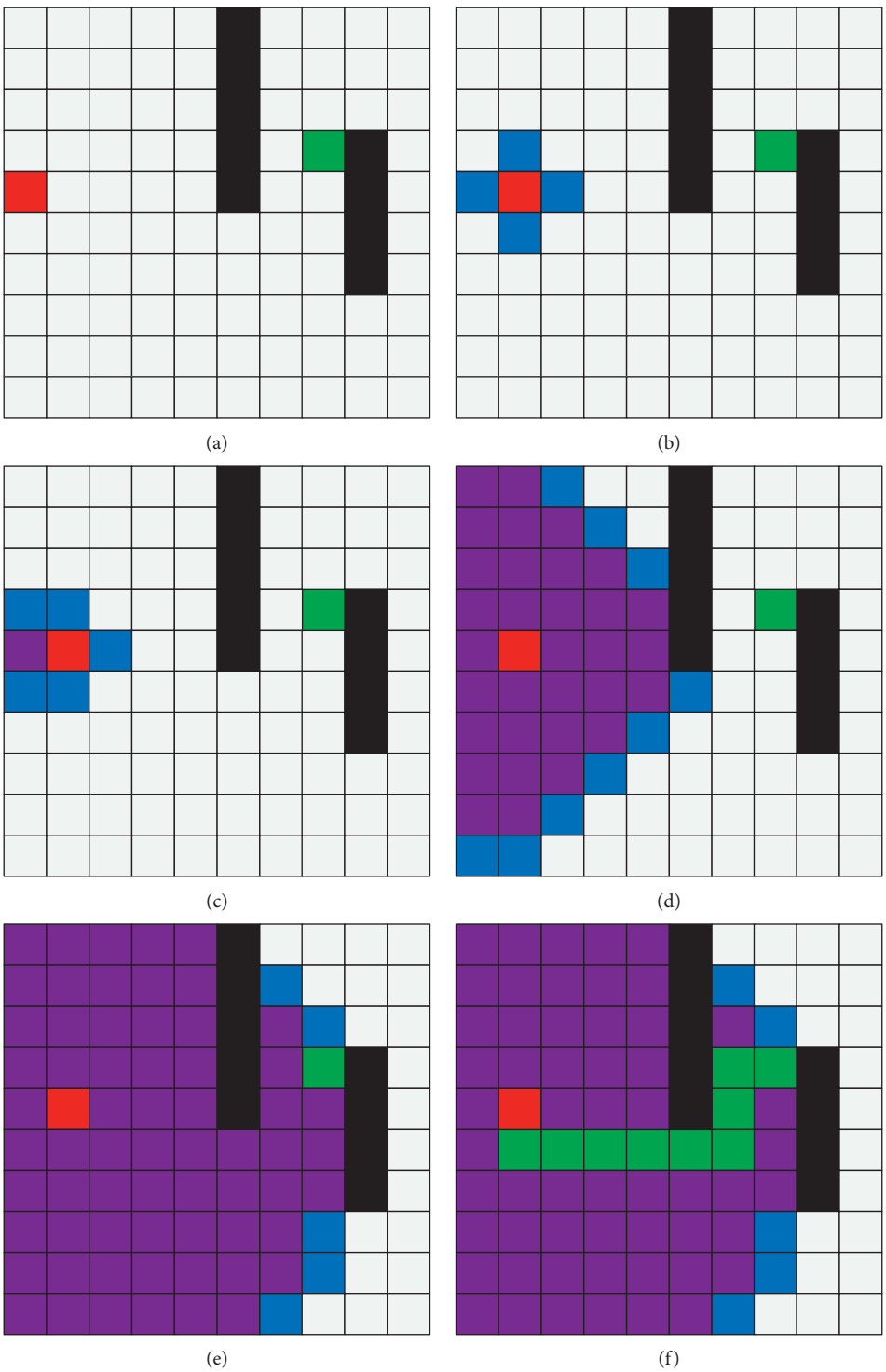

Figure 2: Dijkstra's algorithm path planning process. (a) Process one. (b) Process two. (c) Process three. (d) Process four. (e) Process five. (f) Process six.

Among them, J_i is the derivative of e_i with respect to x_i:

$$J_i = \frac{\mathrm{d}e_i}{\mathrm{d}x_i}. \tag{14}$$

It can be obtained by the formula, and the following formula can be obtained for the objective function of the i-th edge:

$$\begin{aligned} F_i(\tilde{x}_i + \Delta x) &= e_i(\tilde{x}_i + \Delta x)^T \Omega_i e_i(\tilde{x}_i + \Delta x), \\ F_i(\tilde{x}_i + \Delta x) &\approx (e_i + J_i \Delta x)^T \Omega_i (e_i + J_i \Delta x), \\ F_i(\tilde{x}_i + \Delta x) &= e_i^T \Omega_i e_i + 2e_i^T \Omega_i J_i \Delta x + \Delta x^T J_i^T \Omega_i J_i \Delta x, \\ F_i(\tilde{x}_i + \Delta x) &= C_i + 2b_i \Delta x + \Delta x^T H_i \Delta x. \end{aligned} \tag{15}$$

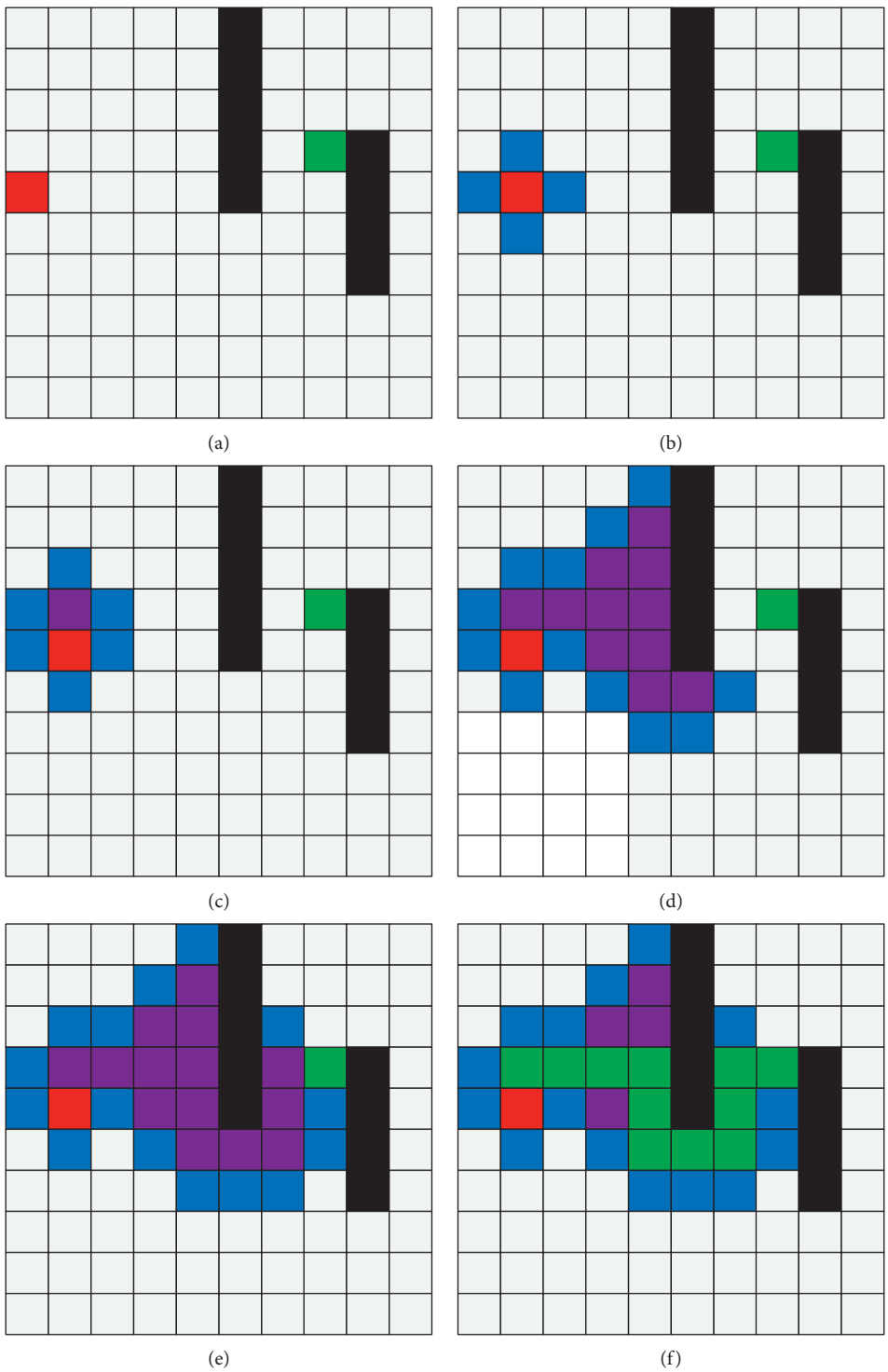

Figure 3: A^* algorithm path planning process. (a) Process one. (b) Process two. (c) Process three. (d) Process four. (e) Process five. (f) Process six.

In the formula, C_i is the integration of terms unrelated to Δx; $2b_i$ is the coefficient of the first-order term; H_i is the coefficient of the quadratic term.

In the above formula, since C_i is an item unrelated to Δx, it is simplified and solved, and when all edges in the SLAM graph model are considered, all edges can be obtained by removing the subscripts of the parameters, and then the incremental equation can be obtained:

$$H\Delta x = -b. \tag{16}$$

When the robot model is running, the number of edges constituting the graph is huge, and there are many

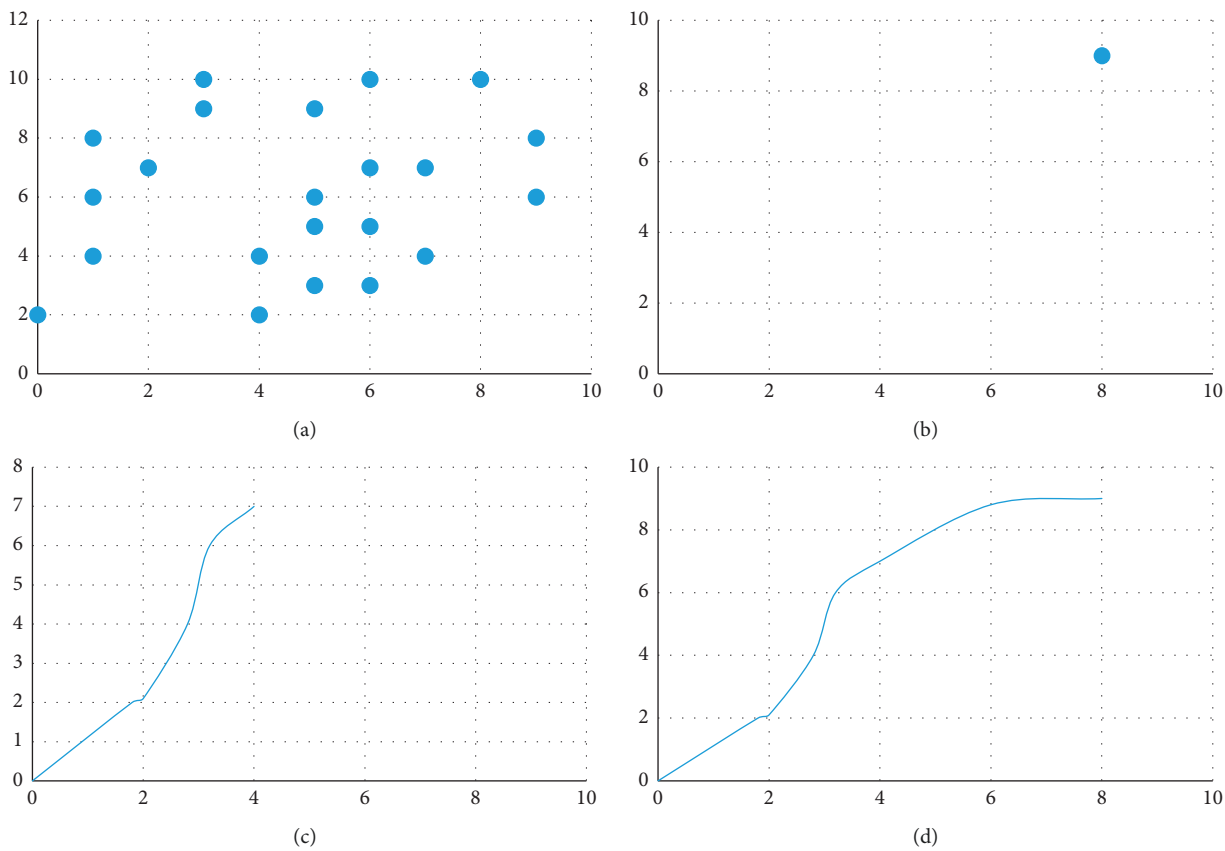

Figure 4: DWA algorithm path planning process.

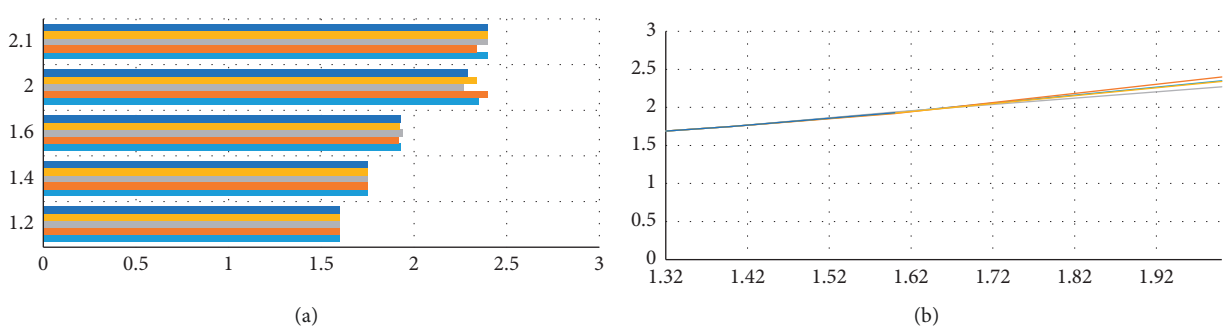

Figure 5: Speed sampling example.

parameters to be solved, but it is sparse, so it is possible to solve it in real time.

The graph-optimized SLAM algorithm, that is, the core formula of Hector SLAM, is solved by the Gauss–Newton method. The formula is as follows:

$$\varepsilon^* = \arg\min_{\varepsilon} \sum_{i=1}^{n} \left[1 - M\left(s_i(\varepsilon)\right)\right]^2. \tag{17}$$

In the formula, $M(s_i(\varepsilon))$ represents the map value corresponding to the grid under the point; $s_i(\varepsilon)$ represents the world coordinate corresponding to the laser point coordinate.

Based on the filtered SLAM, the particle filter algorithm formula is as follows:

$$P\left(x_{1:t}, m | z_{1:t}, u_{1:t-1}\right) = p\left(m | x_{1:t}, z_{1:t}\right) \cdot p\left(x_{1:t} | z_{1:t}, u_{1:t-1}\right), \tag{18}$$

where m is the map, $u_{1:t-1}$ is the chronometer data, $x_{1:t}$ is the robot path, and $z_{1:t}$ is the observation.

4. Validation Experiment

4.1. Dijkstra Algorithm Simulation Verification Experiment. Through the dynamic simulation experiment of the Dijkstra algorithm, one has the following:

(1) By creating a 10×10 grid map as the search workspace, the red square is the starting point of the

search, the green square is the end point of the search, and the black square represents obstacles.

(2) Select the dark red square point as the search point, select four points from the minimum path of the dark red square to join the search range, the wine red square point is the point that has been searched, and the blue square point is the next step to be search point.

(3) Repeat step (2) continuously, finally, search the square of the green endpoint, and the green route connecting the red start point and the green endpoint is the searched path.

Figure 2 shows the tracing process of Dijkstra's algorithm. Figure 2(a), process 1, is the established 10×10 grid map, and the dark red starting point is used as the search center to find its four neighbors up, down, left, and right, making it blue. The color indicates the center to be searched next time, as shown in the second process of 2(b) in the figure, and calculates the distance from them to the starting point; in the third process of 2(c) in the figure, the point to the left of the dark red origin is taken as the new search starting point, the neighbor of the point is changed to blue, the distance from the new neighbor to the origin is calculated at the same time, and finally, the point to the left of the dark red origin is changed to wine red, indicating that the point has been searched. Through continuous outward diffusion, the steps shown in 2(d), process 4, are continuously cycled until the planned green path is found, as shown in 2(f), process 6.

4.2. A^* Algorithm Simulation Verification Experiment. Using the same map as Dijkstra's algorithm in the previous section, the A^* algorithm is dynamically simulated to evaluate its performance. The figure shows the tracing process of the A^* algorithm. Unlike the Dijkstra algorithm, which has the characteristics of nondirectional outward diffusion at the closest distance to the origin, the A^* algorithm uses the evaluation function to select the nearest neighbor to the endpoint as the center of the next search.

Comparing the path planning process of the A^* algorithm in Figure 3 and the path planning process of the Dijkstra algorithm in Figure 2, it can be seen that, in the second process 3(b) of the figure in the initial stage, the execution process of the algorithm is the same as that of the Dijkstra algorithm. However, with the execution of algorithm A^*, the algorithm path begins to step in the direction of the upper right corner under the action of the formula evaluation function until it encounters an obstacle and starts to search up and down, and finally, the searched path is obtained. From the number of grids occupied by blue and red, the time efficiency of A^* algorithm is better than that of the Dijkstra algorithm under this simulation condition.

4.3. DWA Algorithm Simulation Verification Experiment. Through the dynamic simulation of the DWA algorithm, the flowchart of the working effect of the algorithm is verified. In the simulation experiment, the value of the coefficient of the evaluation functions $\alpha = 0.04$, $\beta = 0.3$, and $\gamma = 0.2$ is shown in Figure 4 for the dynamic simulation result of the DWA algorithm. Figure 4(a) represents the obstacle, Figure 4(b) represents the navigation endpoint, Figure 4(c) represents the planned trajectory, and Figure 4(d) green represents the estimated trajectory sampled at different speeds.

When zooming in on the figure, you can see that the trajectory results of the velocity sampling are shown in Figure 5 in a window.

The optimal path is selected through the evaluation function after the sampling of multiple groups of speed. In the simulation process, it can be seen that when the current position of the robot is closer to the obstacle, the smaller $\mathrm{dis}(v.w)$ is, the slower the speed of the robot becomes, which causes $G(v, w)$ to become smaller; on the contrary, the farther the distance is, the larger C is, and the speed of the robot also changes. The faster you go, the bigger $G(v, w)$ becomes. It can be verified that the DWA algorithm can well complete the dynamic obstacle avoidance task so that the robot can safely reach the target point.

5. Conclusion

The path planning algorithm is the key for the robot to move to the target position accurately in the space environment. This paper introduces and compares the path planning algorithm of the robot, that is, the verification of the Dijkstra algorithm and the algorithm in the global route planning algorithm. Validation of the DWA mobile robot algorithm in planning algorithm in robot route planning. By comparing the two algorithms of global planning, the verification experiment shows that the time efficiency of the A^* algorithm is better than that of the Dijkstra algorithm, and the DWA algorithm is verified to be able to complete the dynamic obstacle avoidance task well so that the robot can safely reach the target point. By analyzing and analyzing the DWA dynamic window algorithm, it is described by the formula from the three aspects of the motion model, speed sampling, and evaluation function, experimental simulation is carried out, the relationship between the evaluation function terms is obtained, and the feasibility of the algorithm is verified.

Data Availability

The experimental data used to support the findings of this study are available from the corresponding author upon request.

Conflicts of Interest

The authors declare that they have no conflicts of interest regarding this work.

Acknowledgments

This research was financially supported by Jiaxing Public Welfare Research Project of Jiaxing Science and Technology Bureau (Grant No. 2021AY10072).

References

[1] J. Borenstein, H. R. Everett, and L. Feng, "Mobile robot positioning: sensors and techniques," *Journal of Field Robotics*, vol. 14, no. 4, pp. 231–249, 2015.

[2] T. H. Wagner, A. C. Lo, P. Peduzzi et al., "An economic analysis of robot-assisted therapy for long-term upper-limb impairment after stroke," *Stroke*, vol. 42, no. 9, pp. 2630–2632, 2011.

[3] K. P. Michmizos, S. Rossi, E. Castelli, P. Cappa, and H. I. Krebs, "Robot-aided neurorehabilitation: a pediatric robot for ankle rehabilitation," *IEEE Transactions on Neural Systems and Rehabilitation Engineering*, vol. 23, no. 6, pp. 1056–1067, 2015.

[4] R. Iii, S. K. Jin, and N. J. Cowan, "Nonholonomic modeling of needle steering on behalf of: multimedia archives can be found at: the international journal of robotics research additional services and information for nonholonomic modeling of needle steering," *The International Journal of Robotics Research*, vol. 25, no. 5-6, pp. 509–525, 2017.

[5] S. I. Roumeliotis and G. A. Bekey, "Distributed multirobot localization," *IEEE Transactions on Robotics and Automation*, vol. 18, no. 5, pp. 781–795, 2002.

[6] A. Tewari, A. Srivasatava, and M. Menon, "A prospective comparison of radical retropubic and robot-assisted prostatectomy: experience in one institution," *BJU International*, vol. 172, no. 5, pp. 2106-2107, 2015.

[7] M. Jakimavi¨ius and M. Burinskien, "Route planning methodology of an advanced traveller information system in Vilnius city," *Transport*, vol. 25, no. 2, pp. 171–177, 2010.

[8] J. Krozel, C. Lee, and J. S. Mitchell, "Turn-constrained route planning for avoiding hazardous weather," *Air Traffic Control Quarterly*, vol. 14, no. 2, pp. 159–182, 2006.

[9] J. Dibbelt, T. Pajor, and D. Wagner, "User-constrained multimodal route planning," *ACM Journal of Experimental Algorithmics*, vol. 19, no. 3, pp. 11–19, 2015.

[10] S. Nadi and M. R. Delavar, "Multi-criteria, personalized route planning using quantifier-guided ordered weighted averaging operators," *International Journal of Applied Earth Observation and Geoinformation*, vol. 13, no. 3, pp. 322–335, 2011.

[11] T. Nishi and R. Maeno, "Petri net decomposition approach to optimization of route planning problems for AGV systems," *IEEE Transactions on Automation Science and Engineering*, vol. 7, no. 3, pp. 523–537, 2010.

[12] Y. Zhang, C. Li, and J. Xu, "Traveling in the three-dimensional city: applications in route planning, accessibility assessment, location analysis and beyond," *Journal of Transport Geography*, vol. 19, no. 6, pp. 405–421, 2011.

[13] C. HLscher, T. Tenbrink, and J. M. Wiener, "Would you follow your own route description? Cognitive strategies in urban route planning," *Cognition*, vol. 121, no. 2, pp. 228–247, 2011.

[14] A. Al-Fuqaha, M. Guizani, M. Mohammadi, M. Aledhari, and M. Ayyash, "Internet of things: a survey on enabling technologies, protocols, and applications," *IEEE Communications Surveys & Tutorials*, vol. 17, no. 4, pp. 2347–2376, 2015.

[15] S. Li, L. D. Xu, and S. Zhao, "The internet of things: a survey," *Information Systems Frontiers*, vol. 17, no. 2, pp. 243–259, 2015.

[16] Q. B. Sun, J. Liu, and S. Li, "Internet of things: summarize on concepts, architecture and key technology problem," *Journal of Beijing University of Posts and Telecommunications*, vol. 33, no. 3, pp. 1–9, 2010.

[17] M. Hai, "Formation drillability prediction based on multi-source information fusion[J]," *Journal of Petroleum Science and Engineering*, vol. 78, no. 2, pp. 438–446, 2011.

[18] P. Aarabi and B. V. Dasarathy, "Robust speech processing using multi-sensor multi-source information fusion––an overview of the state of the art," *Information Fusion*, vol. 5, no. 2, pp. 77–80, 2004.

[19] E. P. Blasch, B. V. Dasarathy, and S. Plano, "SPIE proceedings [SPIE defense and security - orlando, FL (monday 12 april 2004)] multisensor, multisource information fusion: architectures, algorithms, and applications 2004 - cognitive fusion analysis based on context," *Proceedings of SPIE - The International Society for Optical Engineering*, vol. 5434, p. 195, 2004.

[20] B. Cai, Y. Liu, Q. Fan et al., "Multi-source information fusion based fault diagnosis of ground-source heat pump using Bayesian network," *Applied Energy*, vol. 114, no. 2, pp. 1–9, 2014.

[21] A. Zanella, N. Bui, A. Castellani, L. Vangelista, and M. Zorzi, "Internet of things for smart cities," *IEEE Internet of Things Journal*, vol. 1, no. 1, pp. 22–32, 2014.

[22] C. Perera, A. Zaslavsky, P. Christen, and D. Georgakopoulos, "Context aware computing for the internet of things: a survey," *IEEE Communications Surveys & Tutorials*, vol. 16, no. 1, pp. 414–454, 2014.

[23] D. Guinard, V. Trifa, S. Karnouskos, P. Spiess, and D. Savio, "Interacting with the SOA-based internet of things: discovery, query, selection, and on-demand provisioning of web services," *IEEE Transactions on Services Computing*, vol. 3, no. 3, pp. 223–235, 2010.

Hindawi
Computational Intelligence and Neuroscience
Volume 2022, Article ID 6420799, 12 pages
https://doi.org/10.1155/2022/6420799

Research Article

Intelligent Traffic Flow Prediction and Analysis Based on Internet of Things and Big Data

Bing Liu,[1] **Tao Zhang**,[1] **and Weicheng Hu**[2]

[1]*Department of Information Engineering, Tongling Polytechnic, Tongling 244061, Anhui, China*
[2]*College of Mathematics and Computer Science, Tongling University, Tongling 244061, Anhui, China*

Correspondence should be addressed to Weicheng Hu; huwc@tlu.edu.cn

Received 16 February 2022; Revised 10 March 2022; Accepted 20 May 2022; Published 15 June 2022

Academic Editor: Guobin Chen

Nowadays, the problem of road traffic safety cannot be ignored. Almost all major cities have problems such as poor traffic environment and low road efficiency. Large-scale and long-term traffic congestion occurs almost every day. Transportation has developed rapidly, and more and more advanced means of transportation have emerged. However, automobile is one of the main means of transportation for people to travel. In the world, there are serious traffic jams in almost all cities. The excessive traffic flow every day leads to the paralysis of the urban transportation system, which brings great inconvenience and impact to people's travel. Various countries have also actively taken corresponding measures, i.e., traffic diversion, number restriction, or expanding the scale of the road network, but these measures can bring little effect. Traditional intelligent traffic flow forecasting has some problems, such as low accuracy and delay. Aiming at this problem, this paper uses the model of the combination of Internet of Things and big data to apply and analyze its social benefits in intelligent traffic flow forecasting and analyzes its three-tier network architecture model, namely, perception layer, network layer, and application layer. Research and analyze the mode of combining cloud computing and edge computing. From the multiperspective linear discriminant analysis algorithm of the combination method of combining the same points and differences between data and data into multiple atomic services, intelligent traffic flow prediction based on the combination of Internet of Things and big data is performed. Through the monitoring and extraction of relevant traffic flow data, data analysis, processing and storage, and visual display, improve the accuracy and effectiveness and make it easier to improve the prediction accuracy of overall traffic flow. The traffic flow prediction of the system of Internet of Things and big data is given through the case experiment. The method proposed in this paper can be applied in intelligent transportation services and can predict the stability of transportation and traffic flow in real time so as to optimize traffic congestion, reduce manual intervention, and achieve the goal of intelligent traffic management.

1. Introduction

At present, almost all major cities have problems such as poor traffic environment [1] and low road efficiency. Large area and long-term traffic congestion occurs almost every day. The extremely congested traffic every day leads to the increase of people's travel time and transportation costs and a great waste of time, energy, and money and increases the pressure of urban life [2]. In the development of urbanization [3], traffic congestion [4] is one of the main urbanization problems that need to be solved. The application of Internet of Things technology [5,6] and big data technology [7] in traditional industries has produced certain economic benefits. In the application of smart transportation and the construction of smart cities [8], traffic data can be quickly collected by using Internet of Things technology, and traffic flow prediction can be realized by using big data technology. Sensor technology [9], as an important data acquisition source in the Internet of Things, can realize fast and stable data transmission and fast storage and analysis [10]. Intelligent transportation can rely not only on the algorithm model [11], but also on the historical data of road traffic. Big data technology is used to process large-scale data and high-dimensional data [12] and capture the data in real time, quickly and effectively. Big data has four characteristics: magnanimity, diversity, efficiency, and

variability. The combination of these four characteristics provides basic support for traffic flow data. Establish the corresponding intelligent traffic flow data analysis system based on big data analysis, extract the historical data of road traffic from the specific traffic system [13], analyze and process these data to form structured traffic flow data, and then store the analyzed structural data in the corresponding target server database [14]. Finally, real-time, effective, and accurate traffic flow data are obtained through Internet of Things technology. This system can quickly analyze the changes of various types of data, accurately predict these changes, and screen the information accordingly. In the intelligent traffic flow prediction model based on intelligent data analysis and application, intelligent technology integration is realized through Internet of Things technology and sensor application [15], such as fiber Bragg grating sensor [16], positioning technology [17], RFID application [18], and wireless sensor technology [19]. How to use big data technology and Internet of Things technology in the field of intelligent transportation has become an important technical means of transportation application in the future. Through intelligent transportation technology, traffic accidents can be handled immediately, cost can be saved, and the system can respond quickly and be handled in time. Under the Internet of Things technology, wireless network information has a strong antiinterference and high positioning accuracy. Therefore, the application of big data and Internet of Things technology in traffic flow forecasting can alleviate urban traffic pressure and is one of the important indicators in realizing smart cities. Therefore, Internet of Things and big data can be widely used in modern cities, and the development of traditional industries can also be realized.

2. Application of Internet of Things and Big Data in Intelligent Traffic Flow Prediction

2.1. Traffic Flow Characteristics. The transportation system is huge and complex, and there are many factors that can cause the poor operation state of traffic flow, such as the changeable weather and the occurrence of accidents. Small changes in the external environment can have a great impact on it, and the performance state of each face is complex, random, and irregular, with obvious dynamic characteristics. Therefore, it becomes very difficult to accurately predict. Hence, it is necessary to comprehensively consider the prediction and analysis of traffic flow, generally from spatial and traffic timeliness. The spatial characteristics of traffic flow means that when observing traffic flow, the parameters of traffic flow at the observation site are inseparable and the traffic state at the observation site is generally directly affected by the overall traffic flow. When the distance of the predicted road section increases, the influence degree decreases; when the distance of the predicted road section decreases, the degree of impact becomes greater.

According to the traffic flow in the past, the change has periodicity, which exists every day, every week, every quarter, and even every year. Looking at the traffic flow every day, it is not in a balanced state as a whole, but obviously has great fluctuations, such as morning peak and evening peak. During these two peak periods, the traffic flow and road congestion are extremely serious compared with the normal time, which is unmatched by the traffic flow in general time. Similarly, if one year is used to analyze the periodicity of traffic flow, the periodicity of traffic flow in each quarter is also very different. Therefore, the traffic flow will roughly show periodic changes due to external factors. Therefore, it is precisely because the traffic flow shows periodic characteristics that the prediction of traffic flow becomes feasible.

The randomness in the time characteristics of traffic flow is mainly reflected in the short-term traffic flow. In the whole transportation system, people mainly manipulate vehicles, whether drivers driving or pedestrians walking on the road, which will affect the whole transportation system. People's behavior cannot be predicted. Sometimes just because of a small action to run the red light, it may cause an irreparable situation; the diversity of vehicle types will also lead to the change of traffic flow. These are unpredictable events, which makes the randomness of traffic flow stronger. Randomness is also a factor that must be considered in real traffic prediction, which increases the difficulty of traffic flow prediction.

Jiao tong traffic flow prediction will predict the traffic flow data of the road section in the past period, process and analyze the real-time dynamic data collected by wireless sensors and other devices, and use the characteristics of the data to predict the traffic flow of the current road section in the future, as shown in Figure 1.

To predict the circulation flow in the future, it must be based on historical data. Firstly, historical traffic data are collected for data preprocessing, the system starts training the data, calculates the prediction model through real-time data, obtains the prediction data, and finally converts the analysis results into charts and other visual results to respond to users.

2.1.1. Traffic Flow Prediction Method. Now, there are generally three methods to realize traffic flow prediction, namely, parameter prediction method, nonparametric prediction method, and combined parameter prediction method, which are shown in Figure 2.

Traffic flow forecasting methods are divided into parametric methods, nonparametric methods, and combined forecasting methods. Among them, parametric methods can be divided into linear and nonlinear styles. The linear method can be subdivided into time series method, historical average algorithm, smoothing algorithm, and filtering algorithm; nonlinear methods can be divided into wavelet analysis, catastrophe theory, and chaos theory; nonparametric methods include support vector machine, nonparametric regression, neural network, and fuzzy logic; combined forecasting method is the combination of two or more forecasting methods to achieve the effect of joint forecasting. It adopts the clustering combination model, decomposition combination model, and prediction result fusion model technology.

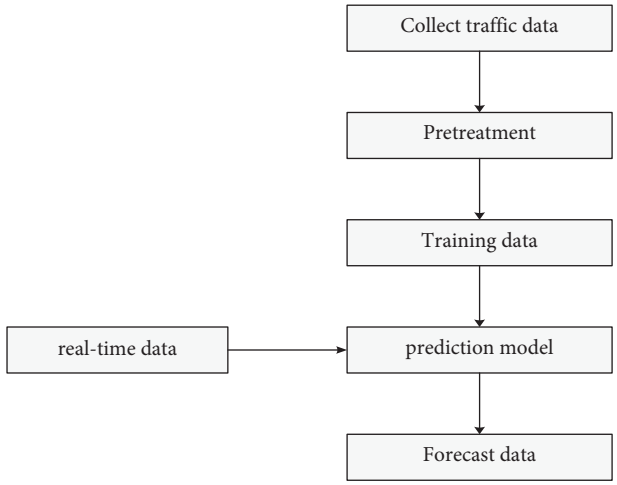

Figure 1: Traffic flow prediction process.

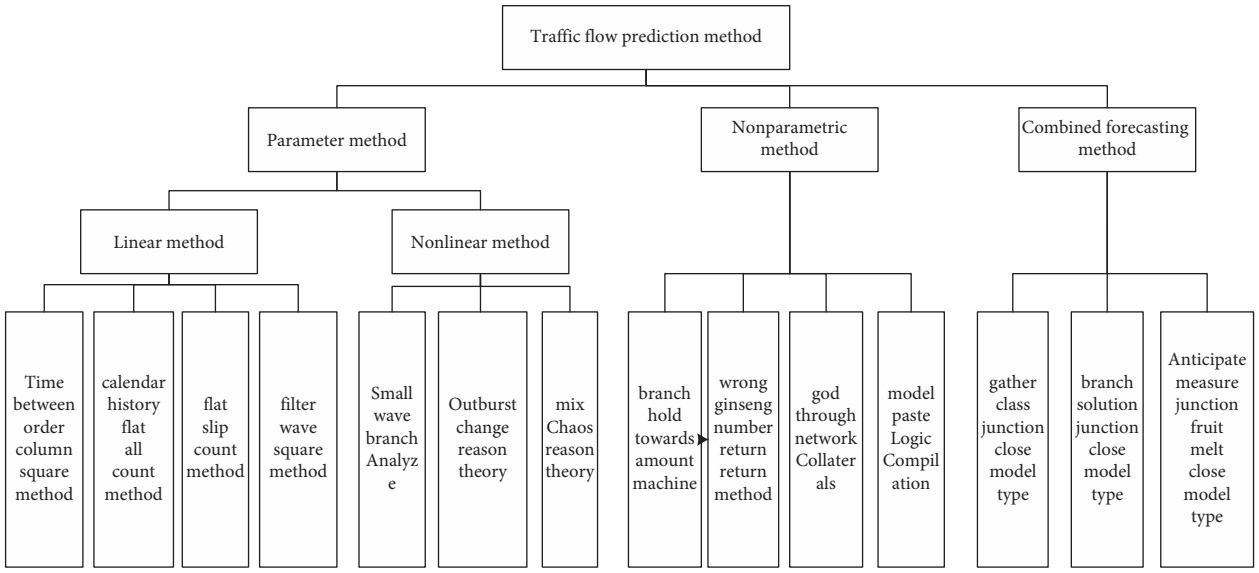

Figure 2: Classification of traffic flow forecasting methods.

2.2. Intelligent Transportation Technology in Internet of Things and Big Data. The application of Internet of Things technology in intelligent transportation has become the main way to relieve traffic pressure. Integrating Internet of Things technology into intelligent traffic flow prediction can make traffic roads smarter and make cities develop faster and more harmoniously. The key technologies are shown in Figure 3.

In Figure 3, intelligent transportation technology in Internet of Things mainly includes data collection, data analysis, data processing, data storage, and data sharing.

The problem to be solved in the road traffic flow data analysis service environment is how to timely analyze the diverse characteristics of traffic flow data, so as to provide accurate services. It should have the ability to enhance service value, mine data value, and reduce response time.

After big data analysis, it will analyze, process, and calculate the object data according to relevant algorithms and provide the service. The basic process of the big data analysis service mode is shown in Figure 4 (online mode) and Figure 5 (offline mode).

This mode has high real-time requirements and slightly small data throughput. The collected data will not be stored, and the results will be calculated directly in memory. Finally, the analysis results will be directly transformed into visual results to respond to the user. For the offline big data service mode, the biggest difference from the online mode is that it will store the collected historical data and real-time data in the disk. When the data needs to be processed, it will load, process, and calculate in the memory, and finally convert the analysis results to the user. This offline service mode is characterized by low real-time requirements and deep mining of data.

2.3. Multiperspective-Based Learning Method. For the same thing, if multiple people describe it, then each person's description methods will be different. Hence, describing the

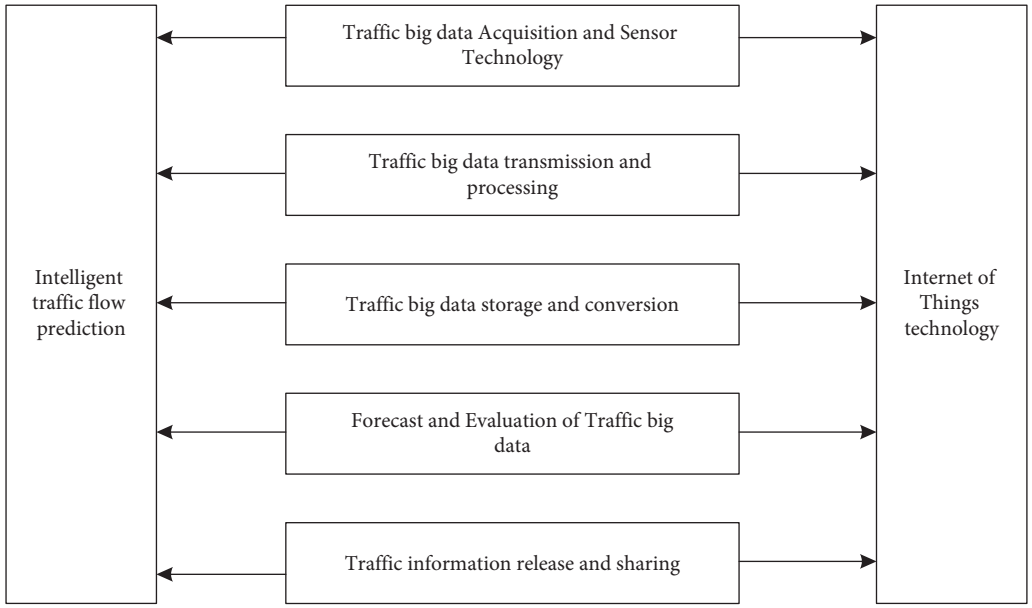

Figure 3: Intelligent transportation technology in Internet of Things and big data.

same data from different angles or ways is the method of multiperspective data learning. Data have multiple feature sets. The data obtained from multiple feature sets have different attributes, and these attributes are revealed from different levels and different perspectives. Such data are called multiperspective data. In multiview data learning, there are various analysis technologies, among which the canonical correlation analysis (CCA) and collaborative training technology are the most representative.

CCA is a multivariate statistical method of the cross-covariance matrix, which reflects the overall correlation through the correlation between various variables. U_1 and V_1 represent two sets of variables and are linearly combined to reveal the dependence of the variables on the whole. According to relevant research, canonical correlation analysis acts on the data represented by two or more perspectives and finds two linear transformations for each perspective. Assuming that there are data sets $\{(x_1, y_1), \cdots, (x_m, y_m)\}$ and $X = [x_1, \cdots x_m], Y = [y_1, \cdots y_m]$, the formula is as follows:

$$\frac{\operatorname{cov}\left(w_x^T X w_y^T Y\right)}{\sqrt{\operatorname{var} w_x^T \operatorname{var} W_y^T Y}} = \frac{w_x^T C_{xy} w_y}{\sqrt{\left(w_x^T C_{xx} w_x\right)\left(w_y^T C_{yy} w_y\right)}}, \tag{1}$$

w_x and w_y are the two projection directions to maximize the linear correlation coefficient, and C_{xy} is defined as follows:

$$C_{xy} = \frac{1}{m} \sum_{t=1}^{m} (x_1 - m_x)\left(y_1 - m_y\right)^T, \tag{2}$$

m_x and m_y are the average of the two perspectives, defined as follows:

$$\begin{aligned} m_x &= \frac{1}{m} \sum_{t=1}^{m} x_1, \\ m_y &= \frac{1}{m} \sum_{t=1}^{m} y_1. \end{aligned} \tag{3}$$

That is, the objective function of typical correlation analysis technology can be obtained:

$$\begin{aligned} &\max\left(w_x, w_y\right) w_x^T C_{xy} w_y, \\ &s.t.\ \ w_x^T C_{yy} w_y = 1. \end{aligned} \tag{4}$$

The corresponding Lagrange function is as follows:

$$\begin{aligned} L\left(w_{x^y} w_{y^y} \lambda_x \lambda_y\right) = w_x^T C_{xy} w_y - \frac{\lambda_x}{2}\left(w_x^T C_{xx} w_x - 1\right) \\ - \frac{\lambda_y}{2}\left(w_y^T C_{yy} w_y - 1\right). \end{aligned} \tag{5}$$

If for w_x and w_y, take the derivative respectively and make it 0, then the formulas are as follows:

$$\begin{aligned} C_{xy} w_y - \lambda_x C_{xx} w_x &= 0, \\ C_{yx} w_x - \lambda_y C_{yy} w_y &= 0. \end{aligned} \tag{6}$$

Using these two formulas, we can get

$$\lambda_y\, w_y^T C_{yy} w_y - \lambda_x w_x^T C_{xx} w_x = \lambda_y - \lambda_x = 0. \tag{7}$$

$\lambda_y = \lambda_x$, If $\lambda_y - \lambda_x = \lambda$, C_{yy} is reversible. Then you can get w_y:

$$w_y = \frac{1}{\lambda} C_{yy}^{-1} C_{yx} w_x \tag{8}$$

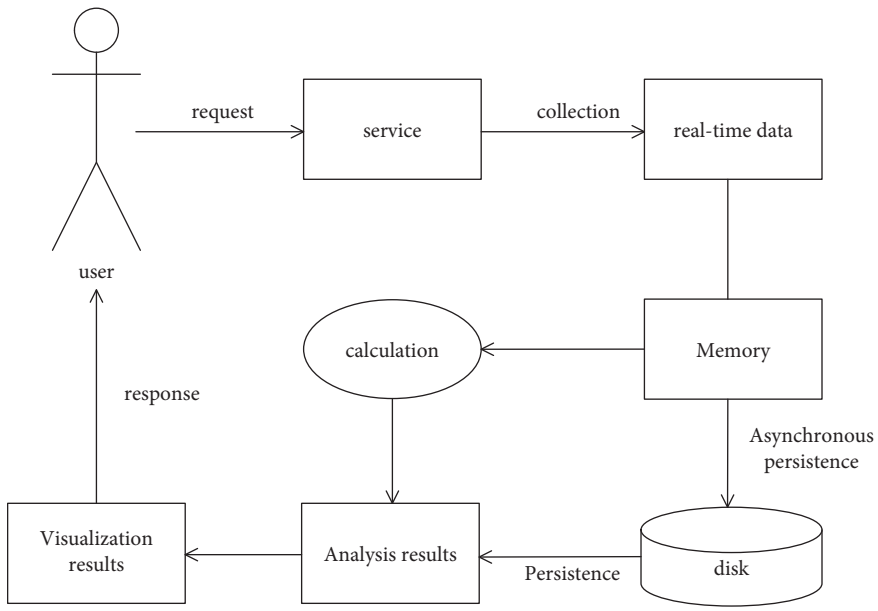

Figure 4: Online big data service mode.

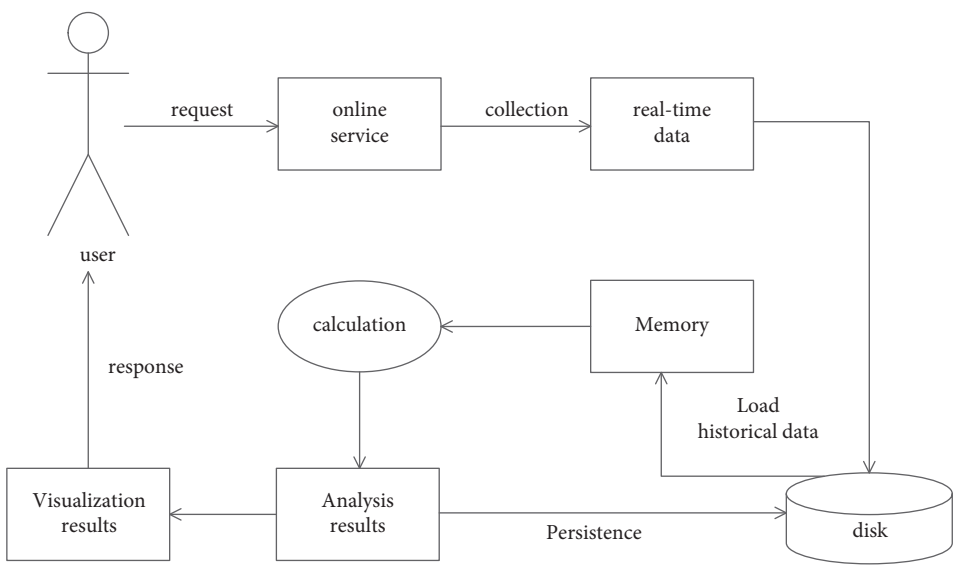

Figure 5: Offline big data service mode.

Similarly, the generalized eigenvalue decomposition problem can be obtained as follows:

$$C_{xy}C_{yy}^{-1}C_{yx}w_x = \lambda^2 C_{xx}w_x. \tag{9}$$

Finally, in order to make λ^2, if the relationship between the eigenvalue and the correlation coefficient is clearer, the rewriting objective function is defined as follows:

$$\begin{aligned} w_x^T C_{xy} w_y &= \frac{1}{\lambda} w_x^T C_{xy} C_{yy}^{-1} C_{yx} w_x, \\ \frac{1}{\lambda} w_x^T \lambda^2 C_{xx} w_x &= \lambda w_x^T C_{xx} w_x = \lambda. \end{aligned} \tag{10}$$

You can get

$$\begin{aligned} w_x^T C_{xy} w_y &= \frac{1}{\lambda} w_x^T C_{xy} C_{yy}^{-1} C_{yx} w_x = \frac{1}{\lambda} w_x^T \lambda^2 C_{xx} w_x \\ &= \lambda w_x^T C_{xx} w_x = \lambda. \end{aligned} \tag{11}$$

λ is a positive correlation solution which affects the correlation of the projection; therefore, the range of λ must vary between $[-1, +1]$.

Finally, according to the calculation results, the biggest feature of using the canonical correlation analysis is that there will be an overfitting of relevant features, and the normalized useful mode will be used, i.e., the function is defined as follows:

$$\frac{w_x^T C_{xy} w_y}{\sqrt{\left((1-\tau_x) w_x^T C_{xx} w_y + \tau_x \|w_x\|^2\right)\left((1-\tau_y) w_y^T C_{yy} w_y + \tau_y \tau_x \|w_x\|^2\right)}}, \tag{12}$$

where τ_x and τ_y are in the change of [0, 1], and the latest statistical analysis believes that regularization is a reasonable standard method to control the projection direction, which will maximize the correlation between the two perspectives and minimize the difference in square loss in each perspective.

2.4. Prediction of Traffic Flow. The so-called traffic flow prediction, through the use of information technology on historical data, finds the rules and predictions of traffic operation, thus effectively reducing communication, congestion, and accidents.

In this paper, the Markov model is used to effectively study and analyze the historical data of AC traffic.

In the Gaussian–Markov model, vectors show normal characteristics.

Mathematical expectations are as follows:

$$E(\varepsilon) = 0. \tag{13}$$

The variance covariance matrix is as follows:

$$\begin{aligned} E(\varepsilon\varepsilon') &= \sigma^2 I \triangle \mathrm{Cov}(\varepsilon), \\ \varepsilon &\sim N\left(0, \sigma^2 I\right). \end{aligned} \tag{14}$$

By calculating the expected value of the random vector Y for formula (1):

$$E(Y \mid X) = XB. \tag{15}$$

The variance covariance matrix is as follows:

$$\mathrm{Cov}(Y) = \sigma^2 I, \tag{16}$$

$$E(b_i) = B_i. \tag{17}$$

In formula (17), b_i is B_i of unbiased estimation.

$$\mathrm{Var}(b_i) = \frac{\sigma^2}{1 - R_i^2}. \tag{18}$$

In formula (18), R_i^2 is the negative correlation coefficient.

K-order multivariate linear regression is defined as follows:

$$\begin{cases} x_{11}, x_{21}, \ldots, x_{k1}, y_1 \\ x_{12}, x_{22}, \ldots, x_{k2}, y_2, \\ . \\ . \\ . \\ x_{1i}, x_{2i}, \ldots, x_{ki}, y_i, \\ . \\ . \\ . \\ x_{1n}, x_{2n}, \ldots, x_{kn}, y_n. \end{cases} \tag{19}$$

The regression model is defined as follows:

$$y_i^* = b_0 + \sum_{i=1}^{k} b_i x_{it}. \tag{20}$$

The least squares method is defined as follows:

$$\begin{pmatrix} S_{11} & S_{12} & \cdots & S_{1k} \\ S_{21} & S_{22} & \cdots & S_{2k} \\ \vdots & \vdots & \vdots & \vdots \\ S_{k1} & S_{k2} & \cdots & S_{1kk} \end{pmatrix} \begin{pmatrix} b_1 \\ b_2 \\ \vdots \\ b_k \end{pmatrix} = \begin{pmatrix} S_{1k} \\ S_{2y} \\ \vdots \\ S_{ky} \end{pmatrix}. \tag{21}$$

3. Optimization and Improvement Algorithm

3.1. Kalman Filtering Algorithm. The Kalman algorithm is realized by using a recursive method to deduce the previous state and the current state of the data. According to the existing prediction model, the Kalman algorithm shows the state and observation equation:

$$\begin{aligned} X_k &= F_{k/k-1} X_{k-1} + G_{k-1} W_{k-1}, \\ L_k &= H_k X_k + V_k. \end{aligned} \tag{22}$$

W_k is dynamic noise, V_k is the observation noise sequence, and its statistical vector is defined as follows:

$$\begin{cases} E[W_k] = 0, \\ E[V_k] = 0, \end{cases} \quad \begin{cases} E\left[W_k W_j^T\right] = Q_k \delta_{kj}, \\ E\left[V_k V_j^T\right] = R_k \delta_{kj}, \end{cases} \tag{23}$$

where Q_k is the variance matrix of dynamic noise,R_k is the variance matrix of observation noise, and δ_{kj} is the Kronecker function.

$$\begin{aligned} \delta_{kj} &= \begin{cases} 0, (k \neq j), \\ 1, (k = j), \end{cases} \\ E\left[W_k V_j^T\right] &= 0, \\ \begin{cases} \widehat{X_0} = E(X_0) = \mu x_0, \\ \widehat{P_0} = \mathrm{Var}(X_0). \end{cases} \end{aligned} \tag{24}$$

X_0 is the set initial value, and the relation between W_k and V_k denotes independence.

$$\begin{cases} E\left[X_0 W_j^T\right] = 0, \\ E\left[X_0 V_j^T\right] = 0. \end{cases} \tag{25}$$

If set target initial state X_0, P_0 is OK, then get X_t Tminimum square difference.

$$\begin{aligned} \widetilde{Z}_{k/k-1} &= Z_k - H(k)\widehat{X}_{k/k-1}, \\ S_{k/k-1} &= E\left[\widetilde{Z}_{k/k-1}\widetilde{Z}^r_{k/k-1}\right] = H(k)P_{k/k-1}H(k)^r + R_k. \end{aligned} \tag{26}$$

Calculated gain is as follows:

$$\begin{aligned} K_{k/k} &= P_{k/k-1}H_k^T H_{k/k-1}^T, \\ \widehat{X}_k &= \widehat{X}_{k/k-1} + K_k\left(Z_k - H_k\widehat{X}_{k/k-1}\right). \end{aligned} \tag{27}$$

3.2. BP Neural Network Algorithm

3.2.1. BP Neural Network Topology. The BP model passes through a multilayer feedforward neural network. The BP network has multilayer hidden units. Most neural networks adopt the change form of the BP network. It is different from perceptron in the network structure. Signal forward transmission is the main feature of the BP network, which is shown in Figure 6.

The realization steps of the BP network can be obtained from the topological structure diagram of the BP three-layer neural network. First, initialize the network, provide training samples, calculate the output layer by layer from the input layer, such as the hidden layer and the output layer, carry out the vehicle output, and then, correct the weight to judge whether the prediction error reaches the error accuracy.

3.3. Kalman-BP Neural Network Algorithm. The neural network prediction method can play a great role in intelligent traffic flow prediction, and it is one of the most important methods. Similar to the neural network prediction method, our method combines the Kalman algorithm and the BP algorithm and gives full play to the advantages of the two algorithms. It mainly introduces the filtering idea into the BP network, and the performance is better after the algorithm is optimized. After the above analysis, we can get the basic flow of neural network prediction as shown in Figure 7.

The prediction process of the neural network can be divided into data preprocessing, network construction, network training, and network prediction. Data preprocessing refers to the input and normalization of data (training data and test data).

4. Experimental Simulation

The experimental data will collect the traffic volume observation data of a certain section of the highway in one year, one week, and one day respectively. The observation scale is one hour traffic flow, a total of 336 total data, 312 training data and 24 test data were obtained. Combining these field collected traffic flow observation data, the experiment will carry out data preprocessing, network construction, network training, and network prediction, and analyze the role of the Kalman filter algorithm in intelligent traffic flow prediction and analysis system from these four aspects.

4.1. Data Analysis. The experiment will start from one month. The changes of traffic flow from three angles of one day and one hour are analyzed. The first is the analysis of the monthly traffic flow change, as shown in Figure 8.

In Figure 8, the traffic flow increased rapidly from January to February, reaching 64000 vehicles in February. From February to August, the growth was relatively stable. It showed a downward trend from August to September and from October to November. The traffic flow from September to October and from November to December is large, and the traffic flow increases rapidly.

Next is the analysis of daily traffic flow change, as shown in Figure 9.

It can be seen from the change in Figure 10 that the traffic flow increases slowly from Monday to Thursday, the traffic flow fluctuates greatly from Thursday to Sunday, the traffic flow on Friday is the least, and the traffic flow on Saturday and Sunday increases sharply.

The analysis of the hourly traffic flow change is shown in Figure 10.

In Figure 10, the hourly traffic flow in a day is less in early morning, gradually increases at 6:00, and reaches the peak from 16:00 to 19:00 with the fastest growth. It means that there is a peak period from 16:00 to 19:00 every day.

Using the traffic flow data of the above three periods as the historical reference data, traffic volume changes periodically in days. The volume first increases gradually, reaches the peak at a certain time, then decreases gradually, and oscillates before reaching the peak. In terms of peak traffic volume, it gradually increases from Monday, increases steadily and slowly on Tuesday, Wednesday, and Thursday, increases sharply on Friday and Saturday, and decreases sharply on Sunday; moreover, the total traffic volume on Friday and Saturday is also larger than usual.

4.2. Comparison of Prediction Error Value. To verify the efficiency of the proposed method, this paper compares the errors between the predicted values and the measured values of the Kalman algorithm, BP algorithm, and Kalman BP algorithm, as shown in Figure 11.

The error value of monthly traffic flow is shown in Figure 12.

Under the monthly traffic flow prediction, the Kalman BP algorithm compared with the BP algorithm and the Kalman algorithm, the Kalman BP algorithm has the lowest error value.

4.3. Algorithm Operation Speed. The operation speed of the algorithm is very important. It is the basis for the algorithm. Its purity means that the system can run correctly and stably, greatly reducing the number of system maintenance, and judging the quality of a system depends on the stability of the algorithm.

Finally, we also compared the operation speed of traffic flow prediction of the three algorithms in three time periods, calculated in milliseconds (MS), as shown in Figures 13–15.

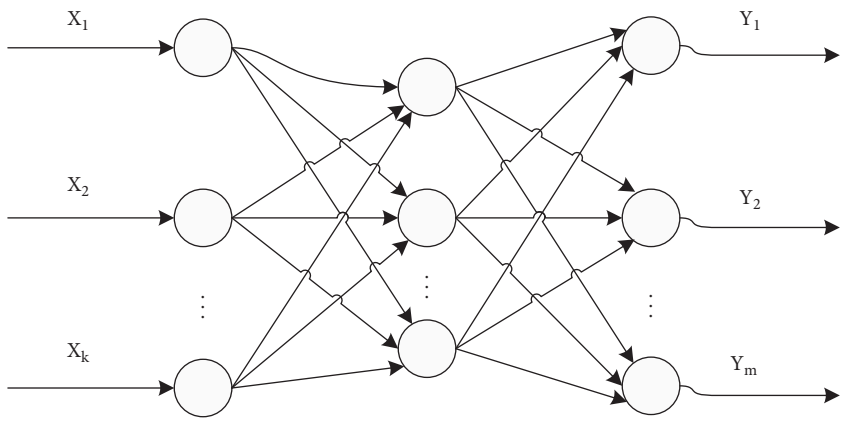

Figure 6: BP network model.

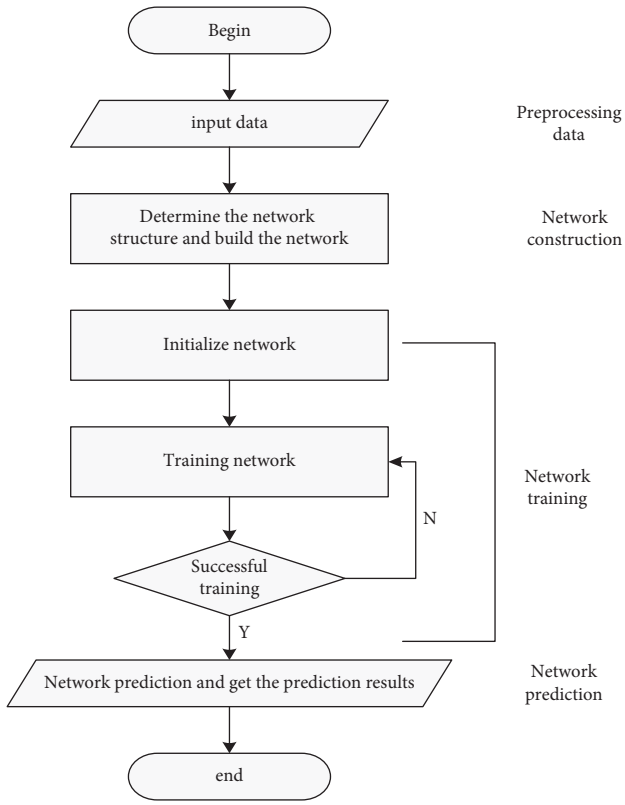

Figure 7: Network prediction process.

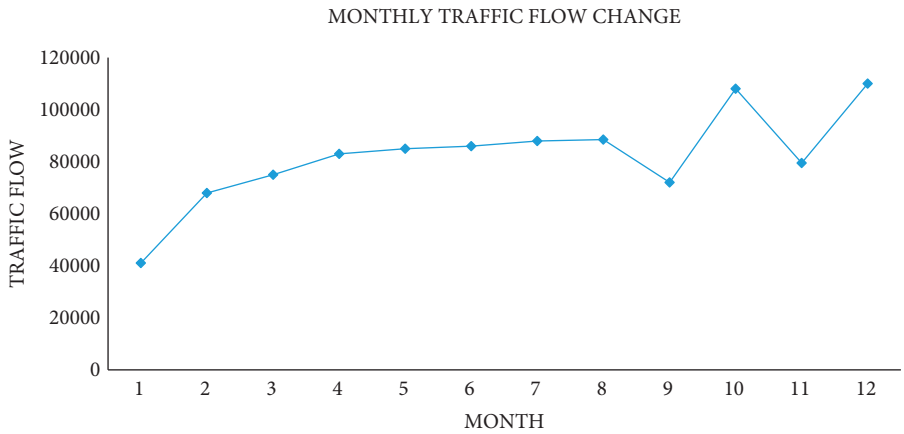

Figure 8: Change of traffic flow in October.

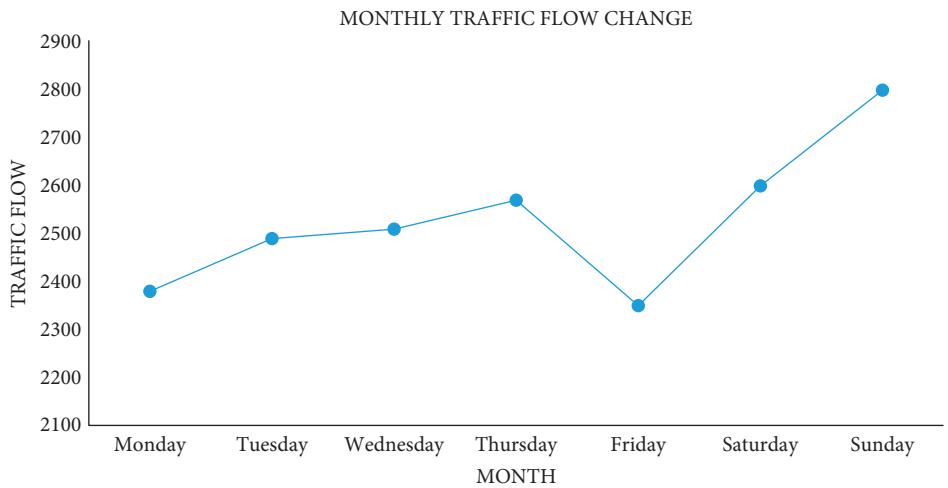

Figure 9: Daily traffic flow change.

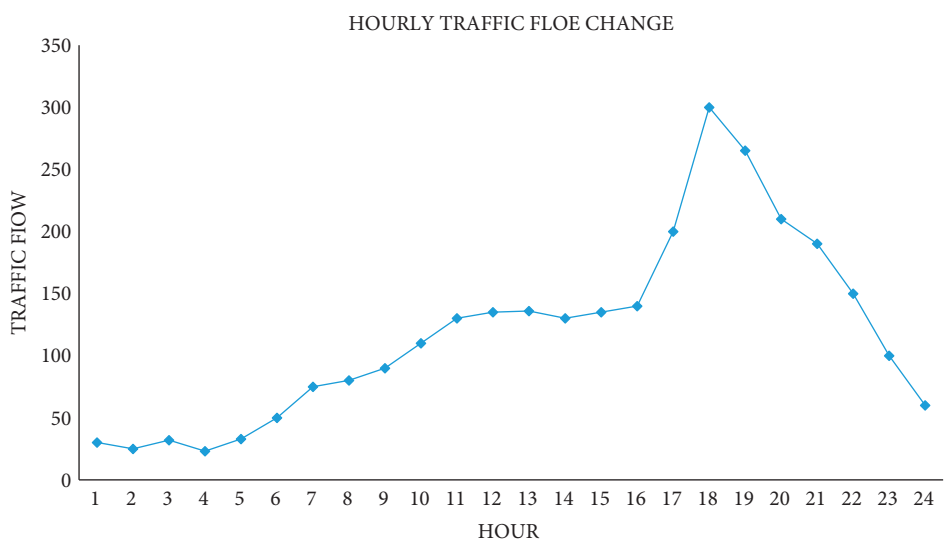

Figure 10: Analysis of the hourly traffic flow change.

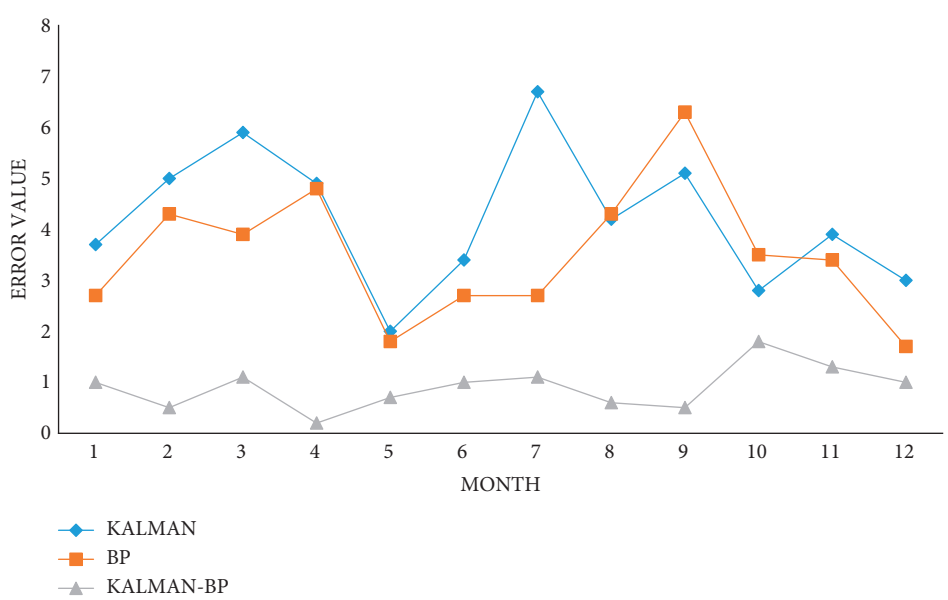

Figure 11: Forecast value of monthly traffic flow.

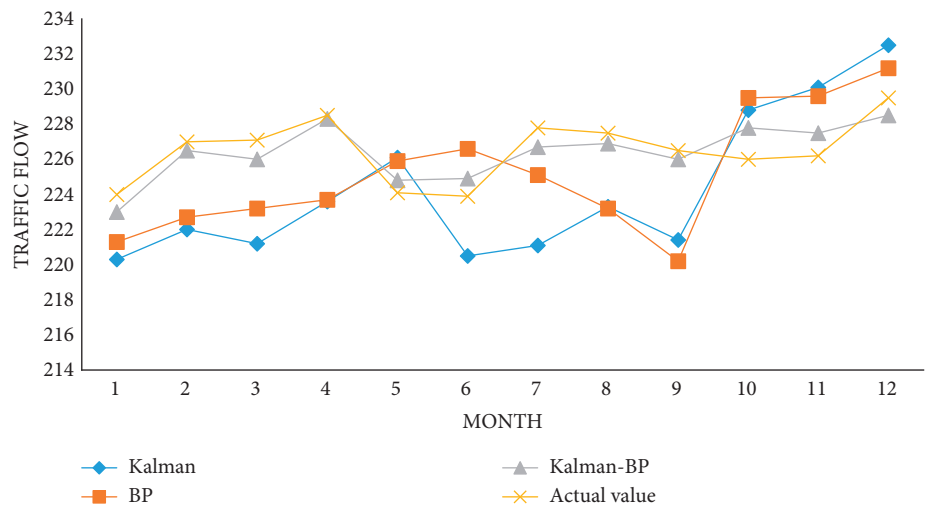

Figure 12: Comparison of monthly traffic flow error values.

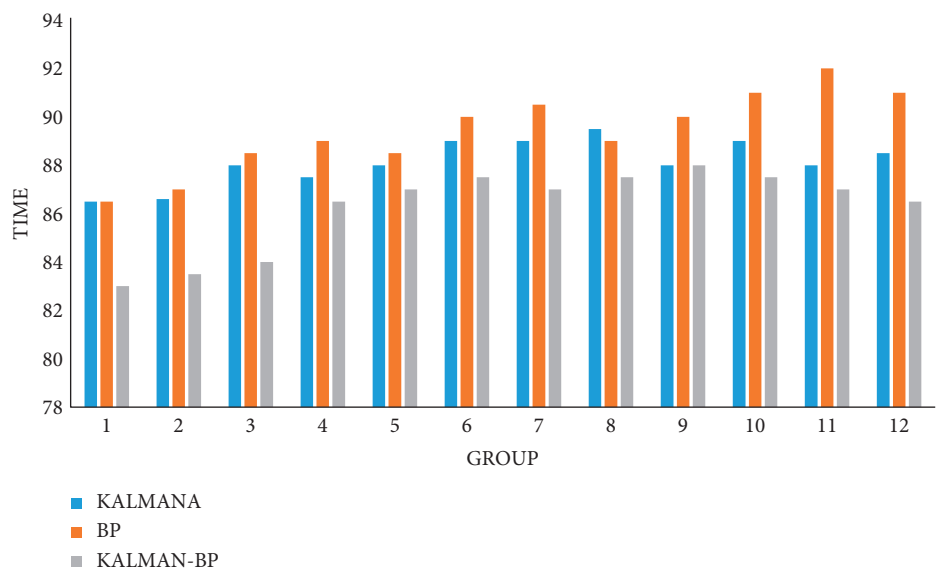

Figure 13: Forecast speed of monthly traffic flow.

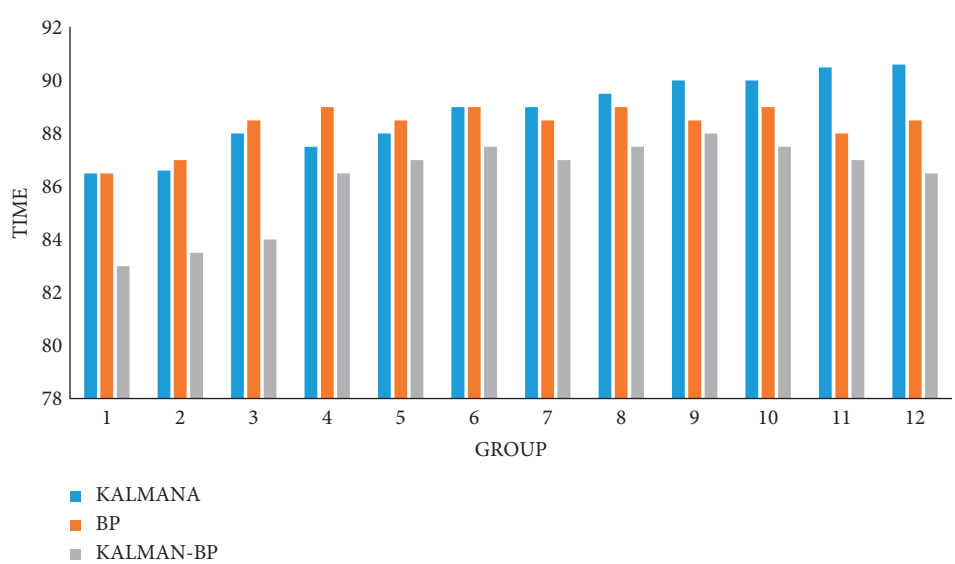

Figure 14: Forecast speed of daily traffic flow.

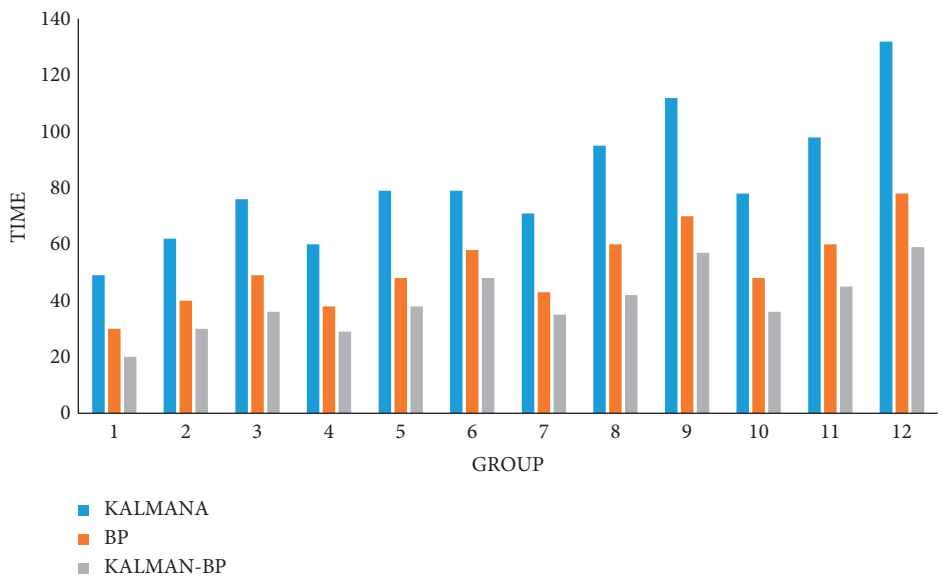

Figure 15: Predicted speed of hourly traffic flow.

5. Conclusion

In the field of intelligent transportation, it is predicted that the current processing research stage will realize the development of intelligent transportation in smart cities. The Kalman-BP combined algorithm proposed in this paper can improve the prediction accuracy of the overall traffic flow and lower the error value. It is pointed out in this paper that there are difficulties in predictive multivariate data fusion, and higher performance optimization algorithms are needed to solve such problems. Future research works, aiming at real-time data for effective prediction, can improve the accuracy of real-time traffic prediction and lower error rate. It also considers multitask and multiplatform data real-time prediction technology supported by Internet of Things, which can be better applied to urban traffic and intelligent optimization of traffic flow.

Data Availability

The experimental data used to support the findings of this study are available from the corresponding author upon request.

Conflicts of Interest

The authors declare that they have no conflicts of interest.

Acknowledgments

This research was supported by the Key Projects of Natural Science Research in Colleges and Universities of Anhui Province, China (KJ2018A0749 and KJ2020A0971) and the Projects of the Professional Construction Fund of Tongling Polytechnic (06202003).

References

[1] P. Anttila, J.-P. Tuovinen, and J. V. Niemi, "Primary NO2 emissions and their role in the development of NO2 concentrations in a traffic environment," *Atmospheric Environment*, vol. 45, no. 4, pp. 986–992, 2011.

[2] R. Sennett, "The uses of disorder : personal identity & city life," *American Political Science Review*, vol. 70, no. 3, pp. 198–987, 1970.

[3] C. L. Fang and D. L. Wang, "Comprehensive measures and improvement of Chinese urbanization development quality," *Geographical Research*, vol. 30, no. 11, pp. 1931–1946, 2011.

[4] K. Saito, S. Inagaki, T. Mituyama et al., "A regulatory circuit for piwi by the large Maf gene traffic jam in Drosophila," *Nature*, vol. 461, no. 7268, pp. 1296–1299, 2009.

[5] T. Lei, F. Lv, J. Liu, and J. Feng, "Research on electrical equipment monitoring and early warning system based on Internet of things technology," *Mathematical Problems in Engineering*, vol. 2022, pp. 1–12, Article ID 6255277, 2022.

[6] L. Hua, J. Zhang, and F. Lin, "Internet of things technology and its applications in smart grid," *TELKOMNIKA Indonesian Journal of Electrical Engineering*, vol. 12, no. 2, pp. 940–946, 2013.

[7] Y. Huang, Z. Yu, and C. Xie, "Study on the application of electric power big data technology in power system simulation," *Proceedings of the Csee*, vol. 35, no. 1, pp. 13–22, 2015.

[8] T. Lancet, "Greener roads: comparing intelligent transportation systems to construction-phase options to reduce emissions and fuel use," *Journal of Pharmacology and Experimental Therapeutics*, vol. 332, no. 1, pp. 153–163, 2011.

[9] K. M. Kendrick, "Intelligent perception," *Applied Animal Behaviour Science*, vol. 57, no. 3-4, pp. 213–231, 1998.

[10] L. Zhang, J. Ma, and C. Zhu, "Theory modeling and application of an adaptive Kalman filter for short-term traffic flow prediction," *Journal of Information and Computational Science*, vol. 9, no. 16, pp. 5101–5109, 2012.

[11] C. E. Brodley, "Addressing the selective superiority problem: automatic algorithm/model class selection," in *Proceedings of the Tenth International Conference on Machine Learning*, pp. 17–24, Amherst, MA, USA, June 1993.

[12] P. L. Peissig, L. V. Rasmussen, R. L. Berg et al., "Importance of multi-modal approaches to effectively identify cataract cases from electronic health records," *Journal of the American*

Medical Informatics Association, vol. 19, no. 2, pp. 225–234, 2012.

[13] A. K. Gupta and P. Redhu, "Analyses of driver's anticipation effect in sensing relative flux in a new lattice model for two-lane traffic system," *Physica A: Statistical Mechanics and Its Applications*, vol. 392, no. 22, pp. 5622–5632, 2013.

[14] R. S. Barga, D. B. Lomet, T. Baby, and S. Agrawal, "Persistent client-server database sessions," *Advances in Database Technology - EDBT 2000*, vol. 1777, pp. 462–477, 2000.

[15] S. Fan, G. Guo, W. Ma, and X. Liu, "Dynamic stability of composite foundation under different area replacement ratio based on intelligent sensing technology," *Cluster Computing*, vol. 22, no. S3, pp. 5931–5940, 2019.

[16] L. Jin, W. We, Z. Hao Zhang et al., "An embedded FBG sensor for simultaneous measurement of stress and temperature," *IEEE Photonics Technology Letters*, vol. 18, no. 1, pp. 154–156, 2006.

[17] W. Kim, D. Shin, D. Won, and C. C. Chung, "Disturbance-observer-based position tracking controller in the presence of biased sinusoidal disturbance for electrohydraulic actuators," *IEEE Transactions on Control Systems Technology*, vol. 21, no. 6, pp. 2290–2298, 2013.

[18] S. Ahuja and P. Potti, "An introduction to RFID technology," *Communications and Network*, vol. 02, no. 03, pp. 183–186, 2010.

[19] J. Song, "The application of WSN technology in the space location system," *Journal of Changchun University*, vol. 2, pp. 633–636, 2011.

Hindawi
Computational Intelligence and Neuroscience
Volume 2023, Article ID 9823751, 1 page
https://doi.org/10.1155/2023/9823751

Retraction

Retracted: The Dissemination and Evaluation of Campus Ideological and Political Public Opinion Based on Internet of Things Monitoring

Computational Intelligence and Neuroscience

Received 19 September 2023; Accepted 19 September 2023; Published 20 September 2023

This article has been retracted by Hindawi following an investigation undertaken by the publisher [1]. This investigation has uncovered evidence of one or more of the following indicators of systematic manipulation of the publication process:

(1) Discrepancies in scope
(2) Discrepancies in the description of the research reported
(3) Discrepancies between the availability of data and the research described
(4) Inappropriate citations
(5) Incoherent, meaningless and/or irrelevant content included in the article
(6) Peer-review manipulation

The presence of these indicators undermines our confidence in the integrity of the article's content and we cannot, therefore, vouch for its reliability. Please note that this notice is intended solely to alert readers that the content of this article is unreliable. We have not investigated whether authors were aware of or involved in the systematic manipulation of the publication process.

Wiley and Hindawi regrets that the usual quality checks did not identify these issues before publication and have since put additional measures in place to safeguard research integrity.

We wish to credit our own Research Integrity and Research Publishing teams and anonymous and named external researchers and research integrity experts for contributing to this investigation.

The corresponding author, as the representative of all authors, has been given the opportunity to register their agreement or disagreement to this retraction. We have kept a record of any response received.

References

[1] X. Xu and B. Sun, "The Dissemination and Evaluation of Campus Ideological and Political Public Opinion Based on Internet of Things Monitoring," *Computational Intelligence and Neuroscience*, vol. 2022, Article ID 8294613, 11 pages, 2022.

Hindawi
Computational Intelligence and Neuroscience
Volume 2022, Article ID 8294613, 11 pages
https://doi.org/10.1155/2022/8294613

Research Article

The Dissemination and Evaluation of Campus Ideological and Political Public Opinion Based on Internet of Things Monitoring

Xiao Xu[1] **and Bei Sun**[2]

[1]*School of International Communication, Communication University of China, Nanjing 211172, China*
[2]*School of E-Sports, Communication University of China, Nanjing 211172, China*

Correspondence should be addressed to Xiao Xu; xux@cucn.edu.cn

Received 11 March 2022; Revised 17 April 2022; Accepted 6 May 2022; Published 14 June 2022

Academic Editor: Guobin Chen

With the advent of the information age, the rapid development of Internet of Things technology makes monitoring methods more flexible and changeable. As an intelligent application, the development of the Internet of Things brings convenience to public opinion monitoring. However, at present, due to the high price of transmission equipment, inconvenient maintenance, information delay, and other unfavorable conditions, real-time and controllable public opinion monitoring cannot be carried out on a large scale, and there are still many deficiencies in campus ideological and political public opinion monitoring. We found an effective transmission method, explored the network energy saving, dig deep into the transmission function of the signal system, and reduced the interference and mutual influence of various transmission accessories. In the application of the Internet of Things, the network public opinion is remotely monitored, the campus public opinion information is mastered, and its dissemination and development orientation are controlled. The exploration and research of online public opinion monitoring are in line with the goal of smart campus, and its theoretical development is constantly enriched.

1. Introduction

The Internet of Things is an emerging information technology revolution [1–5]. As an intelligent application, it has become an extremely important application field. It is an extremely effective tool for monitoring systems [6–9]. Its popularity is increasing year by year, so it is more familiar to the public. The concept of smart campus has gradually gained popularity in recent years [10–12]. It is of great practical significance for ideological and political education to grasp this trend and use the Internet of Things to carry out ideological education work. With the continuous upgrading and expansion of Internet of Things technology, we can realize real-time network remote monitoring. To better meet the needs of campus ideological and political public opinion monitoring [13], public opinion supervision is crucial to campus stability [14, 15]. We use corresponding research methods to improve the supervision of public opinion, conduct real-time mastery and supervision of campus public opinion, and manage and guide it accordingly. The development and application of ideological and political education functions through the development of corresponding modules on the network and the continuous improvement of the functional application of the Internet of Things platform are the embodiment of the comprehensive implementation of the smart campus. The exponential development of Internet platforms has greatly increased the number of online public opinions. In today's information age, the masses have considerable freedom of speech on the Internet, which makes the overall controllability of public opinion information poor. It is necessary to increase the development of public opinion monitoring tools.

2. Overall Design of Campus Public Opinion Dissemination

In the dissemination of campus public opinion information, the dissemination of ideological and political public opinion is one of the important aspects. We need to complete these

tasks: the construction of the campus Internet of Things site, the construction of the energy cycle development system, and the construction of the public opinion monitoring website. Finally, the application of monitoring model to perfect the network environment is established.

When the Internet of Things technology is applied to the construction of smart campuses, it is necessary to fully exploit and utilize the characteristics of the Internet of Things. It makes the task of campus information management in the data age more convenient and effective and can better control the development of public opinion and make it truly effective. The optimization and upgrading of the monitoring function of the Internet of Things conform to the trend of the times and meet the goal of building a smart campus, so that the management and control of campus public opinion can be truly improved.

There are three parts in the campus public opinion dissemination system. One is the monitoring system, including wireless transmission, core control. and sensing operation, which is the core application of the entire system. The second is the appropriate addition of the energy supply system, including the reasonable conversion of natural energy, which can effectively improve the efficiency of energy utilization. The last is the web page display system, which can record and call monitoring data, including time data and location data. The overall design block diagram of campus public opinion dissemination is shown in Figure 1.

2.1. Text Analysis and Calculation of Public Opinion. The following is the application of the TF-IDF method. We can calculate and add vocabulary weights on the basis of the original documents and assign different weights to different words, so as to achieve the division of importance. When a word appears more than average, it can be considered representative, and we perform TF-IDF assignment operation on it. This can make the entire corpus weighted, making it easier to judge the orientation of campus public opinion. This formula can be converted into document feature values for operation when the number of occurrences of words in the article is too large. Specifically, it is a weight addition and subtraction operation for dividing the importance level. The formula for calculating the TF value is as follows:

$$\mathrm{TF}_{i,j} = \frac{n_{i,j}}{\Sigma_k n_{k,j}}. \tag{1}$$

Among them, $\mathrm{TF}_{i,j}$ represents the TF value of the ith word of the jth article, $n_{i,j}$ represents the frequency of the ith word of the jth article, $\Sigma_k n_{k,j}$ represents the frequency of occurrence of all words in the jth article, and k refers to the vocabulary size contained in the jth article. The introduction of the IDF calculation formula allows us to facilitate its calculation process, as shown below:

$$\mathrm{IDF}_{i,j} = \log \frac{|D|}{1 + \left|D_{t_i}\right|}. \tag{2}$$

$\mathrm{IDF}_{i,j}$ can be specific to the IDF value of the ith word in the jth article, $|D|$ represents the total number of text data, and $|D_{t_i}|$ represents the text number of t_i.

The overall calculation formula of the TF-IDF value is as follows:

$$\mathrm{TF-IDF}_{i,j} = \mathrm{TF}_{i,j} \times \mathrm{IDF}_{i,j}. \tag{3}$$

After a large number of TF weight operations [16], extract basic emotional information from text information, so that we can understand the general orientation of public opinion and better study its control methods. Public opinion information is the expression and expression of people's emotions, reflecting the needs of the social masses. The orientation of public opinion information in today's society will cause huge social repercussions, so it is very important to carry out its monitoring work. Public discourse text information is an important aspect, and more attention should be paid to text sentiment analysis.

Naive Bayes is a hypothetical concept [17]. First, assume that the conditions are established, so that the joint behavior turns to differentiation, then gradually solve the probability, and finally apply the conditional probability to calculate.

After multiplying the probabilities, add the maximum likelihood value to solve

$$\begin{aligned} &\mathrm{PX} = x\ ,\ Y = C_k = \mathrm{PY} = C_k P\left(X = x | Y = C_k\right), \\ &\mathrm{PY} = C_k = \frac{\mathrm{count}\left(Y = C_k\right)}{N}. \end{aligned} \tag{4}$$

The prior probability is represented by $\mathrm{PY} = C_k$. The maximum likelihood value proposed above also speaks of it. Usually the value of x is not easy to determine, which brings great difficulty to our calculation, so we have to carry out what-if analysis and use conditional independence and likelihood value to perform calculation operations:

$$\begin{aligned} P\left(X = x | Y = C_k\right) &= P\left(X_1 = x_1, \ldots, X_n = x_n | Y = C_k\right) \\ &= \prod_{i=1}^{n} P\left(X_i = x_i | Y = C_k\right), P\left(X_i = x_i | Y = C_k\right) = \frac{\mathrm{count}\left(X_i = x_i, y_i = c_k\right)}{\mathrm{count}\left(y_i = c_k\right)}. \end{aligned} \tag{5}$$

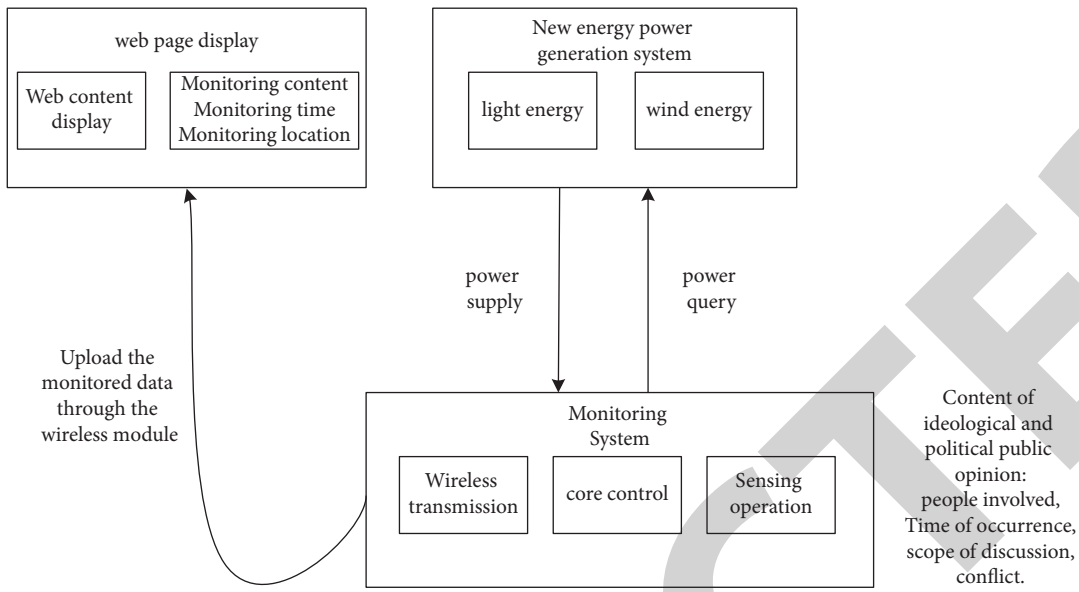

Figure 1: Overall block diagram of campus public opinion communication design.

The posterior probability is then obtained, and the y value is output:

$$y = \arg\max_{C_k} \frac{P(X = x|Y = C_k)\mathrm{PY} = C_k}{P(X = x)}. \quad (6)$$

We can finally get the calculation formula of the classification prediction function by simple conversion:

$$y = \arg\max_{C_k} \mathrm{PY} = C_k \prod_{i=0}^{n} P(X_i = x_i|Y = C_k). \quad (7)$$

After the above calculation is carried out, the text sentiment analysis value can be obtained. Then, take corresponding measures to guide public opinion information to avoid unnecessary losses.

2.2. Storage and Operation of Information. Sentiment analysis work is very important [15, 18–21]. In the following, a series of refinement operations are performed on the public opinion text information, and the lexical sentiment weights are arranged for the text data. Through keyword search, public opinion overview and early warning operations can be performed, and crawler and training parameters can be appropriately added to store and maintain public opinion data. Its design can be drawn from Figure 2:

Because people's words and deeds on the Internet are relatively free [22–24], the speed of dissemination of public opinion information has reached an unimaginable level, and the huge vocabulary increases the difficulty of its storage. For the main body of teachers and students, network tools are used more frequently, so the task of storing public opinions on campus is more difficult. We recommend using MySQL database technology. It has the characteristics of low overhead, high efficiency, and fast speed. It can run in many environments and has good performance in different scenarios. The data hierarchy is interconnected. The differentiated operation of the monitoring system is realized through Mange management, and it also has comprehensive operation monitoring of sessions, threads, and memory. Then, connect to the database protocol communication layer data and implement SQL parsing and optimization operations through the JDBC driver. The classification structure of MySQL database is shown in Figure 3.

Among them, the MySQL statement has the following advantages: MySQL statement has a good shareability, can share and exchange campus public opinion, and adapt to such a huge network public opinion system on campus. MySQL occupies less memory resources, which can facilitate our later cleaning and maintenance work, and we can run operations with less investment. The MySQL language is easy to use, is open source, and has a wealth of applicable platforms, which is convenient for campus personnel to use.

For the data set stored in the database, its reserves are quite huge. We require most of the data to be empty and only extract a small number of clearly representative data as representatives to represent the overall attributes, so as to achieve high efficiency. To identify and analyze public opinion information, we add the model evaluation analysis system to it and propose the precision rate P, recall rate r, F_1, and so on. The following calculated values can be obtained through matrix operations:

$$\begin{aligned} P &= \frac{\mathrm{TP}}{\mathrm{TP} + \mathrm{FP}}, \\ r &= \frac{\mathrm{TP}}{\mathrm{TP} + \mathrm{FN}}, \\ F_1 &= \frac{2\mathrm{TP}}{2\mathrm{TP} + \mathrm{FP} + \mathrm{FN}}, \\ \mathrm{acc} &= \frac{\mathrm{TP} + \mathrm{TN}}{\mathrm{TP} + \mathrm{FP} + \mathrm{TN} + \mathrm{FN}}. \end{aligned} \quad (8)$$

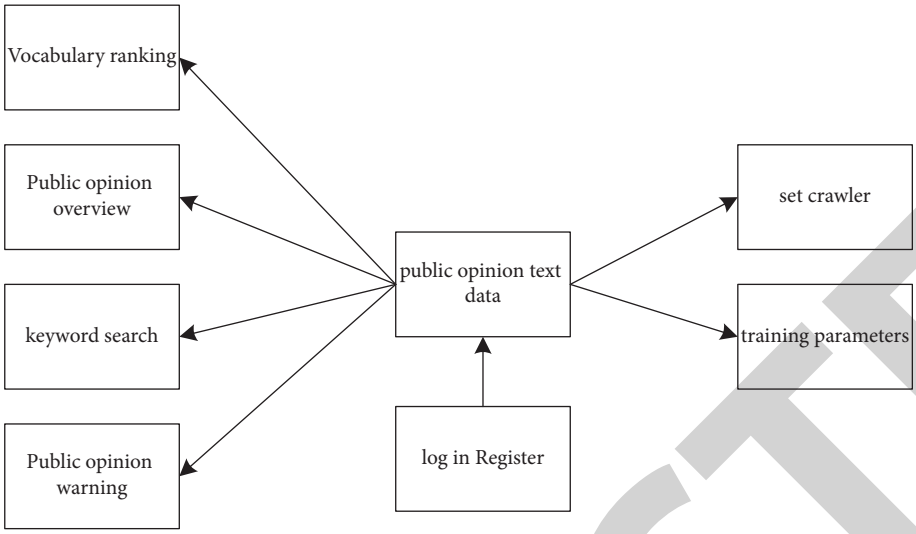

Figure 2: Analysis of public opinion text data.

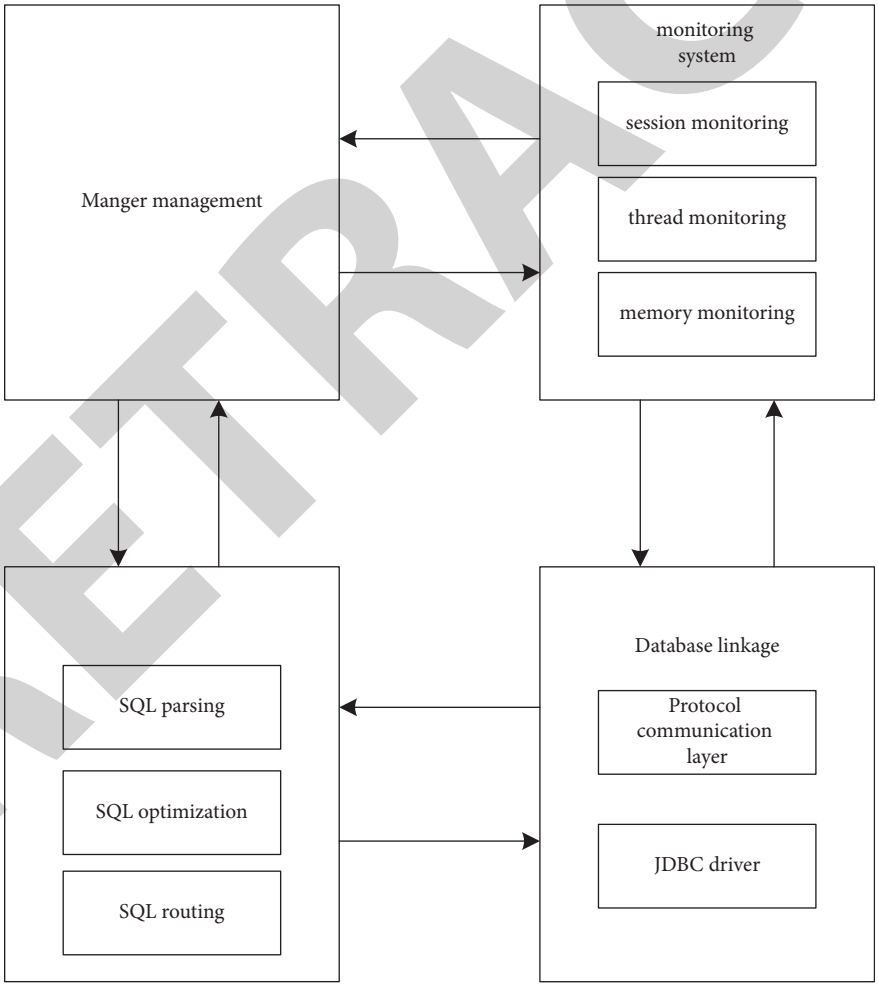

Figure 3: MySQL database implementation flow chart.

P is the overall analysis result of the predictive model, and r is the positive scale of the data. The F_1 value represents the average value of the reciprocal, and acc is the accuracy of the data, which is the proportion of all data. After the abovementioned data storage analysis, the orientation of campus public opinion can be clearly drawn, so that we can conduct more accurate and precise guidance and facilitate the direction of public opinion.

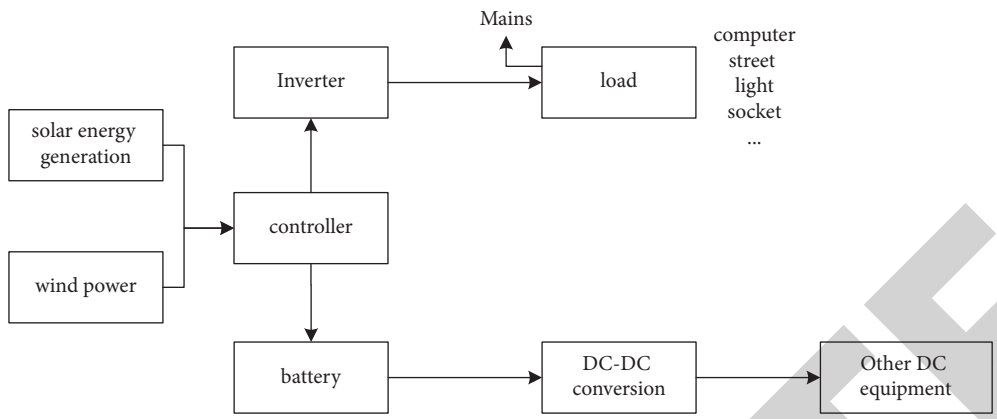

Figure 4: Hardware allocation process of energy supply structure.

3. Model Structure Optimization

3.1. Improvements in Energy Delivery. The power generation efficiency of traditional energy is extremely low, so we have carried out related transformations. The inverter, controller, converter, and battery have been properly adjusted, and the effect has improved. The energy initially flows to the controller and then splits into two to the inverter and battery. The inverter mainly supplies power to the equipment, and the battery stores the backup power. The specific implementation is shown in Figure 4.

3.2. Upgrade of Information Extraction. Generally speaking, the system of public opinion monitoring can be divided into front and rear ends. In the front-end operation, we mainly perform login options, which can roughly preview the public opinion content, watch the ranking of popular topics, search for keywords, etc., which is the main tool for understanding public opinion information. In terms of the back-end, we sequentially carry out the process of data collection, storage, extraction, and analysis and collect statistics on the collected information, so as to achieve effective monitoring of public opinion information. Its system structure diagram is roughly as shown in Figure 5.

Sentiment analysis of text is extremely important. It is worth emphasizing that we individually revamp and optimize the text sentiment analysis work. We introduce the CNN-BILSTM-ATT sentiment classification model. The CNN neural network has great advantages in capturing information in local areas and can perform analysis operations on high-latitude data. Since the object of our processing is the extremely large campus public opinion information group, it is easy to cause data missing when the CNN pooling layer performs data extraction and analysis on it. RNN has the ability of time processing and can effectively complete some difficult problems in time processing. But, at the same time, when RNN encounters such huge data information, its processing ability is also poor. LSTM has a certain ability to forget data, which is extremely important for text work with a huge amount of information. The forgetting ability of LSTM allows us to exclude those neutral words, or words that are not very helpful for analysis. Finally, combining the respective advantages of these models, we concluded that the CNN-BILSTM model can effectively solve this problem and greatly improve the accuracy of data sentiment analysis. Its comprehensive structure is shown in Figure 6.

Introduce the model, adding three gates. The calculations are as follows, each responsible for forgetting filtering, transmitting information, and outputting data. The calculation is as follows:

$$\begin{aligned} f_t &= \sigma\left(w_f \cdot [h(t-1)], x(t)\right] + b_f, \\ i_t &= \sigma\left(w_i \cdot [h(t-1)], x(t)\right] + b_i, \\ \sim c_t &= \tanh\left(w_c \cdot [h(t-1)], x(t)\right] + b_c, \\ c(t) &= f_t * c(t-1) + i_t * \sim c_t, \\ o_t &= \sigma\left(w_o \cdot [h(t-1)], x(t)\right] + b_o, \\ h_t &= o_t * \tanh[c(t)]. \end{aligned} \tag{9}$$

Sequence detection of convolutional kernels is performed in the convolutional layers of the model. We set this value to m and calculate as follows:

$$k_i = \tanh\left(u_i * w' + b\right). \tag{10}$$

Among them, u_i represents the convolution kernel, and $w' = [w_i, w_{i+1} \cdots w_{i+m-1}]$ is a continuous m vocabulary vector.

The output of feature vector calculation at time t is O_t^f, O_t^b. Then, V_t is calculated as follows:

$$V_t = O_t^f + O_t^b. \tag{11}$$

Assign weights to the BILSTM layer to obtain the target weights, which are calculated as follows:

$$U_t = \tanh\left(v_t\right) \tag{12}$$

The final SOFTMAX function can obtain the vector P_t after probabilistic operation and then calculate the weighted average to complete the calculation of each part. The relevant calculations are as follows:

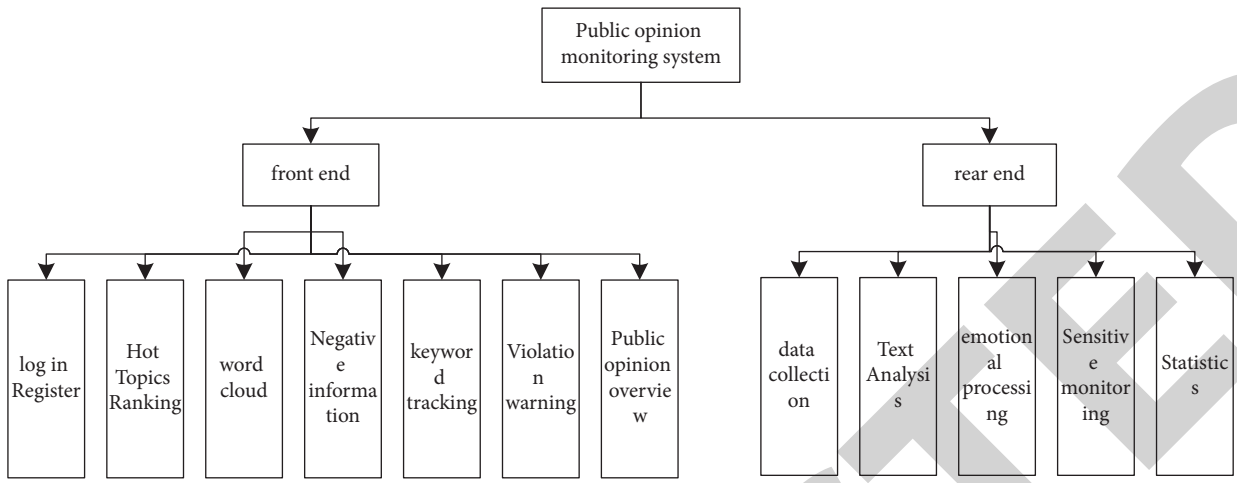

Figure 5: Structure diagram of public opinion monitoring system.

$$P_t = \frac{\exp(U_t)}{\sum_{t=1}^{m} \exp(U_t)},$$
$$a_t = \sum_{t=1}^{m} P_t \cdot V_t. \tag{13}$$

3.3. Optimization of Data Storage. In the overall framework structure of data storage applications, we are mainly dividing it into the following layers, which are user layer, application management layer, application platform support layer, application service layer, and application device layer.

The user layer mainly manages the user's data information. In the application management layer, the system settings, database, and website modules of public opinion can be applied for hierarchical data management. Subsequently, the development of multiplatform systems provides better system support capabilities. The series of platforms mainly include data acquisition and analysis and communication interfaces. Finally, it comes to the service layer, which is the application for the public, including SMS service, pop-up information service, and report download service. Its overall frame structure is shown in Figure 7.

This figure depicts the comprehensive framework of the data storage application and its overall architecture. It can be seen from the figure that the application device serves as the underlying device and has the main objects of the service on it, including short messages, information, and other content. The support layer is its core processing layer, which provides the processing work of information technology. The mutual cooperation of each application layer can finally realize the effective operation of data storage.

When it comes to data storage work, the first thing that comes to our mind is the extremely large number of chaotic information elements. In the face of these massive data information, it is very difficult for us to extract and analyze valuable factors, but we still have some. The approach makes it less complicated to sift through the data for analysis. The RBF neural structure diagram allows us to understand the principle of its data extraction. Its organizational structure is roughly as shown in Figure 8.

$$G(X, c_j) = e^{1/2\sigma_j^2 x - c_j^2},$$
$$y = \sum_{j=1}^{m} \left(G(x, c_j) \times w_j\right). \tag{14}$$

In this formula, m is the unit number of hidden neuron G, the output is Y, and the input is X. c_j and σ_j are the length and width data in the hidden layer.

$$\text{Loss} = \frac{1}{2}(\hat{y} - y)^2,$$
$$c_j = c_j - a\frac{\partial \text{Loss}}{\partial c_j} = c_j + a\frac{w_j}{\sigma_j^2}(\hat{y} - y)G(x, c_j)(x - c_j),$$
$$\sigma_j = \sigma_j - a\frac{\partial \text{Loss}}{\partial \sigma_j} = \sigma_j + a\frac{w_j}{\sigma_j^3}(\hat{y} - y)G(x, c_j)x - c_j^2,$$
$$w_j = w_j - a\frac{\partial \text{Loss}}{\partial w_j} = w_j + a(\hat{y} - y)G(x, c_j), \tag{15}$$

where $\hat{y}$ represents the real result, y is the final result, and a is the learning rate. The RBF neural network data is continuously learned and trained to improve the learning accuracy of data analysis and speed up the learning efficiency on the basis of the machine memory ability. In continuous learning and training, find the best oscillation range. In this way, the maximum learning accuracy is obtained and the most accurate data analysis results are obtained.

4. Experimental Simulation

4.1. Experimental Scheme. At the end of the experiment, we conduct a comparative analysis of the algorithm to verify its practical effect. Research campus public opinion information is the analysis object of the monitoring model. We

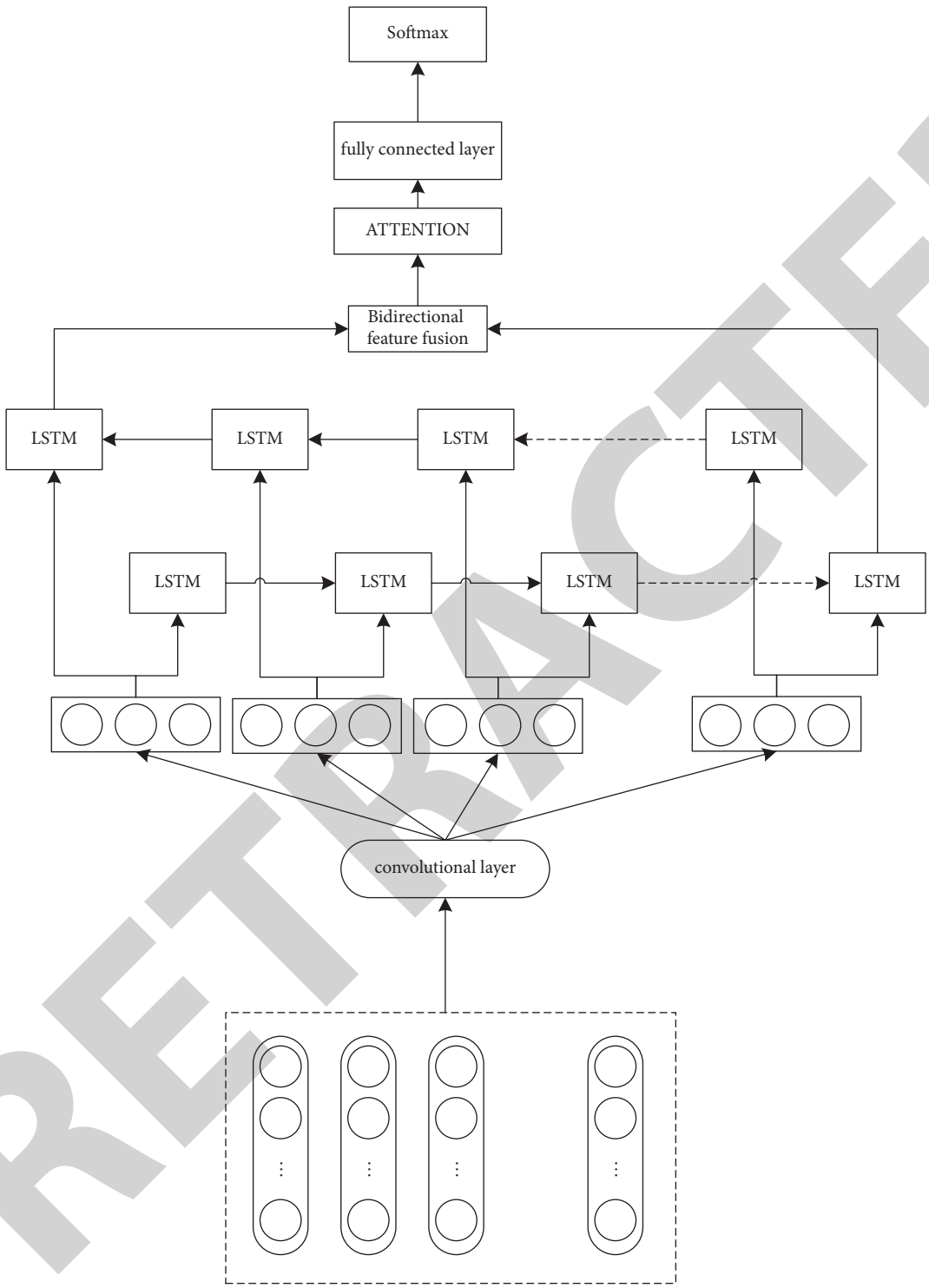

Figure 6: CNN-BILSTM model structure diagram.

compare multiple sets of data and obtain corresponding results by statistics on the efficiency of text sentiment analysis, the amount of text information analysis, and the delay in time transmission. The specific plans are as follows:

Option 1: TF-IDF method and MySQL database screening for public opinion data analysis

Option 2: TF-IDF method combined with MySQL database to provide energy-optimized public opinion data analysis

Option 3: TF-IDF method, public opinion data analysis after introducing CNN-BILSTM-ATT sentiment classification model into MySQL database

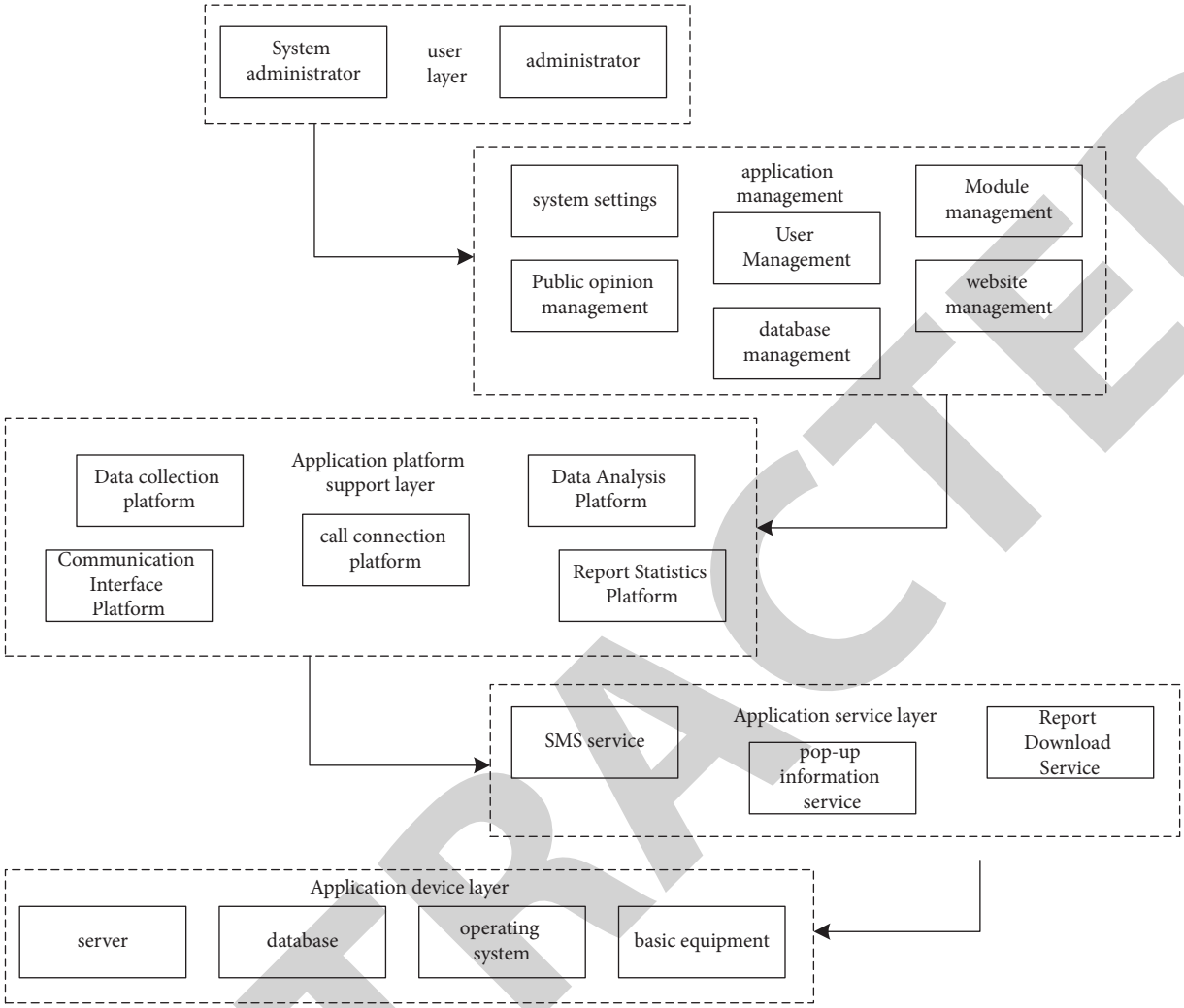

Figure 7: Overall framework of data storage applications.

Scheme 1: TF-IDF method, MySQL database combined with CNN-BILSTM-ATT sentiment classification model and RBF neural network to analyze the final public opinion information

4.2. Public Opinion Analysis and Comparison. Through the design of the above four schemes, we respectively set up a public opinion sentiment analysis experiment with the number of public opinion data information as 200, 500, 1000, and 3000 as the basic amount of data 3000. The results can clearly see the strength of each scheme for sentiment analysis. The specific comparison is shown in Figure 9.

In the following, we will study the time analysis efficiency of various schemes. In the specified unit time, the algorithm analysis amount of schemes 1–4 will be counted, respectively. After comparison, it can be clearly seen that the optimization of scheme 1 has improved significantly. Especially after 4 minutes, the pros and cons of the algorithm are more obvious. The amount of data analysis of scheme 1 is significantly higher than that of other categories. It can be seen more clearly the data analysis ability of our optimized model. The quantitative analysis comparison is shown in Figure 10.

Time efficiency is an important performance metric in any algorithm. The amount of data transmission per unit time of the algorithm is one of the important manifestations. It can be clearly seen from the time delay comparison analysis chart of the four algorithms that the time loss of scheme 1 is significantly lower than that of other algorithms. From left to right, the amount of data selected by the time delay is 100, 300, 500, and 1000, and the specific time loss comparison is shown in Figure 11.

Next, we use the fixed length of public opinion texts as a statistic to explore the efficiency ratio of each scheme to show the distribution of the highest efficiency. Not surprisingly, scheme 1 is the least efficient, while scheme 1 accounts for more than half of the total analysis efficiency, which is equivalent to the sum of the other three algorithms. The specific efficiency distribution is shown in Figure 12.

In the division of market satisfaction based on a fixed number of people, Schemes 1–4 have achieved different results. In the comparative analysis chart, the superiority of option 4 can be clearly seen, and its satisfaction level even

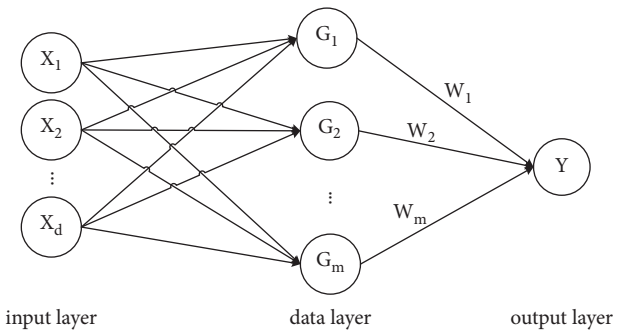

Figure 8: RBF neural network diagram.

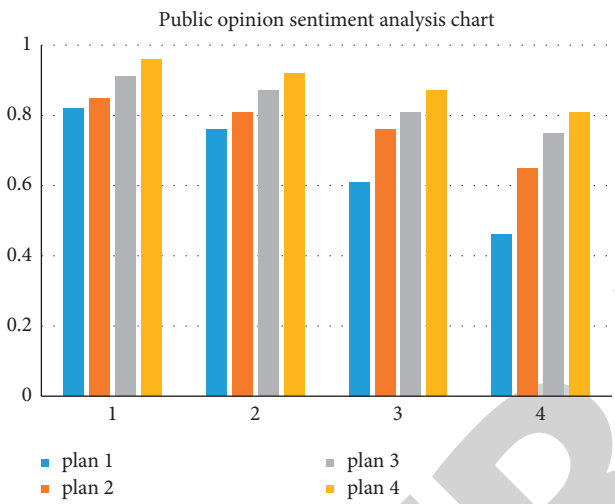

Figure 9: Comparison of public opinion sentiment analysis.

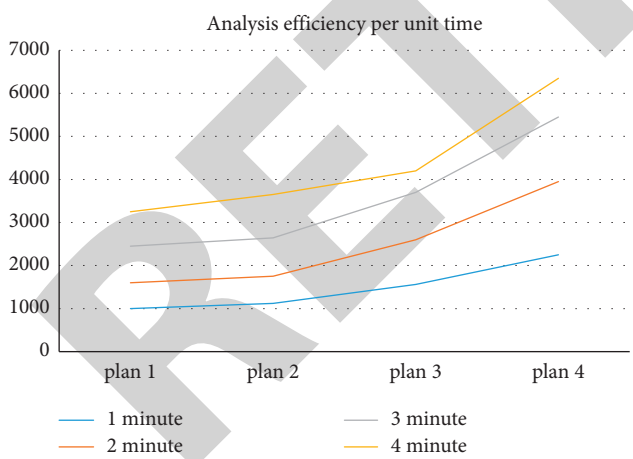

Figure 10: Unit time analysis and comparison chart.

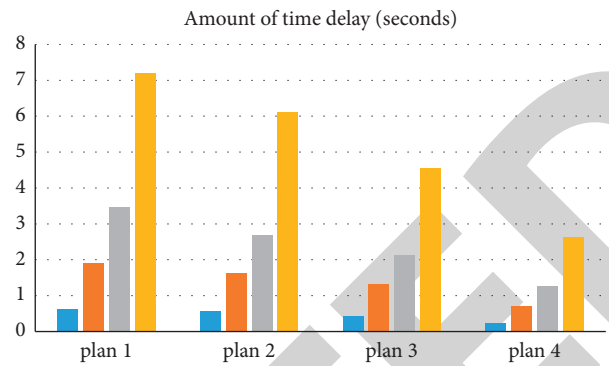

Figure 11: Unit data time delay diagram.

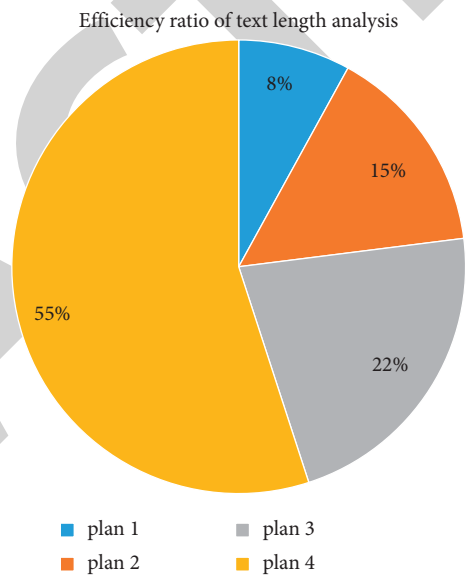

Figure 12: Efficiency ratio of text length analysis.

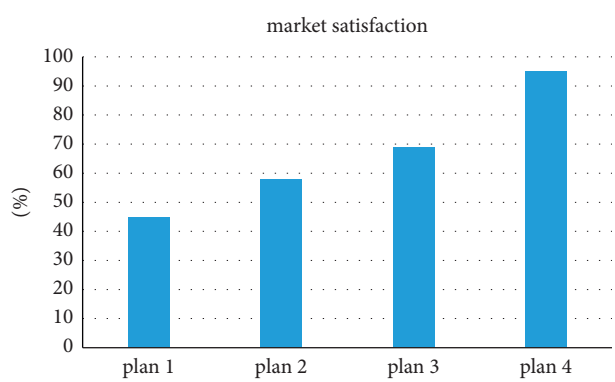

Figure 13: Market satisfaction.

reaches about 95%, which clearly shows the public's recognition of it, specifically as shown in Figure 13.

4.3. Analysis and Evaluation of Public Opinion. Among the numerous information data, we finally obtained two forms through the algorithm collection and analysis, one is the relevant information introduction of the search, and the other is the user's information description. In the search information, we can clearly know the user ID, the completion time of the search, the number of likes and retweets, etc., and even the text content of the search relevance. In the user specific information, we can learn some content, such as name and age. The acquisition of the following information data enables us to quickly understand the direction of public opinion dissemination, which brings great convenience to

Table 1: Search information table.

Id	Primary key
User-id	User ID
Like-num	Likes
Retweet-num	Number of retweets
Keyword	Search keyword
Create-time	First acquisition time
Update-time	Last acquisition time
Target	Search title
Href	Search link
Click	Have hits
Rank	Heat
Tag	Is it relevant

Table 2: User information table.

Field name	Explain
Id	Primary key
Nickname	Username
Gender	User gender
Location	User location
Description	User profile
Keyword	User search content
Talent	User credit
Work	User work information

Table 3: Comprehensive data analysis table.

Data set	Correct rate (%)	Recall (%)
Cluster1	91.02	89.56
Cluster2	94.57	92.65
Cluster3	92.09	96.77
Cluster4	93.25	83.59
Cluster5	98.57	96.64
Cluster6	95.65	91.56

the detection work and more effectively controls the development of public opinion. The details are shown in Tables 1 and 2.

In order to further verify the practical application ability of the public opinion data improvement model, we conducted a comprehensive data collection and analysis experiment, using the optimal algorithm for experimental operation, and running the algorithm under the condition that the optimal parameters are set as the benchmark to obtain the data in Table 3. It can be seen that the accuracy of the analysis of public opinion information in this experiment is very high, with an average of more than 95%. The specific situation is as follows:

5. Conclusion

In today's network information age, with the continuous popularization of network use, the amount of public opinion information is huge, and its management and monitoring are increasingly important. It is necessary to supervise and control the sensitive information and guide the trend of public opinion reasonably. These are all we need to do. In campus public opinion, topics with political tendencies are particularly important. If some negative emotions are added to them, it may affect the public's value orientation and bring about serious social problems. We must take measures to control them. This paper uses TF-IDF method to add and subtract weights and MySQL database and CNN-BILSTM-ATT sentiment classification model, combined with RBF neural network, to extract and analyze public opinion texts. Then, add a text sentiment analysis model for algorithm analysis. Implement the search and supervision of user information, and achieve a comprehensive upgrade of the accuracy of public opinion monitoring. It effectively avoids the serious problems caused by bad public opinion information. After a series of optimizations, it is more in line with the needs of campus public opinion monitoring. The monitoring of campus public opinion is of great practical significance. This paper mainly conducts exploration and research on public opinion text information and does not involve media such as pictures, voice, and video. Since these are also important aspects that reflect the trend of public opinion of the masses, comprehensive consideration of these will also be added in future research to expand public opinion monitoring, depth and width. Through the development of network modules, we improve its functions and continuously promote the construction of smart campuses.

Data Availability

The experimental data used to support the findings of this study are available from the corresponding author upon request.

Conflicts of Interest

The authors declared that they have no conflicts of interest regarding this work.

References

[1] J. Giersch, "Punishing campus protesters based on ideology," *Research & Politics*, vol. 6, no. 4, Article ID 205316801989212, 2019.

[2] Y. Chen and Y. Zhang, "Design and implementation of network educational platform for ideology and politics based on the concept of smart campus," *Revista de la Facultad de Ingenieria*, vol. 32, no. 11, pp. 45–53, 2017.

[3] Y.-p. Ma, X.-m. Shu, S.-f. Shen, and J. G. Q.-y. Song, "Study on network public opinion dissemination and coping strategies in large fire disasters," *Procedia Engineering*, vol. 71, pp. 616–621, 2014.

[4] S. H. Cardoso and R. Sabbatini, "Brain & mind magazine: an on-line multimedia resource for dissemination and evaluation of knowledge in neuroscience," *Proceedings of the Amia Annual Fall Symposium*, vol. 4, p. 921, 1997.

[5] S. Lihi Ben, "Gender, war, and world order: a study of public opinion by richard C. Eichenberg. Ithaca, NY, Cornell University Press, 2019. 204 pp. $49.95," *Political Science Quarterly*, vol. 135, no. 4, 2020.

[6] L. Fan, S. Zhao, and F. Han, "Research on the numerical accuracy of network public opinion propagation model based on Runge-Kutta method," *Journal of Physics: Conference Series*, vol. 1848, no. 1, Article ID 012102, 2021.

Hindawi
Computational Intelligence and Neuroscience
Volume 2022, Article ID 4941617, 10 pages
https://doi.org/10.1155/2022/4941617

Research Article

Intangible Cultural Heritage Management and Protection Based on Spatial Information Technology under the Background of Internet of Things

Jiaxi Sun

Chinese Theatre Arts Department, Shandong University of Arts, Jinan, Shandong 25000, China

Correspondence should be addressed to Jiaxi Sun; z00607@sdca.edu.cn

Received 16 February 2022; Revised 6 April 2022; Accepted 3 May 2022; Published 8 June 2022

Academic Editor: Guobin Chen

Intangible Cultural Heritage does not rely on material forms but is displayed through human inheritance, different tools, and flexible forms, which make the traditional management and protection methods unable to meet the needs of its development. Therefore, this paper puts forward the research on the management and protection of Intangible Cultural Heritage based on spatial information technology under the background of Internet of things and selects sports intangible cultural heritage as an example, combined with GIS technology and virtual reality technology. The analysis of the experimental results shows that the types of Chinese sports intangible cultural heritage are mainly martial arts, lack of water and ice and snow activities. The spatial distribution is uneven, with regional and ethnic differences, and six core density circles are formed in the form of clusters. Ecological environment, declaration system, and project classification are the main influencing factors of the spatial distribution of China's sports intangible cultural heritage. Therefore, in the management and protection of sports intangible cultural heritage, we should not only consider the impact of its ecological environment, but also give it modern function and inheritance form in combination with the needs of modern society while maintaining its connotation and spirit, so as to promote its protection, development, and inheritance.

1. Introduction

Intangible cultural heritage is a concept put forward relative to tangible and objective material cultural heritage. It refers to the cultural heritage created by working people that does not depend on material formation. Intangible cultural heritage has strong cultural value, but due to its intangible characteristics, it is difficult to collect it in museums. Therefore, the protection of intangible cultural heritage is different from the management and protection of other traditional cultural heritage [1]. Although folk cultural institutions have made great contributions to the protection of intangible cultural heritage, the protection of intangible cultural heritage can not ignore the impact of the natural environment and human environment of its birthplace. Only through an in-depth and comprehensive understanding of it can we better understand the significance contained in its spatial information and promote people to have a better understanding of its connotation and carry forward and inherit higher on the basis of maintaining the original national cultural spirit [2]. The formation and development of intangible cultural heritage are closely related to its spatial location, natural environment, humanistic spirit, and other aspects. Therefore, only by comprehensively obtaining its relevant spatial information can we have a relatively complete understanding and interpretation from different angles [3]. At the same time, intangible cultural heritage is special; that is, the characteristics of each intangible cultural heritage are different, and spatial information can not only understand the formation and development of intangible cultural heritage from the objectively existing spatial condition information, but also excavate its social, economic, political, and other significance [4]. Only by understanding and mastering the development

history of intangible cultural heritage can we better protect and manage it and make it better, more comprehensively and more completely showing the implied cultural spirit.

With the development of science and technology and information technology, the management and protection of intangible cultural heritage have a new development direction with the support of new science and technology. Some scholars restored the pictures, videos, words, and other materials of intangible cultural heritage through restoration technology through digital technology and improved the quality of the picture [5]. Other scholars proposed that people should pay attention to the protection and inheritance of intangible cultural heritage. Therefore, relevant materials and resources of intangible cultural heritage should be displayed through the network platform [6]. In addition, the major museums have also built animation models of relevant cultural relics by combining virtual reality technology to realize the 360-degree observable 3D model. The audience can click to obtain the introduction of relevant patterns, colors, and shapes, so as to actively promote China's history and culture and let the audience understand the inheritance significance of Intangible Cultural Heritage [7]. Compared with the traditional management and protection methods of intangible cultural heritage, the management and protection methods combined with modern science and technology can show the whole picture of intangible cultural heritage in a more detailed and clear way. At the same time, the relevant materials obtained through oral or written records can be constructed through modeling, restoration, splicing, and other technologies [8]. The constructed three-dimensional effect model can form a scene database and realize the three-dimensional data preservation of time and space Intangible Cultural Heritage [9]. In addition, the intangible cultural heritage of many ethnic minorities is loosely distributed and has a wide range. It is difficult to collect, record, and preserve relevant information and data in a short time through traditional methods, which improves the difficulty of intangible cultural heritage management and protection [10]. Spatial information technology and Internet of things technology can achieve the purpose of data collection and preservation in a short time, reduce labor costs, and improve the security and reliability of intangible cultural heritage protection [11].

This paper puts forward the research on the management and protection of Intangible Cultural Heritage based on spatial information technology under the background of Internet of things and takes sports intangible cultural heritage as an example, combined with GIS technology and virtual reality technology. The innovative contributions include the uneven distribution of China's sports intangible cultural heritage, showing regional and ethnic differences and forming the group form of six core circles. The impact of intangible cultural heritage on the ecological environment is considered. While maintaining its connotation and spirit, combined with the needs of modern society, give it modern functions and inheritance forms to promote its protection, development, and inheritance. The development of spatial information technology opens up a new way for the management and protection of intangible cultural heritage.

Therefore, this paper puts forward the research on the management and protection of Intangible Cultural Heritage based on spatial information technology under the background of Internet of things. Taking sports intangible cultural heritage as an example, this paper constructs the management and protection system of sports intangible cultural heritage through geographic information system and virtual reality technology in spatial information technology.

2. Difficulties and Problems in the Management and Protection of Intangible Cultural Heritage

Intangible cultural heritage is an important cultural crystallization in the process of human development. It can reflect the way of life in different regions and periods of a country. Its formation and spread have strong particularity. Although the ways of intangible cultural heritage management and protection are constantly developing, it is difficult to protect because of its particularity. First of all, intangible cultural heritage itself does not depend on material forms and is displayed by people through voice, manual, and other means of expression [12]. People are the key factor for the inheritance and development of intangible cultural heritage, but with the continuous development of society, people's education, cultural level, spiritual belief, and other aspects are also changing, which adds uncontrollable influencing factors to the protection and inheritance of Intangible Cultural Heritage [13]. Secondly, the traditional management and protection methods of intangible cultural heritage are relatively unitary, and a complete and systematic protection scheme has not been formed. In case of accidents, many relevant materials are difficult to preserve and restore, resulting in the loss of Intangible Cultural Heritage [14]. In recent years, although modern science and technology have been used in the protection of intangible cultural heritage, there have been many improvements in management and protection. However, there are still some problems such as people's insufficient understanding of intangible cultural heritage and prejudice. They believe that the inheritance of traditional culture does not need to be protected and ignore the historical and cultural connotation dependent on ancient buildings, murals, and other items [15]. Finally, intangible cultural heritage is closely related to local people's lifestyle, cultural environment, and spiritual sustenance. Therefore, much valuable intangible cultural heritage exists in rural areas in remote areas. Due to geographical location, on the one hand, the preservation of these intangible cultural heritage is relatively complete. On the other hand, the way of inheritance limits the development of Intangible Cultural Heritage [16, 17]. As shown in Figure 1, the intangible cultural heritage of some different regions is displayed.

Intangible cultural heritage protection does not have enough communication attraction due to inheritance methods, environmental restrictions, humanistic awareness, and other reasons. Many of them are still transmitted through text, pictures, and videos. It is not intuitive and

Figure 1: Intangible cultural heritage in some different regions.

three-dimensional, which can not fully show the charm of intangible cultural heritage and weaken its attraction to people [18]. At the same time, the offline display channels of intangible cultural heritage are mainly performance and exhibition and guild hall display. The channel is single and can not achieve a comprehensive, perceptible, and touchable experience effect. The commercial value of intangible cultural heritage is not enough to solve the contradiction between survival and development faced by inheritors [19]. At the same time, the inheritors of intangible cultural heritage have relatively weak personal technical foundation and financial ability and lack corresponding innovation consciousness and innovation ability in the process of inheritance, which makes the connotation of intangible cultural heritage unable to meet the spiritual needs of the public, thus limiting its development [20].

3. Genetic Management and Protection System Model of Sports Intangible Culture Based on GIS

Sports intangible cultural heritage, also known as "Living Heritage," is an important part of China's intangible cultural heritage. It not only has extremely important cultural, historical, and scientific values, but also contains the aesthetic consciousness of national traditional culture in various aspects, such as diversified inheritance methods, diversified contents, and flexible display methods, as well as spiritual value and cultural connotation. At the same time, the complex and multifunctional sports intangible cultural heritage has high requirements for the survival and development environment. This specificity makes its management and protection need to be realized through advanced methods and technologies. Therefore, this paper selects geographic information system (i.e., GIS Technology) and virtual reality technology (i.e., VR technology) to support the management and protection of sports intangible cultural heritage. As shown in Figure 2, it is the framework of sports intangible culture genetic management and protection system based on GIS.

As shown in Figure 2, the framework of sports intangible culture genetic management and protection system based on GIS is mainly divided into three layers. It includes visualization technology layer, shared service technology layer, and data management technology layer. The visualization technology layer includes the multimedia interactive platform of sports intangible cultural heritage. The platform constructs context modeling and interaction and knowledge model through scene generation, role generation, and action binding technology. The sharing service layer covers the sharing and service system of sports intangible cultural heritage resources. In the new media era, big data, Internet and technologies have enhanced the scope of effective services sharing. Resource sharing and service system plays an important role in improving the level of competitive sports and promoting the development of national fitness sports industry. Finally, it is the data information management system of sports intangible cultural heritage. Using the most advanced digital technology to protect the ancient intangible cultural heritage is an important means and development direction of global feminine heritage protection and inheritance. The database construction of China's sports well material and cultural heritage resources has reached the requirements of advanced nature, standardization, and expansibility.

3.1. Spatial Distribution Model of Sports Intangible Cultural Heritage Based on GIS. GIS spatial analysis method is to extract and obtain new spatial information through the comprehensive operation of spatial data and attribute data

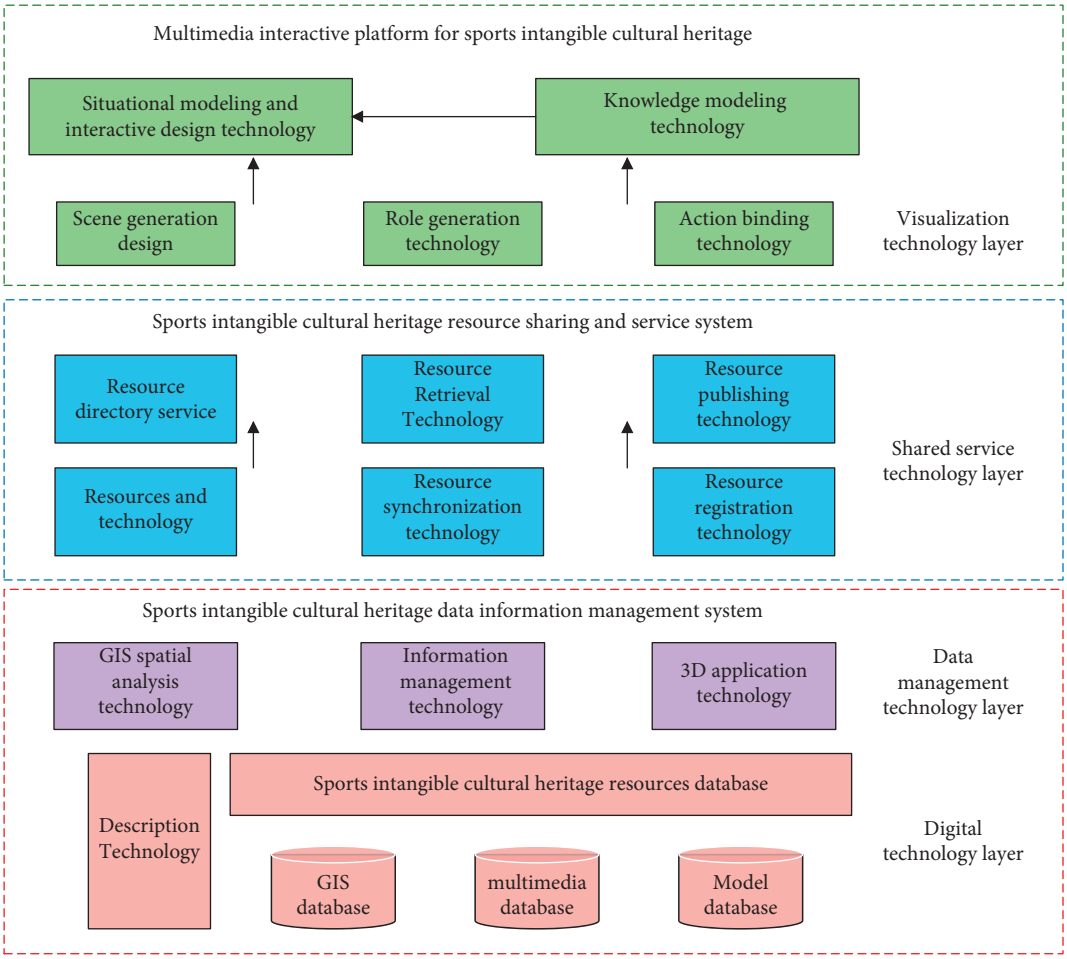

Figure 2: Framework of genetic management and protection system of sports intangible culture based on GIS.

on the basis of the spatial location and morphological characteristics of things in the ground. It mainly includes average nearest neighbor index, standard deviation ellipse, kernel density analysis, and spatial correlation analysis. The average nearest neighbor index is an index to measure the distribution degree of point things in the inner space. The spatial distribution type of sports intangible cultural heritage can be distinguished by the average nearest neighbor index, and its calculation formula is shown in the following formula:

$$\mathrm{ANNI} = \frac{\mathrm{ANNO}}{\mathrm{ANNE}} = \frac{\sum_{i=1}^{n} \min\left(d_{ij}\right)/n}{1/\sqrt[2]{n/A}}. \tag{1}$$

The average nearest neighbor index is expressed as ANNI, the actual nearest neighbor distance is expressed as ANNO, the theoretical nearest neighbor distance is expressed as ANNE, the distance between any sports intangible cultural heritage site and its nearest sports intangible cultural heritage site is expressed as d_{ij}, the number of points is expressed as n, and the area of the study area is expressed as A.

Geographical concentration index measures the concentration degree of element distribution, and the concentration degree of element increases with the increase of its value. Its calculation formula is shown in the following formula:

$$G = 100 * \sqrt{\sum_{i=1}^{n} \left(\frac{x_i}{T}\right)^2}, \tag{2}$$

where the geographical concentration index is expressed as G, the number of sports intangible cultural heritage sites in the i region is expressed as x_i, the total number is expressed as T, and the total number of regions is expressed as n. If G_i is set as the ideal geographical concentration index, the ratio of G and G_i is the geographical concentration degree, expressed as G_r, and its calculation formula is shown in the following formula:

$$G_r = \frac{G}{G_i} = \frac{100 * \sqrt{\sum_{i=1}^{n} \left(x_i/T\right)^2}}{T/n}. \tag{3}$$

When the value of G_r is greater than 1, it means that the distribution of sports intangible cultural heritage sites tends to be concentrated, and the degree of distribution concentration will increase with the increase of G_r value. On the contrary, it means that the distribution of sports intangible cultural heritage sites tends to be uniform.

Let Gini coefficient represents the distribution uniformity of sports intangible cultural heritage in multiscale space, and its value range is [0, 1]. The distribution uniformity of spatial elements increases with the increase of Gini coefficient. The calculation formula is shown in formulas (4) and (5):

$$\text{Gini} = 1 - \frac{1}{n}\left(2\sum_{i=1}^{n-1} W_i + 1\right), \tag{4}$$

$$C = 1 - \text{Gini}. \tag{5}$$

In the formula, the Gini coefficient is expressed as Gini, the uniformity of element distribution is expressed as C, the percentage of spatial elements in all elements in different partitions, the cumulative proportion of the i area sorted in order is expressed as W_i, and the total number of partitions is expressed as n.

Due to the different spatial and scale distribution of intangible cultural heritage elements, the imbalance index can measure the distribution equilibrium degree of spatial elements in different areas, and its value range is [0, 1]. The distribution equilibrium degree of spatial elements increases with the decrease of imbalance index. The calculation formula is shown as follows:

$$S = \frac{\sum_{i=1}^{n-1} Y_i - 50(n+1)}{100n - 50(n+1)}. \tag{6}$$

In the formula, the imbalance index is expressed as S, the number of regions is expressed as n, and the percentage of spatial elements in all elements in i partitions is expressed as Y_i.

And density function can reflect the density of point elements in the neighborhood of the space, that is, the cold and hot spots of elements in spatial distribution. Let the core density of any sports intangible cultural heritage site be x, as shown in the following formula:

$$f(x) = \sum_{i=1}^{n} \frac{1}{\pi r^2} k\left(\frac{d_{\text{is}}}{r}\right). \tag{7}$$

In the formula, the position of the point to be estimated is expressed as x, the search radius is expressed as r, the distance from the point to the center of the circle in the search range with the point to be estimated as the center is expressed as d_{is}, the number of points is expressed as n, and the kernel density equation is expressed as k.

3.2. Visualization of Sports Intangible Cultural Heritage Based on Virtual Reality Technology. 3D registration technology is a 3D registration method of augmented reality system. 3D registration technology is an important aspect of augmented reality system research. The existing 3D registration methods of augmented reality technology use plane signs as positioning benchmarks, and the system structure is complex. Image processing requires a large amount of calculation, which will lead to errors. There is a vision based three-dimensional registration method using three-dimensional markers. This method only needs a color CCD camera to complete the registration of three-dimensional environment and does not need complex image processing operations. This new method can effectively simplify the registration system and algorithm and eliminate the matching error of using multiple sensors. The combination of GIS technology and virtual reality technology can digitally collect and save all kinds of data according to the relevant information of sports intangible cultural heritage. At the same time, the original appearance of sports intangible cultural heritage can be restored through three-dimensional physical modeling or corresponding database, so as to achieve high-precision, real and long-term preservation. In addition, the Virtual Museum of online sports intangible cultural heritage can be built through virtual reality technology, and the virtual scene environment related to sports intangible culture such as information, resource value, protection planning, and management can be built through visualization technology, so as to provide a more intuitive protection and management platform for the management and protection of sports intangible cultural heritage and promote its development and inheritance. This paper uses the virtual reality technology based on Kinect depth camera to realize the construction of three-dimensional model of sports intangible cultural heritage. 3D registration technology is not only the basic technology of VR, but also one of the core technologies. During 3D registration, it is necessary to convert the translation and projection between image plane coordinate system, camera coordinate system, and world coordinate system. Let the point of the world coordinate system be represented by homogeneous coordinates, i.e., $X_w = (x_w, y_w, z_w, 1)^T$, and its corresponding projection on the image plane is represented as $X = (x, y, 1)^T$. The relationship between the two is shown in the following formula:

$$X = PX_w = \lambda KMX_w = \lambda K\begin{bmatrix} R_1 & R_2 & R_3 & R_4 \\ 0 & 0 & 0 & 1 \end{bmatrix} X_w. \tag{8}$$

If X_w is on the surface real plane, $z_w = 0$, formula (8) can be transformed into the following formula:

$$\begin{aligned} x &= \begin{bmatrix} x \\ y \\ 1 \end{bmatrix} = \lambda K\begin{bmatrix} R_1 & R_2 & R_3 & R_4 \\ 0 & 0 & 0 & 1 \end{bmatrix}\begin{bmatrix} x_w \\ y_w \\ 0 \\ 1 \end{bmatrix} \\ &= \lambda K\begin{bmatrix} R_1 & R_2 & T \\ 0 & 0 & 1 \end{bmatrix}\begin{bmatrix} x_w \\ y_w \\ 1 \end{bmatrix} = H_w\begin{bmatrix} x_w \\ y_w \\ 1 \end{bmatrix}. \end{aligned} \tag{9}$$

In the formula, the internal parameters of the camera are expressed as K and the external parameters are expressed as M.

The realization of 3D registration needs to first extract the natural feature points in the real scene and track them accordingly. At the same time, the 3D coordinates of the corresponding feature points are projected in the observation 2D image coordinate system, and the corresponding relationship between them is constructed. Then, the homography matrix of each frame image is obtained to estimate the pose information of the camera, and finally the 3D registration is

realized. The pose information of the camera can be calculated by affine reconstruction technology; that is, when the image plane is known to be in two different viewing angles and the origin and affine base point are also in different viewing angles, affine reconstruction can obtain the corresponding position of the points contained in the two-dimensional image plane in the spatial radial coordinate system. Suppose that a point in the radial coordinates in space is represented as $X = (U, V, W, 1)^T$, the coordinates of the point in the image plane under different viewing angles are represented as $x^1 = \{u^1, v^1, 1\}$, $x^2 = \{u^2, v^2, 1\}$, respectively, and its position in the radial coordinate system can be calculated by the following formula:

$$\begin{bmatrix} u^1 \\ v^1 \\ u^2 \\ v^2 \end{bmatrix} = \begin{bmatrix} u_1^1 - u_0^1 & u_2^1 - u_0^1 & u_3^1 - u_0^1 & u_0^1 \\ v_1^1 - v_0^1 & v_2^1 - v_0^1 & v_3^1 - v_0^1 & v_0^1 \\ u_1^2 - u_0^2 & u_2^2 - u_0^2 & u_3^2 - u_0^2 & u_0^2 \\ v_1^2 - v_0^2 & v_2^2 - v_0^2 & v_3^2 - v_0^2 & v_0^2 \end{bmatrix} \begin{bmatrix} U \\ V \\ W \\ 1 \end{bmatrix} = R_{4*4} \begin{bmatrix} U \\ V \\ W \\ 1 \end{bmatrix}. \tag{10}$$

The corresponding projection of the point in the current image plane is shown in the following formula:

$$\begin{bmatrix} u \\ v \\ 1 \end{bmatrix} = \begin{bmatrix} u_1 - u_0 & u_2 - u_0 & u_3 - u_0 & u_0 \\ v_1 - v_0 & v_2 - v_0 & v_3 - v_0 & v_0 \\ 0 & 0 & 0 & 1 \end{bmatrix} \begin{bmatrix} U \\ V \\ W \\ 1 \end{bmatrix} = M_{3*4} \begin{bmatrix} U \\ V \\ W \\ 1 \end{bmatrix}. \tag{11}$$

The image coordinate system is divided into a two-dimensional rectangular pixel coordinate system and an imaging plane coordinate system with the intersection of the camera optical axis and the image plane as the coordinate origin. Assuming that the physical dimensions of each pixel in the direction of x axis and y axis are $\mathrm{d}x, \mathrm{d}y$, respectively, the transformation relationship of any pixel point in the image under the two coordinate systems is shown in the following formula:

$$\begin{bmatrix} u \\ v \\ 1 \end{bmatrix} = \begin{bmatrix} \frac{1}{\mathrm{d}x} & 0 & u_0 \\ 0 & \frac{1}{\mathrm{d}y} & u_0 \\ 0 & 0 & 1 \end{bmatrix} \begin{bmatrix} x \\ y \\ 1 \end{bmatrix}. \tag{12}$$

Since the manufacturing processes of different cameras are different, the transformation relationship is shown in the following formula:

$$\begin{bmatrix} u \\ v \\ 1 \end{bmatrix} = \begin{bmatrix} \frac{1}{\mathrm{d}x} & s_1 & u_0 \\ 0 & \frac{1}{\mathrm{d}y} & u_0 \\ 0 & 0 & 1 \end{bmatrix} \begin{bmatrix} x \\ y \\ 1 \end{bmatrix}. \tag{13}$$

$s_1 = \tan\gamma$ and γ in the formula represent the oblique distortion angle in the imaging coordinate system.

The position of the camera in any scene is arbitrary, so it is necessary to determine the position of the camera and other objects in space with the help of world coordinates. The transformation relationship between the world coordinate system and the camera coordinate system can be expressed by rotation matrix and translation vector; that is, let the homogeneous coordinate systems of a point under the two coordinate systems be $(X_w, Y_w, Z_w, 1)^T$, $(X_c, Y_c, Z_c, 1)^T$, respectively, and the transformation relationship is shown in the following formula:

$$\begin{bmatrix} X_c \\ Y_c \\ Z_c \\ 1 \end{bmatrix} = \begin{bmatrix} R & t \\ 0^T & 1 \end{bmatrix} \begin{bmatrix} X_w \\ Y_w \\ Z_w \\ 1 \end{bmatrix} = M_1 \begin{bmatrix} X_w \\ Y_w \\ Z_w \\ 1 \end{bmatrix}, \tag{14}$$

where the orthogonal identity matrix is expressed as R, the three-dimensional translation vector is expressed as $t = (t_x, t_y, t_z)^T$, and M_1 is expressed as $4 * 4$.

In the positive virtual reality system, the position of the virtual object needs to be represented through the virtual coordinate system. Therefore, the transformation relationship between the virtual coordinate system and the world coordinate system is shown in the following formula:

$$\begin{bmatrix} X_v \\ Y_v \\ Z_v \\ 1 \end{bmatrix} = \begin{bmatrix} s_x & 0 & 0 & 0 \\ 0 & s_y & 0 & 0 \\ 0 & 0 & s_z & 0 \\ 0 & 0 & 0 & 1 \end{bmatrix} \begin{bmatrix} X_w \\ Y_w \\ Z_w \\ 1 \end{bmatrix} = S \begin{bmatrix} X_w \\ Y_w \\ Z_w \\ 1 \end{bmatrix}. \tag{15}$$

4. Application Experimental Results of Genetic Management and Protection System of Sports Intangible Culture Based on GIS

This paper obtains the data of China's sports intangible cultural heritage according to the relevant database, as shown in Figure 3, which is its main type structure. It can be seen from the results in the figure that China's sports intangible cultural heritage has no international sports intangible cultural heritage at the project level. The main types of classification are mainly the twelve categories in the figure. Although most sports intangible cultural heritage projects can be classified according to the twelve types, the classification of a small number of comprehensive competition projects is not clear, so they are divided into the added new category, namely, folk entertainment. Martial arts are the largest category of sports nonmaterial cultural heritage, accounting for about 60% of the total. The second largest category is folk entertainment, accounting for about 20% of the total. The number of water activities and ice and snow activities is the least, with only one project each. Therefore, overall, among the types of China's sports intangible cultural heritage, Wushu ranks first, other types of activities have a certain quantity distribution, and water activities and ice and snow activities are the most scarce.

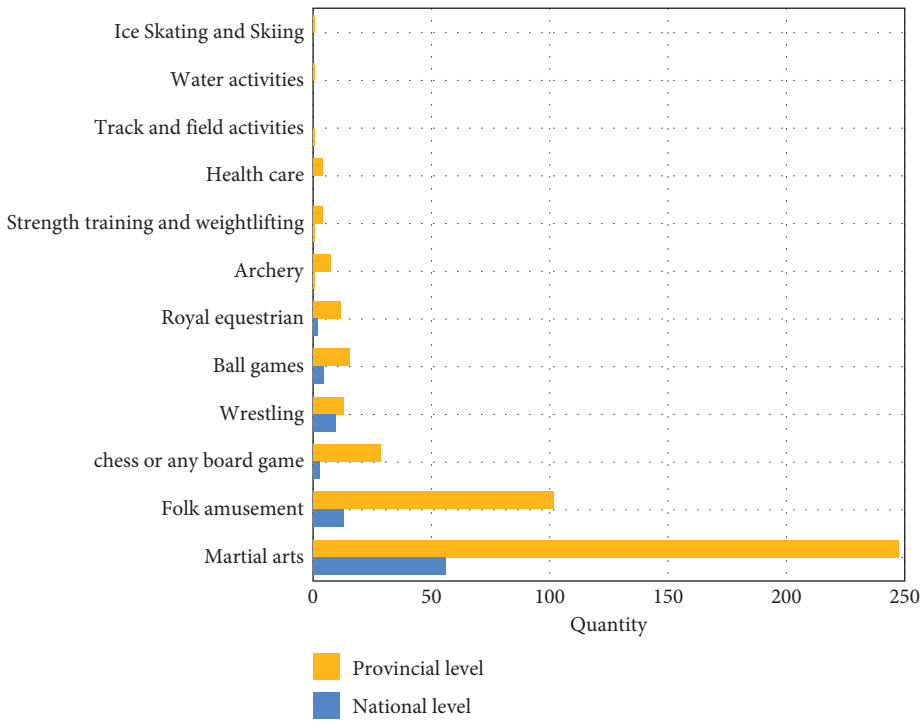

Figure 3: Main types and structure of data of China's sports intangible cultural heritage.

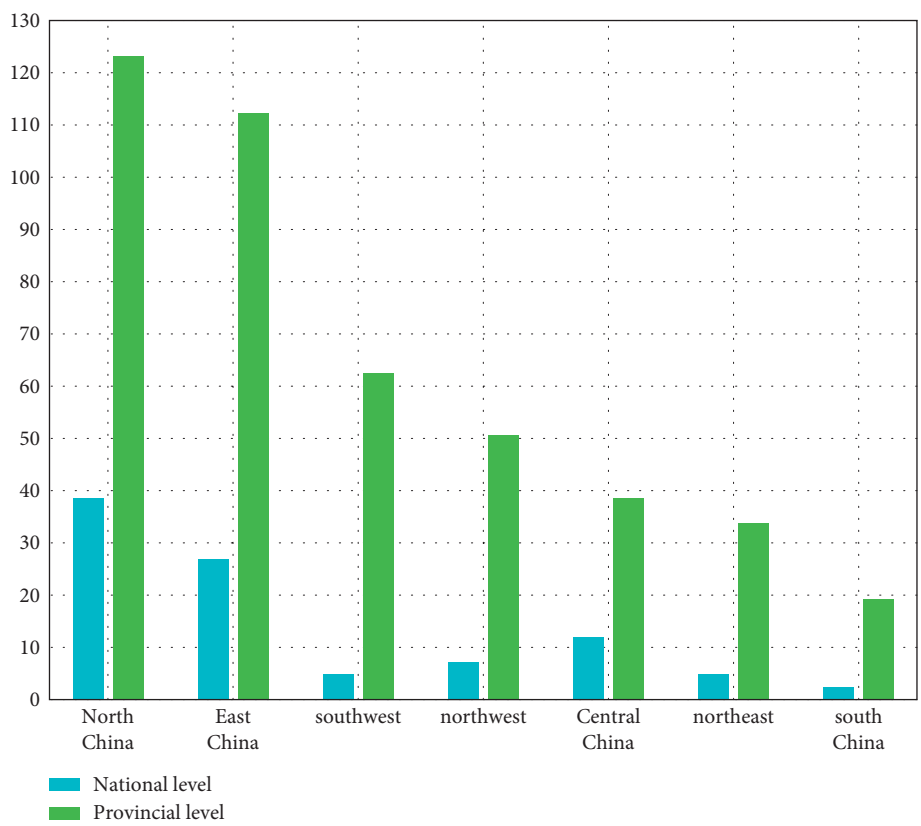

Figure 4: Regional distribution of China's sports intangible cultural heritage.

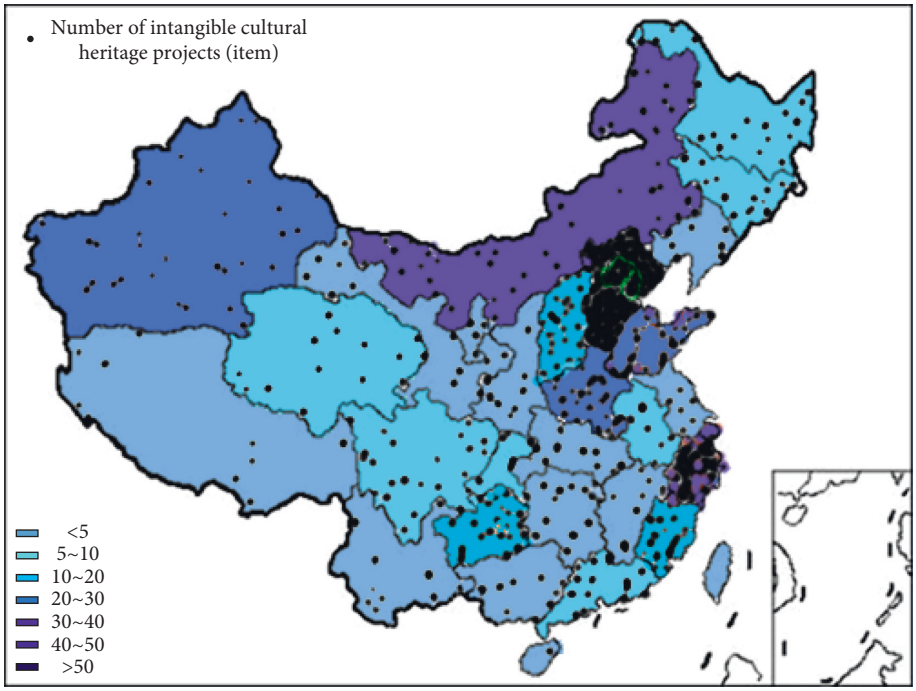

Figure 5: Provincial distribution of China's sports intangible cultural heritage.

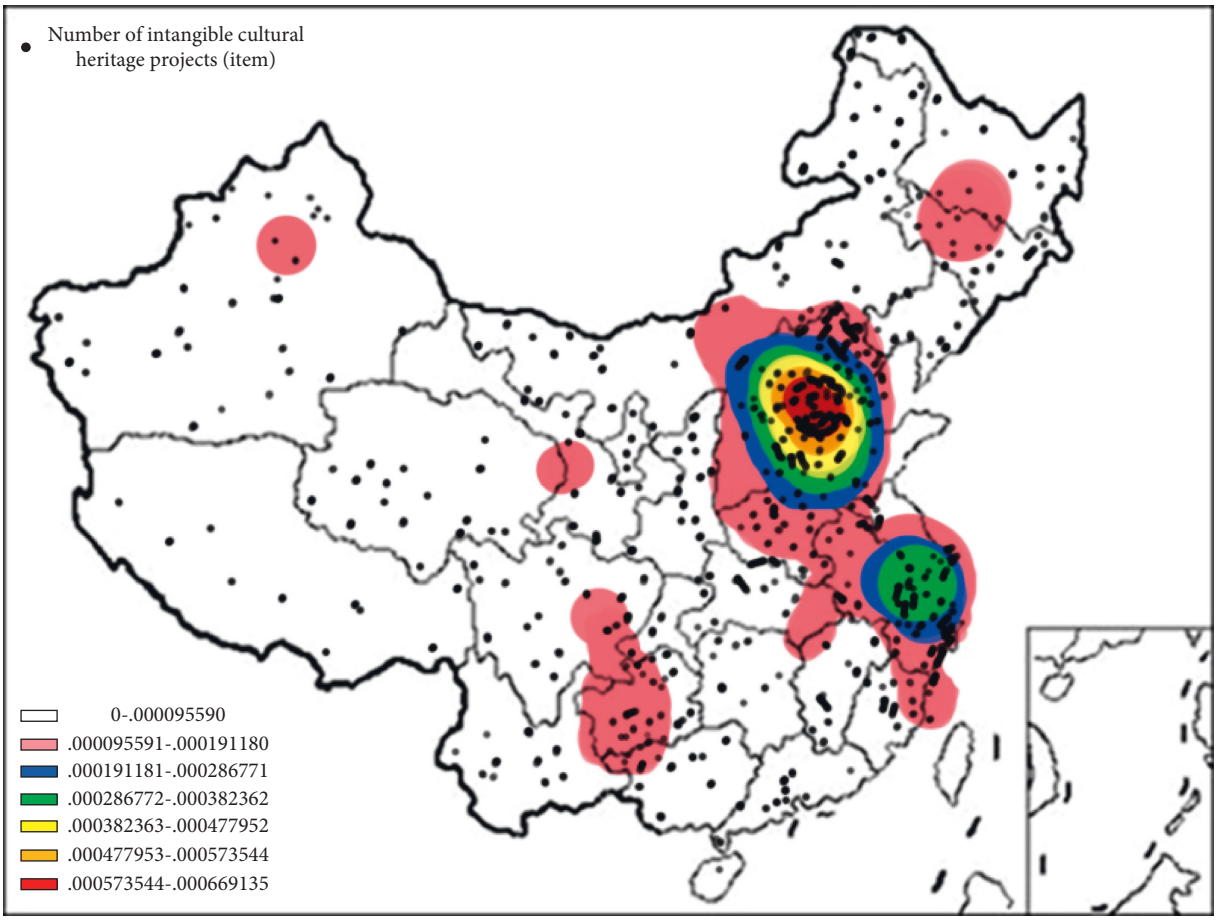

Figure 6: Nuclear density analysis of the distribution of sports intangible cultural heritage resources in China.

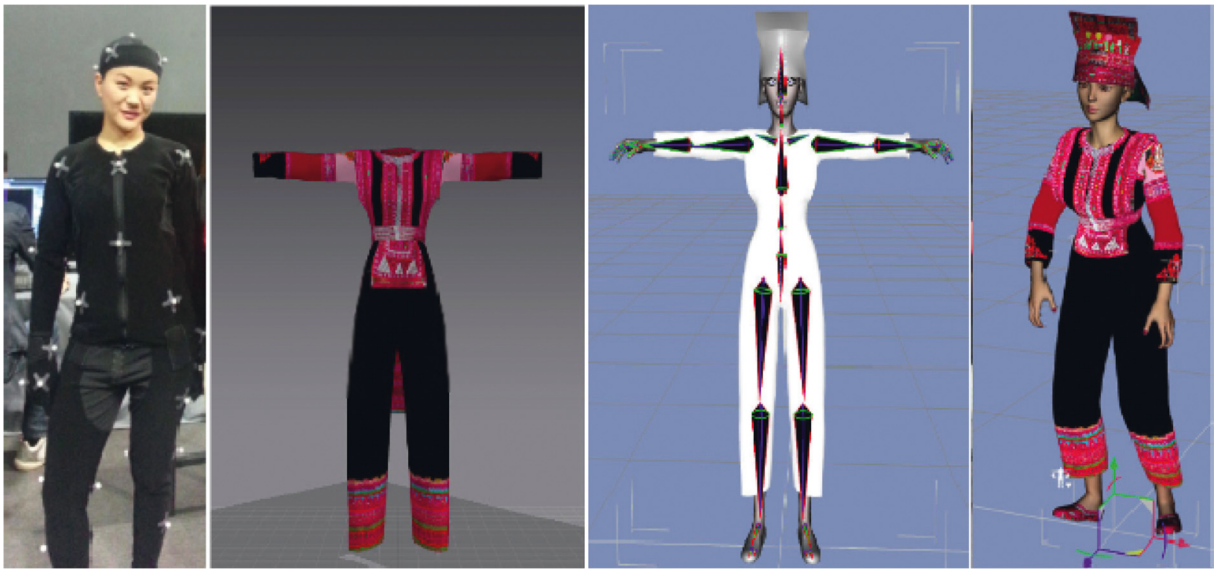

Figure 7: Construction of virtual character image of sports intangible cultural heritage constructed by GIS technology and virtual reality technology.

Figures 4 and 5 show the regional and provincial distribution of China's sports intangible cultural heritage. Different colors represent different quantities of sports intangible cultural heritage. As can be seen from the figure, north and east China contain the largest number of sports intangible cultural heritage, followed by central, southwest, and northwest China, while the northeast and south China contain relatively few sports intangible cultural heritage. At the same time, the quantity of sports waste cultural heritage contained in different provinces and regions is uneven. The most concentrated quantity distribution is Hebei Province and Zhejiang Province, and the relatively small quantity is Jiangsu, Guangxi, and other provinces and regions. It can be seen that China's sports intangible cultural heritage has national differences and is distributed in groups, which can be mainly divided into groups centered on the middle and lower reaches of the Yellow River, groups centered on the middle and lower reaches of the Yangtze River and ethnic groups centered on rich national culture, diverse forms, and regional characteristics.

Figure 6 shows the nuclear density analysis of the distribution of China's sports intangible cultural heritage resources. It can be seen from the results in the figure that the resource distribution of China's sports intangible cultural heritage has formed six core circles, including a high-density core circle with Beijing Tianjin wing as the core area, a subdensity core circle with Zhejiang Province as the core area, and four small core circles with Jilin, Qinghai, Guizhou, and Xinjiang as the core areas, respectively.

To sum up, the influencing factors of the spatial distribution of China's sports intangible cultural heritage mainly include the type of ecological environment, the declaration system of intangible cultural heritage list, and category attribution. The content and form of sports intangible cultural heritage will be restricted by natural environment, social culture, and other factors in the process of its formation and development. China's level by level declaration system enables different sports intangible cultural heritage to obtain fair and fair declaration opportunities and different degrees of protection. In the management and protection of sports intangible cultural heritage, we not only need to consider the impact of its formation and development environment, but also need to carry out more detailed classified management in the existing management system. At the same time, we should combine the sports intangible cultural heritage with modern life, so that it can maintain its own connotation and spirit and have the transformation of modern function and form, so as to obtain better inheritance and development.

As shown in Figure 7, it is the construction of virtual character image of sports intangible cultural heritage constructed by GIS technology and virtual reality technology. The three-dimensional model constructed by virtual reality technology can enable more people to understand and accept the connotation and spirit of sports intangible cultural heritage and promote the protection and inheritance of sports intangible cultural heritage through diversified ways such as offline human-computer interaction, online display, and explanation.

5. Conclusion

Intangible cultural heritage is the crystallization of the development of spiritual civilization of a nation and a country, the result of historical and cultural accumulation, or the witness of the development of human society. Compared with other traditional cultural heritage, intangible cultural heritage has great instability and difficulty in inheritance, protection, and management. The traditional management and protection methods can no longer meet the needs of the development of intangible cultural heritage. The development of spatial information technology opens a new way for

the management and protection of intangible cultural heritage. Therefore, this paper puts forward the research on the management and protection of Intangible Cultural Heritage based on spatial information technology under the background of Internet of things and takes sports intangible cultural heritage as an example. Through the analysis of the experimental results, China's sports intangible cultural heritage lacks international level projects, the ownership of comprehensive competition projects is not clear, the type structure is mainly martial arts, and there is a lack of water and ice and snow activities. At the same time, the distribution of China's sports intangible cultural heritage is uneven, showing regional and ethnic differences, forming six core circles in the form of groups. It can be concluded that the classification of ecological environment type, application system, and project category are the main influencing factors of the distribution of sports intangible cultural heritage. Therefore, in the process of management and protection, we should not only consider the ecological environment needs of sports intangible cultural heritage, but also endow sports intangible cultural heritage with new ways of expression and modern functions in combination with modern life needs and forms, so as to promote its management, protection, and inheritance development.

Data Availability

The data used to support the findings of this study are available from the corresponding author upon request.

Conflicts of Interest

The authors declare that they have no conflicts of interest.

References

[1] W. J. Yan and S. C. Chiou, "The safeguarding of intangible cultural heritage from the perspective of civic participation: the informal education of Chinese embroidery handicrafts," *Sustainability*, vol. 13, no. 9, Article ID 4958, 2021.

[2] L. Cheng and Y. Yuan, "Intellectual property tools in safeguarding intangible cultural heritage: a Chinese perspective," *International Journal for the Semiotics of Law-Revue internationale de Sémiotique Juridique*, vol. 34, no. 03, pp. 893–906, 2021.

[3] S. Huang and J. Liu, "Research on cultural inheritance and inheritor protection in intangible cultural heritage protection: taking Wuming Zhuang Shigong dance inheritance as an example," *Journal of Nanning Normal University (PHILOSOPHY AND SOCIAL SCIENCES EDITION)*, vol. 40, no. 5, pp. 93–99, 2019.

[4] H. Chmil, I. Kuznietsova, M. Mishchenko, O. Oliynyk, and V. Demeshchenko, "Intangible cultural heritage as a resource for consolidating modern Ukrainian society," *Linguistics and Culture Review*, vol. 5, no. S4, pp. 747–760, 2021.

[5] Q. Dang, Z. Luo, C. Ouyang, L. Wang, and M. Xie, "Intangible cultural heritage in China: a visual analysis of research hotspots, frontiers, and trends using citeSpace," *Sustainability*, vol. 13, no. 17, Article ID 9865, 2021.

[6] M. Wang and X. Chen, "Effect evaluation: scientific research on the protection and management of intangible cultural heritage," *Journal of Nanning Normal University (Philosophy and Social Sciences Edition)*, vol. 41, no. 1, pp. 104–110, 2020.

[7] W. Yuan, "Research on the application of virtual reality technology in the protection of Intangible Cultural Heritage," *Industrial & Science Tribune*, vol. 18, no. 16, pp. 41-42, 2019.

[8] Q. Hu, W. Gong, and Y. Hu, "etc. Reverse modeling based on 3D laser scanning point cloud," *Beijing Surveying and Mapping*, vol. 34, no. 3, pp. 352–355, 2020.

[9] Y. Liu and L. I. Xin, "Digital protection research on the minority traditional sports," *Intangible Cultural Heritage*, vol. 36, no. 7, pp. 469–473, 2019.

[10] Y. U. Yang, R. Wang, and Z. Lei, "A case study of northern shaanxi province," *Journal of Human Settlements in West China*, vol. 6, pp. 109–118, 2019.

[11] A. Zhang, Z. Yan, and Z. Hui, "etc. Research on 3D model construction method of ancient buildings based on point cloud data and BIM Technology," *Manufacturing Automation*, vol. 42, no. 1, pp. 122–125, 2020.

[12] C. Gong and C. Wang, "Study on ecological protection model of intangible cultural heritage in Zuojiang River Basin," *Journal of Guangxi Normal University*, vol. 40, no. 3, pp. 76–81, 2019.

[13] Z. Luo and F. Wang, "From cultural symbols to commercial marks: a quantitative analysis of the trademark law protection of intangible cultural heritage in China," *Queen Mary Journal of Intellectual Property*, vol. 11, no. 2, pp. 158–182, 2021.

[14] M. Liu and X. Min, *Improved Design of She People's "Cai-Dai" Weaving Loom Based on the Protection of the Intangible Cultural Heritage in China*, Springer, Berlin, Germany, 2020.

[15] L. Li, M. Li, and T. Deng, "Research on application of digital technology in anhui intangible cultural heritage popularization design-take the manufacture technology of huangshan maofeng tea as an example," *E3S Web of Conferences*, vol. 218, Article ID 04021, 2020.

[16] Z. Guan, "Digital rescue protection of representative inheritors of intangible cultural heritage in the information age," *Journal of Physics: Conference Series*, vol. 1744, no. 4, Article ID 042124, 2021.

[17] G. Zhan, "Application of virtual engine technology in visualization of architectural cultural heritage model," *Tea In Fujian*, vol. 41, no. 5, 67 pages, 2019.

[18] C.-Y. Guo, S.-J. Xu, and G. Luo, "Research on the integration development of sports intangible cultural heritage and national fitness," *IOP Conference Series: Earth and Environmental Science*, vol. 510, no. 3, Article ID 032002, 2020.

[19] Z. Chen, J. Huang, H. Dai, and J. Liu, "Development route analysis of intangible cultural heritage industry of China based on data mining," *Journal of Physics: Conference Series*, vol. 1848, no. 1, Article ID 012040, 8 pages, 2021.

[20] L. Rafianti, A. Suryamah, A. M. E. Putra et al., "Swing the angklung tube in the digital economy era: based on intangible cultural heritage and intellectual property rights perspective," *Indonesian Journal of International Law*, vol. 18, no. 3, p. 2, 2021.

Hindawi
Computational Intelligence and Neuroscience
Volume 2022, Article ID 3772108, 10 pages
https://doi.org/10.1155/2022/3772108

Research Article

Research on Rural Landscape Spatial Information Recording and Protection Based on 3D Point Cloud Technology under the Background of Internet of Things

Li Yue,[1,2] **Zhang Yadong**,[1] **and Chen Jinjin**[1]

[1]*Faculty of Art and Design, Shandong Women's University, Jinan, Shandong 250300, China*
[2]*Universiti Putra Malaysia, Faculty of Design and Architecture, Kuala Lumpur 43100, Malaysia*

Correspondence should be addressed to Li Yue; 29066@sdwu.edu.cn

Received 30 January 2022; Accepted 10 March 2022; Published 2 June 2022

Academic Editor: Guobin Chen

The village with historical and cultural accumulation not only is the witness of the interaction between human activities and natural environment but also contains a lot of intangible cultural heritage. It is an important research object in the history of human social development and has great reference value for the construction of modern Humayun settlements. With the continuous change of modern rural landscape, the traditional engineering drawing cannot meet the needs of people for spatial information measurement. There are some problems such as slow drawing, low precision, and poor benefit, so computer drawing must be used. Therefore, this paper puts forward the research on rural landscape spatial information recording and protection based on 3D point cloud technology under the background of Internet of Things and realizes the recording of rural landscape spatial information through the construction of 3D point cloud spatial information recording model. The experimental results show that the improved unit point cloud spatial information recording model has better feature extraction effect and feature point extraction efficiency, and can classify the point cloud more carefully. At the same time, the scene 3D point cloud classification method based on conditional random field can better deal with the interference factors in the outdoor landscape and show a better classification effect.

1. Introduction

The spatial integration model can effectively identify the spatial form of rural settlements. With the support of continuous data, we can not only dynamically observe the spatial evolution trend of rural settlements but also provide important support for rural land consolidation and rural planning. In terms of regional concept, the broad definition of village refers to the area that does not include cities or primitive uninhabited areas, and rural landscape refers to the food and other renewable natural resources obtained and produced from the natural environment through different farming and animal husbandry in rural areas [1]. In the development of human society, villages have always occupied an important position. Many villages with historical and cultural accumulation have been preserved through the baptism of time [2]. These villages relying on the natural environment not only retain many methods of land use, agricultural technology, and rural culture containing ecological wisdom. Moreover, it is of great value to the research on the history of human social development and also has great inspiration and reference value in the construction of modern human settlements [3]. Therefore, people have new views on the countryside and rural landscape, gradually realize the importance and value of rural landscape, and attribute rural landscape to the important task of heritage protection. However, the rural landscape is not invariable from beginning to end [4]. It has been in a state of continuous change and evolution, and most of the villages are still developing and changing [5]. At the same time, with the promotion of modern urban construction and new rural development, the social structure in the south of the ancient

city of the county has changed, and the rural agricultural production is no longer the traditional farming method, but adopts modern agricultural technology [6]. In order to promote rural construction, many villages have developed corresponding rural tourism industry based on their own natural landscape and cultural landscape, which accelerates the change of rural landscape space [7]. From the perspective of rural landscape heritage protection, it is necessary to obtain the corresponding information from the rapidly changing rural landscape through the spatial information recording method of colleges and universities [8].

Spatial model is a methodology that can solve the spatial problems of rural landscape [9]. It refers to the specific spatial combination formed between different elements in rural landscape [10]. The spatial pattern of rural landscape is formed by the interaction between human activities and natural environment. Its development will be affected by factors such as productivity level, local culture, and natural environment [11]. The value of rural landscape heritage is reflected through the rural landscape spatial model [12]. Therefore, quantitative research on the rural spatial model is conducive to the authenticity, integrity, and diversity of rural landscape heritage protection [13]. Collecting and recording rural landscape spatial information through traditional surveying and mapping technology and spatial expression tools not only has high cost and long cycle time but also is difficult to deal with the rapidly changing rural landscape [14]. At the same time, the utilization rate of the information collected by traditional methods in three-dimensional spatial information is poor, the spatial feature expression effect of rural landscape is not good, and the accuracy of the measured data needs to be improved [15]. The development of point cloud technology has brought a new development direction for the recording and protection of rural landscape spatial information [16]. Point cloud technology includes a series of technologies such as the collection, processing, and visualization of point cloud data, which can vividly describe the three-dimensional coordinate information and reflectivity information of the sampling point data in the dense space of the measurement object and carry out three-dimensional models, lines, surfaces, and images of all kinds of large, complex, standard, or nonstandard entities and real scenes through computers' construction of various map data such as volume [17]. Compared with traditional surveying and mapping methods and spatial expression tools, it can obtain relevant information faster, cover a wider measurement area, collect data with higher accuracy, and have more intuitive expression. These advantages make point cloud technology more advantageous than traditional methods in rural landscape spatial information recording and protection. It can also provide better technical guarantee for the research of rural landscape spatial information recording and protection, and provide an important driving force for the development of rural landscape protection and spatial information [18].

Therefore, this paper puts forward the research on rural landscape spatial information recording and protection based on three-dimensional point cloud technology under the background of Internet of Things, and collects and processes the corresponding data of rural landscape by constructing the spatial information recording model of three-dimensional point cloud technology. This paper is mainly divided into three parts: the first part expounds the development and application of Sanyun point cloud technology; the second part is to build a rural landscape spatial information recording model based on three-dimensional point cloud technology, and improve the accuracy and reliability of rural landscape information collection and processing through the improvement of feature extraction technology and scene three-dimensional point cloud classification technology based on conditional random field; and the third part analyzes the application experimental results of rural landscape spatial information recording model based on three-dimensional point cloud technology.

This paper puts forward the research on rural landscape spatial information recording and protection based on 3D point cloud technology under the background of Internet of Things. The research innovation contributions include the following: the improved unit point cloud spatial information recording model has better feature extraction effect and feature point extraction efficiency, and can classify the point cloud more carefully. The scene 3D point cloud classification method based on conditional random field can better deal with the interference factors in the outdoor landscape, so as to show a better classification effect. In the application of rural landscape spatial information recording, 3D point cloud technology can complete the collection and recording of relevant spatial information in a short time, visualize the spatial information in a variety of ways, and understand the corresponding information more intuitively.

This paper is divided into four parts. Section 1 expounds the research background of rural landscape spatial information based on three-dimensional point cloud technology under the background of Internet of things. Section 2 expounds the citation of relevant literature and explains the wide application of 3D point cloud measurement technology. Section 3 analyzes the construction of rural landscape spatial information recording model based on 3D point cloud technology. Section 4 expounds the application experimental results of rural landscape spatial information recording model based on three-dimensional point cloud technology. Finally, the full text is summarized. The experimental results show that the improved unit point cloud spatial information recording model has better feature extraction effect and feature point extraction efficiency, and can classify the point cloud more carefully.

2. Related Work

With the continuous development of scanning measurement technology and computer technology, 3D point cloud measurement technology has been paid more and more attention and applied in more and more fields. At the same time, the measurement of 3D point cloud technology has gradually developed from the original fixed single location measurement to motion measurement, and has been widely used in the fields of digital city, virtual vision, and so on [19]. According to the working principle of measuring equipment

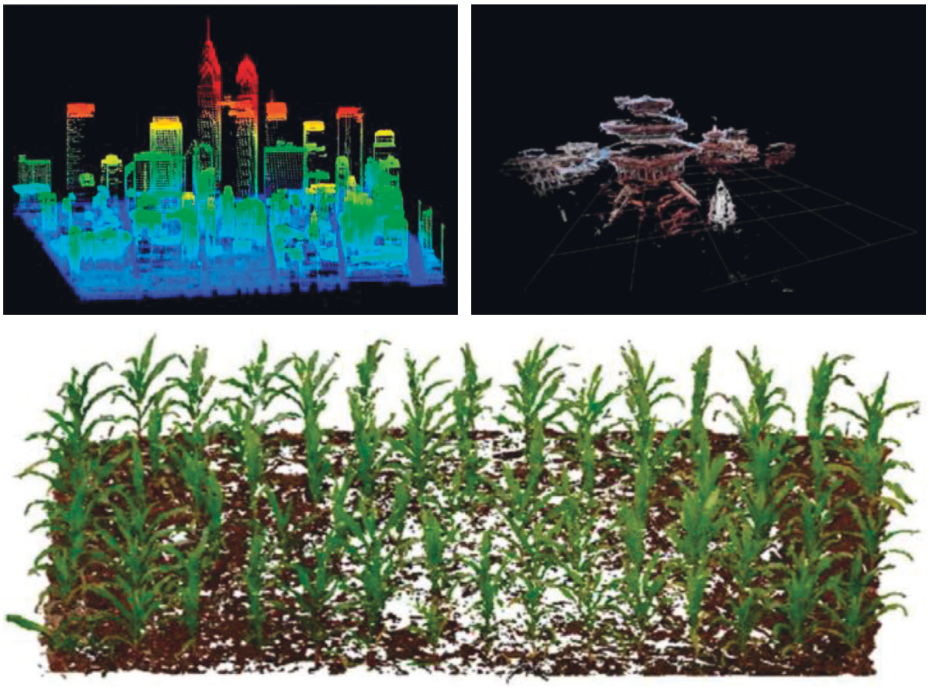

Figure 1: Spatial features and models extracted by 3D point cloud technology.

of 3D point cloud technology, its scanning technology can be divided into manual scanning technology and automatic scanning technology. The manual scanning technology can obtain the relevant information of the scanning object with arbitrary shape, and its accuracy is affected by the operation experience in the scanning process; automatic scanning can obtain relevant information data faster through three-dimensional scanner, which has the advantages of easy operation and automation, but it has certain requirements for the shape of the scanned object [20]. According to the contact between the equipment and the measured object in the data acquisition process of 3D point cloud technology, it can be divided into contact data acquisition method and noncontact data acquisition method. Among them, noncontact data acquisition method is widely used in cultural heritage protection. In the field of international cultural heritage, point cloud technology has become one of the important ways of spatial information recording of heritage sites, in which the representative technologies are lidar technology and digital close-range photogrammetry technology [21]. In China, some scholars have applied 3D point cloud technology to the protection of architectural cultural heritage and pointed out that it has five advantages. First, the noncontact data acquisition method of three-dimensional point cloud technology can reduce the damage to the heritage as much as possible and improve the accuracy of heritage ancient appearance restoration; second, 3D point cloud technology has fast data acquisition speed, which greatly improves the work efficiency, reduces the workload, and saves a lot of labor; third, compared with the traditional measurement methods, the data obtained by 3D point cloud technology have higher accuracy and reduce the accidental error of data; fourth, 3D point cloud technology changes the way of data measurement and improves the security of measurement; fifth, the data record of 3D point cloud technology is more detailed and comprehensive, and the visualization is diversified. Other scholars have recorded and protected the spatial data of Chinese classical garden heritage through three-dimensional point cloud technology, making the corresponding data more comprehensive and accurate [22]. In addition, with the advancement of agricultural modernization, some scholars have applied the three-dimensional point cloud technology to the measurement of farmland crop population growth parameters, which overcomes the limitations of traditional crop parameter measurement and realizes the nondestructive, efficient, and high-precision measurement of crop growth parameters [23]. As shown in Figure 1, the spatial features and models extracted by 3D point cloud technology.

3D point cloud technology obtains a large amount of point cloud data through the equipment and is vulnerable to the influence of the surrounding environment in the process of acquisition, which will have the problems of noise and hole. In order to ensure the accuracy and efficiency of the three-dimensional model of the object, it is necessary to preprocess before model construction. In addition, the lattice quality of point cloud data is the basis of its later classification, recognition, and feature extraction. In the actual environment, it will be affected by technical limitations and the surrounding environment, which will damage the integrity of the obtained point cloud data, and there are problems such as noise, interference points, occlusion in different point cloud areas, and uneven distribution of point cloud. At the same time, the spatial structure of point cloud is usually scattered, which improves the difficulty of defining the regional characteristics of different point clouds.

Therefore, the segmentation and data processing of 3D point cloud has always been a research hotspot in this field. Some studies have proposed a 3D point cloud segmentation method based on set features, which strengthens the curvature expression ability through local weighted curvature feature description method and improves the efficiency and accuracy of edge feature point extraction [24]. In addition, the local partial differential equation is established based on the local finite element of the network to remove the anisotropic abnormal noise in the point cloud data. Some scholars proposed to introduce bilateral filtering in the denoising process to achieve the denoising effect, which has been widely used [25]. At present, there are several commonly used point cloud segmentation methods. The first is the segmentation based on edge characteristics, which determines the boundary data according to the geometric characteristics of point cloud. After determination, it will smoothly connect the point cloud boundary points, so as to obtain multiple point cloud subsets that do not want to intersect with each other and to achieve the effect of segmentation. Therefore, if it is necessary to segment point cloud data, the segmentation effect will be better when the edge characteristics are relatively prominent. The second is the clustering feature-based segmentation algorithm for attribute segmentation according to the feature vector of point cloud data. Generally, the clustering algorithms used include k-means algorithm, fuzzy clustering algorithm, and so on. This kind of algorithm is not easily affected by the spatial properties of point cloud in the process of segmentation and has a relatively stable segmentation effect. However, the most direct factor affecting the segmentation quality of clustering feature-based segmentation algorithm is the selection of point cloud spatial feature vector, and the point cloud spatial density will affect the setting of feature vector threshold to a great extent. The third is a model-based segmentation algorithm based on geometric mathematical model to achieve the purpose of point cloud segmentation through mathematical fitting. The algorithm can be constructed through a large number of mathematical formulas and has superior processing speed. At the same time, the fitting results obtained through the mathematical model will reduce the impact of local noise on the segmentation effect. However, before segmentation, the algorithm needs to classify different models, and then compare and classify the data and models, which means that the segmentation method needs a large number of object models, which is often used for rough segmentation of point cloud data. The fourth is a graph-based segmentation algorithm based on the disorder of point cloud data. The corresponding vertices in the data object graph of point cloud assign different weights that are not similar to the lines between different vertices according to the spatial characteristics, which will directly affect the segmentation results. The fifth is the region growth segmentation algorithm, which divides the point cloud data with similar attributes into independent regions with different attributes within the set threshold range. Different from the point cloud segmentation method based on edge information, the formation of seed points in the region growth segmentation method is based on a variety of spatial attributes of the point cloud and divided into different region subsets with large differences, but the differences in the same region are very small, so it has a more stable resistance to noise. At the same time, the segmentation quality of region growth segmentation method depends on the selection of seed points and the setting of growth criteria. Therefore, the abnormal points in point cloud data have relatively little impact on the segmentation results of point cloud, but their boundary delimitation is generally inaccurate. With the development of 3D point cloud technology, its processing, segmentation, feature extraction, and other technologies in point cloud data are also developing continuously, so as to improve the accuracy and reliability of 3D point cloud technology and provide better data services for the development of various fields.

3. Construction of Rural Landscape Spatial Information Recording Model Based on 3D Point Cloud Technology

Landscape model represents landscape design in the form of micro-entity. The landscape model is made up of the actual objects according to a certain proportion. It is an important tool and carrier for transmitting, explaining, and displaying design projects and design ideas. Therefore, in the model making and design, appropriate materials and processes should be selected according to the uses of different models, and esthetic principles and treatment technology should be considered. Because the landscape model shows the image of an intuitive entity in three-dimensional space, it is convenient for people to study the relationship between a landscape element and the environment. To make a feasible plan, the intuitiveness of the landscape model is also reflected in the integrity of the simulated landscape. It enables the viewer to evaluate and appreciate the complete spatial form and overall environment of the landscape through the model.

The three-dimensional point cloud technology realizes the collection, recording, and visualization of rural landscape spatial information mainly through four steps. First, it is necessary to sort out the landscape characteristics, spatial scope, constituent elements, and other types of information of the measured rural landscape, so as to provide corresponding basis for subsequent research. Second, appropriate methods, technologies, and equipment are used to collect the corresponding spatial information data for the space with different scales, different characteristics, and different accessibility. General rural landscape has diversified scales and rich elements, which need to be coordinated through a variety of equipment. Third, the rural landscape spatial model is constructed through image and point cloud processing software. Fourth, the spatial models of different rural landscapes need to be redeveloped according to different application requirements, such as the extraction of elevations and sections of spatial environment. It can be seen that the data collection of 3D point cloud technology is the basis of the construction, secondary development, and follow-up research of rural landscape spatial information model. The rural landscape is an outdoor landscape, and many factors in

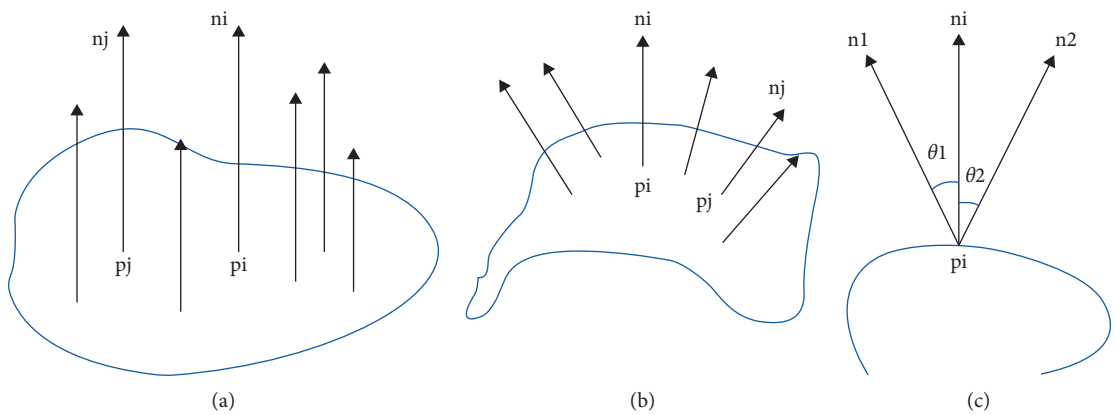

Figure 2: Schematic diagram of normal vector and angle between normal vectors in different surface areas. (a) Plane area. (b) Surface area. (c) Included angle of normal vector.

its surrounding environment have a certain impact on the data acquisition of 3D point cloud technology. Therefore, when building the feature extraction, segmentation, and classification model of 3D point cloud technology, it is necessary to improve the original 3D point cloud model algorithm, so as to achieve the target effect.

3.1. Feature Extraction and Segmentation Model Construction of 3D Point Cloud Technology. This paper adopts the feature point extraction method based on normal vector. The vector perpendicular to the local surface is the surface normal vector, which can describe the local surface direction, and the normal vector of any point on the surface is the normal vector. The idea of feature point extraction method based on normal vector is to solve the normal vectors of all data points contained in the point cloud data model and calculate the included angle between the normal vector of each data point and the normal direction of the corresponding adjacent points. The greater the included angle between the normal vectors, the greater the fluctuation between the corresponding data points and the adjacent point cloud data; that is, it has several sharp features; on the contrary, the smaller the angle between the normal vectors, the smoother the fluctuation between the point cloud data near the data points; that is, it has sparse geometric characteristics. As shown in Figure 2, the angle between normal vector and normal vector in different surface areas is shown. Based on the variation trend of the surface normal vector of the point cloud data, the purpose of selecting the appropriate feature points of the point cloud data can be realized by setting the appropriate threshold.

Let the coordinate of a certain point be p_i, and its k adjacent point set be expressed as $\{p_1, p_2, \ldots, p_k\}$. Solve the mean value of all points, that is, solve its center of gravity o, as shown in the following formula:

$$o = \frac{1}{k}\sum_{i=1}^{k} p_i. \tag{1}$$

The normal vector solution of the least squares fitting surface is to solve the minimum value of formula (2), as shown in the following formula:

$$f = \sum_{Nbh\ d(p_i)} \left\|(p_i - o)\cdot n\right\|. \tag{2}$$

Furthermore, the problem of solving the minimum value of formula (2) is transformed into the problem of solving the minimum eigenvalue of covariance, as shown in the following formula:

$$\begin{bmatrix} \sum_i (x_i - o_x)^2 & \sum_i (x_i - o_x)(y_i - o_y) & \sum_i (x_i - o_x)(z_i - o_z) \\ \sum_i (y_i - o_y)(x_i - o_x) & \sum_i (y_i - o_y)^2 & \sum_i (x_i - o_x)(z_i - o_z) \\ \sum_i (z_i - o_z)(x_i - o_x) & \sum_i (z_i - o_z)(y_i - o_y) & \sum_i (z_i - o_z)^2 \end{bmatrix}. \tag{3}$$

The coordinates of any point in the point cloud data are expressed as x_i, y_i, z_i, and the corresponding center of gravity coordinates is expressed as o_x, o_y, o_z. The minimum eigenvalue λ_0 of the real symmetric matrix in formula (3) is solved, and the eigenvalue is the normal vector of the response point.

Unify the normal vectors with different directions obtained from different point cloud data points in one perspective, and take the change trend of the normal vector of a point, that is, the angle between the normal vector and the normal vector of the corresponding k adjacent point, to calculate the average value, as shown in the following formula:

$$f_i = \frac{1}{k}\sum_{j=1}^{k}\theta_i. \tag{4}$$

The angle between the data point normal vector and its adjacent point normal vector is expressed as θ_{ij}.

From the above formula, it can be seen that the size of neighborhood points has an impact on the calculation time of normal vector and the extraction effect of feature points. Therefore, the optimal neighborhood size is obtained by adding the neighborhood radius constraint method, so as to reduce the impact of noise on the calculation time of normal vector and improve the efficiency of feature point extraction. The neighborhood radius threshold is introduced and expressed as r. Each point selects the nearest k neighborhood

points according to the radius threshold. The expression of the center point of each point is shown in the following formula:

$$c_i = \frac{1}{|k_i|} \sum_{p_{ij} \in N^{k_i}(p_i)} p_{ij}, \tag{5}$$

where the center point is c_i, $\|p_{ij}\| < r$. Calculate the diffusion matrix and eigenvalue of the central point, select the reserved data points, and extract the feature points according to the size of the eigenvalue.

Set the point cloud set as $P = \{p_i\}_{i=1}^{N}$, where the nearest point in the neighborhood of each point is $N^{k_i}(p_i) = \{p_{ij}\}, \quad i \le j \le k_i$, and the incidence matrix of each point is shown in the following formula:

$$C_i = \sum_{p_{ij} \in N^{k_i}(p_i)} \left(p_{ij} - \mathrm{c_i}\right)\left(p_{ij} - \mathrm{c_i}\right)^T. \tag{6}$$

The eigenvalue $\{\lambda_0, \lambda_1, \lambda_2\}, \lambda_0 \le \lambda_1 \le \lambda_2$ and the corresponding eigenvector $\{e_0, e_1, e_2\}$ of the incidence matrix are calculated. Retain the point set according to the set threshold, as shown in the following formula:

$$\frac{\lambda_2(p)}{\lambda_1(p)} < r_{12}, \frac{\lambda_3(p)}{\lambda_2(p)} < r_{23}. \tag{7}$$

The characteristic points of the remaining points are determined by the minimum characteristic value, as shown in the following formula:

$$\rho(p) \approx \lambda_3(p). \tag{8}$$

The eigenvalue of the point is expressed as $\rho(p)$.

In this paper, the method of 3D point cloud segmentation selects the region growth segmentation algorithm, which divides the point cloud data into independent regions with similar attributes according to a certain threshold range, and the attributes of different regions are different. The region growth segmentation algorithm has good robustness, and the algorithm principle is relatively simple and easy to operate. Its segmentation effect depends on the selection of seed nodes and the setting of growth criteria, and will be affected by the threshold setting. Therefore, the region growth segmentation algorithm is improved in the selection of seed nodes and the setting of growth criteria. The improved region growing method realizes region segmentation well and can segment several unconnected parts at the same time. We execute a cycle; that is, the program automatically determines a seed point and divides it. The number of seed points can be controlled by controlling the number of cycles. The program automatically determines the seed points, so that when the threshold and cycle times are determined, the image segmentation effect is certain, and the results can be reproduced. Let the seed node be the point with the smallest curvature, and estimate and sort the curvature of each point contained in the point cloud to be segmented. The average curvature K_h of a point in the surface is calculated as shown in the following formula:

$$2K_h n = \lim \operatorname{diam}(A) \longrightarrow 0 \frac{\nabla A}{A}. \tag{9}$$

The normal vector is expressed as n, an infinitesimal region around the point is expressed as A, the diameter of the region is expressed as $\operatorname{diam}(A)$, and ∇ is the gradient operator of the point. After discretization, the average curvature calculation formula is obtained, as shown in the following formula:

$$K_h(P_i) = \frac{1}{4A_{\min}} \sum j \in N(i)\left(\cos\alpha_{ij} + \cot\beta_{ij}\right)\left(P_i - \mathrm{P_j}\right) \times n. \tag{10}$$

The diagonals connecting edges P_i and P_j are α_{ij} and β_{ij}, respectively.

3.2. 3D Point Cloud Classification of Scene Based on Conditional Random Field. Rural landscape belongs to outdoor scene, and the traditional outdoor point cloud classification method is lack of estimation of 3D point cloud data characteristics of large scale, high complexity, and strong noise outdoor scene. Therefore, this paper selects the scene 3D point cloud classification method based on conditional random field. Each point in the constructed conditional random field based on point cloud represents a node, the random variable is represented as $L = \{L_1, .., L_N\}$, its range is $L_i \in \{l_1, \ldots, l_k\}$, and each point classifies a label and satisfies the scoring function. The point cloud classification task is equivalent to a simple learning problem. The discrimination model to be constructed in the learning process can be proposed from the outdoor scene probability model $P_w(l|x)$. In this model, the dependence between features is expressed by the potential function of the log linear model of the associated Markov model, as shown in formula (11), which is the potential function of a single node

$$\log \varphi_i(l_k) = \omega_n^k \cdot x_i. \tag{11}$$

When the node label is assigned k, the feature weight is expressed as ω_n^k, and the feature vector of three-dimensional space points is expressed as x_i. The similarity of the two connected nodes is expressed by the edge model, and the correlation is expressed by the edge potential function, as shown in the following formula:

$$\log \varphi_{ij}(l_k, l_k) = \omega_e^k \cdot x_{ij}. \tag{12}$$

The two connected nodes are assigned the weight value of the same label, which is expressed as ω_e^k and $\forall l_k \ne l_o$, $\log \varphi_{ij}(l_k, l_o) = 0$. Finally, through the logarithmic model of joint conditional probability, as shown in the following formula:

$$\begin{aligned} \log P_w(y|x) = &\sum_{i=1}^{N}\sum_{k=1}^{K}\left(\omega_n^k \cdot x_i\right) y_i^k \\ &+ \sum_{ij \in E}\sum_{k=1}^{K}\left(\omega_e^k \cdot x_{ij}\right) y_i^k y_j^k - \log Z_w(x). \end{aligned} \tag{13}$$

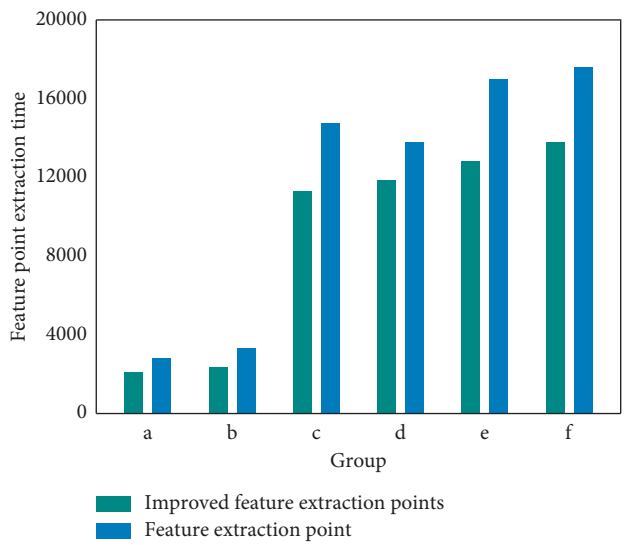

Figure 3: Comparison between the improved feature extraction algorithm and the original feature extraction algorithm in feature point extraction results.

The $Z_w(x)$ calculation formula is as follows:

$$Z_w(x) = \sum_{y} \prod_{i=1}^{N} \varphi_i(y_i') \prod_{ij \in E} \varphi_{ij}(y_i', y_j'). \tag{14}$$

Let the row vector be $w = \{w_n, w_e\}$, $w_n = \{w_n^1, \ldots, w_n^k\}$, $and\ d\ w_e = \{w_e^1, \ldots, w_e^k\}$ and its length be $K(d_n + d_e)$. Redefine y as the column vector $y = \{y_n, y_e\}^T$, $y_n = \{\ldots, y_i^1, \ldots, y_i^k, \ldots\}$, $and\ d\ y_e = \{\ldots, y_{ij}^1, \ldots, y_{ij}^k, \ldots\}$, and its length is $K(N + |E|)$, and then, the size of matrix X is expressed as $K(d_n + d_e) \times K(N + |E|)$, and finally, formula (13) is transformed into the following formula:

$$\log P_w(y|x) = wXy - \log Z_w(x). \tag{15}$$

4. Application Experiment Results of Rural Landscape Spatial Information Recording Model Based on Three-Dimensional Point Cloud Technology

This paper selects a rural landscape for the application experiment of rural landscape spatial information recording model based on three-dimensional point cloud technology, and randomly selects six different rural landscapes for the experiment of feature extraction points. As shown in Figure 3, the improved feature extraction point algorithm is compared with the original feature extraction algorithm in feature point extraction results. As can be seen from the figure, compared with the original feature extraction algorithm, the improved feature extraction algorithm integrating the neighborhood constraint method has significantly improved the feature extraction effect, and the feature extraction time has been greatly reduced. This shows that the improved feature extraction algorithm integrated with neighborhood constraint method can better extract the required data points, greatly improve the extraction efficiency on the basis of improving the extraction effect, and show good application performance in time application.

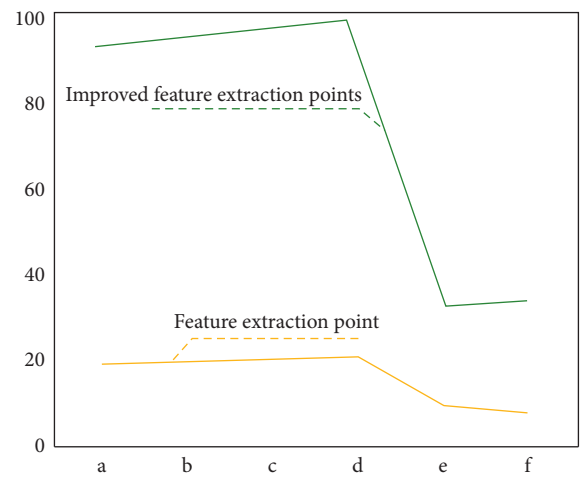

Figure 4: The comparison results of the number of point cloud clusters obtained after segmentation between the improved region growth algorithm and the traditional region growth algorithm.

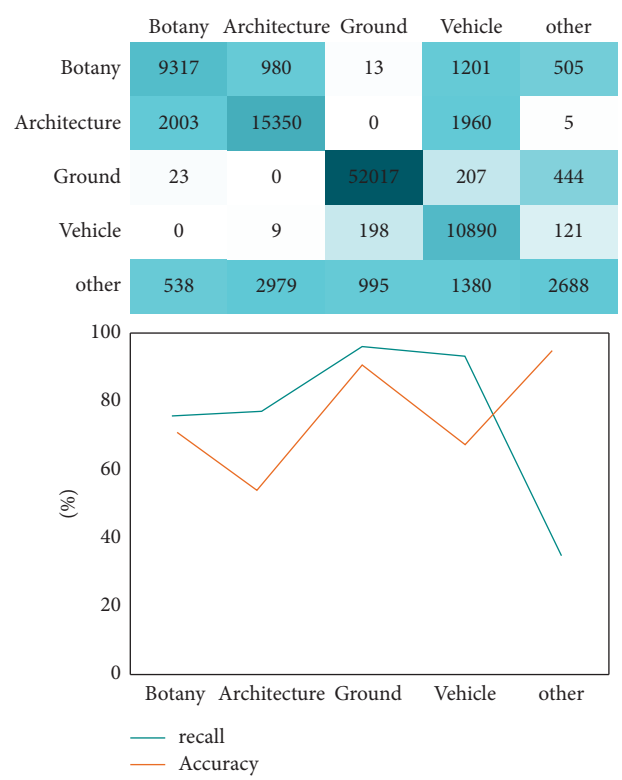

Figure 5: Experimental results of rural landscape point cloud classification based on random forest.

This paper selects three small-scale rural landscapes for the point cloud data segmentation effect test, as shown in Figure 4, which is the comparison result of the number of point cloud clusters obtained after the segmentation of the improved region growth algorithm and the traditional region growth algorithm. It can be seen from the data in the

Figure 6: Experimental results of rural landscape point cloud classification based on conditional random field scene.

figure that compared with the traditional region growth algorithm, the improved region growth algorithm can better segment the image, separate the nonplanar region, and maintain the good boundary. This shows that the improved region growth algorithm can segment more carefully, the quasidetermination of segmentation is better, the performance is more stable, and it can overcome the problem of local region over segmentation.

This paper selects the outdoor scene classification method based on random forest and the scene 3D point cloud classification method based on conditional random field for experimental comparison. As shown in Figures 5 and 6, the experimental results of rural landscape point cloud classification based on random forest and rural landscape point cloud classification based on conditional random field scene are shown, respectively. Random forest is a local classifier related to decision tree, which is composed of many decision trees. When classifying the 3D point cloud of outdoor scene, it is necessary to add category labels to the points contained in each 3D space. Then, the final classification label is selected by voting from the decision tree. Therefore, the outdoor scene classification method based on random forest mainly obtains the classification results according to the characteristics of a single point cloud, which will have some errors due to the voting method. As can be seen from the results in the figure, in terms of recall rate, the classification results of rural landscape point cloud based on conditional random field scene are higher than those of outdoor scene based on random forest. This shows that the scene 3D point cloud classification method based on conditional random field not only considers the local area features of a single point but also takes into account the similarity between adjacent point features and the relationship between points and adjacent areas. The outdoor scene classification based on random forest only infers according to the shape feature description of three-dimensional points. Therefore, the scene 3D point cloud classification method based on conditional random field has the advantages that the outdoor scene classification based on random forest does not have, and shows a better effect in point cloud classification.

As shown in Figure 7, it is the spatial information collection and visualization of a rural landscape obtained through three-dimensional point cloud technology. It can be seen from figure (a) that the three-dimensional point cloud technology can classify and divide the rural landscape in detail according to different attribute characteristics, and record the corresponding spatial information, so as to provide a data basis for further analysis. (b) This figure is the visualization of the laser point cloud model of houses and trees in the countryside, which can intuitively see the profile of buildings and trees and the corresponding centimeter accuracy.

Experiments show that the three-dimensional point cloud technology can quickly collect, quantitatively measure, and analyze the spatial information of different scales in different areas of rural landscape, and express it in a variety of ways. Compared with the traditional surveying and

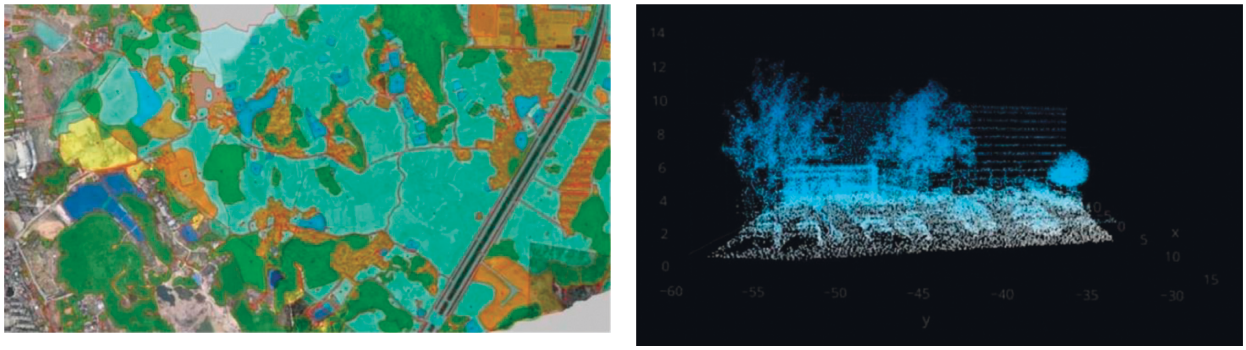

(a) (b)

Figure 7: Spatial information collection and visualization of a rural landscape obtained by 3D point cloud technology.

mapping method, it has a great improvement in measurement accuracy and efficiency. At the same time, the visualization of the spatial model of the rural landscape through the three-dimensional point cloud model saves the cost of manual modeling, and there is no contact between the measured objects in the whole process of data collection, which greatly improves the protection of the relatively fragile elements in the rural landscape.

5. Conclusion

There is a close relationship between the development of human society and rural landscape. Rural landscape is the result of the interaction between human activities and natural environment. It is not only an important carrier of human history and culture, but also its retained intangible cultural heritage, land methods, and agricultural technology have certain research and reference value for human settlements and agricultural development. With the rise of environmental awareness, people pay more and more attention to the protection and research of rural landscape. However, the rural landscape has been changing. The traditional measurement methods have responded to such changes and cannot meet people's needs for rural landscape measurement. With the development of science and technology and information technology, 3D point cloud technology can quickly complete the collection and recording of spatial information without contact. Therefore, this paper puts forward the research on the recording and protection of rural landscape spatial information based on 3D point cloud technology under the background of Internet of Things and records the spatial information of rural landscape through Internet of Things technology and 3D point cloud technology. At the same time, rural landscape belongs to outdoor landscape, and there are many factors that affect the data acquisition of 3D point cloud technology. This paper improves the feature extraction and region growth segmentation algorithm of 3D point cloud. The experimental results show that the improved 3D point cloud feature extraction effect is better, the extraction time is shorter, the point cloud classification can be carried out more carefully, the nonplanar regions can be separated, and the boundary is good. The three-dimensional point cloud classification method based on conditional random field has more classification advantages than the outdoor scene classification based on random forest and can achieve better classification effect. In addition, in the application of rural landscape spatial information recording, three-dimensional point cloud technology can complete the collection and recording of relevant spatial information in a short time, visualize the spatial information in a variety of ways, and understand the corresponding information more intuitively. However, there are still some problems to be solved in this paper. The improved three-dimensional point cloud technology still has a great deficiency, which cannot realize threshold adaptation, and the threshold needs to be given manually. The next step is to start from here and find a solution to realize the program to automatically determine the threshold and obtain better results.

Data Availability

The data used to support the findings of this study are available from the corresponding author upon request.

Conflicts of Interest

The authors declare that they have no conflicts of interest.

References

[1] C. Guo and G. Liu, "Extraction method of apple branch dry point cloud data based on color sampling [J]," *Transactions of the Chinese Society for Agricultural Machinery*, vol. 10, pp. 189–196, 2019.

[2] X. Zhai, zuguan Gong, shaohuan Luo, and J. Wang, "Research on fine segmentation of tree point cloud based on horizontal section method [J]," *Beijing Surveying and Mapping*, vol. 33, no. 3, pp. 270–273, 2019.

[3] D. Avishek, E. Johannes, and H. Michael, "Segmentation of laser point clouds in urban areas by a modified normalized cut method.[J]," *IEEE Transactions on Pattern Analysis and Machine Intelligence*, vol. 41, no. 12, pp. 3034–3047, 2019.

[4] S. Targetti, M. Raggi, and D. Viaggi, "Benefits for the local society attached to rural landscape: an analysis of residents' perception of ecosystem services[J]," *Bio-based and Applied Economics Journal*, vol. 09, 2020.

[5] L. E. Ridding, S. C. L. Watson, A. C. Newton, C. S. Rowland, and J. M. Bullock, "Ongoing, but slowing, habitat loss in a rural landscape over 85 years," *Landscape Ecology*, vol. 35, no. 2, pp. 257–273, 2020.

[6] M. Zhao, H. Zheng, T. Song, L. Cao, junmu Huang, and B. Chen, "Point cloud registration method integrating sampling consistency and iterative nearest point algorithm [J]," *Laser Journal*, vol. 40, no. 10, pp. 45–50, 2019.

[7] S. Xia, "The construction of the protection mechanism of rural landscape in the process of urbanization," *International Journal of Sustainable Development & World*, vol. 28, 2021.

[8] S. Sun, C. Li, P. W. Chee et al., "Three-dimensional photogrammetric mapping of cotton bolls in situ based on point cloud segmentation and clustering," *ISPRS Journal of Photogrammetry and Remote Sensing*, vol. 160, pp. 195–207, 2020.

[9] X. Dai and K. Lu, "Protection and construction strategy of rural landscape based on regional perspective: a case study of wuling town, hunan province," *IOP Conference Series: Materials Science and Engineering*, vol. 780, no. 7, Article ID 072008, 2020.

[10] J. Zhu, L. Wang, C. Zhao, and X. Zheng, "Segmentation of complex building roof point cloud based on region growth algorithm [J]," *Remote Sensing for Land & Resources*, vol. 31, no. 4, pp. 20–25, 2019.

[11] Y. Hu, Y. Wang, and S. Wang, "Scene target 3D point cloud reconstruction technology combining monocular focus stack and deep learning," *IEEE Access*, vol. 8, pp. 168099–168110, 2020.

[12] G. Wu, Q. Zhu, M. Huang, Y. Guo, and J. Qin, "Automatic recognition of juicy peaches on trees based on 3D contour features and colour data," *Biosystems Engineering*, vol. 188, pp. 1–13, 2019.

[13] B. G. Weinstein, S. Marconi, S. A. Bohlman, A. Zare, and E. P. White, "Cross-site learning in deep learning RGB tree crown detection," *Ecological Informatics*, vol. 56, Article ID 101061, 2020.

[14] J. Y. Yang, C. Lee, P. Ahn, H. Lee, E. Yi, and J. Kim, "PBP-net: point projection and back-projection network for 3D point cloud segmentation," 2020, https://arxiv.org/abs/2011.00988.

[15] Q. Li, G. Yang, S. Yan, R. Y. Fan, and C. Wang, "Achieve accurate recognition of 3D point cloud images by studying the scattering characteristics of typical targets," *Infrared Physics & Technology*, vol. 117, no. 20, Article ID 103852, 2021.

[16] G. Piazzi, G. Thirel, C. Perrin, and O. Delaigue, "Sequential data assimilation for streamflow forecasting: assessing the sensitivity to uncertainties and updated variables of a conceptual hydrological model at basin scale," *Water Resources Research*, vol. 57, no. 4, 2021.

[17] T. Reza, K. Mina, and F. Ghasem, "Quantitative structure-critical micelle concentration modeling of anionic gemini surfactants, comparison of MLR, PLS, WNN, and ANFIS models with eigenvalue and correlation ranking methods," *Journal of the Iranian Chemical Society*, vol. 1, pp. 1–9, 2021.

[18] R. Hasanzadeh Fereydooni, H. Siahkali, H. A. Shayanfar, and A. H. Mazinan, "SEMG-based variable impedance control of lower-limb rehabilitation robot using wavelet neural network and model reference adaptive control," *Industrial Robot: The International Journal of Robotics Research and Application*, vol. 47, no. 3, pp. 349–358, 2020.

[19] V. T. Yen, W. Y. Nan, and P. Van Cuong, "Recurrent fuzzy wavelet neural networks based on robust adaptive sliding mode control for industrial robot manipulators," *Neural Computing & Applications*, vol. 31, no. 11, pp. 6945–6958, 2019.

[20] Y. Wang, N. Lin, and N. Zhang, "Application of container building in community ecological environment renewal--taking gejiaying community in wuhan as an example," *IOP Conference Series: Earth and Environmental Science*, vol. 772, no. 1, p. 012082, 2021.

[21] X. R. Wu and Y. Y. Huang, "Adaptive Fractional-Order Nonsingular Terminal Sliding Mode Control Based on Fuzzy Wavelet Neural Networks for Omnidirectional mobile Robot Manipulator," *ISA transactions*, vol. 121, 2021.

[22] Y. Xiao, K. Tian, H. Huang, and J. T. Wang, "Coupling and coordination of socioeconomic and ecological environment in Wenchuan earthquake disaster areas: case study of severely affected counties in southwestern China," *Sustainable Cities and Society*, vol. 71, Article ID 102958, 2021.

[23] M. Xu, X. Chu, Y. Fu, C. Wang, and S. Wu, "Improving the accuracy of soil organic carbon content prediction based on visible and near-infrared spectroscopy and machine learning," *Environmental Earth Sciences*, vol. 80, no. 8, p. 326, 2021.

[24] Y. Tang, X. Wu, H. Chen, T. Zeng, and T. M. Zeng, "Prediction of the antifreeze of the concrete structure based on random forest and wavelet neural network," *IOP Conference Series: Earth and Environmental Science*, vol. 552, no. 1, Article ID 012010, 2020.

[25] O. O. Yashon, C. Y. Rodrick, and N. Alice, "Wachera. "Rainfall and runoff time-series trend analysis using LSTM recurrent neural network and wavelet neural network with satellite-based meteorological data: case study of Nzoia hydrologic basin," *Complex & Intelligent Systems*, vol. 8, pp. 1–24, 2021.

Hindawi
Computational Intelligence and Neuroscience
Volume 2022, Article ID 7766228, 8 pages
https://doi.org/10.1155/2022/7766228

Research Article

Innovative Mode of Logistics Management of "Internet of Things + Blockchain"-Integrated E-Commerce Platform

Hou Yujie and Hao Qiuxia

School of International Business, Qingdao Huanghai University, Qingdao, Shandong 7266000, China

Correspondence should be addressed to Hou Yujie; houyj@qdhhc.edu.cn

Received 4 March 2022; Revised 13 April 2022; Accepted 18 April 2022; Published 29 May 2022

Academic Editor: Guobin Chen

The innovation of logistics management mode plays a great role in promoting the operation timeliness of an e-commerce platform. The question of how to realize the research on the innovation mode of logistics management of the e-commerce platform with the integration of "Internet of things + blockchain" is the current development trend. Based on this, this paper studies the influencing factors of logistics management of an e-commerce platform under the discrete analysis strategy of "Internet of things + blockchain." First, the logistics management analysis model of an e-commerce platform integrating "Internet of things + blockchain" is proposed. The dynamic correlation function is used to simulate the logistics information in the e-commerce platform. Through the extreme value of the dynamic correlation function curve in the detection process, the operation signal is restored, and then its logistics management is analyzed. Second, the influencing factors in the logistics management of the e-commerce platform are analyzed, comprehensive analysis is done by using the "Internet of things + - blockchain" integration model, the dynamic logistics information in the operation of the e-commerce platform is accurately gathered, and the multidimensional hierarchical method is used for quality evaluation. Finally, the effectiveness of the logistics management analysis model of the e-commerce platform is verified by many experiments.

1. Introduction

With the rapid development of the platform, the logistics management system has been greatly improved and gradually developed in the direction of informatization, networking, integration, and automation. This makes the trading activities break the restrictions of time and space and greatly improve the transportation efficiency. E-commerce and logistics management, the so-called e-commerce, generally speaking, refer to business transactions on the network.

Logistics management refers to the use of scientific management methods to coordinate and control logistics activities in a planned and organized way. So that all logistics activities can be carried out smoothly, so as to reduce logistics cost and improve logistics efficiency. The modern logistics management technology is developed on the basis of e-commerce, and there is a very close relationship between them. Logistics management based on e-commerce consumers can directly order the services and products of some enterprises through the platform provided by e-commerce. Then, according to the information provided by customers, the information flow is transmitted to the enterprise. Then, the goods are delivered to consumers through logistics through the material management department. These are the information provided by the e-commerce platform, which not only ensure the development of logistics but also improve consumers' satisfaction with products and services.

China has certain data advantages in the research of logistics management of e-commerce platform, and there are many simulation research methods, including composite logistics simulation, differentiated local simulation, and multiparameter simulation [1]. In addition, in the process of studying the impact of intelligent network on the logistics management of the e-commerce platform, one of the hot

spots is the combination of "Internet of things + blockchain." From the analysis of the impact of the e-commerce platform on efficiency, in addition to the impact on customers' e-commerce platform usage habits, it also involves the logistics management part [2]. At the beginning of the 21st century, quantitative analysis methods began to appear in the research on the logistics management of e-commerce platform and the quantitative analysis methods continued to increase. Since then, the theory of the impact of "Internet of things + blockchain" on the logistics management of e-commerce platform began to pursue a diversified balance [3]. Internationally, the most critical simulation part affecting efficiency lies in the evaluation of the simulation part of the e-commerce platform, and the efficiency of logistics management of the e-commerce platform is improved through corresponding simulation [4]. In this context, based on the improved "Internet of things + blockchain" integration method, this paper puts forward the impact analysis model of logistics management of the e-commerce platform.

This paper studies the logistics management evaluation model of the e-commerce platform integrating "Internet of things + blockchain," which is mainly divided into four chapters. Chapter 1 introduces the research background and research objectives. Chapter 2 introduces the research status of the impact of "Internet of things + blockchain" on the logistics management of the e-commerce platform. Chapter 3 constructs the logistics management evaluation model of the e-commerce platform integrating "Internet of things + blockchain," and adopts the multidimensional composite "Internet of things + blockchain" integration under the multidomain. In Chapter 4, the logistics management impact simulation system of the "Internet of things + blockchain"-integrated e-commerce platform constructed in this paper is tested, and the experimental results are analyzed to draw a conclusion.

Compared with the existing research methods (such as the research method of random construction of sampling data), the innovation of this paper is to propose a discrete analysis system based on the improved "Internet of things + blockchain" fusion. The system can not only realize the daily recording and storage of information and data contained in the operation process of different "Internet of things + blockchain" e-commerce platforms but also make full use of the regional differences in the logistics management process of each e-commerce platform through data comparison and analysis and realize the closed-loop evaluation of logistics management of the e-commerce platform in the process of "Internet of things + blockchain."

2. Related Work

The Internet of things technology has developed rapidly in recent years, and there are more and more application scenarios. With the development needs of the Internet of things technology, blockchain technology also came into being, realizing decentralized digital applications. Relevant domestic logistics engineering and management research institutes have also carried out research on the combination of the Internet of things technology and blockchain technology [5]. Jiang and other scholars summarized and analyzed according to the operation law of the logistics platform and found that there is a problem of low intelligence in the influencing factors of e-commerce platforms on logistics management [6]. Sun and other scholars improved the discrete representation method of e-commerce platforms in the operation process according to the different characteristics and types of logistics information in different regions [7]. Dong and other scholars conducted differentiation analysis according to the process of logistics management of the e-commerce platform and realized the specific representation of the logistics management characteristics of the e-commerce platform according to the fixed key information [8]. Li and other scholars used methods different from conventional ideas to realize the vectorization processing of e-commerce platform signals and used different modes to formulate theoretical evaluation standards and data consistency rules, and studied the operation laws of different types of logistics platforms [9]. De Ku and other scholars summarized the logistics management analysis methods of e-commerce platforms at this stage, classified them according to their identification principles, and analyzed the advantages and disadvantages of different types of e-commerce platforms in the process of logistics management analysis [10]. Gunasekaran A and other scholars have identified the existing logistics management analysis methods of e-commerce platforms with ultrahigh discrimination according to the data information of different types of e-commerce platforms and achieved high accuracy analysis from the aspects of their composition and operation mode [11].

Based on the above research status, it can be seen that there is a lack of research on logistics management analysis of the e-commerce platform combined with intelligent network, and there are few research results [12]. Therefore, although domestic and foreign researchers have done a lot of basic research in the logistics management of the e-commerce platform, the innovation in the research results is relatively insufficient [13]. In addition, in the current research on the innovative mode of logistics management of e-commerce platform, most of them adopt the joint analysis method of simulated data combined with some real data [14]. On the other hand, in the infiltration tool evaluation and optimization of logistics management of the e-commerce platform, the efficiency of the discrete evaluation method adopted is not high, and its internal relevance is weak, resulting in the low transferability of most evaluation models [15]. Therefore, it is of great significance to study the logistics management and discrete evaluation analysis method of the e-commerce platform integrating "Internet of things + blockchain."

3. Methodology

3.1. Application Idea of "Internet of Things + Blockchain" Integration in the Discrete Analysis of Logistics Management of an E-Commerce Platform. The Internet of things technology is an intelligent technology that combines hardware and

software to realize the highly coordinated application of data and resources through interconnection. The Internet of things technology has been applied in different scenarios. Especially in the logistics management process of e-commerce, the comprehensive, coordinated, and unified allocation of logistics data can be realized through the Internet of things technology. In the process of data collection and analysis, the commonly used methods of Internet of things technology are neural network algorithm, mountain climbing algorithm, simulated annealing algorithm, and "Internet of things + blockchain" fusion algorithm [16]. At present, a variety of algorithms have been well applied in many engineering fields such as production scheduling, control engineering, computer vision, neural network, image processing, and accurate query of database information [17]. In addition, different types of optimization methods have emerged in the logistics management of e-commerce platform data, especially in the process of analyzing the logistics management strategy of the e-commerce platform. Among many methods for quantitative analysis of logistics management results of the e-commerce platform, "Internet of things + blockchain" integration has also attracted attention in recent years. This discrete method, combined with a mathematical method and information method, was applied to solve the problems of information systems in the early stage. Therefore, in the process of discrete data analysis and processing, mathematical modeling through the integration of "Internet of things + blockchain" technology is to determine the mathematical relationship between many factors of a gray system. In the process of logistics management analysis of the e-commerce platform, the feature extraction of discrete data is used to distinguish the differences of logistics management between different signals according to the extraction results. By using the blockchain technology, we can realize the high-intensity unified deployment application and information analysis of logistics signal data. Compared with the conventional logistics management analysis method of e-commerce platforms, this signal processing process has significantly improved the accuracy and stability of seepage tool evaluation. In the process of logistics management analysis of e-commerce platforms, the common analysis curve is shown in Figure 1.

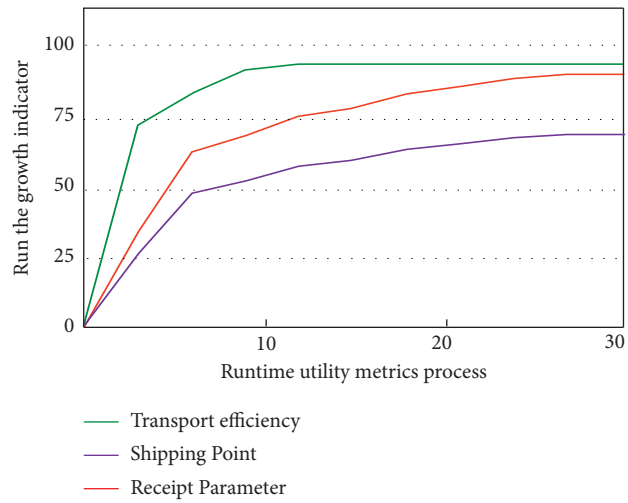

Figure 1: Common evaluation indicators of logistics efficiency.

3.2. Construction Process of the Logistics Management Analysis Model of an "Internet of Things + Blockchain" E-Commerce Platform. The signal processing process of e-commerce platforms by the neural network algorithm is shown in Figure 1. With the deepening of the research on discrete data processing of "Internet of things + blockchain" fusion by scholars, these can be analyzed and processed by using the "Internet of things + blockchain" fusion theory. At the same time, it is also necessary to obtain the key features in the signal through blockchain. The process of the composite synthesis processing algorithm shown in Figure 2.

Building the logistics management analysis model of e-commerce platform requires three steps. The first step is to measure the degree of correlation according to the relationship between factors in the Internet of things nodes. Its basic idea is to sort according to the degree of correlation. In the application, the original data matrix is initialized, and then, the reference data matrix is formulated. The e-commerce platform signal $E_m(t)$ can be marked as follows:

$$E_m(t) = \left[\frac{E_1(t) + E_2(t) + \ldots + E_n(t)}{n}\right]^2. \tag{1}$$

The second step is to calculate the absolute difference between the random subfactor and the main factor. The formula runs as follows:

$$\begin{aligned} \Delta_m(r, t) &= w_m^2(r) - w_n^2(t), \\ \Delta_n(r, t) &= w_n^2(r) + w_m^2(t), \end{aligned} \tag{2}$$

where m and n are two-dimensional neural layers, r represents the reference data column, and t represents the individuals in different data columns. The third step is to calculate the correlation degree $o_m(t)$ between the subfactor and the main factor. The formula is as follows:

$$\left|o_m(t)\right|^2 = \frac{\left|w_t^2(r) - w_t^2(t)\right|}{\sqrt{n}}. \tag{3}$$

3.3. Quantitative Evaluation Process of the Logistics Management Analysis Model of an "Internet of Things + Blockchain" E-Commerce Platform. The quantitative evaluation of the logistics management analysis model of e-commerce platforms is a complex process [18]. This paper analyzes an Internet of things data management system based on the blockchain and shared environment. The system includes data acquisition and storage module, which are used to obtain the Internet of things data and partition the data. The data slice is obtained and stored in the regional server. The hash address corresponding to the data slice is stored on the blockchain, and the smart contract module is used to receive the data transaction request sent by the data consumer and the corresponding hash address. The

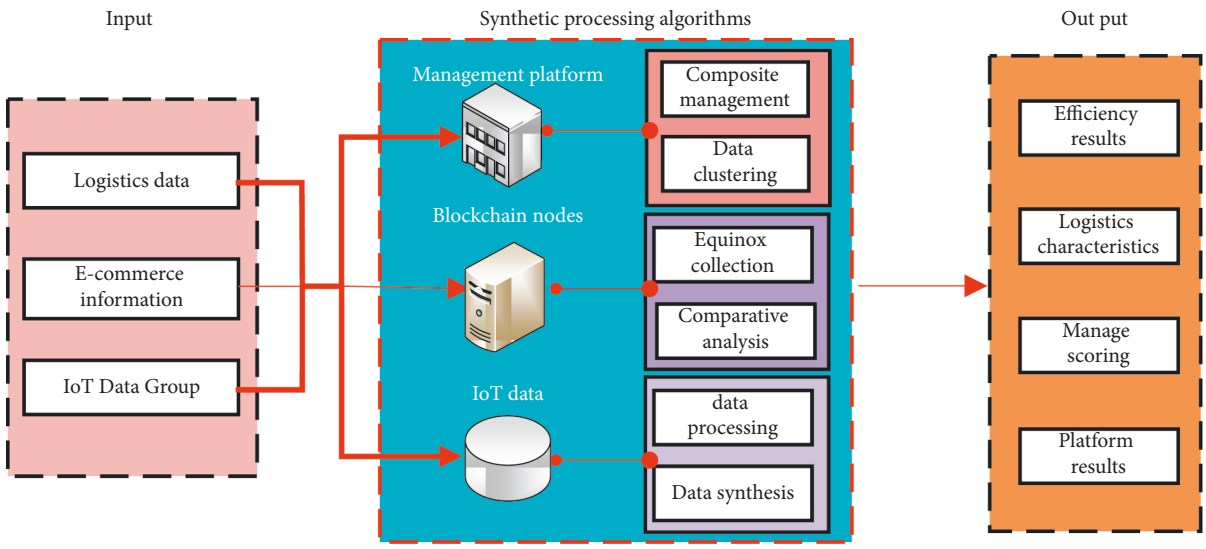

Figure 2: Composite synthesis processing algorithm processing process.

corresponding data slice is obtained according to the hash address and the transaction is executed.

In order to further study the "Internet of things + -blockchain," in the multidimensional hierarchical method using the integration of "Internet of things + blockchain," first the problems are clarified, the system objectives are determined, and the scope of decision-making problems is analyzed, which are generally carried out in the following steps.

The first step is to establish an analytic hierarchy process (AHP) system. Combined with the logistics management research theory of the e-commerce platform and time domain signal analysis, a discrete analysis is carried out in the comprehensive change process of the simulation signal of logistics management of e-commerce platforms, combined with the "Internet of things + blockchain" discrete data simulation system based on an ant colony recursion theory. The feature extraction algorithm is applied to the simulation model of "Internet of things + blockchain," and the logistics management analysis method of the "Internet of things + blockchain" e-commerce platform is established based on the feature extraction algorithm. This link is divided into data collection, data processing, result feedback, and so on. $M(t)$ indicates the feasibility of analytic hierarchy process.

$$M(t) = \frac{c(t) - p(t) + 1}{c(t) + p(t)}, \tag{4}$$

$c(t)$ and $p(t)$ are hierarchical functions. When the corresponding value of critical feasibility is reached, it is recognized as the effective value.

The second step is to determine the analysis indicators according to different logistics management, and then divide the system into different levels. In order to facilitate the calculation, the fusion formula method is adopted. This level division reflects the subordinate relationship of each level, but the importance of each index will not be the same.

$$m(t) = \frac{\sqrt{h(S_k)^2 + n^2}}{n}, \tag{5}$$

where b and c are matrix factors. It is followed by judging whether the model has passed the separation test and whether it can be recognized as the effective value only after meeting the separation test requirements.

The third step is to judge the maximum eigenvalue corresponding to the characteristic matrix in the model λ. The relative importance ranking can be reflected by normalization. Although this structure can reduce the interference of other factors and objectively reflect the influence of differences, there must be a certain degree of separation correlation in the comprehensive comparison. If the same result is produced, the discriminant function $e(h)$ should meet the following conditions:

$$\mathrm{e}(h) = \left(\frac{bw(t) + cw(t)}{i}\right)^2 + bcw(t), \tag{6}$$

where b and c are matrix factors. This is followed by judging whether the model has passed the consistency test and can be recognized as the effective value only after meeting the consistency test requirements.

Using the common reduction mechanism and introducing k for simplification and reconciliation, it can be simplified as follows:

$$\mathrm{e}(h) = k\left(\frac{bw(t) + cw(t)}{i}\right)^2. \tag{7}$$

The fourth step is to conduct consistency inspection. The current scaling method is mainly 9-scale method, and its test function RF(t) running formula is as follows:

$$\mathrm{RF}(t) = \frac{t^2 + 3t + 1}{t^2 + 7 + t^{-1} + t^{-2}}. \tag{8}$$

Finally, we need to improve the above "Internet of things + blockchain" integration and e-commerce platform intervention conditions. In this paper, we mainly improve the blockchain algorithm and use the omega method. This method is simpler to operate. It is only calculated according to the example of importance through the composite comparative analysis. This algorithm has other defects. For example, the business rules and simulation process of e-commerce platforms will directly affect the establishment of the judgment matrix. Affected by subjective factors, it is very prone to objective errors. Therefore, the multidimensional hierarchical method cannot objectively reflect the research problems. It also needs to be evaluated by the fuzzy hierarchical method of "Internet of things + blockchain."

3.4. Design of the Discrete Analysis Model for Logistics Management of an E-Commerce Platform Integrating "Internet of Things + Blockchain". Under the intervention of multilevel coupling factors, in order to study the impact of different discrete data on the logistics management model of e-commerce platforms, the accuracy of simulation is quantitatively analyzed, but in many cases, there is no quantitative data, so it is necessary to quantitatively transform the qualitative data in the simulation process. [19]. In this case, the commonly used functions include a discrete error analysis function, combined covariant function, and so on [20, 21]. The method used in the standard is a comprehensive evaluation function. The results show that this model can effectively reduce the characteristic value of error parameters, improve the accuracy evaluation and cooperation efficiency of logistics management factors of e-commerce platform, and is suitable for different "Internet of things + blockchain," technologies and can also adapt to subjective interference signals in the simulation process of "Internet of things + blockchain" [22].

In the evaluation link of the impact of "Internet of things + blockchain" on the logistics management of human e-commerce platforms, the meaning of data is different, so it is not equivalent to analysis. The original data need to be processed in a dimensionless way, and the proportional transfer method is used in this paper [23]. At present, the behavior decision of IOT terminals depends on the control of the central cloud platform (or edge cloud platform), and its data processing and M2M interaction ability is weak. It can be combined with blockchain, tee (trusted execution environment), and other technologies, which are expected to enhance the intelligence of IOT terminals and make the IOT network have differential distributed intelligence. Blockchain ensures the terminal's identity can be verified and the credibility, reliability, openness, and transparency of data records. If combined with the terminal's hardware computing platform, the terminal can be built into an intelligent platform to complete some local tasks independently. After the normalization process is completed, the relationship between different "Internet of things + blockchain" simulation series can be calculated, and then, the difference between each factor and the main factor at the same observation point can be calculated. The simulation results are shown in Figure 3.

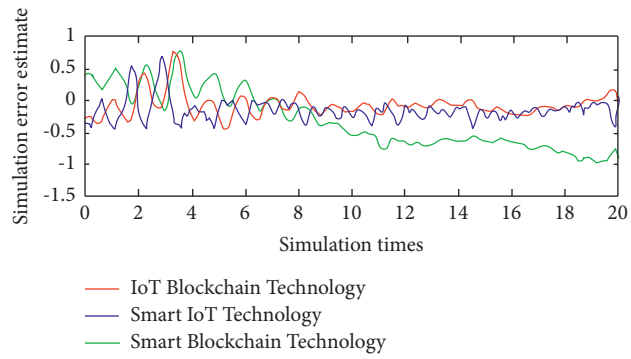

Figure 3: Simulation error estimate.

As can be seen from Figure 3, the logistics management analysis model of e-commerce platforms based on the Internet of things has better stability of simulation results, and its change law is better than that of the other two methods. When comprehensively evaluating the simulation results of the impact of "Internet of things + blockchain" on the logistics management of key customer e-commerce platforms, in most cases, the problem of ranking will be involved. Each evaluation object needs to be ranked first, so it needs to be further compared with the help of gray comprehensive evaluation index.

In order to study the logistics management law of the e-commerce platform under the analysis of Internet of things and blockchain, the hierarchical relationship of gray evaluation index adopted in this article is expressed by set, and its operation formula κ is as follows:

$$\kappa(x) = \sum_{i=1}^{p}\left(\frac{t_{ik} - t_i}{i + k}\right). \tag{9}$$

After the operation formula of its management law is obtained, it is judged. The discriminant of the integration judgment formula $y(t)$ and the characteristic judgment formula $z(t)$ is as follows:

$$\begin{aligned} y(t) &= \sum_{i=1}^{n}\left(\frac{t_{ki}}{k+i} + \frac{t_{kj}}{k+j}\right), \\ z(t) &= \frac{\sum_{i=1}^{n}(t_{ki}/k+i)}{\sum_{i=1}^{n}(t_{ki}/k-i)}. \end{aligned} \tag{10}$$

In the logistics management evaluation function of this e-commerce platform, each secondary indicator will also have its own weight coefficient, which is expressed by different coefficients. The weight vector function of each layer can be classified as $u_1(t)$ or $u_2(t)$. The operation formula is as follows:

$$\begin{aligned} u_1(t) &= \frac{2t^5 + \sqrt{t^2 + 7 + t^{-1}}}{3\sqrt{t^2+1}}, \\ u_2(t) &= \frac{2t^5 - \sqrt{t^2 + 7 + t^{-1}}}{3\sqrt{t^2+1}}, \end{aligned} \tag{11}$$

where t is discrete data.

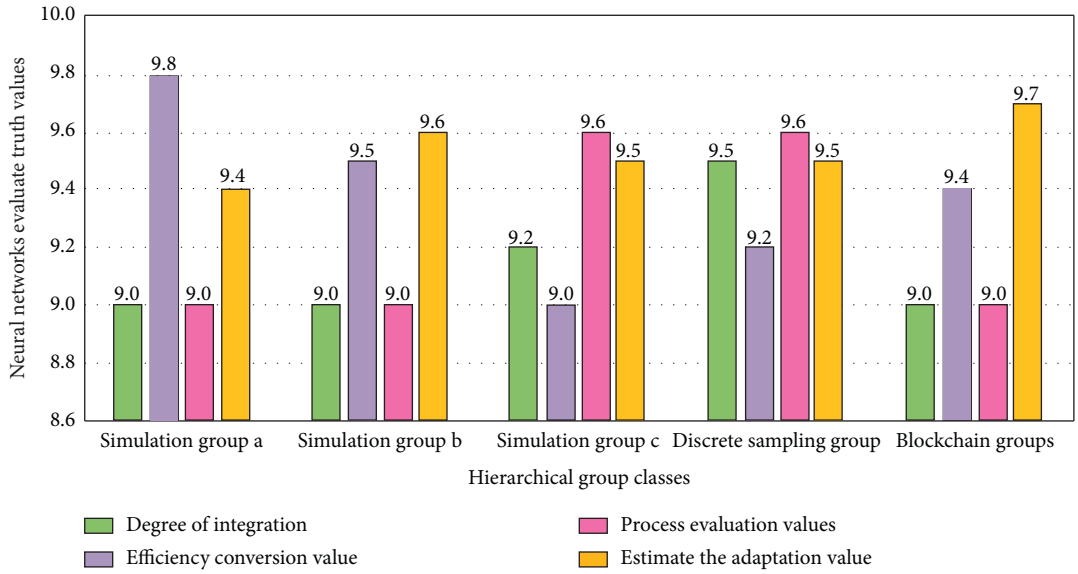

Figure 4: Simulation versus actual evaluation.

The following discriminant is used to judge the classification:

$$P(t) = \sum_{i=1}^{n} \frac{y(t)}{z(t)}. \tag{12}$$

If $P(t)$ is greater than 1, it is classified as $u_1(t)$; otherwise, it is classified as $u_2(t)$.

4. Result Analysis and Discussion

4.1. Evaluation Index of the Discrete Analysis Experiment of Logistics Management of an E-Commerce Platform Integrating "Internet of Things + Blockchain". In this study, the simulation evaluation results of the influencing factors of logistics management of the e-commerce platform under different blockchain nodes are divided into a significant impact and no impact. After determining the classification levels, these levels are assigned and scored, and the ten point assignment method is used to evaluate their integration degree, efficiency conversion value, process evaluation value, and estimated adaptation value. The evaluation results are shown in Figure 4.

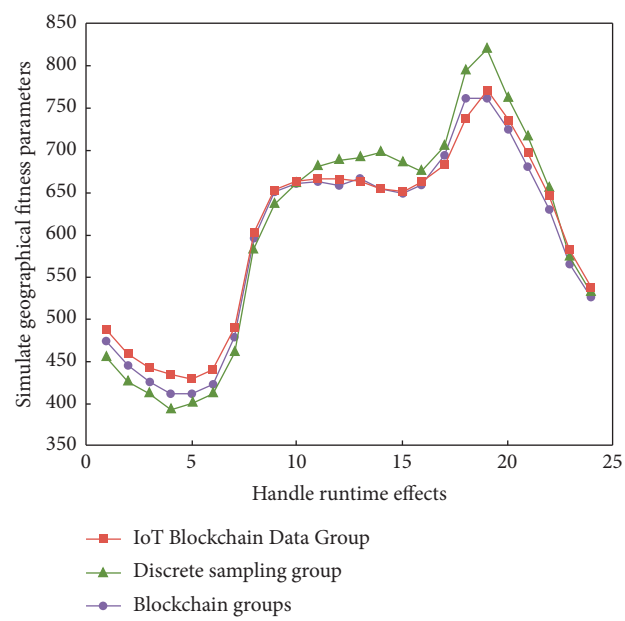

Figure 5: Logistics management analysis of e-commerce platforms.

4.2. Experimental Results and Analysis. Figure 5 shows the experimental results of logistics management analysis of three groups of e-commerce platforms under the optimization of "Internet of things + blockchain." MATLAB software can effectively process the relevant data in this evaluation model.

Figure 6 shows the variation law of proportional error in the discrete analysis of logistics management of different e-commerce platforms by four collection and processing methods under different analysis completion degrees.

As can be seen from Figure 6, with the increase of analysis completion, the accuracy of discrete dynamic analysis corresponding to the four collection and processing methods is different, but presents a similar change law. When the analysis completion degree is the same, the analysis stability and accuracy corresponding to the "Internet of things + blockchain" fusion are the highest, followed by the neural network algorithm. When the completion degree of the four collection and processing methods is 70%, the corresponding analysis accuracy is the highest because the effectiveness of the corresponding cycle analysis times is the highest in the process of discrete dynamic analysis of experimental data.

For example, the characterization of the current data is classified into different types of evaluation criteria, and the evaluation results are refined according to the different characterization criteria of the current e-commerce data [24],

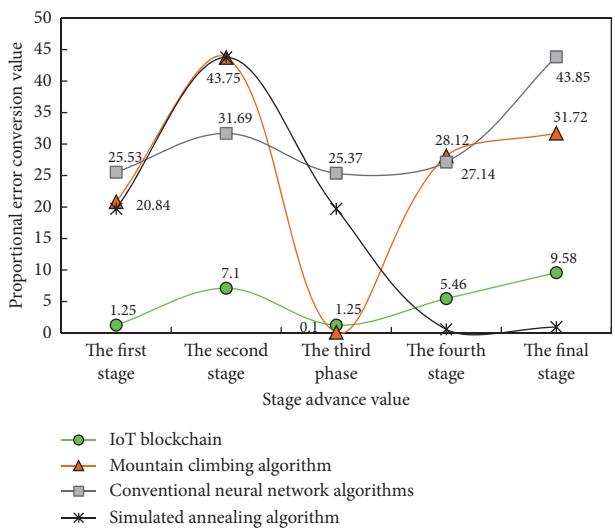

Figure 6: Scale error variation law diagram.

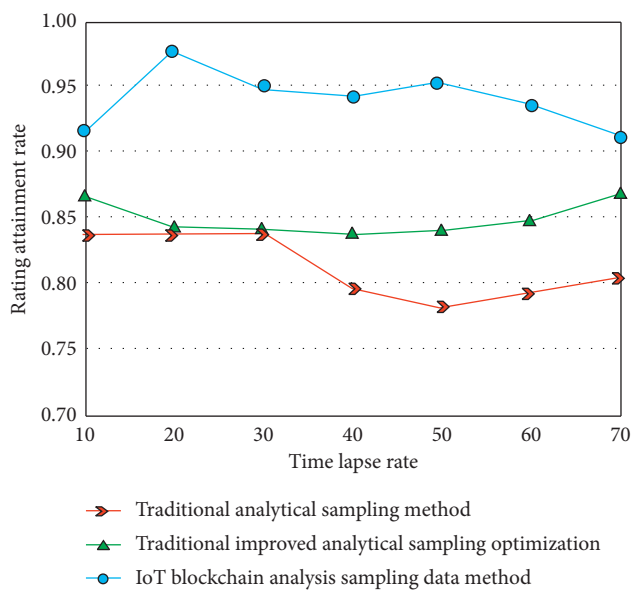

Figure 7: Comprehensive scoring of the logistics management platform.

Finally, the preliminary evaluation and secondary evaluation are carried out according to the known industry reference standards. In this way, the evaluation and analysis of the experimental results can be well completed, which is consistent with the current mainstream evaluation rules and more persuasive and then calculate the weight and score. The experimental simulation analysis results are shown in Figure 7.

As can be seen from Figure 7, the results of the "Internet of things + blockchain" model are more stable with the increase of analysis times and are better than the experimental analysis results of other methods, which shows that compared with the traditional neural network e-commerce platform analysis model and its optimization algorithm, the logistics management analysis model of e-commerce platforms analyzed by the "Internet of things + blockchain" model has a better analysis effect in the logistics management analysis of local e-commerce platform signals. Finally, through model analysis and calculation, it can be concluded that the efficiency improvement rate of this method can reach more than 90, which is better than other collection and analysis methods.

5. Conclusion

The current e-commerce platform has some problems in logistics management, such as less quantitative statistics and large error. Based on this, this paper studies the logistics management analysis model of e-commerce platforms based on the integration and analysis strategy of "Internet of things + blockchain." First, it summarizes the current situation of logistics management analysis of the e-commerce platform and puts forward ideas for improvement and optimization according to its existing problems. Second, through the differences of different types of e-commerce platforms in logistics management, we extract their features and formulate classification strategies. Third, it analyzes the influencing factors of logistics management of the e-commerce platform, makes a comprehensive analysis by using a multidimensional data model, studies the influencing factors involved, and summarizes their influence law and weight ranking in the operation process; Finally, the logistics management analysis model of e-commerce platforms is verified by experiments. The results show that compared with the conventional methods, the logistics management analysis model of e-commerce platforms proposed in this study has a better reliability and lower error rate. However, this study only considers the processing of simulation data, not the elimination of real multidimensional interference signals, so it can be further studied.

Data Availability

The data used to support the findings of this study are available from the corresponding author upon request.

Conflicts of Interest

The authors declare that they have no conflicts of interest.

References

[1] S. Tang, F. Yu, Y. Zhao, Y. Zhou, and W. Deng, "Construction and verification of retinal vessel segmentation innovation mode and optimization strategy of B2C E-commerce logistics distribution under big data," *Sustainability*, vol. 12, 2020.

[2] F. Pollák, M. Konen, and D. Eulovs, "Innovations in the management of E-commerce: analysis of customer interactions during the COVID-19 pandemic," *Sustainability*, vol. 13, 2021.

[3] R. Villa and A. Monzón, "A metro-based system as sustainable alternative for urban logistics in the era of E-commerce," *Sustainability*, vol. 13, 2021.

[4] C. Wang, "Analyzing the effects of cross-border E-commerce industry transfer using big data," *Mobile Information Systems*, vol. 2021, no. 8, pp. 1–12, 2021.

[5] L. Xia and S. Liu, "Intelligent IoT-based cross-border e-commerce supply chain performance optimization," *Wireless Communications and Mobile Computing*, vol. 2021, no. 121, pp. 1–13, 2021.

[6] Y. Jiang, P. Lai, C. H. Chang, K. F. Yuen, S. Li, and X. Wang, "Sustainable management for fresh food E-commerce logistics services," *Sustainability*, vol. 13, 2021.

[7] P. Sun and L. Gu, "Optimization of cross-border e-commerce logistics supervision system based on Internet of things technology," *Complexity*, vol. 2021, no. 4, 11 pages, Article ID 4582838, 2021.

[8] Z. Dong, "Construction of mobile E-commerce platform and analysis of its impact on E-commerce logistics customer satisfaction," *Complexity*, vol. 2021, Article ID 6636415, 13 pages, 2021.

[9] Y. Liu, S. Liang, and R. Ding, "BCG-induced trained immunity in macrophage: reprograming of glucose metabolism: BCG-induced trained immunity by enhanced glycolysis and glutamine-driven tricarboxylic acid cycle in macrophage," *International Reviews of Immunology*, vol. 39, no. 3, pp. 83–96, 2020.

[10] L. I. De-Ku, "The innovation in logistics management in the light of E-commerce," *China Business and Market*, vol. 87, no. 18, pp. 529–531, 2013.

[11] A. Gunasekaran and J. Sarkis, "Research and applications in e-commerce and third-party logistics management," *International Journal of Production Economics*, vol. 113, no. 1, pp. 123–126, 2008.

[12] Y. Abuidris, R. Kumar, and T. Yang, "Secure large-scale E-voting system based on blockchain contract using a hybrid consensus model combined with sharding," *ETRI Journal*, vol. 43, no. 2, 2021.

[13] S. Lee, M. Kim, J. Lee, R. H. Hsu, and T. Q. Quek, "Is blockchain suitable for data freshness? An age-of-information perspective," *IEEE Network*, vol. 35, no. 99, pp. 1–8, 2021.

[14] T. Wang, M. Zhang, C. H. Springer, and C. Yang, "How to promote industrial park recycling transformation in China: an analytic framework based on critical material flow," *Environmental Impact Assessment Review*, vol. 87, no. 5, Article ID 106550, 2021.

[15] H. Huang, Z. Yue, X. Peng et al., "Elastic resource allocation against imbalanced transaction assignments in sharding-based permissioned blockchains," *IEEE Transactions on Parallel and Distributed Systems*, vol. 33, 2022.

[16] Q. Luo, Y. Zhou, W. Hou, and L. Peng, "A hierarchical blockchain architecture based V2G market trading system," *Applied Energy*, vol. 307, 2022.

[17] J. J. Sikorski, J. Haughton, and M. Kraft, "Blockchain technology in the chemical industry: machine-to-machine electricity market," *Applied Energy*, vol. 195, no. JUN.1, pp. 234–246, 2017.

[18] S. Underwood, "Blockchain beyond bitcoin," *Communications of the ACM*, vol. 59, no. 11, pp. 15–17, 2016.

[19] C. Huang, G. Chen, and Y. Gong, "Delay-Constrained buffer-aided relay selection in the Internet of things with decision-assisted reinforcement learning," *IEEE Internet of Things Journal*, vol. 8, no. 99, 2021.

[20] I. Affia and A. Aamer, "An internet of things-based smart warehouse infrastructure: design and application," *Journal of Science and Technology Policy Management*, vol. 13, no. 1, pp. 90–109, 2021.

[21] Xi Chen, "Music emotion analysis based on PSO-BP neural network and big data analysis," *Computational Intelligence and Neuroscience*, vol. 2021, Article ID 6592938, 9 pages, 2021.

[22] A. Rachana Harish, X. L. Liu, R. Y. Zhong, and G. Q. Huang, "Log-flock: a blockchain-enabled platform for digital asset valuation and risk assessment in E-commerce logistics financing," *Computers & Industrial Engineering*, vol. 151, Article ID 107001, 2021.

[23] Z. Liu and Z. Li, "A blockchain-based framework of cross-border e-commerce supply chain," *International Journal of Information Management*, vol. 52, Article ID 102059, 2020.

[24] M. Li, S. Shao, Q. Ye, G. Xu, and G. Q. Huang, "Blockchain-enabled logistics finance execution platform for capital-constrained E-commerce retail," *Robotics and Computer-Integrated Manufacturing*, vol. 65, Article ID 101962, 2020.

Hindawi
Computational Intelligence and Neuroscience
Volume 2022, Article ID 5159448, 9 pages
https://doi.org/10.1155/2022/5159448

Research Article

Research on Town Ecological Landscape Planning and Governance Based on Fuzzy Optimization Method of Internet of Things Technology

Yu Ying, Kunru Jiang, and Meiqi Ren

School of Architecture, Yantai University, Yantai, Shandong 264005, China

Correspondence should be addressed to Yu Ying; 201001001591@ytu.edu.cn

Received 9 February 2022; Revised 12 March 2022; Accepted 21 April 2022; Published 28 May 2022

Academic Editor: Guobin Chen

The current town ecological landscape planning and governance methods are mainly based on the high quality, high energy-saving, and environmental protection effect of the town ecological landscape. How to innovate the town ecological landscape planning and governance process with the help of Internet of things technology and fuzzy optimization method is the current development trend. Based on this, this paper studies the application of Internet of things technology in town ecological landscape planning and management. Firstly, a small town ecological landscape evaluation model based on fuzzy optimization algorithm is proposed. Combined with multivariate matrix transformation function, the authenticity data of ecological landscape are simulated. The original analysis of different types of small town ecological landscape is realized by selecting the multivariate extremum of autocorrelation function curve in the process of planning and governance. Secondly, in the simulation evaluation link, the fuzzy evaluation method is adopted and improved. At the same time, the improved three-dimensional original planning governance model is used to comprehensively analyze the simulation results of three-dimensional landscape planning governance. Finally, by designing fuzzy simulation experiments, the application effects of different Internet of things technologies in town ecological landscape planning and governance are analyzed. The experimental results show that the correlation data indicators of fuzzy optimization methods corresponding to different Internet of things technologies are very different. The application effect of different types of Internet of things technology in ecological landscape planning and governance of small towns is targeted and shows strong regularity.

1. Introduction

The research on the planning and governance of small town ecological landscape in China has been carried out very early, and there are many contents involved. It is analyzed from the perspective of the structure of small town ecological landscape, including local landscape simulation, landscape distribution design, and overall planning [1]. In addition, different designers will also participate in the process of town ecological landscape design. From the perspective of town ecological landscape planning and governance, in addition to the three-dimensional layout of the landscape, it will also involve the functional part of the landscape on town greening. In recent years, Internet of things technology has attracted extensive attention. The core content of town ecological landscape planning and governance process is to quantitatively evaluate the effectiveness of green environmental protection, which is of great significance to promote the diversified development of town ecological landscape planning and governance [2]. On the other hand, the domestic green landscape research institute has also carried out the application research of Internet of things technology, and various application modes are emerging, such as the western town ecological landscape model based on analytic hierarchy process [3]. Under this background, this paper studies the application of fuzzy optimization method based on Internet of things technology in town ecological landscape planning and management.

The innovation of this paper is to propose a small town ecological landscape planning and governance model based on improved fuzzy optimization algorithm. Combined with the Internet of things technology, this paper studies the innovative methods of small town ecological landscape in the design process. On this basis, the landscape planning and governance model can not only realize the differential comparison of three-dimensional landscape in different towns, but also make full use of the location differences between the ecological landscapes of each town to analyze the application of different types of Internet of things technology, so as to realize the closed-loop evaluation of the planning and governance quality of the overall ecological landscape of the town. On the other hand, the HQR difference factor is used to quantitatively describe the data matching degree between each comparison column and reference column and the error calculation of standard data, so as to complete the priority ranking of different types of Internet of things technologies in town ecological landscape planning and governance with quantitative indicators, which can efficiently analyze and extract the factors affecting town ecological landscape planning and governance and realize the application value research and analysis of different landscape planning and governance schemes.

Combined with HQR planning and governance model, this study studies the application of Internet of things technology and fuzzy optimization method in town ecological landscape planning and governance, which is mainly divided into four parts. The first part introduces the general framework and research background. The second part introduces the research status of the application of Internet of things technology and town ecological landscape planning and governance. The third part constructs the three-dimensional planning model of small town ecological landscape based on the fuzzy optimization algorithm in the Internet of things technology, adopts the improved fuzzy optimization algorithm in the time domain mode, and constructs the evaluation index system of different fuzzy optimization methods. In the fourth part, the three-dimensional planning model of small town ecological landscape constructed in this paper is simulated and tested, the results are analyzed, and the conclusion is drawn.

2. Related Work

At present, there are some problems in the research process of town ecological landscape planning and governance, such as low data useful information rate and insufficient intelligence. Therefore, many experts and scholars have studied the scheme of town ecological landscape planning and governance. According to the location differences of different three-dimensional landscapes in different towns, Kyoung et al. put forward targeted improvement strategies for the planning and governance methods of ecological landscapes in different types of towns [4]. Based on the improvement of the standard unit of the small town ecological landscape planning and governance simulation model, Xiu et al. proposed an adaptive model of small town ecological landscape planning and governance based on neural network algorithm and used the normalization method to collect the nodes of the differences in spatial layout of different small towns. The three-dimensional simulation of small town ecological landscape is realized by neural network algorithm [5]. Huiying et al. found that most towns still follow the traditional ideas of town ecological landscape planning and governance in the process of planning and governance, ignoring the utilization of intelligent information technology and the application of green environmental protection materials [6]. According to information technology and small town architecture, Jiang et al. proposed that attention should be paid to the development and construction of small town ecological landscape planning and governance simulation system based on limiting factors and green environmental protection concept, so as to improve the management and attention to effective data information in the process of small town ecological landscape planning and governance [7]. In order to improve the utilization of existing buildings in the process of town ecological landscape planning and governance, Qingyun et al. proposed an innovative collaborative scheme for town ecological landscape planning and governance based on neural network algorithm and related theories [8]. Enrica et al. found that the current small town ecological landscape planning and management scheme often adopts the characteristics of fixed frame input and put forward the method of cluster analysis and processing of data information based on a specific small town to realize the three-dimensional planning and management of landscape [9]. Josefin et al. put forward a new "end-to-end" small town ecological landscape planning, governance, and transformation system through the research and analysis of the value concept and differences of green environmental protection in different locations of small town ecological landscape planning and governance [10]. Alberto et al. have verified the effectiveness of the system in the process of town ecological landscape planning, governance, and transformation through practice. The results show that the innovative town ecological landscape planning, governance, and transformation system has the advantages of high stability and low cost [11]. Lakshika et al. conducted quantitative comparative analysis of ecological landscape planning schemes in different dimensions according to the intelligent sensing strategy in the Internet of things technology and carried out high-accuracy planning and governance according to its internal data relevance [12].

To sum up, it can be seen that, in the current process of town ecological landscape planning and governance, most of the planning and governance schemes and intelligent matching strategies are obtained by mixed analysis of different types of Internet of things technology and IOT technology [13–15]. On the other hand, although the Internet of things technology has produced a variety of matching application strategies in different types of scenarios, it is difficult to produce greater added value in the specific ecological landscape planning process, which is caused by the direct application without adopting the preferred method [16–19]. Based on this, it is of great practical significance to carry out the research on large-scale management of small town ecological landscape based on fuzzy optimization method based on Internet of things technology.

3. Methodology

3.1. Basic Application Idea of the HQR Three-Dimensional Planning Model in Town Ecological Landscape Planning and Governance. HQR model is a commonly used three-dimensional planning method, which usually realizes the three-dimensional reconstruction of the landscape through honor in ecological landscape planning [20]. The HQR three-dimensional planning model is mainly divided into two steps in the process of ecological landscape planning and governance of the town, one is the landscape information input link, and the other is the landscape information utilization link [21].

The process of collecting data from landscape two-dimensional image signals and IOT sensors includes three links. The first process inputs a section of honor or a set of two-dimensional maps of small town landscape. The second link is to infer various parameters in the process of landscape planning through the matching between two-dimensional maps [22]. The principle of HQR model in the process of general ecological landscape planning and governance is shown in Figure 1.

The town ecological landscape planning and governance method based on HQR three-dimensional planning model has been comprehensively developed in recent years, and the three-dimensional space optimization methods in time domain and frequency domain are also emerging. It is difficult for these methods to conduct comprehensive analysis from the perspective of three-dimensional planning [23]. Among many methods for quantitative analysis of ecological landscape simulation results of small towns, HQR three-dimensional planning model has attracted much attention in recent years. This three-dimensional planning method, combined with mathematical methods and information methods, was early applied to solve the problems of three-dimensional restoration of ancient buildings and planning and management of ancient buildings in small towns [24]. Therefore, the planning and management of small town ecological landscape through HQR three-dimensional planning model is to determine the mathematical relationship between many factors of grey system and realize the reconstruction of landscape facilities from 2D to 3D [25, 26].

3.2. Fuzzy Optimization Process of Internet of Things Technology in the HQR Three-Dimensional Programming Model. Based on the HQR three-dimensional planning model described in Chapter 3.1, in order to further realize the efficient planning and governance of the town's ecological landscape through the Internet of things technology, this part first selects the HQR three-dimensional planning model based on the time domain method and selects three characteristic parameters related to the coordination of the town's ecological landscape planning and governance. The hierarchical framework and hierarchical subordination of the whole town ecological landscape simulation design system are clearly defined through the research on three aspects: the zero crossing rate of the collected data of the Internet of things sensor of the landscape two-dimensional image signal, the signal waveform conversion, and the calculation of the filtered excitation signal vector. Therefore, in the application of this study to the ecological landscape planning and governance of small towns, the original two-dimensional design information data is transformed into the corresponding matrix for initialization, and then the reference data column is formulated, marked as

$$x_t^{(0)}(0) = \left\{ \frac{x_1^{(0)}(0), x_2^{(0)}(0), \ldots, x_n^{(0)}(0)}{x_1^{(0)}(0) - 1} \right\}, \tag{1}$$

where $i = 1, 2, \ldots, n$ $x_t^{(0)}(0)$ is different ecological landscape types of small towns.

Secondly, by calculating a sensor data network based on the town landscape planning and governance information and the Internet of things, the absolute difference between the planning factors and governance factors in the town ecological landscape information is calculated, and the formula is expressed as follows:

$$\Delta_t(i, 0) = \left| \left\{ \frac{x_t^{(0)}(i) - x_t^{(l)}(0)}{\sqrt{x_t^{(0)}(i) + x_t^{(l)}(0)}} \right\} \right|, \tag{2}$$

where $i = 1, 2, \ldots, n$ $\Delta_t(i, 0)$ is the absolute difference.

Finally, the correlation degree between the corresponding subfactors and main factors in the HQR three-dimensional planning model is calculated as follows:

$$\zeta_i(0) = \sqrt{\frac{1}{n} \sum_{i=1}^{n} \frac{\min_t \min_t \left| x_t^{(l)}(i) - x_t^{(l)}(0) \right| + \zeta \max_t \max_t \left| x_t^{(l)}(i) - x_t^{(l)}(0) \right|}{\left| x_t^{(l)}(i) - x_t^{(l)}(0) \right| + \zeta \max_t \max_t \left| x_t^{(l)}(i) - x_t^{(l)}(0) \right|}}, \tag{3}$$

where ∂ represents the three-dimensional planning resolution coefficient of the town's ecological landscape. In this process, the formation process of the preliminary treatment scheme for the town's ecological landscape is shown in Figure 2.

3.3. Quantitative Simulation Analysis Process of IOT Technology in the HQR Three-Dimensional Planning Model. In the analytic hierarchy process using the HQR three-dimensional planning model based on IOT (Internet of things) technology, first clarify the problem of selecting the type of

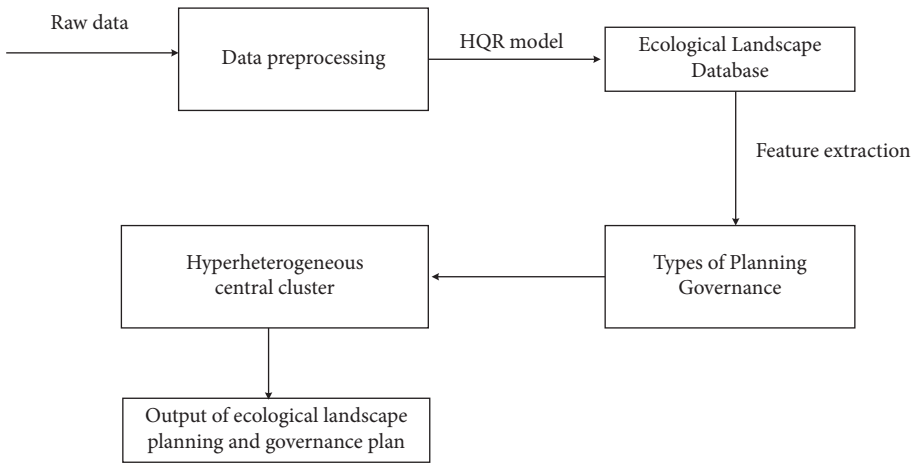

Figure 1: The principle of HQR model in the commonly used ecological landscape planning and governance process.

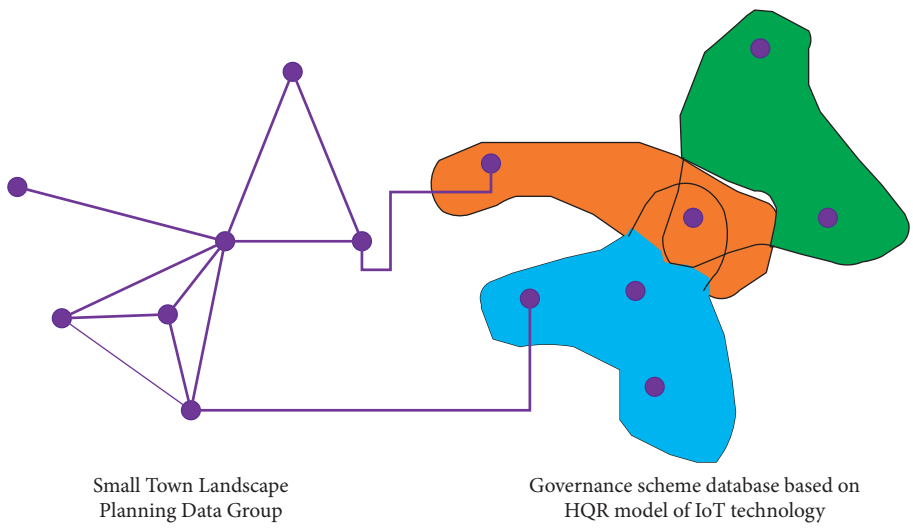

Figure 2: The process of forming the preliminary management plan for the ecological landscape of the small town.

ecological landscape planning and governance of the small town, determine the system governance objectives, and then establish the analytic hierarchy process system. Combined with three-dimensional informatics and three-dimensional visualization system, it makes a unified analysis on the change process of relevant signals in the ecological landscape planning and governance of the small town, learns from the existing simulation system of small town ecological landscape planning and governance based on fish network, and applies the feature extraction algorithm to the parameter setting of Internet of things technology.

The specific details of applying the feature extraction algorithm to the technical parameter setting of the Internet of things include the following: The link is divided into data acquisition, data processing, result feedback, and so on. And according to different angles to determine the various indicators of different Internet of things technologies, the system is then divided into different levels. In order to facilitate calculation, it is often explained in the form of block diagram. If there are many factors involved, the hierarchy can be further decomposed. This hierarchy reflects the subordination of various environmental protection building materials, but the importance of each index will not be the same. The current scaling method is mainly the multidimensional marking method, which divides and registers the indicators, assigns values, establishes a matrix, and then extracts useful information from the matrix. By constructing pairwise judgment matrix and matrix mathematical method, the importance of various physical parameters of different Internet of things technologies is ranked. From the perspective of architecture, too many grades will affect the difficulty of judgment. Therefore, in the process of effectively combining the Internet of things technology and HQR three-dimensional planning model, it is necessary to construct the three-dimensional data level of different building materials in this model. Although this structure can reduce the interference of other factors and objectively reflect the difference of influence, a certain degree of nonheterogeneity is bound to occur in the comprehensive comparison. If the results are consistent, the matrix should meet the following requirements:

$$a_{ij}a_{jk} = a_{ik}. \tag{4}$$

If any two rows of matrix A are proportional, the scale factor is greater than zero. The consistency test of different environmental protection building materials is expressed by *PP*, and the calculation formula can be expressed as

$$PP = \frac{n}{n-1}\lambda_{\max}. \tag{5}$$

After the weight of each index is obtained, the consistency test is carried out, expressed by *b*, and the formula is

$$b_i = \sqrt{\sum_{j=1}^{m} b_{ij}a_j}. \tag{6}$$

The above formula shows that the number of conformance tests needs to be carried out many times before it can be finally determined. Therefore, in the actual calculation, the results of three-dimensional simulation calculation may be inconsistent with the actual situation. The image output after the simulation of the ecological landscape data of the town combined with the improved HQR three-dimensional planning and governance model is shown in Figure 3.

Combined with the method in Figure 2 and the image information in Figure 3, it is not difficult to see that the priority of HQR model for different types of small town ecological landscape planning and governance strategies is different and presents different change laws (the positions of extreme values are inconsistent). This is because the process of small town ecological landscape planning and governance will be affected by subjective factors, which is very prone to objective mistakes. The consistency test cannot be passed, and the physical components of different types of Internet of things technologies are very complex. Therefore, through HQR simulation verification, it is found that this method can promote the interpretation of physical parameters of different types of small town ecological landscape and further improve the simulation quality in the process of small town ecological landscape planning and governance. Therefore, it can not objectively reflect the significance of physical parameters of different Internet of things technologies, and it needs to be evaluated by three-dimensional fuzzy evaluation method. Three-dimensional fuzzy theory has been paid attention to in recent years and has been applied in many fields. This theory is based on set theory. Assuming that the factor domain is represented by *U*, the evaluation level domain is represented by *V*, the membership degree of factor *x* to *v* is represented by *T*, and the fuzzy weight vector is expressed as

$$T = (x_1, x_2, \ldots, x_n), \tag{7}$$

where *x* is the factor value of town landscape planning.

3.4. Simulation Design of Small Town Ecological Landscape System Based on the HQR Model of Internet of Things Technology. In the simulation design of the town ecological landscape system, in order to further study the application of different types of Internet of things technologies in the town ecological landscape planning and governance, this paper first summarizes the disadvantages in the process of traditional town ecological landscape planning and governance and combines the characteristics of different types of Internet of things technologies on the basis of HQR three-dimensional model. Then, the physical parameters of ecological landscape in different towns are analyzed through the output and data input of HQR three-dimensional planning and governance model. On the other hand, in the quality evaluation of different types of small town ecological landscape, the grey numbers used are composed of real numbers, and the weights are also different. The simulation analysis results of different types of small town ecological landscape types before optimization are shown in Figure 4, and the optimized results are shown in Figure 5.

As can be seen from Figures 4 and 5, the corresponding change trend before and after the improvement has not changed significantly, but significant changes have taken place in terms of values. This is because, in the small town ecological landscape simulation design system, the original data are transformed into initial values first, and then the reference data column is formulated. Calculate the relationship or correlation degree of different data columns, and then sort the correlation degree.

In the evaluation of the ecological landscape system simulation design of this small town, the physical data of different types of green town ecological landscape have different meanings, so equivalent analysis cannot be carried out. Calculate the absolute difference between each factor and the main factor at the same observation point, and the formula is expressed as

$$\sqrt{\Delta_t(i,0)} = \left\{ \frac{x_t^{(l)}(i) - x_t^{(l)}(0)}{\sqrt{x_t^{(l)}(i) + x_t^{(l)}(0)}} \right\}. \tag{8}$$

Finally, the correlation between subfactors and main factors of various types of small town ecological landscape is calculated. In the comprehensive evaluation of simulation results, the ranking problem will be involved in most cases. Each evaluation object needs to be ranked first, so grey comprehensive evaluation is also required.

$$R = \begin{bmatrix} \zeta_1(1), \zeta_1(2), \ldots, \zeta_1(n) \\ \zeta_2(1), \zeta_2(2), \ldots, \zeta_2(n) \\ \ldots \\ \zeta_n(1), \zeta_n(2), \ldots, \zeta_n(n) \end{bmatrix}. \tag{9}$$

Sort by *R* value. The evaluation system is established, and then the HQR three-dimensional programming model proposed in this paper is used to determine the weight of each index, improve the accuracy of index weight, and ensure that the weight distribution is more real. The corresponding HQR three-dimensional planning and governance model in this stage analyzes the differentiated characteristics of the ecological landscape of different towns.

After completing the above steps, it is necessary to establish the evaluation matrix, expressed in *O*, expressed as

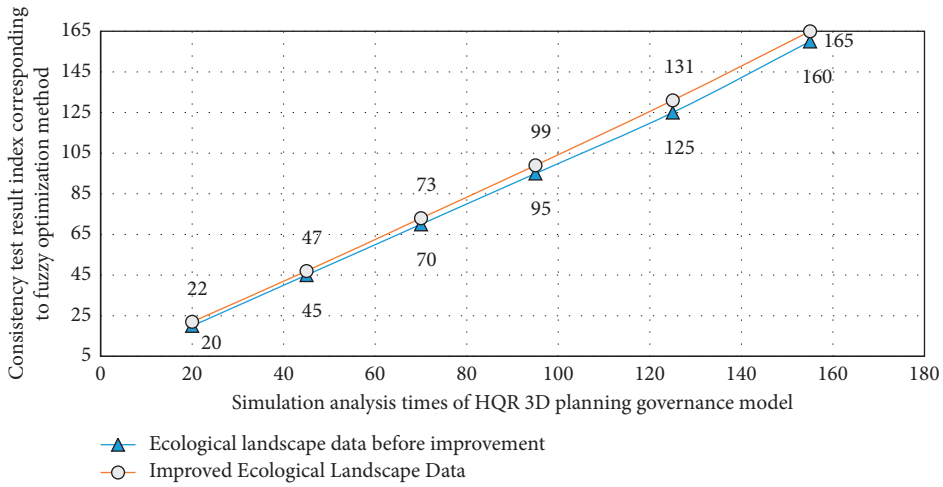

Figure 3: Image of the analysis results of the HQR three-dimensional planning and governance model on the small town ecological landscape data.

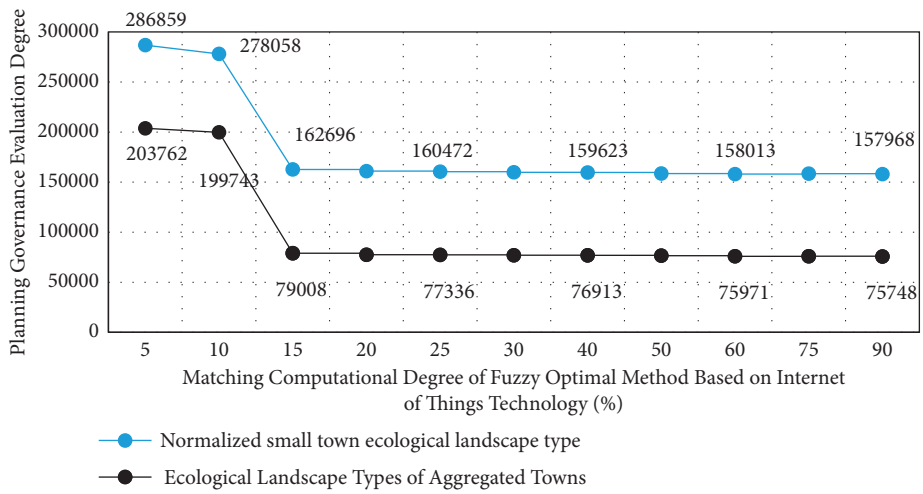

Figure 4: The results of simulation analysis of different types of small town ecological landscape types before optimization.

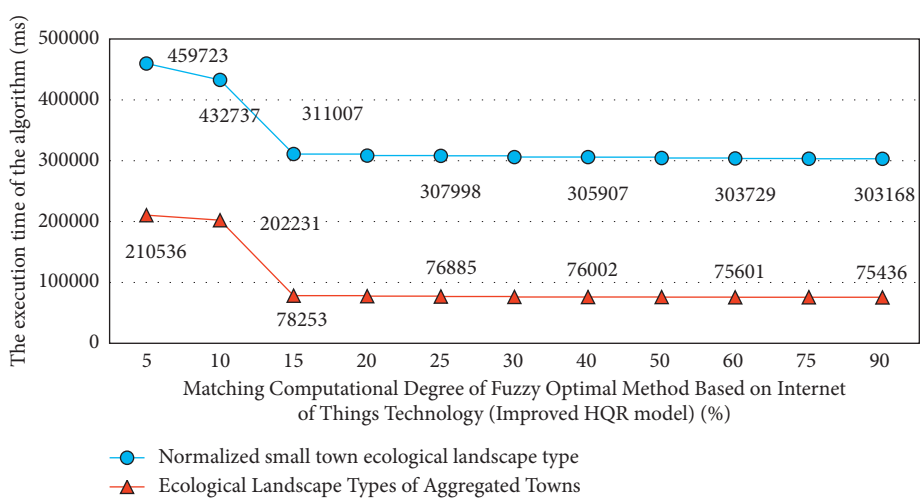

Figure 5: The results of simulation analysis of different types of small town ecological landscape types after optimization.

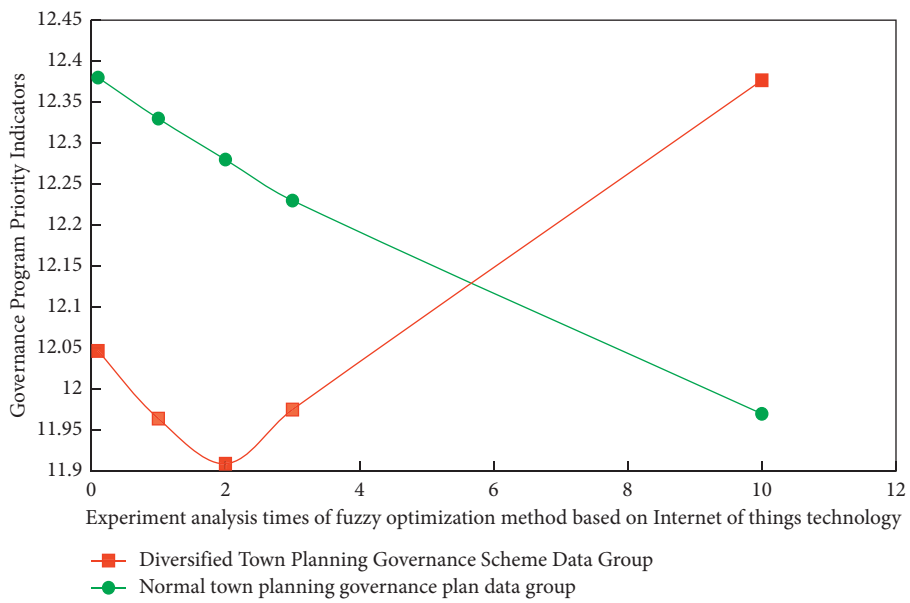

Figure 6: Preliminary experimental results analysis images.

$$O = \left(\frac{\sqrt{r_{i,j}}}{\sqrt{r_{i,j-1}}} \right)_{n \times m}. \tag{10}$$

Combined with the previous design, the comprehensive town ecological landscape simulation design evaluation system is established, and then the comprehensive evaluation is carried out. In the application of fuzzy optimization algorithm based on Internet of things technology, a hierarchical fuzzy evaluation vector C_1^s is calculated, and its formula is

$$C_1^s = \sqrt{W_{C_1} R_{C_1}^s}, \tag{11}$$

where $s = 1, 2, \ldots, p$, and then calculate the secondary evaluation matrix:

$$C_A^s = \left[\frac{B_1^s, B_2^s, B_3^s, B_4^s}{\sqrt{B_1^s + B_2^s}} \right]. \tag{12}$$

In this, $s = 1, 2, \ldots, p$

Then calculate the absolute difference between the subfactors and the main factors of the ecological landscape of different types of green towns at the same time to obtain its correlation error. Calculate the grey correlation coefficient according to the correlation degree between various factors. The calculation formula is

$$\begin{aligned} \zeta_s &= \frac{1}{5} \sum_{j=1}^{s} B_{sj}, \\ P &= (P_1, \ldots, P_m). \\ Z_i &= (Z_{i1}, \ldots, Z_{im}), \end{aligned} \tag{13}$$

P and Z are different types of town ecological landscape planning and management schemes.

4. Result Analysis and Discussion

4.1. Experimental Design Process of Environmental Protection Building Materials in Town Ecological Landscape Planning and Management. When studying the application of Internet of things technology in town ecological landscape planning and governance, relevant differentiation experiments are designed according to different Internet of things technical parameters and planning and governance strategies. Before the experiment, it is assumed that the primary index weight coefficient has been determined, which is expressed by a_1 and greater than 0. Each secondary indicator will also have its own weight coefficient, represented by a_j, and the weight vector is expressed as A_1, which is also greater than zero. The data group of diversified urban planning government plan is set as the experimental group, and the data group of normal urban planning governance plan is set as the control group. In this process, the corresponding experimental results of the fuzzy optimization method based on Internet of things technology for two different town ecological landscape planning and governance schemes are shown in Figure 6.

4.2. Experimental Results and Analysis. Figure 7 is the error analysis process of the experimental results of different types of Internet of things technology in the small town ecological landscape planning and governance simulation model. The relevant data of different types of small town ecological landscape experiments are processed by MATLAB software. Because these index data are very large, in order to facilitate calculation, in the analysis of this study, two different town ecological landscape planning and management schemes are processed in blocks.

From the results of Figures 6 and 7, we can know the comprehensive application of fuzzy optimization methods corresponding to different types of Internet of things

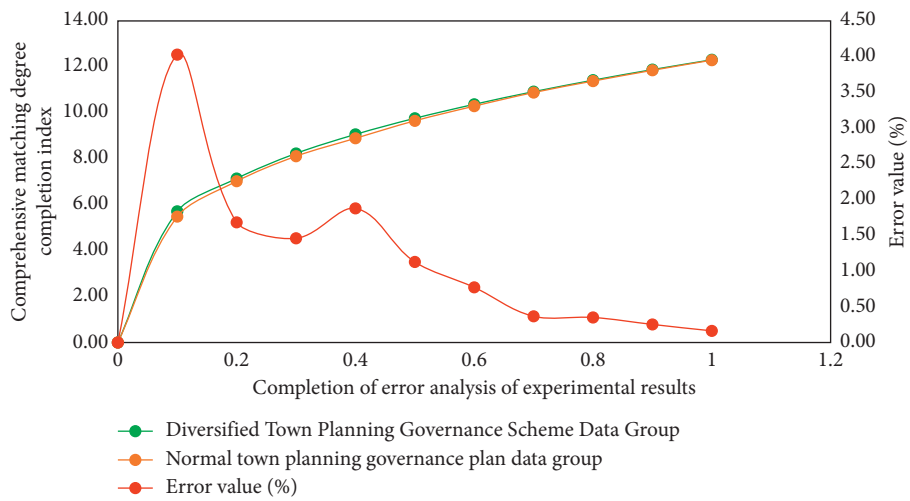

Figure 7: Error analysis of experimental results of simulation model for small town ecological landscape planning and governance.

technologies in the planning and management of ecological landscape of small towns. From the experimental results, it can be seen that similar methods are also used to calculate the evaluation vectors of other indicators, and the difference of grey evaluation matrix is very obvious, and the error can be controlled within 5%. This is because the difference of correlation degree data indicators corresponding to fuzzy optimization methods corresponding to different Internet of things technologies is very obvious. Therefore, the absolute values in the process of ecological landscape planning and governance of different types of small towns are also different. Therefore, the experimental results show that the application effect of different types of Internet of things technologies in ecological landscape planning and governance of small towns is targeted and showed a strong regularity.

5. Conclusion

The current town ecological landscape planning and governance model has the problems of large proportion of subjective factors and low intelligence. Based on this, this paper studies the application of fuzzy optimization method based on Internet of things technology in town ecological landscape planning and management. Firstly, a small town ecological landscape evaluation model based on fuzzy optimization algorithm is proposed. Combined with multivariate matrix transformation function, the authenticity data of ecological landscape are simulated. The original analysis of different types of small town ecological landscape is realized by selecting the multivariate extremum of autocorrelation function curve in the process of planning and governance. Secondly, the fuzzy evaluation method is adopted and improved in the simulation evaluation link. At the same time, the improved three-dimensional original planning and governance model is used to comprehensively analyze the simulation results of three-dimensional landscape planning and governance, and the landscape planning and governance model can not only realize the differential comparison of three-dimensional landscapes of different towns in the design, but also make full use of the location differences between the ecological landscapes of each town to analyze the application of different types of Internet of things technology, so as to realize the closed-loop evaluation of the planning and governance quality of the overall ecological landscape of the town. Finally, by designing fuzzy simulation experiments, the application effects of different Internet of things technologies in town ecological landscape planning and governance are analyzed. However, this study only considers the application of Internet of things technology in town ecological landscape planning and governance and does not consider the application of other materials, so more in-depth research can be carried out.

Data Availability

The data used to support the findings of this study are available from the corresponding author upon request.

Conflicts of Interest

The authors declare that they have no conflicts of interest.

Acknowledgments

This work was supported by "Natural Science Foundation of Shandong Province, China (Grant no. ZR2013EEL021)," "Study on the Complex Cycle of Urban Block Space Form in Coastal Cities of Jiaodong Based on Winter Microclimate Optimization."

References

[1] J. Gong, E. Cao, Y. Xie, C. Xu, H. Li, and L. Yan, "Integrating ecosystem services and landscape ecological risk into adaptive management: insights from a western mountain-basin area, China," *Journal of Environmental Management*, vol. 281, no. 555, Article ID 111817, 2021.

[2] N. C. Armansin, A. J. Stow, M. Cantor et al., "Social barriers in ecological landscapes: the social resistance hypothesis," *Trends in Ecology & Evolution*, vol. 35, no. 2, pp. 137–148, 2020.

[3] J. Xu, H. Zhao, P. Yin, L. Wu, and G. Li, "Landscape ecological quality assessment and its dynamic change in coal mining area: a case study of Peixian," *Environmental Earth Sciences*, vol. 78, no. 24, p. 708, 2019.

[4] A. C. Rai, "Energy performance of phase change materials integrated into brick masonry walls for cooling load management in residential buildings," *Building and Environment*, vol. 199, Article ID 107930, 2021.

[5] A. M. Rashad, M. H. Khalil, and M. H. El-Nashar, "Insulation efficiency of alkali-activated lightweight mortars containing different ratios of binder/expanded perlite fine aggregate," *Innovative Infrastructure Solutions*, vol. 6, no. 3, pp. 156–214, 2021.

[6] H. Coelho-Júnior, B. G. Silva, C. Labre, P. R. Loreto, and L. R. Sommer, "Room-temperature synthesis of earth-abundant semiconductor ZnSiN2 on amorphous carbon," *Scientific Reports*, vol. 11, no. 1, pp. 1–6, 2021.

[7] L. Jiang, Y. Xiong, Y. Wang, and T. Luo, "Soundscape Effects on Visiting Experience in City Park: a Case Study in Fuzhou, China," *Urban Forestry & Urban Greening*, vol. 31, pp. 38–47, 2018.

[8] Q. Du, C. Wu, X. Ye, F. Ren, and Y Lin, "Evaluating the effects of landscape on housing prices in urban China," *Tijdschrift voor Economische en Sociale Geografie*, vol. 109, no. 4, pp. 525–541, 2018.

[9] E. Dall'Ara, E. Maino, G. Gatta, D. Torreggiani, and P. Tassinari, "Green Mobility Infrastructures. A landscape approach for roundabouts' gardens applied to an Italian case study," *Urban Forestry & Urban Greening*, vol. 37, pp. 109–125, 2018.

[10] J. Persson, T. Wang, and J. Hagberg, "Organophosphate flame retardants and plasticizers in indoor dust, air and window wipes in newly built low-energy preschools," *The Science of the Total Environment*, vol. 628-629, pp. 159–168, 2018.

[11] A. Gasparotto, G. Carraro, C. Maccato et al., "WO3-decorated ZnO nanostructures for light-activated applications," *CrystEngComm*, vol. 20, no. 9, pp. 1282–1290, 2018.

[12] L. Weerasundara, D. N. Magana-Arachchi, A. M. Ziyath, A. Goonetilleke, and M. Vithanage, "Health risk assessment of heavy metals in atmospheric deposition in a congested city environment in a developing country: kandy City, Sri Lanka," *Journal of Environmental Management*, vol. 220, pp. 198–206, 2018.

[13] A. Hampe, R. Alfaro-Sánchez, and I. Martín-Forés, "Establishment of second-growth forests in human landscapes: ecological mechanisms and genetic consequences," *Annals of Forest Science*, vol. 77, no. 3, pp. 87–95, 2020.

[14] Y. Wu, L. Huang, C. Zhao, M. Chen, and W. Ouyang, "Integrating hydrological, landscape ecological, and economic assessment during hydropower exploitation in the upper Yangtze River," *The Science of the Total Environment*, vol. 767, Article ID 145496, 2021.

[15] P. Jiang, M. Li, and J. Lv, "The causes of farmland landscape structural changes in different geographical environments," *The Science of the Total Environment*, vol. 685, no. 1, pp. 667–680, 2019.

[16] X. Dai and D. Zhuang, "Geographic planning and design of marine island ecological landscape based on genetic algorithm," *Journal of Coastal Research*, vol. 93, no. 1, p. 524, 2019.

[17] F. Jahanishakib, A. SalmanmahinY, S. H. Mirkarimi, and F. Poodat, "Hydrological connectivity assessment of landscape ecological network to mitigate development impacts," *Journal of Environmental Management*, vol. 296, no. 80, Article ID 113169, 2021.

[18] G. Zegers, E. Arellano, and L. Östlund, "Using forest historical information to target landscape ecological restoration in Southwestern Patagonia," *Ambio*, vol. 49, no. 4, pp. 986–999, 2020.

[19] L. F. Camacho, G. Barragán, and S. Espinosa, "Local ecological knowledge reveals combined landscape effects of light pollution, habitat loss, and fragmentation on insect populations," *Biological Conservation*, vol. 262, no. 10, Article ID 109311, 2021.

[20] Y. M. Rosas, P. L. Peri, M. V. Lencinas, and G. Martinez Pastur, "Potential biodiversity map of understory plants for Nothofagus forests in Southern Patagonia: analyses of landscape, ecological niche and conservation values," *The Science of the Total Environment*, vol. 682, no. 10, pp. 301–309, 2019.

[21] S. M. Jafari and M. R. Nikoo, "Developing a fuzzy optimization model for groundwater risk assessment based on improved DRASTIC method," *Environmental Earth Sciences*, vol. 78, no. 4, p. 109, 2019.

[22] S. I. Han, "Fuzzy supertwisting dynamic surface control for MIMO strict-feedback nonlinear dynamic systems with supertwisting nonlinear disturbance observer and a new partial tracking error constraint," *IEEE Transactions on Fuzzy Systems*, vol. 27, no. 11, pp. 2101–2114, 2019.

[23] R. Ghanbari, K. Ghorbani-Moghadam, and N. Mahdavi-Amiri, "A variable neighborhood search algorithm for solving fuzzy number linear programming problems using modified kerre's method," *IEEE Transactions on Fuzzy Systems*, vol. 27, no. 6, pp. 1286–1294, 2019.

[24] Z. Shi, X. Sun, Y. Cai, and Z. Yang, "Robust design optimization of a five-phase PM hub motor for fault-tolerant operation based on taguchi method," *IEEE Transactions on Energy Conversion*, vol. 35, no. 4, pp. 2036–2044, 2020.

[25] F. Yin and Y. Zhao, "Optimizing vehicle routing via Stackelberg game framework and distributionally robust equilibrium optimization method," *Information Sciences*, vol. 557, no. 7, pp. 84–107, 2021.

[26] X. Liu, "Feature recognition of English based on deep belief neural network and big data analysis," *Computational Intelligence and Neuroscience*, vol. 2021, Article ID 5609885, 10 pages, 2021.

Hindawi
Computational Intelligence and Neuroscience
Volume 2022, Article ID 4572432, 9 pages
https://doi.org/10.1155/2022/4572432

Research Article

Exploration on the Application Path of College English MOOCS Teaching under the Background of Internet of Things

Daoping Xu

School of International Business, Qingdao Huanghai University, Qingdao, Shandong 266427, China

Correspondence should be addressed to Daoping Xu; xudp@qdhhc.edu.cn

Received 9 February 2022; Revised 6 April 2022; Accepted 18 April 2022; Published 21 May 2022

Academic Editor: Guobin Chen

While the development of information and communication technology has brought great changes to social industrial structure and economic development, it has also reshaped people's cognition and thinking modes to a great extent and has paid attention to the field of education under the guidance of technology. The reform of education is taking place. According to the background of the Internet of things, the teaching quality evaluation index is reconstructed with the help of principal component analysis, support vector machine, and fuzzy algorithms, and the application performance and practical results of the improved teaching path are analyzed. The results show that the evaluation accuracy of the improved hybrid algorithm for teaching quality reaches more than 90%, and its evaluation time is far less than that of the SVM algorithm (10.23 s), and it has a good application effect on the evaluation of teaching quality. The increase of students' satisfaction with the improved teaching quality has reached 5.8%, and their professional skills have improved by 6–25 points. After expert evaluation, it is found that the maximum satisfaction frequency of teaching content and teaching effect can reach 96.7% and 91.3%, respectively. Reconstructing the index system of the English path under the background of the Internet of things can better grasp students' learning needs and integrate multiple methods to provide new research ideas for follow-up English teaching.

1. Introduction

Information-based teaching resources and teaching achievements are widely used in education and teaching. As a basic course of higher education teaching, English should always adhere to the principle of innovative teaching in teaching. Since 2018, education informatization 2.0, published by the ministry of education, proposed that innovative research on intelligent education should be actively carried out by using emerging technologies, intelligent devices, and networks, integrate information technology into College English teaching and explore distance teaching from a new perspective. The teaching method of massive open online courses (MOOC/MOOCS) has greatly improved the "individualization" and "personalization" in the teaching process. The innovative teaching method has enriched the teaching activities and mobilized the active participation of students. However, the teaching activity mainly depends on online resources, and the binding force on students is mainly through the compulsory completion of course homework. It cannot be shown that it will make students complete their homework in order to complete the course, which will have a certain impact on students' learning consciousness and the self-binding force of the course. This research reconstructs the teaching path by integrating a variety of algorithms to explore its application performance, which can effectively ensure the completion of its teaching objectives and the improvement of students' professional quality.

By introducing principal component analysis (PCA) and integrating it with a support vector machine, the problem of teaching quality is transformed into a classification problem. The principal component analysis is to extract a set of nonlinear main variable relationships from possibly related data through orthogonal change; that is, to realize data dimensionality reduction for factor analysis. At the same time, the network analysis method is used to reconstruct the indicators affecting the teaching path, and the expert evaluation method is used to score the satisfaction of the index

system, so as to make the improvement of the English MOOCS teaching path more convincing and provide guarantee for the follow-up students' learning quality.

The innovation of this research lies in the combination of principal component analysis and support vector machine to construct the teaching quality index system and adding fuzzy algorithm and expert evaluation to quantitatively reconstruct and analyze the indicators, so as to make the establishment of teaching quality and path more objective and comprehensive, more in line with the teaching concept, and jump out of the subjectivity of the traditional single evaluation method [1].

This paper mainly studies the innovation of the College English MOOCS teaching path under the Internet of things from four aspects. The second part comprehensively discusses some research progress and methods on MOOCS teaching and English teaching methods [2]. The third part introduces principal component analysis and support vector machine, establishes the index system model, optimizes and evaluates the index system with a fuzzy algorithm and expert review, and tests the application performance of the model [3]. The fourth part evaluates the application performance and practical effect of the model, and arranges and analyzes the results [4]. The last part is the summary of the whole article [5].

2. Related Works

Konstantinidis et al. pointed out the role of Internet 0 of things technology in education, summarized the educational concept under the Internet of things, and discussed its future development prospect [6]. In order to better ensure the comfort of learning, Marques et al. put forward an Internet of things solution for noncontact measurement and real-time temperature monitoring, which makes an important contribution to the infrared temperature monitoring system of the Internet of things [7]. Starting from the actual situation of College English teaching, Zhang et al. discuss its countermeasures from the perspective of cultural differences, so as to provide a valuable reference for English teaching [8, 9]. Li et al. have determined the characteristics, platforms, course materials, and methods to promote interaction adopted by MOOC through the teaching situation and relevant cases of previous campus courses, and provided methods for students to provide flexible and personalized campus course learning experiences [10]. Holme et al. analyze whether these resources meet the actual needs of English teachers by investigating and comparing teachers' use of information technology [11]. Hong et al. have changed the difficulties of traditional teaching methods in students' learning of microbiology and adopted a variety of modern multimedia teaching methods to ensure the teaching quality [12] and proposed the collaborative role of computer support and encouraged teachers to actively integrate MOOCs into the improvement of the teaching path [13].

Gao et al. pointed out that the cramming teaching mode of traditional English makes students lack enthusiasm and initiative and advocated the introduction of the MOOC teaching mode to teach students' reading ability and expression ability [14]. Pan et al. study the innovation of MOOC curriculum development and teaching methods, and their opinions on teaching methods and theoretical models help to develop soft skills in MOOC [15]. Hao et al. found that curriculum design is of great significance for MOOC teaching platforms through questionnaires and software simulations, and encouraged the use of information technology tools in the context of distance education and online learning [16]. Dehua et al. proposed that the way of teaching and learning should be handled according to its actual situation [17]. Hilles et al. established a mathematical model of oral English teaching with metacognition and found that the model has a good operational effect in its follow-up simulation test [18]. Corpuz et al. introduce the feasibility of designing a text classification model using two popular and robust algorithms: support vector machine (SVM) and long-term and short-term memory (LSTM), which are used to automatically classify complaints, suggestions, feedback, and praise. The degree of preference between the two algorithms can be attributed to the available data sets and the skills of optimizing these algorithms through feature engineering technology and applying them to practical text classification applications [13]. Hong et al. provided customer evaluation data by analyzing the correlation between airline customer satisfaction based on customer evaluation data. [19]. Mikalef et al. and Wilson introduced fuzzy mathematics and machine learning algorithm to evaluate the application of education and teaching quality model through the functional relationship between teaching quality evaluation index and teaching effect and found that machine learning algorithm has good reliability in evaluation [20, 21]. The pan teams proposed algorithm extraction and emergency division based on English feature rules to predict the control reality established by the algorithm, which has a good application effect [22].

To sum up, it can be found that most researchers begin to pay attention to the improvement of teaching path and teaching quality, integrate computer, and machine algorithms into MOOCS teaching methods, and actively introduce metacognition, support vector machine, and neural network model analysis, but rarely integrate and explore a variety of algorithms [23]. Therefore, by proposing the teaching path exploration integrating multiple algorithms, students can effectively learn with the help of information technology tools and improve their professional quality [24].

3. Research on the Application Path and Model Construction of College English MOOCS Teaching under the Background of Internet of Things

3.1. Reform and Exploration of English Teaching Path under the Background of the Internet of Things. Smart classroom integrates online and offline courses, combines mixed teaching and flipped classroom, and realizes the full monitoring of students' learning process with the help of Internet technology. Build a college English smart classroom teaching system, design the close connection of various teaching

links, realize a series of smart teaching activities such as intelligent resource push and diversified teaching rating, and truly realize the comprehensive personality of College English classroom teaching. Starting from two subjects, students and teachers, this study uses the principal component analysis method to reconstruct the original teaching quality index. Select some data to form training samples, and analyze and calculate the application performance impact of the innovation path according to the weight ratio affecting teaching quality. The construction of its teaching path and mechanism is shown in Figure 1.

MOOC, as a new teaching mode with the development of information technology, is different from the traditional teaching mode in many aspects. The traditional teaching model includes stimulating students' learning motivation, reviewing old knowledge, teaching new knowledge, consolidating exercises and homework. Although traditional teaching also emphasizes the systematicness of knowledge and the two-way nature of teaching, teachers occupy an absolute leading position in teaching. Students only need to cooperate with teachers' teaching activities on the basis of maintaining their initiative. Under MOOC, learners need to choose learning contents, methods, and progress according to their own needs and future development needs and respect the individual differences of students' development. Based on the mastery learning theory, it is believed that learners do not have great differences in learning ability and learning motivation. As long as they study carefully, they can master the learning content.

MOOCS curriculum model re-establishes students' learning methods with the help of online learning resources, breaks through the traditional face-to-face teaching and online teaching methods and has become a more popular teaching method with the advantages of diversified resources and tools, wide audience, and high independent participation. At the same time, the MOOCS course is mandatory to complete a homework assignment, which can ensure the integrity of students' learning process. The main advantage of this model is to obtain higher income with less investment. This teaching method integrates online learning and resource integration and sharing, making teaching resources available and giving learners greater autonomy and creativity. Hierarchical learning progress and rich means of knowledge acquisition can achieve better learning results.

3.2. Construction of English Teaching Model Indicators Based on Principal Component Analysis. The MOOCS teaching mode lacks an overall tracking and supervision mechanism in learning situation analysis, teaching design, and teaching implementation. According to the actual situation of students completing their homework on time, it is difficult to evaluate the overall state of students. The lack of diversity of teaching activities and the process of teaching implementation make there few interaction channels between teachers and students. The index system of teaching quality and teaching path is established by introducing principal component analysis; that is, the weight of each principal component is assigned, which not only reduces the workload

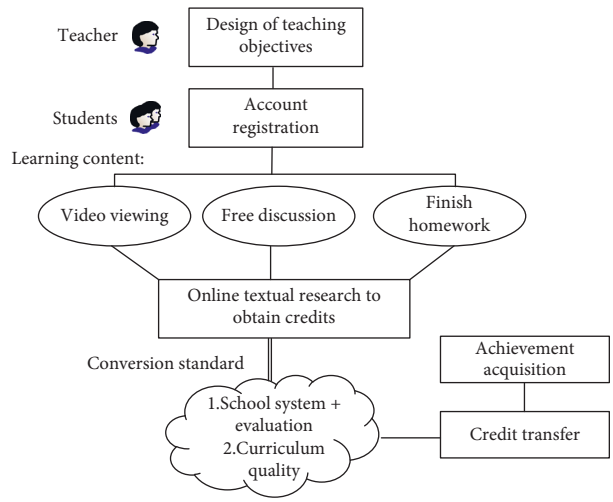

Figure 1: Available MOOCS teaching mode diagram.

but also reduces the interference of human factors in the evaluation process. Its mathematical expression is as follows:

$$xij^{*} = \frac{(xij - \overline{x}j)}{\sqrt{\sigma_{ii}}}, \quad i = 1, 2, \ldots, n;\ j = 1, 2, \ldots, p. \tag{1}$$

Equation (1) is the standardized calculation formula, where xij is the original data of the j index of the i sample, σii is the average value of the j index original data of all samples, and σii is the variance of the j index original data of all samples, so as to obtain the standardized matrix, and calculate the correlation coefficient and variance contribution rate of the matrix to obtain the following equation:

$$\begin{cases} R = [rij]pxp = \dfrac{\left(Z^{T}Z\right)}{n-1}, \\ \dfrac{\sum_{i=1}^{m} \lambda i}{\sum_{i=1}^{p} \lambda i} \geq 85\%. \end{cases} \tag{2}$$

In equation (2), R is the correlation coefficient matrix, where r_{ij} is the correlation coefficient of the original variables x_i and x_j, and Z is the standardization result of the original data matrix. The index system is reconstructed by judging the contribution rate of variance. If the contribution rate is greater than 85%, it shows that the index plays an important role in the evaluation of teaching quality, in which λ_i is the contribution rate of i main component and m is the number of main components. The evaluation destination of teaching quality is the classification problem. The establishment of support vector machine classifier can better improve the evaluation system of the index system, and its calculation formula can be expressed as the following formula:

$$\begin{cases} y1 = \omega^{T}\phi(x) + b, \\ y2 = \min J(\omega, \xi) = \dfrac{1}{2}\|\omega\|^{2} + C\sum_{i=1}^{n} \xi i. \end{cases} \tag{3}$$

Equation (3) is the hyperplane formula established by the support vector machine, where x_i is the evaluation index of English teaching quality, y_i is the grade of English teaching quality, ω is the normal vector of the hyperplane, b is the offset vector, and C is the penalty parameter, that is, the penalty degree of right and wrong samples. At the same time, when dealing with the classification problem of large samples, the classification problem of the support vector machine can be transformed into its dual problem by introducing the langrange multiplier, so as to speed up the running speed. The calculation formula of the hyperplane classification function is shown in the following formula:

$$f(x) = \operatorname{sign}\left(\sum_{i=1}^{l} \alpha i y i k(xi \cdot x)\right) + b. \tag{4}$$

In equation (4), sign represents the symbolic function, α_i represents the langrange multiplier, and $K(x_i, x)$ represents the kernel function, that is, the point product. For the effect evaluation of teaching quality, it is difficult to be accurately analyzed quantitatively. The usual knowledge test is often used to establish the index system. Therefore, it is necessary to introduce the fuzzy mathematics method to convert the values to reduce the subjective fuzziness of experts in the evaluation. The calculation formula of triangular fuzzy numbers is shown in the following formula:

$$\mu_A(x) = \begin{cases} \dfrac{x-m}{n-m}, & m < x < n; \\ \dfrac{x-r}{n-r}, & n < x < r; \\ 0, & \text{other}. \end{cases} \tag{5}$$

$\mu_A(x)$ is the expression of the membership function, where U is the final domain in the function, which is any fuzzy subset, $\mu_{(x)} \in [0, 1]$ is the membership degree of the subset to the final domain, μ is the membership function, and the triangular fuzzy number A is (m, n, r), $\mu_A(x)$ ranges between $[0, 1]$, m, n, r are all real numbers, which are the upper limit, most likely value and lower limit r of A, respectively. Arbitrary triangular fuzzy numbers $A_1(m_1, n_1, r_1)$ and $A_2(m_2, n_2, r_2)$ need to satisfy in the following formula:

$$\begin{cases} A_1 + A_2 = (m_1 + m_2, n_1 + n_2, r_1 + r_2), \\ A_1 - A_2 = (m_1 - m_2, n_1 - n_2, r_1 - r_2), \\ \lambda A_1 = (\lambda m_1, \lambda n_1, \lambda r_1), \\ A_1 \otimes A_2 = (m_1 m_2, n_1 n_2, r_1 r_2). \end{cases} \tag{6}$$

In order to reduce the subjective error of experts in the evaluation, it is necessary to carry out a triangular fuzzy transformation on the expert evaluation results to obtain the specific values that can be calculated, and finally, explain the fuzzy in detail. The application of the center of gravity method, which is less affected by the preference of decision-makers, can make the calculation relatively simple, and its expression formula is shown in the following formula:

$$f = \frac{(r-m) + (n-m)}{3} + m. \tag{7}$$

In equation (7), f represents the clear value obtained by the center of gravity method.

3.3. Establishment of Teaching Innovation Mode under the Integration Path Model. In the current College English teaching process, teachers mainly formulate teaching materials in the selection criteria of teaching materials and rarely involve the recommendation and guidance of expanded literature. In this teaching process, due to inevitable cultural differences and language habits, it is difficult for students to learn basic knowledge and improve their ability, and there are many standards for the evaluation of teaching quality. Some evaluation indicators deviate from student-centered teaching principle and the step-by-step teaching process. Through the introduction of the analytical network process (ANP), the influencing factors are analyzed, and the gray relationship application analysis is carried out on the scores of students after the change of innovation path. The structural diagram of teaching path innovation is shown in Figure 2.

The ANP method is an analysis method based on the analytic hierarchy process. It is applicable to the structural system under the interaction of elements. It has good flexibility in the process of practical application. Through the construction of the weighting matrix, the weighting matrix is obtained after standardizing the device, and the weight value of each influencing factor in the matrix is calculated. Set $T_d = [t_{ij}^D]_{m\times m}, T_c = [t_{ij}]_{n\times n}$ as the primary and secondary index matrix, the standardization process is shown in the following equation:

$$T_c^{11} = \begin{matrix} \cdots \\ c_{11} \\ \cdots \\ c_{1i} \\ \cdots \\ c_{1m_1} \end{matrix} \begin{bmatrix} c_{11} & c_{1j} & \cdots & \cdots & c_{1m_2} \\ t_{11}^{11} & \cdots & t_{1j}^{11} & \cdots & t_{1m_2}^{11} \\ \cdots & \cdots & \cdots & \cdots & \cdots \\ t_{i1}^{11} & \cdots & t_{ij}^{11} & \cdots & t_{im_2}^{11} \\ \cdots & \cdots & \cdots & \cdots & \cdots \\ t_{m_1 1}^{11} & \cdots & t_{m_1 j}^{11} & \cdots & t_{m_1 m_2}^{11} \end{bmatrix}. \tag{8}$$

Equation (8) is the comprehensive influence matrix T_c^{α} taking the submatrix T_c^{11} as an example after standardization. The sum of the elements in row i in T_c^{11} is d_i^{11}. In order to obtain the normalized submatrix $T_c^{\alpha 11}$, divide each element of row i in T_c^{11} by the row sum of row i to obtain the following equation:

$$T_c^{\alpha 11} = \begin{bmatrix} \dfrac{t_{11}^{11}}{d_1^{11}} & \cdots & \dfrac{t_{1j}^{11}}{d_1^{11}} & \cdots & \dfrac{t_{1m_2}^{11}}{d_1^{11}} \\ \cdots & \cdots & \cdots & & \\ \dfrac{t_{i1}^{11}}{d_i^{12}} & \cdots & \dfrac{t_{ij}^{11}}{d_i^{12}} & \cdots & \dfrac{t_{im_2}^{11}}{d_i^{12}} \\ \cdots & \cdots & \cdots & & \\ \dfrac{t_{m_1 1}^{11}}{d_{m_1}^{11}} & \cdots & \dfrac{t_{m_1 j}^{11}}{d_{m_1}^{11}} & \cdots & \dfrac{t_{m_1 m_2}^{11}}{d_{m_1}^{11}} \end{bmatrix}$$

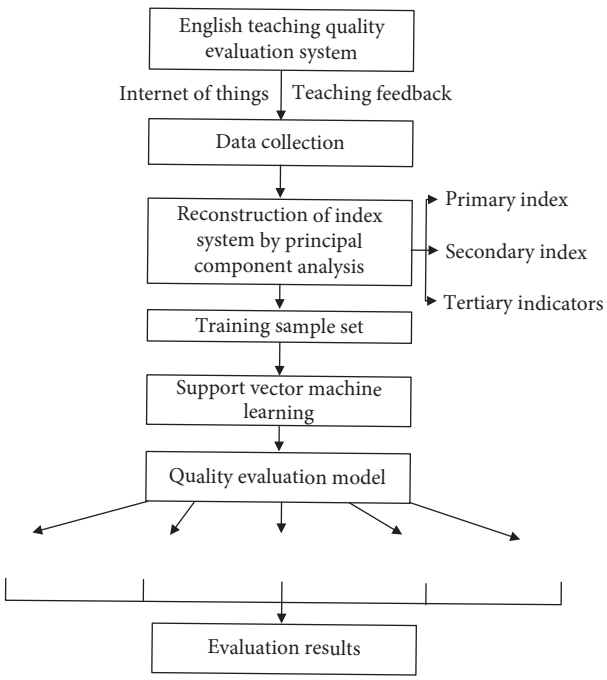

Figure 2: Structural diagram of teaching path innovation.

$$= \begin{bmatrix} t_{11}^{\alpha 11} & \dots & t_{1j}^{\alpha 11} & \dots & t_{1m_2}^{\alpha 11} \\ \dots & \dots & \dots & & \\ t_{i1}^{\alpha 11} & \dots & t_{ij}^{\alpha 11} & \dots & t_{im_2}^{\alpha 11} \\ \dots & \dots & \dots & & \\ t_{m_1 1}^{\alpha 11} & \dots & t_{m_1 j}^{\alpha 11} & \dots & t_{m_1 m_2}^{\alpha 11} \end{bmatrix}. \tag{9}$$

Then transpose the standardized sub matrix and put it into the corresponding position of the matrix to construct the unweighted supermatrix W, set $W_{ij} = (T_c^{\alpha ji})'$, $i = 1, 2, \dots, n$, $j = 1, 2, \dots, n$, and standardize it. After calculating the index of index weight, the weighted super matrix W_w is obtained, as shown in the following equation:

$$W_w = T_d^{\alpha} \times W = \begin{bmatrix} t_{11}^{\alpha\, d} \times W_{11} & \dots & t_{i1}^{\alpha\, d} \times W_{1i} & \dots & t_{1n}^{\alpha\, d} \times W_{1n} \\ \dots & \dots & \dots & & \\ t_{i1}^{\alpha\, d} \times W_{i1} & \dots & t_{ii}^{\alpha\, d} \times W_{ii} & \dots & t_{in}^{\alpha\, d} \times W_{in} \\ \dots & \dots & \dots & & \\ t_{n1}^{\alpha\, d} \times W_{in} & \dots & t_{in}^{\alpha\, d} \times W_{in} & \dots & t_{in}^{\alpha\, d} \times W_{in} \end{bmatrix}. \tag{10}$$

Finally, the limit supermatrix is calculated to obtain the authority until the calculation process converges. If the elements of each row of W_w are equal, it indicates that the matrix is in a stable state, and the obtained matrix is the limit supermatrix W^*. Further determine the weight value of the index, as shown in the following equation:

$$W^* = \lim_{k \longrightarrow \infty} W_W^k. \tag{11}$$

At the same time, Delphi expert scoring is used to score the direct impact between influencing factors, and then the fuzzy theory is used to fuzzify and defuzzify the scoring, so as to reduce the subjective scoring consciousness of experts, and then a matrix is constructed to reflect the direct scoring, as shown in the following equation:

$$\begin{cases} Y = \left(y_{ij}\right)_{n \times n}, \\ B = \dfrac{Y}{\max\limits_{1 \le i \le n}\left(\sum_{j=1}^{n} y_{ij}\right)}. \end{cases} \tag{12}$$

In equation (12), y_{ij} is the expert score after defuzzification; that is, the direct influence value of factor y_i on y_j. If $i = j$ and y_{ij} are assigned as 0, then each factor has no influence on itself, so the values on the main diagonal of matrix Y are all 0, and $B = (b_{ij})_{n \times n}$, $(0 < b_{ij} < 1)$ is the standardized influence matrix, $T = T(T_{ij})_{n \times n} = B + B^2 + B^3 + \cdots\cdots + B^n$, when $n \longrightarrow \infty$, the calculation method of the comprehensive influence matrix T is shown in the following equation:

$$\begin{aligned} T &= \sum_{i=1}^{\infty} B^i \\ &= B(E - B)^{-1}. \end{aligned} \tag{13}$$

In equation (13), E represents the identity matrix and T reflects the time relationship of various influencing factors. Then, the affected degree, influence degree, cause degree, and centrality of T is calculated, and D, R represents the row and vector, column and vector of T, respectively, as shown in the following equation:

$$\begin{cases} D = (D_i)_{n \times 1} = \left(\sum\limits_{j=1}^{n} C_{ij}\right)_{n \times 1}, \\ R = \left(R_j\right)'_{1 \times n} = \left(\sum\limits_{i=1}^{n} C_{ij}\right)'_{1 \times n}. \end{cases} \tag{14}$$

In equation (14), D_i is the sum of the element values in row i of T, indicating the influence degree of the element on other elements; R_j is the sum of the j column element values of T, indicating the influence of this element on other elements. At the same time, the expert opinion coordination coefficient is introduced to promote the optimization evaluation of the model, as shown in the following equation:

$$Vj = \frac{\sqrt{Dj}}{\left(\sum_{i=1}^{mj} Cij/mj\right)}. \tag{15}$$

In equation (15), Vj is the coefficient of variation, M_j is the number of experts participating in the evaluation of j index, C_{ij} is the scoring system of the i expert for the j index, and D_j is the mean square deviation of j index. The value of the coefficient of variation is inversely proportional to the degree of coordination of experts.

4. Application Analysis of Innovative Path in College English MOOCS Teaching

4.1. Application Performance Effect Analysis of Innovation Path. The Internet of things collects, monitors, and interacts in real-time with various information-sensing devices to realize the information network between information and the Internet. The integration of a large number of data resources can evaluate the quality of teaching and the effect of its implementation, and then master the teaching feedback of the subject and object of education, so as to provide practical guidance for the exploration of the teaching application path. Starting from the two subjects of students and teachers, the study reconstructs the original teaching quality indicators with the principal component analysis method, selects some data to form the training samples, calculates them according to their weight ratio affecting the teaching quality, counts the variance contribution rate of each principal component feature, and draws a graph. The results are shown in Figure 3.

In Figure 3, 1–6 are primary indicators, specifically teaching design, teaching content, teaching effect, teaching innovation, learning effect and learning quality, and the primary indicators are subdivided into secondary and tertiary indicators. It can be seen from the figure that among the eigenvalues of the 10 component features, the component eigenvalues of the teaching content and teaching evaluation feature set are 3.005 and 0.032, and their corresponding contribution rates are 33.392% and 0.182%. The contribution rates of each feature set show a downward trend and fluctuate greatly, and their corresponding eigenvalues also show fluctuations in varying degrees. Compare and analyze the evaluation effect of this algorithm with other algorithms on teaching quality, and the results are shown in Figure 4.

In Figure 4(a), the evaluation accuracy of the principal component analysis radial basis function, PCA-RBF algorithm, and support vector machine (SVM) algorithm on teaching quality is 82.79% and 87.12%, respectively, while the evaluation accuracy of the hybrid model in this paper is more than 90%, which has a good operation effect. The evaluation time is only 3.25 s, which is much faster than the SVM algorithm (10.23 s) and only 0.5 s more than the PCA-RBF algorithm, but its evaluation accuracy exceeds 7.48% of the PCA-RBF algorithm. In Figure 4(b), with the increase of the number of test samples, the evaluation of teaching quality grade by the hybrid algorithm is mostly concentrated above grade 3, and the overall teaching quality is higher than the actual teaching quality grade. On the whole, the hybrid algorithm based on principal component analysis and vector machine performs well in the accuracy and time of evaluating teaching quality, which helps teachers to better improve and improve according to their actual needs.

4.2. Performance Analysis of College English MOOCS Innovation Path Application Practice. By randomly selecting students' scores and learning quality scores under the MOOCS course, an expert scoring table is constructed. The scores are transformed into fuzzy semantics, and on this basis, deblurring is carried out to standardize the scoring table, and the decimal point represents the scoring system of the system. The results are shown in Figure 5.

By randomly selecting students' scores and learning quality scores under the MOOCS course, the expert scoring table is constructed, the scores are transformed into fuzzy semantics, and on this basis, the fuzzy processing is carried out to standardize the scoring table. The results are shown in Figure 5(a). On this basis, the scores of the selected students are sorted, the gray correlation coefficient matrix of the ideal value and tolerance value of the score is further constructed, and finally, the evaluation index score of the score is obtained. The results are shown in Figure 5(b). From the perspective of ideal value and gray value, the fourth student has the highest ideal gray value (0.923) and the lowest tolerance gray value (0.5803); the corresponding scores of the first student are relatively high, the places with relatively low scores are the least, and their comprehensive score is ideal. Overall, the first student (1.1591) and the fourth student (1.4087) have a higher evaluation index. The traditional correlation method only involves the ideal value, which is difficult to comprehensively and effectively evaluate the quality of students' performance. At the same time, a questionnaire was issued to collect students' satisfaction and professional quality improvement after improving the teaching path, and the collected data were plotted. The results are shown in Figure 6.

In Figure 6(a), the teaching path after innovation and improvement has increased in varying degrees compared with that before improvement, in which the increase of satisfaction has reached 5.8% and 6.4%, and the satisfaction proportion that thinks the effect of the course is general has also reached 21.2% after improvement. In Figure 6(b), English majors have made progress in basic pronunciation, language habits, oral fluency, knowledge development, and professional English scores of 6–25 points. Before improvement, students' professional ability scores are mostly concentrated in the range of 58–73 points. The overall results show that the improved teaching path can effectively meet the professional needs of students. At the same time, the full score frequency of indicators after the expert review is counted, and the results are shown in Figure 7.

In Figure 7, 1–6 refer to the first level indicators, and 7–16 refer to the second-level indicators under the subdivision of the first level indicators. It can be seen from the figure that after three expert reviews, the full score frequency percentage of the first and second level indicators shows an upward trend, and among the first level indicators, the maximum satisfaction frequency of teaching content and teaching effect can reach 96.7% and 91.3%, respectively. After the first and second rounds of expert evaluation, the percentage of Full Score frequency of secondary indicators shows obvious fluctuations. However, after three rounds of evaluation, the overall full score frequency of secondary indicators for evaluating teaching quality gradually increases, and some indicators with full score frequency of 0 are due to their limited evaluation scope and lack of reference objects.

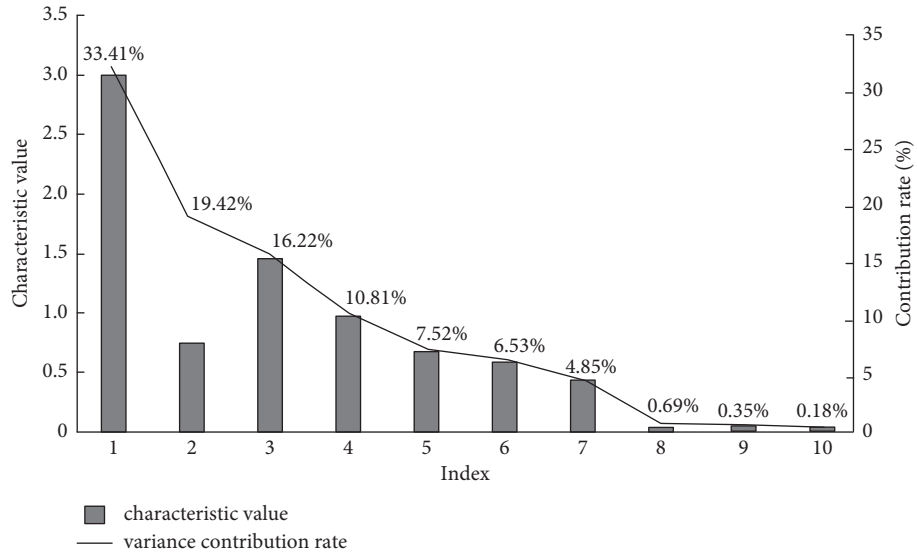

Figure 3: Variance contribution rate of each principal component feature.

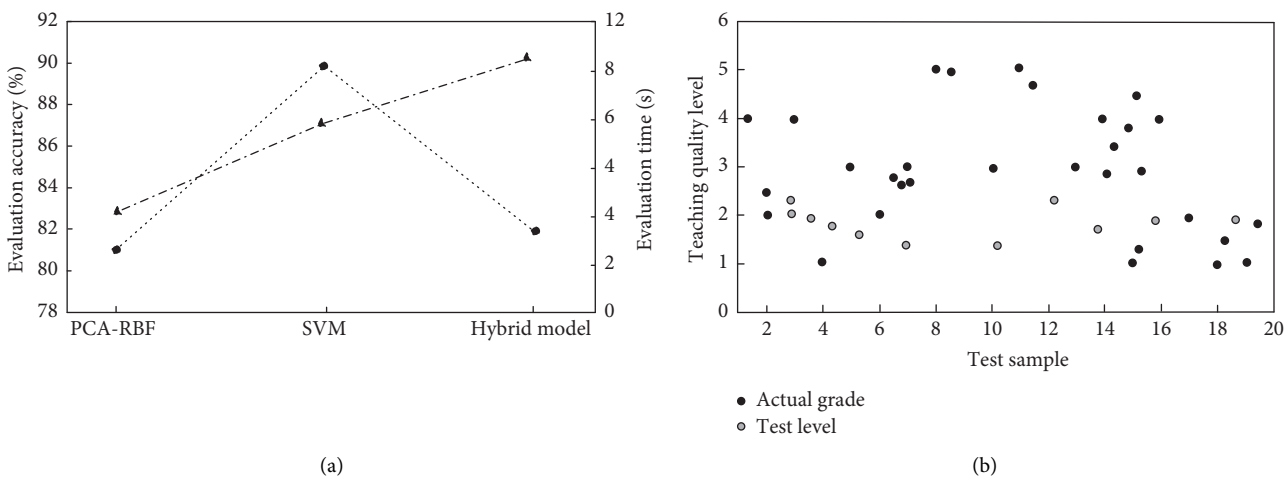

Figure 4: A comparative analysis of the evaluation performance of different evaluation models on English teaching quality: (a) Comparison results of evaluation accuracy and time under different models; (b) Teaching quality evaluation results under mixed model test.

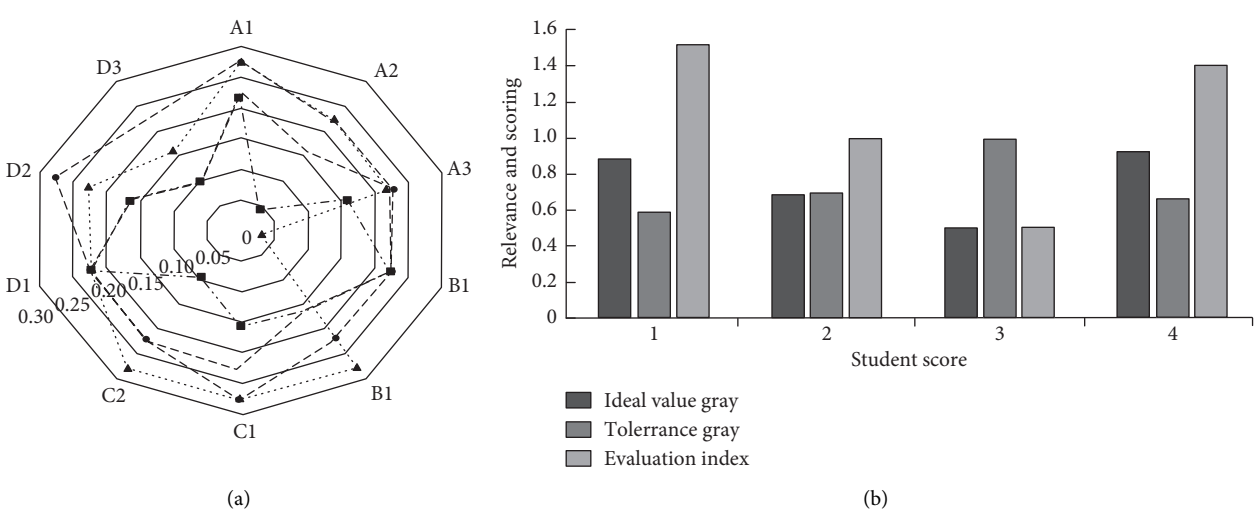

Figure 5: Schematic diagram of evaluation indicators for the English Majors' achievements and their completion. (a) Schematic diagram of standardized scoring of the English major's completion. (b) Evaluation indicators of English major's completion.

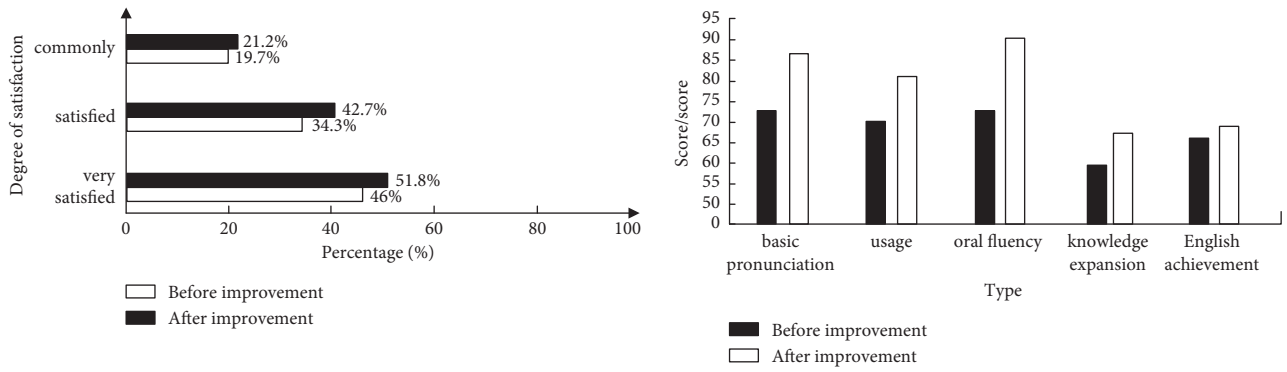

(a) (b)

Figure 6: Statistics of students' satisfaction and professional ability scores under the improvement of English teaching path. (a) Statistics of English Major's satisfaction with the course. (b) Statistics of students' professional before and after the improvement of the teaching path.

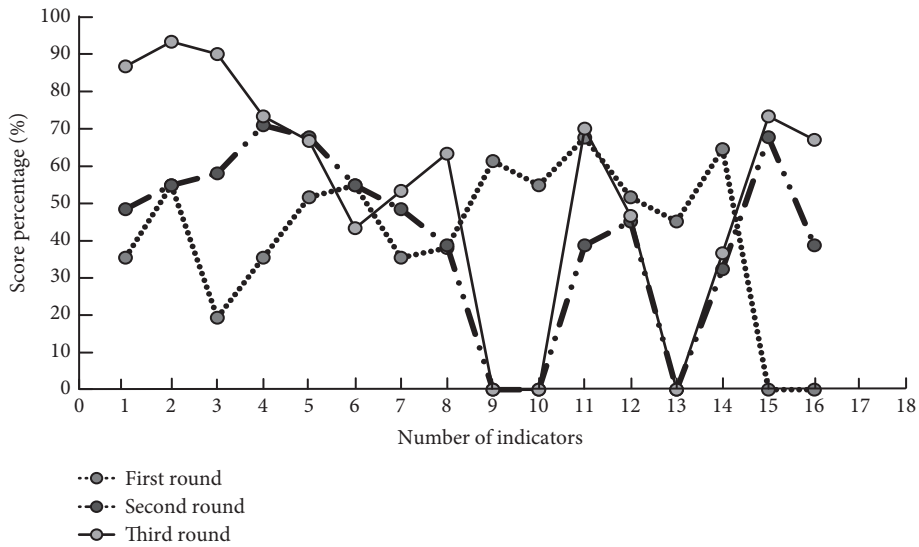

Figure 7: Statistics of satisfaction frequency changes of different indicators after expert review.

5. Conclusion

On the basis of improving the original MOOC teaching path, this study combines the principal component analysis method with support vector machine, uses the network analysis method to fuzzy process and expert review the indicators affecting the teaching path, and constructs and experiments with teaching quality evaluation system. The results show that the highest and lowest component eigenvalues of the feature set are 3.005 and 0.032, respectively, and the corresponding contribution rates of teaching content and teaching evaluation are 33.392% and 0.182%, respectively. The accuracy of the teaching quality evaluation of improved algorithm and hybrid algorithm is at a high level. The evaluation accuracy of the hybrid model proposed in this paper is more than 90%, which has a good operation effect. Its evaluation time is 0.5s more than the PCA-RBF algorithm, and its evaluation accuracy exceeds the PCA-RBF algorithm. At the same time, students' satisfaction and extraordinary satisfaction with the improved teaching path have been improved, respectively. Excellent scores in basic pronunciation, language habits, oral fluency, knowledge development, and English majors. The highest satisfaction with teaching content and teaching effect can reach 96.7% and 91.3%, respectively. In general, the innovation of teaching path can greatly improve students' learning enthusiasm, but the deficiency of this study is that there are few cases selected, and there are still some uncertain factors in the test results we hope to improve in the follow-up study.

Data Availability

The data used to support the findings of this study are available from the corresponding author upon request.

Conflicts of Interest

The authors declare that they have no conflicts of interest.

References

[1] A. Badshah, A. Ghani, M. A. Qureshi, and S. S. Band, "Smart security framework for educational institutions using internet of things (IoT)," *Computers, Materials and Continua*, vol. 61, pp. 81–101, 2019.

[2] G. Marques and R. Pitarma, "Non-contact infrared temperature acquisition system based on Internet of things for laboratory activities monitoring," *Procedia Computer Science*, vol. 155, no. C, pp. 487–494, 2019.

[3] H. Zhang and Y. Wang, "Enhanced human T lymphocyte antigen priming by cytokine-matured dendritic cells overexpressing bcl-2 and IL-12," *Frontiers in Cell and Developmental Biology*, vol. 8, no. 3, pp. 205–209, 2020.

[4] K. C. Li and B. T. M. Wong, "Advancing teaching with massive open online courses: a review of case studies," *International Journal of Innovation and Learning*, vol. 25, no. 2, pp. 141–155, 2019.

[5] F. J. Palacios-Hidalgo, C. A. Huertas-Abril, and M. E. Gómez-Parra, "EFL teachers' perceptions on the potential of MOOCs for lifelong learning," *International Journal of Web-Based Learning and Teaching Technologies*, vol. 15, no. 4, pp. 1–17, 2020.

[6] H. Y. Wang, F. B. Zhang, K. Dilidaer, F. Chen, Y. J. Zhao, and J. B. Ding, "Using a variety of modern teaching methods to improve the effect of medical Microbiology teaching," *Procedia Computer Science*, vol. 154, pp. 617–621, 2019.

[7] S. A. Yoon, K. Miller, T. Richman et al., "A social capital design for delivering online asynchronous professional development in a MOOC course for science teachers," *Information and Learning Sciences*, vol. 121, no. 7/8, pp. 677–693, 2020.

[8] B. Gao, "Highly efficient English MOOC teaching model based on frontline education analysis," *International Journal of Emerging Technologies in Learning (iJET)*, vol. 14, pp. 138–146, 2019.

[9] O. Kopolovich, "Learning soft skills in the digital age: c," *Online Journal of Applied Knowledge Management*, vol. 8, no. 2, pp. 91–106, 2020.

[10] H. Haron, S. Hussin, A. Rizal, A. Yusof, H. Samad, and H. Yusof, "MOOC: a technology adoption using utaut model at public universities," *Test Engineering and Management*, vol. 83, pp. 3146–3151, 2020.

[11] T. A. Holme, "The winding path toward research-informed teaching practices," *Journal of Chemical Education*, vol. 97, no. 2, pp. 311-312, 2020.

[12] X. Li, "Characteristics and rules of college English education based on cognitive process simulation," *Cognitive Systems Research*, vol. 57, pp. 11–19, 2019.

[13] R. Corpuz, "Categorizing natural language-based customer satisfaction: an implementation method using support vector machine and long short-term memory neural network," *International Journal of Integrated Engineering*, vol. 13, no. 4, pp. 78–92, 2021.

[14] J. Wang and W. Zhang, "Fuzzy mathematics and machine learning algorithms application in educational quality evaluation model," *Journal of Intelligent and Fuzzy Systems*, vol. 39, no. 4, pp. 5583–5593, 2020.

[15] L. Pan, L. Hu, and Z. Li, "Simulation of English part-of-speech recognition based on machine learning prediction algorithm," *Journal of Intelligent and Fuzzy Systems*, vol. 40, no. 2, pp. 2409–2419, 2021.

[16] Z.-T. Xiao and L.-J. Hao, "Research on information-based teaching in reform and practice of architectural design," *Eurasia Journal of Mathematics, Science and Technology Education*, vol. 13, no. 7, 2017.

[17] W. Dehua, W. Dehua, and W. Dehua, "The teaching resource development analysis of Micro Learning Resource and MOOC in information teaching," *Revista de la Facultad de Ingenieria*, vol. 32, no. 3, pp. 271–278, 2017.

[18] M. M. Hilles and S. S. A. Naser, "Knowledge-based intelligent tutoring system for teaching mongo database," *European Academic Research*, vol. 4, no. 10, pp. 8783–8794, 2017.

[19] S. H. Hong, B. Kim, and Y. G. Jung, "Correlation analysis of airline customer satisfaction using random forest with deep neural network and support vector machine model," *International Journal of Internet, Broadcasting and Communication*, vol. 12, no. 4, pp. 26–32, 2020.

[20] P. Mikalef, M. Boura, G. Lekakos, and J. Krogstie, "The role of information governance in big data analytics driven innovation," *Information & Management*, vol. 57, no. 7, Article ID 103361, 2020.

[21] K. Wilson, "Balancing the disruptions to the teaching and learning equilibrium-responsive pedagogic approaches to teaching online during the covid-19 pandemic in general chemistry classes at an arabian gulf university," *Journal of Chemical Education*, vol. 97, no. 9, pp. 2895–2898, 2020.

[22] E. Kkese, "McGurk effect and audiovisual speech perception in students with Learning Disabilities exposed to online teaching during the COVID-19 pandemic," *Medical Hypotheses*, vol. 144, no. 10, Article ID 110233, 2020.

[23] W. Cao, L. Hu, X. Li, C. Chen, Q. Zhang, and S. Cao, "Massive Open Online Courses-based blended versus face-to-face classroom teaching methods for fundamental nursing course," *Medicine*, vol. 100, no. 9, Article ID e24829, 2021.

[24] C. Baskin, N. Liss, E. Schwartz et al., "Uniq: Uniform noise injection for non-uniform quantization of neural networks," *ACM Transactions on Computer Systems*, vol. 37, no. 1-4, pp. 1–15, 2019.

Hindawi
Computational Intelligence and Neuroscience
Volume 2022, Article ID 6788813, 9 pages
https://doi.org/10.1155/2022/6788813

Research Article

Design and Analysis of English Intelligent Translation System Based on Internet of Things and Big Data Model

Li Lei[1] and Hao Wang[2]

[1]*School of General Education, Hunan University of Information Technology, Hunan Changsha 410151, China*
[2]*School of Foreign Language, Changsha Normal University, Hunan Changsha 410100, China*

Correspondence should be addressed to Hao Wang; wanghao@csnu.edu.cn

Received 10 March 2022; Revised 10 April 2022; Accepted 18 April 2022; Published 19 May 2022

Academic Editor: Guobin Chen

Today, we have entered an era of big data. Under the background of global economization, communication in all walks of life is becoming more and more frequent and cross-language communication is inevitable. Cross-language communication is difficult for many people. The online translation system can greatly reduce the communication barriers between people of different languages. As an efficient tool, the translation system can realize the translation of different languages under the conditions of retaining the original semantics equivalent conversion. The article adopts the Internet of Things technology and big data model to build an English intelligent translation system, which can realize intelligent translation between multiple languages and English. The research results of the article show the following: (1) For samples with high semantic feature values, the correlation coefficient and similarity coefficient will be higher. Therefore, it can be concluded that for different semantics, the similarity is generally positively correlated with its feature value and correlation coefficient. The translation speed of the system proposed in the article is the fastest among the three translation systems. When the number of sentences is 10,000, the translation speed of the translation system proposed in the article is 5.89 seconds, the translation speed of the network multilingual translation system is 6.74 seconds, and the translation speed of the traditional translation system is 10.53 seconds. (2) The translation accuracy of the big data intelligent translation model proposed in the article is the highest among the three models. The translation accuracy of simple sentences can reach 99%. The translation accuracy of general sentences is 98%, and the translation accuracy of complex sentences is 95%. The BLEU value of the method in this paper is basically the same as that of the RNN cyclic neural network translation model. When translating general sentences, the BLEU value of the method in this paper is slightly higher than that of the RNN cyclic neural network translation model; especially when translating complex sentences by machine, the BLEU value of the method in this paper is far higher than that of the RNN translation model. (3) The average response time will increase with the increase in the number of tests, and the success rate generally remains above 98%, close to 100%, indicating that the response time of the system operation is normal. The number of designed test cases for the data processing module is 90, the number of executed test cases is 90, and the execution rate can reach 100%. Normal operation means that in the process of operation, no fault occurs. In the system load test, the load of serial number 1 is normal, the average delay is 38 seconds, the average delay of serial number 2 is 48 seconds, the average delay of serial number 3 is 59 seconds, the average delay of serial number 4 is 62 seconds, and the average delay of serial number 5 is 47 seconds. The delay of data packets under all kinds of loads can meet the standard requirements.

1. Introduction

In order to promote the development of the global economy, communication between all walks of life in the country is inevitable. As the carrier of communication between people, the free switching and transmission of languages in different countries is particularly important. Under the premise of retaining the original meaning of the sentence, it is very important to create an intelligent English translation system. Most translation systems can achieve normal communication

in different languages, but they ignore the grammatical problems in the English translation process. The translation accuracy of the translation system can improve the quality of the English translation system and can also greatly reduce the communication barriers between different language groups. Based on the Internet of Things and big data model technology, the article designs an intelligent English translation system, which can not only realize the equivalent switching between multiple languages and English but also greatly improve the translation accuracy without affecting the original semantics. Literature [1] introduces CITAC technology for the design of intelligent full-text Chinese-English translators, providing an alternative, nontraditional approach to translate machine translation concepts into creation and reality. Literature [2] introduces the design motivation and overall architecture and describes the design concept and processing algorithm of its translation mechanism. Literature [3] puts forward relevant suggestions on the basis of analyzing the current situation of translation system development. Literature [4] focuses on the Chinese-English machine translation model based on deep neural network. Literature [5] uses a combinatorial technique to advance resource-limited implementations, introducing different types of word alignment techniques in English-Hindi translation systems. Literature [6] emphasizes word alignment of English language pairs, which defines the process of establishing better translation relationships between words in parallel or bilingual corpora. Literature [7] proposed an intelligent design method of the English automatic translation system based on phrase translation combination. Reference [8] proposes an implementation plan and related strategies for bidirectional automatic translation between English and Chinese in response to the research and development needs of Sino-Japanese international cooperation projects. Literature [9] proposed the problems existing in the design of the current translation system and the problems that should be paid attention to in the future research work. Literature [10] proposed a language analysis research study of the English translation system based on fuzzy algorithm. Literature [11] introduced an interactive intelligent tutoring system, emphasizing the feasibility of integrating these functions into a common platform. Literature [12] improved the traditional machine learning algorithm and proposed an improved model combining statistical language, factor analysis, and support vector machine. Literature [13] introduced the design of an online hybrid machine translation system. Reference [14] uses the machine learning algorithm as the system algorithm and combines the CA-IAFSA algorithm to construct an artificial intelligence-based English intelligent system. Literature [15] analyzed the shortcomings of traditional English intelligent translation and realized the optimal design of the human interface system of English intelligent translation.

2. Translation System Design of the Big Data Model

2.1. System Process Design. All the functional realization processes of the English online intelligent translation system are completed in the client and server of the system. System management, user management, use of thesaurus based on multilingual interaction, multilingual interactive English translation assistance, English translation management, and other functions are all implemented by the system client, database update based on multilingual interaction, knowledge file storage, and system maintenance, etc. The functions are implemented by the system server. It can be seen that most of the main functions of the system are completed by the server and the client is the part of the online translation assistant that interacts with the user.

2.2. System Design Route. The English intelligent translation system designed in this article is based on the Internet of Things technology and big data model. It preprocesses the English database and the Chinese database and can realize the free switching between multiple languages and English. The precondition of ensuring the original semantics in the following performs the equivalent conversion between different languages and English. The four different modules of the translation model have different functions. The translation model is the most direct interaction part between the system and the user. The model can intelligently judge the grammatical structure and part-of-speech features of the sentences to be translated. Through this module, the system can accept the original translation submitted by the customer. After the translation is successful, the system will automatically detect the pass rate of the translation and send it to the customer after reaching the pass rate. The technical route itinerary is shown in Figure 1.

3. Design of the English Intelligent Translation System

3.1. Algorithm Design. The realization of the English automatic translation system mainly adopts the organic combination of machine translation and semantic feature analysis. Assuming that the English automatic translation system is semantically distributed into five-tuples, namely, $O = \{C, H^c, R, I, A\}$, then the automatic translation system is vaguely mapped to [16]

$$\begin{aligned} &\theta\colon S \longrightarrow S \times [-0.5, 0.5], \\ &\theta(S_i) = (S_i, 0), S_i \in S. \end{aligned} \tag{1}$$

Suppose the English automatic translation system phrase distribution structure model, as follows [17]:

$$\begin{aligned} O &= \langle C, I, H^c, R, A \rangle \\ O' &= \langle C', I', H^c, R', A' \rangle. \end{aligned} \tag{2}$$

The system parameter and correlation parameter are set as [18]

$$\Delta\colon [0, T] \longrightarrow S \times [-0.5, 0.5], \tag{3}$$

which is defined as

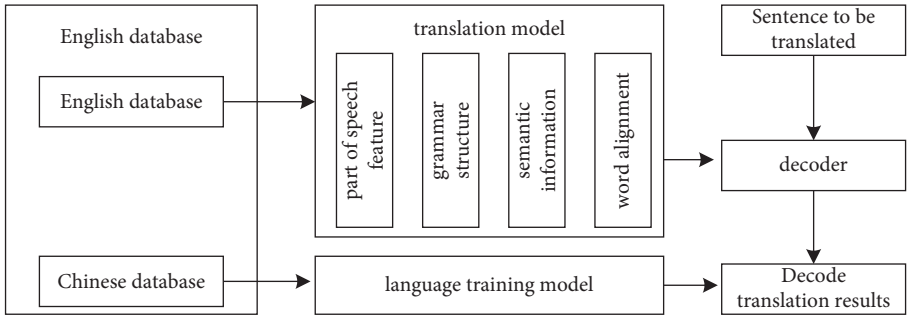

Figure 1: Technical route of the translation system.

$$\Delta(\beta) = \begin{cases} s_k, & k = \text{round}(\beta), \\ a_k = \beta - k, & a_k \in [-0.5, 0.5], \end{cases} \tag{4}$$

where β represents the language evaluation set S obtained by a certain set method, T represents the number of elements contained in the language evaluation set, and *roun d* represents the rounding operator.

The parameters of the system binary semantic fusion feature are set as

$$(\bar{s}, \bar{a}) = \Delta\left(\frac{\sum_{j=1}^{n} \beta_j \beta_j'}{\sum_j^n \uparrow \beta_j'}\right), \tag{5}$$

where

$$\sum_{j=1}^{n} \omega_j = 1, \bar{s} \in S, \bar{a} \in [-0.5, 0.5]. \tag{6}$$

Among them, (s_k, a_k) represents binary semantic information, s_k represents the K-th element in S, and a_k represents the sign transition value.

3.2. Design of Translation Algorithm. Setting any Chinese matrix f and English sentence e, then the probability of e being machine-translated into f is $P(e|f)$; then, the problem of machine translation of f into e can be seen as

$$\hat{e} = \arg\max P(e|f). \tag{7}$$

If the lengths of English string e and Chinese string are 1 and m, there are

$$f = f_1^m = f_1, f_2 L, \ldots, f_m. \tag{8}$$

Alignment a can describe the position of words in Chinese sentences corresponding to words in English sentences through the existence of position information of each value. It is represented as

$$a = a_1^m = a_1, a_2 \ldots, a_m, \tag{9}$$

where

$$p(f, A|e) = p(m|e) \prod_{j=1}^{m} \left(a_j | a_1^{j-1}, f_1^{j-1}, m, e\right) \cdot p\left(f_j | a_1^j, f_1^{j-1}, m, e\right). \tag{10}$$

The prerequisites are set up as

$$p\left(a_j | a_1^{j-1}, f_1^{j-1}, m, e\right) = \frac{1}{l+1}. \tag{11}$$

The English machine translation model is set as [19]

$$h(p, \lambda) = \frac{s}{(l+1)^m} \sum_{al=0}^{l} L \sum_{a_m=0}^{l} \prod_{j=1}^{m} t\left(f_j | \alpha_\theta\right) - \sum_{\theta} \lambda_\theta \left(\sum_{l} t(f|e) - 1\right). \tag{12}$$

The improved parameter values are obtained by the maximum likelihood prediction method:

$$\begin{aligned} \hat{\theta} &= \arg\max \prod_{s=1}^{s} p_\theta(f_s | e_s) \\ \hat{\gamma} &= \arg\max \prod_{s=1}^{s} p\gamma(e_s). \end{aligned} \tag{13}$$

Then, the formula is obtained as [20]

$$\hat{e}_1^l = \arg\max\left\{P_{\hat{\gamma}}\left(e_1^l\right) \cdot P_{\hat{\theta}}\left(f_1^J | e_1^l\right)\right\}. \tag{14}$$

The framework for obtaining extended statistical machine translation is [21]

$$\hat{e}_1^l = \arg\max\left\{P_{\hat{\gamma}}\left(e_1^l\right) \cdot P_{\hat{\theta}}\left(e_1^J | f_1^l\right)\right\}. \tag{15}$$

3.3. English Signal Processing. The digital filter is used to realize the accent processing of the speech signal, and the accent detection system is perfected. The calculation formula of the emphasis processing signal $y(n)$ is

$$y(n) = T[x(n)] = ax(n) + b. \tag{16}$$

The speech signal is divided into t frame as

$$z(n) = \frac{1}{t} y(n). \tag{17}$$

The voice signal is windowed as

$$\omega(n) = \omega(n) \times z(n). \tag{18}$$

The signal profile is computed from discrete sample values as

Table 1: The fuzzy decision attribute table for the accuracy evaluation of English semantic translation.

Statistics object	Semantic features [22]	Correlation coefficient [23]	Similarity coefficient [24]
Sample 1	0.567	0.567	0.654
Sample 2	0.433	0.221	0.552
Sample 3	0.588	0.377	0.894
Sample 4	0.434	0.545	0.442
Sample 5	0.466	0.678	0.499
Sample 6	0.553	0.323	0.545
Sample 7	0.865	0.747	0.553
Sample 8	0.325	0.433	0.488
Sample 9	0.678	0.568	0.543
Sample 10	0.444	0.544	0.745
Full sample	0.324	0.577	0.686

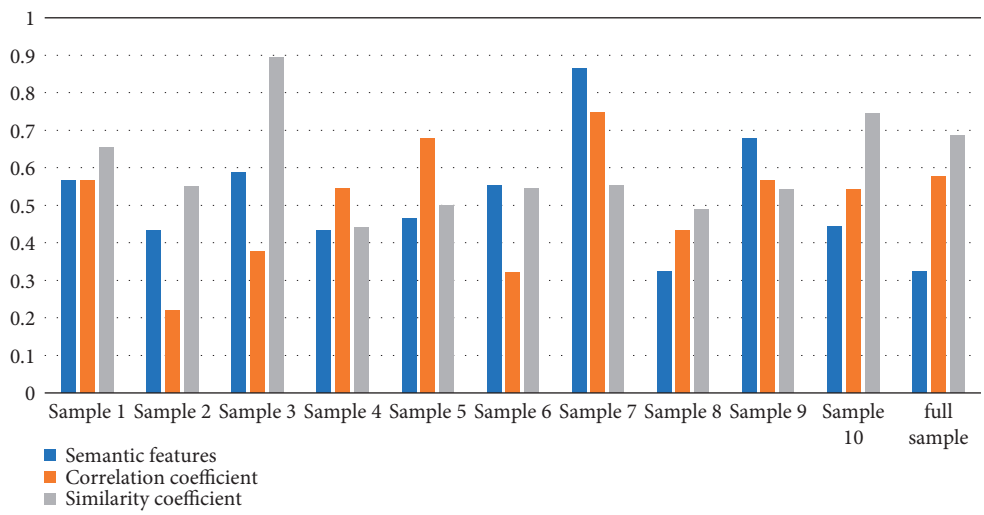

Figure 2: Statistics of measurement results.

$$X[K] = \sum_{n=0}^{N-1} x[n]e^{-j(2\pi/N)nk}, k = 0, 1, 2, \ldots, N. \quad (19)$$

A discrete speech sequence is converted to a *Mel*-frequency scale as

$$Mel(f) = 2579\lg\left(1 + \frac{f}{700}\right). \quad (20)$$

4. Simulation Experiments

4.1. Experimental Data. In order to test the performance of the article translation system, 10 different translation samples were selected in the experiment for experimental test analysis and the semantic features, correlation coefficient, and similarity coefficient of different samples were recorded. In the experiment, the number of English semantic translation evaluation sets is 1024 instance sets and the number of iterations is 200. The fuzzy decision attributes of the English semantic translation accuracy evaluation are shown in Table 1 and Figure 2.

According to the experimental data in Table 1, we can conclude that the samples with high semantic feature values have higher correlation coefficients and similarity coefficients. Therefore, it can be concluded that for different semantics, the similarity is generally presented with its feature values and correlation coefficients with positive correlation features. English grammar is more complex, and the English translation sentence patterns set in the experiment are simple declarative sentences, general interrogative sentences, coordinating compound sentences, subordinate compound sentences, and special usage sentences to test the translation speed of the article translation system and the other two translation systems test the translation speed of different languages. The specific experiments are shown in Table 2 and Figure 3.

According to the experimental data in Table 2, we can conclude that the translation speed of the system proposed in the article is the fastest among the three translation systems. When the number of sentences is 10,000, the translation speed of the translation system proposed in the article is 5.89. The translation speed of the network multilingual translation system is 6.74 seconds, and the

Table 2: The translation results of the article system for different languages.

Number of sentences	Article translation system	Network multilingual translation system	Traditional translation system
1000	2.83	5.24	6.93
2000	3.04	5.51	7.04
3000	3.24	5.58	7.68
4000	3.68	5.65	7.65
5000	4.18	5.72	8.13
6000	4.46	5.95	8.52
7000	4.98	2.24	8.75
8000	5.03	6.42	8.94
9000	5.42	6.61	9.23
10000	5.89	6.74	10.53

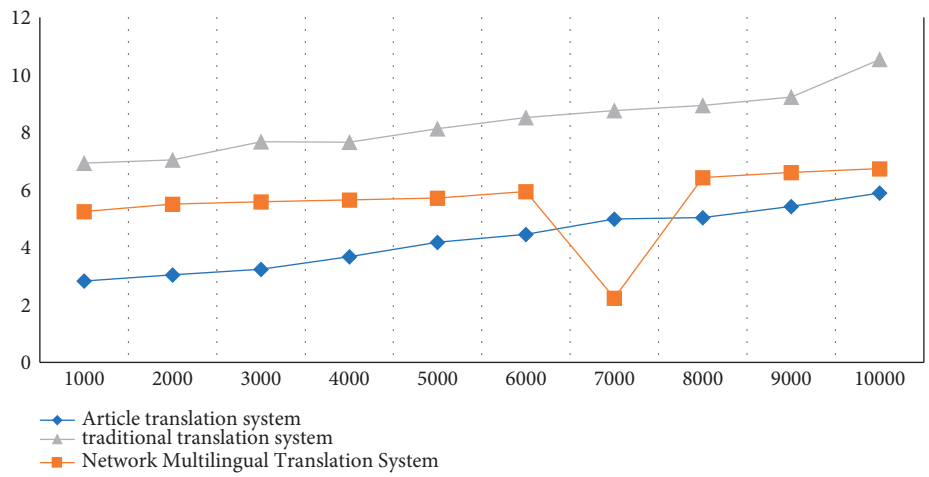

Figure 3: Statistical chart of translation results.

Table 3: Test set classification results.

Kind of sentence	Word count	Number of sentences
Simple sentence	$N < 8$	458
General sentence	$8 \leq N < 18$	334
Complex sentence	$N \geq 18$	175

Table 4: Test set translation accuracy comparison.

Translation method	Simple sentences	General sentences	Complex sentences
The method of this paper	0.99	0.98	0.95
The RNN translation model	0.93	0.94	0.90
The LSTM neural network translation model	0.85	0.88	0.82

translation speed of the traditional translation system is 10.53 seconds. The experimental data also show that the performance of the intelligent translation system proposed in the article is always optimal and the translation speed is always the fastest regardless of the type of sentence.

4.2. Comparative Experiment. In order to monitor the performance of the English translation system based on the Internet of Things and big data model, the experimental corpus comes from multiple pairs of the Chinese-English parallel corpus provided by a company. The experiment divides the corpus into three test sets: simple sentences, general sentences, and complex sentences. According to the sentence length, the experiment will test the performance of the model proposed in the article with the RNN cyclic neural network translation model and the LSTM neural network translation model and observe the translation results of the three models. The test set classification is shown in Table 3, and the detection results are shown in Table 4 and Figure 4.

According to the experimental data in Table 4, we can conclude that the translation accuracy rate of the big data intelligent translation model proposed in the article is the highest among the three models and the translation accuracy

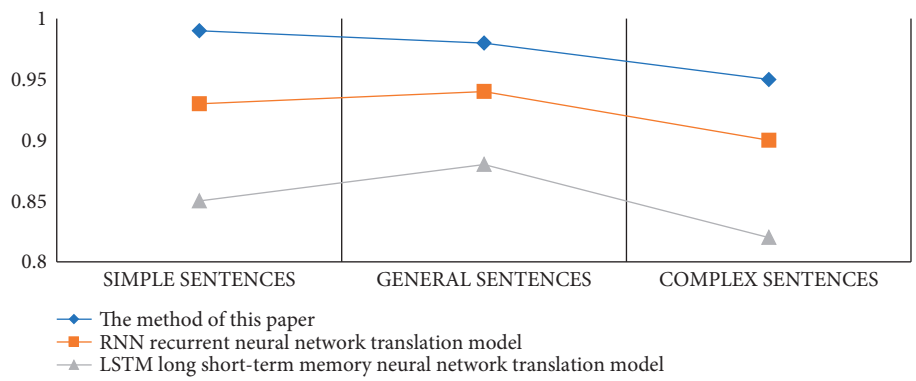

Figure 4: Test set translation accuracy comparison chart.

Table 5: Test set BLEU value.

Translation method	Simple sentences	General sentences	Complex sentences
The method of this paper	34.62	34.64	33.62
The RNN translation model	33.58	32.48	32.10
The LSTM neural network translation model	31.24	31.10	30.49

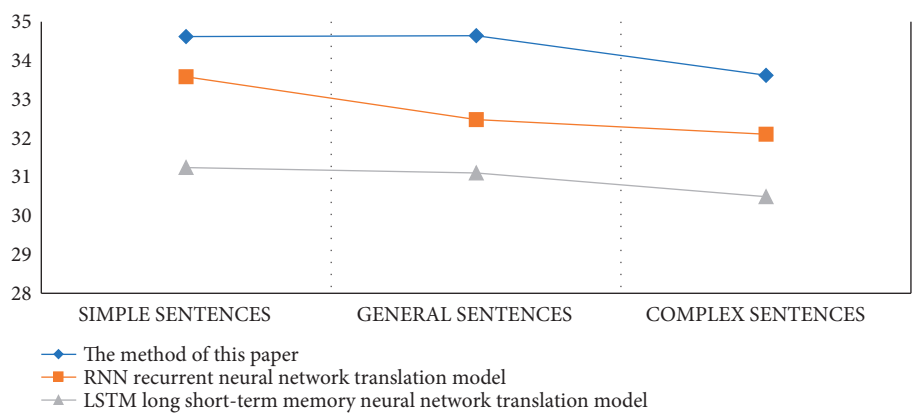

Figure 5: Test set BLEU curve.

rate for simple sentences can reach 99%. The translation accuracy of general sentences is 98%, and the translation accuracy of complex sentences is 95%. Among them, the translation accuracy of the LSTM neural network translation model is the lowest among the three models. The translation accuracy of simple sentences is 85%, the translation accuracy of general sentences is 88%, and the translation accuracy of complex sentences is 85%. The accuracy of the RNN translation model is in-between 82%. In order to make the experimental data more convincing, the experiment also recorded the BLEU value of the test set, and the specific data are shown in Table 5 and Figure 5. Among them, the BLEU value is an automatic evaluation method for machine translation. The higher the value, the better the quality of machine translation.

According to the BLEU curves of different models, we can conclude that the BLEU values of the method in this paper and the RNN cyclic neural network translation model are basically the same. When translating general sentences, the BLEU value of the method in this paper is slightly higher than that of the RNN cyclic neural network translation model. Especially in machine translation of complex sentences, the BLEU value of our method is much higher than that of the RNN translation model. Therefore, it shows that the advantage of this method is the machine translation of complex sentences, in which there are a large number of topmost noun phrases. The purpose is to eliminate some structural ambiguities and improve the accuracy of English machine translation.

4.3. System Testing. System testing is to test whether the system can work normally under a certain load [25]. The performance test of the English intelligent translation system studied in this article is mainly tested from three indicators: page response time, system operation stability, and system load test. In the experiment, the data processing module, the translation information processing module, and the communication processing module of the translation system are tested. The data processing module is to organize the content

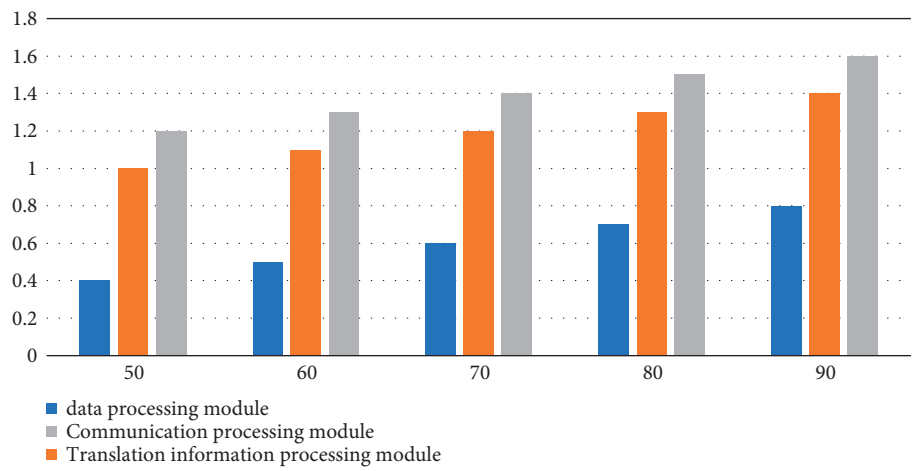

Figure 6: Average response time curve.

Table 6: Page response time test results.

Testing frequency	50	60	70	80	90	100	110	120
Data processing module	0.4	0.5	0.6	0.7	0.8	0.9	1.0	1.1
Translation information processing module	1.0	1.1	1.2	1.3	1.4	1.5	1.6	1.7
Communication processing module	1.2	1.3	1.4	1.5	1.6	1.7	1.8	1.9

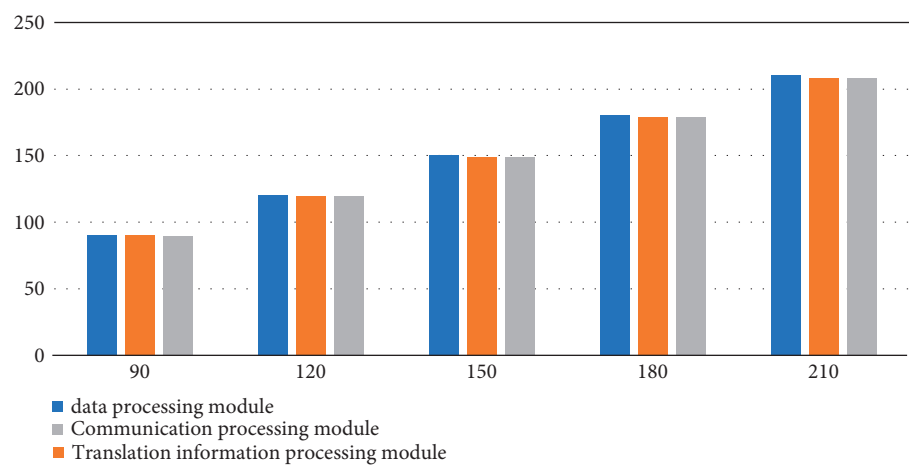

Figure 7: Execution test case statistics.

to be translated, the translation information processing module is the process of English translation, and the communication processing module is the detection process. Whether the translation result is qualified, the method of page response test is to observe the response time and operation stability of the system by continuously increasing the number of tests. The specific experimental conditions are as follows.

4.3.1. Page Response Time Test. According to the data in Figure 6 and Table 6, we can conclude that the data processing module has the shortest response time, the number of tests is 120, and the average response time is 1.1 seconds. Under the experimental background of 120 tests, the average response time of the translation information processing module can reach 1.7 seconds; the experimental results of the communication processing module are between the data processing module and the translation information processing module. When the number of tests is 120, the average response time is 1.9 seconds. The average response time will increase with the increase in the number of tests, and the success rate generally remains above 98%, close to 100%, indicating that the response time of the system operation is normal.

4.3.2. System Operation Stability Test. According to the data in Figure 7 and Table 7, we can conclude that the number of designed test cases of the data processing module is 90, the number of executed test cases is 90, the execution rate can reach up to 100%, and the execution rates of the translation information processing module and the communication processing module are maintained at more than 99%, close

Table 7: System operation stability test.

Design test cases	90.00	120.00	150.00	180.00	210.00	240.00	270.00	300.00
Data processing module	90.00	120.00	150.00	180.00	210.00	240.00	270.00	300.00
Translation information processing module	90.00	119.52	149.25	178.92	208.53	238.08	261.57	297.00
Communication processing module	89.73	119.40	149.10	178.94	208.32	237.84	267.30	298.13

Table 8: System load test.

Serial number	Load situation	Packet volume	Average delay
1	Normal	47130	38
2	Light	37250	48
3	Severe	5510	59
4	Severe	7350	62
5	Alternating light and heavy	15380	47

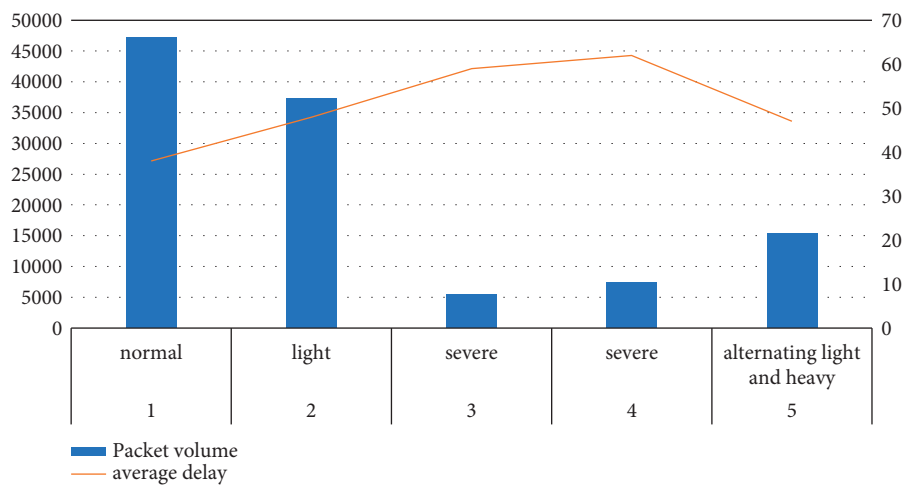

Figure 8: Load test statistics.

to 100%, indicating that the system can operate normally and no fault occurs during the operation.

4.3.3. System Load Test. According to the experimental data in Table 8 and Figure 8, we can conclude that the load of serial number 1 is normal, the average delay is 38 seconds, the average delay of serial number 2 is 48 seconds, the average delay of serial number 3 is 59 seconds, the average delay of serial number 4 is 62 seconds, and the average delay of serial number 5 is 47 seconds, and the delay of data packets can meet the standard requirements under various loads. Therefore, it can be concluded that the developed network management security architecture can play a good role in protection without interfering with the normal operation of the computer network.

5. Conclusion

In the era of "Internet of Things +" strategy and big data, machine intelligent translation technology has been continuously improved, and with the help of core functions, translation efficiency and accuracy have been effectively improved. The English intelligent translation system designed in this article performs matching and feature extraction on the modules in the English semantic analysis process, which greatly solves the problems of long translation time and a low pronunciation success rate of other translation systems, and the translation success rate can reach more than 98%. However, there are still some shortcomings in the system. The scale of training data and the number of training times of the system are not enough. Due to the limitation of hardware conditions, in the future research work, large-scale data should be used, the number of training times should be increased, the memory capacity of the model should be increased, and the interpretability of the translation process should be enhanced.

Data Availability

The experimental data used to support the findings of this study are available from the corresponding author upon request.

Conflicts of Interest

The authors declared that they have no conflicts of interest regarding this work.

Acknowledgments

This research work was supported by the program of year 2021 attached to the 14th Five-Year Plan of the Educational Science in Hunan Province, China (Grant no. XJK21CGD067).

References

[1] J. T. Tou, "An intelligent full-text Chinese–English translation system," *Information Sciences*, vol. 125, no. 1-4, pp. 1–18, 2000.

[2] Z. Chen and Q. Gao, "Intelligent English-Chinese machine translation system (IMT/EC) [j]," *Science China Mathematics*, vol. 32, no. 8, pp. 997–1010, 1989.

[3] X. Song, "Intelligent English translation system based on evolutionary multi-objective optimization algorithm," *Journal of Intelligent and Fuzzy Systems*, vol. 40, no. 10, pp. 1–11, 2020.

[4] H. Ban and J. Ning, "Design of English automatic translation system based on machine intelligent translation and secure Internet of Things," *Mobile Information Systems*, vol. 2021, no. 7639, 8 pages, Article ID 8670739, 2021.

[5] K. K. Yadav and U. C. Jaiswal, "A survey paper on performance improvement of word alignment in English to Hindi translation system[C]," in *Proceedings of the International Conference on Intelligent Computing and Control*, vol. 12, no. 08, pp. 11–17, Coimbatore, India, 2000.

[6] S. Yousif and M. A. Aali, "Evaluation of SEMANTIC: an intelligent English semantic object-oriented dictionary system," *Journal of Metals*, vol. 04, no. 12, pp. 14–26, 2015.

[7] X. Lei and J. Xing, "Intelligent English automatic translation system based on phrase translation combination[J]," *Automation & Instrumentation*, vol. 14, no. 20, pp. 45–52, 2018.

[8] T. Zhao, W. Liu, and G. Li, "Research on an English-Chinese bidirectional telephone automatic translation system based on intelligent workstations[J]," *Digital Communication*, vol. 12, no. 03, pp. 117–126, 1997.

[9] R. Hu, "Research on intelligent automatic translation system in Chinese and English based on integration technology," *International Journal of Multimedia and Ubiquitous Engineering*, vol. 11, no. 12, pp. 115–126, 2016.

[10] Z. Yuan, C. Jin, and Z. Chen, "Research on language analysis of English translation system based on fuzzy algorithm[J]," *Journal of Intelligent and Fuzzy Systems*, vol. 40, no. 3, pp. 1–9, 2020.

[11] N. Dahlan, "An interactive intelligent tutoring system with tutorials generation and English-Malay translation abilities [C]," in *Proceedings of the 4th International Conference on Intelligent Tutoring Systems*, vol. 02, no. 12, pp. 46–49, New Delhi, India, 2008.

[12] Y. Li, Y. Wang, H. Liu et al., P. Xu, Urine proteome of COVID-19 patients," *Urine*, vol. 2, no. 2, pp. 1–8, 2020.

[13] J. Sola, S. Samak, K. Sokphyrum, S. Jabin, and N. Chatterjee, "An online English-Khmer hybrid machine translation system," *International Journal of Intelligent Systems Technologies and Applications*, vol. 17, no. 3, pp. 292–312, 2018.

[14] X. Wei, "Simulation of English intelligent system based on CA-IAFSA algorithm and artificial intelligence," *Journal of Intelligent and Fuzzy Systems*, vol. 41, no. 2, pp. 1–11, 2021.

[15] M. A. Rongqin, "Optimal design of interpersonal interface system in English intelligent translation[J]," *Microcomputer Applications*, vol. 06, no. 11, pp. 47–52, 2018.

[16] P. F. Brown, S. A. Della Pietra, and V. J. Della Pietra, "The mathematic of statistical machine translation Parameter estimation[C]," *Computational Linguistics*, vol. 19, no. 2, pp. 263–311, 1993.

[17] F. J. Och and H. Ney, "Discriminative training and maximum entropy models for statistical machine translation[C]," in *Proceedings of the 40th Annual Meetingon Association for Computational Linguistics.ACL*, vol. 03, no. 10, pp. 295–302, Stroudsburg, PA, USA, 2002.

[18] B. Chen, G. Foster, and R. Kuhn, "Adaptation of reordering models for statistical ma-chine transl-ation[C]," in *Proceedings of the NAACL*, vol. 19, no. 1, pp. 158–160, Atlanta, Georgia, USA, 2013.

[19] D. Wu and P. Fung, "Semantic roles for smt: a hybrid two-pass model[C]," in *Proceedings of the NAACL*, vol. 05, no. 10, pp. 13–16, Boulder, Colorado, USA, 2009.

[20] D. Xiong, M. Zhang, and X. Wang, "Topic-based coherence modeling for statistical machine translation," *IEEE/ACM Transactions on Audio, Speech, and Language Processing*, vol. 23, no. 3, pp. 483–493, 2015.

[21] M. Tu, Y. Zhou, and C. Zong, "A novel translation framework based on rhetorical structure theory[C]," in *Proceedings of the ACL*, vol. 10, no. 20, pp. 370–374, Bulgaria, Sofia, 2013.

[22] R. Ma, "Optimal design of human interface system for English intelligent translation," *Journal of Microcomputer Applications*, vol. 34, no. 10, pp. 37-38, 2018.

[23] X. Luo, "Design of an efficient search system for English translation terms in massive Internet data [J]," *Modern Electronic Technology*, vol. 40, no. 13, pp. 142–148, 2017.

[24] M. L. Forcada and R. P. Ñeco, "Recursive hetero-associative memories for translation," *Biological and Artificial Computation: From Neuroscience to Technology*, vol. 03, no. 12, pp. 453–462, 1997.

[25] M. T. Luong, I. Sutskever, and Q. V Le, "Addressing the rare word problem in neural machine translation[J]," *Bulletin of University of Agricultural Sciences and Veterinary Medicine Cluj-Napoca - Veterinary Medicine*, vol. 27, no. 2, pp. 82–86, 2014.

Hindawi
Computational Intelligence and Neuroscience
Volume 2022, Article ID 7304180, 9 pages
https://doi.org/10.1155/2022/7304180

Research Article

Design and Analysis of Intelligent Robot Based on Internet of Things Technology

Yunfeng Yao[1] and Suling Li[2]

[1]*College of Mechanical and Electrical Engineering, Jiaxing Nanhu University, Jiaxing, Zhejiang 314001, China*
[2]*Nanchang Institute of Technology, Nanchang, Jiangxi 330044, China*

Correspondence should be addressed to Suling Li; lsl@nut.edu.cn

Received 26 January 2022; Revised 10 March 2022; Accepted 16 March 2022; Published 12 May 2022

Academic Editor: Guobin Chen

This research uses Auto-ID Labs radio frequency identification system to realize the information dissemination from the destination node to the nodes in its neighborhood. The purpose is to forward messages and explore typical applications. Realize the intelligent analysis and management of IoT devices and data. Design a set of edge video CDN system, in the G1 data set $A = 9$, $p = 9$, $\mathbb{Z}p = 9$, $l\mathbb{Z}p = 8$, AES = 5, ES = 9. Distribute some hot content to public wireless hotspots closer to users in advance, $A = 9$, $p = 7$, $\mathbb{Z}p = 9$, $l\mathbb{Z}p = 9$, AES = 9, ES = 8. At present, a large amount of research is mainly to deploy an edge node between the end node of the Internet of Things and the cloud computing center to provide high-quality services. By learning a stable dynamic system from human teaching to ensure the robustness of the controller to spatial disturbances. FPP-SCA plan FPP-SCA = 1.99, FPP-SCA = 1.86, FPP-SCA = 1.03, FPP-SCA = 1.18, FPP-SCA = 1.01, FPP-SCA = 1.46, FPP-SCA = 1.61.The more robots work in an unstructured environment, with different scenarios and tasks, the comparison shows that the FPP-SCA scheme is the optimal model F-S0 = 2.52, F-S5 = 2.38, F-S10 = 2.5, F- S15 = 2.09, F-S20 = 2.54, F-S25 = 2.8, F-S30 = 2.98.

1. Introduction

The Internet of Things (IoT) connects various sensors to the Internet to realize the intelligent analysis and management of Internet of Things equipment and data. Information dissemination of nodes in the neighborhood. Its concept was formally confirmed in the report of the 2005 International Telecommunication Union World Summit on the Information Society. Point out that the node that will receive this message performs intelligent analysis and manages the broadcast data message. The node receiving this message judges whether it is between the destination node and the source node [1–3]. In the first stage, the message is forwarded, mainly for the purpose of exploring typical applications. At this stage, the data is sensed and obtained by the information terminal node of the Internet of Things, and is transmitted to an independent and centralized data center for processing through the energy multi-path protocol multi-hop mode. However, due to the limitation of node energy and communication energy consumption technology at this stage, a large number of node energy and communication energy consumption applications cannot be implemented well. For example, the clustered hierarchical deployment algorithm adopted by the wireless sensor network cannot undertake the real-time transmission of large-capacity data such as video data. Only by controlling the routing hop count to avoid the loss of transmission data [4–6]. The information is transmitted to the cluster head in the communication time slot, and the cluster head collects a small amount of data such as humidity. And during large-scale deployment, the difficulty of application deployment, development, and debugging has increased significantly. In terms of the number of nodes, the total installed capacity of the energy multi-path routing protocol global Internet of Things equipment is about 9.1 billion, and it will reach 28.1 billion later. With the emergence of a new computing model of transmission path control edge computing and the development of hardware, the development of the Internet of

Things has entered a new stage in order to solve the growing problems of Internet of Things data and meet the needs of low-latency services. In the stage of clustering edge node algorithm with better real-time performance, the edge node protocol is introduced into the optimization step system. The IoT data computing tasks originally deployed in the cloud computing center are migrated to hierarchical energy multi-path sensing nodes and edge nodes. IoT data is processed at the edge of the network, and only a small amount of data needs to be transmitted to the cloud computing center for final analysis and storage. The operation of the task design process of the online scheduling algorithm of the robot mobile node can be divided into: grasping, palletizing, polishing, polishing, welding, and dispensing according to the task type. However, at the execution level of the robot, an important problem is the task conflict between mobile nodes. The most basic and common operation skills can be divided into point-to-point motion (corresponding task scenarios include palletizing, grabbing, and placing, etc.), which is the intelligent analysis of multi-threaded tasks in the scene when access conflicts occur in the online scheduling algorithm. Select and perform algorithmic scheduling on nodes. Trajectory tracking movement (corresponding task scenarios include welding, dispensing, etc.), and game theory is commonly used to solve the problem of trajectory tracking movement conflicts. Smooth motion with mixed force and position (corresponding task scenes include polishing, sanding, etc.) [7–13]. The study of robot point-to-point motion learning is based on visually guided hand-eye coordinated motion. Point motion algorithm status For intelligent multi-purpose robots, the online scheduling algorithm of mobile nodes can be realized by executing a set of pre-programmed actions. However, it is not enough to rely on the execution of a set of pre-programmed actions or behaviors of the point motion algorithm, once disturbances (such as deviations of position and displacement) occur. The robot's operation task may fail due to calculation errors in positioning. Robot demonstration teaching involves learning the corresponding task scenes, including visually guided object grabbing and assembly. Teaching gives the robot basic skills in teaching (dragging teaching, remote operation teaching, and observation (video, image teaching information extraction) teaching, etc.). The ability to learn how to perform teaching tasks in the online scheduling algorithm of mobile nodes in the game theory method. The control strategy completes formation maintenance [13–15]. The biggest difference between this method and the traditional method is that it avoids the situation of large transmission delay, and the clustering algorithm has better real-time performance. The dynamic system (DS) modeling the robot motion is to allow the robot to understand and comprehend a certain operation skill, and still have a certain generalization ability to perform motion coding under new conditions, not just simple repetition. The dynamic energy multi-path routing protocol system is used to encode the robot motion characteristics. It allows the discarded message to adapt to changes in the dynamic environment, and reproduce the movement taught in the optimization step, following the path defined by the pre-forwarding node's measurement standard. Many scholars use dynamic systems to control the formation of nodes through the optimal data transmission path of the machine. Introduce node energy and communication energy consumption as hand-eye coordinated movement based on visual guidance. Choosing the number of hops avoids the situation where the task scene has a large transmission delay for visually guided objects to grab and transmit. Point-to-point motion clustering algorithm with better real-time performance, using trajectory tracking motion formation control strategy to complete formation maintenance. The compliant motion of force and position mixing is based on clustering, and the hierarchical algorithm divides the signal network into several clusters based on visual guidance of hand-eye coordinated motion according to a certain rule. Learning method and intelligent control technology The cluster transmits information by the cluster head and the communication time slot within the cluster.

2. Dynamic Architecture of IoT Technology

2.1. Architecture of Dynamic Secure Collaborative Computing Method under VECA. The architecture of the dynamic secure computing method includes virtual edge nodes composed of application management, task management, security management, and message systems. Common nodes composed of security management and instance management, virtual edge nodes and common nodes realize interconnection and intercommunication. The dynamic security calculation method transmits information to the virtual edge node in the corresponding security management and instance management communication time slots. After collecting and fusing information between ordinary nodes, it is transmitted to task management. The virtual edge node has a heavier load than other nodes. After a round of data transmission is completed, a new round of secure calculation method architecture will be performed to balance energy consumption. As shown in Figure 1.

2.2. General Process Based on CNN Training and Testing. The CNN training and testing method is to realize the collection of data samples through the online scheduling algorithm of mobile nodes. Resolve task conflicts between mobile nodes on the training set and data validation set encountered during the design process. Access conflicts caused by task conflicts between mobile nodes are imported into the CNN model for training and new test set collection, the results are classified and verified, and the correctness and error rates of the results are verified. The method often involved in resolving conflicts is the line scheduling algorithm. It mainly includes the application of analyzing wireless sensor networks to model the interaction between players with conflicting interests. To compete for limited network resources such as energy and bandwidth. as shown in Figure 2.

2.3. Joint Transmission of Information and Power. The battery capacity of wireless information and power combined transmission sensor equipment is limited. In order to save

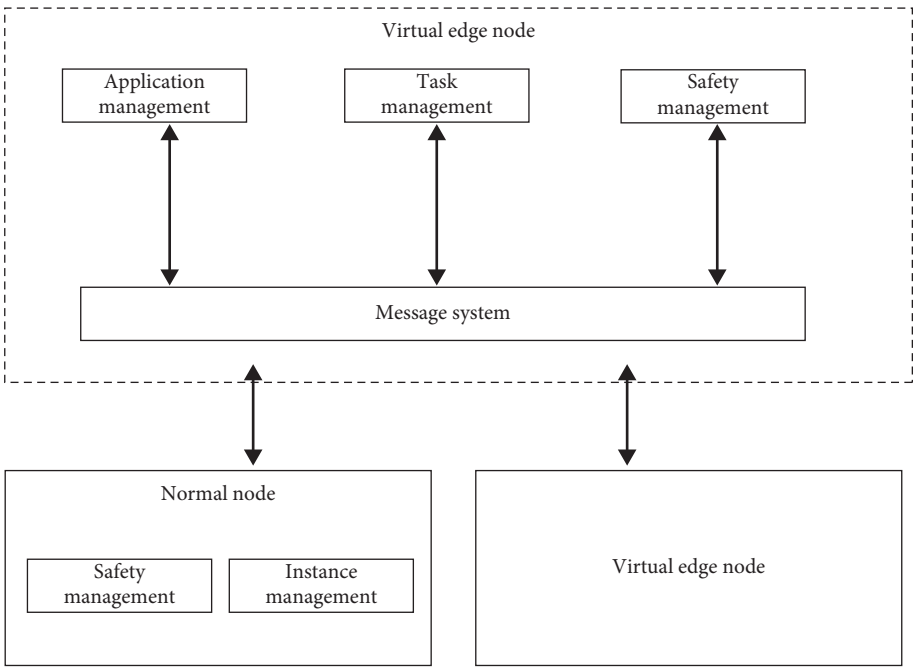

Figure 1: Architecture of dynamic secure collaborative computing method under VECA.

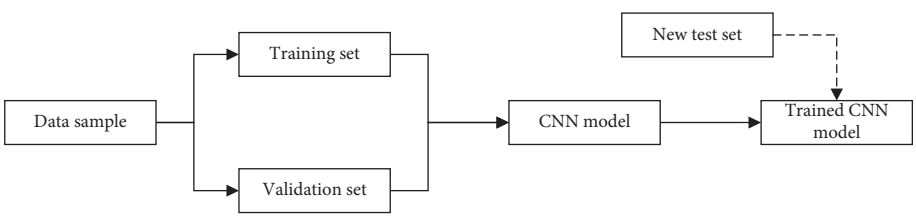

Figure 2: CNN training test.

costs and facilitate the distribution of its battery capacity, the battery capacity is usually relatively small, and it is inconvenient to replace the battery, which may be dangerous, costly, and sometimes not feasible. In the natural environment, energy exists in many forms, is widely distributed, and has infinite supply. It can be obtained, developed and utilized in large quantities without any extra effort. However, the implementation of energy harvesting technology is not simple. In order to effectively convert energy and effectively use energy, many factors need to be considered. Since each dimension is separated in the modeling process, it is difficult to generalize a learned dynamic system to other different shapes of motion. The stability estimation of dynamic system (SEDS) method is to ensure the robustness of the controller to spatial disturbances by learning a stable dynamic system from human teaching. SEDS uses Gaussian mixture model to model the motion, and ensures the global asymptotic stability of the dynamic system by introducing stability constraints derived from the Lyapunov function. The SEDS method provides a theoretical framework to ensure the global asymptotic stability of the learning dynamic system. This method has certain reference significance for solving the robustness problem of the nonlinear dynamic system.

3. Application of IoT Technology in Smart Robots

3.1. FPP-SCA [16–19]. Information dissemination from the destination node to the nodes in its neighborhood

$$X_j = X_i + \text{visual} * \text{rand}(). \tag{1}$$

CDN system

$$\begin{aligned} X_i^+ &= X_i + \text{rand}() * \text{step} * \frac{X_j - X_i}{\left\| X_j - X_i \right\|}, \\ X_i^+ &= X_i + \text{rand}() * \text{step} * \frac{X_m - X_i}{\left\| X_m - X_i \right\|}. \end{aligned} \tag{2}$$

IoT devices

$$\begin{aligned} \text{visual} &= V_{\max} - \frac{V_{\max} - V_{\min}}{i_{\max}} * i, \\ \text{step} &= S_{\max} - \frac{S_{\max} - S_{\min}}{i_{\max}} * i. \end{aligned} \tag{3}$$

Intelligent analysis of IoT data

$$F = \left[\frac{1}{N}\sum_{i}^{N}\sum_{j}^{K}\left(O_{ij} - y_{ij}\right)^2\right]^{-1}. \tag{4}$$

The Internet of Things in the Cloud Computing Center

$$\begin{aligned} \beta &= H_1\left(c_1, c_2, c_3, c_4, c_5, ke\left(h_0, g_3\right)^t\right), \\ CT &= \left\{c_1, c_2, c_3, c_4, c_5, \beta, S, \mathrm{SEnc}_{\mathrm{key}}\left(M\right)\right\}, \\ \mathrm{rct} &= \mathrm{Enc}\left(\mu, S\prime, r, \mathrm{fun}_r\right). \end{aligned} \tag{5}$$

3.2. SNRS [20–23].

$$\begin{aligned} u_{i,r,0} &= g_2^{r_i,r,1}R^{-1}, \\ RK_{i,S\longrightarrow S',r} &= \left\{u_{i,r,-1}, u_{i,r,0}, u_{i,r,1}, \ldots, u_{i,r,n}, \mathrm{rct}, S\right\}. \end{aligned} \tag{6}$$

Robot execution layer

$$\begin{aligned} ID_j &\in S\left(j = 1, 2, \ldots, n\right), \\ c &= \frac{e\left(\prod_{j=1}^{n} u_{i,r,j}, c_2\right)}{c_3^{u_{i,r,-1}} c_4^{f\left(u_{i,r,-1}\right)} e\left(c_1, u_{i,r,0}\right)}. \end{aligned} \tag{7}$$

Hierarchical energy multipath perception

$$CT' = \left\{c_1, c_2, c_3, c_4, c_5, \beta, c_6, \mathrm{rct}, S', \mathrm{SEnc}_{\mathrm{key}}\left(M\right)\right\}. \tag{8}$$

Intelligent sorting

$$\begin{aligned} e\left(h_0, g_3\right)^t &= \frac{e\left(\prod_{j=1}^{n} u_{i,r,j}, c_2\right)}{c_3^{u_{i,r,-1}} c_4^{f\left(u_{i,r,-1}\right)} e\left(c_1, u_{i,r,0}\right)}, \\ \hat{s} &= H_1\left(c_1, c_2, c_3, c_4, e\left(h_0, g_3\right)^t\right), \\ ke\left(h_0, g_3\right)^t &= \frac{c_5}{e\left(h_0, g_3\right)^{\hat{s}}}. \end{aligned} \tag{9}$$

Intelligent management of IoT data

$$\begin{aligned} k &= \frac{ke\left(h_0, g_3\right)^t}{e\left(h_0, g_3\right)^t}, \\ e\left(h_0, g_3\right)^{t_{d-1}} &= \frac{c_6^{d-1}}{e\left(c_1^{d-1}, R_d^{-1}\right)}. \end{aligned} \tag{10}$$

3.3. SDR [24, 25].

$$P_{\mathrm{avg}} = \sum_{i=1}^{N}\frac{C_i V\left(\alpha\right)^2 AF\left(\alpha\right)}{2}. \tag{11}$$

Robot demonstration teaches learning

$$\begin{aligned} M &= \frac{B - \min\left(B\right)}{\max\left(B\right) - \min\left(B\right)}, \\ \mathrm{precision}\left(i\right) &= \frac{\mathrm{TP}_i}{\left(\mathrm{TP}_i + \mathrm{FP}_i\right)}. \end{aligned} \tag{12}$$

Robot trajectory tracking

$$\mathrm{recall}\left(i\right) = \frac{\mathrm{TP}_i}{\left(\mathrm{TP}_i + \mathrm{FN}_i\right)}. \tag{13}$$

Edge computing

$$\begin{aligned} F1 - \mathrm{Score}\left(i\right) &= \frac{2 \times \mathrm{Pr}_i \times \mathrm{Re}_i}{\left(\mathrm{Pr}_i \times \mathrm{Re}_i\right)}, \\ \Phi_B &= \mu \mathrm{NIS} \cos\theta. \end{aligned} \tag{14}$$

Robot teaches from

$$\begin{aligned} &\log f_0\left(e^y\right), \\ &\log f_0\left(e^y\right) \le 0, \quad i = 1, \ldots, m, \\ &\log h_1\left(e^y\right) \le 0, \quad i = 1, \ldots, M, \\ &C = B \times \log_2 \det\left(I_{N_R} + \frac{\mathrm{E}_s HH^H}{N_0}\right). \end{aligned} \tag{15}$$

4. Simulation Experiment

4.1. Edge Computing. The research work of edge computing revolves around data downlink services. A set of edge video CDN system is designed, in the G1 data set $A = 9$, $p = 9$, $\mathbb{Z}\mathrm{p} = 9$, $l\mathbb{Z}\mathrm{p} = 8$, AES = 5, ES = 9. Distribute some hot content to public wireless hotspots closer to users in advance, $A = 9$, $p = 7$, $\mathbb{Z}\mathrm{p} = 9$, $l\mathbb{Z}\mathrm{p} = 9$, AES = 9, ES = 8. At present, a large amount of research is mainly to deploy an edge node between the end node of the Internet of Things and the cloud computing center to provide high-quality services. As shown in Table 1 and Figure 3.

4.2. TSP Algorithm. Regarding the multi-route IoT nested non-cooperative problem, even if it is not a large-scale network individual, it may be selfish. The number of variables is also very large, and the solution is in the best interest. It is very difficult to directly deviate from the established solution. The conversion to the energy-constrained TSP algorithm is to convert the refusal forwarding mTSP into the standard freight forwarding dilemma TSP, which can solve the pure strategy set Si and the revenue function μi. The algorithm designed for TSP can solve it by deviating from the Nash equilibrium. The basic parameter variables are shown in Table 2 and Figure 4.

4.3. Data Values of Different Scenarios. Energy model In order to effectively complete the data transmission and charging tasks of the sensor node, the mobile node needs to reach the sensor node for energy replenishment before the

Table 1: Edge computing.

	A	p	$\mathbb{Z}$p	$l\mathbb{Z}$p	AES	ES
$\mathbb{G}1$	9	9	9	8	5	9
$\mathbb{G}2$	7	9	10	6	9	6
$\mathbb{G}T$	6	8	10	5	7	8
$l\mathbb{G}1$	5	10	5	8	9	8
$l\mathbb{G}2$	8	7	10	10	8	7
$l\mathbb{G}$	9	7	9	9	9	8

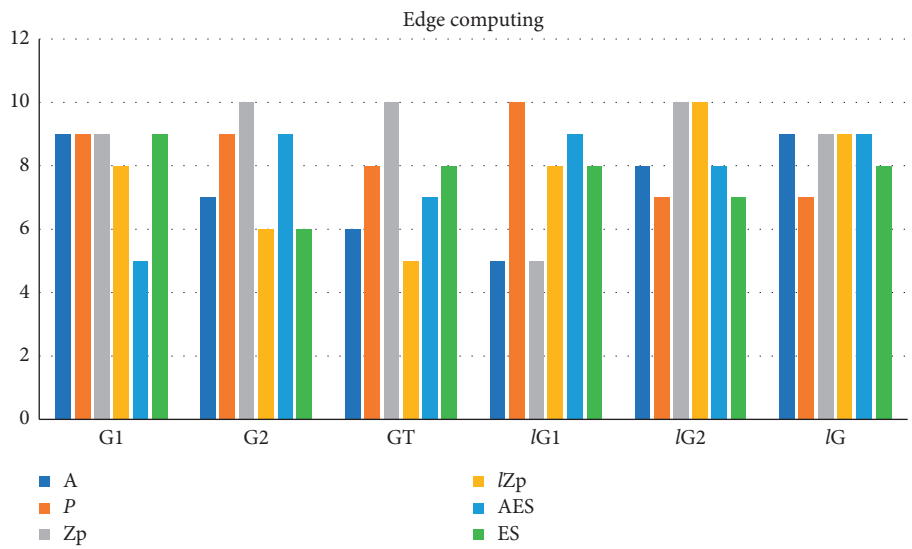

Figure 3: Edge computing.

Table 2: TSP algorithm.

	System	Participants	Architecture	Confidential computing	Dynamic task unloading	Automatic expansion
Cloud	18	17	18	10	17	19
Edge	15	14	13	12	19	17
End	14	13	10	11	18	15
PaaS	15	15	14	12	13	11
IaaS	20	12	10	19	10	10

sensor node does not have enough power to continue working. In the FPP-SCA scheme, $\beta = 0.3$ SNRs is 0.21, $\beta = 0.5$ SNRs is 0.29, $\beta = 0.7$ SNRs is 0.19, $\beta = 0.3$ SNRs is 0.08, $\beta = 0.5$ SNRs is 0.79, $\beta = 0.7$ SNRs is 0.89. When a sensor node receives a beacon signal from a mobile node in the distance-based energy loss model, according to the strength of the beacon signal, the distance required for the sensor node to send data to the mobile node can be estimated. When $\beta = 0.3$, the SNRs is 0.77, When $\beta = 0.5$, SNRs is 0.71, when $\beta = 0.7$, SNRs is 0.63, when $\beta = 0.3$, SNRs is 0.3, when $\beta = 0.5$, SNRs is 0.79, and when $\beta = 0.7$, SNRs is 0.68. As shown in Table 3 and Figure 5.

The location of sensor nodes can be known in advance. Independent scheme, FPP-SCA scheme, low-complexity scheme, SDR scheme. These nodes are used as relays to collect the information monitored by the static nodes and charge these sensor nodes. In the independent scheme, $S = 0$, ID = 1.51, $S = 5$, ID = 1.47, $S = 10$, ID = 1.98, $S = 15$, ID = 1.92, $S = 20$, ID = 1.77, $S = 25$, ID = 1.09. By learning a stable dynamic system from human teaching to ensure the robustness of the controller to spatial disturbances. FPP-SCA scheme FPP-SCA = 1.99, FPP-SCA = 1.86, FPP-SCA = 1.03, FPP-SCA = 1.18, FPP-SCA = 1.01, FPP-SCA = 1.46, FPP-SCA = 1.61. As shown in Table 4 and Figure 6.

4.4. Model Comparison. Comparing the independent scheme, FPP-SCA scheme, low complexity scheme, and SDR, it is found that the global asymptotic stability can ensure that the system responds appropriately and quickly to the disturbances that the robot may encounter during the movement. More and more robots work in unstructured environments, with different scenarios and tasks. The comparison shows that the FPP-SCA scheme is the optimal model F-S0 = 2.52, F-S5 = 2.38, F-S10 = 2.5, F-S15 = 2.09, F-S20 = 2.54, F-S25 = 2.8, F-S30 = 2.98. As shown in Table 5 and Figure 7.

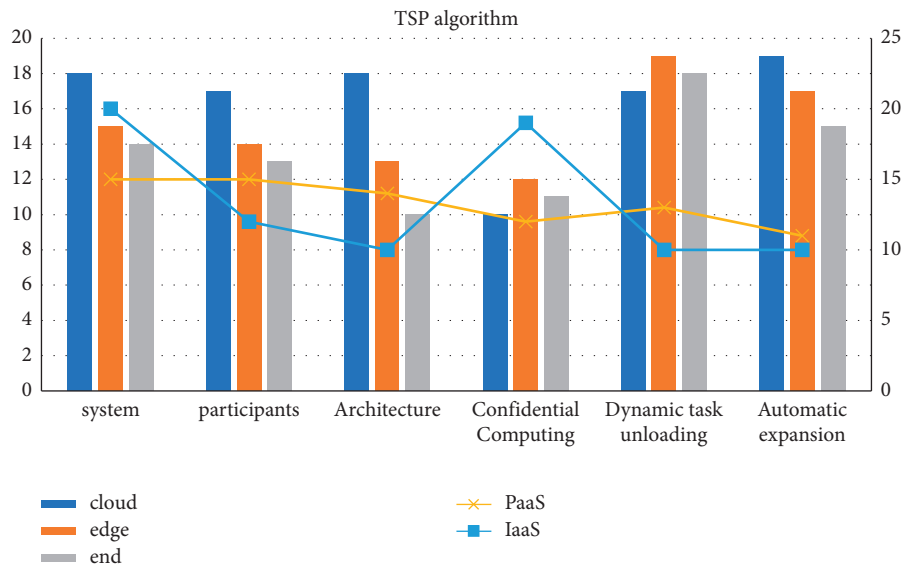

Figure 4: TSP algorithm.

Table 3: Data values of different schemes.

	FPP-SCA program			Low-complexity solution		
SNRS(dB)	$\beta = 0.3$	$\beta = 0.5$	$\beta = 0.7$	$\beta = 0.3$	$\beta = 0.5$	$\beta = 0.7$
0	0.21	0.29	0.19	0.08	0.79	0.89
5	0.02	0.97	0.27	0.30	0.80	0.44
10	0.60	0.06	0.37	0.15	0.66	0.30
15	1.00	0.47	0.31	0.20	0.42	0.15
20	0.12	0.36	0.63	0.09	0.24	0.22
25	0.21	0.42	0.59	0.76	0.03	0.30
30	0.77	0.71	0.63	0.30	0.79	0.68

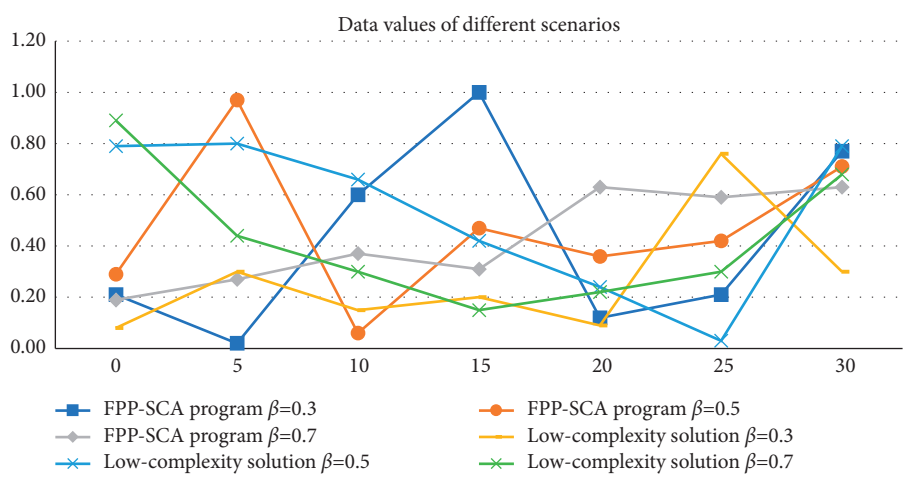

Figure 5: Data values of different scenarios.

Robots need to master new skills frequently and quickly. Therefore, the learning speed of the algorithm is also an important evaluation index for the study of teaching learning algorithms. Fast learning algorithms can make sports learning more efficient. In the FPP-SCA scheme model, AM, $N = 0.99$, BM, $N = 1.99$, CM, $N = 0.58$, DM, $N = 0.55$, EM, $N = 1.92$, FM, $N = 1.82$. The FPP-SCA project model uses dynamic motion primitives to improve the accuracy of DMP modeling. An autonomous dynamic system model of human motion is established,

Table 4: Sensor nodes.

SNRS(dB)	Independent program	FPP-SCA program	Low-complexity solution	SDR solution
0	1.51	1.99	1.72	1.66
5	1.47	1.86	1.42	1.08
10	1.98	1.03	1.74	1.34
15	1.92	1.18	1.10	1.47
20	1.77	1.01	1.19	1.77
25	1.09	1.46	1.06	1.26
30	1.72	1.61	1.21	1.70

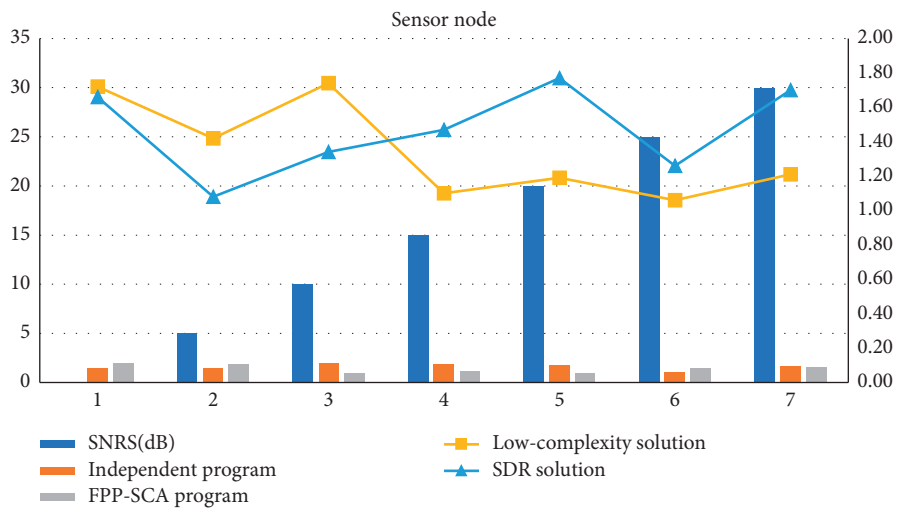

Figure 6: Sensor node.

Table 5: Model comparison.

SNRS(dB)	Independent program	FPP-SCA program	Low-complexity solution	SDR solution
0	2.66	2.52	2.31	2.57
5	2.69	2.38	2.59	2.46
10	2.28	2.50	2.88	2.82
15	2.97	2.09	2.51	2.56
20	2.09	2.54	2.22	2.88
25	2.18	2.80	2.30	2.12
30	2.09	2.98	2.71	2.88

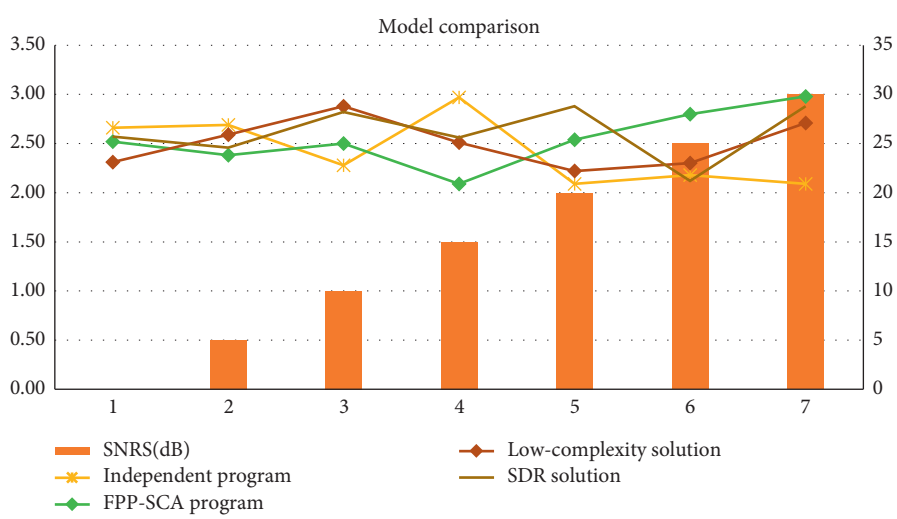

Figure 7: Model comparison.

Table 6: Simulation experiment data.

SNRS(dB)	FPP-SCA program			Low-complexity solution		
	$A^{M,N}$	$B^{M,N}$	$C^{M,N}$	$D^{M,N}$	$E^{M,N}$	$F^{M,N}$
0	0.99	1.99	0.58	0.55	1.92	1.82
5	1.21	0.85	0.91	1.44	0.26	1.25
10	0.88	1.77	0.34	0.71	1.75	0.89
15	0.84	0.11	0.10	1.59	1.87	0.38
20	1.12	1.01	0.40	1.28	1.87	1.32
25	0.75	0.88	1.14	0.23	1.69	1.87
30	1.30	0.00	1.16	1.33	1.45	1.24

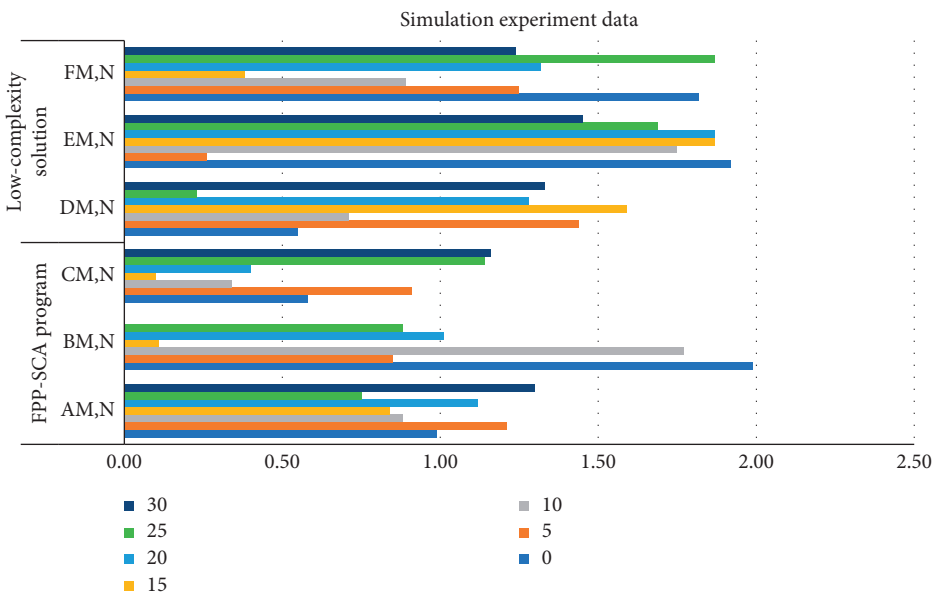

Figure 8: Simulated experimental data.

and stability is achieved through a combination of linear and nonlinear dynamic systems. The dimensions of low complexity algorithms are all separated, AM, $N = 1.3$, BM, $N = 0$, CM, $N = 1.16$, DM, $N = 1.33$, EM, $N = 1.45$, FM, $N = 1.24$. As shown in Table 6 and Figure 8.

5. Conclusion

This research uses Auto-ID Labs radio frequency identification system to realize the information dissemination from the destination node to the nodes in its neighborhood. The purpose is to forward messages and explore typical applications. Realize the intelligent analysis and management of IoT devices and data.

Design a set of edge video CDN system, in the G1 data set $A = 9$, $p = 9$, $\mathbb{Z}p = 9$, $l\mathbb{Z}p = 8$, AES = 5, ES = 9. Distribute some hot content to public wireless hotspots closer to users in advance, $A = 9$, $p = 7$, $\mathbb{Z}p = 9$, $l\mathbb{Z}p = 9$, AES = 9, ES = 8. At present, a large amount of research is mainly to deploy an edge node between the end node of the Internet of Things and the cloud computing center to provide high-quality services.

Data Availability

The experimental data used to support the findings of this study are available from the corresponding author upon request.

Conflicts of Interest

The authors declare that they have no conflicts of interest regarding this work.

References

[1] Y. J. Choi, Y. W. Lee, and B. G. Kim, "Residual-based graph convolutional network for emotion recognition in conversation for smart internet of things," *Big Data*, vol. 9, no. 4, pp. 279–288, 2021.

[2] C. Liao and L. Nong, "Smart city sports tourism integration based on 5G network and internet of things," *Microprocessors and Microsystems*, Article ID 103971, 2021.

[3] H. Yu, L. T. Yang, X. Fan, and Q. Zhang, "A deep residual computation model for heterogeneous data learning in smart Internet of Things," *Applied Soft Computing*, vol. 107, no. 5, Article ID 107361, 2021.

[4] N. Tariq, F. A. Khan, and M. Asim, "Security challenges and requirements for smart internet of things applications: a comprehensive analysis," *Procedia Computer Science*, vol. 191, no. 1, pp. 425–430, 2021.

[5] T. Ahmad and D. Zhang, "Using the internet of things in smart energy systems and networks," *Sustainable Cities and Society*, vol. 68, no. 1, Article ID 102783, 2021.

[6] S. Ju, Y. Sun, and Y. Su, "Internet of things smart medical system and nursing intervention of glucocorticoid drug use," *Microprocessors and Microsystems*, vol. 83, no. 3, Article ID 104008, 2021.

[7] Z. Akhavan, M. Esmaeili, D. Sikeridis, and M. Devetsikiotis, "Internet of things-enabled passive contact tracing in smart cities," *Internet of Things*, no. 1533, Article ID 100397, 2021.

[8] L. Ferretti, F. Longo, G. Merlino, M. Colajanni, A. Puliafito, and N. Tapas, "Verifiable and auditable authorizations for smart industries and industrial Internet-of-Things," *Journal of Information Security and Applications*, vol. 59, Article ID 102848, 2021.

[9] X. Zhao, H. Askari, and J. Chen, "Nanogenerators for smart cities in the era of 5G and Internet of Things," *Joule*, vol. 5, no. 6, 2021.

[10] K Peng, M Li, H Huang, C. Wang, and S. Wan, "Security challenges and opportunities for smart contracts in internet of things: a survey," *IEEE Internet of Things Journal*, vol. 8, no. 99, p. 1, 2021.

[11] A. Gehlot, S. S. Alshamrani, R. Singh, and M. Rashid, "Internet of things and long-range-based smart lampposts for illuminating smart cities," *Sustainability*, vol. 13, no. 11, 2021.

[12] P. Spachos, I. Papapanagiotou, and K. Plataniotis, "Micro-location for smart buildings in the era of the internet of things: a survey of technologies," *Techniques, and Approaches*, vol. 83, no. 3, pp. 10–28, 2021.

[13] S. Nižetić, Š. Petar, and L. P. Diego López-de-Ipiña González-de, "Internet of Things (IoT): opportunities, issues and challenges towards a smart and sustainable future," *Journal of Cleaner Production*, vol. 274, Article ID 122877, 2020.

[14] U. Pujaria, P. Patil, N. Bahadure, and M. Asnodkar, "Internet of things based integrated smart home automation system," in *Proceedings of the 2nd International Conference on Communication & Information Processing (ICCIP)*, Tokyo, Japan, May 2020.

[15] M. H. Kabir, "Convergence platform of cloud computing and internet of things (IoT) for smart healthcare application," *Journal of Computer and Communications*, vol. 8, no. 8, pp. 15–28, 2020.

[16] C. Morgan, "Can smart cities Be environmentally sustainable? Urban big data analytics and the citizen-driven internet of things," *Geopolitics, History, and International Relations*, vol. 12, 2020.

[17] M. Beshley, N. Kryvinska, M. Seliuchenko, and M. Beshley, "End-to-End QoS "smart queue" management algorithms and traffic prioritization mechanisms for narrow-band internet of things services in 4G/5G networks," *Sensors*, vol. 20, no. 8, 2020.

[18] S. Din and A. Paul, "RETRACTED: erratum to "Smart health monitoring and management system: toward autonomous wearable sensing for Internet of Things using big data analytics [Future Gener. Comput. Syst. 91 (2019) 611-619]," *Future Generation Computer Systems*, vol. 108, pp. 1350–1359, 2020.

[19] A Nathoo, G Bekaroo, T Gangabissoon, and A. Santokhee, "Using tangible user interfaces for teaching concepts of internet of things: usability and learning effectiveness," *Interactive Technology and Smart Education*, vol. 17, 2020.

[20] E. A. Wilhelm, "Smart learning ecosystem design for delivering data-driven thinking in STEM education," *Smart Learning Environments*, vol. 8, 2021.

[21] T. Lim, C. S. Ong, H. P. Tan, and R. Belani, "Designing a smart internet of things solution for point of use water filtration management system in residential, commercial and public settings," *Test Engineering and Management*, vol. 83, pp. 12561–12568, 2020.

[22] F. Zafar, A. Khan, A. Anjum, C. Maple, and M. A. Shah, "Location proof systems for smart internet of things: requirements, taxonomy, and comparative analysis," *Electronics*, vol. 9, no. 11, p. 1776, 2020.

[23] M. M. Khan, M. Fahim, A. A. Habibullah, N. Tabassum, and A. Sarker, "Research and development of a smart internet-of-things–based system to monitor and prevent household gas wastage," *Multidisciplinary Digital Publishing Institute P*, vol. 67, no. 23, pp. 12–18, 2020.

[24] A. O. Almagrabi, "A pervasive controlled access with privacy delegation design for smart internet of things applications," *Measurement*, vol. 172, no. 2, Article ID 108875, 2020.

[25] W. Choi, J. Kim, S. Lee, and E. Park, "Smart home and internet of things: a bibliometric study," *Journal of Cleaner Production*, vol. 301, Article ID 126908, 2021.

Hindawi
Computational Intelligence and Neuroscience
Volume 2022, Article ID 7153260, 9 pages
https://doi.org/10.1155/2022/7153260

Research Article

Construction of Enterprise Financial Information Intelligent Processing Innovation Model Based on Internet of Things Technology

Mei Ding

Zhushan College, Qingdao Huanghai University, Qingdao, Shandong 266427, China

Correspondence should be addressed to Mei Ding; dingm@qdhhc.edu.cn

Received 28 February 2022; Revised 17 March 2022; Accepted 2 April 2022; Published 6 May 2022

Academic Editor: Guobin Chen

The application of Internet of Things technology provides conditions for the systematization of enterprise financial data and the intellectualization of financial management. In this study, support vector machine (SVM) algorithm and genetic algorithm (GA) are combined to obtain the innovation model of enterprise financial information intelligent processing based on GA-SVM optimization algorithm. Nine factors affecting enterprise financial information processing from 2010 to 2018 are selected as influencing factors, and according to the idea and method of data modeling, the simulation experiment of enterprise financial information intelligent processing model is carried out with MATLAB. The results show that the average fitness of GA-SVM is close to the best fitness, indicating that each individual in the population is near the optimal solution. The RMSE of GA-SVM is 0.35%, and the root mean square error obtained is greater than this value, which shows that the application effect of GA-SVM is significantly better than that of SVM using cross validation method, and it is more suitable for precision prediction. At the same time, it also reflects that the optimization of SVM parameters by GA is reliable. The algorithm can be better applied in the intelligent processing of enterprise financial information and can provide a certain reference for enterprises in the financial management based on the Internet of Things.

1. Introduction

With the development trend of China's market economy in full swing, the Internet of Things technology has developed rapidly and has become one of the key technologies applied by various enterprises [1]. The development of enterprises is inseparable from advanced technology, especially the financial management of enterprises [2]. In the era of Internet of Things, enterprise financial information management has become the key to enterprise development. Enterprises must update traditional concepts and make full use of advanced Internet of Things technology in order to effectively complete financial management [3]. The Internet of Things is a system based on the Internet, which realizes the connection between things and realizes monitoring at any time through modern radio frequency identification, infrared induction, and wireless communication technologies [4]. Internet of Things technology is widely used in major industries, which can effectively supervise enterprise financial information, realize the whole process management of enterprise financial information, make enterprise financial information processing more efficient, timely, and reliable, and finally improve the efficiency of enterprise financial management [5].

For the innovation model of enterprise financial information intelligent processing, this research combines the related technologies of genetic algorithm (GA) and support vector machine (SVM), introduces the genetic algorithm GA into the SVM parameters of support vector machine, and constructs the innovation model of enterprise financial information intelligent processing according to the idea and method of data modeling. Finally, MATLAB is used for simulation experiment.

This study mainly adopts the combination of research methods and simulation experiments, takes the idea of

system engineering and complexity theory as the direction, extracts the data affecting enterprise financial information processing from 2010 to 2018, adopts the method of normalized data, and constructs the innovation model of enterprise financial information intelligent processing according to the idea and method of data modeling, The purpose is to improve the operation speed of the model and ensure the accuracy of the system.

The research content of this paper mainly includes four parts. The second part is the research status of genetic algorithm (GA-SVM) for support vector machine optimization at home and abroad. The third part mainly introduces the research algorithm. The first section describes the design of GA-SVM algorithm, and the second section discusses the implementation of GA-SVM algorithm. The fourth part preprocesses the influencing factors, empirically analyzes the GA-SVM algorithm, and compares the results with the traditional SVM algorithm. The results show that the application effect of GA-SVM is significantly better than that of SVM using cross validation method, and it is more suitable for precision prediction.

2. Related Works

In recent years, Internet of Things technology has been applied more and more in enterprise financial information processing, and researchers at home and abroad have also conducted in-depth research on this technology. Luthra et al. used grey relational analysis (GRA) and analytic hierarchy process (AHP) to analyze the challenges faced by the adoption and diffusion of the Internet of Things in India, so as to help practitioners and decision makers remove the obstacles to the successful adoption and promotion of the Internet of Things [6]. Wang R and others designed a new inventory pledge financing mode according to the special functions of Internet of Things technology and the business process of inventory financing mode. The results show that the risk loss value gap caused by various loss events in the Internet of Things combined with supply chain financial inventory pledge financing mode is large, among which the external fraud loss is the largest. Finally, it is found that the supply chain financing mode based on Internet of Things technology effectively reduces the operational risk [7]. Lopez BS and others analyzed the impact of artificial intelligence and Internet of Things technology on the change of business process management system. The Internet of Things allows you to deliver information, improve control and automation, and provide opportunities to optimize your company's operating costs [8]. Wen C. and others use distributed search engine technology to customize the web crawler to obtain the required bank card and transaction data from the multisource heterogeneous data of the Internet of Things financial industry, design the corresponding spark parallel algorithm to preprocess the data, and establish the inverted table and secondary index document, which provides a data source for the big data analysis platform. The results show that this method can significantly reduce the probability of banks formulating the first and second error rates and effectively reduce the losses caused by improper credit regulations when evaluating the credit risk of Internet of Things financial financing [9].

Genetic support vector machine algorithm (GA-SVM) has been highly valued by many relevant professionals. Dayma A. et al. proposed a content-based image retrieval system based on genetic support vector machine algorithm (GA-SVM). Users retrieve images by sending query images, extract visual features to retrieve query images, and implement it in MATLAB environment to verify the superiority of performance [10]. Yang et al. used GA-SVM to analyze the dissolved oxygen fault of water quality monitoring system. The results show that the optimized values of penalty coefficient and parameters after iteration are 2.1649 and 5.3312, respectively, and GA-SVM has good accuracy [11]. Yin et al. proposed a symbol detection method based on GA-SVM to deal with this problem from different angles and transformed the symbol decoding process into a numerical calculation process. The results show that compared with the traditional method of calculating threshold decoding symbols, GA-SVM improves the bit error rate (BER) performance of CBWCS, simplifies the symbol detection process, and eliminates the process of channel identification and threshold calculation [12]. Zhaia et al. proposed a hybrid method combining genetic algorithm (GA) and support vector machine (SVM). Genetic algorithm is used to mine key factors, and support vector machine is used to calculate the fitness function of genetic algorithm. Using the survey data of China Aviation Industry Corporation (AVIC), the effectiveness of the proposed hybrid method is experimentally analyzed. The experimental results show that the hybrid genetic support vector machine method proposed in this paper can be used as an alternative to the exploration of key factors [13]. Through the research of domestic and foreign scholars on genetic algorithm and support vector machine, it can be seen that the research method of combining genetic algorithm and support variable machine is the main research direction in the future. Therefore, this study mainly discusses the establishment of enterprise financial information intelligent processing innovation model, uses GA-SVM model algorithm to evaluate the processing of enterprise financial information, and uses MATLAB software to simulate and verify the algorithm.

3. Intelligent Financial Information Processing Model Based on GA-SVM Optimization Algorithm

3.1. GA-SVM Optimization Algorithm. Support vector machine can find the best scheme between learning ability and complexity according to the model with limited sample information, so as to obtain the minimum confidence range and empirical risk and obtain better generalization ability and statistical law when the statistical samples are incomplete [14]. Support vector machine (SVM) is a two-class classification model. Its basic model is the linear classifier with the largest interval defined in the feature space. Support vector machine also includes kernel technique, which makes it an essentially nonlinear classifier. The learning strategy of

support vector machine is interval maximization, which can be formalized as a problem of solving convex quadratic programming, which is also equivalent to the minimization of regularized hinge loss function. The learning algorithm of support vector machine is an optimization algorithm for solving convex quadratic programming. The training of SVM needs to train the optimization of a quadratic programming. If the data capacity is large, it will cause a very large amount of computation of SVM [15]. If the training data is simply reduced, it will not only have a great impact on the accuracy and training effect of the classifier, but also affect the selection of parameters. The index selection of kernel function and penalty function also affects the prediction accuracy and model classification. Generally, the parameter indexes are continuously selected artificially and through repeated experiments, but human experience will cause certain subjectivity of the experiment and high time cost. The traditional support vector machine design process [16] is shown in Figure 1.

In this study, the parameter selection and kernel function of SVM are optimized by GA. The potential parallelism and global optimality of GA are not available in traditional algorithms. The implementation steps of GA are shown in Figure 2 [17]. This study uses the advantages of GA, proposes an improved method of SVM algorithm, and establishes a new GA-SVM algorithm model. The kernel function of GA-SVM takes the radial basis function, the model parameters are globally optimized and genetically coded by the real number coding method, and the final model parameters of GA-SVM adopt the searched optimal kernel parameter and penalty parameter C [18].

The specific ideas of GA-SVM model design are as follows: firstly, encode the parameters of SVM model. The process of finding the optimal kernel parameter and penalty parameter C is a complex parameter continuous optimization problem. In this study, the real number coding method is adopted to avoid repeated coding and decoding in the operation process. It can also solve the problem of limited binary coding length, so as to improve the accuracy and performance of genetic algorithm. If the penalty parameter C is large enough, it will lead to "over learning" of the model algorithm. At this time, the SVM model assigns all training samples to categories with large sample size.

SVM, which is based on the principle of structural risk minimization and statistical theory, is selected as a new machine learning method to effectively regress and classify nonlinear and linear data. SVM algorithm includes linear and nonlinear algorithms. When the data in the data set is linearly separable or approximately linearly separable, it maximizes a linear classifier through hard interval or soft interval. When the data set has a nonlinear structure, the nonlinear SVM is learned by maximizing the soft interval and using the kernel technique. For example, given a two-dimensional plane,

$$T = \{(x_1, y_1), (x_2, y_2), \ldots, (x_N, y_N)\}. \tag{1}$$

In (1), $x_i \in R^n$, $y_i\{+1, -1\}$, $i = 1, 2, \ldots, N$ and x_i represent eigenvectors, y_i is the class mark of x_i, and (x_i, y_i) represents sample points. Thus, it is extended to the n-dimensional hyperplane, where B represents the scalar and W represents the weight vector. By adjusting the scalar and weight vector, SVM searches the hyperplane on the side of the largest edge, as follows:

$$\begin{aligned} H_1&: W \cdot X + b \geq 1, y_i = +1, \\ H_2&: W \cdot X + b \leq 1, y_i = -1. \end{aligned} \tag{2}$$

The sample satisfying the above formula on the hyperplane H_1 or H_2 is the support vector. It is necessary to maximize the spacing and support the hyperplane, so it can be optimized twice, as follows:

$$\min_{W,b} \frac{1}{2}\|W\|^2, \tag{3}$$

$$y_i(W \cdot x_i + b) \geq 1, \quad i = 1, 2, \ldots, N. \tag{4}$$

The optimal solutions W^* and b^* can be obtained from (4), and the linear separable SVM and separation hyperplane can be obtained, as follows:

$$W^* \cdot x + b^* = 0. \tag{5}$$

Separate the decision function, as follows:

$$f(x) = \operatorname{sign}(W^* \cdot x + b^*). \tag{6}$$

If the decision data set is not linearly separable, there are two cases: linear approximate separability and nonlinear. When the data is linearly separable, the relaxation variable ξ_i needs to be introduced to make it reach the "separable" state, and the quadratic optimization representation is shown as follows:

$$\min_{W,b,\xi} \frac{1}{2}\|W\|^2 + C\sum_{i=1}^{N} \xi i, \tag{7}$$

$$y_i(W \cdot x_i + b) \geq 1 - \xi, \quad i = 1, 2, \ldots, N. \tag{8}$$

Among them, $\xi_i \geq 0$, $i = 1, 2, \ldots, N$. The optimal solution is obtained. The separation hyperplane and the separation decision function are shown in the following equations:

$$W^* \cdot x + b^* = 0, \tag{9}$$

$$f(x) = \operatorname{sign}(W^* \cdot x + b^*). \tag{10}$$

For the nonlinear data set, it needs to be transformed into a linear problem in the high-dimensional feature space for solution. The kernel function is used to replace the instance inner product in the nonlinear classification, the kernel function $K(x, z) = \phi(x) \cdot \phi(z)$. Accordingly, the obtained nonlinear SVM is shown in the following equation:

$$f(x) = \operatorname{sign}\left(\sum_{i=1}^{N} \alpha_i^* y_i K(x, x_i) + b^*\right). \tag{11}$$

The radial basis kernel function (RBF) is shown in the following equation:

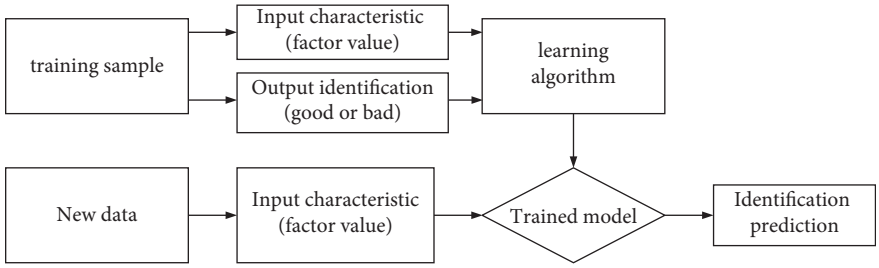

Figure 1: Traditional SVM design process.

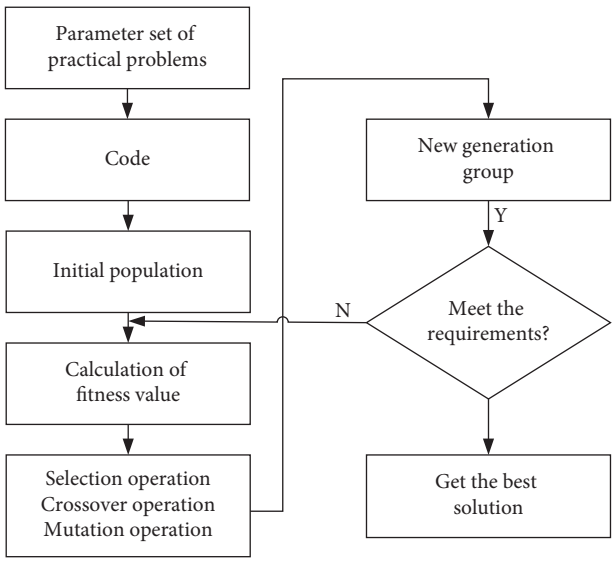

Figure 2: Implementation steps of genetic algorithm.

$$K(x, x') = \exp\left(\frac{\|x - x'\|^2}{2\sigma^2}\right). \tag{12}$$

In (12), $K(x, x')$ represents the radial basis kernel function, x and x' are two training points, and σ represents the kernel function, that is, the width in the function direction, the mean square deviation of the Gaussian function, and the σ value directly proportional to the function width.

Through the experimental verification of RBF kernel function, it can be seen that the value of σ has a close correlation with $\|x - x'\|^2$. If the minimum distance between training samples is much larger than σ, $\sigma \longrightarrow 0$. If the minimum distance between training samples is much smaller than the σ value, then $\sigma \longrightarrow \infty$. This study determines the search space for σ value, with the interval value being $[\min(\|x - x_j\|^2 \times 10^{-2}), \max(\|x - x_j\|^2 \times 10^{-2})]$, and further reduces the search range in this interval to determine a more accurate range.

Penalty coefficient C is mainly used to constrain Lagrange factor A. When the value of penalty coefficient C reaches a certain value, the constraint on a will fail. At this time, the complexity of SVM in data subspace will become the largest, and its generalization ability and empirical risk will not be changed. In this study, a new search method of c-interval is proposed. It can be seen from $0 \le a_l, a_i^* \le C/l; \quad i = 1, 2, \ldots\ldots, l$ that if $C \ge 0$, first select a large enough C, and then apply the SVM model of this value to solve $a_i \quad (i = 1, 2, \ldots\ldots, n)$, where n represents the number of training samples. At this time, if $C_1 = \max(a_i)$ and $C_1 < C$, then the upper bound of C's search boundary is C_1, indicating that a_i is still constrained by C. At this time, a larger capacity C should be selected to support SVM model training until C is much greater than C_1. Therefore, the interval of C search can be confirmed, and the interval is $(0, C_1)$.

Then, the fitness function of genetic algorithm is designed. According to the experimental object of this study, a genetic fitness function is proposed as follows:

$$F(\sigma, C) = \frac{1}{\text{Error}}. \tag{13}$$

In (13), error represents the misclassification rate of the training sample set of SVM model. When the classification error of SVM model on the test sample is higher, the parameter chromosome fitness is smaller. Then, there is genetic operation, which includes selection operation, crossover operation, and mutation operation. The sorting of individuals in the population of the selection operation is carried out according to the fitness, and then the selected probability P_i of individuals is calculated, as shown in the following equation:

$$P_i = r \times (1 - r)^{i-1}. \tag{14}$$

In (14), r represents the selection probability of the first individual, and i represents the individual sorting sequence number. The selection probability has nothing to do with the fitness value, but only with the ranking of individuals in the population. Cross operation is a cross operation mode, which mainly applies the linear combination mode. If x_1 and x_2 chromosomes are crossed, it is shown in the following formula:

$$\begin{cases} x_1 = ax_1 + (1 - a)x_2, \\ x_2 = ax_2 + (1 - a)x_2. \end{cases} \tag{15}$$

In (15), a represents a random number and [0,1]. Mutation operation is to randomly select one of the mutation bits j in the mutated chromosome and transform the mutation bit j into a random number $U(a_i, b_i)$. a_i represents the upper limit of the variation bit, and b_i represents the lower limit of the variation bit, as shown in the following equation:

$$x_j = \begin{cases} U(a_i, b_j), & (i = j), \\ x_i, & (i \neq j). \end{cases} \tag{16}$$

3.2. Construction of Intelligent Processing Model of Enterprise Financial Information. After designing the GA-SVM algorithm, this study proposes an enterprise financial information intelligent processing model based on GA-SVM algorithm. The specific implementation steps are shown in Figure 3. Firstly, the regression model of support vector is designed to determine the values of kernel parameters and penalty coefficients. The individual length of GA is determined, m chromosomes are randomly generated by real number coding, and the initial population $P(t)$ of genetic algorithm is formed. According to the gene sequence, select the selection strategy to combine the factors. The SVM program is used to calculate the individuals in the initial population, find out the predicted value, check whether it corresponds to the sample, calculate the misclassification rate of the test sample, and finally calculate the chromosome individual fitness $F(\sigma, C)$. Repeat operation m times to calculate the fitness value of each individual of the initial population. In order to get the next generation population, crossover, mutation, and selection operators are implemented. The optimal individual is selected and the grid search is carried out near the optimal individual to search the optimal parameter combination. According to the criterion mode of whether the iteration ends or not, if not, continue the iteration and return to recalculate the individual fitness value of chromosome until the conditions are met. Then, the solution of parameter inversion is the optimal individual in the population. The optimal parameter combination, that is, kernel parameters and penalty parameters, is brought into the support vector regression machine program, and a model is created to predict and analyze the data in the sample.

The performance of SVM is determined by the rationality of parameter selection. At present, the conventional method of selecting parameters has great defects, and human factors will lead to the inaccuracy of parameter selection. Using crossover algorithm to select parameters is often accompanied by a huge amount of calculation, and its algorithm is cumbersome. Genetic algorithm has strong search and robust performance and plays a great role in global optimization, which makes the adaptability of genetic algorithm very strong and is widely used in various fields.

After determining the basic data, it is necessary to preprocess the data to increase the accuracy of the model and reduce the prediction error, make the network training faster, and avoid the occurrence of over training. Data normalization is the main work of preprocessing. This operation is to control the data within a certain range by using a certain function or method, such as converting all the data into 0 ~ 1. This operation is mainly to eliminate the differences between training data. In MATLAB, there are the following normalization methods: first, postmnmx, premnmx, mapminmax, tramnmx, and scaleforsvm; second, trastd, poststd, prestd. The third is programming in MATLAB. There are two programming algorithms, namely, the maximum and minimum method and the mean variance method [19]. For the error measurement in the data, this study adopts the root mean square error and relative error analysis method, where RMSE represents the root mean square error and RE represents the relative error [20].

By preprocessing the influencing factors, the GA-SVM algorithm is empirically analyzed and compared with the traditional SVM algorithm. The results show that the application effect of GA-SVM is obviously better than cross validation SVM, and it is more suitable for precision prediction.

4. Experimental Design and Analysis

This study uses the financial data of 132 enterprises in a region in 2019, excluding 30 abnormal data, and the number of effective data samples is 102. The following factors are selected as influencing factors, including accounts receivable turnover rate, operating cash to total debt ratio, return on net assets, quick ratio, current ratio, cost profit ratio, working capital to total assets ratio, main business profit ratio, total asset turnover rate, etc., and the data affecting enterprise financial information processing from 2010 to 2018 are extracted [21, 22].

Firstly, the results and errors of BP neural network prediction are analyzed. It can be seen that the errors are less than 10%, which meets the prediction requirements, as shown in Figure 4(a) [23, 24]. In the analysis of SVM prediction model, the first eight influence factors are used as the input vector, and the ninth influence factor is used as the output vector to establish the SVM model, and the simulation test is carried out on MATLAB [9,25]. The Gaussian radial kernel function is selected as the kernel function predicted in this study, and the parameters of SVM are selected by cross validation. The parameters are $\sigma = 0.02$, $g = 0.105$, $C = 256$. The prediction results are shown in Figure 4(b).

Figure 4(b) shows the prediction results of SVM. Next, this method will be compared with GA-SVM prediction model. For the selection of prediction data of GA-SVM model, the data from 2010 to 2014 are selected as training samples and the data from 2015 to 2019 are selected as test samples to obtain the fitness of optimization parameters of GA, as shown in Figure 5.

The data from 2010 to 2014 are selected as training samples and the data from 2015 to 2019 are selected as test samples to obtain the fitness of GA optimization parameters, as shown in Figure 5. As can be seen from Figure 5, the average fitness is very close to the best fitness, indicating good results. Comparing the prediction results of SVM model and GA-SVM model, the fitting value selects the data from 2010 to 2014, and the prediction value selects the data from 2015 to 2019. The results show that the prediction errors of SVM model and GA-SVM model are very small, both less than 1%, which meet the prediction requirements. The prediction results of SVM model and GA-SVM model are better than BP neural network.

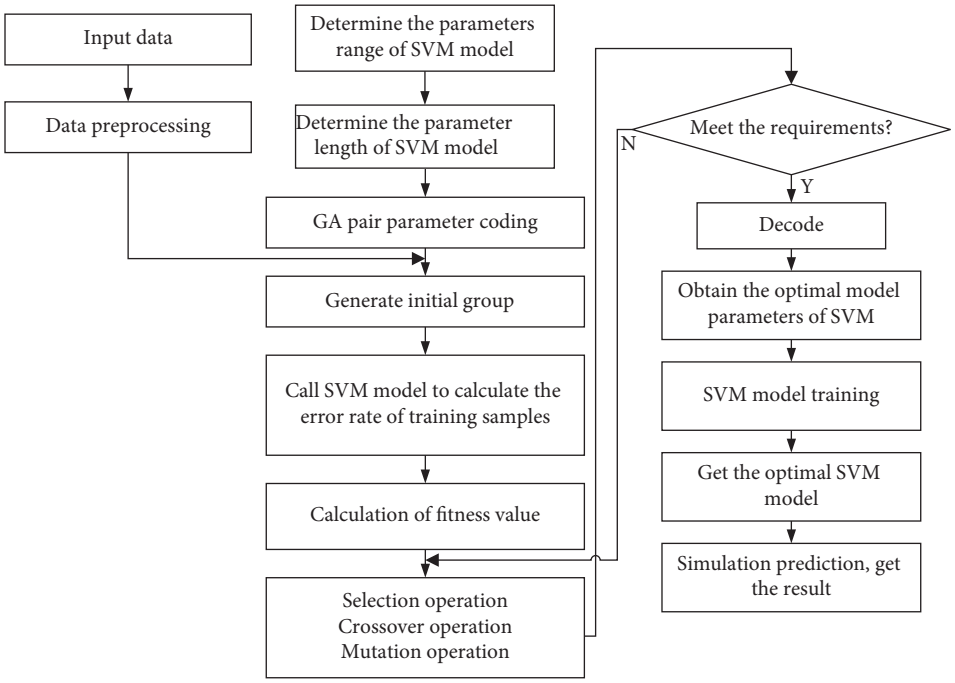

Figure 3: Implementation steps of GA-SVM algorithm.

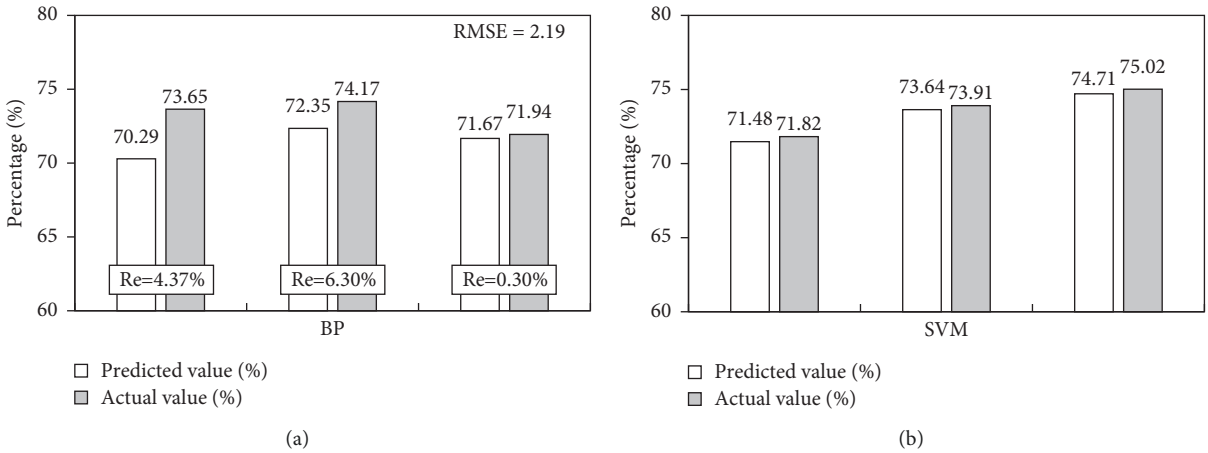

Figure 4: Prediction results and error analysis of BP neural network and SVM. (a) BP neural network. (b) Support vector machine.

The RMSE of GA-SVM is 0.35, and the root mean square error is greater than this value, which shows that the application effect of GA-SVM is obviously better than that of SVM with cross validation method, and it is more suitable for accuracy prediction. At the same time, it also reflects that the genetic algorithm is reliable for the optimization of support vector machine parameters. The error comparison between SVM model and GA-SVM model is shown in Figure 6.

In order to further verify the effectiveness of the model, the factor fat is introduced into the program_ 1, FAT_ 2, and FAT_ 3, the functional relationship between financial security and various factors is mined, and the optimal number of nodes, tree structure diagram, variation evolution and crossover probability change diagram, and fitting optimization diagram of individual algorithm are obtained in the calculation process for simulation and empirical analysis. After the program is simulated, the dynamic change trend of levels, nodes, and goodness of fit of the structure tree is obtained, as shown in Figure 7.

As can be seen from Figure 7, with the increase of genetic algebra, the goodness of fit will continue to improve. However, after 34 generations, the efficiency of evolution began to remain unchanged, and the current optimal individual was recorded, including the number of nodes of the individual structure and the depth of the tree. FAT of all data samples_ 1, FAT_ 2, FAT_ The value of 3 is introduced into the optimal structural calculation to obtain the observation of enterprise financial standards and the fitting of theoretical values, as shown in Figure 8.

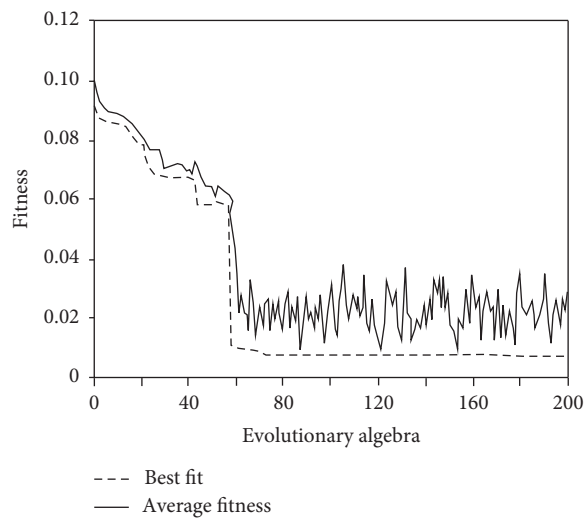

Figure 5: Fitness curve of genetic algorithm optimization.

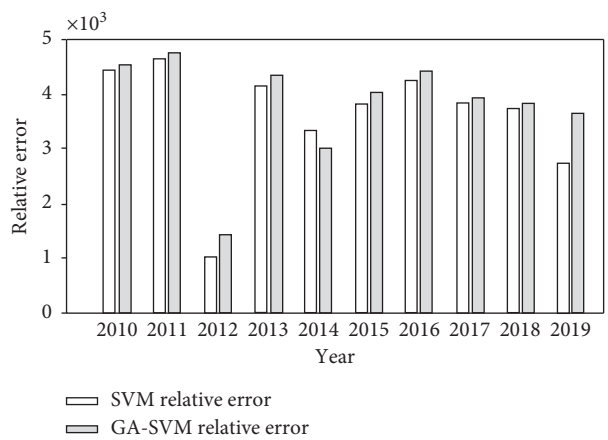

Figure 6: Error effect comparison between GA-SVM and SVM.

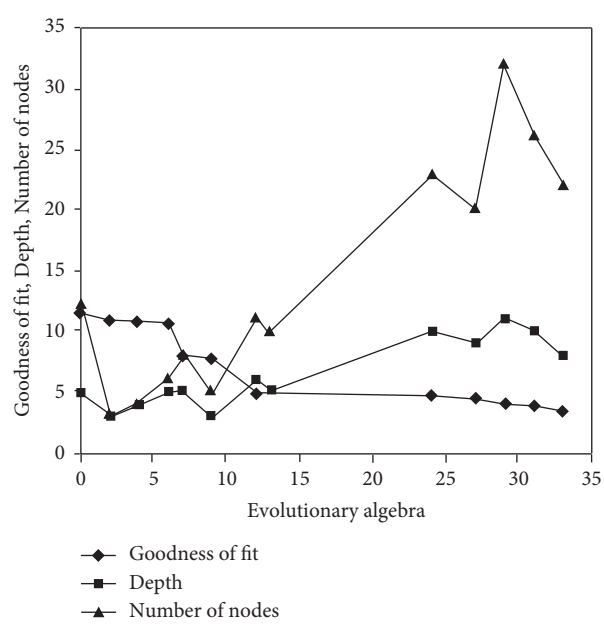

Figure 7: The relationship between fitting degree and tree nodes and layers.

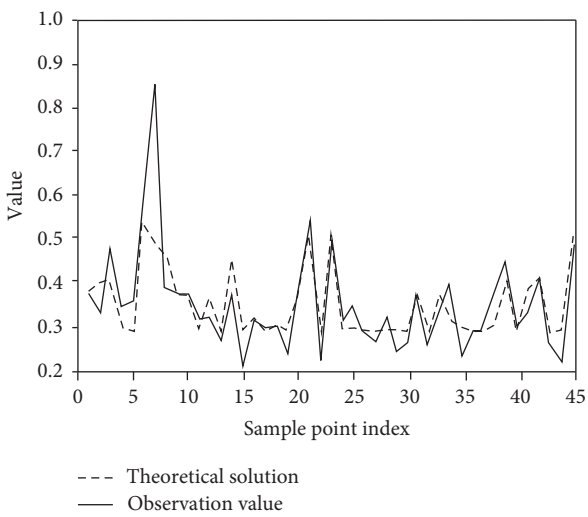

Figure 8: Training sample fitting effect chart.

As can be seen from Figure 8, the evaluation model proposed in this study reflects the ups and downs in the process of financial data processing. Using the model to test the sample data, the accuracy of the model is 87.51%. The experimental results fit the financial data well.

By comparing the prediction results of SVM model and GA-SVM model, the fitting value selects the data from 2010 to 2014, and the prediction value selects the data from 2015 to 2019. The results show that the prediction errors of SVM model and GA-SVM model are very small, both less than 1%, which meet the prediction requirements. The prediction results of GA-BP model and SVM-BP model are better than those of SVM-BP model. This shows that the algorithm has a high practical application in enterprises.

5. Conclusion

In this paper, a GA-SVM optimization algorithm model based on Internet of Things is established for enterprise financial information management, and the simulation experiment is carried out on MATLAB platform. The results show that the Gaussian radial kernel function is selected as the kernel function predicted in this paper, and the parameters of SVM are selected by cross validation. The parameters are = 0.02, $g = 0.105$, $C = 256$. For the selection of prediction data of GA-SVM model, the data from 2010 to 2019 are selected as training samples and the data from 2011 to 2015 are selected as test samples. The value of average fitness of GA-SVM is close to the best fitness, indicating that each individual in the population is near the optimal solution, reflecting the good effect of the algorithm. The RMSE of GA-SVM is 364.062, and the root mean square error obtained is greater than this value, which shows that the application effect of GA-SVM is significantly better than that of SVM using cross validation method, and it is more suitable for precision prediction. At the same time, it also reflects that the optimization of SVM parameters by GA is reliable. This study also has some shortcomings. Due to many influencing factors of enterprise financial management, this study only selects some as the research. In the future research, we will pay more attention to the selection of influencing factors of the model.

Data Availability

The data used to support the findings of this study are available from the corresponding author upon request.

Conflicts of Interest

The author declares that there are no conflicts of interest.

References

[1] C.-P. Tang, T. C.-K. Huang, and S.-T. Wang, "The impact of internet of things implementation on firm performance," *Telematics and Informatics*, vol. 35, no. 7, pp. 2038–2053, 2018.

[2] Y. Cao, "Research on application of the Internet of things technology in financial leasing of intelligent manufacturing enterprises," *International Journal of Advanced Manufacturing Technology*, vol. 107, no. 4, pp. 1061–1070, 2020.

[3] S. Kompella and C. Kam, "Special issue on age of information," *Journal of Communications and Networks*, vol. 21, no. 3, pp. 201–203, 2019.

[4] M. Kim, W. Jo, J. Kim, and T. Shon, "Visualization for internet of things: power system and financial network cases," *Multimedia Tools and Applications*, vol. 78, no. 3, pp. 3241–3265, 2018.

[5] X. Zhang and Y. Wang, "Research on prepaid account financing model based on embedded system and internet of things," *Microprocessors and Microsystems*, vol. 82, no. VI, Article ID 103935, 2021.

[6] S. Luthra, D. Garg, S. K. Mangla, and Y. P. Singh Berwal, "Analyzing challenges to Internet of Things (IoT) adoption and diffusion: an Indian context," *Procedia Computer Science*, vol. 125, pp. 733–739, 2018.

[7] R. Wang, C. Yu, and J. Wang, "Construction of supply chain financial risk management mode based on internet of things," *IEEE Access*, vol. 7, no. 99, pp. 323–332, 2019.

[8] B. S. Lopez and A. V. Alcaide, "Blockchain, artificial intelligence, internet of things to improve governance, financial management and control of crisis: case study COVID-19," *SocioEconomic Challenges*, vol. 4, no. 2, pp. 78–89, 2020.

[9] C. Wen, J. Yang, L. Gan, and Y. Pan, "Big data driven Internet of Things for credit evaluation and early warning in finance," *Future Generation Computer Systems*, vol. 124, no. 4, 2021.

[10] A. Dayma, A. Shrivastava, A. K. Saxena, and M. Manoria, "Support vector machine (linear kernel) and interactive genetic algorithm-based content image retrieval technique," *Lecture Notes in Networks and Systems*, vol. 34, pp. 151–159, 2018.

[11] P. Yang, Z. Li, Z. Li, Y. Yu, J. Shi, and M. Sun, "Studies on fault diagnosis of dissolved oxygen sensor based on GA-SVM," *Mathematical Biosciences and Engineering*, vol. 18, no. 1, pp. 386–399, 2021.

[12] H.-P. Yin and H.-P. Ren, "Direct symbol decoding using GA-SVM in chaotic baseband wireless communication system," *Journal of the Franklin Institute*, vol. 358, no. 12, pp. 6348–6367, 2021.

[13] L. Zhai, J. Qin, and L. Yu, "Hybridizing support vector machines into genetic algorithm for key factor exploration in core competence evaluation of aviation manufacturing enterprises," *Filomat*, vol. 30, no. 15, pp. 4191–4198, 2016.

[14] M. Gholipour, A. Toroghi Haghighat, and M. R. Meybodi, "Hop-by-Hop congestion avoidance in wireless sensor networks based on genetic support vector machine," *Neurocomputing*, vol. 223, pp. 63–76, 2016.

[15] F. Zhu and J. Wei, "Localization algorithm in wireless sensor networks based on improved support vector machine," *Journal of Nanoelectronics and Optoelectronics*, vol. 12, no. 5, pp. 452–459, 2017.

[16] J. Xu, W. Tan, and T. Li, "Predicting fan blade icing by using particle swarm optimization and support vector machine algorithm," *Computers & Electrical Engineering*, vol. 87, no. 1, Article ID 106751, 2020.

[17] P. Panikkath, P. K. Sarkar, and S. Krishnaswamy, "A technique of solving an ill-posed inverse problem of neutron spectrum unfolding using a genetic algorithm search within Monte Carlo iterations," *The European Physical Journal Plus*, vol. 136, no. 4, pp. 1–18, 2021.

[18] P. B. Kumar and D. R. Parhi, "Intelligent hybridization of regression technique with genetic algorithm for navigation of humanoids in complex environments," *Robotica*, vol. 38, no. 4, pp. 565–581, 2020.

[19] J. Gedong, X. Ping, Y. Jun, M. Xuesong, and M. Lei, "Thermal error modeling with dirty and small training sample for the motorized spindle of a precision boring machine," *International Journal of Advanced Manufacturing Technology*, vol. 93, no. 1-4, pp. 571–586, 2017.

[20] M. Jing, C. Long, C. Ke-Li, and H. Be-sheng, "Qualitative and quantitative analysis of amber adulteration using near infrared spectroscopy based on support vector machine," *Journal of Chinese Medicinal Materials*, vol. 40, no. 1, pp. 32–37, 2017.

[21] L. Cleofas-Sánchez, J. S. Sánchez, V. García, and R. M. Valdovinos, "Associative learning on imbalanced environments: an empirical study," *Expert Systems with Applications*, vol. 54, pp. 387–397, 2016.

[22] G. Prenat, K. Jabeur, P. Vanhauwaert, and G. Di Pendi, "Ultra-fast and high-reliability SOT-MRAM: from cache replacement to normally-off computing," *IEEE Transactions on Multi-Scale Computing Systems*, vol. 2, no. 1, pp. 49–60, 2017.

[23] Y. Zelenkov, E. Fedorova, and D. Chekrizov, "Two-step classification method based on genetic algorithm for bankruptcy forecasting," *Expert Systems with Applications*, vol. 88, pp. 393–401, 2017.

[24] I. N. Hanitra, F. Criscuolo, N. Pankratova, S. Carrara, and G. D. Micheli, "Multi-channel front-end for electrochemical sensing of metabolites, drugs, and electrolytes," *IEEE Sensors Journal*, vol. 20, no. 7, p. 1, 2019.

[25] Z. Y. Chen, "Research on financial violations of listed companies based on decision tree and random forest algorithm," *Modern Finance*, vol. 449, no. 7, 2020.

Hindawi
Computational Intelligence and Neuroscience
Volume 2022, Article ID 8193800, 9 pages
https://doi.org/10.1155/2022/8193800

Research Article

Integration Path Analysis of Traditional Media and New Media Based on Internet of Things Data Mining

Yinuo Liu

Liaocheng University, Liaocheng, Shandong 710016, China

Correspondence should be addressed to Yinuo Liu; weijianguo@lcu.edu.cn

Received 9 February 2022; Revised 12 March 2022; Accepted 2 April 2022; Published 6 May 2022

Academic Editor: Guobin Chen

With the development of information technology, the influence of traditional media is weakening day by day. In view of this, based on the Internet of things data mining technology, this study improves the k-means algorithm, and designs a new media precision marketing system, which combines new media with traditional media and provides a new marketing model for traditional media. The results show that the accuracy of the improved k-means algorithm finally reaches about 93%, which is much higher than that of similar algorithms. It can be seen that the improved k-means algorithm has better performance. In the application experiment, this study can effectively find the new media activities with the highest user preference, and the impact of the two websites' application of precision marketing system on users has also increased. It can be seen that the precision marketing system designed this time is more effective.

1. Introduction

The integration of new media and traditional media is an inevitable trend. On the one hand, it is driven by policies. As we all know, in recent years, traditional media have been greatly impacted by new media, resulting in the bankruptcy of paper media and brain drain. Therefore, the state strategically hopes and requires the traditional media to change in time and continue to dominate public opinion. On the other hand, facing the changes of media environment and users' reading and viewing habits, traditional media must also carry out self-revolution and media integration. In the era of mobile Internet, not only new channels, platforms, and products have been added, but people have been changed, demand, and consumption behavior have changed significantly, and the competitive logic of media has evolved.

With the development of modern information technology, the impact of traditional media industry on users is constantly challenged by new media technology. Users prefer fast and online media experience. In the past, the audience and market of traditional media were gradually severely squeezed (peiulis y.2021) [1]. This change in the media ecological environment has greatly weakened the advantages of traditional media such as newspapers, magazines, and television in channels and production resources, making it difficult for them to obtain the first opportunity in terms of real-time and entertainment in the process of new media competition. At the same time, compared with new media, the more institutionalized operation mode of traditional media industry is also lack of flexibility (Topbas b.2021) [2]. Using Internet of things, data mining technology and new media technology can help traditional media make up for their shortcomings and find a more feasible development model in the new media environment.

In order to make up for the shortcomings of traditional media in marketing mode, this study uses Internet of things data mining technology and new media technology to establish a precision marketing system for traditional media. The system is divided into three parts: data processing, business processing, and display system. Internet of things data mining and personalized recommendation are the main processing modules. The design of personalized recommendation module combines collaborative filtering algorithm, while the design of data mining module is based on the improvement of K-means algorithm. Particle swarm optimization algorithm is used to improve the selection

effect of its initial clustering center, so as to achieve better data mining effect.

This study has two main innovations. The first innovation is to use particle swarm optimization algorithm to improve the k-means algorithm, improve its initial clustering center selection ability, and then make the improved k-means algorithm achieve better clustering effect. The second innovation is to use collaborative filtering algorithm and improved k-means algorithm to establish a new media precision marketing system, so that the model has the functions of data mining and personalized recommendation and overcomes the disadvantages of traditional media in marketing mode.

This study is mainly divided into four parts. The first part introduces the research background and existing research results in related fields, and leads to the research content of this study; the second part is the elaboration of the precision marketing model of new media; the third part is the demonstration and analysis of the experimental results of this study; and the fourth part is the conclusion of this study and the prospect of the future.

2. Related Works

Compared with traditional media, new media has higher flexibility and timeliness, richer channels, and stronger market advantages. Lu Jie and others investigated new media from three aspects: art and touch, art and tactile symbols, and tactile symbols in new media art. Finally, they proposed a new media research method with touch symbols as the core and a method of using art to benefit society (Lu *x* and others., 2019) [3]. The nazmine team collected data from 500 students through a questionnaire survey to understand how new media technology affects the interaction mode of Multan youth. Young people prefer to communicate through digital media technology, which increases their sense of isolation (nazmine and others. 2021) [4]. It combines advanced marketing concepts such as relationship marketing, viral marketing and event marketing, and puts forward a set of effective new media marketing strategies. The results show that new media marketing strategy can increase information coverage and interactivity, achieve more convenient communication, and improve marketing efficiency (MA t.2019) [5]. Wang *R* team conducted computer-aided interactive research on visual communication technology in new media and proposed an intelligent visual art creation form suitable for the development of the intelligent era. The results show that digital technology can improve the practical effect of digital media art from three aspects: visual expression, auditory expression, and audio-visual integration (Wang r.2021) [6].

As a mature clustering algorithm in the field of Internet of things data mining, K-means algorithm has been widely and deeply applied in all walks of life. Morais fo and others combined density functional theory calculation with K-means clustering algorithm to study the stability mechanism of eight atom binary metal clusters. The results show that the energy stability of binary clusters increases with the increase of the energy interval between the highest occupied molecular orbital and the lowest unoccupied molecular orbital (Morais fo and others. 2021) [7]. Sudarsono BG team determines the number and scale of scholarships through K-means clustering algorithm. The results show that this method more effectively divides students into four scholarship categories (Sudarsono BG and others. 2021) [8]. The method of mining voters by age (faminiag and others. 2029) and other types of social data was successfully applied by faminiah and others. Muhajir *m* and others used K-means clustering algorithm based on mixed data analysis between data observation and satellite imaging to generate more specific and up-to-date climate regions. Updated seasonal regions can provide more comprehensive data support for future government planning (muhajir *m* and others. 2021) [9]. Sintiya's team designed a hierarchical k-means algorithm by combining k-means algorithm with hierarchical method. The results show that this improvement can improve the selection ability of initial clustering centers of K-means algorithm and provide data support for policy zoning in poor areas (sintiya *s* and others. 2021) [10].

It can be seen that although the Internet of things data mining algorithm and new media technology have made great progress in recent years, there are few studies on the application of data mining algorithm to the integration of new media and traditional media, but traditional media is also an indispensable part of the current media ecological environment. Therefore, this study is based on the Internet of things data mining technology, and combines new media with traditional media to lay a foundation for the integrated development and new development of all kinds of media.

3. Establishment of New Media Precision Marketing Model for Traditional Media

3.1. Establishment of New Media Precision Marketing System Architecture for Traditional Media. Great changes in the media industry have weakened the influence of traditional media, but the timeliness and accuracy of new media on the Internet of things can provide customers with personalized positioning and services, so as to help the traditional media industry segment and re-expand the consumer market (Qureshi IH and others. 2018) [11]. The establishment of traditional media precision marketing system is based on the marketing needs of traditional media, which can be divided into three categories: data acquisition and management needs, marketing business needs, and non-functional needs. The data collection and management requirements of the Internet of things are mainly user data and external data. User data is the basic attribute and behavior of users. In the architecture of most Internet companies, acquiring users is the work of the promotion and channel departments, and the next action is the user behavior to be performed by our operation. However, user conversion payment and user autobiography are the later behavior. Therefore, it is considered as the basic skill of user operation to make users active and retain users. Attributes such as geographical environment and time environment can represent user groups, while user characteristics such as attempt behavior and consumption preference can accurately locate user

preferences. The combination of the two can extract the market outline of consumers; marketing business needs mainly include the distribution needs of market channels, user personalized recommendation needs, and implementation strategy needs. Non-functional requirements are mainly the security and performance requirements of the system. According to the above requirements, the framework of traditional media and new media precision marketing system established in this study is shown in Figure 1:

The system in Figure 1 is mainly composed of three parts: presentation layer, business layer, and data layer. The data layer is the most basic underlying system, that is, the data acquisition part, which is mainly divided into internal data acquisition and external data acquisition. The internal data is such as website data and software data, and the external data is mainly industry data and competitive data. By collecting and transforming internal and external data, you can build user's result labels. Prepare for the next personalized release, and adjust the external environment according to the needs of users. The business layer is mainly divided into business and data processing. Data processing uses data mining algorithm to process the data collected by the data layer. The business part realizes the specific business according to the processed data, that is, the segmentation of marketing channels, the formation of user personalized recommendations, and the fine management of core business. The main function of the presentation layer is to show the data collected and analyzed by the data layer and the business layer in the form of charts or personalized advertisements. It is the embodiment layer of the system. The order of the whole system from left to right is from the presentation link to the basic link. In the new media precision marketing system, the most important modules are two parts, one is the data mining module, and the other is the personalized recommendation module. In this study, in the personalized recommendation module, collaborative filtering algorithm is used to weight the processed user data, so as to judge the user's preference for goods, as shown in Figure 2:

Collaborative filtering algorithm is one of the most effective recommendation algorithms so far. It can be divided into heuristic and model-based algorithms according to different modes. This study adopts heuristic collaborative filtering algorithm (Han x and others. 2021) [12]. As shown in Figure 2, the heuristic collaborative filtering algorithm is divided into user-based cf (user CF) method and item-based cf (item CF) method. The system designed this time adopts the user CF method for personalized recommendation among the direct recommendations between users, and the item CF method for personalized recommendation based on user behavior. User CF is a method for searching similar users based on user history information. Its similarity calculation mainly selects Pearson correlation coefficient and cosine similarity as the main method. The formula of Pearson correlation coefficient is

$$s(u,v) = \frac{\sum_{i \notin I_u \cap I_v} \left(r_{u,i} - \overline{r}_u\right)\left(r_{v,i} - \overline{r}_v\right)}{\sqrt{\sum_{i \notin I_u \cap I_v} \left(r_{u,i} - \overline{r}_u\right)^2} \sqrt{\sum_{i \notin I_u \cap I_v} \left(r_{v,i} - \overline{r}_v\right)^2}}. \quad (1)$$

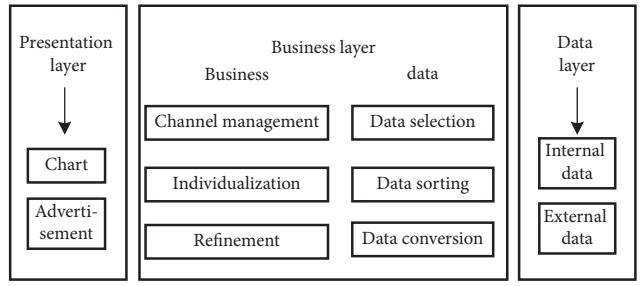

Figure 1: New media precision marketing system architecture.

The item is represented by i, u and v represent the user, I_u and I_v, respectively, represent the evaluation item set of two users, r_u and r_v, respectively, represent the average score of two users, $r_{u,i}$ represents the score of user u on item i, and $r_{v,i}$ represents the score of user v on item i. The cosine similarity formula is

$$s(u,v) = \frac{r_u \cdot r_v}{\|r_u\|_2 \|r_v\|_2}. \quad (2)$$

In addition, it is also necessary to calculate the prediction score of user u on the products without scoring. The prediction score of user u on the item i is

$$p_{u,i} = \overline{r}_u + \frac{\sum_{u' \in N} s(u,u')\left(r_{u',i} - \overline{r}'_u\right)}{\sum_{u' \in N} \left|s(u,u')\right|}, \quad (3)$$

where $s(u,u')$ represents the similarity between u and u' users. At the same time, item CF is calculated in a similar way:

$$sim(i,j) = \mathrm{corr}_{i,j}. \quad (4)$$

Then we can get

$$\mathrm{sim}(i,j) = \mathrm{corr}_{i,j} = \frac{\sum_{u \in U}\left(R_{u,i} - \overline{R}_u\right)\left(R_{u,i} - \overline{R}_u\right)}{\sqrt{\sum_{u \in U}\left(R_{u,i} - \overline{R}_i\right)^2}\sqrt{\sum_{u \in U}\left(R_{u,j} - \overline{R}_j\right)^2}}, \quad (5)$$

where $sim(i,j)$ represents the similarity between i and j, and $corr_{i,j}$ represents the correlation. Therefore, the user u's predicted score $P_{u,i}$ for item i is:

$$P_{u,i} = \frac{\sum_{j \in N} \mathrm{sim}(i,j) \cdot r_{u,j}}{\sum_{j \in N} |\mathrm{sim}(i,j)|}, \quad (6)$$

where N represents the item set similar to item i, and $r_{u,j}$ represents the user u's score on item j.

3.2. Model of Improved K-Means Clustering Algorithm in Precision Marketing Mode of New Media. K-means algorithm is widely used, and its idea is simple and easy to understand. And K-means algorithm is a clustering algorithm which is easy to implement. K-means algorithm has many advantages, such as simple idea and fast convergence speed. In the clustering analysis of large-scale data sets, the clustering algorithm is more efficient and excellent. In the data mining module of new media precision marketing

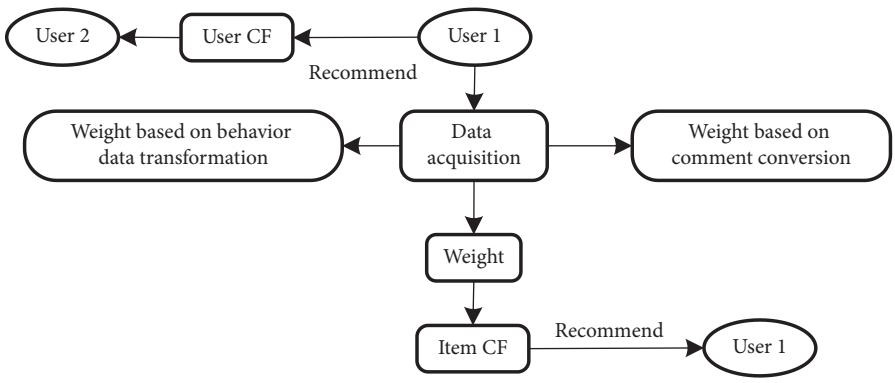

Figure 2: Processing flow of personalized recommendation module.

system, this study uses K-means clustering algorithm to extract and classify the characteristics of customers. The algorithm flow is shown in Figure 3:

Clustering itself is to divide a data set into several data clusters, reduce the difference between data classes in the same data cluster as much as possible, and increase the difference between data classes in different clusters as much as possible (Xu *n* and others. 2021) [13]. Assuming that there is a set $A = \{a_1, a_2 \ldots a_n\}$, which is divided into k clusters $\{c_1, c_2 \ldots c_k\}$, there are

$$X = C_1 \cup C_2 \ldots \cup C_k. \tag{7}$$

X represents the result set after clustering, then it can further include

$$C_i \cup C_j = \varnothing (1 \le i, \quad j \le K, \quad i \ne j). \tag{8}$$

K-means algorithm calculates the distance between different data objects in the clustering process to judge the approximation between them. The clustering center can be described as

$$C = \left\{c_j | c_j = \left(c_{j1}, c_{j2}, \ldots c_{jd}\right), \quad j = 1, 2, \ldots K\right\}. \tag{9}$$

The Euclidean distance between x_i and c_i can be expressed as

$$Dis\left(x_i, c_j\right) = \sqrt{\sum_{n=1}^{d} \left(x_{in} - c_{jn}\right)^2}, \quad i = 1, 2, \ldots, n; j = 1, 2, \ldots, K. \tag{10}$$

x_i and c_i are defined as follows:

$$\begin{cases} x_i = \left(x_{i1}, x_{i2}, \ldots, x_{id}\right), \\ c_j = \left(c_{j1}, c_{j2}, \ldots, c_{jd}\right). \end{cases} \tag{11}$$

In order to prevent the wrong selection of the initial clustering center in the clustering process, the particle swarm optimization algorithm is used to optimize the k-means algorithm. The particle swarm optimization algorithm is a method based on the group information transmission mode of bird swarm, which uses the information sharing of individuals in the group to convert the motion mode of the whole group from disordered motion to ordered motion in a certain solution space, so as to obtain the optimal solution of the problem (maihemuti *s* and others. 2021) [14]. A group contains a whole group of different individuals. These individuals are the particles in the particle swarm. The particles begin to fly at random speed in space. With the change of time, the position of the particles will change

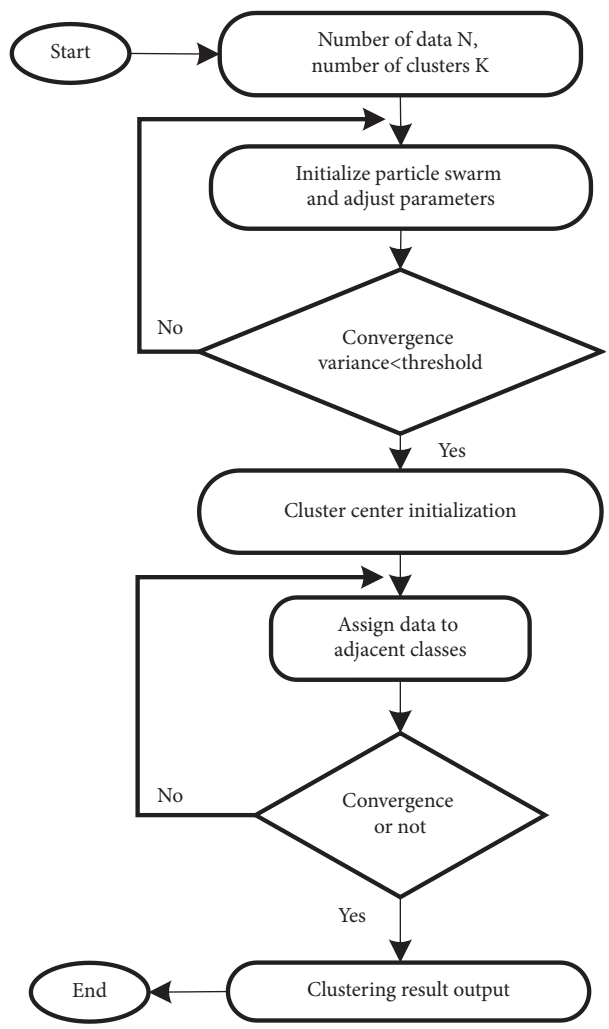

Figure 3: K-means algorithm flow.

constantly. These particles that change their position continuously are the feasible solution of the problem. Find the best initial clustering center through the global search ability of particle swarm optimization algorithm. In the clustering process, it is necessary to calculate the average value of all data objects in each data class:

$$\overline{x}_i = \sum_{x \in C_i} \frac{x}{|C_i|}. \tag{12}$$

Then the function value of the sum of squares of errors can be calculated:

$$E = \sum_{i=1}^{k} \sum_{x \in C_i} \left| x - \overline{x}_i \right|^2. \tag{13}$$

The particle swarm search starts from the random position in space, and each particle starts to adjust itself according to the existing information, and then constantly approaches the global optimal solution. The search performance of this particle swarm can be judged by the fitness function of the current particle position. Based on formula (13), the fitness function of particle swarm optimization can be defined as

$$f(x) = \sum_{j=1}^{k} \left(\sum_{x \in C_j} \left\| X_i - C_j \right\| \right), \tag{14}$$

where $f(x)$ represents the fitness of particles, X_i represents the data sample, and C_j represents the cluster center. Because the two algorithms need to be converted in the clustering process, that is, the particle swarm optimization algorithm is used to find the initial clustering center of the data, and the k-means algorithm is used in the subsequent clustering analysis process, the two algorithms need to be switched, and the switching time is mainly measured by the convergence variance of the particle swarm optimization algorithm:

$$\sigma^2 = \frac{1}{m \sum_{i=1}^{m} \left[f(x_i) - f_{\text{avg}} \right]^2}, \tag{15}$$

where σ represents the convergence degree variance, m represents the particle swarm size, $f(x_i)$ represents the particle fitness, and f_{avg} represents the mean value of particle fitness. If the convergence degree variance reaches a very small state, it means that the particle swarm is still in the convergence state. Even if the particles are allowed to continue to iterate, a better solution cannot be obtained, and the redundant iteration range will waste computing time. Therefore, the best time for the system to change from particle swarm optimization algorithm to k-means algorithm is when particle swarm optimization reaches the convergence state. After data classification, users can be divided into different clusters according to different dimensions such as region, age and preference, and then personalized recommendation between customers, customer behavior, and customers can be carried out based on customer preference clusters.

4. Application Effect Analysis of New Media Precision Marketing Model for Traditional Media

4.1. Performance Analysis of Improved K-Means Clustering Algorithm. In the application experiment, this study analyzes the new media activities with the highest user preference. Two websites are randomly selected to discuss the impact of precision marketing system on users. This study analyzes the application effect of the new media precision marketing model for traditional media from two angles. The first angle is the performance analysis of the improved k-means clustering algorithm in this study, and the second angle is the application effect analysis of the new media precision marketing model for traditional media. In the analysis part of improved k-means clustering algorithm, firstly, the selection ability of improved k-means clustering algorithm for initial clustering center is analyzed, as shown in Figure 4:

Figure 4 shows the comparison of the initial clustering center selection effect between the traditional K-means algorithm and the improved k-means algorithm designed this time. It can be seen that although there are some obvious set categories in the overall distribution of the initial clustering center data points randomly selected by the traditional K-means algorithm, there are still individual data points in other data point sets, and this phenomenon occurs more frequently. Almost every data point category is mixed with other types of data points, and the category boundary between data points is not obvious. The initial clustering center data points selected by the improved k-means algorithm designed in this study form a set of data points with clear boundaries. There is almost no case that the data points are mixed between other types of data points, and the clustering effect is very obvious. It can be seen that the improved k-means algorithm in this study can reflect a stronger clustering effect when selecting the initial clustering center, and then obtain a high-quality initial clustering center. The selection performance of clustering center is much better than that of the unmodified k-means algorithm. The comparative analysis of clustering errors between different clustering algorithms is shown in Figure 5:

Figure 5 shows the comparison of clustering errors among the traditional K-means algorithm, d-means algorithm, and the improved k-means algorithm designed in this study. The clustering errors are compared from four aspects: the highest value, the lowest value, the average value, and the standard deviation. It can be seen that in the highest value, the clustering error of the traditional K-means algorithm is 46.89%, and the error of the improved k-means algorithm is 42.73%; At the lowest value, the clustering error of the traditional K-means algorithm is 4.28%, and the error of the improved k-means algorithm is 1.14%; On the average, the clustering error of the traditional K-means algorithm is 0.36%, and the error of the improved k-means algorithm is 0.04%; In terms of standard deviation, the clustering error of traditional K-means algorithm is 9.32%, which is the largest, while the error of improved k-means algorithm is 5.61%, which is the smallest. It can be seen that the clustering error

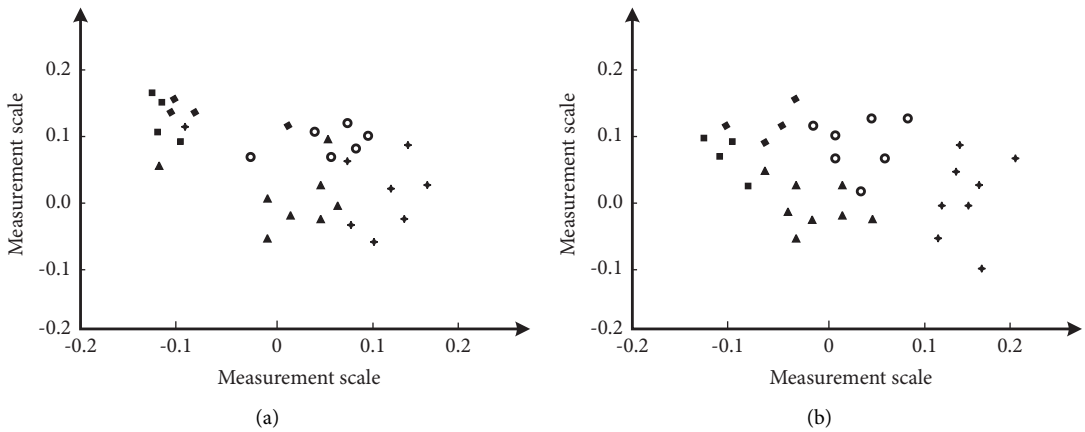

Figure 4: Effect drawing of initial cluster center. (a) k-means. (b) Improved k-means.

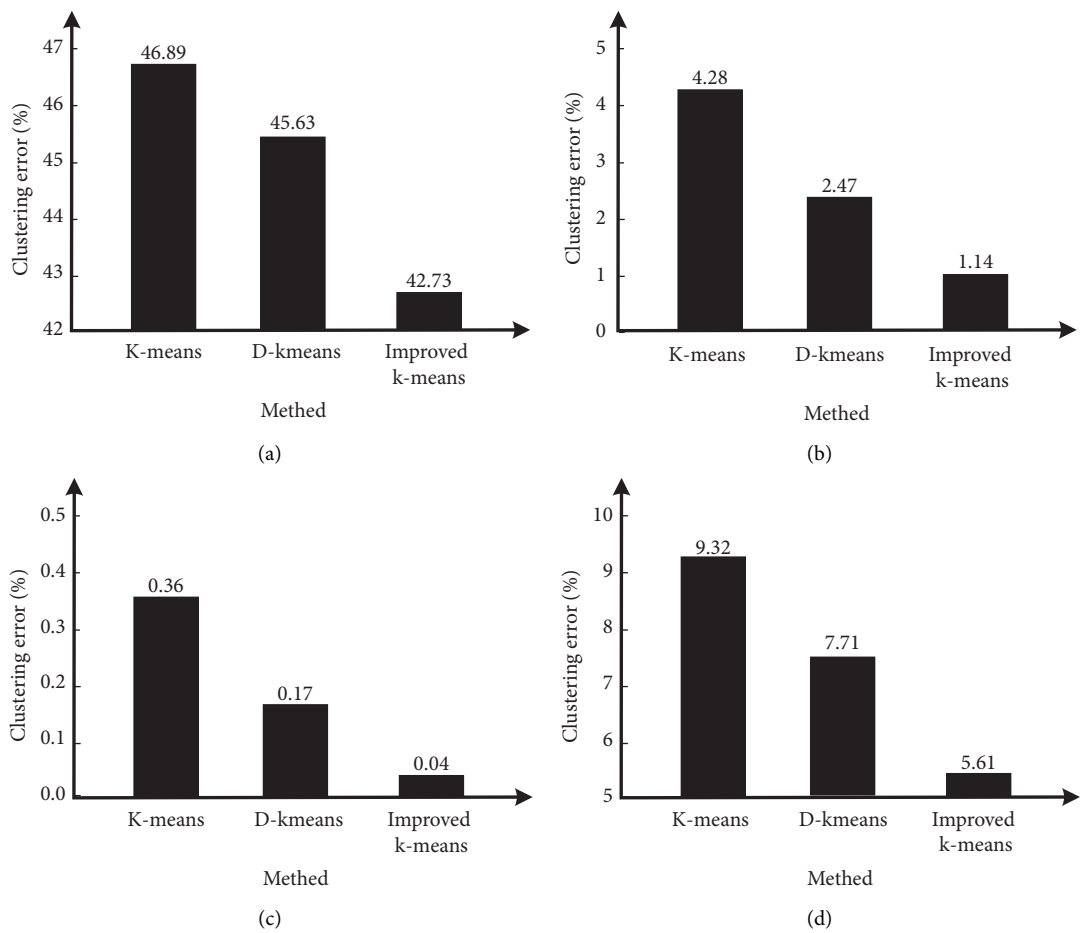

Figure 5: Comparative analysis of clustering errors. (a) Max. (b) Mean. (c) Min. (d) STD.

of the improved k-means algorithm is the smallest of the three clustering algorithms in the four aspects of the highest value, the lowest value, the average value, and the standard deviation of the clustering error, and the clustering performance is the best. The comparison between running time and running accuracy is shown in Figure 6:

Figure 6 shows the comparison of running time and accuracy of n-kmeans, d-kmeans, K-means, and the improved k-means algorithm designed in this study. It can be seen that in terms of running time, with the increase of K value, the three running time broken lines show an overall upward trend, in which the position of K-means broken line is the highest, the interval is between 0s and 100s, and the fluctuation is the most frequent in the rising process, while the position of the improved k-means algorithm designed in this study is the lowest, the interval is between 0s and 60s,

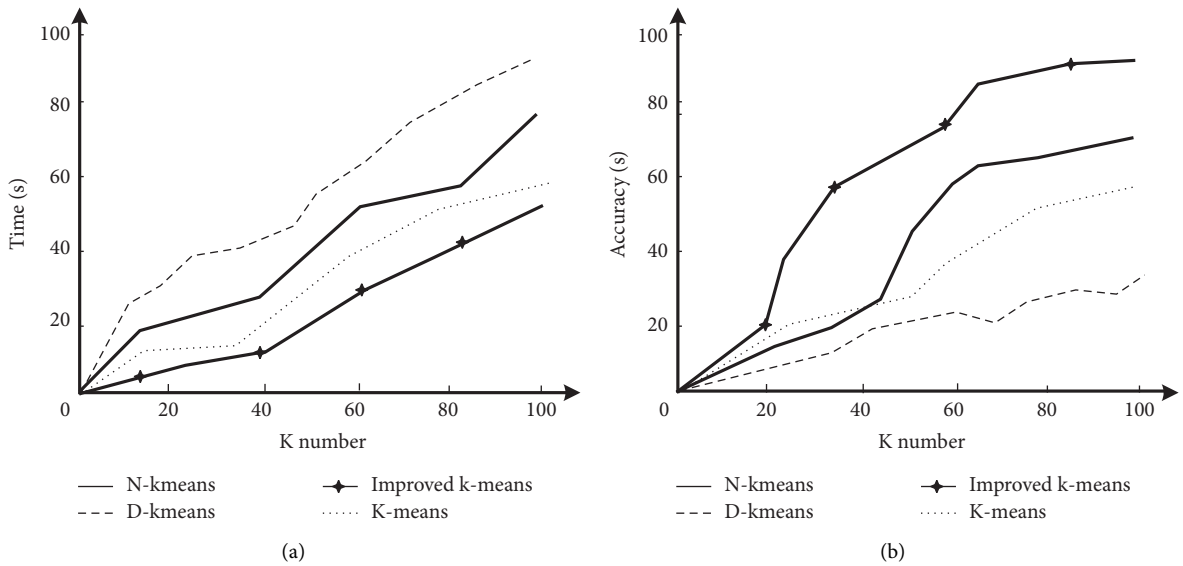

Figure 6: Comparative analysis of running time and accuracy of clustering error. (a) Run time comparison. (b) Comparison of transportation accuracy.

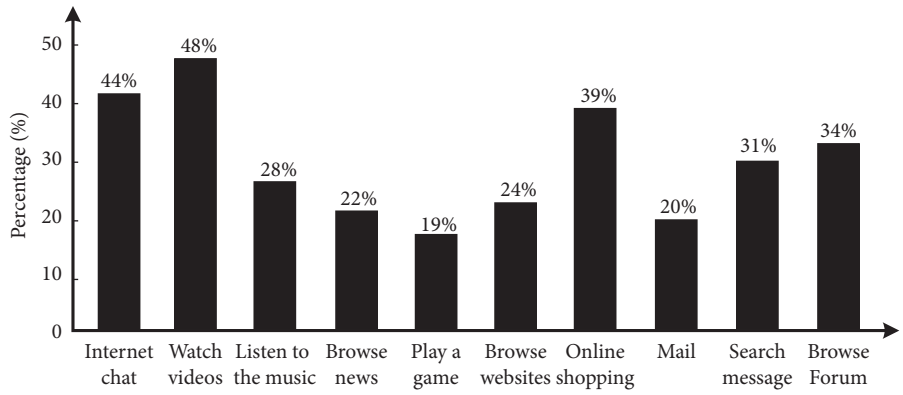

Figure 7: Network preference data.

and the fluctuation is the most stable in the rising process, It can be seen that in terms of running time, the algorithm designed in this study takes less time and has a stronger performance; in terms of accuracy, the broken line position of the improved k-means algorithm in this study is the highest. After the K-value reaches 20, it enters an obvious rising period, and the accuracy finally reaches about 93%. It can be seen that the improved k-means algorithm has the strongest performance in running accuracy.

4.2. Application Effect Analysis of New Media Precision Marketing Model for Traditional Media. In the part of application effect analysis, this study is mainly divided into two parts: user preference data in new media activities and user access data on different websites. The preference data of users on the network is shown in Figure 7:

Figure 7 shows the preference performance of users in various new media activities. It can be found that the three activities with the strongest user preference in new media activities are watching video, online chat, and online shopping. Among them, 48% of users prefer watching video, 44% of users prefer online chat, and 44% of users prefer online shopping. When making personalized recommendation, it is suitable for advertising design and online recommendation from the above three aspects. Among them, the users who prefer to watch video are the most. Therefore, the recommendation in video is the most likely to attract the attention of users and has the highest marketing efficiency. Among all new media activities, online games, e-mail, and news browsing activities have lower preference. Among them, online game users account for 19%, e-mail users account for 20%, and news browsing users account for 22%, among which online game activities account for the lowest proportion, Therefore, when making marketing recommendations to users, advertising and marketing push in relevant activities should be avoided as far as possible, and the marketing efficiency of relevant activities is low. The analysis of access data for different websites is shown in Figure 8:

For all enterprises, whether traditional enterprises or Internet plus enterprises, the drainage and publicity of new

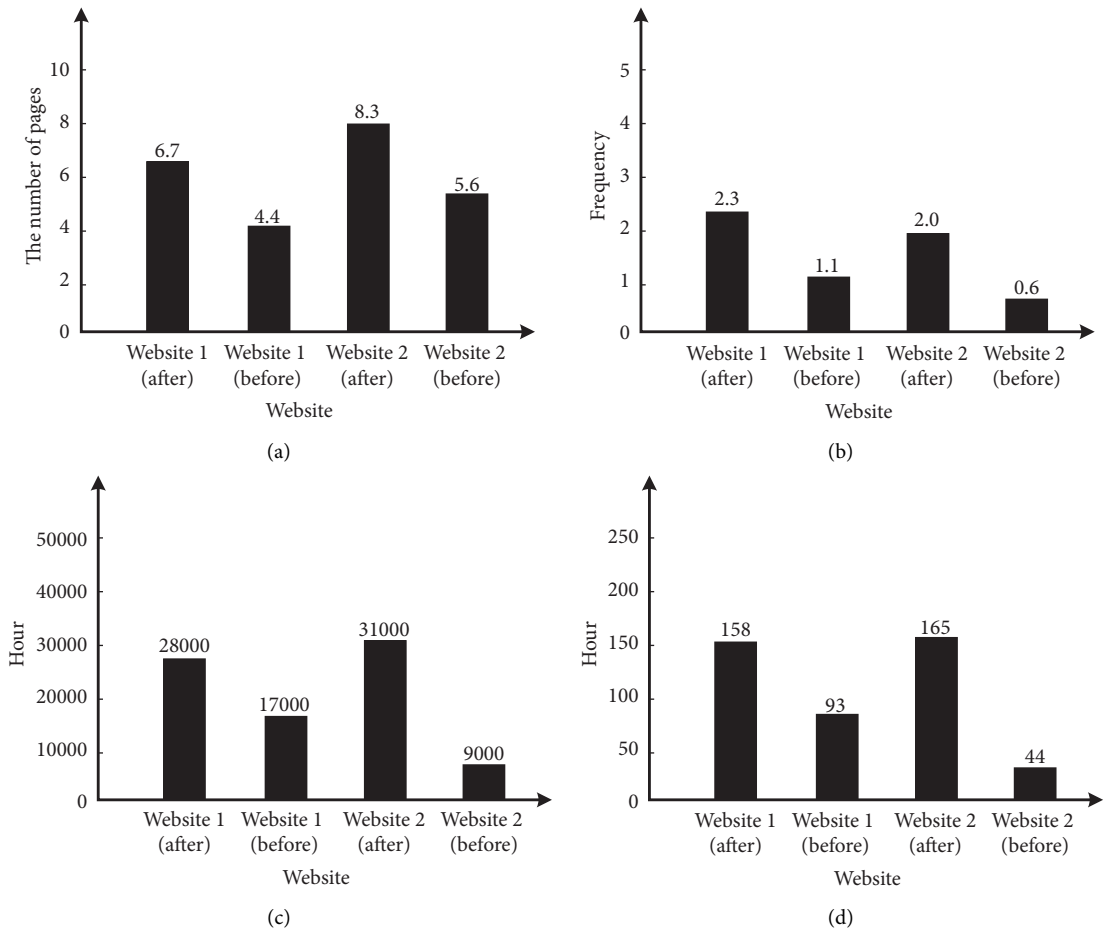

Figure 8: Website access data. (a) Page views per capita per day. (b) Per capita visits per day. (c) Average daily effective browsing time. (d) Per capita browsing time in a single day.

media platforms is very important. If an enterprise can skillfully use new media marketing, it can attract traffic to the greatest extent and obtain the trust of intended customers, which is twice the result with half the effort for enterprise sales and publicity [15].

This study first numbers the website, and then analyzes the changes in its use of precision marketing system and the influence level of new media marketing on users. Figure 8(a) shows the analysis of page views per capita in a single day. It can be seen that the page views per capita in a single day of website 1 increased from 4.4 to 6.7 after using the precision marketing system, while the page views per capita in a single day of website 2 increased from 5.6 to 8.3 after using the precision marketing system; Figure 8(b) shows the analysis of per capita visits per day. It can be seen that the per capita visits per day of website 1 increased from 1.1 to 2.3 after using the precision marketing system, while the per capita visits per day of website 2 increased from 0.6 to 2.0 after using the precision marketing system; Figure 8(c) shows the analysis of daily effective browsing time. It can be seen that the daily effective browsing time of website 1 increases from 17000 hours to 28000 hours after using the precision marketing system, while the per capita visits of website 2 in a single day increase from 9000 hours to 31000 hours after using the precision marketing system; Figure 8(d) shows the analysis of the per capita effective browsing time in a single day. It can be seen that the per capita effective browsing time in a single day of website 1 increases from 93 hours to 158 hours after using the precision marketing system, while the per capita effective browsing time in a single day of website 2 increases from 44 hours to 165 hours after using the precision marketing system. To sum up, the four indicators used in this analysis have increased after the adoption of the new media precision marketing system. Compared with website 1, website 2 has a greater growth rate, and the data of both websites have increased. It can be seen that the precision marketing system designed in this study has certain universality.

5. Conclusion

As a new form of media, new media can provide accurate marketing solutions for traditional media from the perspective of Internet of things data technology and promote the development of traditional media. Aiming at the shortcomings of K-means algorithm, this study improves k-means algorithm from the perspective of initial clustering center and particle swarm optimization algorithm, and

combines it as a data mining tool and collaborative filtering algorithm as a personalized recommendation tool. On this basis, a new media precision marketing system is designed for traditional media, namely traditional media customer data mining and personalized recommendation marketing. The results show that the improved k-means algorithm is better than similar algorithms in clustering error and running time, its accuracy finally reaches about 93%, and the overall performance is also significantly better than other algorithms. In the application test, the new media precision marketing system successfully found the user's favorite new media activity, namely video viewing, accounting for 48%. After using the new media precision marketing system, the impact of the two websites on users has increased significantly. It can be seen that the system designed in this study has certain effectiveness and universality. However, this study also needs to simulate and verify the proposed optimization algorithm, and this part needs to be further elaborated in future research.

Data Availability

The data used to support the findings of this study are available from the corresponding author upon request.

Conflicts of Interest

The authors declare that they have no conflicts of interest.

Acknowledgments

The study was supported by "Science and Technology Project of China Railway Corporation, China (Grant no. 1341324011)".

References

[1] Y. Peiulis, "TV media change in the aspect of remediation theory," *Informacijos Mokslai*, vol. 91, pp. 26–40, 2021.

[2] B. Topbaş, "Adaptation of traditional media organs in video content: new media example: ct," *Turkish Online Journal of Design Art and Communication*, vol. 11, no. 2, pp. 393–402, 2021.

[3] J. Lu, D. K. Su, Y. Ro, and H. G. Kim, "New media art research focused on tactile symbols," *TECHART Journal of Arts and Imaging Science*, vol. 6, no. 2, pp. 14–20, 2019.

[4] K. A. Nazmine, K. Z. Chishti, and K. T. Hannan, "New media technologies and society: a study ON the impact OF new media technology ON interaction patterns OF youth," *Tianjin Daxue Xuebao (Ziran Kexue yu Gongcheng Jishu Ban)/Journal of Tianjin University Science and Technology*, vol. 54, no. 5, pp. 66–77, 2021.

[5] T. Ma, "Identification of new media technology factors and research on big data in the tourism industry," *ICIC Express Letters*, vol. 13, no. 4, pp. 279–285, 2019.

[6] R. Wang, "Computer-aided interaction of visual communication technology and art in new media scenes," *Computer-Aided Design and Applications*, vol. 19, no. S3, pp. 75–84, 2021.

[7] F. Orlando Morais, K. F. Andriani, and J. L. F. Da Silva, "Investigation of the stability mechanisms of eight-atom binary metal clusters using DFT calculations and k-means clustering algorithm," *Journal of Chemical Information and Modeling*, vol. 61, no. 7, pp. 3411–3420, 2021.

[8] B. G. Sudarsono and S. P. Lestari, "Clustering pbyummm K-means," *JURNAL MEDIA INFORMATIKA BUDIDARMA*, vol. 5, no. 1, pp. 258–263, 2021.

[9] M. Muhajir, N. Ismail, S. Syahreza, and A. V. H. Simanjuntak, "Pemutakhiran zmpam data blending b non-h K-means clustering," *Jurnal Fisika Flux: Jurnal Ilmiah Fisika FMIPA Universitas Lambung Mangkurat*, vol. 18, no. 1, pp. 35–41, 2021.

[10] S. Sintiya, T. G. Laksana, and N. A. F. Tanjung, "Kombinasi single linkage d K-means clustering upwdkp," *Journal of Innovation Information Technology and Application (JINITA)*, vol. 3, no. 1, pp. 17–27, 2021.

[11] I. H. Qureshi and S. Z. Zahoor, "Social media marketing and brand equity: a literature review," *Social Science Electronic Publishing*, vol. 16, pp. 47–64, 2018.

[12] X. Han, Z. Wang, and H. J. Xu, "Time-weighted collaborative filtering algorithm based on improved mini batch K-means clustering," *Materials, Computer Engineering and Education Technology*, vol. 105, pp. 309–317, 2021.

[13] N. Xu, R. B. Finkelman, S. Dai, and C. M. Xu, "Average linkage hierarchical clustering algorithm for determining the relationships between elements in coal," *ACS Omega*, vol. 6, no. 9, pp. 6206–6217, 2021.

[14] S. Maihemuti, W. Wang, H. Wang, and J. Wu, "Voltage security operation region calculation based on improved particle swarm optimization and recursive least square hybrid algorithm," *Journal of Modern Power Systems and Clean Energy*, vol. 9, no. 1, pp. 138–147, 2021.

[15] G. Fajriansyah, "Analisis daftar pemilih tetap pada hasil rekapitulasi KPU berdasarkan usia menggunakan algoritma K-means (studi kasus:kota bandar lampung)," *Electrician*, vol. 15, no. 1, pp. 39–53, 2021.

Hindawi
Computational Intelligence and Neuroscience
Volume 2022, Article ID 4637180, 8 pages
https://doi.org/10.1155/2022/4637180

Research Article

Study on Discrete Dynamic Modeling of College Students' Innovative Employment Security Mechanism under the Environment of Internet of Things

Liming Gu [1] **and Xue Chen** [2]

[1] *Chengdu Normal University, Chengdu, 610000, Sichuan, China*
[2] *Chengdu Experimental School, Chengdu, 610000, Sichuan, China*

Correspondence should be addressed to Liming Gu; 521026@cdnu.edu.cn

Received 7 February 2022; Revised 11 March 2022; Accepted 19 March 2022; Published 15 April 2022

Academic Editor: Guobin Chen

The innovative mechanism of college students' employment security is a series of security measures implemented by the state and society to solve the mismatch between the scale growth of college graduates and the jobs provided by the society. In order to promote the development of emerging Internet of things technologies, users can find interesting and valuable information from a large number of data sets and use this information to meet the needs of users. This article mainly studies the historical development trend and discrete dynamic modeling and analysis technology of college students' innovative employment security mechanism under the environment of Internet of things. Using two different modeling methods of Bayesian network and BP neural network, this article makes discrete dynamic modeling on the influencing factors and employment security mechanism of college students' employment, so as to improve the college biological network innovation employment security mechanism and better help college students' employment.

1. Introduction

China has the largest number of college graduates in the world. The scale of higher education in China is unmatched by any other country, and the number of colleges and universities is in the forefront of all countries. However, the increase in the number of college students not only brings great opportunities and talent dividends to the country but also brings a series of challenges and social problems, the most important of which is the employment of graduates. The number of college students is growing, but the employment cannot match the growth rate of college students, resulting in a considerable number of graduates facing the dilemma of unemployment once graduation, and the "lying flat" and "gnawing the old" are growing day by day. At the same time, although some college students find jobs, they cannot give full play to their professional strengths, and the post functions do not match the skills they master Tengrong [1]. In view of the above situation, the Chinese government has paid full attention to it, adopted a series of employment security measures for college students, and adopted different and flexible assistance policies for different implementation objects, such as students, universities, and enterprises Kurszewska et al. [2].

In recent years, with the continuous development of computer, Internet, Internet of things, and various new sensors, information and data circulating in various fields have attracted more and more attention from all walks of life Zhang [3]. Nowadays, the way of data generation extends to all fields of society. Almost everything will produce information data, and these information data are finally collected and counted to form a huge data set, referred to as "big data" Pang et al. [4]. It mainly refers to the data set whose data scale exceeds that obtained, saved, and processed by traditional data management software. It can analyze and process big data, collect and extract from massive and

scattered data, so as to obtain valuable information for users, and then conduct discrete dynamic modeling to associate with college students' employment security Zhu [5]. Discrete dynamic modeling technology is also very practical. It is suitable for most fields and belongs to a comprehensive cutting-edge technology. With the continuous exploration and promotion of personnel in various fields, the technology has made great progress and has been successfully applied in various fields Pirbhulal et al. [6]. For example, the e-commerce platform uses the user search and browsing record data to recommend the products that users expect to buy, establish relevant models, and promote user consumption. The public security system uses all the monitoring data to obtain all kinds of information of the suspect, master its whereabouts, and make the big data play a major role in the reconnaissance work Cui [7].

This article mainly consists of three parts. The first part introduces the development status of University Biological Networking Innovation and employment security mechanism and discrete dynamic modeling algorithm. The second part analyzes the application of discrete dynamic modeling method in employment security mechanism under the background of Internet of things and puts forward scientific and reasonable suggestions by combining Bayesian network algorithm, grey analysis method, and BP neural network with today's College Students' employment security system. The third part analyzes and compares the research results, establishes relevant discrete dynamic models, finds out the hidden relationship between the calculation data and the employment security mechanism and the employment status of college students, and puts forward effective suggestions to improve the security mechanism.

2. Related Work

The concept of big data has long been mentioned. As early as the last century, Toffler, a futurist, mentioned the word "big data" in his works Tang et al. [8]. At the beginning of this century, analysts pointed out that the number of big data of the group is diverse. McKinsey formally defined the concept of big data Wang et al. [9]. After that, the United States released a report on big data Internet of things analysis technology, marking that big data Internet of things analysis and processing technology has become a technology at the level of national science and technology strategy Zhang et al. [10]. Since then, the development and maturity of computer, Internet, and other technologies have provided fertile ground for the seeds of big data Internet of things analysis technology to thrive.

The United States is the first country to upgrade the discrete dynamic modeling technology from the civil field to the national strategic level. Through the "three-step" plan, it has formed a technology leader ahead of other countries in various fields in the country Liu et al. [11]. The "three-step" plan mainly includes the following contents: first, accelerate the research of discrete dynamic modeling and analysis technology and realize the application of discrete dynamic modeling and analysis in some fields of the Internet of things Zhang and Liu [12]. Then, aiming at the derivative problems brought by discrete dynamic modeling technology, a series of regulations are implemented. Finally, strengthen the construction of discrete dynamic modeling production system to enhance the country's competitiveness in the field of data analysis.

On the development of discrete dynamic modeling and analysis technology, Britain has absorbed the valuable experience of the United States. According to the needs of the country and the people, strengthen the investment in data research and development and focus on the application of Internet of things analysis in advanced fields Pu [13]. In addition, the UK government strongly advocates digital strategy to improve the employment problem in the country.

As a neighbor of China, South Korea has the world's leading network transmission speed and the popularity of intelligent devices, which also brings its inherent advantages in the development of the Internet of things Meng et al. [14]. Under the policy of "creative economy," various departments of the Korean government cooperate to speed up the development of discrete dynamic modeling and analysis technology. By 2016, South Korea had introduced a policy based on discrete dynamic modeling technology to meet the opportunities and challenges brought by global digitization.

China also focuses on developing discrete dynamic modeling technology. At the Fifth Plenary Session of the 18th CPC Central Committee, the government took the development of big data Internet of things as a national strategy Shumin and Liu [15]. The Ministry of industry and information technology has also formulated an industrial development plan for the development of discrete dynamic modeling and made different policy arrangements for different periods.

The above is the development history of discrete dynamic modeling analysis and processing technology and its development status in various countries.

3. Methodology

3.1. Model Construction of Bayesian Network Algorithm in College Students' Innovative Employment Security Mechanism. The original method can only understand the impact of policies through simple manual prediction and actual implementation. Nowadays, the vigorous development of Internet of things analysis technology provides us with new research methods. In the process of proposing and applying the innovative employment security mechanism for college students, it is necessary to consider the role, influence, and effectiveness of the corresponding security mechanism after practical application.

We can use the Internet of things technology. The security mechanism is to collect and analyze the employment information of college students after the implementation of the employment security mechanism and the employment information that does not enjoy the security and carry out dynamic data prediction modeling, so as to infer the weight of the impact of different college students' employment security mechanisms on the employment situation and improve the effectiveness of the employment security mechanism. This article uses Bayesian network algorithm to

predict and analyze the security mechanism of College Students' innovative employment. Before that, the Bayesian theorem is briefly introduced, mainly including the following concepts:

(1) Random test

Random test refers to the test that cannot know all the results in advance before the event occurs. All the results obtained from the random test constitute the sample space Ω of the test. The sample space contains all events.

(2) Probability

The probability of occurrence of event X in the sample space is called probability, and the value is $p(x)$. The probability satisfies the following conditions:

$$\begin{aligned} P(\Omega) &= 1, \\ P(X) &\geq 0, \\ P(X \cup Y) &= P(X) + P(Y),\ X \cap Y = \varnothing. \end{aligned} \tag{1}$$

(3) Joint probability

The combination probability that contains all multiple random variables and satisfies their respective probabilities. For multiple random variables, the joint probability is

$$P(X_1, \ldots, X_n), \tag{2}$$

of which

$$\sum_{X_1,\ldots,X_n} X_1, \ldots, X_n = 1. \tag{3}$$

(4) Conditional probability refers to the probability that event x occurs under the condition that event y has occurred, which can be expressed as

$$P(X|Y) = \frac{P(X,Y)}{P(Y)}. \tag{4}$$

(5) Bayesian theorem:

$$\begin{aligned} P(Yi|X) &= \frac{P(X,Yi)}{P(X)} \\ &= \frac{P(Yi)P(X|Yi)}{\sum_{i=1}^{n} P(Yi)P(X|Yi)}. \end{aligned} \tag{5}$$

Bayesian theorem can obtain unknown posterior probability through the determined prior probability. When you cannot determine the probability of an event, you can use the probability of other related events to infer the probability of the event.

Bayesian network is mainly composed of $(X, A, \varnothing)$. The first two parts (X, A) is a directed acyclic graph structure, and X is the set of nodes in Bayesian network. These sets can be observable variables, hidden variables, or unknown variables. Two variables with causality will produce a directed arrow connecting two nodes. After the two nodes are connected with each other, the conditional probability values of the two nodes can be obtained. A is the set of arrows in the network.

The following figure is a common Bayesian network diagram.

The structure diagram of Bayesian network is shown in Figure 1. In the figure, the one issuing the arrow is called the parent node, and the arrow refers to the child node. For example, a is the parent node of B. A parent node can have multiple child nodes, and a child node can also have multiple parent nodes. The arrow represents that the two are interrelated. Therefore, through Bayesian network, we can deduce a and h from C, or C from a and H.

X is the set of nodes in Bayesian network, which can be observable variables, hidden variables, or unknown variables. Two variables with causality will produce a directed arrow connecting two nodes. After the two nodes are connected with each other, the conditional probability values of the two nodes can be obtained. A is the collection of arrows in the network.

Conditional independence has been assumed in Bayesian networks, that is, a parent node is given, which will be independent of all its nondescendant nodes. Therefore, the joint probability of all nodes in Bayesian network is the product of the conditional probability of each node.

$$P(X_1, \ldots, X_n) = \prod_{i=1}^{n} P(Xi|X_1, \ldots, X_n) = \prod_{i=1}^{n} P(Xi|\pi(Xi)). \tag{6}$$

Therefore, as long as the directed graph model of Bayesian network is constructed, the relationship between each node can be obtained, and then, the probability distribution of nodes can be obtained by determining the parameter ø.

According to the Bayesian network algorithm, we can build a structure diagram, mark the end node as employed and unemployed college students, and its related parent node can be set as individual information of college students, such as gender, education, and skills. Then, according to the collected employment information of college students in a certain year in a certain region and the probability of different security mechanisms to help college students obtain employment, the data are input into the model. Through this model, we can obtain the relationship between graduates' employment and employment security policy and individual factors, so as to get the rated relationship between them.

3.2. BP Neural Network Combined with Discrete Dynamic Modeling of Internet of Things to Construct the Evaluation Model of College Students' Innovative Employment Security Mechanism. With the continuous expansion of the scale of college graduates, it is particularly important to innovate the employment security mechanism to alleviate the employment pressure of college students. How to find the mechanism with the highest quality and the best effect among many security mechanisms is related to the optimization and structural adjustment of employment security mechanism.

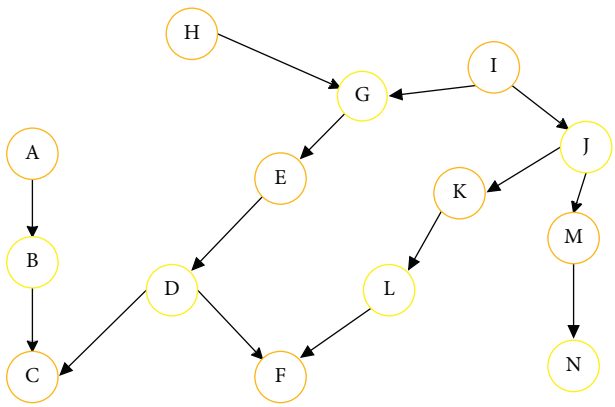

Figure 1: Bayesian network structure diagram.

There are many quality evaluation models of employment security mechanism, which can be roughly divided into the following three categories: subjective evaluation model, objective evaluation model, and subjective and objective evaluation model. Among them, the subjective evaluation model is the evaluation of College Students' innovative employment security mechanism by professional researchers in this field. This approach often varies widely in terms of results, personal feelings, and persuasion. The objective evaluation model uses this algorithm to evaluate the innovative employment security mechanism of college students. This method does not include personal subjective views, and all evaluation results depend on input parameters. Compared with the subjective evaluation model, the evaluation effect of this model is better. However, the goal model often uses only one algorithm, and the employment security mechanism of college students is composed of a variety of security measures. A single algorithm is difficult to reflect the quality evaluation of all mechanisms. The third subjective and objective evaluation model combines the advantages of the first two evaluation models and has high evaluation accuracy, but at the same time, the modeling speed of the model is the slowest and the efficiency is the lowest.

In order to evaluate the quality of college students' innovative employment security mechanism with higher accuracy and efficiency, this article uses BP neural network method to build a model and analyze its evaluation effect.

BP neural network is a popular and mature algorithm. The principle is to carry out forward propagation after inputting data. If the expected result cannot be obtained in the output layer, the error will be propagated back to the input layer and the weight of neurons will be adjusted to repeat continuously to obtain the expected result.

This article combines the two analysis methods to evaluate the employment security mechanism of college students. The main steps are as follows:

Firstly, collect the employment data of college students and the data of employment security mechanism, preprocess the data, eliminate some wrong information, construct the corresponding model using grey analysis method and BP neural network algorithm, obtain the employment rate data of college students under different employment security mechanisms, and then adjust their weights by linear regression, Finally, the optimal evaluation model of college students' employment security mechanism is obtained, and the flow chart is shown in the figure below.

As shown in Figure 2, there are two methods to build the model of college students' employment security mechanism. First, preprocess the collected data and eliminate accidental data to reduce the error after analysis. There are four extracted feature vectors: employment area, salary, specialty matching, and working hours. These four features are respectively input into the neural network training mode for training to see whether the results meet the accuracy requirements. If the accuracy requirements are not met, the parameters are adjusted again and input into the neural network system for training. If the results meet the accuracy requirements, the characteristics that have the greatest impact on college students' employment will be output. After many experiments and simulations, it can be concluded that the salary has the greatest impact, and the other orders are region, working time, and major matching. Through this mechanism, we can put forward more reasonable suggestions on the employment security system of college students.

4. Result Analysis and Discussion

4.1. Bayesian Network Algorithm in College Students' Innovative Employment Security Mechanism Model Construction and Result Analysis. Finding new directions and ideas for college students' innovative employment through algorithm analysis is the development trend of big data of the Internet of things. The training sample set is constructed based on the data samples collected in recent years. Combined with the previous experience, the Bayesian network model can be constructed and the corresponding parameters can be obtained. If you have complete data, you can evaluate the Bayesian function by scoring and summing the obtained local data. At this time, the overall structure of Bayesian network will not be affected by this part of data. Therefore, we only calculate local data. For example, if random variables and training sets are defined respectively, the scoring function can be decomposed into

$$Sj = \sum_{i=0}^{m-1} wij\, xi + bj,$$

$$xj = f(Sj), \tag{7}$$

$$\text{score}(BN\colon D) = \sum_{i=1}^{N} \log\left(P_{BN}(X_i) - \frac{\log_2 N}{2} \text{Dim}[G] \right).$$

Through the above processing, we use two typical Bayesian networks. When the number of nodes is 8, the maximum number of node states is 2. When the training set is set to 1000, 2000, and 3000, the relationship between the data default rate can be obtained according to the time required for the algorithm to run, as shown in Figure 3.

It can be seen from the picture that when the default rate reaches 30%, the correlation between running time and the

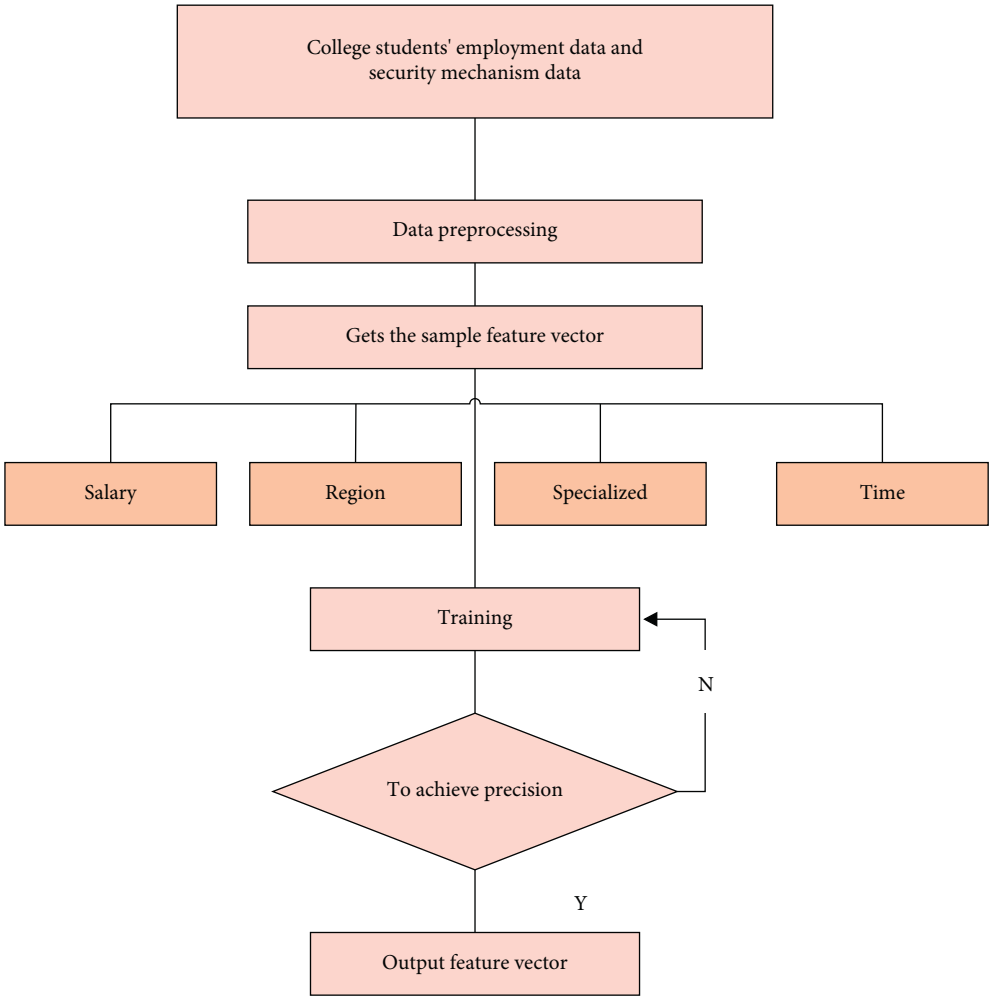

Figure 2: Processing flow chart.

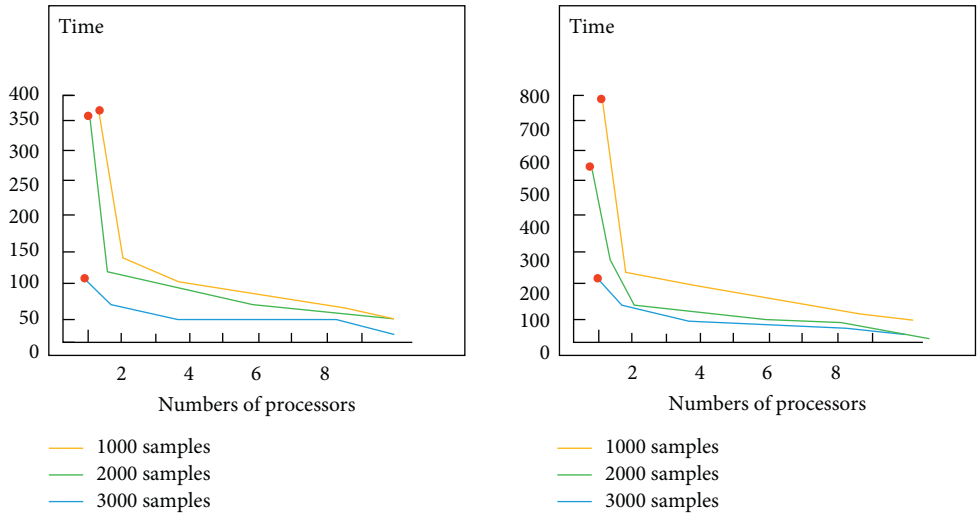

Figure 3: Result comparison chart.

number of samples is almost negligible. In the graph of 1000 sample points, when the default rate is equal to 10, there is more than 1800 seconds of serial running time.

Through comparison, it is found that when using pl-em algorithm in Bayesian network, it can well reduce the communication overhead and is suitable for large sample

learning. However, in the case of M nodes, the communication overhead will increase with the increase in the number of nodes, so the performance of this algorithm will be reduced.

Therefore, although pl-em algorithm is an effective method to learn Bayesian network, it also has great disadvantages. In particular, the huge amount of calculation required in the process of posterior probability calculation should be reasonably modified according to the selected inference engine.

When Bayesian network is used to deal with such uncertainty, it needs to be applied to the method of probability for reasoning. This method is also called Bayesian network calculation, that is, the posterior probability distribution $P(x|e)$ is calculated using conditional probability. Bayesian network inference methods are divided into accurate inference and approximate inference, but it is proved that both methods are NP complete problems. Inference is carried out through the method of joint tree. The main principle is message passing using union tree.

The largest clique in the union tree determines the complexity of its reasoning, and it is also a core problem that we need to solve in Bayesian network using probability method. The triangulation operation of constructing the union tree can directly determine the size of the clique. Therefore, using the optimal triangulation operation can make the probability reasoning more accurate, and the order of BN's moral graph determines the optimal triangulation operation. Therefore, the root of making probability inference more accurate is to solve the optimal triangulation and find the optimal deletion ranking problem.

First build a union tree, then find the largest clique, and use VC to represent the variables in the clique to obtain the potential function of the clique:

$$\phi_c = \prod_{X \in Vc} P(X|pa(X)). \tag{8}$$

Then, the potential function of the union tree is established as follows:

$$\phi_{JT} = \frac{\prod c \subset C\phi C}{\prod s \subset S\phi S}. \tag{9}$$

The clique generated by the triangulation operation can represent the weight of the joint tree, and the weight of the above clique can be obtained as follows:

$$w(C) = \prod_{i=1}^{k} w(v_i). \tag{10}$$

The operation tree weights are as follows:

$$w(JT) = \log_2 \sum_{C} w(C). \tag{11}$$

The main implementation of this algorithm is to convert BN into joint tree and then use the message transmission of joint tree, so as to improve the inference accuracy of uncertain events using Bayesian network. By inputting the employment data information of college students, individual information of college students, such as family environment and mastery of work skills, and the type data of college students' innovative employment security mechanism into the network model, we can obtain the relevance of college students' individual factors to the choice of innovative employment security mechanism and employment. The results show that individuals with higher education are more inclined to choose the policy of providing employment information, and they are easier to find a job. The lower the educational background and female college students are more inclined to the system and policy of job provision.

4.2. BP Neural Network Combined with Discrete Dynamic Modeling of Internet of Things to Construct the Evaluation Model of College Students' Innovative Employment Security Mechanism

4.2.1. Experimental Data. In this experiment, we select the number of graduates from 50 colleges and universities in 2019 and the four most popular employment security policies for college students. The four policies are as follows: (i) provide employment information, (ii) provide labor security agency services, (iii) provide employment opportunities, and (iv) provide employment skills training. And the number of college students successfully employed after obtaining a certain policy as the sample data, as shown in Figure 4.

The figure above shows the statistics of college students' employment in recent years. It can be seen from the picture that with the increase in samples, a peak will appear every time a certain number is reached, as shown by the yellow dotted line in Figure 4.

4.2.2. Result Analysis. 100 employed samples are selected from the sample database, and the corresponding classification marks are made according to whether the samples accept four kinds of college students' innovative employment security mechanisms.

(1) Determine the Analysis Sequence. In this step, we need to calculate the factors reflecting all the characteristics of the whole system as the reference sequence and then get the factors affecting the system as the comparison sequence. Here, we take the employment number of college students as the reference series and the employment number of college students under different security systems as the comparison series.

(2) Dimensionless. Because the dimensions referenced by each factor in the system will be different, it will be difficult to compare, and the results will be error. Therefore, we need to deal with each factor dimensionless to make it a unified reference standard.

(3) Obtain Correlation Coefficient. Correlation degree is the degree of shape difference between data curves, which can also be regarded as the fitting degree between them. The difference between curves affects the magnitude of correlation degree and the difference in correlation coefficient ρ is

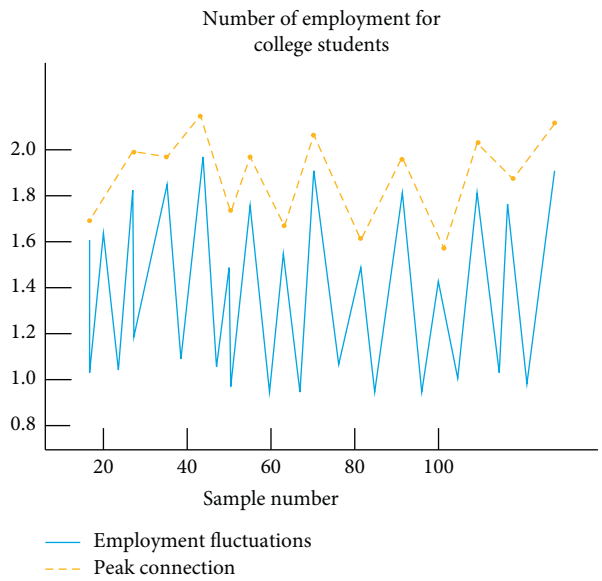

Figure 4: Employment number of college students.

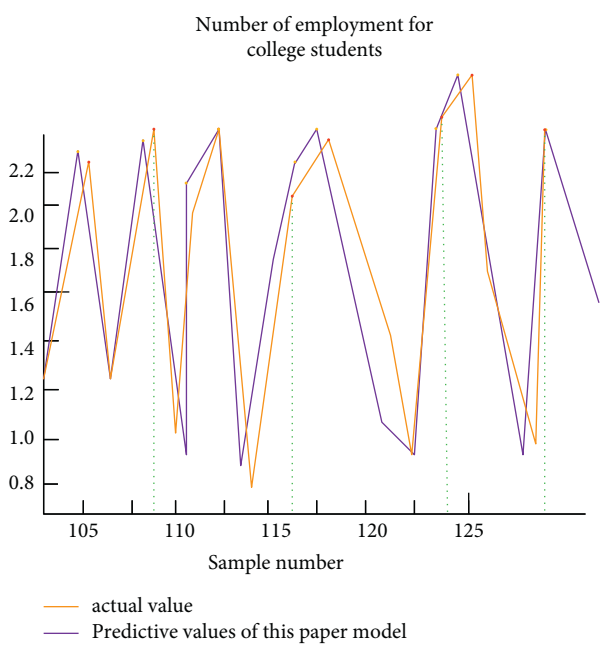

Figure 5: Projected employment figure.

the resolution coefficient. It has a negative correlation with resolution, ρ. The value range is between 0 and 1, usually 0.5.

(4) Get Relevance. The correlation coefficients of a system are different at different times, so there are multiple values of the coefficient. For the convenience of calculation and comparison, the average value of each point is used here.

(5) Sort by Relevance. Rank the correlation between four different employment security systems and college students' employment. The greater the correlation degree value indicates that the employment security system can better help college students obtain employment.

The calculation shows that among the four main college students' employment security mechanisms, the largest value is to provide employment information and then to provide jobs, employment skills training, and understanding labor security agency services. It can be concluded that among the employment security mechanisms, the one that has the greatest impact on the successful employment of college students is to provide employment information.

In addition, this article uses BP neural network algorithm to predict the number of college students after the implementation of college students' employment security mechanism, and the results are shown in Figure 5.

According to the figure, after importing the employment data of college students into BP neural network algorithm for training, the predicted employment number of graduates is roughly consistent with the actual data, but there is still a certain error, which is caused by the insufficient number of training samples.

5. Conclusion

This article mainly studies the historical development trend and discrete dynamic modeling and analysis technology of college students' innovative employment security mechanism under the background of the Internet of things. In this article, two different modeling methods, Bayesian network and BP neural network, are used to conduct discrete dynamic modeling on the influencing factors and employment security mechanism of college students' employment and find out four factors affecting college students' employment. Also get the main factors affecting college students' employment. In short, the formulation and improvement of employment security mechanism is a multidimensional and multilevel problem. Whether we can help graduates get employed smoothly is not only related to the type and implementation of the security mechanism but also closely related to the graduates' personal factors, family environment, and other factors. When formulating the employment security system for college students, the state should consider the factors such as regions, colleges, and universities and the working skills mastered by students and then analyze the specific problems. We will adjust employment security mechanisms and policies to achieve a balance between supply and demand in the talent market. This article has some innovative contributions, but there are still multidimensional and multilevel issues to discuss the formulation and improvement of employment security mechanism. Therefore, further research and analysis are needed in the future research.

Data Availability

The data used to support the findings of this study are available from the corresponding author upon request.

Conflicts of Interest

The authors declare that they have no conflicts of interest.

References

[1] G. Tengrong, "An analysis and countermeasures of economic and management college graduates' current employment status," *Journal of Qujing Normal University*, vol. 39, no. 4, 60 pages, 2020.

[2] A. Kruszewska, S. Nazaruk, and K. Szewczyk, "Polish teachers of early education in the face of distance learning during the COVID-19 pandemic - the difficulties experienced and suggestions for the future," *Education*, vol. 50, no. 3, pp. 304–315, 2022.

[3] W. Jiang, "Problems and countermeasures of ideological and political management of college students based on network information," *Journal of Physics: Conference Series*, vol. 1744, no. 4, Article ID 042005, 2021.

[4] E. Pang, M. Wong, C. H. Leung, and J. Coombes, "Competencies for fresh graduates' success at work: perspectives of employers," *Industry and Higher Education*, vol. 33, no. 1, pp. 55–65, 2019.

[5] J. Chu, J. Liu, and S. Liu, "Research and countermeasure analysis of college students' employment issues," *Open Journal of Social Sciences*, vol. 8, no. 1, pp. 129–138, 2019.

[6] S. Pirbhulal, V. Gkioulos, and S. Katsikas, "Towards integration of security and safety measures for critical infrastructures based on bayesian networks and graph theory: a systematic literature review," *Signals*, vol. 2, no. 4, pp. 771–802, 2021.

[7] Y. Z. Wang, S. Zhou, and X. M. Ou, "Development and application of a life cycle energy consumption and CO2 emissions analysis model for high-speed railway transport in China," *Advances in Climate Change Research*, vol. 12, no. 2, pp. 270–280, 2021.

[8] J. Tang, Y. Zhao, and L. Yuan, "Design of large passenger flow early warning and response scheme for large railway passenger station -- Taking Beijing West Railway Station as an example," *China work safety science and technology*, vol. 12, no. 2, pp. 143–147, 2016.

[9] J. Wang, L. Sun, H. Zhao, and Y. Wang, "ARIMA-BP integrated intelligent algorithm for China's consumer price index forecasting and its applications," *Journal of Intelligent and Fuzzy Systems*, vol. 31, no. 4, pp. 2187–2193, 2016.

[10] J. F. Zhang, J. D. Jiao, and L. P. Sn, "A modeling approach for early-warning of water bloom risk in urban lake based on neural network," *China Environmental Science*, vol. 37, no. 5, pp. 1872–1878, 2017.

[11] F. Liu, G. Lin, and C. Shen, "CRF learning with cnn features for image segmentation," *Pattern Recognition*, vol. 48, no. 10, pp. 2983–2992, 2015.

[12] C. Zhang and J. Liu, "The research and implementation of the cylinder stamping character recognition algorithm," *Machine and hydraulics*, vol. 46, no. 13, pp. 37–41, 2018.

[13] L. Zhang, Y. C. Liang, and D. Niyato, "6G visions: mobile ultra-broadband, super internet-of-things, and artificial intelligence," *China Communications*, vol. 16, no. 8, pp. 1–14, 2019.

[14] Q. Liu, Y. Zhang, and J. Yang, "The relationship of morphological-hemodynamic characteristics, inflammation, and remodeling of aneurysm wall in unruptured intracranial aneurysms," *Translational Stroke Research*, vol. 13, no. 1, pp. 88–99, 2022.

[15] W. Shumin and J. Liu, "Survey on policy cognition of orientation normal university students with public funds at the junior middle school starting point and undergraduate level in Hunan province," *Journal of Higher Education*, vol. 60, no. 09, pp. 62–65, 2018.

Hindawi
Computational Intelligence and Neuroscience
Volume 2022, Article ID 8469945, 8 pages
https://doi.org/10.1155/2022/8469945

Research Article

Analysis Model of Spoken English Evaluation Algorithm Based on Intelligent Algorithm of Internet of Things

Nan Xue

School of Foreign Languages, Xidian University, Xi'an, Shanxi 710071, China

Correspondence should be addressed to Nan Xue; xuenan@xidian.edu.cn

Received 4 January 2022; Revised 23 January 2022; Accepted 28 January 2022; Published 27 March 2022

Academic Editor: Guobin Chen

With the in-depth promotion of the national strategy for the integration of artificial intelligence technology and entity development, speech recognition processing technology, as an important medium of human-computer interaction, has received extensive attention and motivated research in industry and academia. However, the existing accurate speech recognition products are based on massive data platform, which has the problems of slow response and security risk, which makes it difficult for the existing speech recognition products to meet the application requirements for timely translation of speech with high response time and network security requirements under the condition of network instability and insecurity. Based on this, this paper studies the analysis model of oral English evaluation algorithm based on Internet of things intelligent algorithm in speech recognition technology. Firstly, based on the automatic machine learning and lightweight learning strategy, a lightweight technology of automatic speech recognition depth neural network adapted to the edge computing power is proposed. Secondly, the quantitative evaluation of Internet of things intelligent classification algorithm and big data analysis in this system is described. In the evaluation, the evaluation method of oral English characteristics is adopted. At the same time, the Internet of things intelligent classification algorithm and big data analysis strategy are used to evaluate the accuracy of oral English. Finally, the experimental results show that the oral English feature recognition system based on Internet of things intelligent classification algorithm and big data analysis has the advantages of good reliability, high intelligence, and strong ability to resist subjective factors, which proves the advantages of Internet of things intelligent classification algorithm and big data analysis in English feature recognition.

1. Introduction

There are many research achievements in speech recognition, mainly including different speech recognition, feature extraction and recognition in complex environment, and real-time classification of a variety of speech [1]. In the conventional methods of speech recognition, voiceprint recognition and speech recognition are mostly used for multidimensional analysis, but the accuracy of this analysis method is greatly affected by environmental noise [2]. In recent years, in order to improve the accuracy of speech recognition, most scholars have improved speech recognition methods and data analysis strategies, including language recognition methods, database processing strategies, and so on [3]. However, there are some problems in speech feature recognition, such as low efficiency, large error, and inconsistent model [4]. In addition, the speech recognition technology and estimation algorithm adopted in different application scenarios are also quite different [5]. Based on this background, this paper proposes an oral English recognition method based on the integration of intelligent classification algorithm of Internet of things and big data analysis.

This paper studies the English text and English feature recognition system based on Internet of things intelligent classification algorithm and big data analysis, which is organized as follows. Section 1 introduces the research background and overall framework of this study. Section 2 introduces the research status of speech recognition and oral feature evaluation at home and abroad. Section 3 adopts the intelligent classification algorithm of the Internet of things based on lightweight learning strategy, constructs the

automatic speech and oral recognition model based on the intelligent classification algorithm of the Internet of things and big data analysis, and proposes the intelligent evaluation model of the effect of oral English recognition. Section 4 verifies the reliability of the spoken English and English feature recognition system constructed in this paper, analyzes the experimental results and errors, and draws a conclusion.

Compared with the existing research results (the speech recognition method is only limited to the feature recognition of audio), the innovation of this paper is to propose the application of intelligent classification algorithm based on the Internet of things in speech recognition technology and the quantitative analysis of oral English evaluation algorithm. Through the daily recording and storage of different oral English data, make full use of the semantic differences between different oral English features and integrate the key data Information comparison and analysis to realize the closed-loop evaluation of oral English in the process of recognition.

2. Related Work

In recent years, a lot of research has been carried out on speech intelligent recognition, and some scientific research achievements have been made [6]. Calandruccio and other scholars improved the information input mode of the existing oral English evaluation model, proposed an English speech analysis model based on multidimensional genetic algorithm, used the multidimensional dispersion strategy to collect the data signals of the English feature recognition model, and realized the information normalization processing of the data signals through the Shenjing network algorithm [7]. Yazdani and other scholars put forward targeted evaluation strategies for the identification of different spoken English according to the differences in oral English expression [8]. Gupta and other scholars found that most speech recognition models still follow the traditional speech evaluation strategy and ignore the use of Internet of things technology and data twin technology. Therefore, the current oral English analysis models often adopt the characteristics of freeze frame input and propose a method of clustering analysis and processing of oral English data information based on characteristic regions, achieving high-quality evaluation of oral English recognition [9]. In order to improve the accuracy of speech recognition, Hovsepyan and other scholars proposed an innovative method of speech recognition based on neural network algorithm and Internet of things topology theory [10]. By studying and analyzing the semantic differences of spoken English in different scenarios, Gla and other scholars put forward a new "point-to-point" ladder evaluation system of spoken English and verified the effectiveness of the speech recognition system in the process of different spoken English recognition through practice [11]. Aiming at the problem of high error rate in speech recognition technology, Hülsmeier et al., combined with multivariate screening strategy and mesh analysis method, proposed an environment fusion recognition method based on Internet of things intelligent algorithm [12].

To sum up, it can be seen that in the process of recognizing spoken English, current speech recognition systems mostly use speech recognition technology to innovate in speech feature extraction, while ignoring its internal speech relevance and innovation [13, 14]. In addition, in terms of English feature recognition, although it can realize the local feature recognition of most spoken English, there is still no universal speech recognition intelligent model with high recognition accuracy [15–17]. On the other hand, most of the current research results focus on the speech recognition model with the intelligent analysis dimension as the core, and there are few speech recognition models combined with the intelligent algorithm of the Internet of things.

3. Methodology

3.1. Application of Internet of Things Intelligent Algorithm in the Construction of English Feature Recognition Model. In the application of speech recognition model, most speech recognition technologies are combined with quantitative analysis methods, audio acquisition methods, and information methods. In the early stage, their combined model was applied to audio recognition of information system [18]. In recent years, the intelligent classification algorithm and big data analysis strategy of the Internet of things have been fully applied in many industries, mainly to solve the identification of specific targets in specific scenarios and realize the efficient analysis and quantitative evaluation of environmental information by collecting environmental information and converting environmental information into characteristic data. Figure 1 shows the commonly used theoretical methods and their implementation process [19]. The intelligent classification algorithm of the Internet of things has a similar idea of big data analysis and modeling, mainly by determining the mathematical relationship between many factors in different types of data, then extracting and classifying the differentiated features of the data, and then conducting intelligent analysis according to the known rules and matching strategies, so as to complete the multidimensional fusion of data [20]. In recent years, with the deepening of the research on intelligent classification algorithm and big data analysis of the Internet of things, its application in various fields is also gradually increasing, so speech recognition is starting to combine with more algorithms [21]. For example, in the fields of medicine, science and technology, transportation, agriculture, economy, and so on, it can be combined with the hardware sensors in the Internet of things to complete the collaborative processing and quantitative analysis of data in different dimensions [22].

Based on the intelligent algorithm of Internet of things, combined with the main characteristics of spoken English, relying on speech recognition technology and spoken language database, the quantitative evaluation of spoken English can be realized by adopting the process of "audio collection-noise removal-feature extraction-text recognition-semantic extraction." Based on this, the construction process of this intelligent model is as follows.

The first step is to measure the degree of relevance according to the relationship or similarity between oral

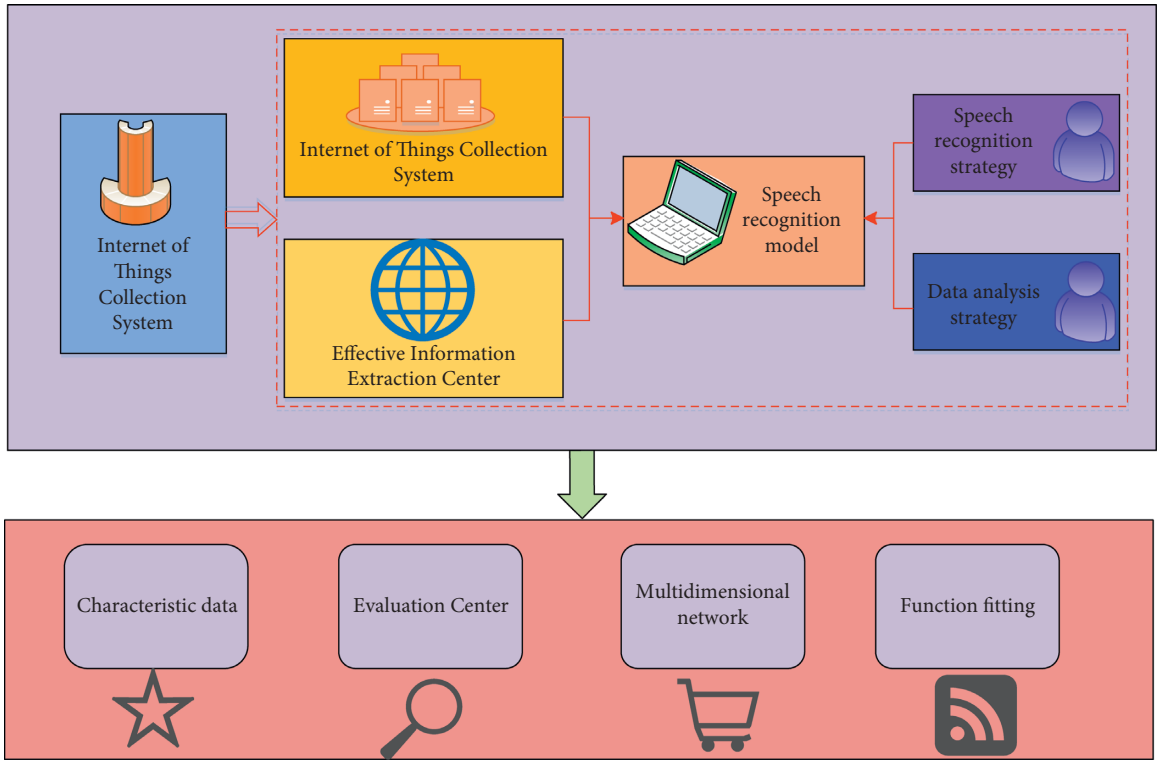

Figure 1: Theoretical methods and implementation processes often used in intelligent algorithms of the Internet of things.

English and environment, mainly by combining the speech recognition strategy model to realize the feedback analysis of its accuracy. In the application of this model, the original spoken English data matrix is initialized, and then the reference data column is formulated and characterized by data. As shown in formula (1), the demand condition on one side is expressed, the actual value of the individual corresponding to the other side is Q_{erca}, the average value of all individuals on the other side is Q'_{erca} the maximum value corresponding to the largest individual is $Q_{\max}$, and the minimum value corresponding to the smallest individual is $Q_{\min}$.

$$M(x) = Q_{erca}^{e-1}\left(\frac{Q_{erca} + Q_{\min}}{Q_{\max} - Q_{\min}}\right)^{x}. \quad (1)$$

In the feature recognition formula (formula (1)) of spoken English, the calculation condition of evaluation accuracy is $(Q_{erca} - Q_{\min}/Q_{\min}) \leq 1$ and the expression of accuracy $Q'(x)$ is

$$Q'(x) = \frac{Q_{erca}^{e-1}}{x/x-1}\left(\frac{Q_{erca} + Q_{\min}}{Q_{\max} - Q_{\min}}\right)^{x}. \quad (2)$$

The English feature recognition accuracy formula (formula (2)) shows that when the satisfaction calculation condition is $(Q_{erca} - Q_{\min}/Q_{\min}) \geq 1$, the coincidence expression $W(x)$ of the corresponding oral English evaluation algorithm is

$$W(x) = \frac{(Q_{erca} + Q_{\min}/Q_{\max} - Q_{\min})^{ex}(x - de^{x}/x + 1)}{e^{x} - 1}, \quad (3)$$

where d is the environmental factor and e^{x} is the time factor.

3.2. Construction of Oral English Evaluation Function in Big Data Analysis Strategy Based on Intelligent Classification Algorithm of Internet of Things. After the coupling analysis of oral English by using the intelligent classification algorithm of the Internet of things, its internal relevance and direct data coupling have a good dimension. Oral test directly detects the examinee's language performance, with strong subjectivity and low reliability. This paper discusses the feasibility of constructing a scientific oral evaluation system from the quality indicators of reliability and validity, combined with the oral examination links such as test construct, information feed and output, and examination form and score. Therefore, it is also necessary to construct the oral English evaluation function on the basis of the above research. The construction principle is the internal relevance analysis strategy of data, and its evaluation process of data is shown in Figure 2.

In the above oral English evaluation model, we can judge the accuracy of oral English through different dimensions. Although this evaluation method can reduce the interference of other factors and objectively reflect the difference of influence, there will be a certain degree of misjudgment in the evaluation of spoken English, resulting in inaccurate final evaluation results. If the low probability misjudgment factors in the process of speech recognition are not considered, the solution value of the objective function is the smallest. It shows that the voice evaluation function value is the best, and the data analysis and classification process are shown in Figure 3.

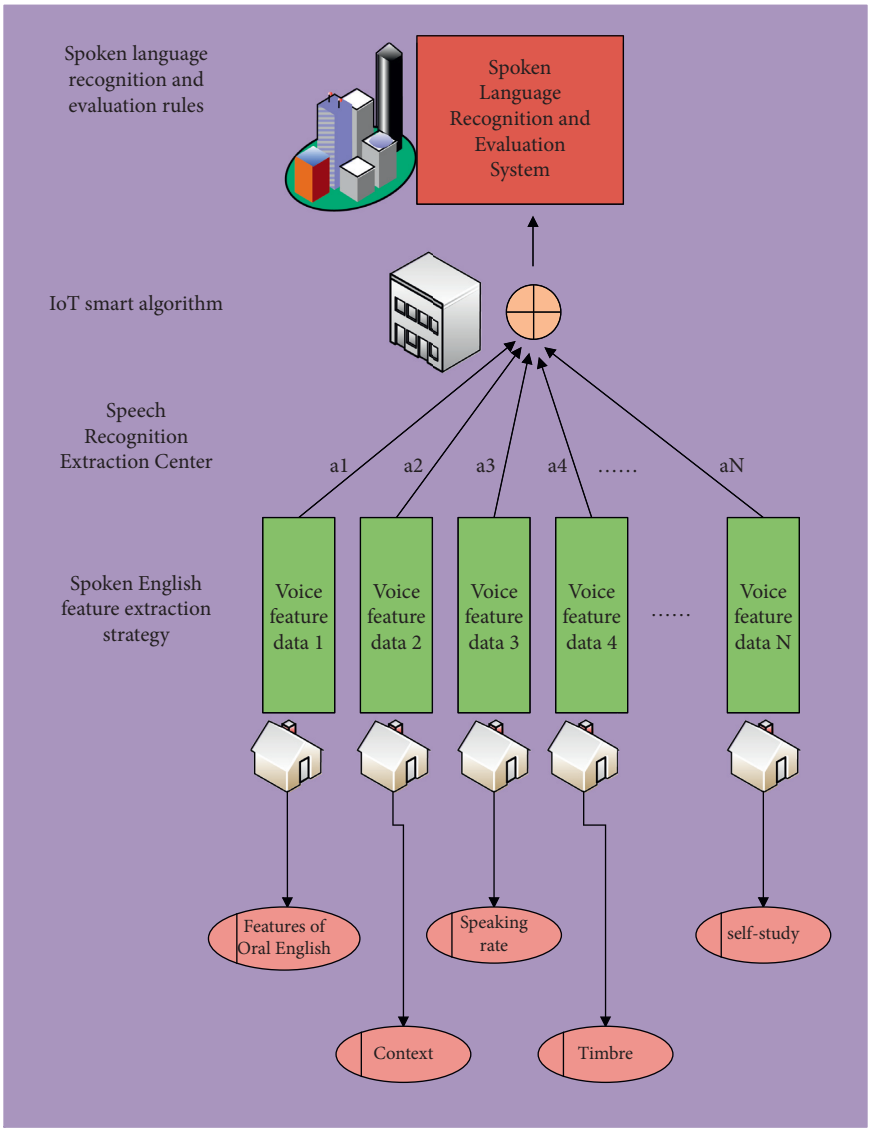

Figure 2: The evaluation process of spoken English data.

As can be seen from Figure 3, with the increase of oral complexity in 10 groups of data, its internal relevance and accuracy have improved, especially in the evaluation of oral English in complex environment. If the vector of the second matrix is H_i, the single extreme value can be set to F_i, and the set extreme value can be set to T_i. The relationship between one-dimensional equation and two-dimensional equation in algorithm calculation is as follows:

$$T_i = \frac{\lambda^2}{\lambda^2 + 2}\sqrt{\frac{H_i + F_i}{\lambda}},$$
$$T'_i = \frac{\lambda^2}{\lambda^2 + 2}\sqrt{\frac{H'_i + F'_i}{\lambda}} + \frac{\sqrt{x - w^2\lambda/x + 1}}{\lambda}, \tag{4}$$

where w is the multidimensional weight of the evaluation function. In order to further remove the noise factors in the environment, the calculation formula can be expressed as

$$T_i = \frac{\left(\lambda^2/\lambda^2 + 2\right)\sqrt{H_i + F_i/\lambda}}{H_i^2 + F_i^2},$$
$$T'_i = \frac{\left(\lambda^2/\lambda^2 + 2\right)\sqrt{H'_i + F'_i/\lambda} + \left(\sqrt{x - w^2\lambda/x + 1}\,/\lambda\right)}{H_i^2 + F_i^2}. \tag{5}$$

The calculated accuracy results under different evaluation degrees are shown in Figure 4.

It can be seen from the evaluation results in Figure 4 that under different degrees of oral complexity, there are important differences in the internal relevance and data consistency in the process of language recognition technology. For example, when the evaluation completion degrees are 0.49, 0.69, and 0.83, the difference in the corresponding accuracy is very obvious, basically showing the law of equal difference sequence. This is because the optimization method based on the intelligent algorithm of the Internet of

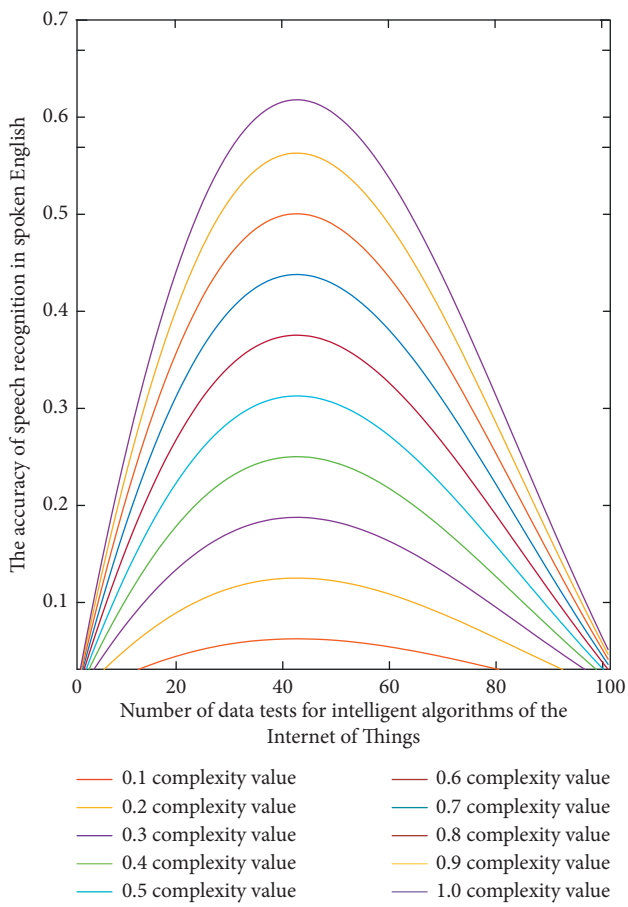

Figure 3: Analysis of the accuracy of the speech recognition of spoken English in different complexities of the intelligent algorithm of the Internet of things.

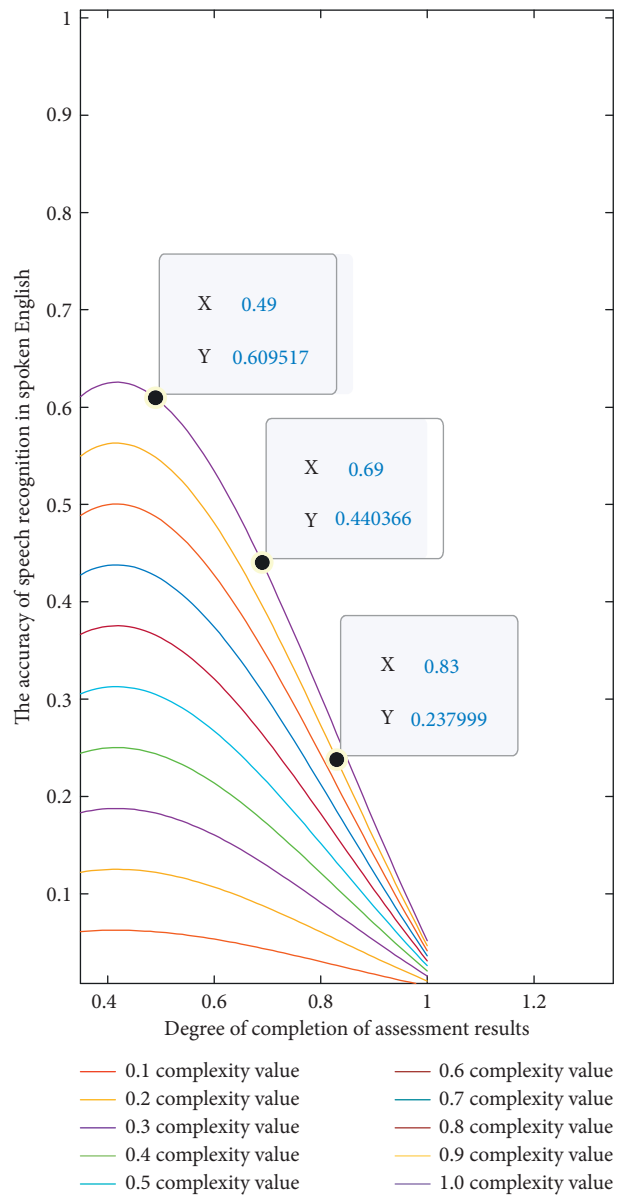

Figure 4: Calculation flowchart for detecting changes in English text.

things mainly makes cyclic iterative judgment by setting the threshold. When the cyclic result meets the set threshold requirements, the corresponding final result can be output. In this experiment, the program is written in MATLAB language. The iterative automatic threshold algorithm is used to realize the global threshold segmentation and local threshold segmentation of the intelligent algorithm. Using the results of global threshold segmentation, the edge detection of the picture is realized, and the data information in the algorithm is enhanced.

The optimization model of speech recognition based on intelligent algorithm of Internet of things adopts the optimization idea of greedy iterative algorithm. Compared with the conventional quantitative evaluation method, this iterative method can have higher reliability and smaller evaluation error with the increase of evaluation times. However, after optimization, the objectivity of the evaluation can be greatly changed. Therefore, in this optimized evaluation method, through three-dimensional simulation verification, the three-dimensional simulation results are shown in Figure 5.

As can be seen from Figure 5, with the increase of simulation times, different types of speech samples can quickly characterize their internal relationship under the same denoising conditions, which is also in line with the expected simulation results and simulation rules. In the evaluation process of simulation results, the red color represents the worse evaluation results, and the blue color represents the better evaluation results. Assuming that the factor universe is represented by discrete function and the evaluation level universe is represented by time value, the vector expressions of the evaluation function before denoising $S_i(x)$ and after denoising $S_i'(x)$ are, respectively,

$$S_i(x) = \frac{\sqrt{1 - xe^x/x + e^x}}{xe^x + 2e^{x-1}},$$
$$S_i'(x) = \frac{\sqrt{xe^{1-x} + e^x/1 + e^x}}{x - 2 + xe^{x-1}}. \quad (6)$$

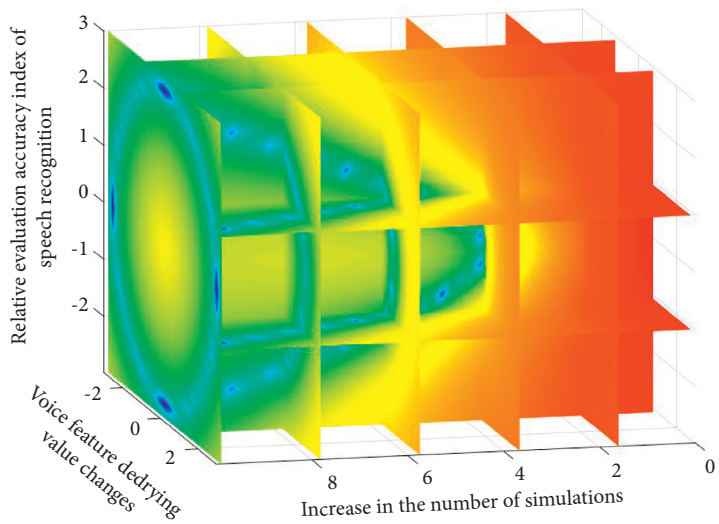

Figure 5: Analysis of 3D simulation results under the intelligent algorithm of the Internet of things.

3.3. Simulation Solution Process of English Text and English Feature Recognition Model. After analyzing and summarizing the characteristics of spoken English, it is necessary to calculate the relationship or correlation degree of different simulation data columns with the help of its internal correlation and the type of spoken English evaluation strategy and then sort the correlation degree. The three-dimensional simulation results of the data corresponding to the English feature recognition model in this link are shown in Figure 6.

It can be seen from the results in Figure 6 that in the process of simulation analysis of different data types, a variety of data gradually change from unstable to stable, and the result orientation of their recognition effect is also significantly different because different data types contain different English features.

In the process of identifying spoken English, the meaning of spoken English in different environments is also different, so equivalent analysis cannot be carried out, and the original data need to be processed dimensionless. After calculating the absolute difference between each factor and the main factor at the same observation point, it is also necessary to calculate the correlation degree between each subfactor and the main factor in the simulation process. When comprehensively evaluating things, the problem of ranking will be involved in most cases. Each evaluation object needs to be ranked first, so grey comprehensive evaluation is also required. The formula is

$$T(x) = \frac{\sqrt{1 + e^{1-x}/1 - e^{1+x}} + \sqrt{e^{1-x}/1 + xe^{x}}}{\sqrt{1 + xe^{x}}}. \tag{7}$$

The optimized function expression is

$$T'(x) = \frac{\sqrt{1 + e^{1-x}/1 - e^{1+x}} - \sqrt{e^{1-x}/1 + xe^{x}}}{1 + \sqrt{x + xe^{x}}}. \tag{8}$$

Combined with the intelligent algorithm based on the Internet of things, use the improved algorithm and data analysis strategy proposed in this study to determine the weight of each index, improve the accuracy of index weight, and ensure that the weight distribution is more real. Select a reasonable evaluation level. The evaluation coupling function $R(x)$ is

$$R(x) = x\sqrt{\frac{1}{x + xe^{x}}}. \tag{9}$$

The optimized coupling function is

$$R'(x) = \frac{x + e^{x}}{3xe^{x-1}}\sqrt{\frac{e^{x} - 1}{x + xe^{x}}}. \tag{10}$$

After calculating the coupling degree, the solution result $D(x)$ can be expressed as

$$D(x) = \sqrt{\frac{R(x) + T(x) + S_i(x)}{xe^{x}}}. \tag{11}$$

4. Experimental Design and Analysis Process of English Feature Recognition Model

4.1. Experimental Design. After processing based on the intelligent algorithm of the Internet of things, the feature information in oral English can be clustered, so that the corresponding noise in the oral expression environment can be effectively reduced, so as to better improve the recognition rate and accuracy of oral English. Then, the data information obtained by the self-learning machine learning algorithm is convoluted, and its internal correlation analysis is realized through decoupling analysis. During the experiment, many types of oral English samples are required (for example, British English and American English) which are input into the Internet of things for machine learning and feature extraction, and then the three features are fused. After the fused features are obtained, the convolution network and intelligent algorithm of the Internet of things are further used for feature extraction and processing, so as to obtain the final output of spoken English recognition results.

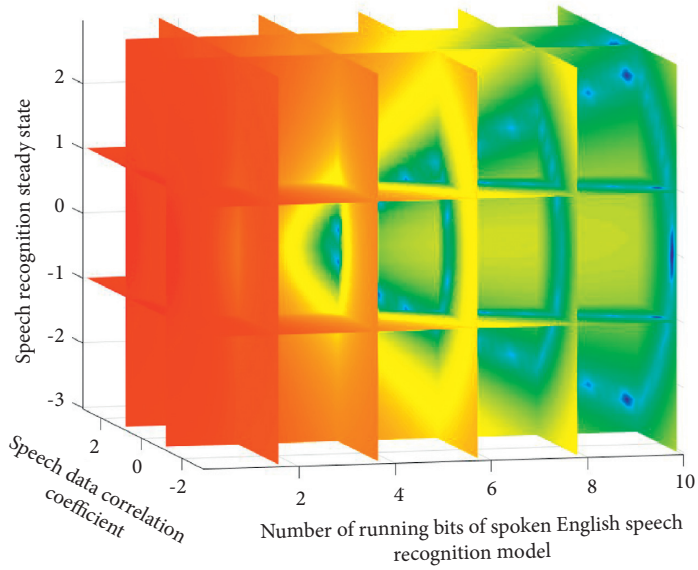

Figure 6: Three-dimensional simulation results of data corresponding to the English feature recognition model.

Before the formal experiment of the recognition model, it is necessary to determine the characteristic parameters of spoken English. According to the experimental samples, the recognition and evaluation rules of oral English are determined, and the characteristic parameters of English features are selected. The experimental process is shown in Figure 7. The tested objects are intelligently classified through the Internet of things. A total of no less than 1000 types of repeated screening and classification are carried out, and the average classification results are used as the preliminary experimental reference index.

4.2. Experimental Data Processing and Result Analysis. Figure 7 shows the score detection results of the spoken English evaluation algorithm. The relevant data in the speech feature recognition score detection model are analyzed and processed by MATLAB software and Python compiler.

As can be seen from the evaluation results in Figure 7, under different evaluation conditions (t data), with the increase of the number of experiments, the evaluation accuracy of the first single oral English experiment data (x data) will be improved to a certain extent, but for two-dimensional (y data) and three-dimensional (D data) data, with the increase of the number of experiments, the evaluation results also show a relatively stable trend (gathered in a certain range), so it has good stability, which also shows that the evaluation index of the identification system has high reliability and stability. Therefore, it can be seen from the experimental results that different types of data fluctuate greatly in the evaluation accuracy because different types of English speakers are different in the process of multiple screening and classification of experimental data. The stability and timbre characteristics of language data groups are different, and the English features involved in different data groups are different, and the initial feature parameter screening will also fluctuate. However, with the increase of

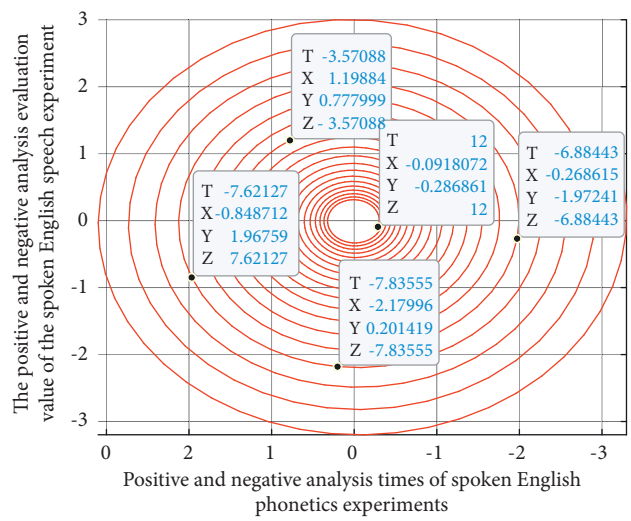

Figure 7: Scoring test results of spoken English assessment algorithm.

the number of experiments, its volatility will weaken and its stability will enhance, so the accuracy of its evaluation will be higher and higher.

In addition, the evaluation index system of the oral evaluation system of the speech recognition technology based on the intelligent algorithm of the Internet of things refers to the speech recognition evaluation standard, which is divided into three levels, of which there are four secondary indicators, namely, the recognition score of the oral English evaluation algorithm, the oral meaning score, the accuracy score of oral feature recognition, and the discrimination score of oral regional features. Each evaluation index of spoken English is divided into different three-level indicators. The English feature recognition score has five three-level indicators, which can comprehensively reflect the recognition accuracy of spoken English.

5. Conclusion

This paper studies the application of intelligent classification algorithm based on Internet of things in the analysis of oral English evaluation algorithm based on speech recognition technology. The experimental results show that the spoken English feature recognition system based on Internet of things intelligent classification algorithm and big data analysis has the advantages of good reliability, high intelligence, and strong ability to resist subjective factors. It proves the advantages of Internet of things intelligent classification algorithm and big data analysis in English feature recognition. This paper solves the problems of large proportion of subjective factors and low degree of intelligence in English text and English feature recognition methods. However, this study only considers the processing of oral feature signals but does not consider the elimination of noise. The future research work can be deeply studied from two aspects: homologous audio separation and error evaluation methods.

Data Availability

The experimental data used to support the findings of this study are available from the corresponding author upon request.

Conflicts of Interest

The author declares that there are no conflicts of interest.

References

[1] N. Giroud, M. Keller, and M. Meyer, "Interacting effects of frontal lobe neuroanatomy and working memory capacity to older listeners' speech recognition in noise," *Neuropsychologia*, vol. 158, Article ID 107892, 2021.

[2] J. Meng, P. Pan, Z. Yang et al., "Degradable and highly sensitive CB-based pressure sensor with applications for speech recognition and human motion monitoring," *Journal of Materials Science*, vol. 55, no. 7, 2020.

[3] I. Speck, M. C. Ketterer, S. Arndt, A. Aschendorff, T. F. Jakob, and F. Hassepass, "Comparison of speech recognition and localization ability in single-sided deaf patients implanted with different cochlear implant electrode array designs," *Otology & Neurotology*, vol. 42, 2021.

[4] C. Rodman, A. C. Moberly, E. Janse, D. Başkent, and T. N. Tamati, "The impact of speaking style on speech recognition in quiet and multi-talker babble in adult cochlear implant users," *Journal of the Acoustical Society of America*, vol. 147, no. 1, pp. 101–107, 2020.

[5] J. A. Skidmore, K. J. Vasil, S. He, and A. C. Moberly, "Explaining Speech Recognition and Quality of Life Outcomes in Adult Cochlear Implant Users: Complementary Contributions of Demographic, Sensory, and Cognitive Factors," *Otology & Neurotology*, vol. 41, 2020.

[6] Z. Song, "English speech recognition based on deep learning with multiple features," *Journal of Computers*, vol. 102, no. 99, pp. 1–20, 2020.

[7] L. Calandruccio, P. A. Wasiuk, E. Buss et al., "The effect of target/masker fundamental frequency contour similarity on masked-speech recognition," *Journal of the Acoustical Society of America*, vol. 146, no. 2, pp. 1065–1076, 2019.

[8] R. Yazdani, J.-M. Arnau, and A. Gonzalez, "A low-power, high-performance speech recognition accelerator," *IEEE Transactions on Computers*, vol. 68, no. 12, pp. 1817–1831, 2019.

[9] M. Gupta, S. S. Bharti, and S. Agarwal, "Gender-based speaker recognition from speech signals using GMM model," *Modern Physics Letters B*, vol. 33, no. 35, Article ID 1950438, 2019.

[10] S. Hovsepyan, I. Olasagasti, and A. L. Giraud, "Combining predictive coding and neural oscillations enables online syllable recognition in natural speech," *Nature Communications*, vol. 11, no. 1, 2020.

[11] G. Li, S. Liang, S. Nie, W. Liu, and Z. Yang, "Deep neural network-based generalized sidelobe canceller for dual-channel far-field speech recognition," *Neural Networks*, vol. 141, pp. 225–237, 2021.

[12] D. Hülsmeier, M. R. Schdler, and B. Kollmeier, "DARF: a data-reduced FADE version for simulations of speech recognition thresholds with real hearing aids," *Hearing Research*, vol. 404, no. 2, Article ID 108217, 2021.

[13] S. V. Blackley, V. D. Schubert, F. R. Goss, W. Al Assad, P. M. Garabedian, and L. Zhou, "Physician use of speech recognition versus typing in clinical documentation: a controlled observational study," *International Journal of Medical Informatics*, vol. 141, Article ID 104178, 2020.

[14] D. Hülsmeier, A. Warzybok, B. Kollmeier, and M. René Schädler, "Simulations with FADE of the effect of impaired hearing on speech recognition performance cast doubt on the role of spectral resolution[J]," *Hearing Research*, vol. 395, no. 6, Article ID 107995, 2020.

[15] K. V. C. Martins, M. V. S. Goffi-Gomez, R. K. Tsuji, and R. F. Bento, "Do the minimum and maximum comfortable stimulation levels influence the cortical potential latencies or the speech recognition in adult cochlear implant users?" *Hearing Research*, vol. 404, no. 5, Article ID 108206, 2021.

[16] G. Chen, L. Wang, and M. M. Kamruzzaman, "Spectral classification of ecological spatial polarization SAR image based on target decomposition algorithm and machine learning," *Neural Computing & Applications*, vol. 32, no. 10, pp. 5449–5460, 2020.

[17] S. Zahra Tajalli, M. Mardaneh, E. Taherian-Fard et al., "DoS-resilient distributed optimal scheduling in a fog supporting IIoT-based smart microgrid," *IEEE Transactions on Industry Applications*, vol. 56, no. 3, pp. 2968–2977, 2020.

[18] M. Alshehri, A. Bhardwaj, M. Kumar, S. Mishra, and J. Gyani, "Cloud and IoT based smart architecture for desalination water treatment," *Environmental Research*, vol. 195, no. 5, Article ID 110812, 2021.

[19] A. Poniszewska-Maranda, D. Kaczmarek, N. Kryvinska, and F. Xhafa, "Studying usability of AI in the IoT systems/paradigm through embedding NN techniques into mobile smart service system," *Computing*, vol. 101, no. 11, pp. 1661–1685, 2019.

[20] H. Igarashi, M. Fukuda, Y. Konno, and H. Takano, "Abscopal effect of radiation therapy after nivolumab monotherapy in a patient with oral mucosal melanoma: a case report," *Oral Oncology*, vol. 108, Article ID 104919, 2020.

[21] M. A. Tahir, H. Huang, A. Zeyer, R. Schlüter, and H. Ney, "Training of reduced-rank linear transformations for multilayer polynomial acoustic features for speech recognition," *Speech Communication*, vol. 110, pp. 56–63, 2019.

[22] X. Liu, "Feature recognition of English based on deep belief neural network and big data analysis," *Computational Intelligence and Neuroscience*, vol. 2021, no. 6, Article ID 5609885, 10 pages, 2021.

Hindawi
Computational Intelligence and Neuroscience
Volume 2022, Article ID 1266332, 11 pages
https://doi.org/10.1155/2022/1266332

Research Article

Research on Image Feature Extraction Algorithm of the Egg and Egg White Protein Thermal Gelation Based on PCA/ICA

XinCi Liu[1] **and Chang Zhao**[2]

[1]*School of Food Engineering, Harbin University of Commerce, Harbin 150028, China*
[2]*School of Food Engineering, Heilongjiang Vocational College for Nationalities, Harbin 150066, China*

Correspondence should be addressed to XinCi Liu; lxc@s.hrbcu.edu.cn

Received 10 November 2021; Revised 6 December 2021; Accepted 15 December 2021; Published 26 March 2022

Academic Editor: Yang Gu

With the rapid development of the computer field in recent years, a series of major breakthroughs have been made in the field of computer vision. The key technologies in image feature recognition, face recognition, image understanding, pattern recognition, and machine learning have been rapidly applied and developed. The research and application of this field provide efficient and convenient means. However, for traditional physical and chemical experimental research, parameter adjustment is time-consuming and costly. In response to the phenomenon, this article starts with the study of the characteristics of the egg white protein thermal gelation image and explores the extraction of external features presented by the optimal parameters of the coagulation image under the thermal coagulation state of the egg white protein, based on the classic PCA and ICA—image feature extraction algorithm and its improved algorithm, respectively. Experiment and simulation research on several image feature extraction algorithms under different egg white solidification states are carried out, and the efficient recognition method and accuracy of the image under the optimal egg white protein thermal gelation state are discussed. It has important reference significance for the research of optimal image feature extraction in the future high-efficiency experimental research.

1. Introduction

Image feature extraction is a process of extracting multiple unique attributes from the preprocessed image target, so that the extracted features reflect the characteristics of the image target as much as possible. This technology is the basis for image object classification, recognition, tracking, and other computer vision-related applications. It is a key link in the image processing process, as well as a key technology for image understanding, pattern recognition, and machine learning. In the image feature extraction, the gray-scale feature of the image pixel and the statistical feature of the pixel's gray-scale value are the most easily obtained features. Extracting images of the best physical and chemical experimental state, avoiding the need to coordinate various parameters in the past, and finding the best state to spend a lot of time and manpower cost have important reference significance. The optimal state image is often produced in physics and chemistry research, and the optimal solution of each parameter is determined by the characteristics of the algorithm. In recent years, with the rapid development of the computer field, a series of major breakthroughs have been made in the field of computer vision, providing efficient and convenient means for research and application in various fields. This thesis starts with the image feature research of the egg white protein thermal gel. Based on the classic PCA and ICA image feature extraction algorithms, as well as several existing improved algorithms, experimental simulation studies are carried out on these image feature extraction algorithms.

2. Related Work

Feature extraction is one of the most fundamental problems in the field of pattern recognition. Extracting effective discrimination features is a prerequisite for solving the problem

of target classification and recognition. The research of feature extraction mainly has the following two purposes: one is to find the most discriminative description between targets, so that different types of targets can be separated from each other; and the other is to compress the dimensionality of target data under certain circumstances.

According to whether it can be linearly separable, the feature extraction methods can be divided into two types: one is the linear feature extraction method, and the other is the nonlinear feature extraction method [1]. To date, for the problem of linear separable feature extraction, people have given many solutions, including principal component analysis [2, 3] (PCA), independent component analysis [4] (ICA), factor analysis (FA), locality preserving projections [5] (LPP), linear discriminant analysis [6] (LDA), local feature analysis (LFA), multidimensional scaling (MDS) is the most classic and widely used method in linear feature extraction algorithms. The linear feature extraction method is easy to understand and easy to implement. It has been successfully applied to various problems such as face recognition, character recognition, speech recognition, and text classification. Aiming at the problem of complex nonlinear separable feature extraction, the introduction of nuclear technology has become one of the important methods to solve. The core idea is to project in a low-dimensional space so that it is linearly separable and then use linear methods for processing.

Principal component analysis is a classic feature extraction algorithm. As early as 1873, Beltrami and Jordan independently derived PCA on the basis of singular value decomposition (SVD). In 1933, the geometric description and algebraic description of PCA were given. In 1967, Jeffers used PCA in practical situations and not just as a dimensionality reduction tool. Jian Yang et al. proposed two-dimensional principal element analysis in 2004 [7–10] (two-dimensional principle component analysis—2DPCA). There is no need to convert a two-dimensional image matrix into one-dimensional data, so it does not change the neighboring relationship of image pixels, which can more accurately estimate the covariance matrix of the image. In recent years, with the widespread application of tensors, Haiping Lu et al. proposed multilinear principal component analysis [2, 11, 12] (MPCA), which extended PCA from one-dimensional vector space to multidimensional tensor space.

Independent component analysis, as an extension of PCA, focuses on the high-order statistics between the data, so that the high-order statistics between the transformed components are independent, and can reflect the essential characteristics of the data. In 2006, Hyvarinen proposed Fast ISA, a fast algorithm for ISA, which has good convergence and reduces the running time of the algorithm. In 2009, Hyvarinen used ISA in the feature extraction and analysis of natural images, which well reflected the essential characteristics of natural images. Scholars at home and abroad [13–18] have developed rapidly in the past 10 years on the algorithm and application of ICA, such as the Computational Neurobiology Laboratory of the Department of Biology, University of California, the Computer and Information Science Laboratory of Helsinki University of Technology in Finland, the Riken Institute of Brain Science in Japan, and the Intelligent Perception and Image Understanding of the Ministry of Education in Xidian University.

The task of image feature extraction is to map data samples in a high-dimensional space to a low-dimensional feature space, so that the statistical correlation between the extracted features is as small as possible, and the separability between different types of features is a certain classification, which is best maintained or enhanced in advance. Principal component analysis considers that the image has a Gaussian distribution, focuses on the two-dimensional statistics of the image, and decorrelates the image. Independent component analysis not only involves the second-order correlation between the images, but also relates to the high-order independence—which is an extension of PCA. The previous research on white protein in egg mainly stayed on the microscopic study of characteristics, and these lacked the study of characteristics to reflect the changes of its parameters. This article will use PCA and ICA to enhance the advantages of the distinguishing ability of characteristics to varying degrees. Corresponding research is also an important development direction for future research on microfeature parameter extraction. This article will use PCA and ICA to enhance the advantages of the distinguishing ability of characteristics to varying degrees. Corresponding research is also an important development direction for future research on micro-feature parameter extraction.

3. Image Feature Analysis of Thermal Gelation of the Egg White Protein

3.1. Experimental Method

3.1.1. Egg White Preparation. First, the egg whites of fresh eggs were separated manually, then stirred with a high-speed disperser (speed 35r/s) for 20 minutes, allowed them stand for 1 hour to discard the bottom umbilical cord and other impurities, and finally placed in a refrigerator at 4 °C for later use.

3.1.2. Moisture Content Determination. Moisture content was determined by oven-drying method.

3.1.3. Preparation of Gel and Determination of Gel Strength. The egg white was diluted with distilled water to the set concentration. According to GB 2760–2007 Food Additives Hygiene Standard, after the addition of food additives or ingredients below the allowable amount to the above diluted egg white, 35 mL was taken into a 50-mL beaker, sealed with plastic wrap, and used after heating in a water bath for a certain period of time. It is cooled in an ice-water bath, placed in a refrigerator at 4 °C for 14 hours, and then taken out for use (Christ Det al., 2005).

The coagulation strength of the egg white expressed was tested by P0.5 probe of the physical property tester with the measured hardness, parallel sample (n = 6) (Valerie Lechevalier et al. 2007). The measurement conditions are as follows:

Speed before test: 5 mm/s;
Testing speed: 1 mm/s;
Speed after measurement: 5 mm/s;
Compression ratio: 50%;
Trigger force: 5g.

3.1.4. Differential Scanning Calorimetry. Netzsch DSC 204 F1 differential scanning calorimetry (DSC) was used to study the thermal characteristics of the egg whites. Pure metal indium (99.99%) was used to correct the enthalpy and temperature of the instrument. 20 mg of egg white sample was weighed with a solid content of 10% into a 25 μl aluminum crucible. Then, the sample is sealed and the distilled water of the corresponding quality is used as a reference. The temperature is increased from 30 °C to 100 °C at a heating rate of 2 °C·min^{-1}. The whole process is carried out under dry N2, the flow rate of purge gas is 20 ml·min^{-1}, and the flow rate of shielding gas is 60 ml·min^{-1} (Yoshinori Mine, 1996).

3.2. Image Feature Analysis of Thermal Gelation of the Egg White Protein. The egg white begins to thicken at 60 °C, but when the gel temperature is lower than 70 °C, the gel strength formed is extremely low. It can be seen from Figure 1 that the gel strength increases with the setting between 80 °C and 90 °C. The temperature of the gel increases; the strength of the gel does not increase at a temperature greater than 90 °C and remains basically stable, but the pores in the gel gradually increase, and a large number of pores are generated at 100 °C, and a relatively stable gel strength value cannot be measured. Considering that it is necessary to obtain a gel with high gel strength and to ensure stable test results, the gel temperature for the following tests is selected as 90 °C.

It can be seen from Figure 2 that when the gel temperature is 90 °C, when the gel time is less than 30 minutes, the gel strength increases with the increase of the gel time; the fresh egg white and the egg white with a solid content of 10% are all congealing. When the gel time is 30 minutes, the gel solidification transition reaches the maximum; after 30 minutes, the gel solidification transition remains stable and no longer increases with the extension of the gel time, but the gel turns brown when the gel time is greater than 50 minutes. Based on the above research conclusions, for the convenience of image feature research, for the subsequent research on the egg and egg white protein thermal gelation image feature extraction algorithm, the egg white with a solid content of 10%, gel temperature of 90 °C, gel time of 30 min, and image feature recognition are selected. The image features in this state are stable, and the best egg gel state can be judged by direct recognition, which can provide a reference for relevant experimental research with efficient research methods.

4. Analysis of Feature Extraction Algorithm of the Egg and Egg White Protein Thermal Gelation Image Based on PCA/ICA

4.1. Feature Extraction of Thermal Gelation Image of the Egg and Egg White Protein Based on PCA

4.1.1. PCA. The classic PCA-based image feature extraction algorithm directly performs feature extraction on the pixel gray level of the image, which is easy to understand and easy to implement, but only considering the pixel gray value information cannot meet the feature extraction of complex images. The PCA algorithm is improved through image pre-transformation, one-dimensional to multidimensional, and block sub-models. The structure information of the image is used to greatly reduce the dimension of the image matrix during operation. At the same time, the image is decomposed by wavelet transform and wavelet is used. The coefficient describes the image, which can effectively extract detailed information and reduce the complexity of subsequent calculations. Wavelet PCA [19] first uses wavelet transform to preprocess the image to obtain a wavelet image that is much smaller than the original image dimension, and then uses the PCA algorithm for feature extraction, which can effectively extract the main features of the image and reduce the algorithm complexity.

The purpose of the PCA algorithm is to find an optimal feature subspace, so that the observation data are projected under this feature subspace, and the component with the largest variance is obtained. It is to find an orthogonal transformation matrix W, so that after orthogonal transformation of the multidimensional data, the new components after transformation are not related to each other.

Suppose $X = (x_1, x_2, \ldots, x_n)^T$ is an n-dimensional random variable, and its mean value can be expressed as follows:

$$\overline{x} = \frac{1}{N}\sum_{n-1}^{N} x_n. \tag{1}$$

After de-averaging X, the component obtained by PCA processing can be expressed as $y_i = w_i^T X$. The feature extraction process of PCA can be described as when the observation data are projected into the feature space, first by looking for w_1, $y_1 = w_1^T X$ has the largest variance, and y_1 is called the first principal component (PC1). Next, by looking for w_2, $y_2 = w_2^T X$ has the second largest variance, and y_1 and y_2 are not correlated, and y_2 is called the second principal component (PC2). By analogy, $y_k = w_k^T X$ has the kth largest variance and is uncorrelated with the previously determined $y_1, y_2, \ldots y_{k-1}$. Then y_k is called the kth principal component (PC k) Until all principal components are found $\{y_i | i = 1, 2, \ldots n\}$. Figure 3 shows the principal component directions of a set of two-dimensional zero-mean random data, where X_1 and X_2 are the original coordinate directions, PC1 and PC2 are the principal component directions after

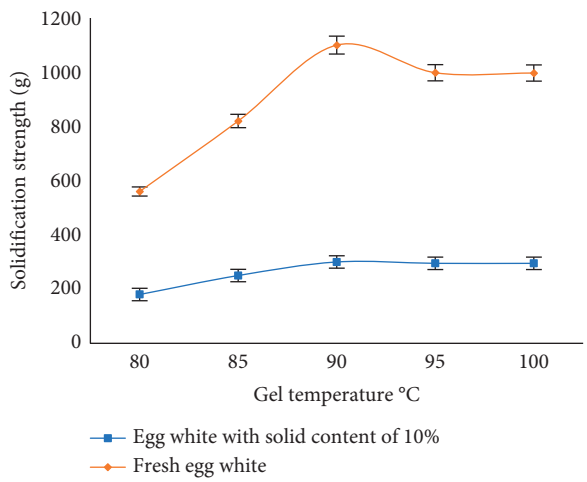

Figure 1: The influence of gel temperature on the gel strength of the egg white.

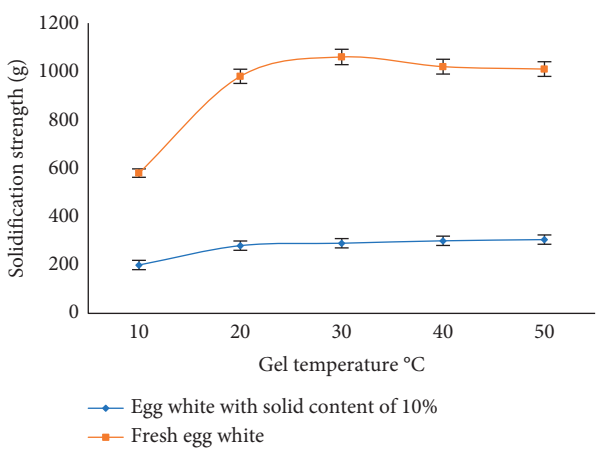

Figure 2: The effect of gel time on the gel strength of the egg white.

PCA processing, and PC1 and PC2 are not correlated with each other.

In fact, a few principal components can meet the demand for data information, that is, the orthogonal transformation matrix $\{w_i = i = 1, 2, \ldots, n\}$, the subscript $p \leq n$ in $w = (w_1, w_2, \ldots, w_p)$, and the principal component is $Y = (y, y_2, \ldots, y_P)$. PCA outputs a few principal components that are not related to each other, which retains the main information of the data and realizes data compression and second-order redundant data removal.

For general natural data, the covariance matrix $C = E[\mathrm{XX}^T]$ is usually a positive definite matrix, and there must be a singular value decomposition $C = \mathrm{UVU}^T$, where $U = (u_1, u_2, \ldots, u_n)$ is the covariance matrix. An orthogonal matrix composed of eigenvectors, $V = \mathrm{diag}\ (\lambda_1, \lambda_2, \ldots, \lambda_n)$, is a diagonal matrix composed of eigenvalues corresponding to the eigenvectors. When the eigenvalue satisfies $\lambda_1 > \lambda_2 > \cdots > \lambda_n$, the basis vector of U constitutes the optimal projection matrix of PCA. After the observation data are projected accordingly, the components are not correlated with each other, and the variance of each component is equal to the corresponding characteristic value. The minimum mean square error of the reconstructed data can be expressed as follows:

$$\varepsilon_{m_i n} = \sum_{i-p+1}^{n} \lambda_i. \tag{2}$$

In the image feature extraction, the image is firstly vectorized, and the image f(x, y) with the size of $m \times n$ is connected end-to-end to form a vector χ of mn ×1, as shown in Figure 4.

Assuming that the image training set has M training samples, vectorize them to get: $\{\chi_i | i = 1, 2, \ldots, M\}$. Then the average vector of M images is as follows:

$$\mu = \frac{1}{M} \sum_{i=1}^{M} \chi_i. \tag{3}$$

Then the covariance matrix of the training image set can be expressed as follows:

$$\begin{aligned} C &= \frac{1}{M} \sum_{i=1}^{M} (\chi_i - \mu)(\chi_i - \mu)^T \\ &= \frac{1}{M} \mathrm{XX}^T. \end{aligned} \tag{4}$$

Since the size of XX^T is $mn \times mn$, for example, the size of the image in the egg white protein image database is 112×92. The high dimensionality of XX^T makes the calculation of the eigenvectors of the covariance matrix very complicated, and the size of $X^T X$ is $M \times M$, usually the number of samples is less than 1000. Assuming that λ and η are an eigenvalue of XX^T and the corresponding eigenvector, there are:

$$X^T X \eta = \lambda \eta. \tag{5}$$

Multiply both sides of the equation by X at the same time to get:

$$\left(\mathrm{XX}^T\right) X \eta = \lambda X \eta. \tag{6}$$

It can be seen that when the eigenvalues of XX^T and $X^T X$ X are the same, the eigenvector is $X\eta$. Therefore, the eigenvalues and eigenvectors of the image covariance matrix are calculated by this method.

The feature vectors are sorted according to the size of the feature value. The feature vector corresponding to the larger the feature value is more able to reflect the image feature, and the size of the feature value decreases exponentially. The image corresponding to the feature vector is called a feature sub-image. Figure 5 is the six-feature sub-images obtained by PCA of the egg and egg white protein image database in the case of five training samples. From left to right, the feature value gradually becomes smaller. It can be seen that the smaller the feature value, the more blurred the feature description and the less information it contains.

4.1.2. Wavelet PCA. The classic PCA-based image feature extraction algorithm directly performs feature extraction on the pixel gray level of the image, which is easy to understand and easy to implement, but only considering the pixel gray

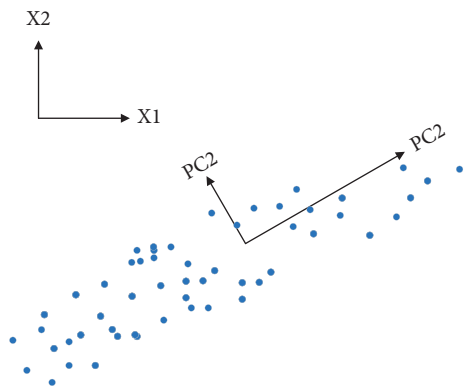

Figure 3: Schematic diagram of principal components of two-dimensional random data.

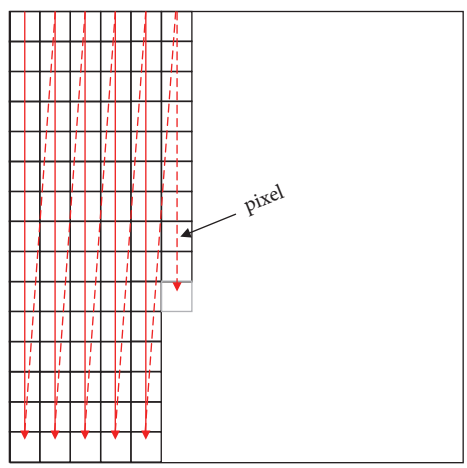

Figure 4: Schematic diagram of image matrix vectorization.

value information cannot meet the feature extraction of complex images. Using wavelet transform to decompose the image and describing the image with wavelet coefficients can effectively extract detailed information and reduce the complexity of subsequent calculations. Wavelet PCA [19] first uses wavelet transform to preprocess the image to obtain a wavelet image that is much smaller than the original image dimension, and then uses the PCA algorithm for feature extraction, which can effectively extract the main features of the image and reduce the algorithm complexity.

Let $f(x)$ be the original signal, the continuous wavelet transform can be expressed as

$$\mathrm{CWT}(a,\tau) = \frac{1}{\sqrt{a}} \int_{-\infty}^{\infty} f(x)\psi\left(\frac{x-\tau}{a}\right)\mathrm{d}x. \tag{7}$$

Among them, ψ is the mother wavelet function, a is the scale variable, and τ is the position variable.

The discrete wavelet transform can be defined as follows:

$$\mathrm{CWT}(j,k) = \frac{1}{\sqrt{2^j}} \int_{-\infty}^{\infty} f(x)\psi\left(\frac{x}{2}-k\right)\mathrm{d}x. \tag{8}$$

Among them, ψ is the mother wavelet function, j is the scale variable, and k is a constant.

The image $f(x,y)$ is two-dimensional data, which needs to be decomposed by two-dimensional discrete wavelet transform. The image after two-dimensional discrete wavelet transform can be expressed as follows:

$$f(x,y) = \sum_{p\cdot q} c_{p,q}\varphi_{p,q} + \sum_{p\cdot q} d^1_{p,q}\psi^1_{p,q} + \sum_{p,q} d^2_{p,q}\psi^2_{p,q} + \sum_{p,q} d^3_{p,q}\psi^3_{p,q}. \tag{9}$$

Among them, $c_{p,q}$, $d^1_{p,q}$, $d^2_{p,q}$, and $d^3_{p,q}$ are two-dimensional discrete wavelet coefficients, and $c_{p,q} = f, \varphi_{p,q}$, $d^1_{p,q} = f, \psi^1_{p,q}$, $d^2_{p,q} = f, \psi^2_{p,q}$, and $d^3_{p,q} = f, \psi^3_{p,q}$. $\varphi_{p,q}$ is the scaling function in the two-dimensional discrete wavelet transform; p and q are the horizontal and vertical displacement marks of the scaling function, respectively; $\varphi_{p,q}(x,y) = \varphi_p(x)\varphi_q(y)$. $\psi^1_{p,q}$, $\psi^2_{p,q}$, $\psi^3_{p,q}$ are two-dimensional wavelet functions, which are as follows:

$$\begin{aligned} \psi^1_{p,q} &= \varphi_p(x)\varphi_q(y), \\ \psi^2_{p,q} &= \varphi_p(x)\varphi_q(y), \\ \psi^3_{p,q} &= \varphi_p(x)\varphi_q(y). \end{aligned} \tag{10}$$

Four sub-band images can be obtained after one-layer decomposition of two-dimensional discrete wavelet transform. Among them, the LL sub-band image retains the low-frequency components of the original image, which is also called a smooth image; HL retains the horizontal details of the original image; LH retains the vertical details of the original image; and HH retains the oblique edge details of the original image. Figure 6 is the result of one-layer wavelet transformation of the egg white thermal gel image in the egg white protein image database using the dB2 wavelet of the Daubechies wavelet series. Usually, we replace the original image with the LL sub-band image after wavelet decomposition for PCA feature extraction. The LL sub-band image is much smaller than the size of the original image matrix, which can effectively improve the real-time performance of the algorithm.

4.2. Feature Extraction of the Egg and Egg White Protein Thermal Gelation Image Based on ICA Algorithm

4.2.1. ICA. ICA was proposed to solve the problem of blind source separation [20] (BSS). It has developed into a multidimensional signal processing technology. In terms of image feature extraction, it is an extension of PCA, focusing on image The high-order statistical characteristics make the components of the transformed image independent of each other and make more effective use of the essential characteristics of the image.

The research of ICA algorithm originates from blind source separation, which is a process of recovering independent source signals from the source signal only from the observation signal according to the statistical characteristics of the input source signal when the source signal and the transmission channel parameters are unknown. When the ICA algorithm is applied to image feature extraction, it realizes the separation of images and generates a set of

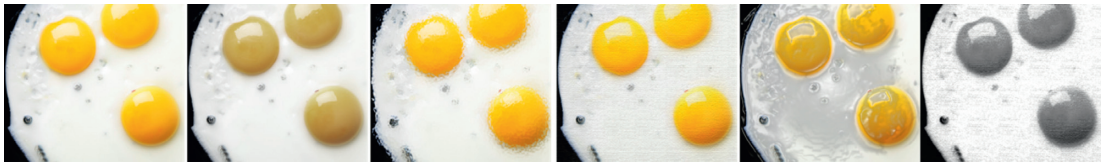

Figure 5: Example of the egg and egg white protein.

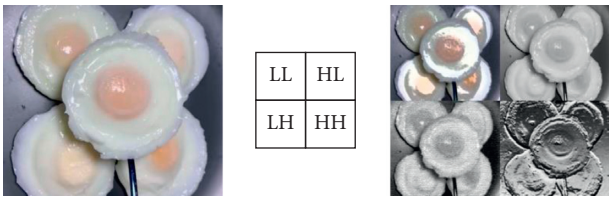

Figure 6: Image wavelet decomposition.

independent source images, and uses these source images as a set of base images of the image set, that is, the images in the image set can be composed of these independent base images. The linear superposition of the image under different combination coefficients minimizes the redundancy of the image pixel gray value and extracts the essential characteristics of the image.

Let $s = [s_1, s_2, \ldots s_m]^T$ be m unknown independent source signals with zero-mean value, and $X = [x_1, x_2, \ldots x_n]^T$ are n random observation signals formed by linear mixing of source signals. Then there are

$$X = \mathrm{AS}. \tag{11}$$

And is

$$x_i = \sum_{j=1}^{m} a_{ij} s_j. \tag{12}$$

Among them, $i = 1, 2, \ldots, n$, $j = 1, 2, \ldots, m$, $A = [a_1, a_2, \ldots, a_n]$ is a full-rank matrix of size $n \times m$.

Let $Y = [y_1, y_2, \ldots, y_m]$ be the estimated signal, then

$$\begin{aligned} Y &= \mathrm{WS} \\ &= \mathrm{WAS}. \end{aligned} \tag{13}$$

Among them, W is called the unmixing matrix. When WA is the identity matrix, the estimated signal is an independent source signal, and because the non-Gaussian nature of random variables is closely related to statistical independence. According to the central limit theorem, when a group of random variables with the same mean and variance act together, the result will be close to the Gaussian distribution, that is, the non-Gaussian of the source signal is stronger than that of the observation signal. Therefore, when the non-Gaussian is maximized, the estimated signal is closer to the source signal. The ICA algorithm uses the unmixing matrix corresponding to the strongest non-Gaussian as the projection direction that ICA seeks based on the high-order statistical characteristics of X to estimate the independent source signal S and realize the separation of the independent sources. Figure 7 is a simple diagram of the ICA model. Figure 8 is an example of ICA used for blind source separation. Figure 7(a) uses four basic signals such as sinusoidal signals as independent source signals. Figure 7(b) is the result of linearly mixing the source signal as the observation signal. Figure 7(c) is the estimated signal separated by ICA. It can be seen from Figure 8 that the ICA algorithm can be effectively used for blind source separation.

The ICA algorithm is different from the PCA algorithm, which regards the signal as a Gaussian distribution and only focuses on the second-order statistics of the signal, but focuses on the high-order statistics of the signal to study the independent relationship between the signals, so the ICA algorithm is more in line with the essential characteristics of image data. Since Hyvarinen et al. published a milestone paper in 1995 and proposed the Fast ICA algorithm, the algorithm has received extensive attention and has been applied to brain signals, speech signals, target detection, image processing, and other fields.

The two-dimensional image is vectorized to form an image signal. It can be considered that the image signal is formed by a set of linear aliasing of statistically independent base images. The base images are separated by the Fast ICA algorithm to form a feature subspace. Each image is in the feature subspace. Projection in the space achieves the purpose of extracting image features.

The feature selection after the independent component feature extraction is an important factor in determining the subsequent classification and recognition of the image. How to use fewer features to quickly obtain a higher classification and recognition rate is a key issue to test the feature extraction algorithm. In the actual feature extraction of images, it is required that the extracted features have as large a difference as possible for images that do not belong to the same category and as small as possible for images that belong to the same category. Since the signals separated by Fast ICA are disordered, the intra-class distance function is introduced to optimize the features.

Assuming that the image set has M types of images, and each type of image is composed of N images, U_j is called the mean value of the distance within the jth feature of the M type, which can be expressed as follows:

$$U_j = \frac{1}{\mathrm{MN}(N-1)} \sum_{i=1}^{M} \sum_{u=1}^{N} \sum_{\substack{v=1 \\ v \neq u}}^{N} \left| a_{(i-1)N+u,j} - a_{(i-1)N+v,j} \right|. \tag{14}$$

Among them, $a_{i,j}$ is the j features of the ith image. In the same way, the mean value V_j of the distance between classes of the jth feature M class can be expressed as follows:

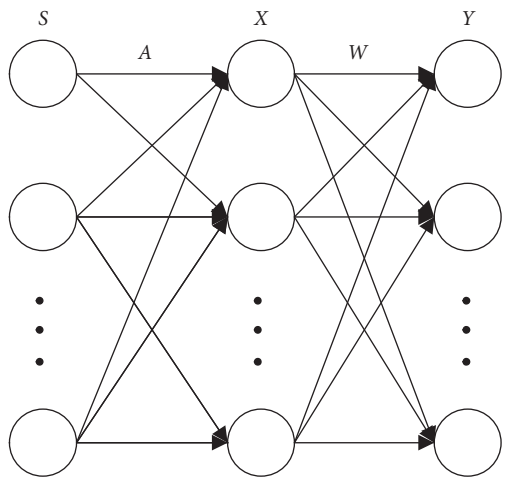

Figure 7: Schematic diagram of ICA model.

$$U_j = \frac{1}{\mathrm{MN}(N-1)} \sum_{p=1}^{M} \sum_{\substack{q=1 \\ q \neq p}}^{N} \left| \frac{1}{N} a_{(p-1)N+u,j} - \frac{1}{N} a_{(q-1)N+v,j} \right|. \tag{15}$$

The evaluation factor β_j of the jth feature is expressed as follows:

$$\beta_j = \frac{U_j}{V_j}. \tag{16}$$

The value of β_j reflects the accuracy of the jth feature for classification. When β_j is small, it means that the distance between classes is greater than the distance within the class, which makes it easier to distinguish different classes. On the contrary, when β_j is large, it means that the distance between classes is larger. The distance is greater than the distance between classes, and it is not easy to classify. Therefore, the evaluation factors of all features can be sorted, and some features with fewer evaluation factors that are most conducive to target classification are selected as the most characteristic set for the final classification.

4.2.2. Subpattern-ICA. The Subpattern-ICA algorithm is based on the ICA algorithm with the selection of the objective function, image preprocessing, and feature optimization. First, the training set image is divided into blocks, as shown in Figure 9, the image is equally divided into multiple sub-blocks without overlapping, and then the corresponding sub-blocks are vectorized to form the training set sub-model. Usually, the local change trend in the image is not the same, so the classification contribution of each training set sub-model to the entire training set is not the same, and due to factors such as occlusion, expression, lighting, the reliability of the classification of each training set sub-model is also inconsistent. So Subpattern-ICA introduces the concept of adaptive weights. After using PCA independently for each training set sub-model, each training set sub-model is classified and recognized, and the classification recognition rate is obtained and normalized as the weighted value of the classification rate of each submodel in the final classification voting stage. Figure 10 is a visualization of the three images in the egg white protein image database and the median image and average image in the database as the test images to calculate the weights of each sub-model. The lighter the color in the figure, the greater the weight, and the greater contribution to the overall classification rate.

The main steps of the Subpattern-ICA algorithm are as follows:

Step 1. The training image set is divided into N sub-blocks, and the corresponding sub-blocks form a sub-model;

Step 2. Use the Fast ICA algorithm to obtain the characteristic projection matrix for each sub-block model;

Step 3. Project the image in the sub-model with the corresponding feature projection matrix to extract features;

Step 4. Divide the test image set image into N sub-blocks according to Step 1. Each sub-block image uses the feature projection matrix of the corresponding training sub-model in step 2 to extract features, and uses the nearest neighbor method to compare the test images based on the sub-model image features The set of sub-block images are classified, and the normalized sum of the votes of each sub-model is used to determine which category the test image set images belong to.

The Subpattern-ICA algorithm uses the idea of sub-patterns to limit the impact of each sub-block image on the overall image within the sub-block image, so that even if the image has serious lighting, expression, and occlusion changes, the changes are reflected in the sub-block image. It will not interfere too much in the feature extraction and classification of the image as a whole. This improves the algorithm's robustness to local changes and improves the algorithm's feature extraction effect.

5. Results

5.1. Simulation Experiment and Result Analysis. The hardware configuration of the PC used in this article is as follows: the CPU model is Intel's Core IS 6600K, the main frequency is 3.SGHz, and the memory is 16 GB DDR4; the software environment is as follows: MATLAB version 2021a; the algorithm is tested on the egg white gel image database. The experiment is used to compare the performance of feature extraction between PCA and Wavelet PCA algorithms, as well as ICA and Subpattern-ICA. In the experiment, three random division methods were selected for the image set of the egg white gel database to verify the feasibility of the algorithm. In the experiment, the nearest neighbor method was used as the classifier, and all the experimental results were averaged after being executed ten times.

5.2. Simulation Experiment and Result Analysis. The egg white protein image database is obtained by crawler extraction based on the characteristics of the image through big data, including rich images of a variety of egg white

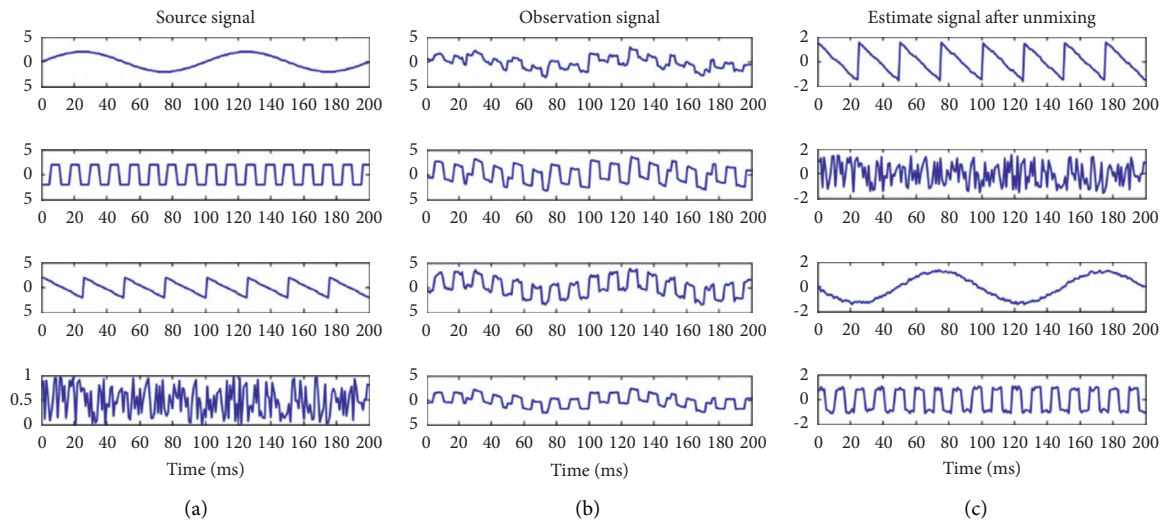

Figure 8: An example of ICA used for blind source separation.

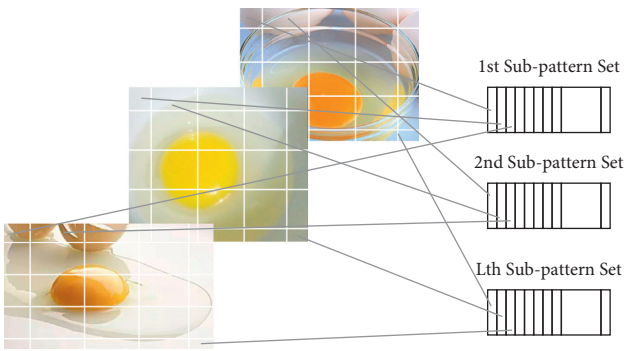

Figure 9: Block diagram.

proteins in different states, totaling 10,000 images. The gray level of the original egg white is 256, with a total of 320×243 pixels. In this experiment, all the images are first cropped to a size of 128×128.

Figure 11 shows 10 images of the egg white state in the egg white protein image database. In this experiment, the egg white protein image database is used as the input image set, and P images in different states of the egg white are randomly selected to form the training image set, and the remaining images are used as the test image set images. The values of P are 1, 4, and 5, that is 1 train, 4 train, and 5 train.

It can be seen from Table 1 that the recognition rate of all algorithms will increase as the number of training increases. Overall, the recognition rate of Wavelet PCA is higher than that of PCA, while the recognition rate of 2DPCA is higher than that of Wavelet PCA and PCA. This is because Wavelet PCA first uses wavelet transform to extract the detailed information of the image, while PCA only uses the gray information of the image. In addition, 2DPCA uses the image matrix as a whole for covariance calculation, taking into account the structural information of the image, which is more effective. It is more representative of the image, and the recognition rate is higher. It can be seen from Figure 12 that the egg white protein image database has changes under the influence of light, and 2DPCA is more effective in such high-change images. Since 2DPCA is different from the other two algorithms in calculating the feature dimension, Figure 12 here shows the curve of the recognition rate of Wavelet PCA and PCA with the feature dimension in the two cases of 1 train and 5 train.

It can be seen from the figure that in Strain, the two algorithms are relatively stable and remain unchanged after reaching a higher recognition rate. It can be seen that Wavelet PCA maintains a leading position compared with PCA. In the 1 train with a small number of samples, Wavelet PCA is also better than PCA.

In this experiment, the egg state image database is the egg white protein image database, and the sub-databases with characteristic types and obvious characteristics are used as the input image set. P images of each egg white in the solidification state at different temperatures are randomly selected to form the training image set. The remaining images are used as test images and the value of P is S, which is recorded as Strain. Figure 13 shows the variation curve of the recognition rate of ICA and Subpattern-ICA with the feature dimension under 5 train. It can be seen from the figure that in the 5 train, both algorithms can achieve a higher recognition rate in a smaller feature dimension, and remain unchanged, with good robustness. However, it can be clearly seen from the figure that when the number of dimensions is small, the recognition rate of Subpattern-ICA stays ahead of ICA and can reach stability faster.

Table 2 shows the classification and recognition results of ICA and Subpattern-ICA in Strain. It can be seen from the table that the recognition rate of these two algorithms will increase with the increase of the feature dimension. On the whole, the recognition rate of Subpattern-ICA is higher than that of ICA. This is because Subpattern-ICA first divides the first image into blocks, and each sub-block uses ICA for feature extraction. It takes into account the structural information of the image but is not sensitive to local changes and can better represent the image, so the recognition rate is higher.

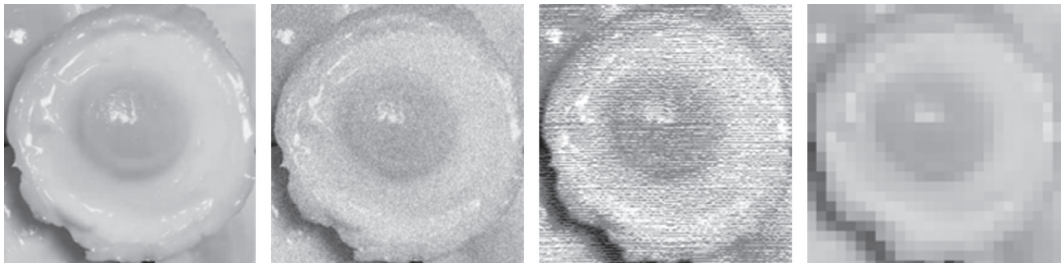

Figure 10: Schematic diagram of adaptive weights.

Figure 11: Ten image state samples of egg whites in the egg white protein image database.

Table 1: In the egg white protein image database, the highest recognition rate obtained after each algorithm is stabilized (%).

Egg white protein image database	1 train	4 train	5 train
PCA	43.07	62.00	63.89
Wavelet PCA	45.47	62.57	62.55

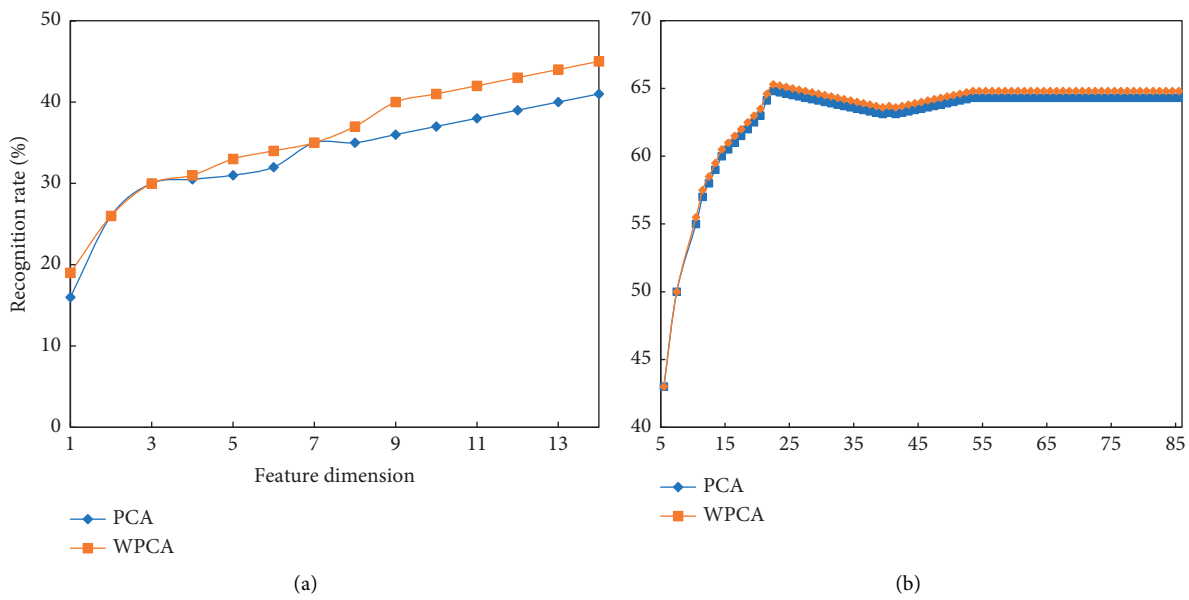

Figure 12: The recognition result of the algorithm in the egg white protein image database. (a) 1 train (b) 5 train.

Consistent with the experimental results of the egg state image database in Experiment 1, it can be seen from Table 3 that the recognition rate of these two algorithms will increase with the increase of the feature dimension. On the whole, the Subpattern-ICA algorithm can better represent the image, the recognition rate is higher than that of the ICA algorithm, and it can quickly reach stability, and has good robustness.

It can be seen from the above two experimental results that the above two algorithms can be used for image feature extraction, and the recognition rate of the Subpattern-ICA algorithm and the image feature extraction proposed in this section are better.

The PCA-based image feature extraction algorithm is a classic image feature extraction algorithm. After the image matrix is vectorized, the covariance matrix is eigenvalue decomposed, and the eigenvector is used as the feature projection matrix. The algorithm is simple and easy to implement, and has been widely used in various fields. Usually, the image is a two-dimensional matrix, and the dimensionality of the image will be very high after vectorization. The direct use of feature extraction makes the algorithm too complex, resulting in unsatisfactory image extraction. On this basis, before using PCA for feature extraction, Wavelet PCA first performs wavelet

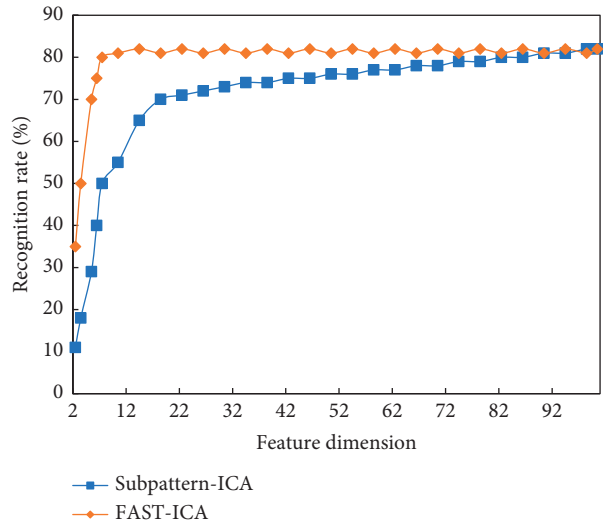

Figure 13: The recognition result in the image database of the egg state of the algorithm.

Table 2: In the egg state image database, the recognition rate corresponds to the feature dimension (%).

Egg state image database	10	20	30	40	50	60	70	80	90	100
ICA	55.5	69.65	76.95	81.05	83.45	85.15	85.95	87.15	87.75	88.8
Subpattern-ICA	85.6	87.55	88.35	89.3	89.65	89.65	89.75	89.65	89.75	89.45

Table 3: In the egg white protein image database, the recognition rate corresponds to the feature dimension (%).

Egg white protein image database	10	20	30	40	50	60	70	80	90
ICA	60.13	64.4	65.13	65.07	64.8	64.53	65.33	66.67	66.53
Subpattern-ICA	64.8	66.53	66.8	67.07	67.2	67.2	67.2	67.2	67.2

transformation on the image to extract wavelet coefficients, which greatly reduces the data dimension used for PCA. This algorithm has good feature extraction effect for images with low changes.

The image feature extraction algorithm based on ICA realizes the separation of images, generates a set of independent source images, and uses these source images as a set of base images in the image space to perform feature extraction on the images. The algorithm considers the high-order statistics of the image, which is more in line with the non-Gaussian nature of the image. But the disadvantage is that the algorithm still needs image vectorization processing, ignoring the internal structure information of the image, and the iterative speed is too slow when the algorithm constructs the objective function and optimizes the objective function, which affects the real-time performance of the algorithm. Based on this, Subpattern-ICA is proposed, which uses the idea of sub-patterns to divide the image into sub-patterns, and then uses ICA for feature extraction for each sub-pattern independently, and finally uses adaptive-weighted voting to determine the classification of the image. The algorithm uses the structural information of the image, improves the robustness of the algorithm for local changes, and improves the feature extraction effect.

6. Conclusion

This article tries to find the optimal parameter combination through traditional parameter adjustment, studies the physical and chemical changes in the egg white, and obtains the optimal parameters through different image state characteristics during the change. This article focuses on the thermal gelation of the egg white protein. In the image feature extraction algorithm, through the analysis of the simulation experiment results, Wavelet PCA is obtained by extracting wavelet coefficients, which greatly reduces the data dimensionality used for PCA, has a good feature extraction effect for images with low changes, and improves the complexity of the PCA algorithm. The improved PCA algorithm is too high, resulting in unsatisfactory image feature extraction. The improved algorithm Subpattern-ICA uses the idea of sub-patterns to divide the image into sub-patterns, uses the structural information of the image, improves the robustness of the algorithm for local changes, and improves the feature extraction effect. Through this research, it can be seen that PCA and ICA have enhanced the distinguishing ability of features to varying degrees, which can enrich the connotation of image feature extraction and solve the problem of image extraction in different states. In addition, the number of image data extracted by the algorithm

used in this article is complicated. When the algorithm is simulated and verified, there will inevitably be shortcomings. In the future, similar research should establish an infrared database for feature extraction and classification in the laboratory to verify the feasibility of the algorithm.

Data Availability

The dataset can be accessed upon request.

Conflicts of Interest

The authors declare that they have no conflicts of interest.

References

[1] M. A. Carreira-Perpinan, "A review of dimension reduction techniques," Technical Report CS-96-09, Department of Computer Science, University of Sheffield, Sheffield, England, 1997.

[2] I. T. Jolliffe, *Principal Component Analysis*, Springer-Verlag, NY, USA, 2002.

[3] J. Shlens, *A Tutorial on Principal Component Analysis*, NY, USA, 2009.

[4] A. Hyvärinen and E. Oja, "Independent component analysis: algorithms and applications," *Neural Networks*, vol. 13, no. 4-5, pp. 411–430, 2000.

[5] X. F. He and P. Niyogi, "Locality preserving projections," *Neural Information Processing Systems*, vol. 16, pp. 153–160, 2003.

[6] K. Etemad and R. Chellappa, "Discriminant analysis for recognition of human face images," *Journal of the Optical Society of America. A*, vol. 14, no. 8, pp. 724–1733, 1998.

[7] A. M. Martinez and A. C. Kak, "PCA versus LDA," *IEEE Transactions on Pattern Analysis and Machine Intelligence*, vol. 23, no. 2, pp. 228–233, 2001.

[8] D. Zhang and A. F. Frangi, "Two-dimensional pca: a new approach to appearance-based face representation and recognition," *IEEE Transactions on Pattern Analysis and Machine Intelligence*, vol. 26, no. 1, pp. 131–137, 2004.

[9] P. Nagabhushan, D. S. Guru, and B. H. Shekar, "Visual learning and recognition of 3D objects using two-dimensional principal component analysis: a robust and an efficient approach," *Pattern Recognition*, vol. 39, no. 4, pp. 721–725, 2006.

[10] W. Zuo, D. Zhang, and K. Wang, "An assembled matrix distance metric for 2DPCA-based image recognition," *Pattern Recognition Letters*, vol. 27, no. 3, pp. 210–216, 2006.

[11] L. Xang, "On image matrix based feature extraction algorithms," *IEEE Transactions on Systems, Man and Cybernetics, Part B (Cybernetics)*, vol. 36, no. 1, pp. 194–197, 2006.

[12] H. P. Haiping Lu, K. N. Plataniotis, and A. N. Venetsanopoulos, "MPCA: m principal component analysis of tensor objects," *IEEE Transactions on Neural Networks*, vol. 19, no. 1, pp. 18–39, 2008.

[13] H. Wang and N. Ahuja, "A tensor approximation approach to dimensionality reduction," *International Journal of Computer Vision*, vol. 76, no. 3, pp. 217–229, 2008.

[14] C. M. Chen, S. Q. Zhang, and Y. F. Chen, "Face recognition based on MPCA," in *Proceedings of the International Conference on Intelligent Mechatronics and Automation (ICIl-VIA)*, vol. 1, pp. 322–325, Montreal, Canada, May 2010.

[15] G. Wu, P. Zhang, and R. Wang, "Independent component analysis and its application status in image processing," *Computer Engineering and Applications*, vol. 44, no. 23, pp. 172–177, 2008.

[16] J. Han, K. Chi, and Y. Yeon, "Aquaculture feature extraction from satellite image using independent component analysis," *Machine Learning and Data Mining in Pattern Recognition*, vol. 3587, pp. 660–666, 2005.

[17] Q. H. Huang, S. Wang, and Z. Liu, "Improved algorithm of image feature extraction based on independent component analysis," *Electronic Engineering*, vol. 34, pp. 121–125, 2007.

[18] J. Y. Gan and C. Z. Li, "Face recognition based on wavelet Transform,Two-dimensional principal component analysis and independent component analysis," *Pattern Recognition and Artificial Intelligence*, vol. 20, pp. 377–381, 2007.

[19] Q. Jiao, "Face recognition method based on wavelet and PCA," in *Proceedings of the 33rd China (Tianjin) 2019 IT, network, information technology, electronics, instrumentation Innovative Academic Conference Proceedings*, Tianjin Institute of Electronics, Tianjin Institute of Instrumentation: Tianjin Institute of Electronics, 2019.

[20] X. Jiao, "General approach to blind source separation," *IEEE Transactions on Signal Processing*, vol. 44, no. 3, pp. 562–571, 1996.

Hindawi
Computational Intelligence and Neuroscience
Volume 2022, Article ID 8799247, 10 pages
https://doi.org/10.1155/2022/8799247

Research Article

Research and Forecast Analysis of Financial Stability for Policy Uncertainty

Zhiyi Dai [1] **and Zhengming Zhou** [2]

[1] *School of Business, Shanghai University of Finance and Economics, Yangpu District, Shanghai 200433, China*
[2] *School of Finance, Shanghai University of Finance and Economics, Yangpu District, Shanghai 200433, China*

Correspondence should be addressed to Zhiyi Dai; daizhiyi1234567@163.sufe.edu.cn

Received 26 January 2022; Revised 20 February 2022; Accepted 25 February 2022; Published 24 March 2022

Academic Editor: Guobin Chen

The instability of financial market will have a great impact on money, bonds, and stocks and affect the economic development of society and people's lives. Therefore, it is very necessary for us to study and predict the financial stability. According to the forecast results, we will analyze and make a series of preparatory measures. First, we make a series of analyses on the structure and significance of policy uncertainty and financial stability. This paper introduces the advantages and disadvantages of the P/L model, the KLS signal method, and the BP neural network model for financial stability early warning, It is clearly pointed out that the BP neural network is more reliable and accurate, Then, the BP neural network, the ant colony algorithm, and the genetic algorithm are used to predict the opening price, closing price, highest price, and lowest price of KDJ index of Cathay Pacific Group's 5-day data. Compared with the real value, we find that the BP neural network is almost the smallest in forecasting the opening price and closing price, or the lowest price and the highest price, and has good stability, which once again proves the feasibility of applying the BP neural network to the research and prediction of financial stability.

1. Introduction

The stability of financial market can prevent the possibility of financial crisis. The instability of financial market will bring impact to the securities market, affect people's economic life, and bring bad experience to people's life, so we should always need to care the stability of the market. Uncertainty in economic policy can cause many inconveniences and impacts especially on decision-making including financial intermediaries. By examining the impact on whether the total amount of bank credit will increase. We should have a look on the total amount of credit that will increase or decrease, and then analyze the data owned by the bank entity level. This paper studies and analyzes whether the policy uncertainty will affect the loans of financial intermediaries. The above effects may be attributed to loan demand, which is related to load sheet conditions, or loan supply, which is related to its financial constraints. After analysis and research, we find that it has big bag effect on bank credit become more. Similarly, loan supply factors will obviously have an advantage to determine the impact of goals to a certain extent [1]. Finally, it is concluded that high economic policies will inhibit the growth of overall credit, mainly through bank loans, which will slow down the possible consistency of American economic recovery to a certain extent. This paper investigates the influence of EPU on cross-border mergers and acquisitions. The results show that a high level of domestic EPU will hinder the number and volume of transactions in a certain part, but the host country has moderated this effect positively through its own better conditions. For cross-border M&A, the survey shows that with the same high level of EPU, the target country hinders the entry CBA transactions, while the acquiring country increases the number of its transactions. Finally, an EPU with a larger growth rate will have a lower stock recovery rate compared with the two countries with a smaller growth rate. The results show that if we want to have better transnational investment, we should try our best to reduce the uncertainty of economic policies [2]. Through a macroeconomic model with asset prices, this paper analyzes how several indicators are affected by the central bank's robustness, namely, optimal monetary policy, economic dynamics, and

performance. Based on the worst-case model, it is shown that the increase of conservatism preference requires the optimal nominal interest rate to make a series of more positive responses to inflation. The results show that increasing conservatism preference can strengthen the response of current and expected inflation, asset prices, and output to its shocks, but this has almost no impact on commodity demand and financial market shocks [3]. This paper discusses the factors that determine have a question on what can deicide the financial institutions, finds that the policy instability is very important for the proper control of financial system risks, has a significant impact on the target, and it may have an impact on the target through its changed lending behavior and risk-taking ability [4]. This journal points out that economic uncertainty has made a significant contribution to financial risk management, and uncertainty impacts the market and is the decisive factor of banking expansion. Through some dynamic characteristics and forecasting variables, a practical method is constructed, which is mainly based on the price of liquidity factors, to achieve the prediction of interval volatility. It also points out that the uncertainty of China's economic policy and its impact on Taiwan and Hong Kong have a certain impact on their finance [5].We discusses the influence of target on earnings management in Japan and proves that it is negatively correlated with earnings management, that is to say, when EPU is increased, administrators may reduce earnings management. After further analysis of different entities, it is found that the relationship between the two objectives will be less significant under the company with the main bank, which is consistent with the view that the management will have relatively little room to improve the quality of objectives when the EPU is higher. We found similar results when we added analysts to report this indicator. Finally, we find that with the different influencing factors of policy uncertainty, the impact of EPU will also change, and the exposure degree of each enterprise will be different [6]. This paper analyzes and discusses how EPU affects configuration efficiency. The research found that it affected the market value of nearly 25% of the companies, but 90% of them were affected by it and the investment decreased. EPU will distort the signal of capital market, which may aggravate the conflict of interest between managers and investors [7]. We have a question on how the target will influence the investment and capital cost and then try to find an answer. Using a news-based index, looking at 21 countries, we find that a high EPU will reduce the intensity of target negative relationship, and this increase in EPU will reduce the sensitivity of investment to capital cost to a certain extent, whether it is in more opaque countries, enterprises with low analyst coverage or no credit rating. It is said that the answer to the question we started to ask is yes [8].This paper makes an extended research on what kind of influence the target will have on the spread in different ways mechanism of policy by analyzing the relationship between speculators' trust in financial market stability, exchange rate growth and economic development, and the volatility between them. The heterogeneity of error is used to estimate the uncertainty, the results are compared with the literature, and the causes of the financial crisis are obtained. It is found that the low tide of macroeconomic fluctuation will not directly produce the low tide driven by financial stability [9]. This paper points out that the deregulation of financial market will increase the frequency of currency crisis. At present, crisis prediction and financial stability detection are still in their infancy. This paper discusses whether the application of visualization tools based on neural networks will be beneficial to monitoring, mainly self-organizing mapping, which takes time points as benchmarks to intuitively introduce economic indicators and the vulnerability of impending crises. The results show that SOM can be used as a dynamic visualization tool for early warning signals of currency crisis [10].Taking the financial distress data of listed companies in China as research samples, the BP neural network model is trained and tested. The results show that the optimized model improves the prediction accuracy and stability to a certain extent. This study not only have a good outcome on test but also provides new ideas and measures on what we hope it become better [11]. This paper establishes a model related to financial stability. This defines that unregulated private money creation and excessive short-term debt issuance by intermediaries may lead to externalities. Moreover, it can adjust this situation by open market operation. Finally, the model well explains how monetary policy affects practical activities such as bank loans, that is, other trading media can not be controlled by the central bank except banks create money, but this is based on the situation that prices are not adjusted by friction [12]. Faced with the weakness of the existing measurement of financial stability. Too much reliance on macro stress testing, but the "ambiguity" in measurement will not hinder its progress towards the framework. The main features of its framework are strengthening the prudent orientation of supervision; systematically solve the procyclical problem; reduce the burden of measuring financial stability risks in real time; and establish institutional arrangements that draw on the relative expertise of the various authorities involved in safeguarding, in particular financial regulators and central banks [13]. By evaluating the impact of policy uncertainty on China, we find that its increase can reduce investment, mainly for export entry and technological upgrading, and on the contrary, it will reduce real income, which is mainly brought by trade flows and consumers. Through this analysis and research on the export boom before and after China's entry into WTO, it is concluded that the reduction of TPU is a very important policy. We construct a theoretically consistent TPU measure, which not only estimates more than one quarter to about one-third of China's exports to the United States but also estimates a series of effects after removing TP, including welfare benefits for American consumers, and finds that it is similar to the benefits obtained from newly imported varieties [14]. This paper points out that reasons have two. One is the growth of government expenditure, tax revenue, and supervision. Second, the aggravation of political polarization has an impact on its decision-making process and policy choice. Evidence shows that these two reasons have played a certain role in this [15].

2. Basic Overview

2.1. Policy Uncertainty. Policy uncertainty mainly refers to one of the one of the goals in the article (EPU). In this context, the fluctuation of financial market is a good

reflection of the changes in the economic situation at that time, which will have an impact on the expectations of investors and consumers. The composition of EPU in each country is different. The United States mainly includes three parts: news index, tax law failure index, and economic forecast difference index; Europe and China are news indexes. Economic policy uncertainty can be used to explain the change of leverage ratio of listed companies, which has a long impact on it and will aggravate the differentiation of leverage ratio in places with serious financial repression. Time has proved that the rise of policy uncertainty will bring many influences, such as the rise of leverage ratio of state-owned enterprises and the decline of nonstate-owned enterprises. Economic policy uncertainty is closely related to financial market stability, which can increase unemployment rate, increase inflation, and have a negative impact on financial market.

2.2. Financial Stability. Financial stability, most people regard it as the stability of financial institutions, which is mainly the stability of banks, or we can also understand that the main and most financial institutions in the financial system operate steadily without affecting market confidence. On the contrary, financial instability is mainly manifested as the fragility of financial intermediaries or abnormal fluctuations in asset prices, which is also an important basis for monitoring financial stability. Obviously, financial stability is a state, which refers to a state in which a country's financial system runs smoothly without much fluctuation. The exchange rate transmission mechanism of financial stability is shown in Figure 1.

The characteristics of financial stability are

2.2.1. Global. It plays an overall role and is an important provider and defender of some components in the financial institution system. At the same time, banks are the core of financial stability, and its foothold should be a role in maintaining the stability of the whole macro-financial system.

2.2.2. Dynamics. As a state, financial stability is obviously not static and unchangeable, it is constantly changing and developing, and it is a dynamic state. It needs to make corresponding changes with the development of economy and finance. Its internal brother structure adjusts and interacts with each other to form a systematic liquidity system with regulation and control to adapt to the ever-changing financial situation.

2.2.3. Benefit. The stability of the financial system can bring more investment opportunities to enterprises and promote the efficiency of transforming savings into investment.

2.2.4. Comprehensive. Financial stability needs different policies, measures and behaviors, such as monetary policy, financial supervision, and real economy.

There are two important conditions to judge whether finance is stable: price stability and bank stability. The financial stability evaluation system is shown in Figure 2.

2.3. BP Neural Network. BP neural network is one of the most widely used neural network models at present. It is a network model based on error back propagation algorithm. The learning process mainly consists of two processes: forward propagation of signals and back propagation of errors.

In forward propagation, the input of samples is transmitted through the input layer, processed by each hidden layer, and then transmitted to the output layer. If the reality of the output layer does not match the expectation, it is necessary to turn to the back propagation stage of error in time. In the back propagation stage, the input will pass through the hidden layer in a certain form and then reverse transmit to the input layer, and the error will be given to all the units in each layer in the form of equal sharing, so that the error signal means that there will be no gaps in each layer, and this signal can be used as the basis for correcting the weights of each unit.

2.3.1. Transfer Function of BP Neural Network. It mainly adopts a non-linear transformation function-S function, which itself and its derivatives are continuous. The expression of unipolar S-type function is as follows:

$$f(x) = \frac{1}{1 + e^{-x}}. \tag{1}$$

The expression of bipolar S-type function is as follows:

$$f(x) = \frac{1 - e^{-x}}{1 + e^{-x}}. \tag{2}$$

2.3.2. Learning Algorithm of BP Neural Network. This algorithm takes a three-layer perceptron as an example. When the network output is not equal to the expected output, it will output error E, which is defined as follows:

$$E = \frac{1}{2}(d - O)^2 = \frac{1}{2}\sum_{k=1}^{\iota}\left(d_k - o_k\right)^2. \tag{3}$$

2.3.3. Training Decomposition of BP Neural Network. This process is mainly to adjust two parameters: weight and offset, which are divided into the following two parts:

The output layer calculation formula is as follows:

$$I_j = \sum_{i=1} w_{ij} o_j + \theta_j. \tag{4}$$

After random initialization, each weight randomly takes the real number between [–1, 1], and each offset takes the real number between [0, 1], and then starts forward transmission.

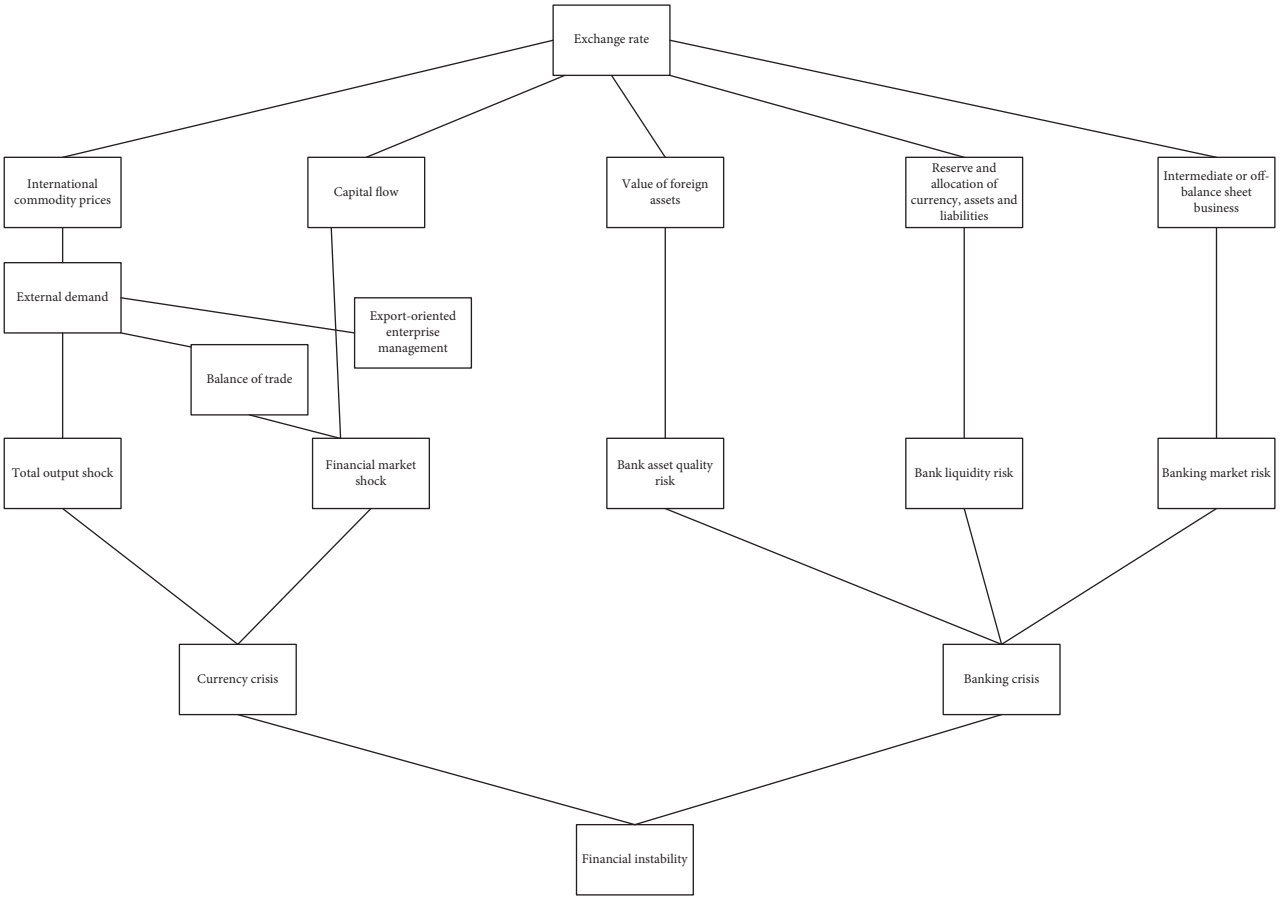

Figure 1: Exchange rate transmission mechanism of financial stability.

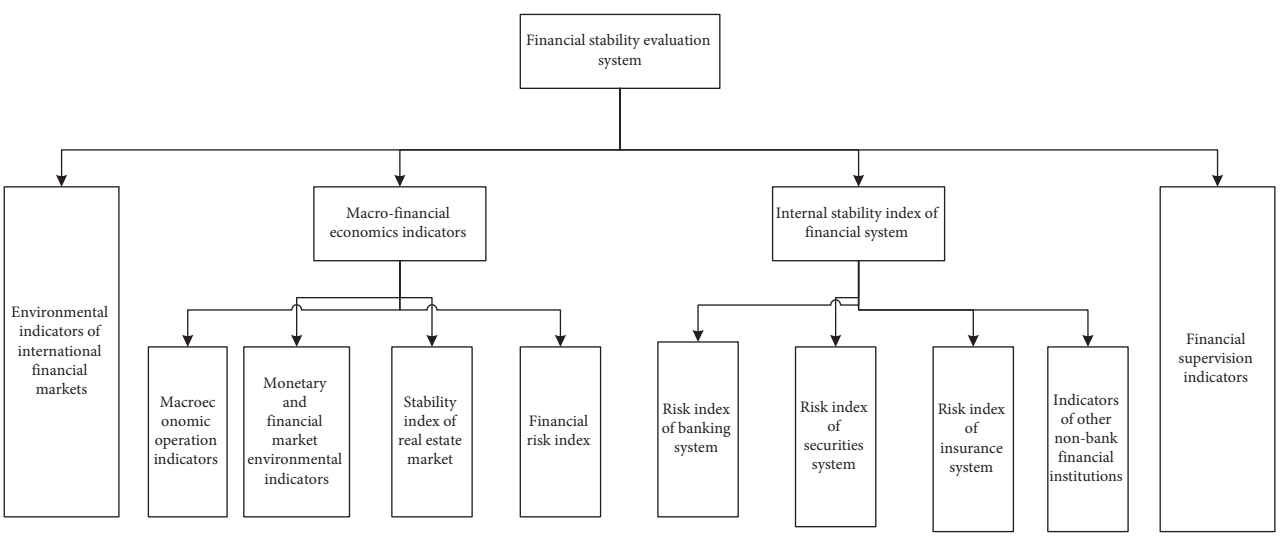

Figure 2: Financial stability evaluation system.

$$o_j = f\left(I_j\right) = \frac{1}{1 + e^{I_j}}. \tag{5}$$

After calculating the output value, we are equivalent to completing the forward transmission part.

For the output layer:

$$E_j = O_j\left(1 - O_j\right)\left(T_j - O_j\right), \tag{6}$$

where E_j represents the error value generated by the Jth node and the output value completed by the Jth node, it is responsible for completing the task of recording the output value. For example, for the classification of two categories, it is stipulated that 01 represents category 1 and 10 represents category 2. If a record belongs to category 1, its $T_1 = 1, T_2 = 0$.

The hidden layer in the middle is calculated by accumulating the errors of all nodes in the next layer according to the weight, and the calculation formula is as follows:

$$E_j = O_j\left(1 - O_j\right)\sum_k E_k W_{jk}, \tag{7}$$

where W_{jk} represents the weight value from the node j of the current layer to the node k of the next layer, and E_k represents the error rate of the node k of the next layer.

The rules for updating weights are as follows:

$$\begin{aligned} \Delta W_{ij} &= \lambda E_j O_i, \quad 0 \le \lambda \le 1, \\ W_{ij} &= W_{ij} + \Delta W_{ij}. \end{aligned} \tag{8}$$

It indicates the speed of learning. The larger its value, the faster the training convergence, but it also has certain disadvantages, that is, it is easy to fall into the local optimal solution. On the contrary, the smaller its value, although the convergence speed is slow, it can approach the global optimal solution step by step.

After completing the above operation update, the bias should also be updated, and its update rules are as follows:

$$\begin{aligned} \Delta\theta_j &= \lambda E_j, \\ \theta_j &= \theta_j + \Delta\theta_j. \end{aligned} \tag{9}$$

When the number of iterations reaches the maximum value, we set or the prediction accuracy of the training set on the network, and the training will be terminated.

2.3.4. Specific Algorithm Flow Chart of BP Neural Network Operation. The Specific Algorithm Flow Chart of BP Neural Network Operation is as Follows in Figure 3

3. Choice of Early Warning Model of Financial Stability

3.1. P/L Probabilistic Model. Its expression is as follows:

$$\begin{cases} P\{Y = 1\} = (X, \alpha), \\ P\{Y = 0\} = (X, \alpha), \end{cases} \tag{10}$$

where the probability of 1 means that the financial crisis will occur, 0 means that the financial crisis will not occur, X is the inducing factor of the financial crisis, and α is a vector of the parameter.

The advantages of this model are easy to understand and simple to operate, and the probability of financial crisis in different countries can be compared from a horizontal perspective. However, the cumulative time and examples show that this model does not consider the differences of different countries repeatedly, which makes its prediction seriously deviated and lacks certain effectiveness.

3.2. KLS Signal Method. This signal model is more applied to the early warning of currency crisis, which mainly consists of the following four comprehensive early warning indicators:

(1) Sum all the basic alerts, and the expression is

$$I_t^1 = \sum_{t=1}^{n} S_t^i, \quad I_t^1 \in [0, n],\ i = 1, 2, 3 \ldots n. \tag{11}$$

It indicates whether the I index will exceed the safety threshold in T period, and its values are only 0 and 1.

(2) Consider the weights of different indicators into early warning indicators

$$I_t^2 = \sum_{t=1}^{n}\left(SM_t^i + 2SE_t^i\right), \quad I_t^2 \in (0, 2n], \tag{12}$$

where SE_t^i is a strong signal and SM_t^i is a weak signal, and the weight value of the strong signal is twice that of the weak signal.

(3) This comprehensive early warning index holds that the outbreak of crisis is not achieved overnight, but a process of accumulation. We regard the time point when the safety threshold is exceeded as the signal of crisis and assume that the time of the model is 8 months, and the expression is as follows:

$$I_t^3 = \sum_{t=1}^{n} S_{t-s,t}^i, \tag{13}$$

where $S_{t-s,t}^i$ means that he will have an early warning at any time point between [t-s, t], and its values are only 0 and 1, 1 means that it will happen, and 0 means that it will not happen.

(4) Considering the different situations of each early warning indicator, the expression is as follows:

$$I_t^4 = \sum_{t=1}^{n} \frac{S_t^i}{w^i}, \tag{14}$$

where W represents interference ratio, which is mainly for weight, and comprehensive index can be obtained by weighting.

Compared with the P/L model, this model has a better effect and development. However, because many indicators of this model are determined and carried out by historical data, subjectivity will be strong and there will be certain limitations.

3.3. BP Neural Network Model. The basic process of the BP neural network model mainly includes three parts: initial network creation, learning and training, and early warning. The algorithm flow chart is shown in Figure 4.

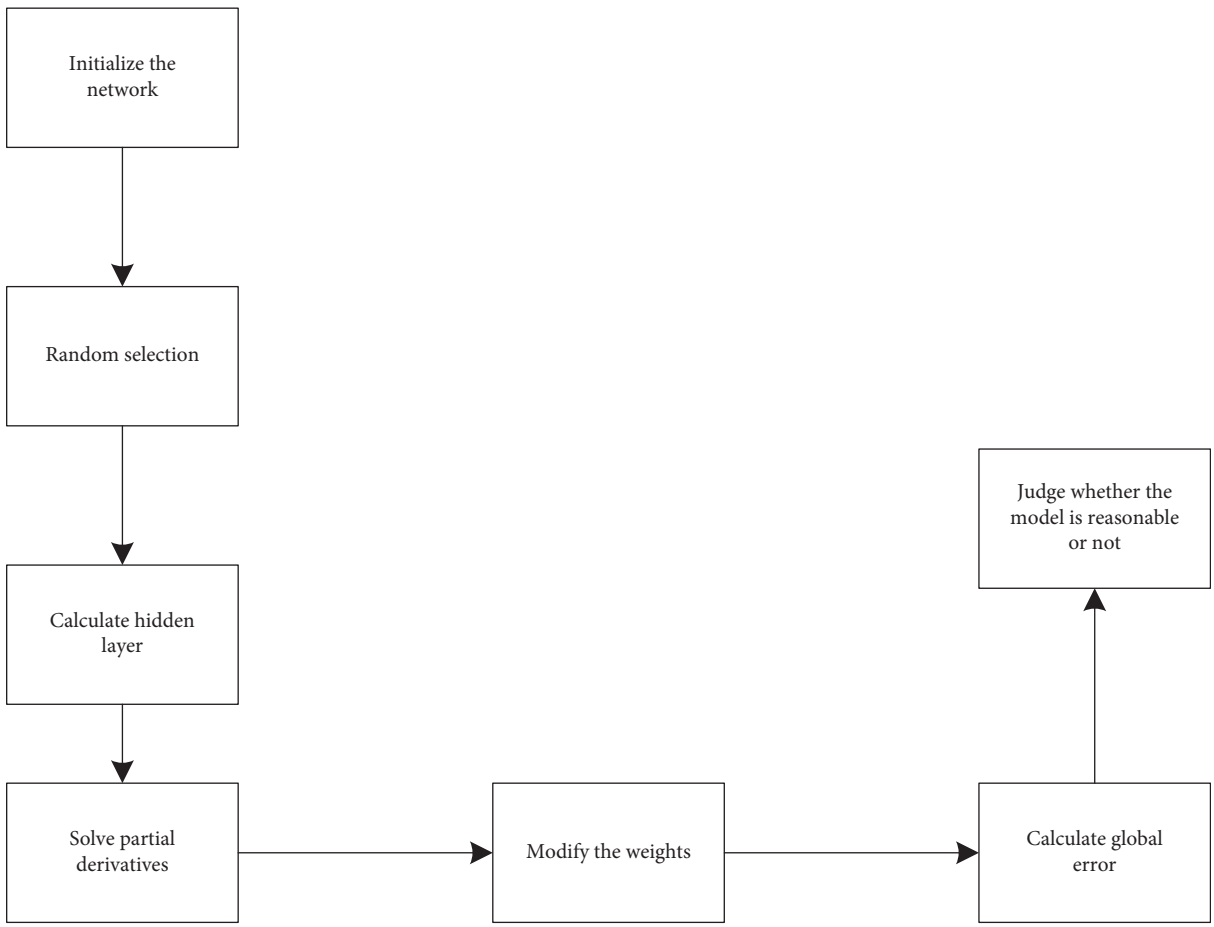

Figure 3: Algorithm flow chart of BP neural network.

3.3.1. Initial Network Creation. This part needs to be combined with the specific problem of determining the specific number of nodes (n, l, m) in the input layer, hidden layer, and output layer of the model.

The input layer inputs the data of the hidden layer as H_j, and the value of the hidden layer is Y_k. The calculation formula is as follows:

$$\begin{cases} H_j = x_1 w_{1j} + x_2 w_{2j} + \cdots + x_n w_{nj} = \sum_{i=1}^{n} x_i w_{ij}; \quad h_j = f_1(H_j), \\ Y_k = h_1 w_{1k} + h_2 w_{2k} + \cdots + h_l w_{lk} = \sum_{j=1}^{l} h_j w_{jk}; \quad y_k = f_2(Y_k), \end{cases} \quad i = 1, 2, \ldots, n; j = 1, 2, \ldots, l; k = 1, 2, \ldots, m, \tag{15}$$

where x_i is the input data, w_{ij} is the connection weight input to the hidden layer, h_j is the passed value, the weight from the hidden layer to the output layer is w_{jk}, y_k represents the output value, and f_1 and f_2 are the conversion functions of two layers outside the input layer. This conversion function generally uses the Sigmoid function, which is a nonlinear function, including log and tan, which have the advantage of converting the values on $(-\infty, +\infty)$ to (0, 1) and (–1, 1), respectively.

3.3.2. Carry Out Study and Training. Because the actual output is not completely consistent with the expected output, there are errors between them. Assume their error as

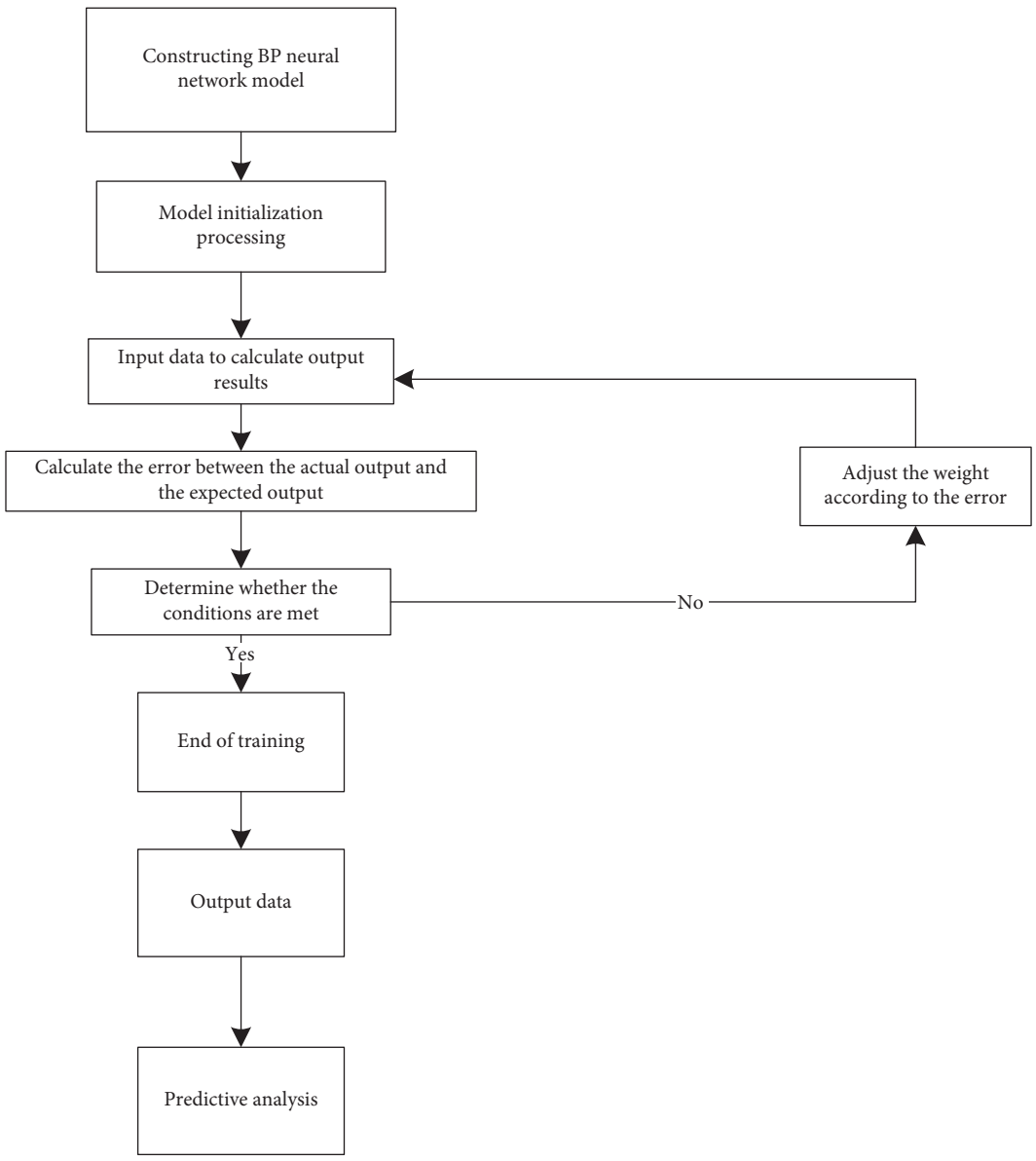

Figure 4: Algorithm flow chart of BP neural network.

E and optimize it by using the mean square error minimization method, which is defined as follows:

$$E = \frac{1}{2}\sum_{k=1}^{m}\left(y_k^* - y_k\right)^2, \tag{16}$$

where y_k^* represents the desired output.

Back propagate the error, and you can get:

$$E = \frac{1}{2}\sum_{k=1}^{m}\left(y_k^* - f_2\left(Y_k\right)\right)^2 = \frac{1}{2}\sum_{k=1}^{m}\left(y_k^* - f_2\left(\sum_{j=1}^{l} h_j w_{jk}\right)\right)^2. \tag{17}$$

By back propagating to the input layer, you can get:

$$\begin{aligned} E &= \frac{1}{2}\sum_{k=1}^{m}\left\{y_k^* - f_2\left[\sum_{j=1}^{l} w_{jk} f_1\left(H_j\right)\right]\right\}^2 \\ &= \frac{1}{2}\sum_{k=1}^{m}\left\{y_k^* - f_2\left[\sum_{j=1}^{l} w_{jk} f_1\left(\sum_{i=1}^{n} x_i w_{ij}\right)\right]\right\}^2. \end{aligned} \tag{18}$$

In this calculation process, the weight value will constantly change and adjust, so as to achieve a function of reducing error terms. When using gradient descent algorithm to optimize this process, its adjustment amount should be proportional to the negative gradient of error terms, and the following formula can be obtained:

$$\Delta w_{jk} = -\eta \frac{\partial E}{\partial w_{jk}} = -\eta \frac{\partial E}{\partial Y_k} \frac{\partial Y_k}{\partial w_{jk}}, \quad j = 1, 2, \ldots, l;\ k = 1, 2, \ldots, m,$$
$$\Delta w_{ij} = -\eta \frac{\partial E}{\partial w_{ij}} = -\eta \frac{\partial E}{\partial H_j} \frac{\partial H_j}{\partial w_{ij}}, \quad j = 1, 2, \ldots, n;\ k = 1, 2, \ldots, l, \tag{19}$$

where the normal range of the learning rate is (0, 1), and the minus sign in the formula indicates that the gradient shows a downward trend, so that $\delta_k^y = -(\partial E/\partial Y_k)$, $\delta_j^h = -(\partial E/\partial H_j)$, then the expression of the adjustment amount of the weight value can be rewritten into the following form:

$$\Delta w_{jk} = \eta \delta_k^y h_j;$$
$$\Delta w_{ij} = \eta \delta_j^h x_i. \tag{20}$$

Therefore, the following results can be calculated:

$$\delta_k^y = -\frac{\partial E}{\partial Y_k} = -\frac{\partial E}{\partial y_k} \frac{\partial y_k}{\partial Y_k} = -\frac{\partial E}{\partial y_k} f_2'(Y_k),$$
$$\delta_j^h = -\frac{\partial E}{\partial H_j} = -\frac{\partial E}{\partial h_j} \frac{\partial h_j}{\partial H_j} = -\frac{\partial E}{\partial H_j} f_2'(Y_k). \tag{21}$$

The output layer can be obtained by the above formula:

$$\frac{\partial E}{\partial y_k} = -(y_k^* - y_k). \tag{22}$$

At the same time, the hidden layer formula can be obtained:

$$\frac{\partial E}{\partial h_j} = -\sum_{k=1}^{m} (y_m^* - y_k) f_2'(Y_k) w_{jk}. \tag{23}$$

Substituting formulas (22) and (23) and deriving S function satisfies $f'(x) = f(x)(1 - f(x))$, the following formula can be obtained:

$$\delta_k^y = (y_k^* - y_k) y_k (1 - y_k),$$
$$\delta_j^h = \sum_{k=1}^{m} (y_k^* - y_k) f_2'(Y_k) w_{jk} h_j (1 - h_j). \tag{24}$$

Therefore, to sum up, we can get the relevant formula of weight adjustment:

$$\Delta w_{jk} = \eta \delta_k^y h_j = \eta (y_k^* - y_k) y_k (1 - y_k) h_j,$$
$$\Delta w_{ij} = \eta \delta_j^h x_i = \eta \sum_{k=1}^{m} \delta_k^y w_{jk} h_j (1 - h_j) x_i. \tag{25}$$

Through a series of quantitative analysis, the final weight adjustment formula is as follows:

$$w_{jk}^{t+1} = w_{jk}^t + \Delta w_{jk},$$
$$w_{ij}^{t+1} = w_{ij}^t + \Delta w_{ij}. \tag{26}$$

Finally, when the actual output meets the expected output, the training can be finished.

3.3.3. (3) Issue an Early Warning. Input data to the trained BP neural network model for prediction, and then according to the output results of the model for a series of analysis of financial crisis and financial stability.

4. Feasibility Experimental Study of BP Neural Network

4.1. Preprocessing Data Model. For data processing, we generally normalize the index data, so that the later processing is more convenient and the convergence speed can be accelerated. Normalization means that after processing our data in a specified way, it will limit them to the required range. Our input value and target value both stipulate that they can only fall in the range of [0, 1].

The data adopted in this paper come from the securities network software and takes the 5-day KDJ index data of individual stocks Yatai Group. We record the opening price, the highest price, the lowest price, and the closing price data, predict them, respectively, first, and compare the actual output results with the real values to get the results. The forecast data of the opening price of Yatai Group's 5-day KDJ index by different algorithms is shown in Table 1.

Its closing price forecast is shown in Table 2.

The highest price forecast is as follows in Table 3.

Its lowest price forecast is shown in Table 4.

4.2. Experimental Comparison Results. The prediction results of BP neural network, ant colony algorithm, and genetic algorithm for several different indexes of Yatai Group are as follows: Figures 5–7.

The forecast results of Yatai Group's 5-day KDJ index opening price are compared in Figure 5.

From Figure 5, we can see that the BP neural network is relative to the other two algorithms, In addition to the fourth day, the prediction error is larger than that of ant colony algorithm and genetic algorithm, and its prediction value is closer to the real opening value at other times, followed by ant colony algorithm and genetic algorithm. Their errors are not much different from the real value, but they are slightly worse than BP neural algorithm.

The forecast results of Yatai Group's 5-day KDJ index closing price are compared in Figure 6.

It can be seen from Figure 6 that the error value between the daily closing value and the real value predicted by BP is the smallest, which is very close to the change curve of the real value, followed by ant colony algorithm with smaller error value, and finally genetic algorithm.

The prediction results of the highest price of Yatai Group's 5-day KDJ index are compared in Figure 7.

Table 1: Forecast data of opening price of Yatai Group's 5-day KDJ index.

Yatai	Opening price				
True value	7.66	8.01	8.04	8.10	8.21
BPneural network	7.599	7.956	8.035	8.156	8.198
Ant colony algorithm	7.588	7.920	8.030	8.144	8.193
Genetic algorithm	7.578	7.900	8.034	8.166	8.200

Table 2: Forecast data of closing price of KDJ index in 5 days of Yatai Group.

Yatai	Closing price				
True value	7.66	8.03	8.01	8.12	8.23
BPneural network	7.600	8.001	8.02	8.116	8.208
Ant colony algorithm	7.599	7.999	8.009	8.134	8.193
Genetic algorithm	7.588	7.930	7.999	8.146	8.200

Table 3: Forecast data of the highest price of KDJ index in 5 days of Yatai Group.

Yatai	Maximum price				
True value	8.02	8.11	8.06	8.20	8.25
BPneural network	8.019	8.109	8.050	8.186	8.238
Ant colony algorithm	8.011	8.010	8.009	8.194	8.293
Genetic algorithm	8.012	8.200	8.01	8.196	8.270

Table 4: Forecast data of the lowest price of Yatai Group's 5-day KDJ index.

Yatai	Lowest price				
True value	7.66	7.78	7.99	8.01	8.10
BPneural network	7.600	7.880	8.000	8.006	8.080
Ant colony algorithm	7.599	7.990	7.009	8.034	8.430
Genetic algorithm	7.588	7.930	7.999	8.046	8.200

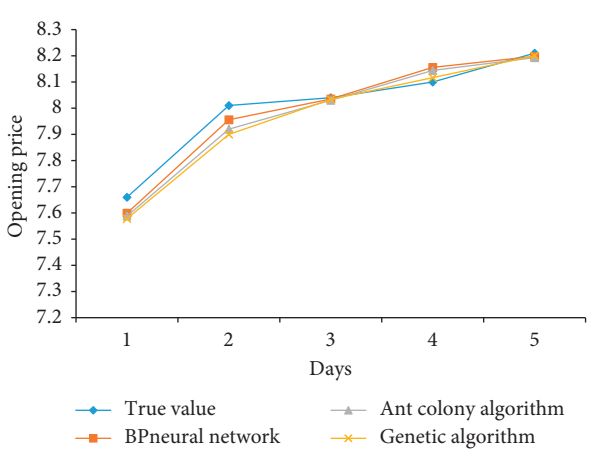

Figure 5: Comparison of opening price forecast results.

It can be seen from Figure 7 that the predicted value of the BP neural network is almost completely consistent with the real value the next day, but both ant colony algorithm and genetic algorithm have large error values, and their two

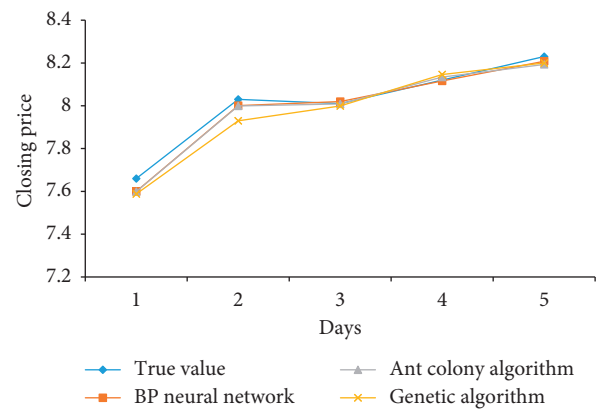

Figure 6: Comparison of closing price forecast results.

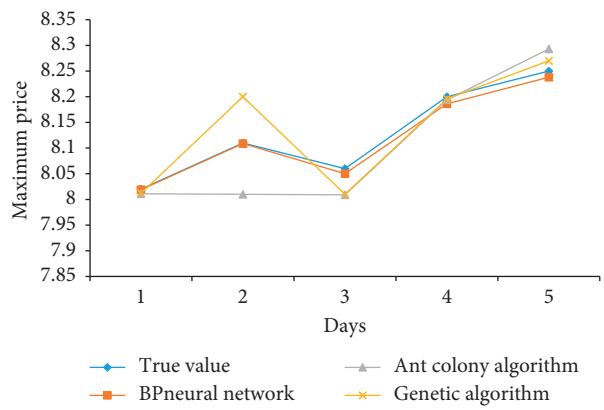

Figure 7: Comparison of the highest price forecast results.

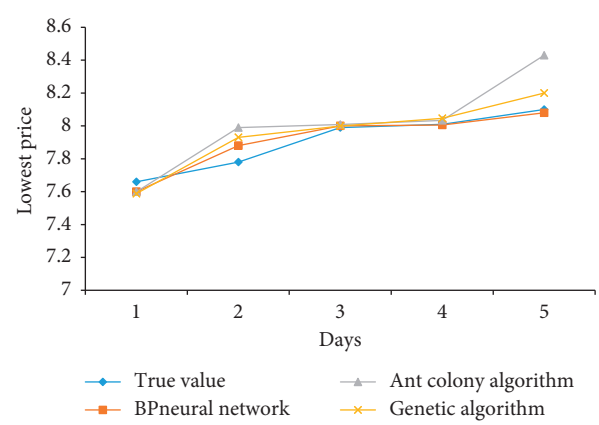

Figure 8: Comparison of lowest price prediction results.

algorithms have large error fluctuations, while the BP neural network has relatively small and stable error.

The prediction results of the lowest price of Yatai Group's 5-day KDJ index are compared in Figure 8.

Through Figure 8, we can also see that the BP neural network has the smallest error value among the three

algorithms, genetic algorithm at this time, and ant colony algorithm at last.

5. Conclusion

It is very feasible to apply the BP neural network to the research and prediction analysis of financial stability. Its three-layer structure can be arbitrarily approximated to any nonlinear continuous function, which has certain advantages in dealing with complex problems and can predict data results more accurately and reliably; he also has a high degree of self-learning and self-adaptability, which will provide stronger explanatory power than other algorithms; he also has efficient data analysis ability and can obtain strong practicability; and its fault tolerance makes it have stronger practical ability. All these advantages provide a good support for it to successfully predict financial stability with smaller errors.

Data Availability

The experimental data used to support the findings of this study are available from the corresponding author upon request.

Conflicts of Interest

The authors declare that they have no conflicts of interest.

References

[1] M. D. Bordo, J. V. Duca, and C. Koch, "Economic policy uncertainty and the credit channel: aggregate and bank level U.S. Evidence over several decades," *Working Paper Series*, vol. 26, pp. 1–38, 2016.

[2] K. Paudyal, C. Thapa, S. Koirala et al., "Economic policy uncertainty and cross-border mergers and acquisitions," *Journal of Financial Stability*, vol. 78, p. 56, 2021.

[3] M. Dai and E. Spyromitros, "Monetary policy, asset prices and model uncertainty," *Macroeconomic Dynamics*, vol. 16, no. 5, 2008.

[4] C.-C. Lee, C.-C. Lee, J.-H. Zeng, and Y.-L. Hsu, "Peer bank behavior, economic policy uncertainty, and leverage decision of financial institutions," *Journal of Financial Stability*, vol. 30, pp. 79–91, 2017.

[5] S. Hammoudeh and M. Mcaleer, "Advances in financial risk management and economic policy uncertainty: an overview," *International Review of Economics & Finance*, vol. 40, pp. 1–7, 2015.

[6] H. Kim and Y. Yasuda, "Economic policy uncertainty and earnings management: evidence from Japan," *Journal of Financial Stability*, vol. 56, no. 2, Article ID 100925, 2021.

[7] O. Guedhami, S. Mansi, D. Reeb et al., "Economic policy uncertainty and allocative distortions," *Journal of Financial Stability*, vol. 56, no. 4, Article ID 100923, 2021.

[8] D. Wolfgang, E. G. Sadok, and G. Omrane, "Policy uncertainty, investment, and the cost of capital," *Journal of Financial Stability*, vol. 39, pp. 28–45, 2018.

[9] C. Guerello, "The effect of investors' confidence on monetary policy transmission mechanism," *The North American Journal of Economics and Finance*, vol. 37, pp. 248–266, 2016.

[10] P. Sarlin, "Visual monitoring of financial stability with a self-organizing neural network," in *Proceedings of the International Conference on Intelligent Systems Design & Applications*, IEEE, Cairo, Egypt, November 2011.

[11] R. Lei and H. Liu, "Financial distress prediction using GA-BP neural network model," *International Journal of Economics and Finance*, vol. 13, no. 3, 2021.

[12] A. Koronowski, "Monetary policy and financial (In)Stability," *Contemporary Economics*, vol. 4, no. 2, 2010.

[13] C. Borio and C. M. Drehmann, "Towards an operational framework for financial stability: "fuzzy" measurement and its consequences," *Social Science Electronic Publishing*, vol. 15, no. 9, pp. 3295–3303, 2009.

[14] K. Handley and N. Limo, "Policy uncertainty, trade and welfare: theory and evidence for China and the U.S." *Cepr Discussion Papers*, vol. 107, no. 9, pp. 2731–2783, 2013.

[15] S. R. Baker, N. Bloom, B. Canes-Wrone, S. J. Davis, and J. Rodden, "Why has US policy uncertainty risen since 1960?" *The American Economic Review*, vol. 104, no. 5, pp. 56–60, 2014.

Hindawi
Computational Intelligence and Neuroscience
Volume 2022, Article ID 7474581, 10 pages
https://doi.org/10.1155/2022/7474581

Research Article

Analysis of Sports Video Intelligent Classification Technology Based on Neural Network Algorithm and Transfer Learning

Han Guangyu

Physical Education Institute, Xinxiang Medical University, Xinxiang 453003, Henan, China

Correspondence should be addressed to Han Guangyu; 031013@xxmu.edu.cn

Received 28 December 2021; Accepted 28 January 2022; Published 24 March 2022

Academic Editor: Guobin Chen

With the rapid development of information technology, digital content shows an explosive growth trend. Sports video classification is of great significance for digital content archiving in the server. Therefore, the accurate classification of sports video categories is realized by using deep neural network algorithm (DNN), convolutional neural network (CNN), and transfer learning. Block brightness comparison coding (BICC) and block color histogram are proposed, which reflect the brightness relationship between different regions in video and the color information in the region. The maximum mean difference (MMD) algorithm is adopted to achieve the purpose of transfer learning. On the basis of obtaining the features of sports video images, the sports video image classification method based on deep learning coding model is adopted to realize sports video classification. The results show that, for different types of sports videos, the overall classification effect of this method is obviously better than other current sports video classification methods, which greatly improves the classification effect of sports videos.

1. Introduction

As a branch of artificial intelligence, more and more different methods are emerging with the increasing development of theory, and they play an important role. Deep learning is one of the more popular areas. The development of DNN is driven by the continuous breakthroughs and innovations of deep learning. DNN is the most commonly used architecture in deep learning [1]. The concept of deep learning was first proposed by Hilton et al. in 2006. In recent years, it has shined in various fields, making it a hot topic in the AI field [2]. The main idea of deep learning is to simulate the neural structure of the human brain. It is hoped that the machine can process the received data like a human. The realization process is to extract features from the data through multiple nonlinear stages [3]. However, when we actually want to solve a problem by using machine learning algorithm, whether we use shallow machine learning algorithm or deep learning algorithm, we are faced with some practical conditions, such as the lack of data and information and the difference between training data and practical application data, resulting in poor model construction and poor practical application effect [4]. This is because traditional machine learning requires that the data of learning and the data of actual application scenarios should meet the same statistical characteristics, and it means that whenever there is a new application scenario, it is necessary to collect enough annotation information to make the traditional machine learning methods play an effective role, which will consume a lot of manpower, material resources, and time cost [5]. With the rapid development of machine learning in recent years, people pay more and more attention to this problem, and transfer learning, one of the learning methods to solve this problem, has become a very active research field [6].

The goal of transfer learning is to use existing knowledge to deal with problems in different but related fields, so as to realize the transfer of knowledge between related fields. It is an intelligent learning method similar to human basic learning ability. Just like in real life, we humans can judge whether the new problems we face are related to the previous accumulation and whether we can adopt the knowledge learned before through the knowledge we have learned or accumulated before [7]. Psychologists have found that, in

order to realize transfer learning, it is certainly necessary for the two fields or learning materials to have common factors, and the transfer effect is proportional to the common factors, and the more the common factors, the better the transfer effect. Of course, there are common factors and different factors, which may also cause negative transfer and affect learning [8]. Sports video is a very important resource in video. Sports programs have hundreds of millions of loyal viewers all over the world. The classification of sports video has become the focus of many researchers. Sports video intelligent classification technology can not only intelligently classify and sort out massive sports video data and reduce people's workload, but also provide people with better spiritual enjoyment in daily life. It is also the basis of intelligent radio and television intelligent classification. Therefore, sports video intelligent classification technology can be widely used in sports video management, retrieval, query, and other fields and has broad development prospects and great value [9]. At present, the traditional transfer learning method is mainly to find a common feature space and map the data in two domains into the feature space by mapping function, so as to make the data distribution difference between the two domains as small as possible while maintaining the original characteristics of the data as much as possible and then train the classifier on these mapped data [10]. Existing sports video classification technologies pay more attention to the extraction of video features. It can be seen that feature extraction is the key to sports video classification. Researchers have proposed different feature models for classification in terms of motion, color, edge, etc., but different features. The role played in sports videos is different. Some features have a good classification effect. Obviously, the features extracted by these methods are not more expressive than those extracted by deep learning, and the deep transfer learning technology can better meet the end-to-end needs in practical applications. [11].

Video features mainly focus on motion, color, brightness, edge, texture, audio, etc. These features are mainly used in the classifier in a separate way, or in a simple linear fusion (horizontal); that is, different feature vectors are used in a linear combination according to the law. This fusion method improves the classification performance to a certain extent. However, most of them separate different features and ignore the semantic relationship between features [12]. In order to establish more connection and fusion between features, this paper proposes an intelligent sports video classification technology based on DNN and transfer learning and makes an in-depth study on the field of sports video classification. The third paragraph introduces the video region feature extraction and processing and migration learning video classification system architecture. Block brightness comparison coding and block color histogram are proposed, which reflect the brightness relationship between different regions in the video and the color information in the region. The fourth paragraph introduces the transfer learning of DNN. The algorithm of maximum mean difference (MMD) is proposed for migration learning. The fifth paragraph introduces the classification and experimental results of migration learning sports video images based on deep learning coding model. On the basis of obtaining the features of sports video images, the sports video image classification method based on deep learning coding model is adopted to realize sports video classification. In order to analyze the effectiveness of the method classification in the article, the sports videos are set to be figure skating, badminton, and yoga in order. Due to the supervised fine-tuning, the parameters of each layer of the deep learning network can be adjusted in the form of error back-propagation to optimize the classification effect.

Through the analysis of traditional transfer learning algorithm and DNN transfer learning algorithm, this paper studies a video classification transfer learning algorithm based on DNN. Innovation contributions include the following: (1) It solves the problem that the target domain data has no label and domain adaptation. (2) It provides different suggestions for automatic classification for the rapidly increasing amount of sports video data. (3) To improve the effect of sports video classification, a sports video classification method based on DNN and transfer learning is proposed. The classification accuracy, recall, and maximum value of this method are better than the comparison method, and a better classification effect of sports video is achieved.

2. Related Work

Many data mining and machine learning algorithms have achieved great success in many fields (such as classification, regression, and clustering). However, most of these algorithms have a common assumption: the training set and the test set are in the same feature space and obey the same distribution. Zhang et al. [13] point out that, with the passage of time and the adjustment of application scenarios, the training data collected before may be out of date. It is a pity to discard these out-of-date data, but the adjustment of scenarios leads to differences in statistical characteristics between training data and application data, resulting in poor model effect. Ma et al. [14] indicate that traditional machine learning does not have the ability to transfer learning. Whenever a new application scenario is encountered, the process of data collection, training, and verification will be carried out again. For example, every time we learn something from "nothing," then every time we learn, we will spend a lot of energy. Migration learning can make full use of outdated data to ensure that the target model has better effect, thus reducing the cost of data collection in new target tasks. Moradzadeh et al. [15] proposed a method called joint distributed adaptation. They assume that the marginal distributions of the source and target domains are different from the conditional probability distributions, and the target domain has no data annotations. This method looks for a linear transformation, so that the edge distribution of the transformed data can be as close as possible, and the conditional probability distribution difference is also as small as possible. The method to measure the degree of the difference in the data distribution is still the maximum mean difference. Compared with TCA, this method requires iteration and the source domain needs to be labeled. However, the

method proposed in [16] has a hyperparameter, that is, the number of subspaces, which means that the user cannot know how many intermediate points should be found. Mahmoud et al.[17] proposed a geodesic stream-core method to solve the problem of choosing several intermediate points.

Qiu et al. [18] show that principal components are used to reduce the dimensionality of video visual and audio features to describe video content, and time series of motion features are used to distinguish motion event classifications in football sports videos. Chen et al. [19] studied the classification of simple sports in sports videos by detecting some motion modes in video frames, such as running, jumping, translation, and zooming of the serve lens. Liu et al. [20] show that some knowledge in the source domain is obtained by training the source convolution neural network on the ImageNet dataset beforehand, and then the network is migrated and studied on the image classification datasets Calteech-101 and Catech-256, respectively, which improves the classification accuracy by 40% compared with traditional training methods. Zhang et al.[21] show that, by studying the transfer learning effect of different layer features of convolutional neural networks, it is found that the transfer learning ability of lower layer features is weaker than that of higher layer features. Wang et al. [22] studied the combination of video and audio features to classify videos and experimentally studied the effect of principal component analysis (PCA) on feature dimension reduction but failed to solve the correlation between features, and the fusion scheme of two types of features was slightly insufficient. Migration learning solves the problem of insufficient training of neural networks with small samples, while greatly reducing the training cost of the network. This paper takes sports video classification as the focus of research and applies convolutional neural networks to a broader field. Therefore, the research of transfer learning is one of the current development trends. Researchers are committed to finding better video features or using multifeature fusion methods to classify videos, while improving the performance of the classifier and the accuracy of classification.

3. Video Classification

3.1. Extraction and Processing of Video Area Features. Video area features are divided into (BICC) and block color histograms, which reflect the brightness relationship between different areas in the video and the color information within the area. The algorithm framework is shown in Figure 1.

For each type of video, the brightness distribution of the frame is relatively uniform and there is a certain brightness difference between the target in the frame and its surrounding environment. The human visual system distinguishes the object by the brightness difference between the target in the frame and its surrounding environment, and BICC is obtained by comparing the average brightness between blocks [23]. BICC reflects the brightness relationship between intraframe blocks and has strong anti-interference ability for different video segments of the same kind of video due to factors such as brightness and darkness.

Assuming that the frame size is $M\times N$, each frame is divided into log×seven blocks, and the size of each block is $h\times u$, where $h = M/k$, $u = N/k$, and x_i represents the i-th pixel in the block The brightness value of each block is $\overline{X(l)}, l \in [1, k\times k]$; then

$$\overline{X(l)} = \sum_{i=1}^{h\times u} \frac{x_i}{(h\times u)}. \tag{1}$$

If the block brightness comparison coded value is expressed as y, the result of the brightness comparison between the m-th block and the nth block in a frame can be expressed as (2), where $1 < m < K\times K$, $2 < n < K\times K$-1.

$$y\left[(m-1)\times(k\times k)+n+\frac{m(m+1)}{2}\right] = \begin{cases} 1 & \text{if}\,\overline{X(m)} > \overline{X(n)}, \\ 0 & \text{otherwise.} \end{cases} \tag{2}$$

According to formula (2), the frame can be coded by 0 and 1 according to the block brightness mean value comparison.

For some videos, there is no obvious difference in brightness, but there is a significant difference in color distribution, such as volleyball and table tennis videos, which can be used for video classification by dividing video frames into blocks and counting their color histograms. The extraction process of block color histogram is as follows.

Assuming that the frame size is $M\times N$, the frame is divided into $k\times k$ blocks, and the size of each block is $h\times u$, where $h = M/k$, $u = N/k$, and x_{ir}, x_{ig}, and x_{ib}, respectively, represent the i-th block in the block. The value of the R, G, and B components corresponds to the pixel point, P represents the number of straight squares, and $\mathrm{HIST}_{m,n,p}$ represents the color histogram of the nth block in the frame, where $m \in \{r, g, b\}, n \in [1, k\times k], p \in [1, P]$, p_m represent the quantization range of the color component m corresponding to the p square, but

$$\mathrm{HIST}_{m,n,p} = \sum_{i=1}^{h\times u}\left(x_{i,m,n} \in p_m\right). \tag{3}$$

Features are extracted based on video frame blocks. When there are more block partitions and more histograms in the BlockHist histogram, the dimension of the extracted feature vector is higher. Therefore, PCA is used to reduce the dimension of the extracted features to speed up the processing.

3.2. Migration Learning Video Classification System Architecture. Convolutional neural network (CNN) is a neural network architecture for image classification, which usually includes convolution layer and pooling layer. The loss function and accuracy are reported on the test set of each CNN architecture. Loss function: how far is the difference between the prediction and the actual results? The greater the predicted value, the worse the accuracy of the

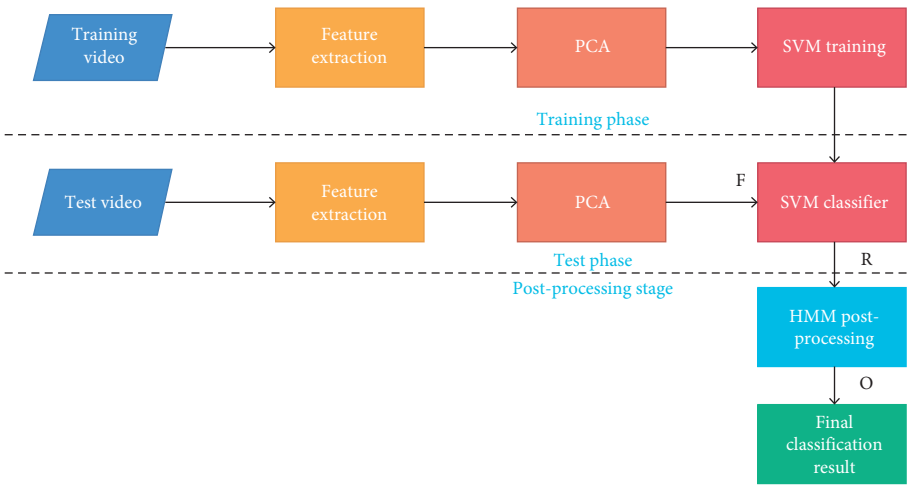

Figure 1: Video classification frame diagram.

model fitting data points. Accuracy of test set is the accuracy of the model's prediction of test set data.

With the development of artificial intelligence technology, video classification technology is needed in various fields, such as face recognition, video location, and so on. On the one hand, with the advent of the Internet age, although the available target domain data that can fully meet the target tasks cannot be collected, enough original digital videos that are similar or related can be collected, and it is easier to train a source convolutional neural network that can better complete the video classification tasks [24]. In addition, DNN has gradually become a research hotspot in recent years, and the convolutional neural network, as a star in the field of video classification, has also made progress that cannot be ignored. Compared with other traditional video classification methods, it has a better classification accuracy. Therefore, most of the current fields are keen to complete video classification tasks through deep convolutional neural networks from many aspects such as processing speed, classification accuracy, and user experience. According to the functions of video classification related systems, the realized video classification system can be divided into three parts, namely, network training, network migration, and network testing [25]. The overall functional framework of the system is shown in Figure 2.

Network migration module is the core part of the whole system. For convolution models that are already available, the network training module can be almost unused, loaded directly with existing parameters, and then used. The migration module also has superparameter settings, which include not only the learning rate and iteration rate, but also the ratio of convolution layer and full-connection layer parameter changes and the K selection function. Task mapping is the mapping of the source and target tasks when changing the top-level classifier structure of the source domain model according to the target domain tasks, which makes the modification of the network more reasonable. The process of retraining the new network by the fine-tuning function is similar to that of the network training model, except that K selection algorithm is added in the process, and

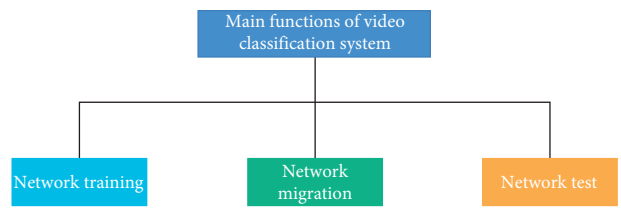

Figure 2: The overall framework of the system.

only some parameters are adjusted. The network test module has an evaluation method for the constructed convolutional neural network, so as to know whether the model meets the task research and how to modify the network.

The main workflow of migration learning video classification system is the training, migration, and testing process of convolutional neural network, in which whether the training process is carried out depends on whether there are trained available model parameters. The following describes the workflow of the system in the form of a flowchart, as shown in Figure 3.

4. DNN Transfer Learning

Fully connected neural network model (DNN) is also called deep neural network in some cases. Different from traditional perceptron, each node has an operation relationship with all nodes in the next layer, which is the meaning of "fully connected" in the name. The middle layer in the above figure also becomes a hidden layer. Fully connected neural network usually has multiple hidden layers. Adding a hidden layer can better separate data. However, too many hidden layers will also increase the training time and produce overfitting.

On the other hand, since the last feature of a neural network, such as the last layer of a convolution layer, must be related to a particular dataset, assuming that the last layer of the network is the softmax layer and that the entire network has been trained on a dataset, the output of the softmax layer must be closely related to that dataset, so make this feature special [26].

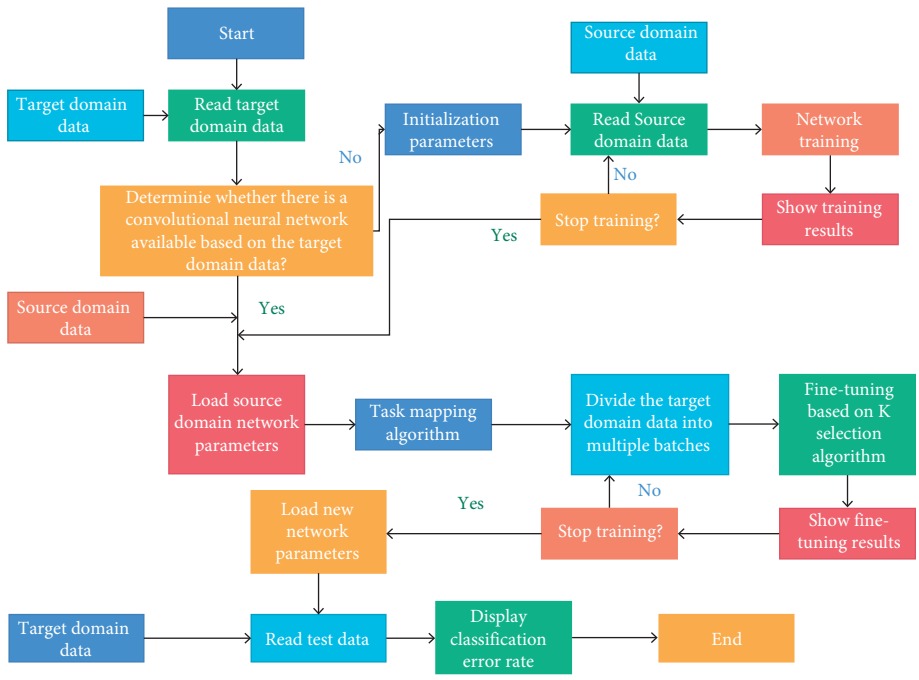

Figure 3: Work flowchart of video classification system.

The first two modules of VGG13 network can be fixed (not counting pooling layer, but the first four layers) because the first few layers of DNN trained on image data set are all common features. These network layers have been trained on ImageNet data set and can be used to extract common features on source domain and target domain [27]. The domain adaptation problem is difficult to solve because the target domain data has no label. In order to solve this problem, many methods try to limit the error value of the target domain to the error of the source domain plus a difference value. MMD is one of the methods, and its formula is

$$\mathrm{MMD}[F,p,q]=\left[\sup_{f\in F}\left(E_p[f(x)]-tE_pn[f(y)]\right)\right]. \tag{4}$$

Among them, F is the space where the function f is located, the distribution of x is p, and the distribution of y is q. Equation (4) means the upper bound of the difference between the expected value $E_p[f(x)]$ and $E_q[f(y)]$ after random projection of the data x on the source domain and the data y on the target domain through the function f. Obviously, when $p=q$, that is, when the distributions of x and y are the same, no matter how the function f is projected, the expectation will be the same, so in the case of $p=q$, MMD is 0. However, if p_q, and the function space F is rich enough, the MMD will never be zero. Its value is determined by the function in function space F which makes the distribution difference between the X and Y projections the greatest. It is important to note that if the function space F is too rich and f has too many possibilities to take values, MMD can easily be infinite, so the function space F needs to be constrained. F is proved to be the best when F is the unit ball in the reproducing kernel Hilbert space (i.e., space less than or equal to 1 from the origin). At this point, the formula for MMD^2 becomes

$$\begin{aligned}\mathrm{MMD}^2[F,p,q]&=\left[\sup_{\|f\|_H\le 1}\left(E_x[f(x)]\right)-E_Y[f(y)]\right],\\&=\left[\sup_{\|f\|_H\le 1}\langle\mu_p-\mu_q,f\rangle_H\right]^2,\\&=\left\|\mu_p-\mu_q\right\|_H^2.\end{aligned} \tag{5}$$

An important property of (5) is that $p\neq$q if and only if $\mathrm{MMD}^2=0$. Because a single kernel function may not be optimal, if a single kernel is used, it can be Gaussian kernel or linear kernel, but the disadvantage is obvious: it is impossible to know which kernel is good. Therefore, multikernel maximum mean error (MK-MMD) is used for feature mapping, and the kernel is weighted by m different Gaussian kernels, and the weight is β_u, and the formula is

$$K=\left\{k=\sum_{u=1}^{m}\beta_u k_u:\ \beta_u\ge 0,\forall u\right\}. \tag{6}$$

The restriction on the coefficient β_u ensures that the obtained k is unique, so that the measurement method for the difference between the source domain and the target domain is determined to be MK-MMD.

In general convolution networks, the characteristics will eventually change from general to special before the last layer, and this transformation will become larger and larger as the number of layers of the network goes deeper to the full-connection layer. In other words, deep networks are almost specialized by specific tasks in the full-connection layer. If there is not enough data in the target domain for

supervised learning, the full-connection layer cannot be trained directly in the target domain. Since the source domain is labeled, train the entire network on the source domain to improve its accuracy on the source domain. At the same time, use MK-MMD to make the data on the source domain be on the output of the fully connected layer and the target domain. The output difference of the data on the fully connected layer is as small as possible, so as to reduce the distribution difference between the data of the source domain and the data of the target domain after feature mapping, so as to achieve the purpose of migration learning. The experimental results are shown in Figures 4 and 5.

As shown in Figure 6, it can be seen that, in different stages of training, the accuracy of models with different fine-tuning depths is ranked consistent.

After carefully observing and analyzing the fine-tuning results at different depths, we find that the highest accuracy will first increase with the deepening of fine-tuning layers, then reach the highest at a certain depth, and then gradually decrease, showing a single peak curve. As shown in Figures 7 and 8, it can be observed that each curve has only one peak. For example, the peak of the GoogLeNet model of SUN397 is 4inceptions, and the peak of the GoogLeNet model of FOOD101 is 8inceptions. The peak of the AlexNet model of FoOD101 is 3 FCs+3convs. This shows that when starting the comparison from the smallest depth, once the highest accuracy rate of the next larger depth is not higher than the previous one, then the previous smaller depth is the best fine-tuning training depth. This kind of accuracy does not fluctuate with the change of the fine-tuning depth and is very suitable for iteratively finding the optimal solution without falling into the local optimum.

So you can think of an iterative approach to finding the best fine-tuned training depth. However, this method does not utilize the model weights that have been previously trained for each additional depth but instead retrains a model for a new fine-tuning depth.

According to the experimental results in Figures 9 and 10, using Places365_GoogLeNetfeature on SUN397 data set has better fitting effect on training set than ImageNet_GoogLeNetfeature and has higher accuracy on test set. Places365 is a scene dataset with 1.8 million pictures, SUN397 is also a scene dataset, and ImageNet is a large image dataset related to objects. Therefore, the more similar the new data is to the data used in the pretraining model, the higher the accuracy of the model after transfer learning.

5. Sports Video Image Classification and Experimental Results

5.1. Transfer Learning Sports Video Image Classification Based on Deep Learning Coding Model. On the basis of acquiring the characteristics of the sports video image's key chain frame, the sports video image classification method based on the deep learning coding model is adopted to realize the sports video classification. The specific detailed process is as follows:

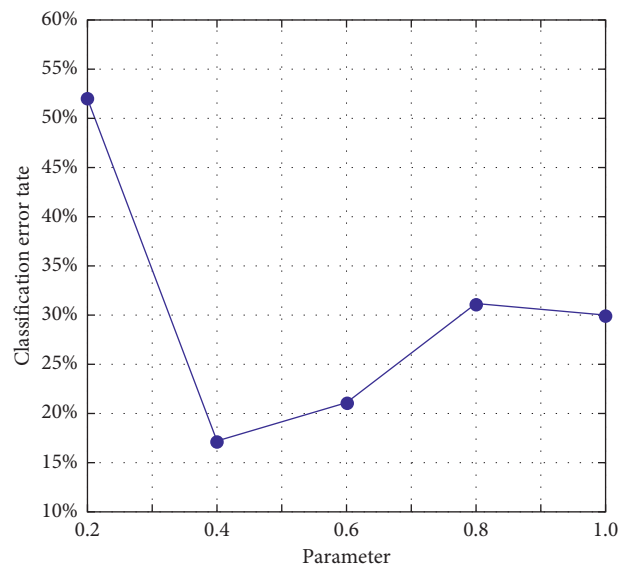

Figure 4: The impact of K selection on migration results.

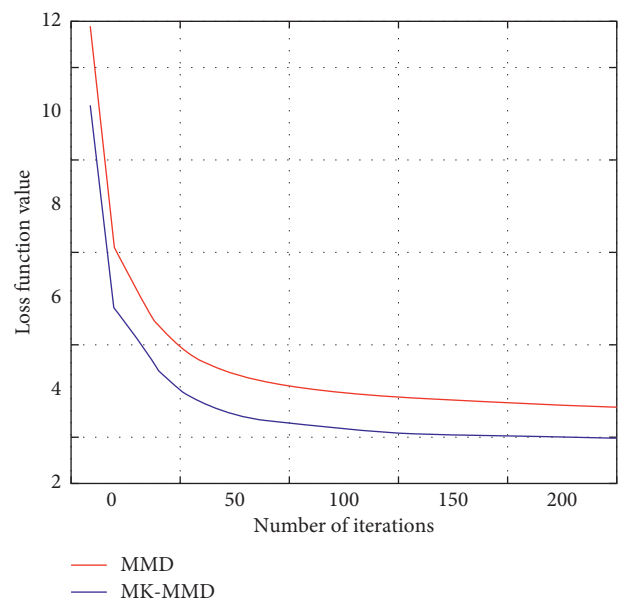

Figure 5: Two transfer learning loss functions.

(1) Set the feature library of sports video images to be linked to $G = \{g_1, g_2, \cdots, g_m\}$, and M represents the number of features

(2) Use unsupervised restricted Boltzmann machine (RBM) to encode G; use CD algorithm to obtain convergence parameter codebook and become a complete dictionary

(3) Use the kind label information of training data to spread the errors of the dictionary acquired by learning nonforward, supervise the learning of RBM network, and then optimize the acquisition of G-code to get the optimized visual dictionary and description coefficient

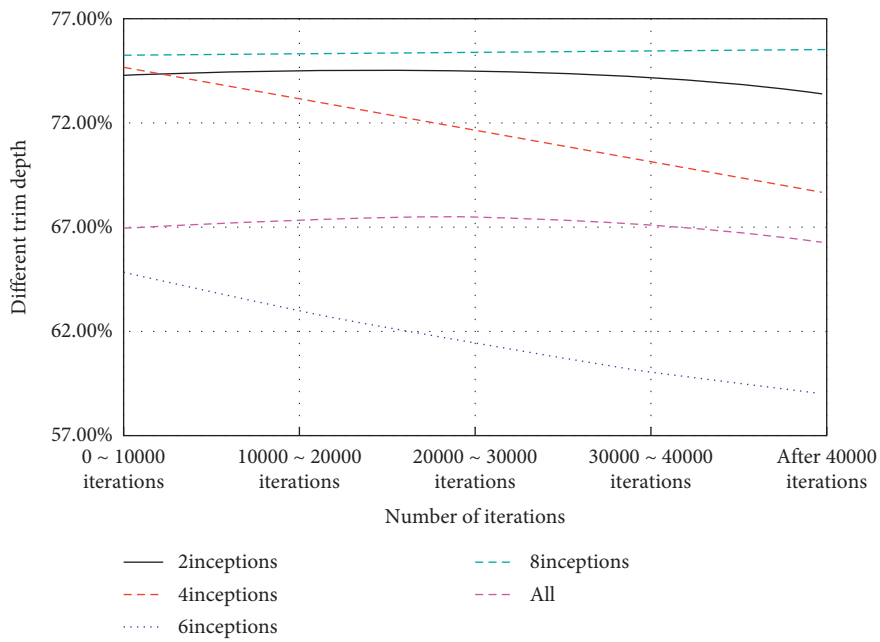

Figure 6: The accuracy of the FOOD101 GoogLeNet model with different fine-tuning depths in different training stages.

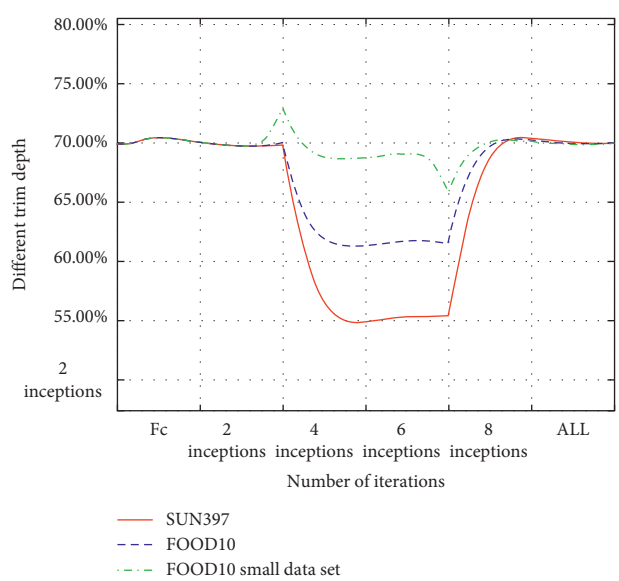

Figure 7: The accuracy of the three data sets under different fine-tuning depths of GoogLeNet.

(4) Rub the support vector machine classifier with the deep learning coding vector of the training sports video image to realize sports video classification

G is coded by using multilayer restricted Boltzmann machine and becomes an exemplary visual dictionary. According to the spatial information of G, the neighboring G features are set as the input of RBM, and the RBM is trained by CD fast algorithm to obtain the hidden stack features. Then, the adjacent hidden layer features are regarded as the input of the lower RBM, and the output dictionary is obtained. Among them are ϖ_1 and ϖ_2. Belonging to the connection weight of RBM, RBM has a visible layer and a hidden layer, and neurons based on the same level in RBM do not have a connection relationship. During network training, the hidden layer and the explicit layer of the RBM are connected according to the conditional probability distribution. The conditional probability of the explicit layer and the hidden layer is

$$q(s_i|y) = \text{sigmoid}\left(c_i + \sum_{j=1}^{i} \varpi_{ji} y_i\right),$$
$$q(y_i|s) = \text{sigmoid}\left(b_i + \sum_{j=1}^{i} \varpi_{ji} s_i\right). \quad (7)$$

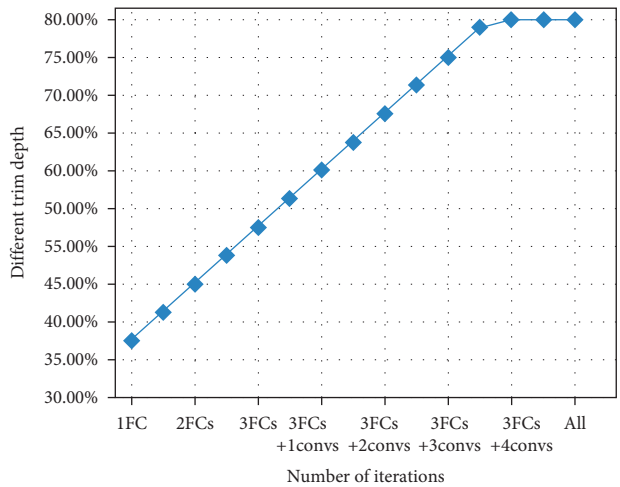

Figure 8: The accuracy of FOOD101 under different fine-tuning depths of Alex Net.

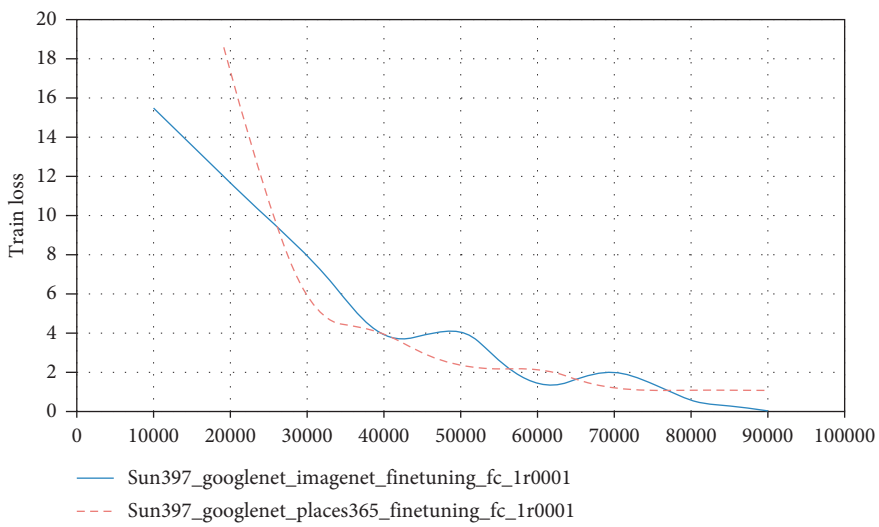

Figure 9: Train loss change curve during training.

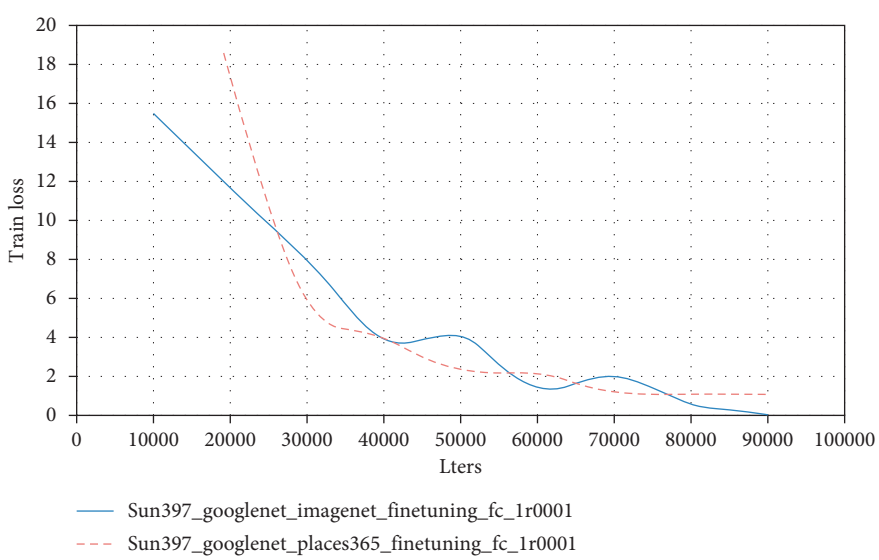

Figure 10: Test accuracy change curve during training.

Table 1: The key frame miss rate of sports video images of the method in the article.

Number of extractions	Figure skating	Badminton	Yoga
1	0.03	0.03	0.02
2	0.03	0.03	0.02
3	0.02	0.03	0.02
4	0.02	0.03	0.03
5	0.02	0.04	0.03
6	0.03	0.04	0.03
7	0.02	0.03	0.04
Mean value	0.02	0.03	0.03

In the formula, y_i and s_i describe the feature layer and encoding layer of sports video in turn, that is, the explicit layer and the hidden layer in RBM.

Using CD algorithm, RBM is quickly learned to improve the convergence efficiency of parameters, and the amount of update to obtain weights is ϖ_{ji}:

$$\Delta\varpi_{\mathrm{ji}} = \phi\left(\langle y_i s_i\rangle_{\mathrm{data}} - \langle y_i s_i\rangle_{\mathrm{model}}\right). \tag{8}$$

Among them, ϕ describes the learning speed. Using CD algorithm can get the latest parameters of sports video features until the parameters converge and get the initial visual dictionary.

5.2. Experimental Results. In order to analyze the effectiveness of the method classification in the article, the sports videos are set to be figure skating, badminton, and yoga in order.

When the method in the test article recognizes the three types of sports videos of figure skating, badminton, and yoga, the comprehensiveness of the key frames of the video images is extracted, and the missed recognition rate is the evaluation index. The results are shown in Table 1.

The data in Table 1 shows that when the method is used to identify the three types of sports videos: figure skating, badminton, and yoga, the average miss rate of extracting video image keyframes is less than 0.03, which indicates that the method in this paper can extract the key frame features from sports video images in an all-round way. Three sports videos were imported into the Caltech image collection to test the interference of different visual point sizes on the methods in this paper. With the increasing scale of sports video visual dictionary, the classification accuracy of the proposed method also increases. When the scale of sports video visual dictionary reaches 2000 MB, the classification accuracy of the proposed method is stable at 0.98. In order to test the influence of supervised fine-tuning on the classification effect of the proposed method, there are fine-tuning and no fine-tuning in the test. There is a significant difference between supervised fine-tuning and unsupervised fine-tuning. Supervised fine-tuning can improve the classification accuracy of methods in the text. This is because supervised fine-tuning can use the form of error backpropagation to adjust the parameters of each layer of the deep learning network to optimize the classification effect.

6. Conclusions

By analyzing the traditional transfer learning algorithm and DNN transfer learning algorithm, this paper studies a DNN based video classification transfer learning algorithm and designs it as a video classification system based on convolutional neural network. The first two modules of vgg13 network can be fixed because the first several layers of DNN trained on the image data set are common features. These network layers have been trained on ImageNet datasets and can be used to extract common features on source and target domains. Because the target domain data has no label, the domain adaptation problem is difficult to solve. How to automatically classify these sports videos has become a hotspot and difficulty in current research. In order to improve the effect of sports video classification, a sports video classification method based on DNN and transfer learning is proposed. In the classification process of this method, supervised fine-tuning is introduced to improve the classification accuracy of this method. The experimental results show that, for figure skating, badminton, and yoga sports videos, the classification accuracy, recall, and maximum value of this method are better than the comparison method, and a better sports video classification effect is achieved.

Data Availability

The experimental data used to support the findings of this study are available from the corresponding author upon request.

Conflicts of Interest

The author declares that there are no conflicts of interest regarding this work.

References

[1] R. Duan, T. Kawahara, M. Dantsuji, and J. Zhang, "Articulatory modeling for pronunciation error detection without non-native training data based on DNN transfer learning," *IEICE - Transactions on Info and Systems*, vol. E100.D, no. 9, pp. 2174–2182, 2017.

[2] A. H. Vo, L. Hoang Son, M. T. Vo, and T. Le, "A novel framework for trash classification using deep transfer learning," *IEEE Access*, vol. 7, pp. 178631–178639, 2019.

[3] Y. Shen, Z. Huang, S. Jiang, and B. Hu, "A combined recommendation algorithm of MF and DNN with transfer learning," *Journal of Air Force Early Warning Academy*, vol. 33, no. 02, pp. 62–67, 2019.

[4] H. Tong, J. Chu, and J. Shen, "Image classification technology based on convolutional neural network," *Science and Technology Vision*, vol. 000, no. 032, pp. 36-37, 2017.

[5] Y. Yang, J. Sun, and S. Yu, "Aircraft target recognition based on transfer learning of convolutional neural network," *Modern Radar*, vol. 41, no. 12, pp. 35–39, 2019.

[6] Z. Kastrati, A. S. Imran, and A. Kurti, "Integrating word embeddings and document topics with deep learning in a video classification framework," *Pattern Recognition Letters*, vol. 128, no. Dec, pp. 85–92, 2019.

[7] Z. Kang, B. Yang, Z. Li, and P. Wang, "OTLAMC: an online transfer learning algorithm for multi-class classification,"

Knowledge-Based Systems, vol. 176, no. JUL.15, pp. 133–146, 2019.

[8] N. Dif, M. O. Attaoui, Z. Elberrichi, M. Lebbah, and H. Azzag, "Transfer learning from synthetic labels for histopathological images classification," *Applied Intelligence*, vol. 52, no. 2, pp. 1–20, 2022.

[9] F. Zhang and J. Yan, "Cloud image classification method based on deep convolutional neural network," *Xibei Gongye Daxue Xuebao/Journal of Northwestern Polytechnical University*, vol. 38, no. 4, pp. 740–746, 2020.

[10] Z. Zhang, "Research on sports video content classification based on artificial intelligence technology," *Modern Electronic Technology*, vol. 043, no. 009, pp. 58–61, 2020.

[11] D. Pan and W. Guan, "Sports video classification method based on hidden Markov model," *Journal of Natural Science of Xiangtan University*, vol. 39, no. 001, pp. 73–77, 2017.

[12] Li Chen, H. Fei, and H. Li, "Analysis of information geometry measurement of internal migration of DNN," *Journal of Hunan University: Natural Science Edition*, vol. 046, no. 002, pp. 97–104, 2019.

[13] L. Zhang and L. Cao, "Research on video description method based on deep transfer learning," *Journal of Testing Technology*, vol. 32, no. 05, pp. 80–86, 2018.

[14] Z. Ma, H. Yu, W. Chen, and J. Guo, "Short utterance based speech language identification in intelligent vehicles with time-scale modifications and deep bottleneck features," *IEEE Transactions on Vehicular Technology*, vol. 68, no. 1, pp. 121–128, 2019.

[15] A. Moradzadeh and N. R. Aluru, "Transfer-learning-based coarse-graining method for simple fluids: toward deep inverse liquid-state theory," *Journal of Physical Chemistry Letters*, vol. 10, no. 6, pp. 1242–1250, 2019.

[16] R. K. Samala, H.-P. Chan, L. Hadjiiski, M. A. Helvie, C. D. Richter, and K. H. Cha, "Breast cancer diagnosis in digital breast tomosynthesis: effects of training sample size on multi-stage transfer learning using deep neural nets," *IEEE Transactions on Medical Imaging*, vol. 38, no. 3, pp. 686–696, 2019.

[17] H Mahmoud, A Alharbi, and D Khafga, "Breast cancer classification using deep convolution neural network with transfer learning," *Intelligent Automation & Soft Computing*, vol. 29, no. 3, pp. 803–814, 2021.

[18] N. Qiu, X. Wang, P. Wang, S. Zhou, and Y. Wang, "Research on convolutional neural network algorithm combined with transfer learning model," *Computer Engineering and Applications*, vol. 56, no. 5, pp. 43–48, 2020.

[19] C. Lifu, W. Hong, C. Xianliang, G. Zhenghua, and J. Zhiwei, "Convolutional neural network SAR image target recognition based on transfer learning," *Chinese Space Science Technology*, vol. 038, no. 006, pp. 45–51, 2018.

[20] L. Xiaodong, C. Xinbao, Y. Guanghui, and L. Peng, "Exploration of ball sports target tracking methods in sports video," *Popular Science and Technology*, vol. 20, no. 01, pp. 114–116, 2018.

[21] Y. Zhang, "Research on the classification of sports video types based on machine learning technology," *Microcomputer Applications*, vol. 36, no. 11, pp. 46–48, 2020.

[22] Y. Wang, M. Liu, and W. Yan, "Ant colony optimization algorithm to optimize support vector machine video classification," *Modern Electronic Technology*, vol. 043, no. 001, pp. 56–58, 2020.

[23] D. Liu, X. Wang, and M. Liu, "Research on olympic video classification mechanism based on Lagrangian gauss transform," *Optoelectronics Letters*, vol. 30, no. 10, pp. 104–109, 2019.

[24] Y. Zhou and B. Yang, "Sports video athlete detection using convolutional neural network," *Journal of Natural Science of Xiangtan University*, vol. 39, no. 001, pp. 95–98, 2017.

[25] E. Deniz, A. Sengür, Z. Kadiroglu, Y. Guo, V. Bajaj, and U. Budak, "Transfer learning based histopathologic image classification for breast cancer detection," *Health Information Science and Systems*, vol. 6, no. 1, pp. 1–7, 2018.

[26] G. Zhou, Z. Zeng, J. X. Huang, and T. He, "Transfer learning for cross-lingual sentiment classification with weakly shared deep neural networks," in *Proceedings of the 39th International ACM SIGIR Conference on Research and Development in information Retrival*, vol. 2016, pp. 245–254, Pisa, Italy, July 2016.

[27] G. Chen, J. Qi, C. Tang, Y. Wang, Y. Wu, and X. Shi, "Analysis and research of key genes in gene expression network based on complex network," *Complexity*, vol. 2020, pp. 1–12, Article ID 8816633, 2020.

Hindawi
Computational Intelligence and Neuroscience
Volume 2022, Article ID 6755053, 9 pages
https://doi.org/10.1155/2022/6755053

Research Article

Image Recognition and Extraction of Students' Human Motion Features Based on Graph Neural Network

Jianguo Liu, Kai Ji, and Yan Jing

School of Physical Education, Wuhan Sports University, Wuhan, Hubei 430079, China

Correspondence should be addressed to Kai Ji; 2015041@whsu.edu.cn

Received 22 December 2021; Accepted 4 February 2022; Published 24 March 2022

Academic Editor: Guobin Chen

In order to improve students' overall subhealth behavior, teenagers' physical health problems have attracted more and more attention. The state clearly requires students to increase the number and frequency of exercise in school. In order to study the physical changes in the process of students' sports and the impact on their health caused by a sports injury, a student human motion feature image recognition based on a graph neural network is proposed in this paper. This paper combines image recognition technology with graphic neural network management and uses image recognition technology to detect and track targets. It also analyzes the health changes of students in sports and the influencing factors of physical subhealth in classroom learning. The results show that image recognition technology can accurately analyze the process of cervical spine injury and sports injury in students' classroom activities. It provides accurate experimental data for analyzing students' physical health and effective suggestions for promoting students' healthy development. Compared with the traditional image recognition and analysis results, the advantage of using a graph neural network to manage the detection and tracking results is that a graph neural network is used to manage the detection and tracking results, and the visual expression of students' physical health test data is completed.

1. Introduction

With the rising demand of people's life, the quality of life is also undergoing benign changes. More and more people have begun to pay attention to health problems [1]. Due to the focus on the cultivation of teenagers, most countries began to pay attention to students' physical health and physical changes [2]. We analyze the current situation of physical health of contemporary primary and secondary school students and find that most of the students' physique has decreased. The reason may be that schools and educational staff do not pay attention to students' physical development, and students' family environment and students' own lack of health concept [3]. According to the survey, the overall development of primary and middle school students' comprehensive quality is lower, and the physical health problems are mainly reflected in overweight, height is not up to the age standard, subhealth, cervical spine damage, physical injury, and so on. Due to the complexity of the school environment and the imbalance of students' healthy development, we should ensure the premise of students' normal development and improve their own physical quality [4, 5].

Factors affecting students' physical health due to the deep influence of exam-oriented education, the original concept can not be changed immediately [6]. Therefore, it virtually increases the overall burden of students, resulting in neglect of physical health [7]. Secondly, the lack of sports equipment is also the reason affecting physical health. In school physical education, cultivating students to cultivate physical exercise is an important link in the development of moral character and comprehensive quality. Finally, there are family factors. Students' physical health problems are inseparable from their family environment [8, 9]. Most parents only know that they pay attention to students' academic development and do not pay attention to students'

physical quality. Based on the above situation, we need to further study and analyze students' physical health [10]. Image recognition technology has developed rapidly and has been applied in many fields. Image recognition specifically includes character recognition, image recognition processing, object recognition, human tracking recognition, etc. [11, 12]. We found that the application of image recognition technology in paying attention to the changes in students' physical health has achieved effective research results. Due to the interference of various background factors in the recognition process, image recognition technology can also solve the problems such as judgment error in the process of manual recognition [13]. Human identification of information elements is inefficient and can not process a large number of image data. Image recognition technology can obtain the most intuitive data information through the analysis and ranking of a large number of data and store the data information. When people need to identify and analyze an aspect, they can directly obtain the changes of reference data [14].

This paper discusses and analyzes the changing factors of students' physical health. The innovative contributions of this paper are as follows: (1) Compared with the traditional recognition technology, we use the red marker aggregation region for local capture. This method greatly improves the accuracy and efficiency of image recognition. (2) This paper focuses on students' cervical health problems in classroom activities and analyzes the change trend of cervical spine through students' learning time and bow image acquisition. (3) The graph neural network algorithm is used to manage and distribute the information data after image recognition. This enables students' health data to be displayed intuitively and can be fed back to testers faster when storing data. The experimental results show that most students have physical and subhealth problems. Image recognition technology can quickly extract feature points in the classroom environment and other interference backgrounds and track and identify students' behavior targets.

This paper is mainly divided into three parts. The first part is to understand the advantages of image recognition technology and the development status of various countries and put forward the research content of this paper. The second part first studies the physical changes and injuries of students in the process of sports by using image recognition technology combined with graph neural network management data. Finally, it studies the subhealth problems and the changes of cervical and vertebral health produced by students in the process of learning in the classroom environment by using image recognition technology. The third part analyzes the results of the research on students' physical health problems after using image recognition technology and graph neural networks to manage data.

2. Related Work

Due to the call of the corresponding countries, most schools began to pay attention to the health problems of students. When analyzing and studying students' physical health, we can obtain students' health change data through character behavior tracking and image processing through image recognition technology [15]. Now the transmission speed of artificial image recognition technology is accelerating, which can meet the research needs of the medical field, education field, and military field. And gradually convert from the traditional two-dimensional image mode to multidimensional image mode [16, 17]. Finally, it is combined with virtual simulation technology to form an intelligent multidimensional image recognition technology. At present, image recognition technology has the advantages of large storage and rapid processing of graphic information to obtain feature points [18]. However, with the continuous in-depth exploration of human body detection, target tracking, motion tracking, and other functions, the traditional image recognition technology can not meet the processing and storage of a large amount of data [19]. Therefore, we need to add dynamic network management after graph neural network optimization to manage and store the information after identification and processing and finally realize the visualization of data results [20].

The United States is in a leading position in the research of image recognition technology. From the perspective of the traffic field, combined with vehicle recognition function, it improves the efficiency of traffic management [21]. In road environment detection, different types of roads and vehicle driving conditions are quickly analyzed through image recognition, then fed back the processing results to the traffic management system for road coordination and control.

The UK combines image recognition technology with cloud computing to realize image upload, processing, classification, and other functions [22, 23]. They will obtain the pixel values of the image for analysis and classification and conduct the image edge range test to determine the image size. Finally, the real contrast and similarity of images are calculated uniformly so as to judge the problems of duplicate images in cloud network platforms.

Germany mainly applies this technology to food safety. Due to the species of bacteria, the food image is small [24]. The background of the acquired image is most complex, so it can not accurately distinguish the key content and interference factors. This leads to low accuracy of image recognition. Therefore, fine-grained image recognition is proposed to analyze the strain style, which improves the accuracy of food safety detection.

China has applied image recognition technology in the field of industrial converter automation. It can realize the control and detection of tapping results [25]. The spectrum is analyzed by image recognition to improve the range and accuracy of the cutting area. Finally, realize automation and improve efficiency. They also applied this technology to analyze tunnel traffic on the expressway. It reduces the traffic accidents caused by terrain, light, traffic flow, and other factors in the tunnel scene. Based on the research status of the above countries, this paper proposes to study and analyze the students' physical health status and influencing factors by combining image recognition technology with graph neural network management technology.

3. Research on Students' Physical Health Problems in Classroom and Sports Based on Image Recognition Technology and Graph Neural Network Management

3.1. Research on the Changes of Students' Physical Health after Exercise Based on Image Recognition Technology and Graph Neural Network Management. Subhealth means that the body has no obvious diseases, but the health state is not very good, and the physical condition is on the edge of health and disease. The main causes of adolescent students' subhealth are a heavy academic burden and great employment pressure. The social environment leads to the emergence of an inferiority complex, improves students' physical quality, pays more attention to physical health, and so on. The main causes of subhealth of young students and their sports countermeasures have a very important impact on the physical health of young students, which can effectively improve the enthusiasm of young people to exercise and improve their physical quality. Moreover, through the popularization of some subhealth knowledge, teenagers can pay more attention to subhealth and their own health. At present, many primary and middle school students generally have physical quality problems such as subhealth, and there are many influencing factors of physical health. With more and more students' myopia, heart injury, and sports injury, schools and researchers began to focus on the influencing factors and the healthy development of students. The traditional recognition technology has some problems, such as low success rate, long analysis time, and small storage environment. We propose an image recognition automatic tracking technology to analyze the movement changes and injuries of students in different intensity sports. After acquiring the image target of the student activity range, the target image of the student activity is extracted by segmenting the original image, and filtering and excluding the result to obtain the center distance position of the image. Finally, the pixel classification of motion action is carried out to establish the model. Before tracking and detecting the movement process, first deploy a student physical health system, as shown in Figure 1.

According to the function of the system in Figure 1, students' sports and other activities are detected and analyzed in real time. Wavelet transform is required to extract the target of student action image, which is expressed as follows:

$$A(i,j)(k,l) = \|B(i,j) \cdot C(k,l)\|, \tag{1}$$

where $A(i,j)(k,l)$ is the filtering result of the human body target image after being processed by the filtering network structure. $B(i,j)$ is the moving image target and $C(k,l)$ is the small filter combination. Next, you need to define the centralization of nonstationary moving images within the active range:

$$E_{pq} = \sum_x \sum_y (x-\bar{x})^p (y-\bar{y})^q D(x,y). \tag{2}$$

In the formula, (x, y) is the central coordinate of the action image. In order to accurately analyze the image, four matrices need to be defined. They represent translation, rotation, scale invariance, etc. According to the matrix change results, calculate the normalized center distance of the human action diagram under different exercise intensity, and the formula is as follows:

$$\eta_{pq} = \frac{E_{pq}}{E_{00}^{\gamma}}, \gamma = \frac{p+q}{2} + 1, p+q = 2, 3, 4... \tag{3}$$

In this paper, the center distance of students' action images is analyzed by vector classification method. It is assumed that at any time, the pixel probability in the action image is expressed as follows:

$$p\left(G_{ij}^t\right) = \sum_{s=K,L} p_s\left(G_{ij}^t | \theta_{ij,s}^t\right). \tag{4}$$

In the formula, G_{ij}^t is the pixel in the target result graph at a certain time. $p_s(G_{ij}^t|\theta_{ij,s}^t)$ represents the probability that image pixels exist before and after the environment. At any time, the pixel environment mixing model within the student's activity range can be expressed as follows:

$$p_b\left(G_{ij}^t\right) = \sum_K w_{ij,b,k}^t \times \eta\left(G_{ij}^t, \mu_{ij,b,k}^t, \sum_{ij,b,k}^t\right). \tag{5}$$

In the formula, K is the number of pixel colors of the action image expressed by the hybrid model. $w_{ij,b,k}^t$ is the weight value in the action image background at any time. The weight value satisfies the following formula:

$$\sum_k w_{ij,b,k}^t = 1. \tag{6}$$

After getting the action background image, compare the difference between the number of action image frames of students under different intensity exercise and the background. The human motion image target is obtained, which is expressed as follows:

$$p_u(y) = I_h \sum_{i=1}^n k\left(\left\|\frac{y-x_i}{h}\right\|^2\right)\delta[b(x_i)-u]. \tag{7}$$

In the formula, I_h is the normalization factor, u is the target eigenvalue of the action image, and y is the central pixel of the image. According to the above formula, the student motion feature data are calculated and extracted, and finally, the student motion target model is constructed. Then, the physical data of athletes are analyzed, and the sports injury images of students are obtained. The motion injury image is converted to gray scale. Compared with traditional color images, byte representation can be performed according to pixels. The corresponding brightness is generated according to the bytes. When the three brightnesses are the same, it is a gray image. On the contrary, when the values are different, it is a color image. The gray value conversion formula is as follows:

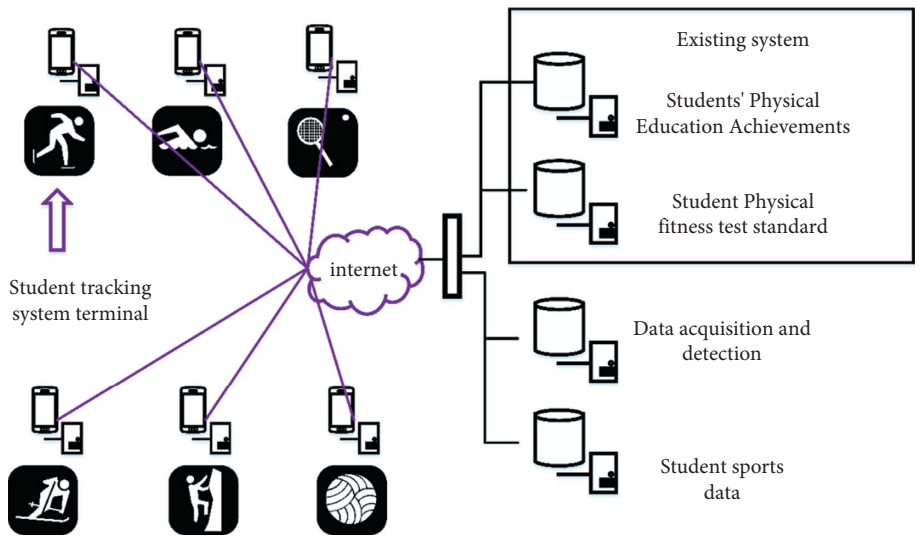

Figure 1: Structure diagram of student physical health system.

$$\text{Gray}(i, j) = 0.299 \cdot R(i.j) + 0.587 \cdot G(i.j) + 0.114 \cdot B(i.j). \quad (8)$$

After conversion, the bitmap pixel representation of the image remains unchanged. Therefore, the above gray conversion is mainly to improve the damage identification effect. The comparison between the original image and gray image before and after conversion is shown in Figure 2.

It can be seen from Figure 2 that by comparing the original image with the gray coefficient image, it is concluded that the injury parts in sports are mainly reflected in the hip joint, knee joint, and ankle joint. Therefore, the analysis of students' physical health can clearly identify the location of sports injury and improve their health. In order to distinguish the damage of students' local activities and improve the accuracy, it is necessary to extract the features of local range structure. We need to carry out nonhealth positioning according to mathematical modeling and defining threshold. The expression formula is as follows:

$$E(C) = [aE_{in}(C) + \beta E_{es}(C)]\text{Gray}(i, j), \quad (9)$$

where a and β represent weighted values, $E_{in}(C)$ and $E_{es}(C)$ represent external and internal values, respectively. After obtaining the damage range, the damage location is initialized and identified according to the transformation analysis method. After obtaining the contour range, a numerical matrix is established according to the number of pixels. To improve the accuracy of recognition position, the images need to be arranged as feature vectors. The formula is expressed as follows:

$$u = \frac{1}{m}\sum_{i=1}^{m} x_i \cdot E(C). \quad (10)$$

In this paper, the eigenvectors are arranged in a decreasing way. After the arrangement, you need to select the nonzero vector, calculate the covariance matrix according to the following formula, and select 60% of the eigenvalue to save most of the damaged images.

$$u_i = A\frac{1}{\sqrt{\lambda_i}} x \cdot v_i \cdot \mu. \quad (11)$$

Finally, all the moving image samples of students to be recognized are projected into the spatial model, and the projection coefficient is calculated according to the following formula:

$$y_i = U^T \cdot u_i. \quad (12)$$

Then calculate the distance for all image samples to be recognized and training data according to the following formula. The selected minimum distance value sample is the preliminary identification result.

$$d(x, y) = \left[\sum_{i=1}^{n} (x_i - y_i)^2\right]^{1/2}, \quad (13)$$

where n represents the number of training samples and $d(x, y)$ represents the European distance.

Through the above formula, the damage of students in the process of sports is calculated to detect physical health and other problems. In order to further analyze whether the students' overall physical health meets the standards, we input the training and identified data into the graph neural network management. Graph neural networks can extract features from the European spatial data calculated above so as to obtain the data we need. The structure of the neural network is shown in Figure 3.

As can be seen from Figure 3, the spectral domain graph convolution network and spatial domain are combined. Be able to recognize the signal of the diagram for processing. The graph convolution network is used in this paper. Compared with other graph neural network structures, it can process the updated feature points and has higher efficiency, more flexibility, and versatility. We define graph convolution as the product of signal and filter function, and the expression is as follows:

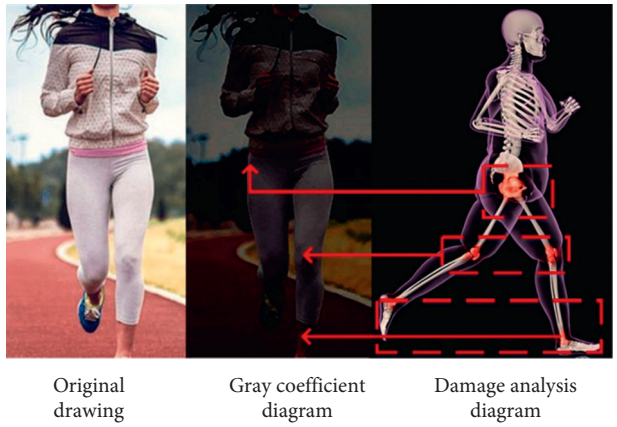

Figure 2: Comparison between the original image and gray image.

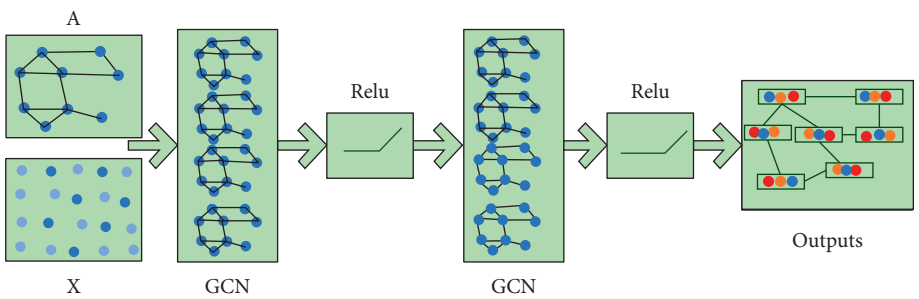

Figure 3: Figure structure diagram of neural network.

$$g_\theta^* x = U g_\theta U_x^T. \tag{14}$$

g_θ is the filter function and x is the signal of the image node. Finally, the eigenvalues of the function matrix are formed into a diagonal matrix for approximate processing, and the expression is as follows:

$$h^{(l)} = \sigma\left(\bar{D}^{1/2}\bar{A}\bar{D}^{1/2}h^{(l-1)}W^{(l-1)}\right), \tag{15}$$

where σ is the nonlinear activation function and $W^{(l-1)}$ is the numerical matrix of graph convolution network. In this paper, the feature data after image recognition is managed by a graph neural network, which has faster operation efficiency and accuracy than the traditional recognition algorithm. It can accurately analyze the changes of students' physical health.

3.2. Research on Cervical Spine Health Problems of Students' Classroom Activities Based on Image Recognition Technology. As an important way of processing image information in the computer field, image recognition technology plays different roles in people's life. Based on the image recognition technology, this paper analyzes the students' classroom activities and detects the students' overall physical health. This paper investigates the problems of students, such as cervical subhealth. The factors affecting the reading time and exercise time of the cervical spine were analyzed and discussed. The results showed that 60% of the students had mild cervical spondylosis and other complications caused by cervical vertebra. Figure 4 shows the comparison of the change rate of cervical subhealth between students' reading time and exercise time.

It can be seen from Figure 4 that most students spend two to three hours reading, and the impact on cervical subhealth is very significant. The increase of exercise time will reduce the change rate of cervical subhealth. The effect of the cervical subhealth change is the greatest between 1.5 hours and 2 hours. According to the above situation, we will detect the process of students in class and obtain the students' class state image at each time for recognition. The target color histogram model is used to convert the position of the feature box to locate the center position of the target in the current image. In this paper, the target tracking optimization algorithm camshift algorithm is used to identify the video area. Compared with the traditional tracking and recognition algorithm, it can improve the target tracking accuracy and effectively reduce the error. Facing the complex classroom environment, we can provide conditional feedback to the original algorithm according to the color feedback method. We extract the red pixels in the classroom area for color clustering to obtain the contour and center coordinates of the red target. The experimental process and feedback results are shown in Figure 5.

Students' goals can be tracked through local color feedback. Secondly, according to the needs of the experimental environment, students wear the same color uniforms for classroom activities. We mark the student's class clothes

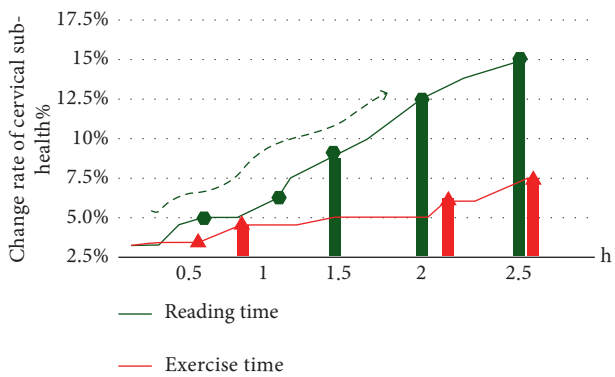

Figure 4: Comparison of the subhealth change rate of cervical spine between reading time and exercise time.

Classroom activity map | Red area map | Cervical flexion recognition

Figure 5: Experimental process and feedback results.

for easy detection. Mark the area between the head and the coat in the image, and use the above pixels to gather the target areas respectively. Eliminate the interference factors of black and environment so as to detect the changes of cervical spine bending during students' learning. Compared with traditional target tracking algorithms, the accuracy of camshift algorithm used in this paper is shown in Figure 6.

It can be seen from Figure 6 that the traditional target tracking and recognition algorithm can not improve the accuracy with the increase of image feature points. The camshift algorithm used in this paper can improve the detection accuracy in the case of a large number of pixel features. When we start the classroom monitoring mode to obtain students' local images, we analyze the local changes of students' cervical spine according to the image recognition technology to judge whether there are subhealth problems. Therefore, image recognition technology can realize the local analysis of students' physical health and obtain accurate detection data.

4. Analysis of Research Results of Students' Physical Health Problems in Class and Exercise Based on Image Recognition Technology

4.1. Analysis of Students' Physical Health Changes during Exercise Based on Image Recognition Technology. In the process of tracking and recognizing of students' human action images, based on the students' activity subject and environment model, this paper uses mathematical modeling and classification to construct the structure model of image gray value. Judge the samples of students' moving images in each frame, and finally remove the optimal value according to the peak point to realize the simultaneous recognition, tracking, and classification of multiple targets. Firstly, we use the active contour model, morphological operation model, and image recognition model to compare and analyze. Verify the speed and clarity of the image extraction time of the three methods, and the comparison results are shown in Figure 7.

As can be seen from Figure 7, in the same extraction time change, the image recognition technology has the highest definition for image processing. The average sharpness reaches 98%, while the extraction time of the contour model and morphological model is slow, and the average sharpness is also low. In order to further verify the effect of the recognition method studied in this paper, we compare the student sports injury recognition rate with the actual injury value at the same image feature points, as shown in Figure 8.

It can be seen from Figure 8 that the actual damage value is basically consistent with the identification effect. The image recognition effect can improve the damage range and accuracy to the actual result range and meet the basic requirements of detecting students' physical health.

4.2. Analysis of Research Results of Cervical Spine Health Problems in Students' Classroom Activities Based on Image Recognition Technology. In this paper, the same number of

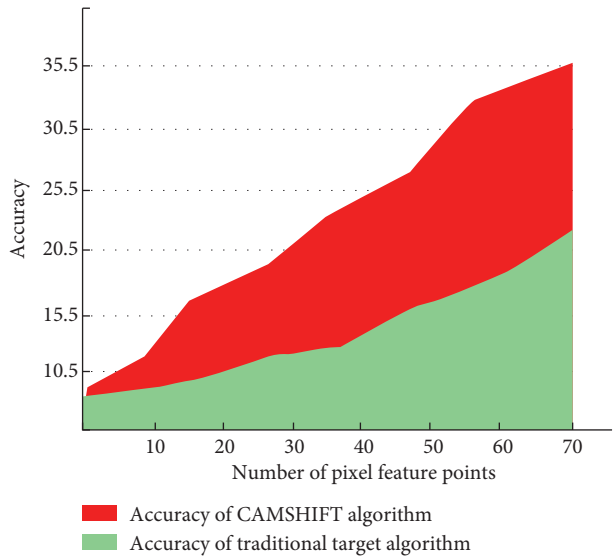

Figure 6: Comparison of accuracy between traditional target tracking algorithm and CAMSHIFT algorithm.

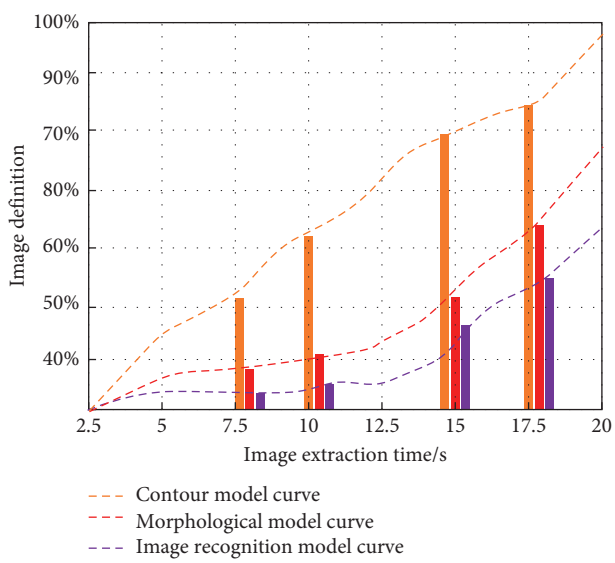

Figure 7: Comparison of image extraction time and definition in three ways.

students are randomly selected from different schools for experimental research. The ratio of male to female is 1 : 1. The tracking detection is divided into three stages according to age: high school, junior middle school, and primary school. Experiments show that students bow their heads every five minutes in the data feedback obtained by image recognition technology. The average time to look up is 10 to 15 minutes. If calculated at the same time, the number and total intensity of high school students' heads are more than primary and secondary school students. In order to more clearly reflect the changes of the data, we compared the ratio of the number and average duration of head lowering of middle school students in the three stages to the cervical subhealth ratio, as shown in Figure 9.

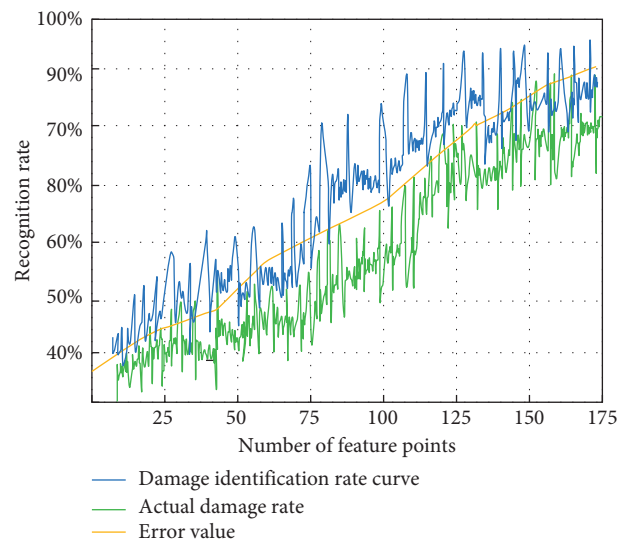

Figure 8: Comparison between damage identification rate and actual damage value.

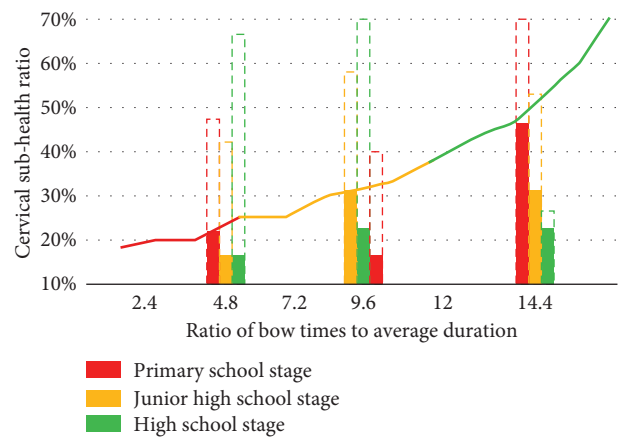

Figure 9: Comparison of the ratio of the number of times of head lowering, the average length of time, and the cervical subhealth ratio of students in the three stages.

As can be seen from Figure 9, the ratio of the bow to the duration of students in senior high school changes greatly, and the resulting subhealth problems are more serious. The initial proportion of primary schools is higher, but with the increase of learning time, the learning efficiency of primary school students is significantly reduced. The hidden proportion of high school students is higher, so the subhealth problem is more serious. Finally, according to the image recognition results of students' school activity detection, this paper forms a change curve affecting students' physical health, as shown in Figure 10.

It can be seen from Figure 10 that the horizontal is the time consumed by students in this activity, and the vertical is the change of students' physical health. Most students' physical function and quality are continuously declining in the state of continuous learning. With the increase of physical exercise, their physical health is also improved. The increase of students' meal time can also alleviate the decline

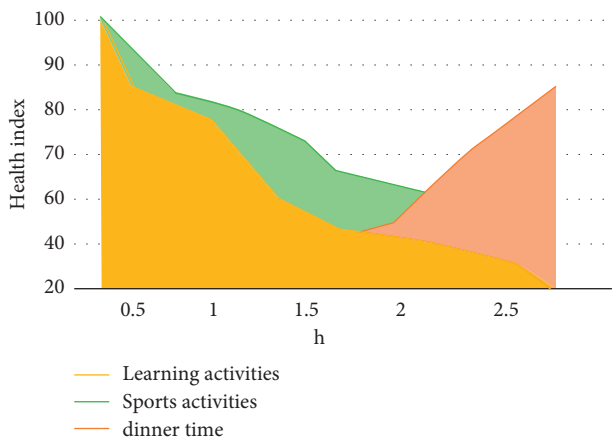

Figure 10: Chart of changes affecting students' physical health.

of physical function caused by learning. According to the analysis of students' physical health according to their sports and classroom activities, the students' cardiopulmonary function level is general. The failure rate of boys is lower than the overall level, indicating that boys' cardiopulmonary function is better than girls. The overall sensitivity and flexibility of girls are higher than the overall average level. The overall weight change of students is relatively uniform, and a small number of students are underweight and overweight.

5. Conclusion

With the continuous emergence of subhealth problems in adolescents, China focuses on the physical health problems of students in the learning stage. Long term study, reading, and writing will lead to an increase in the incidence of the cervical spine and other diseases. Abnormal posture and overtraining in sports will also lead to physical injury. This paper explores and analyzes the changing factors of students' physical health. It mainly uses the image recognition technology to track and recognize the students' action behavior in the process of movement and processes the recognition data in gray scale. Compared with the traditional recognition technology, we use the red mark aggregation region for local capture. This method greatly improves the accuracy and efficiency of image recognition. This paper also pays attention to students' cervical health problems in classroom activities and analyzes the change trend of the cervical spine through students' learning time and low head image capture. Finally, the information data after image recognition is managed and distributed by a graph neural network algorithm. This makes the students' physical health data can be displayed intuitively and can be fed back to the tester more quickly when storing the data. Finally, the experimental results show that most students have physical and subhealth problems. Image recognition technology can quickly extract feature points in the classroom environment and other interference backgrounds, and track and recognize students' behavior targets. Based on the above situation, we need to pay more attention to the healthy development of students. According to the local characteristics of image recognition and analysis, carry out quality education.

Data Availability

The experimental data used to support the findings of this study are available from the corresponding author upon request.

Conflicts of Interest

The author declare that they have no conflicts of interest regarding this work.

References

[1] W. Xiaoxiao and P. Xia, "Research on the relationship between students' physical health and physical exercise," *Sporting goods and technology*, vol. 17, pp. 47-48, 2021.

[2] Y. Liang, "Research on students' physical health test on physical education teaching reform in secondary vocational colleges," *Research on ice and snow sports innovation*, vol. 15, pp. 141-142, 2021.

[3] F. Chen and X. Mei, "Examination and optimization path of College Students' physical health," *Journal of Weinan Normal University*, vol. 36, no. 8, pp. 68–74, 2021.

[4] S. Yang, "Research on monitoring and utilization of students' physical health data based on smart phones," *Sports science and technology literature bulletin*, vol. 29, no. 8, pp. 3–5, 2021.

[5] J. Yin, "Research on the evolution of college physical education reform from the perspective of students' physical health," *Research on ice and snow sports innovation*, vol. 13, pp. 109-110, 2021.

[6] Y. Wu, *Research on the Establishment of College Students' Physical Health Data Evaluation index*, Sun Yat sen University, China, Guangdong, 2021.

[7] M. Lin, W. Sun, D. sun, Y. Li, and Y. Zheng, "Application of image recognition technology based on deep learning in defrosting system," *Office automation*, vol. 26, no. 17, pp. 22–24, 2021.

[8] J. Zhou, C. Xiong, Y. Liu, and w. Shen, "Design of complete inspection equipment for surface quality of special-shaped glass based on image recognition," *Machine tool and hydraulic*, vol. 49, no. 16, pp. 123–126, 2021.

[9] J. Chen, L. Zhu, S. Zhang, and W. Huang, "Comparative study on the recognition effect of RGB and multispectral images on banana nitrogen deficient leaves," *Modern agricultural equipment*, vol. 42, no. 4, pp. 21–28, 2021.

[10] X. Li, G. Wang, L. Li, X. Wang, J. Jing, and K. Zhang, "Object recognition method based on rgb-d image," *Journal of Xi'an University of engineering*, vol. 35, no. 4, pp. 55–70, 2021.

[11] M. Pan, "Application of image recognition in fruit and vegetable classification and recognition," *Modern agricultural science and technology*, vol. 16, pp. 257–259, 2021.

[12] C. Li, "Vehicle identification technology in adverse weather environment," *Electronic Technology*, vol. 50, no. 8, pp. 194-195, 2021.

[13] L. Zhang and D. Li, "Research and application of image recognition technology in electrolytic aluminum production," *Special Casting and Nonferrous Alloys*, vol. 41, no. 8, pp. 968–973, 2021.

[14] G. Liu, J. he, and Y. Yang, "Research on insulator fault detection method based on image recognition and intelligent

algorithm," *Electric porcelain arrester*, vol. 4, pp. 191–195, 2021.

[15] R. Yang, B. Jun, J. Su et al., "Discrimination of Tobacco Maturity Based on the integration of near infrared spectroscopy and image recognition technology," *Journal of Hunan Agricultural University*, vol. 47, no. 4, pp. 406–411, 2021.

[16] J. Shen and L. sun, "Research on substation nuclear phase inspection manipulator based on image recognition," *Electrical application*, vol. 40, no. 8, pp. 48–55, 2021.

[17] Yu Ren, X. Xie, T. Wang, P. Qiao, and Y. Chen, "Bearing fault diagnosis method based on deep learning waveform image recognition," *Journal of Naval University of Engineering*, vol. 33, no. 4, pp. 76–82, 2021.

[18] A. N. S. I. Pan, S. Xu, S. Cheng, and Y. she, "Breast mass image recognition based on svgg16," *Journal of Central South University for Nationalities (NATURAL SCIENCE EDITION)*, vol. 40, no. 4, pp. 410–416, 2021.

[19] Z. Zhang, Y. Li, Z. Liu, and T. Zhang, "Application of deep learning in fine-grained image recognition," *Journal of Beijing University of Technology*, vol. 47, no. 8, pp. 942–953, 2021.

[20] Z. Zhou and B. Cao, "Overview of military application of image target recognition and tracking technology," *Application of electronic technology*, vol. 47, no. 8, pp. 26–29, 2021.

[21] Yu Wang, "Application of neural network in image semantic segmentation," *Light industry science and technology*, vol. 37, no. 9, pp. 74-75, 2021.

[22] S. P. Li, S. Qi, S. Lin, X. Liu, and H. Chen, "A review of graph neural network and its application in the field of communication network," *Journal of Beijing University of Technology*, vol. 47, no. 8, pp. 971–981, 2021.

[23] S. Wu, "Relation selection graph neural network based on meta path," *Modern computer*, vol. 22, pp. 30–37, 2021.

[24] Bo Tan and Z. Wang, "Small traffic sign recognition algorithm based on multi-scale regional convolution neural network," *Modern electronic technology*, vol. 44, no. 15, pp. 59–64, 2021.

[25] H. Chen, X. Ding, and Y. Liu, "Overview of target detection algorithms based on deep learning," *Journal of Beijing Union University*, vol. 35, no. 3, pp. 39–46, 2021.

Hindawi
Computational Intelligence and Neuroscience
Volume 2022, Article ID 6807106, 10 pages
https://doi.org/10.1155/2022/6807106

Research Article

Concrete Application of Computer Virtual Image Technology in Modern Sports Training

YongHui Chi[1] and Jun Li[2]

[1]*Jilin University of Architecture and Technology, Changchun, Jilin Province 130114, China*
[2]*Office of Teaching Construction and Quality Control, Chengdu Technological University, Chengdu, Sichuan Province 611730, China*

Correspondence should be addressed to Jun Li; ljun1@cdtu.edu.cn

Received 5 January 2022; Revised 6 February 2022; Accepted 16 February 2022; Published 8 March 2022

Academic Editor: Yang Gu

The efficiency of basketball shooting training has always been an urgent problem to be solved in basketball sports. Applying computer virtual image technology to basketball sports training is the key to improve basketball shooting ability and improve the effect of basketball sports training. Therefore, based on the design of basketball shooting automatic recognition system based on the background difference method, this study puts forward the specific application of computer virtual image technology in modern sports training. By analyzing the techniques of image denoising, image detection, and image calibration, a goal detection algorithm for modern sports basketball shooting training is designed. Firstly, the camera is used for image capture, the RGB image is converted into gray image, and the median filter is used to suppress the noise in the image. Then, the background difference method is used to detect the moving region, and the background modeling is combined with the mean method. After obtaining the background reference model, the image is differentiated, the gray image after image difference is binarized, and then the binary image is postprocessed by morphological middle closure operation. Finally, the image calibration technology is used to extract the basketball feature information. Through the region segmentation algorithm, the basketball shooting part is segmented and judged, so as to realize the basketball shooting training goal detection. The experimental results show that the proposed method has a good effect on basketball shooting training goal detection and can effectively improve the detection accuracy and efficiency.

1. Introduction

The development of computer virtual image technology provides convenience for life. At present, computer virtual image technology is added to many devices in life [1–3]. With the rapid development of computer virtual image technology, moving target detection technology in video has been more and more widely used [4, 5]. Especially, in the application of modern sports training in recent years, the image processing technology in video includes image acquisition, processing, and image secondary display. Similarly, with the rapid development of the times, more and more requirements for video processing applications have been put forward. Moving target detection work is involved in many engineering application projects, but the moving target has a certain degree of difficulty in moving target detection due to the strong time-varying speed and uncertain path [6, 7]. Among them, the basketball special automatic test is an engineering application of sports target detection. The basketball special automatic test is one of the main content needed for the current sports professional basketball talent training test and basketball sports. Basketball goal recognition is the key technology of basketball special automatic test. Accurate and timely judgment of basketball goals has an important practical value.

At present, scholars in related fields have made some progress in basketball shooting detection. Yu and Liu [8] proposed an automatic feature detection method of the basketball shooting teaching image based on artificial intelligence. Starting from the decomposition of basketball

shooting teaching actions, the practical attributes of basketball shooting teaching images are defined, and a standardized image detection environment based on artificial intelligence is constructed according to the essentials of basketball shooting actions. The feature of basketball shooting teaching image is extracted, the feature scale value of basketball shooting action is calculated, and the feature description principle of automatic detection is combined to complete the automatic detection of basketball shooting teaching image features. This method has certain validity. Yang et al. [9] proposed a three-dimensional multiviewpoint basketball player detection and location method based on probability occupancy. Combine player detection based on deep learning and player positioning based on occupancy rate to extract the characteristics of three-dimensional multiview basketball players. The Bayesian model of a new positioning algorithm is used to detect and locate basketball players' game images by using the foreground information of the fisheye camera. This method has high reliability.

Xie [10] designed an automatic shooting recognition system based on the background difference method. The design and application of the system are tested by experimental analysis, sampling survey, and data analysis. Firstly, the relevant information of the background difference method is collected, and the algorithm flow and modeling method of the background difference method are understood. Secondly, relevant tests are designed according to the characteristics of shooting. Then, an automatic recognition system is designed for experimental research. By sampling 8 basketball players for data observation and analysis, the results are obtained. The accuracy of the basketball shooting automatic recognition system reaches 89%, which can basically meet the requirements. Therefore, based on this research, this study puts forward the specific application of computer virtual image technology in modern sports training. Using computer virtual image technology, a goal detection algorithm for modern sports basketball shooting training is designed. The basketball shooting training images are captured and preprocessed, the background difference method is used to detect the motion area for background modeling, and the images are processed by difference and binarization before postprocessing. By extracting the basketball feature information, segmenting the basketball shooting part, and making judgments, the basketball shooting training goal detection is realized. The basketball shooting training goal detection effect of this method is better, and the detection accuracy and efficiency can be effectively improved.

2. Computer Virtual Image Technology

The number of virtual images from "brightest" to "darkest" is divided according to the gray level. The larger the dynamic range is, the richer the level can be represented and the wider the color space it contains. With the rapid development of computer technology, both software and hardware have developed to a very high level. However, for users who pursue higher quality, the development of computer is endless, especially, the requirements of image quality. In order to further improve the quality of some aspects of the virtual image and make it close to the real environment as much as possible, the computer virtual image technology is studied. The specific processing process is image denoising, image detection, and image calibration. The specific analysis is as follows.

2.1. Image Denoising Technology. Because the noise in different images has differences in characteristics and spectral distribution, different denoising methods are formed. The mean filtering method and the median filtering method are the two most typical denoising methods in the spatial domain.

2.1.1. Mean Filtering Method. It uses the average brightness value or weighted value of all pixels in the neighborhood of gray jump points to replace the original jump pixel value, remove abnormal pixels, and realize image smoothing, so as to eliminate noise [11, 12]. The mathematical form of mean filtering is as follows:

$$g(x, y) = \frac{\sum_{i=1}^{mn} e_i d_i}{\sum_{i=1}^{mn} e_i}, \tag{1}$$

where d_i is the neighboring pixel value of the jumping pixel $g(x, y)$, e_i is the weighting coefficient of the neighboring pixel, that is, the template coefficient, and mn is the number of weighting coefficients, that is, the template size. If the neighborhood is larger, the image will be blurry accordingly. The average filter template is generally selected as the following size:

$$e = \frac{1}{9}\begin{bmatrix} 1 & 1 & 1 \\ 1 & 1^* & 1 \\ 1 & 1 & 1 \end{bmatrix}. \tag{2}$$

The position with an asterisk is the jumping pixel point, that is, the jumping point is at the center of the template. The equal weighting coefficient makes the pixels in the neighborhood play the same smoothing effect. Small amount of calculation and simplicity are the biggest characteristics of this filtering, but the smoothed image inevitably reduces the sharpness, especially the edges and details are the most obvious.

2.1.2. Median Filter. It is a kind of the nonlinear smoothing filter, which can effectively suppress abrupt noise by using ranking statistical theory [13–15]. Working principles of the median filter are as follows: determine a pixel as the central position, sort the gray values of other surrounding pixels according to the size relationship, and take the intermediate value to replace the pixel value at the central position. A square neighborhood formed on the basis of the central pixel is called a window. The noise smoothing of the image is realized by moving the window. Median filtering algorithm can eliminate isolated noise points and reduce the fuzziness of the image.

In the one-dimensional case, if $b_1, b_2, ..., b_n$ is a set of original signal sequences and assuming that $b_1, b_2, ..., b_n$ is already an ordered sequence from large to small, then the median of this set of original signal sequences is defined as

$$k = median\{b_1, b_2, ..., b_n\} = \left\{ \begin{array}{c} b\left(\frac{n+1}{2}\right) \\ \\ \frac{1}{2}\left(\frac{bn}{2} + \frac{bn}{2} + 1\right) \end{array} \right\}. \quad (3)$$

When there is a large isolated noise at the center of the slope change, the median filtering of this type of signal can completely eliminate the noise. When the noise is not isolated, but two consecutive equal values, the median filter can still completely filter out the noise in this case. At this point, the median filter has a much better effect than the neighborhood average smoothing.

In the two-dimensional case, the median filter takes the median value of the pixel gray value in the two-dimensional window as the new value at the center of the window, and its mathematical expression is

$$G(m, n) = median[f(i, j)] \quad (4)$$

or

$$G(m, n) = median[f(m - i, n - j)]. \quad (5)$$

Commonly used two-dimensional window shapes include cross window, X-shaped window, and square window. Commonly used processing windows for two-dimensional median filtering are shown in Figure 1.

2.2. Image Detection Technology

2.2.1. Background Difference Method. The background difference method uses the difference between the pixel gray corresponding to the current frame image and the background image to detect the moving target [16–18]. The operation flow of the background difference method is shown in Figure 2.

Assuming that the background frame image used in the background difference method is static, that is, the background frame will not change with the number of image frames, $b(i, j)$ is used to represent the background image, $\mu(i, j, l)$ is defined as the image sequence, and (i, j) in the image sequence is set as the position coordinate of the image. Among them, l is the number of frames in the image sequence, and the gray value of the selected image in the image sequence is used to make the difference with the gray value in the background image, and a difference image $\mu_d(i, j, l)$ moving target is expressed as

$$\mu_d(i, j, l) = \mu(i, j, l) - b(i, j). \quad (6)$$

2.2.2. Interframe Difference Method. The interframe difference method is a method to obtain the contour of the moving target by frame difference between two consecutive frames extracted from video sequence [19–21]. The operation flow of the interframe difference method is shown in Figure 3.

The τ picture in the video sequence is recorded as frame σ, and the $\tau - 1$ picture is regarded as frame $\sigma - 1$. The corresponding images are represented by H_τ and $H_{\tau-1}$, respectively, and the gray values of pixel points are represented by $H_\tau(i, j)$ and $H_{\tau-1}(i, j)$, respectively. The gray values of pixel points of two adjacent frames are subtracted to obtain the absolute value, and the two frames of differential images are expressed as

$$\kappa_\tau(i, j) = \left|H_\tau(i, j) - H_{\tau-1}(i, j)\right|. \quad (7)$$

2.3. Image Calibration Technology. In order to obtain the size of the object and its corresponding position in the image from the video image, the relationship between the corresponding points in the object and the corresponding points in the image can be determined. The common method is image calibration technology [22–24]. The image calibration technology is divided into traditional camera calibration and camera self-calibration.

(1) The traditional camera calibration method has certain requirements for the camera model, and the size and shape of the calibration object should be processed under the known condition. The internal and external parameters of the camera model can be obtained by mathematical transformation and calculation.

(2) The camera self-calibration method does not require a specific calibration object, but is calibrated according to the positional relationship between the surrounding image and the corresponding image captured during the movement of the camera. Camera self-calibration methods can be further divided into camera automatic visual calibration technology, using basic matrix and essential matrix self-calibration technology, etc. Self-calibration technology is very flexible, but immature. Because there are too many unknowns, it is difficult to get stable results.

There are also differences in the selection of traditional camera calibration methods and camera self-calibration methods for different occasions. For example, for some occasions that require high accuracy and the parameters do not change frequently, traditional calibration techniques can be used. For communication, virtual reality, and other occasions where the accuracy is not high, the camera self-calibration method can be used.

3. Goal Detection Algorithm in Modern Sports Basketball Shooting Training

Through the further study of computer virtual image technology, this study puts forward the goal detection algorithm of modern sports basketball shooting training. The algorithm implementation flow is shown in Figure 4.

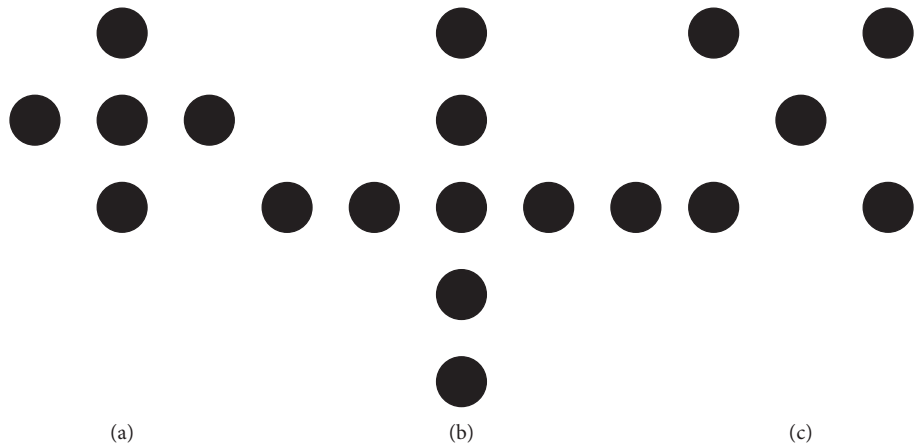

Figure 1: Common processing windows for two-dimensional median filtering.

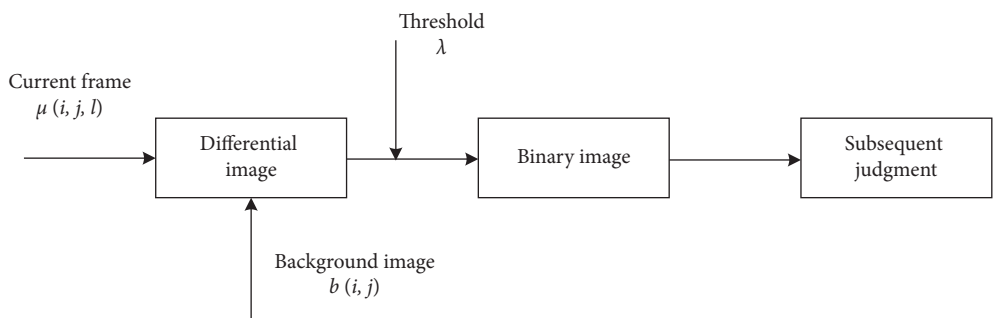

Figure 2: Background difference method operation flowchart.

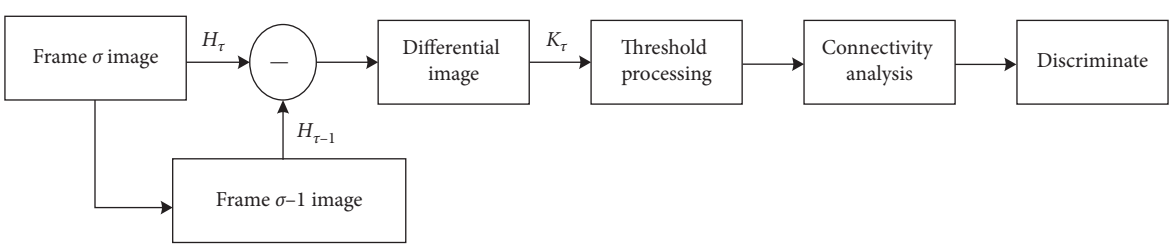

Figure 3: Interframe difference method operation flowchart.

3.1. Image Capture and Preprocessing. In the process of basketball shooting training goal detection, the image capture position is very important. Whether the camera is installed properly directly affects the accuracy of detection. To this end, use the recorded TestOne video to detect and determine the installation position of the camera is set above the basket, and the camera installation position is directly opposite to the basket for image capture, which can completely capture the basketball goal process. Because the format of the video is RGB24, the color space parameters are not needed during the detection process, so after the image is acquired, the RGB image is converted to a grayscale image, thereby reducing the system memory usage and increasing the processing speed [25].

The image captured by the camera is easily disturbed and polluted by noise in the process of transmission, conversion, and storage, which will make the useful information in the image unable to be extracted. Therefore, after capturing and converting the image, this paper uses the median filter [26, 27] to suppress the noise in the image. In order to perform median filtering on a pixel point on an image, the pixel values of the desired pixel in the mask and its neighborhood must be sorted to determine the median, and the median is given to the pixel point, which is expressed as follows:

$$G(m,n) = media[f(m,n)]. \tag{8}$$

3.2. Background Modeling. When using the background difference method to detect a moving area, the background reference model must first be prepared. Because the

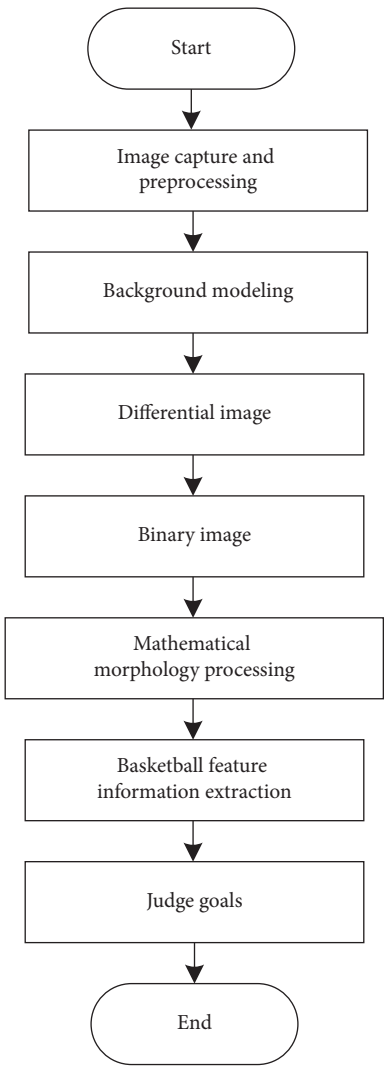

Figure 4: Algorithm implementation flowchart.

environment of the scene is relatively simple and the influence of other objective factors is small, this study adopts the mean value method for background modeling. The multiframe images captured by the camera in a period of time are accumulated, and then, the accumulated value is divided by the number of captured frames, and finally, the average value is obtained, and the obtained average value is used as the background reference model. The mathematical expression is expressed as

$$W_n = \frac{(z_n + z_{n-1} + \ldots + z_{n-N+1})}{N}, \tag{9}$$

where N is the number of frames to be averaged, $(z_n + z_{n-1} + \ldots + z_{n-N+1})$ is the continuous N frame image saved by the system including the current frame, and W_n is the background model established by the system when the n frame image is collected. Due to the influence of the lighting changes in the scene and other factors and the background model updated according to the scene for a long time, it will cause the moving target to not be detected [28, 29]. Therefore, the obtained background model W_n must be updated at regular intervals, and the update calculation formula is

$$W_n = W_{n-1} + \frac{(z_n - z_{n-N})}{N}. \tag{10}$$

Formula (10) shows that the new background model is based on the background model W_{n-1} obtained in the previous calculation, and the current frame z_n and z_{n-N} frame are recursively obtained, thus realizing the update of the background model. Obviously, if the selected image frame N value (the more image frames) is larger, the background reference model W_n obtained is closer to the real background in the scene.

3.3. Image Difference. After the background modeling is completed, the foreground area is the area where the difference value of the current image minus the background image is greater than a specific threshold. Direct subtraction is generally good, but it is poor when the foreground and background are very similar, the noise is very loud, and there are shadows. At this time, the difference between the background area and the foreground area is relatively small, so it is difficult to select the threshold [30, 31]. For this reason, after the reference model is obtained, the image in the video can be differentiated to obtain the moving area in the image and separate the background in the image. For grayscale images, the following formula is used to perform differential operations indirectly:

$$\begin{aligned} &\gamma(a,b) = 1 - \frac{2\sqrt{(a+1)(b+1)}}{(a+1)+(b+1)} \times \frac{2\sqrt{(256-a)(256-b)}}{(256-a)+(256-b)}, \\ &0 \le \gamma(a,b) \le 1, \\ &0 \le a(i,j), b(i,j) \le 255, \end{aligned} \tag{11}$$

where $a(i,j)$ and $b(i,j)$ are the gray value of the current image and the background image at the pixel point (i,j), respectively. This formula can alleviate the impact of a particularly large or small pixel gray value.

3.4. Binarization Processing. After the image is differentiated, although some parameters of the image can be extracted, further processing of the image is required. In order to be able to quickly and accurately extract the position and appearance information of the basketball feature from the video image sequence, then it is necessary to binarize the gray image after image difference and to convert the gray image to binarization. First, a segmentation threshold value needs to be given, the gray value of the points in the grayscale image is compared with the given segmentation threshold value, and the grayscale image is converted into a binary image according to the result of the comparison. For this reason, the maximum interclass difference method [32, 33] is used to extract the threshold value in the grayscale difference image.

First, assume that the range of gray values in the entire image is $[0, L-1]$, and the number of pixels with gray values of i in the gray image is c_i; then, N can be expressed as

$$N = \sum_{i=0}^{L-1} n_i. \tag{12}$$

The occurrence probability of each gray value is

$$\sum_{i=0}^{L-1} m_i = 1. \tag{13}$$

The points in the grayscale image are divided into two regions V_0 and V_1 by the segmentation threshold λ. V_0 is composed of points with grayscale value $[0, \lambda - 1]$, and V_1 is composed of points with grayscale value $[\lambda, L-1]$. Then, the probabilities of regions V_0 and V_1 are, respectively,

$$M_1 = \sum_{i=\lambda}^{L-1} m_i = 1 - M_0, M_0 = \sum_{i=0}^{\lambda-1} m_i. \tag{14}$$

The average gray levels of regions V_0 and V_1 are, respectively,

$$U_0 = \frac{1}{M_0} \sum_{i=0}^{\lambda-1} m_i = \frac{U(\lambda)}{M_0}, \tag{15}$$

$$U_1 = \frac{1}{M_1} \sum_{i=\lambda}^{\lambda-1} m_i = \frac{U - U(\lambda)}{1 - M_0}, \tag{16}$$

where U is the average gray level of the entire image:

$$U = \sum_{i=0}^{L-1} m_i = \sum_{i=0}^{\lambda-1} m_i + \sum_{i=\lambda}^{L-1} m_i = M_0 U_0 + M_1 U_1. \tag{17}$$

The total variance of the two regions is

$$\omega_B^2 = M_0 M_1 (U_0 - U_1)^2. \tag{18}$$

Let λ take values sequentially within the range of $[0, L-1]$ grayscale values so that the threshold λ, when the total variance ω_B^2 of the two regions is the largest, is the optimal region segmentation threshold in the grayscale image.

3.5. Mathematical Morphology Processing. After the gray image is processed by binarization, there will be many holes and gaps. In order to restore the basketball to its original shape and fill the hole, according to the effect of image difference and binarization, morphological closure operation [34–36] needs to be used for postprocessing of the binarized image. The closed operation can not only connect the disconnected adjacent targets in the binary image but also smooth the contour in the image.

First, the binary image is expanded, and then, the image is corroded. The definition is as follows:

$$\alpha \cdot \beta = (\alpha \oplus \beta) \Theta \beta, \tag{19}$$

where β represents a structural element, α represents an image, and $\alpha \cdot \beta$ represents β which performs a closed operation on the image α.

3.6. Basketball Feature Information Extraction. After the above steps and calculations and after the image is processed by mathematical morphology, the image calibration technology can be used to extract the basketball feature information. Basketball $x_{\min}, x_{\max} y_{\min}, y_{\max}$ is the minimum and maximum pixel coordinates in the X, Y direction, and it is also the basis for calculating other feature information. The total number of diameter pixels in the direction is denoted by $B_P(X)$and$B_P(Y)$, and the calculation method is

$$\begin{Bmatrix} B_P(X) = x_{\max} - x_{\min} \\ B_P(Y) = y_{\max} - y_{\min} \end{Bmatrix}. \tag{20}$$

The corresponding pixel in the image and the actual corresponding size of the object are mainly obtained through the calculation of the calibration coefficient B_T, which is a very important parameter in identifying goals, and the calculation of the basketball diameter is mainly obtained through B_T. Only when B_T can be obtained accurately can we calculate some basketball parameters more accurately and judge basketball shots more accurately. In the image, a diameter line segment is marked in the basketball box, and two coordinate points $(x_1, y_1)$and(x_2, y_2) are obtained at both ends of the line segment. The total number of pixels R_P between the two points on the line segment can be obtained by the straight line calculation formula:

$$R_P = \sqrt{(x_2 - x_1)^2 + (y_2 - y_1)^2}. \tag{21}$$

The corresponding relationship between the length and the pixels established by the actual size of the basketball frame diameter L and the total number of pixels of the basketball frame diameter in the image is

$$B_T = \frac{L}{R_P}. \tag{22}$$

Through the above extraction and calculation of basketball feature information, the basketball position can be determined.

3.7. Judging the Goal Method. The most important parameter for judging whether a basketball scores a goal is the actual size of the basketball diameter B_R in the image when the basketball is shooting:

$$B_R = \frac{B_P(X) + B_P(Y)}{2} B_T. \tag{23}$$

The basketball shooting part is segmented by the area segmentation algorithm. When the basketball corresponding pixel is not detected in the basketball shooting and when the basketball shooting enters the basket, the total number of pixels in the X, Y direction of the basketball will be different. The ratio coefficient Q of the total number of pixels in this

direction can be used to determine whether all basketball shots have entered the basket, which is expressed as

$$Q = \frac{B_P(X)}{B_P(Y)}. \tag{24}$$

The method to judge the goal is to compare and analyze the eigenvalues of basketball calculated above. There are three conditions to judge whether a goal is scored. If any of the conditions are not met, it will be deemed that the basketball is not scored, and the image will be captured again for detection.

Condition 1. The calculated size of $B_P(Y)$ or $B_P(X)$ must be less than 24 cm. If it is larger than 25 cm, it means that the basketball is still above the ball frame and has not been put into the basketball frame.

Condition 2. Comparing $B_P(Y)$ and $B_P(X)$, if the ratio coefficient of the two is $Q > 1.1$ or $Q < 1.1$, it is possible to detect only the noise in the image or only a part of the basketball, indicating that the basketball is not all above the basket.

Condition 3. If the above two conditions are met, compare B_R with the diameter B_T of the basketball goal obtained in the debugging process. When $B_R < B_T$, it is judged that the ball is scored, and R_P is automatically incremented by 1.

In the detection, the basketball shooting is judged through these three conditions. If the goal is judged, it will be delayed by 0.3 ms. This is because, after the goal, it is still possible to detect the basketball judged as after the goal. Then, the purpose of the delay is to wait for the previous one to pass through the basket, so as to avoid misjudgment. Through the above analysis, the computer virtual image technology is used to collect the basketball shooting image, and the image preprocessing is completed by establishing the background reference model, image difference, binarization processing, and mathematical morphology processing. On this basis, the basketball characteristic information is proposed and the goal determination method is designed to realize the basketball shooting goal detection in modern sports training.

4. Experimental Simulation and Analysis

4.1. Set up the Experimental Environment. In order to verify the effectiveness of the specific application of computer virtual image technology in modern sports training, simulation experiments are carried out in MATLAB. The operating environment is set in the GUIDE integrated environment of the MATLAB software GUI interface. In Intel Core i5-7200U@2.50 GHz CPU, 4G memory, Window 7 32 bit operating system, install this plug-in MCRInstaller.exe or MATLAB software and video decoder. In the process of basketball shooting, due to the fast movement of basketball, the basketball will hit the basket or backboard during the shooting process, causing the phenomenon of shooting jitter. For this reason, from the aspects of real-time, frame rate, and anti-shake, the camera model and CMOS sensor parameters are selected, as shown in Table 1.

4.2. Analysis of the Effect of Basketball Shooting Training Goal Detection. According to the above simulation environment and parameter settings, a basketball shooting training goal detection simulation experiment is carried out. Using the proposed method, through the recorded shooting video TestOne (640 × 480), the 46th, 85th, and 109th frames of basketball shooting training goal images are detected, and the basketball shooting training goal detection of the proposed method is obtained. The effect is shown in Figure 5.

According to Figure 5, the proposed method can effectively detect the basketball shooting training goal image, capture the goal track of the basketball shooting training image in frames 46, 85, and 109, and judge the basketball shooting training goal image. It can be seen that the basketball shooting training goal detection of the proposed method is better.

4.3. Analysis of the Accuracy of Goal Detection in Basketball Shooting Training. In order to further verify the basketball shooting training goal detection accuracy of the proposed method, the detection accuracy is taken as the evaluation index. The higher the detection accuracy is, the higher the detection accuracy is. The calculation formula is as follows:

$$A_c = \frac{P_z}{P_j} \times 100\%, \tag{25}$$

where P_z represents the number of correctly detected goals and P_j represents the number of detected goals. The number of shots is set to 45. The methods of [8], the methods of [9], and the proposed methods are used to detect the basketball shooting training goal image, respectively. The comparison results of the detection accuracy of basketball shooting training goals of different methods are calculated according to formula (25), as shown in Figure 6.

It can be seen from Figure 6 that when the number of shots is 40, the average detection accuracy of basketball shooting training goals of the methods of [8] is 81.2%, the average detection accuracy of basketball shooting training goals of the methods of [9] is 74.5%, and the average detection accuracy of basketball shooting training goals of the proposed method is as high as 92.8%. It can be seen that the accuracy of basketball shooting training goal detection of the proposed method is high, which can effectively improve the accuracy of basketball shooting training goal detection. The main reason is that this method uses the background difference of the basketball shooting image in advance to improve the accuracy of basketball shooting training goal detection.

4.4. Analysis of the Efficiency of Goal Detection in Basketball Shooting Training. On this basis, the detection efficiency of the proposed method is verified. Taking the detection time as the evaluation index, the shorter the detection time, the higher the detection efficiency of the method. Using the

Table 1: Set model parameters.

Project	Model	Free drive (M30 A)
Video camera	Image resolution	640 × 480
	Frame rate	60 frames/sec
	Interface protocol	USB2.0
	Image data format	YUV422
	Programmable control	Brightness, contrast, hue, saturation, etc.
CMOS sensor	Pixel size	$6 \times 6\,\mu$m
	Photosensitive size	$3984 \times 2953\,\mu$m
	Sensitivity	3.0 V/Lux-sec (550 nm)
	Spectral response	310–1070 nm affixed IR650 filter

(a) (b) (c)

Figure 5: Basketball shooting training goal detection effect of the proposed method.

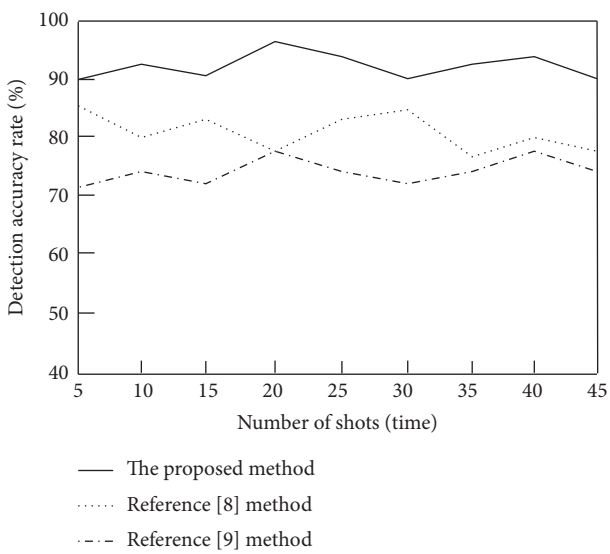

Figure 6: Comparison results of goal detection accuracy of basketball shooting training with different methods.

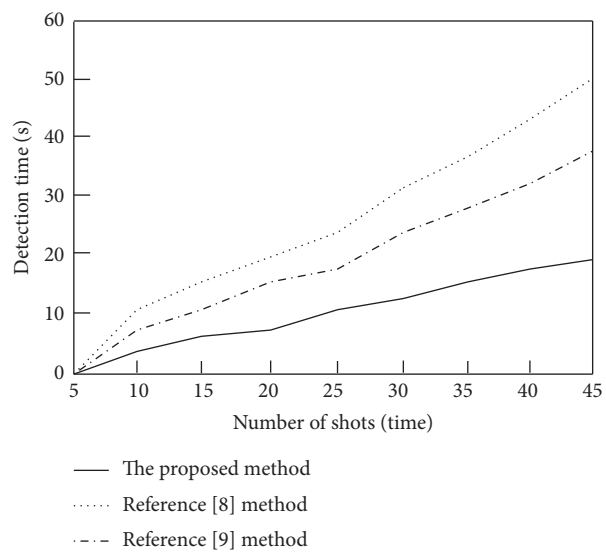

Figure 7: Comparison results of goal detection efficiency of basketball shooting training with different methods.

methods of [8], the methods of [9], and the proposed methods, the basketball shooting training goal images are detected, and the comparison results of the detection efficiency of basketball shooting training goals of different methods are obtained, as shown in Figure 7.

It can be seen from Figure 7 that, with the continuous increase of shooting times, the goal detection time of basketball shooting training with different methods increases. When the number of shots reaches 45, the basketball shooting training goal detection time of the methods of [8] is 50 s and the basketball shooting training goal detection time of the methods of [9] is 37.5 s, while the basketball shooting training goal detection time of the proposed method is only 19.2 s. Therefore, the basketball shooting training goal detection time of the proposed method is short, which can effectively improve the basketball shooting training goal

detection efficiency. The main reason is that this method accurately locates the goal position through image calibration, reduces the interference of background and other factors in the detection process, and improves the detection efficiency.

5. Conclusion

Taking basketball shooting training as the research object, this study completes the application research of computer virtual image technology in basketball shooting training from three aspects: image denoising, image detection, and image calibration. The experimental results show that this method gives full play to the advantages of computer virtual image technology, improves the accuracy and efficiency of goal detection in modern sports basketball shooting training, and has a good effect of goal detection in basketball shooting training. However, this method is only applied in basketball shooting training goal detection. The next research is to apply and analyze it in other aspects of basketball training or other sports, expand the algorithm, and further improve the application universality of the proposed method.

Data Availability

The raw data used to support the findings of the study can be obtained from the corresponding author upon request.

Conflicts of Interest

The authors declared that they have no conflicts of interest regarding this work.

References

[1] B. He, "Video teaching of piano playing and singing based on computer artificial intelligence system and virtual image processing," *Journal of Ambient Intelligence and Humanized Computing*, vol. 105, no. 1, p. s12652, 2021.

[2] W. Zhou and Z. Fu, "Adoption of bio-image technology on rehabilitation intervention of sports injury of golf," *The Journal of Supercomputing*, vol. 77, no. 10, pp. 11310–11327, 2021.

[3] Y. Yang, T. Chen, W. Wu, and H. Zheng, "Modelling the stability of a soil-rock-mixture slope based on the digital image technology and strength reduction numerical manifold method," *Engineering Analysis with Boundary Elements*, vol. 126, no. 5, pp. 45–54, 2021.

[4] J. Wang and Y. Li, "A rapid detection method for dim moving target in hyperspectral image sequences," *Infrared Physics & Technology*, vol. 102, no. 11, p. 102967, 2019.

[5] X. Yu, G. Cui, J. Yang, and L. Kong, "MIMO radar transmit-receive design for moving target detection in signal-dependent clutter," *IEEE Transactions on Vehicular Technology*, vol. 69, no. 1, pp. 522–536, 2019.

[6] Y. Yu, B. Liu, Z. Chen, Z. Li, A macro-pulse photon counting lidar for long-range high-speed moving target detection," *Sensors*, vol. 20, no. 8, pp. 2204–2209, 2020.

[7] D. Zhang, L. Gao, T. Teng, and Z. ia, "Underwater moving target detection using track-before-detect method with low power and high refresh rate signal," *Applied Acoustics*, vol. 174, no. 4, p. 107750, 2020.

[8] S. Yu and J. Liu, "Automatic detection of image features in basketball shooting teaching based on artificial intelligence," *Lecture Notes of the Institute for Computer Sciences, Social Informatics and Telecommunications Engineering*, Springer, vol. 340, no. 12, , pp. 165–175, Cham, 2020.

[9] Y. Yang, M. Xu, W. Wu, R. Zhang, and Y. Peng, "3D multiview basketball players detection and localization based on probabilistic occupancy," *2018 Digital Image Computing: Techniques and Applications (DICTA)*, vol. 12, no. 10, p. 8615798, 2018.

[10] F. Xie, "Design of basketball shot automatic recognition system based on background difference method," *2021 International Conference on Big Data Analytics for Cyber-Physical System in Smart City*, vol. 103, no. 1, pp. 65–75, 2022.

[11] B. Delibas and B. Koc, "A method to realize low velocity movability and eliminate friction induced noise in piezoelectric ultrasonic motors," *IEEE*, vol. 25, no. 6, pp. 2677–2687, 2020.

[12] C. Shao, P. Kaur, and R. Kumar, "An improved adaptive weighted mean filtering approach for metallographic image processing," *Journal of Intelligent Systems*, vol. 30, no. 1, pp. 470–478, 2021.

[13] S. X. Jiang, R. G. Zhou, W. W. Hu, and Y. C. Li, "Improved quantum image median filtering in the spatial domain," *Nternational Journal of Theoretical Physics*, vol. 58, no. 1, pp. 2115–2133, 2019.

[14] A. Gupta and D. Singhal, "Global median filtering forensic method based on pearson parameter statistics," *IET Image Processing*, vol. 13, no. 12, pp. 2045–2057, 2019.

[15] J. Chen, Y. Zhan, H. Cao, and G. Xiong, "Iterative grouping median filter for removal of fixed value impulse noise," *IET Image Processing*, vol. 13, no. 6, pp. 946–953, 2019.

[16] H. Liu, T. Hiraoka, T. Hirayama, and D. Kim, "Saliency difference based objective evaluation method for a superimposed screen of the HUD with various background," *IFAC-PapersOnLine*, vol. 52, no. 19, pp. 323–328, 2019.

[17] K. Zhang, K. Yang, S. Li, and H.-B. Chen, "A difference-based local contrast method for infrared small target detection under complex background," *IEEE Access*, vol. 7, no. 8, pp. 105503–105513, 2019.

[18] Ju Jianguo and X. Jinsheng, "Moving object detection based on smoothing three frame difference method fused with RPCA," *Multimedia Tools and Applications*, vol. 78, no. 21, pp. 29937–29951, 2019.

[19] S. M. Fadl, Q. Han, and Q. Li, "Inter-frame forgery detection based on differential energy of residue," *IET Image Processing*, vol. 13, no. 3, pp. 522–528, 2019.

[20] P. Selvaraj and M. Karuppiah, "Inter-frame forgery detection and localisation in videos using earth mover's distance metric," *IET Image Processing*, vol. 14, no. 4, pp. 4168–4177, 2020.

[21] T. Li, B. Jiang, D. Wu, X. Yin, and H. Song, "Tracking multiple target cows' ruminant mouth areas using optical flow and inter-frame difference methods," *IEEE Access*, vol. 7, no. 12, pp. 185520–185531, 2019.

[22] X. Ding, "Research on camera calibration technology based on deep neural network in mine environment. 2020 international conference on computer vision," *Image and Deep Learning (CVIDL)*, vol. 68, no. 12, p. 51233, 2020.

[23] M. Mäkelä, P. Geladi, M. Rissanen, L. Rautkari, and O. Dahl, "Hyperspectral near infrared image calibration and regression," *Analytica Chimica Acta*, vol. 1105, no. 4, pp. 56–63, 2020.

[24] Q. Deng, Q. Xu, and N. Wang, "Digital image displacement calibration simulation based on gray gradient regularization," *Computer Simulation*, vol. 38, no. 02, pp. 365–369, 2021.

[25] A. Girdhar, H. Kapur, and V. Kumar, "A novel grayscale image encryption approach based on chaotic maps and image blocks," *Applied Physics B*, vol. 127, no. 3, pp. 1–12, 2021.

[26] Y. Chen, S. Zu, Y. Wang, and X. Chen, "Expression of Concern: deblending of simultaneous source data using a structure-oriented space-varying median filter," *Geophysical Journal International*, vol. 221, no. 3, p. 2052, 2020.

[27] L. Dong, C. Wang, M. Zhang, D. Wang, and X. Liang, "Blended noise suppression using a hybrid median filter," *normal moveout and complex curvelet transform approach. Studia Geophysica et Geodaetica*, vol. 64, no. 4, pp. 241–254, 2020.

[28] W. Song, Y. Wang, D. Huang, A. Liotta, and C. Perra, "Enhancement of underwater images with statistical model of background light and optimization of transmission map," *IEEE Transactions on Broadcasting*, vol. 66, no. 1, pp. 153–169, 2020.

[29] F. G. Claude-André, "A cosmic UV/X-ray background model update," *Monthly Notices of the Royal Astronomical Society*, vol. 30, no. 2, pp. 1–22, 2020.

[30] X. Rotllan-Puig and A. Traveset, "Determining the minimal background area for species distribution models: MinBAR package," *Ecological Modelling*, vol. 439, no. 1, p. 109353, 2021.

[31] J. Mao, Z. Zhao, and C. Wang, "The unique iterative positive solution of fractional boundary value problem with q-difference," *Applied Mathematics Letters*, vol. 100, no. 2, p. 106002, 2019.

[32] H. G. Sun, Z. Wang, J. Nie, Y. Zhang, R Xiao, Generalized finite difference method for a class of multidimensional space-fractional diffusion equations," *Computational Mechanics*, vol. 67, no. 1-2, pp. 1–16, 2020.

[33] K. Sayevand, J. T. Machado, and V. Moradi, "A new non-standard finite difference method for analyzing the fractional Navier-Stokes equations," *Computers & Mathematics with Applications*, vol. 78, no. 5, pp. 1681–1694, 2019.

[34] A. Me, B. Ye, and B. Mm, "Segmentation of handwritten Arabic graphemes using a directed convolutional neural network and mathematical morphology operations," *Pattern Recognition*, vol. 122, no. 2, p. 108288, 2021.

[35] N. Madrid, M. Ojeda-Aciego, J. Medina, and I. Perfilieva, "L-fuzzy relational mathematical morphology based on adjoint triples," *Information Sciences*, vol. 474, no. 2, pp. 75–89, 2019.

[36] X. Tian, L. Chen, and X. Zhang, "Classifying tree species in the plantations of southern China based on wavelet analysis and mathematical morphology," *Computers & Geosciences*, vol. 151, no. 7, p. 104757, 2021.

Hindawi
Computational Intelligence and Neuroscience
Volume 2022, Article ID 1586006, 8 pages
https://doi.org/10.1155/2022/1586006

Research Article

Analysis of Ice and Snow Path Planning System Based on MNN Algorithm

YinZhe Jin [1,2] and Bai Li [3]

[1] *Post-Doctoral Research Center of Skiing Teaching and Training Base, Harbin Sport University, Harbin, Heilongjiang, China*
[2] *School of Sports Science, Lingnan Normal University, Zhanjiang, Guangdong, China*
[3] *School of Kinesiology and Health Promotion, Dalian University of Technology, Dalian, Liaoning, China*

Correspondence should be addressed to YinZhe Jin; 41804427@xs.ustb.edu.cn

Received 23 December 2021; Accepted 20 January 2022; Published 5 March 2022

Academic Editor: Yang Gu

Traditional ice and snow path planning methods still have internal environmental problems in intelligent path planning, such as weak innovation ability, imperfect management, long planning path, unreasonable security structure, and low degree of specialization. Therefore, more and more ice and snow sports lovers are eager to solve this problem. This paper designs a path planning method based on three-dimensional ice and snow model. The path planning method of moving snow and ice based on MNN (Multiclass Neural Networks) algorithm is studied from many aspects. MNN algorithm is used for comprehensive analysis and evaluation. The mobile phone provides data information on key nodes, air resistance, momentum change, ice and snow movement track, and so on. The results show that the ice and snow path planning system based on MNN algorithm designed in this paper has the advantages of high feasibility, high data accuracy, and good prediction effect and can effectively improve the efficiency of ice and snow path planning.

1. Introduction

According to the survey, the research on ice and snow movement track in sports mainly focuses on the movement type, path planning method, and optimal movement strategy and rarely constructs the change law of movement path process and intelligent algorithm [1]. On the other hand, some foreign scholars have begun to reconstruct the track of ice and snow in sports, which is used to analyze the tactical strategy between teams in sports, and have verified the effectiveness of the track of ice and snow through experiments [2]. At present, the existing sports path planning model provides a lot of reconstruction methods, but there are few targeted breakthroughs in ice and snow sports [3]. In this context, this paper proposes a path planning model of sports ice and snow based on MNN algorithm.

The innovation of this paper lies in the MNN algorithm and ice snow motion path planning algorithm. On this basis, we can make full use of the difference information in the ice and snow movement, carry out multivariate analysis on different types of ice and snow movement data information, combine with MNN algorithm factors, standardize the identification of the path information generated in the process of ice and snow movement, and realize the intelligent planning and correct guidance of ice and snow path according to the characteristics and objectives of ice and snow movement.

This paper studies the construction of intelligent path planning guidance system of ice and snow sports, which is mainly divided into four parts. The first chapter introduces the research background and the general arrangement of this chapter. The second chapter introduces the research status of ice and snow sports and path planning factors. In the third chapter, the dynamic tracking and intelligent path planning model of ice and snow movement based on MNN algorithm is constructed. The Laplace factor method is used to construct the ice and snow movement path planning guidance system and related evaluation system. In Chapter 4, the

dynamic tracking and path planning model of ice and snow movement constructed in this paper is verified by experiments, and the conclusion is drawn.

2. State of the Art

Since entering the 21st century, there are some problems in the research of ice and snow sports in China, especially in the path planning and intelligent dynamic tracking of ice and snow sports [4]. Based on the sphere kinematics theory and intelligent recognition method, Zenke et al. proposed a method for reconstructing the trajectory of ice and snow movement. According to different types of ice and snow movement rules, they constructed a normalized insurance path planning method [5]. Zhang et al. put forward a unified model of ice and snow movement path based on variational strategy, aiming at the safety and optimal path problems in the process of ice and snow movement, which can solve the problem of multiple dispersion in the process of traditional ice and snow movement [6]. P. Thieberger et al. proposed an antidisturbance optimal planning method for ice and snow sports path based on the types of athletes in ice and snow sports and the low efficiency of cooperation in ice and snow sports [7]. Based on the video tracking strategy, Wang et al. analyzed the path data generated in the process of ice and snow movement according to the genetic algorithm and unified different types of analysis methods. The results were applied to the path planning scheme of ice and snow movement, and the results showed that this method can significantly improve the efficiency of path planning of ice and snow movement [8]. Qi et al. put forward an improved multiangle path optimization analysis model in order to improve the aesthetic effect of athletes in the process of ice and snow sports and obtain the path information of key nodes from common ice and snow sports rules [9]. Bragazzi et al., from the perspective of the planning of the starting point and end point of the path, innovated the determination of the path planning scheme of ice and snow sports and proposed a semiautomatic online path planning method, which can realize remote detection and path planning with the help of cloud computing technology and has certain application value [10]. Fischer et al. scholars analyzed different types of ice and snow movement process from the path planning analysis level and proposed a path optimization analysis method based on ice and snow movement trajectory feedback mode, which can provide the best path planning scheme according to the characteristics of ice and snow movement [11]. In order to reduce the error rate of ice and snow movement in the path planning process, K. W. Guo et al. adopted the multifactor improved strategy docking model and designed verification experiments to verify the stability and reliability of the model in the ice and snow movement path planning process [12]. According to the different types of ice and snow sports, scholars such as Mohammad used different modes of differentiated path analysis methods to classify the types of path planning, then analyzed their differences, and obtained the optimal path scheme according to their shortest distance [13]. Grattarola et al. put forward a path optimization planning model based on firefly tracking algorithm according to the specific ice and snow movement path law, which has the advantages of strong stability and good reliability [14]. According to the characteristics of ice and snow movement path, Miles et al. improved the path planning strategy and proposed an intelligent path planning method based on super-high selection [15]. The research of Janson et al. shows that different types of path optimization strategies can be adopted according to the differences of ice and snow movement; that is, the differences in different path planning schemes can be quickly identified first, and then the common path planning standard schemes can be analyzed point-to-point, and the analysis result data can be converted to the path signal, and the final path planning scheme can be output [16]. Saeed et al. make path planning strategies for different types of ice and snow sports according to their uniqueness. This method can quickly give the shortest path recommendation scheme according to the type of ice and snow sports and the target demand [17].

To sum up, it can be seen that the current ice and snow sports generally have low degree of intelligence, weak applicability, and many restricted conditions in the path planning, which is the same with the study [18, 19]. On the other hand, although there have been many research results in ice and snow sports, there are still many problems in the path planning and guidance of ice and snow sports and few path planning models involving intelligent algorithms [20, 21]. Therefore, it is of great significance to carry out the ice and snow movement path planning method combined with intelligent algorithm.

3. Methodology

3.1. Application of MNN Algorithm in Intelligent Path Planning of Ice and Snow Sports. At present, genetic algorithm, neural network algorithm, mutual nearest neighbor algorithm, and MNN (multiclass neural network) algorithm are widely used in path planning [21–23]. The so-called mutual nearest neighbor algorithm refers to the process of finding the nearest data in a group of random samples propagating in the state space, replacing the integral operation with the sample mean value, and then obtaining the solution set of the optimal function [24–26]. As long as the global path point contains spatial position information, it can also contain attitude information, which does not need to be related to time, but time information can be considered in local planning. Here, it is specified that the track point is also a kind of path point, that is; when the time constraint is added to the path point information, it can be called a track point. From this point of view, trajectory planning is a kind of path planning. When the path planning process needs to meet the longitudinal and transverse dynamic constraints of ski objects, it becomes trajectory planning. Path planning and trajectory planning can be expressed in both state space and Cartesian coordinate system. In the process of path tracking, the reference path curve can be independent of time parameters. During tracking control, it can be assumed that the unmanned vehicle advances at a constant speed at the current speed, and the driving path approaches the

reference path with a certain cost rule. In trajectory tracking, the reference path curve is related to time and space, and the unmanned vehicle is required to reach a preset reference path point within the specified time.

In the research on the optimal solution of the track and path planning of ice and snow sports, in the application process based on MNN algorithm, aiming at the path planning strategy of ice and snow sports, this paper first designs the MNN algorithm based on the influence degree of multidimensional factors. The cloud path location tracking network with strong pertinence is used to formulate the optimal path planning scheme of ice and snow movement and determine the characteristic ice and snow movement trajectory and path planning process. The data processing process of MNN algorithm is shown in Figure 1.

3.2. Construction of Intelligent Path Planning Model for Ice and Snow Sports Based on MNN Algorithm. In this model of ice and snow sports path planning based on MNN algorithm, an online guidance scheme based on intelligent path planning strategy is constructed by using three characteristic parameters related to ice and snow sports path and trajectory. Through the research on the track collection, speed control, starting point and end point information, and data analysis strategy in the ice and snow movement, the internal relations of the factors in the whole ice and snow movement path planning guidance system are clearly defined, and the processing process is shown in Figure 2.

The basic steps of building the intelligent path planning model of ice and snow sports can be divided into three steps.

In the first step, we need to find multiple path related optimal detection information with high similarity in morphology and structure from the existing ice and snow motion detection network and then carry out local video tracking to realize the dynamic tracking of the ball in the process of space movement. The tracking function $K(s)$ is

$$K(s) = \frac{3s^3 + 3s^2 + 4s + 1}{\sqrt{5s + 2}}. \tag{1}$$

The tracking function $K'(s)$ optimized by adding dynamic aggregation factor t is

$$K'(s) = \frac{\sqrt{3s^3 + 3s^2 + 4s + 1/\sqrt{5s + 2}}}{t + 3}, \tag{2}$$

where s is the track data of ice and snow movement and t is the dynamic aggregation factor. In this process, three groups of different types of data are analyzed, and the simulation results are shown in Figure 3. As can be seen from Figure 3, with the increase of data dimension, the tracking function values of different groups of data show a similar change law, and with the increase of data dimension, it shows a gradually increasing trend.

The second step is to reduce the error in the process of path planning and optimal scheme formulation and improve the guidance efficiency of ice and snow movement trajectory and path analysis. In this process, we need to use the discriminant function to judge the planning efficiency. The discriminant function $Q(s)$ before optimization is

$$Q(s) = \frac{\sqrt{3s^3 + 3s^2 + 4s + 1}}{s}. \tag{3}$$

After adding anti-interference factor e, the optimized discriminant function $Q'(s)$ is

$$Q'(s) = \frac{\sqrt{5s^3 + 5s^2 + 3s + 1}/3s + 1}{e + 3}, \tag{4}$$

s is the trajectory data of ice and snow movement; e is the anti-interference factor.

In the third step, according to the difference of position dynamic stability of different types of ice and snow sports, the position of athletes can be updated dynamically:

$$T(s) = \frac{7s^3 + 7s^2 + 5s + 3}{s + 5s^{-1}}. \tag{5}$$

The location function with dynamic update strategy is

$$T'(s) = \frac{\sqrt{7s^3 + 7s^2 + 5s + 3/s + 5s^{-1}}}{r^s + s + s^{-1}}, \tag{6}$$

s is the trajectory data of ice and snow movement; r is the dynamic change factor. In this way, after several interactive cycles of two-way gait information, the best strategy data will be obtained according to the data analysis method, and the specific path trajectory information in line with the lowest normal ice and snow movement trajectory will be generated; that is, the data vector value of the normal boundary of an ice and snow movement path position signal and the longitude and latitude coordinates of the known position information will be compared and analyzed. In this way, the information analysis and recording of ice and snow movement track, path scheme, and coordinate longitude and latitude can be realized under the condition of "MNN algorithm." The simulation results are shown in Figure 4. As can be seen from Figure 4, with the increase of simulation times, the corresponding coincidence index of ice and snow movement trajectory (according to the commonly used empirical value, the maximum value of coincidence is 2.85) shows a gradually increasing trend, which is also in line with the law of ice and snow movement in path planning.

In MNN algorithm, the longitude and latitude analysis function $P(s)$ and trajectory analysis function $H(s)$ are

$$\begin{aligned} P(s) &= \frac{9s^3 + 7s^2 + s^x + 5}{3s^x + 5s^{-1} + 1}, \\ H(s) &= \frac{7s^{x+1} + 7s^x + 7s^{x-1} + 9}{3s^x + 5s^{x-1} + 3}. \end{aligned} \tag{7}$$

s is the track data of ice and snow movement and x is the longitude and latitude information. The ice and snow movement path planning mode based on the longitude and latitude coordinate information of the path can also realize the self storage and cloud computing functions of the data information generated in this process. Therefore, the more the accumulated historical data of ice and snow movement trajectory and path location information, the stronger the self-learning ability and intelligent planning guidance

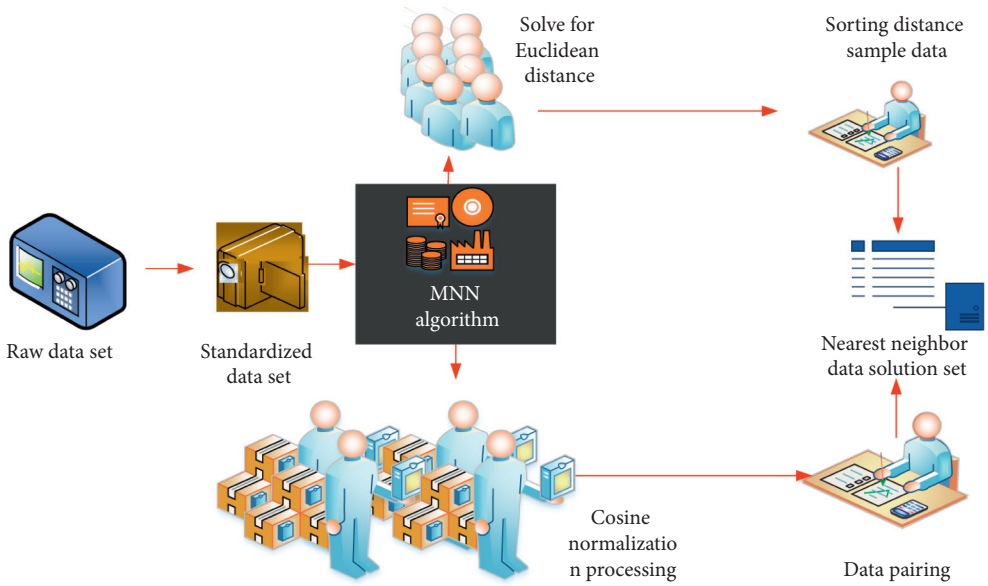

Figure 1: Data processing process under the MNN algorithm.

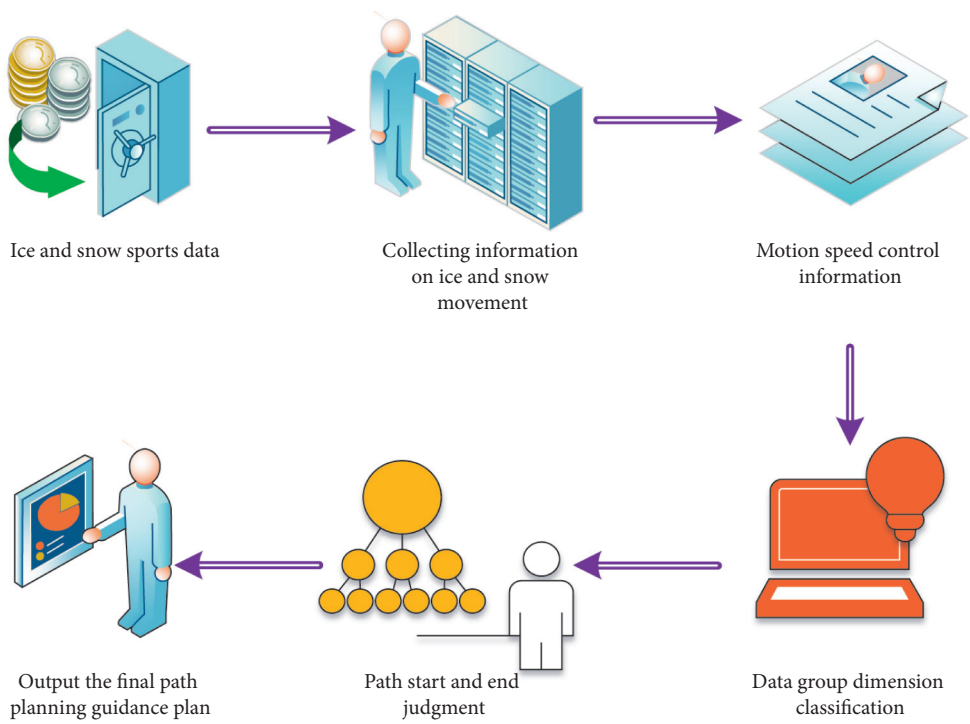

Figure 2: Processing process of ice and snow movement path planning guidance system.

scheme of the system. This adaptive path planning and tracking method can complete the intelligent path planning and error rate control of ice and snow movement with high accuracy. The analytic simulation results of this ice and snow movement path planning model for two different target path planning schemes are shown in Figure 5. According to the simulation results in Figure 5, it can be seen that, with the control of the error rate, the intelligent degree of the path planning solution, whether it is time first or distance first, tends to rise first and then fall. Therefore, it can be considered that the path planning solution has little effect on time or distance.

3.3. Different Ice and Snow Sports Path Planning Guidance Scheme and Optimization Improvement Strategy. In the process of reconstructing the trajectory of ice and snow, because different object will produce different deviations in the process of space motion, especially in the real-time dynamic position signal processing of balls, we use MNN

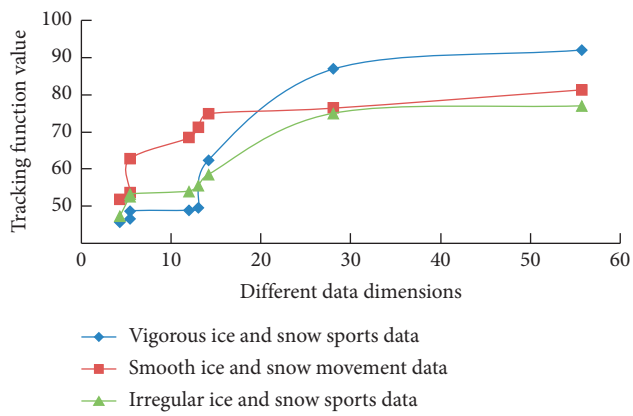

FIGURE 3: Simulation analysis results of different ice and snow sports data.

algorithm with adaptive characteristics. In order to improve the effect of different ice and snow movement path planning by MNN algorithm, it is necessary to optimize the MNN algorithm, and the optimization process is realized by the partial local method. In the process of distribution, the threshold value E is selected according to the following criteria:

$$r(s) = \frac{1}{\sqrt{5s^t + 5s^{t-1} + 3s}},$$
$$e(s) = \frac{r}{\sqrt{5s^{t+r} + 5s^{t-r} + 3s^r}}, \tag{8}$$
$$E = \frac{e + r}{e^{t+r} + e^{t-r} + e^r}.$$

s is the trajectory data of ice and snow movement, t is the eigenvalue information, $r(s)$ is the result of the first distribution, and $e(s)$ is the result of the multiple distribution.

In the process of tracking and reconstructing the track of ice and snow movement, MNN algorithm needs to select its motion feature in the process of spatial motion analysis for probability state, that is, the selection of ice and snow motion feature factor based on the whole crowd target, and then detect and analyze according to different path feature functions, whose path feature function $M(s)$ is

$$M(s) = \frac{\sqrt[3]{3s^{t+1} + 3s^t + 2s^{t-1} + 8}}{\sqrt{5s^t + 5s^{t-1} + 8}}. \tag{9}$$

After adding the tracking condition, the path characteristic function $M'(s)$ is

$$M'(s) = \frac{t + s^2}{t - s} + \frac{\sqrt[3]{3s^{t+1} + 3s^t + 2s^{t-1} + 8}}{\sqrt{5s^t + 5s^{t-1} + 8}}, \tag{10}$$

where s is the track data of ice and snow movement and t is the eigenvalue information. In the aspect of path planning for ice and snow sports, this model will use the existing ice and snow sports big data and the path planning information database stored in the cloud, combined with the data analysis factor, to analyze the adaptive disturbance of the limit weight value obtained from the optimized MNN algorithm, and then use the MNN algorithm to subdivide specific ice and snow sports information. According to the differences of different types of ice and snow movement paths, the integrity of them is sorted, and then the sorting results are discretized according to different weight indexes, and the path factors related to the optimization strategy are marked, and the marking results are transmitted to the optimal path planning scheme database. The expressions of the standard function $B(s)$ and the discrete weight solving function $J(s)$ of the optimal path planning scheme are as follows:

$$B(s) = \frac{t^{2s} + s^{2t}}{t^s - s^t},$$
$$J(s) = \frac{t^{2s} - s^{2t}}{\sqrt{t^s + s^t}} + \frac{B^t(s) + tB(s)}{B^{2t}(s) - tB(s)}, \tag{11}$$

where s is the track data of ice and snow movement and t is the eigenvalue information. The simulation results of path selection and the number of scattered points are shown in Figure 6.

As can be seen from Figure 6, with the increase of the number of key points of the path, the scattered points of the path in the four different schemes also show different changing rules with obvious characteristics. This is because MNN algorithm first selects the data coding for the ice and snow trajectory and then classifies the different types of parameter data groups. Then the MNN algorithm is used to solve the local optimization of the processed path database, and the internal change law is analyzed. In order to realize the optimization of the path selection process, we will form the vector matrix group with key characteristics from the path parameters and other information generated in the process of ice and snow movement and input it into the path planning guidance model. These vector groups produce different vector eigenvalues according to the different path trajectories of ice and snow movement. Therefore, the spatial position of the original ice and snow movement in the process of path selection is analyzed by using the transformed matrix sequence.

4. Result Analysis and Discussion

4.1. Experimental Process of Ice and Snow Path Planning Guidance Model Based on MNN Algorithm. Before the beginning of the experiment, we set up a model of ice and snow trajectory reconstruction and path planning based on the characteristic parameters and path differences. The model centers on the dynamic movement process of ice and snow athletes and takes the differences of different ice and snow trajectories and different path schemes as the core evaluation index. The reconstruction effect and path planning strategy of ice and snow trajectory are evaluated. The experimental process is shown in Figure 7.

As can be seen from Figure 7, with the increase of the number of dynamic signals (the number of experiments), the completion degree of path planning gradually increases until it becomes stable. This is because the more the number of

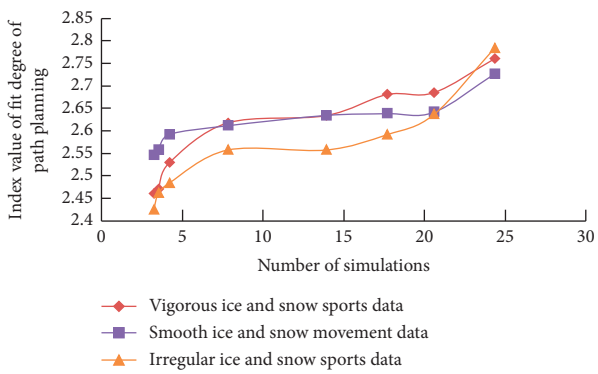

Figure 4: The coincidence index of ice and snow trajectory under different simulation times.

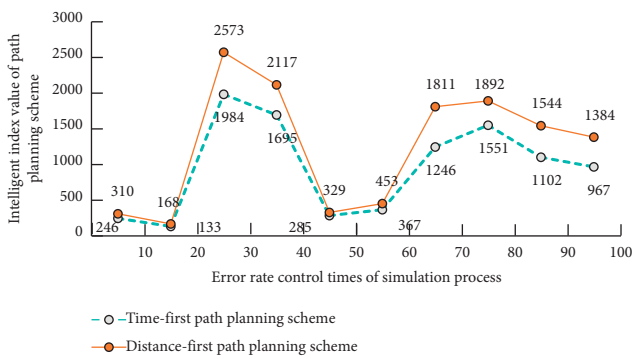

Figure 5: Analytical simulation results of path planning schemes for two different goals.

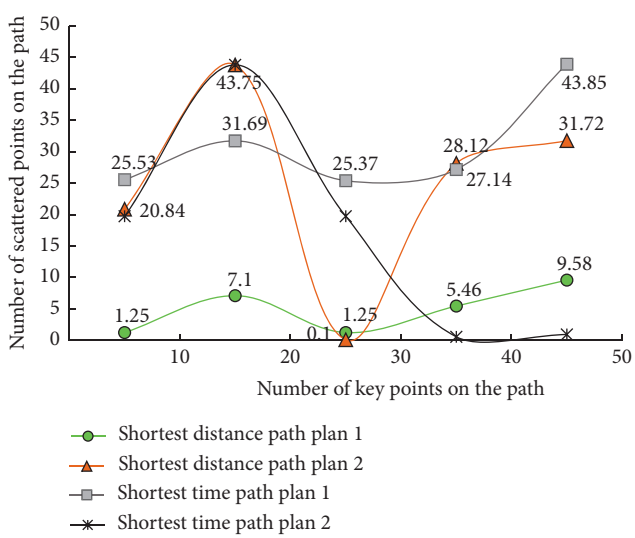

Figure 6: Reconstruction model of volleyball sports track based on filtering algorithm.

signals, the more the amount of calculation required, and so the higher the degree of coincidence. Moreover, the MNN algorithm has better reliability and data stability. Compared with other methods, it also has better scientific reference in the error control of the optimal solution of the path. This is because in the ice and snow movement path planning model, different ice and snow movement trajectories, and path data are taken as the experimental objects. Through the tracking process of different ice and snow movement tracks, the intelligence and convenience of ice and snow movement path planning scheme are evaluated. It is mainly based on the automatic analysis strategy and multidata comparison method of conventional ice and snow sports path planning at the big data level. Then, through the detection and quantitative processing of the motion data in ice and snow movement, the analysis of different types of ice and snow movement trajectories and the planning and feasibility prediction of the optimal path are realized. On this basis, with the help of the idea of nearest neighbor strategy, the optimal path planning guidance for different types of ice and snow sports is realized and displayed by three-dimensional visualization method. This is also an innovation of the intelligent analysis model based on MNN algorithm in the research of real-time path planning and intelligent data processing methods of ice and snow sports.

4.2. Analysis of Experimental Results. The stability test results of the experimental results of snow and ice trajectory reconstruction based on MNN algorithm and other path planning methods are shown in Figure 8, and the evaluation results of the snow and ice path planning guidance model based on MNN algorithm and other path planning methods are shown in Figure 9.

It can be seen from Figures 8 and 9 that, with the increase of the number of experiments, the stability of the overall path planning is significantly improved. This is because, with the increase of the number of experiments, certain error data will be eliminated in each calculation process (which can be judged according to the coincidence degree) and in the process of analyzing the experimental results. We find that, in the process of feature extraction, the reconstruction of ice and snow trajectory is based on the data stored in the hardware of traditional detection equipment, and the detection process is mainly direct contact detection, while the noncontact real-time motion space signal detection is rare. Therefore, in the detection of ice and snow movement, a standard evaluation model of ice and snow movement trajectory data is determined in advance (in order to determine the key detection nodes). Therefore, this paper studies the processing object based on the spatial position change of the ball randomly selected from the local ice and snow movement set of multiple targets to be detected. By comparing and analyzing the real-time analysis model of the ball's spatial position and the big data system of sports ice and snow trajectory, it is easy to know that, in the process of the change of the two ball's spatial position, if there is a high degree of structural similarity in the group, the numerical difference of the ice and snow trajectory between them is very small. This shows that the accuracy of this model is very high.

Finally, this study takes two similar ice and snow movement path schemes in sports as a group of tracking research objects, and a random ice and snow movement path as the control object. One of the groups is that the ice and snow movement path is known (the ice and snow movement path and other information are known). The other group is

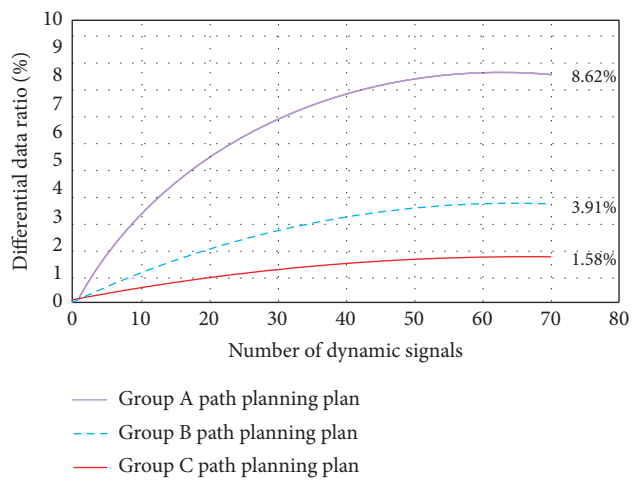

Figure 7: Experimental process of intelligent planning of ice and snow sports path.

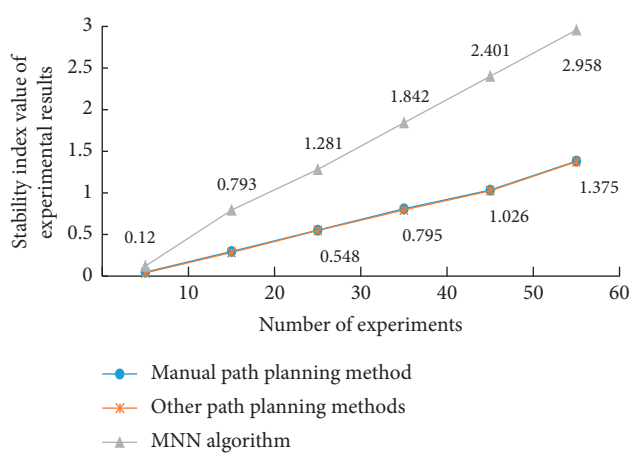

Figure 8: Stability of experimental results under different experimental times.

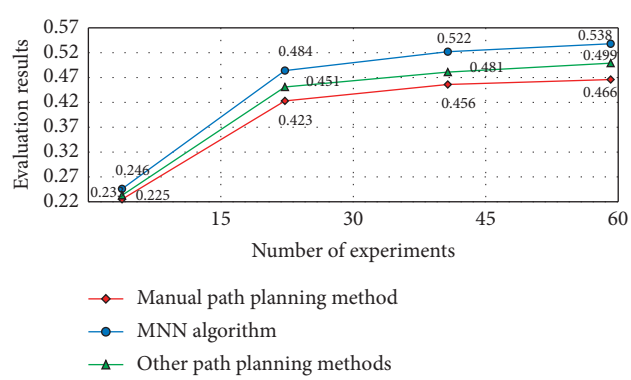

Figure 9: Evaluation results of different guidance models for path planning of ice and snow sports.

that the track of ice and snow movement is unknown (the initial track and path of ice and snow movement are known, but the details of the specific motion path are unknown). It is found that there is a high similarity in the process of reconstructing the ice and snow trajectory in the two kinds of data, and the error is 1.2% and 2.3%, respectively. In the guidance scheme of ice and snow path planning based on MNN algorithm, the intelligent path planning scheme given by MNN algorithm is in good agreement with the real optimal path planning scheme. Therefore, the research results of this experiment show that the ice and snow movement path planning model based on MNN algorithm combined with the characteristics of ice and snow movement and data reliability, intelligent planning for different types of ice and snow movement path planning scheme, and its high degree of coincidence, in line with the actual application needs. Therefore, the experimental results show that the ice snow path planning method based on MNN algorithm can be applied to the dynamic analysis of ice snow trajectory and the guidance of the optimal path allocation after the game.

5. Conclusion

In recent years, there are many problems in the research of ice and snow sports, such as the inefficient path planning of ice and snow sports, less application scope, and so on. Therefore, the reform of traditional ice and snow sports path planning method is more and more urgent. Based on this, this paper studies the path planning model of ice and snow sports based on MNN algorithm and designs the dynamic tracking method of intelligent path planning of ice and snow sports based on the three-dimensional trajectory model. Through the research of three aspects in the process of ice and snow movement, the ice and snow movement path planning guidance system based on the minimization strategy is constructed. Finally, the MNN algorithm and the optimized iterative data analysis model are used to analyze the characteristics of the screening results and the intelligent path planning process. The experimental results show that the model can make full use of the intelligent path planning strategies of different types of ice and snow sports, achieve the integrity of the intelligent path of ice and snow sports, efficiently carry out the customized analysis of the factors affecting the ice and snow sports path planning, and improve the efficiency of path planning. However, this paper only focuses on the path planning method of ice and snow movement and does not take the directional capture efficiency and the potential impact of error into account. Therefore, the ice and snow movement path planning model has some room for improvement.

Data Availability

The experimental data used to support the findings of this study are available from the corresponding author upon request.

Conflicts of Interest

The authors declare that they have no conflicts of interest regarding this work.

References

[1] Z. Zhang, C. Y. Park, C. L. Theesfeld, and O. G. Troyanskaya, "An automated framework for efficiently designing deep convolutional neural networks in genomics," *Nature Machine Intelligence*, vol. 3, no. 5, pp. 392–400, 2021.

[2] H. Hewamalage, C. Bergmeir, and K. Bandara, "Recurrent neural networks for time series forecasting: Current status and future directions," *International Journal of Forecasting*, vol. 37, no. 1, pp. 388–427, 2021.

[3] D. K. Dewangan and S. P. Sahu, "RCNet: road classification convolutional neural networks for intelligent vehicle system," *Intelligent Service Robotics*, vol. 14, no. 2, pp. 199–214, 2021.

[4] P. Elnaz, P. Elham, and A. Nizamettin, "Gene selection using hybrid binary black hole algorithm and modified binary particle swarm optimization," *Genomics*, vol. 111, no. 4, p. 9, 2018.

[5] F. Zenke and T. P. Vogels, "The remarkable robustness of surrogate gradient learning for instilling complex function in spiking neural networks," *Neural Computation*, vol. 33, no. 4, pp. 899–925, 2021.

[6] A. Zhang, Z. Xiang, and T. Jin, "Exploring influence of different gait trajectories on major muscle fatigue of a lower human limb," *Mechanical Science & Technology for Aerospace Engineering*, vol. 10, no. 5, pp. 41–45, 2018.

[7] P. Thieberger, D. Gassner, R. Hulsart et al., "Fast readout algorithm for cylindrical beam position monitors providing good accuracy for particle bunches with large offsets," *Review of Scientific Instruments*, vol. 89, no. 4, Article ID 043303, 2018.

[8] J. Wang, Y. Yang, T. Wang, R. S. Sherratt, and J. Zhang, "Big data service architecture: a survey," *Journal of Internet Technology*, vol. 21, no. 2, pp. 393–405, 2020.

[9] C.-C. Qi, "Big data management in the mining industry," *International Journal of Minerals, Metallurgy and Materials*, vol. 27, no. 2, pp. 131–139, 2020.

[10] N. L. Bragazzi, H. Dai, G. Damiani, M. Behzadifar, M. Martini, and J. Wu, "How big data and artificial intelligence can help better manage the COVID-19 pandemic," *International Journal of Environmental Research and Public Health*, vol. 17, no. 9, p. 3176, 2020.

[11] C. Fischer, Z. A. Pardos, R. S. Baker et al., "Mining big data in education: affordances and challenges," *Review of Research in Education*, vol. 44, no. 1, pp. 130–160, 2020.

[12] K. Guo, F. Xu, Y. Wang, Y. Liu, and Q. Dai, "Robust non-rigid motion tracking and surface reconstruction using L_0 regularization," *IEEE Transactions on Visualization and Computer Graphics*, vol. 24, no. 5, pp. 1770–1783, 2018.

[13] J. Xia, J. Wang, and S. Niu, "Research challenges and opportunities for using big data in global change biology," *Global Change Biology*, vol. 26, no. 11, pp. 6040–6061, 2020.

[14] D. Grattarola and C. Alippi, "Graph neural networks in TensorFlow and keras with spektral [application notes]," *IEEE Computational Intelligence Magazine*, vol. 16, no. 1, pp. 99–106, 2021.

[15] C. Miles, A. Bohrdt, R. Wu et al., "Correlator convolutional neural networks as an interpretable architecture for image-like quantum matter data," *Nature Communications*, vol. 12, no. 1, pp. 3905–3907, 2021.

[16] L. Janson, B. Ichter, and M. Pavone, "Deterministic sampling-based motion planning: Optimality, complexity, and performance," *The International Journal of Robotics Research*, vol. 37, no. 1, pp. 46–61, 2018.

[17] J. Saeed and S. Zeebaree, "Skin lesion classification based on deep convolutional neural networks architectures," *Journal of Applied Science and Technology Trends*, vol. 2, no. 1, pp. 41–51, 2021.

[18] Y. Singh, S. Sharma, R. Sutton, D. Hatton, and A. Khan, "A constrained A ∗ approach towards optimal path planning for an unmanned surface vehicle in a maritime environment containing dynamic obstacles and ocean currents," *Ocean Engineering*, vol. 169, no. DEC.1, pp. 187–201, 2018.

[19] Y. Wu, "Coordinated path planning for an unmanned aerial-aquatic vehicle (UAAV) and an autonomous underwater vehicle (AUV) in an underwater target strike mission," *Ocean Engineering*, vol. 182, no. 15, pp. 162–173, 2019.

[20] S. Khanra, A. Dhir, and M. Mäntymäki, "Big data analytics and enterprises: a bibliometric synthesis of the literature," *Enterprise Information Systems*, vol. 14, no. 6, pp. 737–768, 2020.

[21] R. H. Hamilton and W. A. Sodeman, "The questions we ask: Opportunities and challenges for using big data analytics to strategically manage human capital resources," *Business Horizons*, vol. 63, no. 1, pp. 85–95, 2020.

[22] N. An and W. Qi Yan, "Multitarget tracking using Siamese neural networks," *ACM Transactions on Multimedia Computing, Communications, and Applications*, vol. 17, no. 2s, pp. 1–16, 2021.

[23] H. Sun, M. T. Xu, X. Q. Wang et al., "Comparison thigh skeletal muscles between snowboarding halfpipe athletes and healthy volunteers using quantitative multi-parameter magnetic resonance imaging at rest," *Chinese Medical Journal*, vol. 131, no. 9, pp. 1045–1050, 2018.

[24] J. Halverson, A. Maiti, and K. Stoner, "Neural networks and quantum field theory," *Machine Learning: Science and Technology*, vol. 2, no. 3, Article ID 035002, 2021.

[25] A. B. Çolak, "An experimental study on the comparative analysis of the effect of the number of data on the error rates of artificial neural networks," *International Journal of Energy Research*, vol. 45, no. 1, pp. 478–500, 2021.

[26] P. D. Thanh, H. T. T. Binh, and T. B. Trung, "An efficient strategy for using multifactorial optimization to solve the clustered shortest path tree problem," *Applied Intelligence*, vol. 50, no. 4, pp. 1233–1258, 2020.

Hindawi
Computational Intelligence and Neuroscience
Volume 2022, Article ID 2199166, 8 pages
https://doi.org/10.1155/2022/2199166

Research Article

Dynamic Monitoring of Football Training Based on Optimization of Computer Intelligent Algorithm

Jin Gang

Physical Education Department, Northeastern University, Shenyang, Liaoning 110000, China

Correspondence should be addressed to Jin Gang; jingang@pe.neu.edu.cn

Received 29 December 2021; Revised 19 January 2022; Accepted 31 January 2022; Published 28 February 2022

Academic Editor: Guobin Chen

Nowadays, with the development of computer science and technology, computer intelligent algorithms are more and more widely used in various industries. Every calculation formula in the computer intelligent algorithm has systematic logic and singleness, in order to expound the dynamic algorithm of football training optimized by the computer intelligent algorithm in detail. In this paper, the monitoring system using the computer intelligent algorithm can dynamically observe people or objects and systematically analyze them. This paper mainly studies the research of a football training dynamic monitoring system based on the computer intelligent algorithm and the design and optimization of the computer intelligent dynamic monitoring system in football training. Finally, the overall composition of the computer intelligent dynamic monitoring system and the application of the optimized computer intelligent dynamic monitoring system to the analysis of sample data are studied.

1. Introduction

Computer intelligent dynamic monitoring technology is widely used, and then it has evolved various types of intelligent dynamic monitoring methods over time. Therefore, it is not a simple task to thoroughly master computer intelligent dynamic monitoring technology (Viviana et al., 2021) [1]. With the development of the computer intelligent dynamic monitoring system, many relevant researchers have made technical improvements and functional upgrades to this kind of system. With the development of society, computer intelligent dynamic monitoring technology has also been innovated in the research process. Nowadays, although the development of computer intelligent dynamic monitoring technology has not reached idealization, there are often difficult technical problems to overcome (Kwon et al., 2021) [2]. However, the development prospect of computer intelligent dynamic monitoring technology in today's society and even in the future society is very broad, and this technology can also promote the development of intelligent technology. The development of computer intelligent dynamic monitoring technology is also the focus of today's society (Bai et al., 2021) [3]. This also makes the computer intelligent dynamic monitoring technology applied to more industries in today's society.

At present, relevant researchers who study computer intelligent dynamic monitoring technology are very mature in both theoretical cognition and specific means of use. Computer intelligent dynamic monitoring technology mainly originated in the 1950s, and its earliest monitoring form is data collection and analysis (Shao et al., 2021) [4]. After three stages of technical change, the traditional data monitoring has evolved into single machine data monitoring and finally into today's networked computer intelligent monitoring mode. In the process of building the computer intelligent dynamic system, the system function is mainly to implement application requirements such as data acquisition, storage, processing, and analysis (Fan and Zhao, 2021) [5]. Compared with the stand-alone monitoring system, the networked computer intelligent dynamic monitoring system achieves the system functions of data integration and processing and long-distance data transmission (Li et al., 2021) [6]. At the same time, you can also analyze multiple types of data at the same time. Computer intelligent monitoring technology not only helps to improve the system's ability to analyze data but also reduces the human labor force. This

technology is also becoming more and more important in the application of various industries (Wang et al., 2021) [7].

This paper mainly studies the dynamic monitoring system of football training based on the computer intelligent algorithm. Innovation contributions include as follows: (1) In this paper, the monitoring system using the computer intelligent algorithm can dynamically observe people or objects and systematically analyze them. In the upgrade of the system algorithm, it is mainly enhanced in the part of human condition monitoring. (2) Only by ensuring the correctness of monitoring data, we can reduce the workload of the system and ensure the stability of the whole system. In order to improve the correctness of monitoring data, feature extraction algorithm and state recognition algorithm are added. (3) The performance and stability of the intelligent dynamic monitoring system designed in this paper are verified by specific experiments. The experimental results also prove that the dynamic monitoring system optimized by the computer intelligent algorithm can be applied to football training.

This paper is mainly composed of three parts. The first part is the application of computer intelligent monitoring technology in football training and the development status of computer intelligent monitoring technology in various countries. The second part is the design and research of the football training dynamic monitoring system under the computer intelligent algorithm and the intelligent algorithm optimization design of the football training dynamic monitoring system. The third part is the result analysis of the dynamic monitoring system of football training under the computer intelligent algorithm and the optimization result analysis of the intelligent algorithm of the dynamic monitoring system of football training.

2. Related Work

Computer intelligent dynamic monitoring system appeared before World War II. It was the most common dynamic monitoring system in the early stage of development. The traditional dynamic monitoring system mainly carries out a brief analysis of data manually (Shohei et al., 2021) [8]. In the middle stage of development, the form of technology stays in the single-machine mode. In this system mode, the data acquisition ability has been significantly improved, but it does not absolutely reflect the collection and sharing of data. The computer intelligent dynamic detection system in the later stage of development is integrated with network and wireless communication technology, which not only solves the data collection processing but also improves data sharing (Zhang et al., 2021) [9]. The development of the computer intelligent dynamic monitoring system also provides a solid development foundation for relevant researchers and enriches the internal functions of the computer intelligent dynamic monitoring system. Then, based on the development of computer hardware, the data tasks processed by the computer intelligent dynamic monitoring system are becoming more and more complex. After the emergence of the intelligent dynamic monitoring system, it is applied to monitor a bridge structure for the first time. Its main task is to monitor and evaluate the abnormal data.

In the United States, computer intelligent monitoring technology is mainly used to monitor hospital patients' heart rate, blood pressure, and other data information. With the popularity of medical devices, the United States is also developing in the field of medical industries. The medical industry itself is a special group serving the masses, and there are many patients with different diseases every day (Lund et al., 2021) [10]. It is impossible for the only service personnel in the hospital to pay attention to the patient's data information all the time. With the advent of computer intelligent monitoring technology, relevant researchers have conducted a series of experiments (Xu et al., 2021) [11]. It is found that this technology can be combined with the data information of hospital patients and transmit the data summary results to the computer screen, which also reduces the task of medical staff.

Germany mainly applies computer intelligent monitoring technology to the automobile manufacturing industry. Germany ranks first in the field of automobile manufacturing in the world, and the quality of cars made in Germany is very high. Besides, high-quality automobile production is inseparable from computer intelligent monitoring technology. Germany applied the computer intelligent monitoring technology to monitor the internal parameter data of automobile parts for the first time and achieved great success (Loogen et al., 2021) [12]. This success also makes the computer intelligent monitoring technology popular all over the German country. In the process of autoparts manufacturing, the data are automatically collected and classified by the computer intelligent monitoring system so that the relevant quality inspection personnel can observe more intuitively. The combination of computer intelligent monitoring technology and the automobile manufacturing industry not only reduces the expenditure but also reduces the emergence of unqualified parts.

France has widely applied computer intelligent monitoring technology to the breeding industry. Nowadays, scientific breeding methods can not only bring more considerable income to farms but also reduce the probability of animal diseases. As we all know, animal husbandry in France accounts for a large proportion in the whole social industry (Xiang and Xiang, 2020) [13]. Part of the reason for the large proportion is that there are a lot of lawns in France, which also leads to a lot of farms and pastures in France. However, when computer intelligent monitoring technology is not applied to the breeding industry, there are often phenomena such as nonstandard feeding and large-scale illness of livestock [14]. Once this phenomenon occurs, it means that the farm will lose a lot of money. The emergence of computer intelligent monitoring technology can automatically record the daily food intake and exercise of individual livestock. Once the data deviation is large one day, measures can be taken in time to avoid capital loss, which also reflects the importance of computer intelligent monitoring technology.

China applies computer intelligent monitoring technology to the field of logistics industries. Because computer intelligent monitoring technology has the function of automatic classification of data, it can quickly classify packages in the face of a large number of express packages. The

classified package can accurately deliver the express to the buyer, and the delivery time of the express package is also shortened (Xian et al., 2020) [15]. Computer intelligent monitoring technology is also widely used in other fields in China and has brought positive results to various industries, which also makes computer intelligent monitoring technology valued by mankind.

The above content is the development history of the computer intelligent monitoring system and the application of this technology in various countries.

3. Methodology

3.1. Design of Dynamic Monitoring System for Football Training under Computer Intelligent Algorithm. Nowadays, the dynamic monitoring system has achieved the systematic analysis of the information data generated in the process of sports. This paper mainly studies the systematic analysis of the relevant data of football training under the computer intelligent monitoring system. The purpose of designing the computer intelligent monitoring system is to better monitor people or things and then process the collected data information to get the final required data results. In the process of monitoring football training, it is essentially monitoring athletes. Therefore, the design of the dynamic monitoring system for football training under the computer intelligent algorithm in this paper combines dynamics and machine science. These two contents can be integrated with the dynamic monitoring system and can also give play to its internal expertise in information and data processing. Through the high-speed processing ability of data and information, the internal performance of the computer intelligent dynamic monitoring system is comprehensive. The structure of the dynamic monitoring system after combining the two learning methods is shown in Figure 1.

As can be seen from Figure 1, the dynamic monitoring system mainly includes three modules: data acquisition, storage, and data analysis. The data acquisition module cannot be completed by the intelligent dynamic monitoring system itself. The sensor needs to be worn on the football player. The data information generated by football players in the training process will be output to the intelligent dynamic monitoring system through sensors. The data storage system included in the system can automatically store the input data. It can also perform simple data processing, such as deleting incomplete data and noise data. Then, the system analyzes the data information in the database one by one. The data analysis operation is multidimensional, and the data can be systematically analyzed from different angles. Finally, the analysis result data are displayed by the visual method, which can also make the system users have a good user experience.

Each module in the system mainly relies on the network for real-time communication. After connecting through the network, the whole intelligent dynamic monitoring system is formed. In the data acquisition module, the main component used is the sensor. The main purpose of the sensor is to collect the data information of football players and transmit data information. Because the collected data type is a physical variable, the data transmission mode in this paper mainly adopts the wireless transmission mode, and the data collected by the sensor are also sent by the wireless controller. The sensor also processes the data, and the processing flow has its own characteristics. The flow of data processing in networked sensors is shown in Figure 2.

It can be seen from Figure 2 that the sensor can collect data on temperature, pressure, and speed. All kinds of internal sensors can get high-precision sensing data and also have the characteristics of high temperature resistance and waterproof. The connection between the sensor and the controller is mainly based on the communication protocol inside the controller, which can keep the sensor in the mode of high-speed operation and high-speed transmission. The data transmission part inside the sensor is mainly connected with the intelligent dynamic monitoring system through the data interface.

In the data storage module of the system, the main purpose is to put the obtained data information into the system. The data in the system cannot be completely correct, and the phenomenon of data missing often occurs. The internal intelligent algorithm of the system can complete or retrieve the missing data. In the data analysis module of the system, the main analysis methods are mechanical analysis and detecting abnormal data. In the process of mechanical analysis of data, it is to judge the force. The analysis of mechanics in the intelligent dynamic monitoring system is also the focus of this paper.

In the process of physical and mechanical analysis, it is mainly to combine the collected element data related to mechanics. After the combined data model is obtained, the speed of physical and mechanical analysis data can be accelerated. The basic construction equation in physical mechanics is as follows:

$$\rho i \frac{\partial^2 u_i^t}{\partial T^2} = \int_H f\left(\xi^t\right) dV_j + b_i. \tag{1}$$

From the above equation, the acceleration existing in the data element can be obtained, and the force used in this expression is mainly composed of many element nodes. The nodal volumes of elements are the same, which is also conducive to the calculation of acceleration. The damage function describing the lack of data is also added to the whole computer intelligent dynamic monitoring system. The damage function studied in this paper mainly adds polynomial damage function to the ordinary damage function, which also makes the whole research more convincing. Because the process of calculating the damage function will slow down the data processing speed of the whole system, an OpenMP shared thread parallel algorithm is added to solve this problem. With the addition of the algorithm, the running speed of the whole detection system has also been greatly improved. The above content is the overall design concept of the football training dynamic monitoring system under the computer intelligent algorithm.

3.2. Intelligent Algorithm Optimization Design of Football Training Dynamic Monitoring System. In the optimization process of the intelligent algorithm of the football training

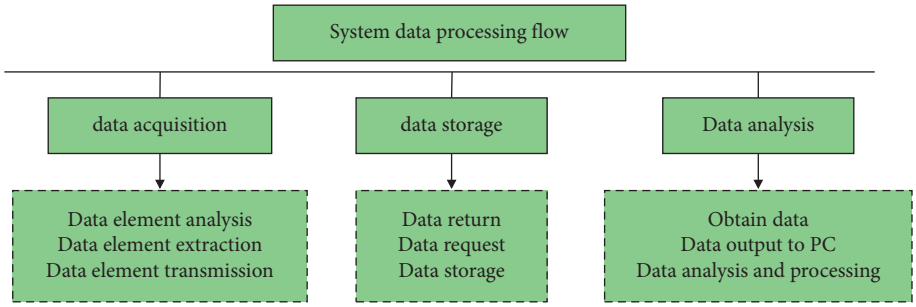

Figure 1: Structure flowchart of computer intelligent monitoring system.

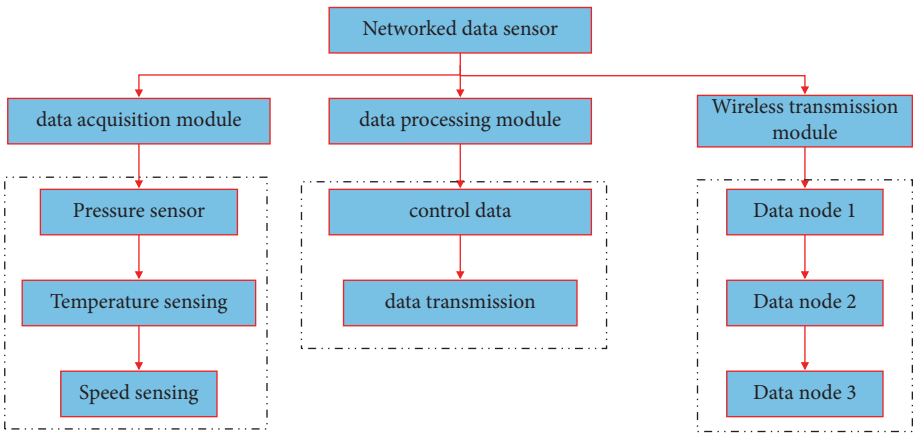

Figure 2: Specific design flowchart of system processing data under networked sensor.

dynamic monitoring system, the optimization method is adopted for the algorithm in the dynamics module. Considering that the environmental factors of football players in the training process may affect the monitored data information, it is necessary to improve the accuracy and overall scale of data processing in the computer intelligent dynamic monitoring system. To meet the functional requirements of the intelligent dynamic monitoring system, we need to constantly find suitable algorithms so as to improve the overall work efficiency of the system. The above contents have given the dynamic construction equation. When applied in the system, the construction equation is changed to the following formula:

$$\rho i \frac{\partial^2 u_i^t}{\partial T^2} = \int_H f\left(\xi^{t+1}\right) dV_j + b_i. \tag{2}$$

It can be seen from the above formula that the internal time of the formula has specific significance. With the displacement generated inside the data node, the force contained in it will also change. After the introduction of time, the continuous analysis of data by the intelligent dynamic monitoring system can be truly realized. Different intelligent recognition algorithms will also affect the collected data. In order to avoid data deviation and result error, this paper identifies the motion state of football players. The specific identification algorithm is as follows:

$$SVM_1 = \sqrt{a_{x,t}^2 + a_{y,t}^2 + a_{z,t}^2}, \tag{3}$$

in which, because this paper studies the monitoring and recognition of the motion state generated by the human body, the collection of data information of football players' legs and feet is particularly important in this study. Because the data monitoring of football training itself has periodicity, the use of the above function can reduce the data coverage between the same data. In order to more accurately collect the data of legs and feet, the following formula is used:

$$\mathrm{CSVM}_t = \mathrm{Max}\left(\mathrm{SVM}_t\right)\text{-}\mathrm{Min}\left(\mathrm{SVM}_{t-k}\right). \tag{4}$$

By bringing the parameters into the above formula, more accurate data information of football players' sports state can be obtained. From the above formula, it can be seen that in the process of monitoring data, the change of acceleration during movement is the core of data acquisition. By calculating the change value of acceleration, the training state of football players can be judged. If the overall data are in a balanced trend, it is normal training; on the contrary, athletes are breaking through their own limits. In order to avoid the influence of environmental factors during monitoring, the following formula is added:

$$CSVM_{t+k} \leq 0.2g. \tag{5}$$

By solving the above equation, the influence of noise on the collected data can be reduced. Considering that human beings cannot always be in a static state, the static state can only be formulated by setting parameters. In this paper, through repeated numerical analysis, 0.2 is finally selected as the experimental parameter. After reducing the influence of environmental factors, the error of the computer intelligent automatic detection system in data processing can be reduced. The error comparison of the computer intelligent monitoring system is shown in Figure 3.

As can be seen from Figure 3, the computer intelligent monitoring system studied in this paper has greatly reduced the probability of error due to the adoption of new algorithms for human motion state recognition. However, the common dynamic monitoring system has a very high probability of error, and it is not within the standard error. From the comparison of error probability between the ordinary dynamic monitoring system in the figure above and the computer intelligent monitoring system studied in this paper, it can be seen that the computer intelligent monitoring system studied in this paper has good performance and can better ensure the accuracy of data analysis results.

In the detection process of football training, a new human recognition algorithm is added to the intelligent dynamic monitoring system. As the name suggests, the recognition algorithm is to calculate the actions of the human body. Among them, the time series needs to be modeled and calculated within the system, and the relevant formulas are as follows:

$$X(t) = \rho_1 X(t-1) + \rho_2 X(t-2) + \ldots + \rho_p X(t-p) + \zeta(t-1),$$
$$X(t) = \rho(t-1,t)X(t-1) + \zeta(t-1),$$
$$J = \sum_{k=1}^{N} \zeta^2(t-1) = \sum_{k=1}^{N} [X(t) - \rho(t-1,t)X(t-1)]^2. \tag{6}$$

The above formula constructs the state space model of football players. Based on the total data collected by the system, the deviation derivative of J to ρ is calculated. The relevant formula is as follows:

$$\frac{\rho J}{\partial \rho}\Big|_{\rho=\widehat{\rho}} = 0,$$
$$-2\sum_{k=1}^{N} X(t) - \widetilde{\rho} X(t-1)X(t) = 0, \tag{7}$$
$$\sum_{k=1}^{N} \widehat{\rho}[X(t-1)]^2 = \sum_{k=1}^{N} X(t)X(t-1).$$

After calculating the deviation derivative of the data, the least square algorithm needs to be added to estimate the data. The formula is as follows:

$$\widetilde{\rho}(t-1,t) = \left(M^T M\right)^{-1} M^T Z. \tag{8}$$

In the process of football training, players have been in motion. When training a specific action, the action will be repeatedly trained. This repetitive training can also regard the human body as a stable state. The accuracy of the monitoring system can be greatly improved by estimating the error. Since the monitoring data type is nonlinear, it is also necessary to establish a discrete state equation and calculate its state. The specific formula is as follows:

$$\begin{cases} X(t) = \rho(t-1,t)X(t-1)\zeta(t-1), \\ Y(t) = H(t)X(t)V(t). \end{cases} \tag{9}$$

In the above three formulas, firstly, the state equation is established to calculate the state of the data; then, the type of state is replaced by the function according to the calculated state quantity, and finally, the data are classified by the Kalman filter recurrence formula. After optimizing the intelligent algorithm in the dynamic monitoring system, the system can accurately judge the action characteristics and state of players in the process of football training and monitor and calculate the action data.

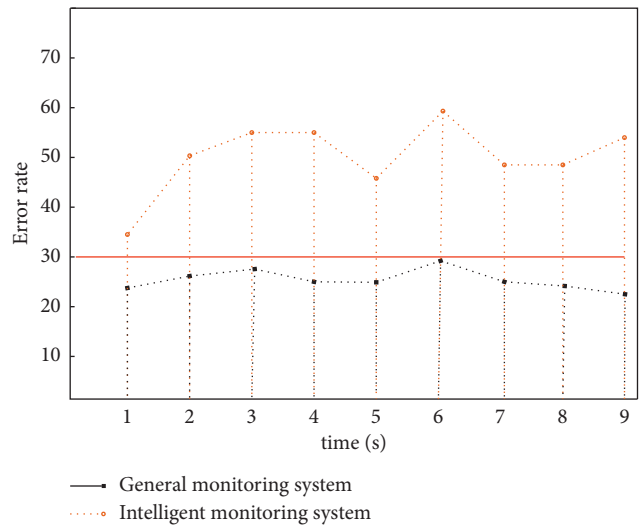

Figure 3: Error comparison diagram of computer intelligent monitoring system.

4. Result Analysis and Discussion

4.1. Result Analysis of Dynamic Monitoring System for Football Training under Computer Intelligent Algorithm. In order to further verify the dynamic monitoring system of football training under the computer intelligent algorithm, this paper analyzes the data by using different monitoring systems. We first select 200 groups of football training process data as sample data and then input the sample data into three monitoring systems, respectively. The purpose of this experiment is to judge whether the performance of the intelligent dynamic monitoring system studied in this paper is practical through the high and low data processing capacity of each system. In the process of this experiment, through the repeated analysis of 200 groups of sample data within the system and the cooperative operation between various modules within the system, the result data are finally transmitted to the computer PC. Through the above

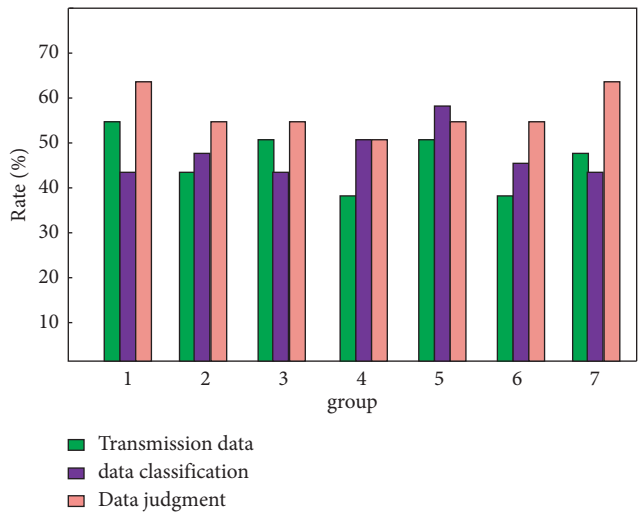

Figure 4: Performance test comparison diagram of three types of monitoring systems.

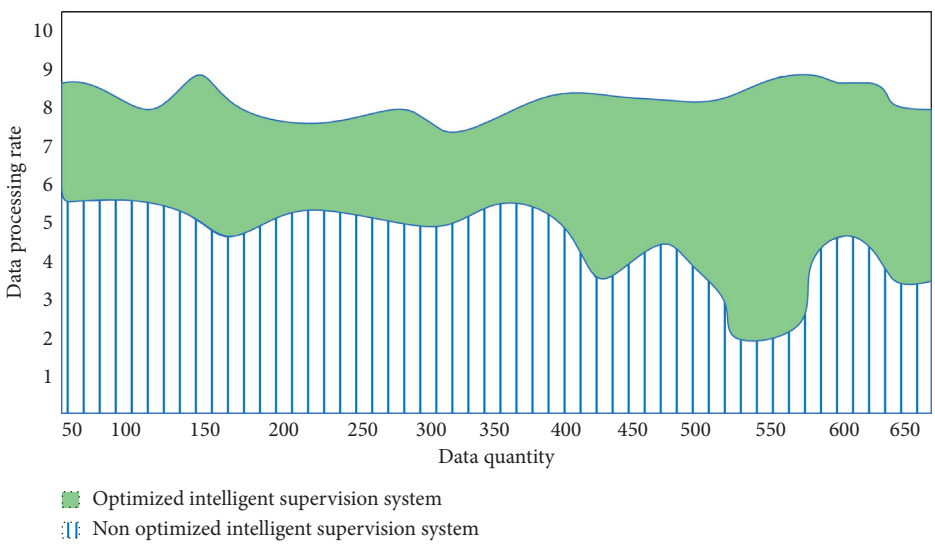

Figure 5: Data processing rate diagram of optimized detection system.

dynamic monitoring and processing of football training data under the computer intelligent algorithm, the best system can be clearly distinguished. The performance test comparison results of three types of monitoring systems are shown in Figure 4.

As can be seen from Figure 4, the computer intelligent dynamic monitoring system studied in this paper has the highest efficiency of 65% in processing football training sample data. Compared with a traditional monitoring system and an ordinary dynamic monitoring system, the computer intelligent dynamic monitoring system studied in this paper has better data processing ability and does not consume too much human resources in the whole process of the experiment. Therefore, the computer intelligent dynamic monitoring system has considerable social practicability in terms of data processing ability. This further proves that the computer intelligent dynamic monitoring system studied in this paper can be applied to football training and has good application performance.

4.2. Analysis of Intelligent Algorithm Optimization Results of Football Training Dynamic Monitoring System. After optimizing the intelligent algorithm, the football training dynamic monitoring system does reduce the phenomenon of data error. However, it is far from enough to judge the performance of the optimized intelligent dynamic monitoring system only from the error level. In order to further verify whether the new monitoring system studied in this paper can maintain or exceed the performance of the original system, thirteen groups of different sample data are selected in this experiment, which contains a variety of different types of data information. Compared with a single type of data information, using different types of data information as sample data can better reflect the excellent data processing ability of a system. During this experiment, the main purpose is to observe whether the system can maintain the stability and high-speed processing capacity of the system in the face of massive data. Finally, the system

processes the overall trend of sample data transmission to the computer PC, as shown in Figure 5.

As can be seen from Figure 5, the results of the non-optimized system are very obvious compared with the optimized system. It can be seen from the picture that the whole system has a significant downward trend in the process of data processing. The main reason for this trend is the function disorder between modules in the system, which leads to the serious decline of data processing rate, which also proves that there is an unstable problem in the non-optimized system. On the contrary, the optimized intelligent dynamic monitoring system not only has high-speed data processing capacity but also the trend of data processing of the whole system in the figure is very stable. This also proves that the optimized intelligent dynamic monitoring system can still run smoothly in the face of massive data. It can also be seen that the dynamic monitoring system optimized by the computer intelligent algorithm has a wide development space in football training.

5. Conclusion

This paper mainly makes systematic experimental research on computer intelligent dynamic monitoring technology. Firstly, the history and development of computer intelligent dynamic monitoring technology are introduced. Secondly, the computer intelligent dynamic monitoring system is designed, and its structure construction and algorithm upgrading are described in detail. We understand that the first simulation test has its own meaning and function, and ensure that each module can run normally. In the upgrade of the system algorithm, it is mainly enhanced in the part of human condition monitoring. Compared with a traditional monitoring system and an ordinary dynamic monitoring system, the computer intelligent dynamic monitoring system studied in this paper ensures the correctness of monitoring data, reduces the workload of the system, and ensures the stability of the whole system. In order to improve the correctness of monitoring data, the feature extraction algorithm and the state recognition algorithm are added. Finally, the performance and stability of the intelligent dynamic monitoring system designed in this paper are verified by specific experiments. The experimental results also prove that the dynamic monitoring system optimized by the computer intelligent algorithm can be applied to football training. However, this paper still lacks a detailed description of intelligent dynamic monitoring system equipment. The research needs to change and monitor according to the changes of external factors such as environment, and the array synchronization operation needs to be further elaborated, which needs to be further supplemented in future research.

Data Availability

The data used to support the findings of this study are available from the corresponding author upon request.

Conflicts of Interest

The authors declare that they have no conflicts of interest.

Acknowledgments

This work is supported by the Research on Intelligent Teaching Mode of Football Based on Virtual Simulation (L20BED007), the Necessary Qualities of Referees in Modern Football Match (20111SLYJ1-023), and the Research and Practice of Football Training Intelligent Teaching under the Background of Informationization (DDJFZ202005).

References

[1] A. Viviana, D. Vale Luke, M. Pearce, O. Evgenia, and L. Liudmila, "Aspects of economic costs and evaluation of health surveillance systems after a radiation accident with a focus on an ultrasound thyroid screening programme for children," *Environment International*, vol. 156, p. 156, 2021.

[2] I H. Kwon, K. I. Young, and H. M. Beom, P. June-Woo, L. Sang-Won, and L. T. Geol, Real-time heart rate monitoring system for cardiotoxicity assessment of daphnia magna using high-speed digital holographic microscopy," *Science of the Total Environment*, vol. 780, p. 780, 2021.

[3] H. Bai, J. Zhao, C. Ma et al., "Impact of RNA degradation on influenza diagnosis in the surveillance system," *Diagnostic Microbiology and Infectious Disease*, vol. 100, no. 4, 2021.

[4] S. Shao, N. Kubota, K. Hotta, and S. Takuya, "Behavior estimation based on multiple vibration sensors for elderly monitoring systems," *jaciii*, vol. 25, no. 4, 2021.

[5] S. Fan and Q. Zhou, "Multi-agent system for tunnel-settlement monitoring: A case study in Shanghai," *Displays*, vol. 69, 2021 prepublish.

[6] D. Li, B. Qin, W. Liu, and L. Deng, "A city monitoring system based on real-time communication Interaction module and intelligent visual information collection system," *Neural Processing Letters*, vol. 53, 2021 (prepublish).

[7] F. Wang, R. Wang, C. Xie, J. Zhang, Li Rui, and L. Liu, "Convolutional neural network based automatic pest monitoring system using hand-held mobile image analysis towards non-site-specific wild environment," *Computers and Electronics in Agriculture*, vol. 187, p. 187, 2021.

[8] S. Shohei, N. Ishimura, M. Hironobu et al., "Evaluations of gastric acid pocket using novel vertical 8-channel ph monitoring system and Effects of Acid Secretion Inhibitors," *Journal of neurogastroenterology and motility*, vol. 27, no. 3, 2021.

[9] T. Zhang, Y. Zhao, W. Jia, and C. Mu Yen, "Collaborative algorithms that combine AI with IoT towards monitoring and control system," *Future Generation Computer Systems*, vol. 125, 2021 (prepublish).

[10] J. J. Lund, T. T. Chen, G. E. LaBazzo, S. E. Hawes, and S. J. Mooney, "The association between three key social determinants of health and life dissatisfaction: a 2017 behavioral risk factor surveillance system analysis," *Preventive Medicine*, vol. 153, Article ID 106724, 2021.

[11] R. Xu, C. Wang, X. Yao, X. Gao, Z. Zhu, and B. Chen, "A portable sitting posture monitoring system based on a pressure sensor array and machine learning," *Sensors and Actuators: A. Physical*, vol. 331, 2021.

[12] J. Loogen, A. Müller, A. Balzer et al., "An illuminated respiratory activity monitoring system identifies priming-active compounds in plant seedlings," *BMC Plant Biology*, vol. 21, no. 1, p. 324, 2021.

[13] M. Xiang and M. Xiang, "Design of intelligent agricultural greenhouse monitoring system based on 5G network cloud platform," *Journal of Physics: Conference Series*, vol. 1578, no. 1, 2020.

[14] S. Feng, K. Wen, Y. Si, X. Guo, and J. Zhang, "Theoretical studies on thermally activated delayed fluorescence mechanism of a series of organic light-emitting diodes emitters comprising 2, 7-diphenylamino-9, 9-dimethylacridine as electron donor," *Journal of Computational Chemistry*, vol. 39, no. 31, pp. 2601–2606, 2018.

[15] J. Xian, M. Zeng, R. Zhu et al., "Design and implementation of an intelligent monitoring system for household added salt consumption in China based on a real-world study: a randomized controlled trial," *Trials*, vol. 21, no. 1, p. 349, 2020.

Hindawi
Computational Intelligence and Neuroscience
Volume 2023, Article ID 9825316, 1 page
https://doi.org/10.1155/2023/9825316

Retraction

Retracted: Research on Piano Performance Optimization Based on Big Data and BP Neural Network Technology

Computational Intelligence and Neuroscience

Received 19 September 2023; Accepted 19 September 2023; Published 20 September 2023

This article has been retracted by Hindawi following an investigation undertaken by the publisher [1]. This investigation has uncovered evidence of one or more of the following indicators of systematic manipulation of the publication process:

(1) Discrepancies in scope
(2) Discrepancies in the description of the research reported
(3) Discrepancies between the availability of data and the research described
(4) Inappropriate citations
(5) Incoherent, meaningless and/or irrelevant content included in the article
(6) Peer-review manipulation

The presence of these indicators undermines our confidence in the integrity of the article's content and we cannot, therefore, vouch for its reliability. Please note that this notice is intended solely to alert readers that the content of this article is unreliable. We have not investigated whether authors were aware of or involved in the systematic manipulation of the publication process.

Wiley and Hindawi regrets that the usual quality checks did not identify these issues before publication and have since put additional measures in place to safeguard research integrity.

We wish to credit our own Research Integrity and Research Publishing teams and anonymous and named external researchers and research integrity experts for contributing to this investigation.

The corresponding author, as the representative of all authors, has been given the opportunity to register their agreement or disagreement to this retraction. We have kept a record of any response received.

References

[1] X. Liu, "Research on Piano Performance Optimization Based on Big Data and BP Neural Network Technology," *Computational Intelligence and Neuroscience*, vol. 2022, Article ID 1268303, 10 pages, 2022.

Hindawi
Computational Intelligence and Neuroscience
Volume 2022, Article ID 1268303, 10 pages
https://doi.org/10.1155/2022/1268303

Research Article

Research on Piano Performance Optimization Based on Big Data and BP Neural Network Technology

Xueying Liu

Cai Jikun Conservatory of Music, Minjiang University, Fuzhou, Fujian Province 350108, China

Correspondence should be addressed to Xueying Liu; 1728@mju.edu.cn

Received 7 December 2021; Accepted 19 January 2022; Published 22 February 2022

Academic Editor: Guobin Chen

At present, there are many chess styles in piano education, but there is a lack of comprehensive, scientific, and guiding teaching mode. It highlights many educational problems and cannot meet the development requirements of piano education at this stage. However, the piano scoring system can partially replace teachers' guidance to piano players. This paper extracts the signal characteristics of playing music, establishes the piano performance scoring model using Big Data and BP neural network technology, and selects famous works to test the effect of the scoring system. The results show that the model can test whether the piano works fairly. It can effectively evaluate the player's performance level and accurately score each piece of music. This not only provides a reference for the player to improve the music level but also provides a new idea for the research results and the application of new technology in music teaching. This paper puts forward reasonable solutions to the problems existing in piano education at the present stage, which is helpful to cultivate high-quality piano talents. Experiments show that the application of Big Data technology and BP neural network to optimize the piano performance scoring system is effective and can score piano music accurately. This paper studies the performance scoring system and gets the model after training, which can replace music teachers and alleviate the shortage of music teachers in the market.

1. Introduction

In recent decades, Chinese people's material life has seen abundant growth with the rapid economic development, and their aspiration for better spiritual life has been increasing and has become urgent. Therefore, more people choose to learn musical instruments, especially, piano. Nowadays, most piano learners are teenagers. One in every five families will send their children to learn piano performance, thus increasing the number of piano grading examinees year by year. However, the number of professional piano teachers is limited, so teachers become scarce resources, and due to the long-time neglect of art education in China, the imbalance of supply and demand has become more serious.

Big Data technology refers to the application of Big Data to the technological problems' solution. Big Data refers to data sets that are too large in scale to access, store, manage, and analyze with the traditional database software tools, featured by massive data size, rapid data flow, various data types, and low-value density [1, 2]. BPNN (back propagation neural network) is proposed by Rumelhart and McClelland et al., in 1986, which is a multilayer feed-forward NN (neural network) trained by error BP (back propagation) algorithm, and it has become the most widely used NN at present [3, 4].

BPNN is considered to be the most commonly used prediction method. The general structure of BPNN model is shown in the figure below. It is composed of input layer, hidden layer, and output layer, in which the hidden layer transmits important information between input layer and output layer. BPNN is the most basic neural network. Its output results adopt forward propagation, and the error adopts back propagation. BPNN has the function of supervised learning. Under the background of Big Data, the piano performance scoring system is built using the BPNN technology. First, in the introduction, the situation of the piano education market in China is introduced. Second, in the related works, the previous research is reviewed. Furthermore, in the method part, a scoring model based on Big

Data and BPNN technology is constructed. Then, the test results of the proposed scoring model are discussed in the result section. Finally, the conclusion is summarized. The innovation here is to optimize the traditional NN model through the combination of Big Data technology and the BPNN model and to use the most appropriate algorithm to establish a performance evaluation model so that the performance evaluation of each piece of music is more accurate and sufficient. The research results provide a new perspective for computer technology to promote people's work and life.

This paper extracts the signal characteristics of playing music, establishes the piano performance scoring model using Big Data and BPNN technology, and selects famous works to test the effect of the scoring system. This paper is divided into five parts. The first part expounds the research background. At this stage, the development of piano education cannot meet the development requirements. However, the piano scoring system can partially replace teachers' guidance to piano players. In the second part, some references are cited to illustrate the extraction of signal characteristics of playing music and the establishment of piano performance scoring model using Big Data and BPNN technology. The third part establishes the piano performance scoring system and studies the functions of Big Data technology, BPNN technology, piano music feature extraction, performance scoring, and so on. In the fourth part, the performance of the scoring system is tested, and the notes, music bar score, and the whole music bar score are detected. Finally, the full text is summarized.

2. Related Works

In the context of Big Data, DL (deep learning) technology is widely used in all walks of life. At present, many experts and scholars have researched the application of DL technology. For example, Han et al. proposed an education development and evaluation model of intelligent learning environment, which integrated intelligent learning environment into learning ecology and education environment [5]. Liu et al. put forward an advanced regional cognitive ability training mode and applied DL in regional cognitive teaching through five teaching strategies: typical geographical real situation type, geographical depth problem type, interdisciplinary project type, emotion knowledge integration experience type, and field practice type of high-order thinking [6]. Maria et al. personalized online learning using Moodle in learning management systems, which improved students' academic performance and helped find students with difficulties [7]. Carin suggested a method using DL to integrate medical practice automation with medical education [8]. Ruhalahti et al. constructed the teacher's training assistance method using DL and inspired the thinking on the new development stage of designing and creating collaborative, self-management, and dialogue knowledge process [9]. Elbir et al. established a music scoring and recommendation model based on NN technology, which described music and score music with vectors [10]. Liu et al. proposed a combined algorithm for dam deformation prediction based on two traditional models and an optimized model, which combined two subalgorithms: GM (Grey Model) (1, 1) and BPNN [11]. Dekel et al. built the statistical basis and performance analysis of a new scoring system based on Naive Bayes classifier and 11-item validation questionnaires to test pain level [12]. Huang et al. suggested three different performance evaluation models: (a) a CNN (convolutional neural network) model using a simple time-series input, including aligned pitch contour and score. (b) A joint embedding model that could learn joint potential space of pitch contour and score. (c) A CNN model based on distance matrix, and the model of distance matrix between pitch contour and the score could predict the evaluation level [13]. He proposed a vocal music teaching system to automatically determine the level of piano players. The algorithm flow of the system was designed in detail with the principle of NN technology. The performance features of vocal music were extracted using Fourier transform and its improved function, and the key modules of the system were designed according to the system framework and data processing flow [14]. Chen et al. studied the application of DL in environmental monitoring and built a DL model for air pollution prediction using BPNN [15]. To sum up, Big Data, NN technology, and DL technology are used in all walks of life, especially, in education, which can alleviate teachers' burden by partly replacing their works.

The aforementioned research of Big Data technology and BPNN technology in different fields has proven that the related algorithms have been much matured and can be used in piano performance scoring systems. Meanwhile, different types of CNN result in different data accuracy. Here, the BPNN model is optimized, combined with Big Data technology, to make the scoring system model more effective.

3. Construction of Piano Performance Scoring System

3.1. Big Data Technology. Big Data refers to the data set that cannot be captured, managed, and processed by conventional software tools within a period. It is a massive, highly growing, and diversified information asset that needs a new processing mode to have stronger decision-making power, insight, and process optimization ability.

The biggest feature of Big Data is the huge amount of data. Traditional data processing software, such as Excel and MySQL, cannot analyze data well. Thus, the technology used in Big Data for data storage, processing, and calculation is completely different, such as Hadoop and Spark. Within the enterprise, the process of data production, storage, analysis, and application are interrelated, thus forming an overall Big Data architecture [16]. The basic architecture of Big Data is shown in Figure 1.

Generally, for Big Data technology, before the final view of data report or the use of data for algorithm prediction, data will go through the following processing steps [17].

(a) Data collection: it means to synchronize the data and logs generated by the application programs to the Big Data system.

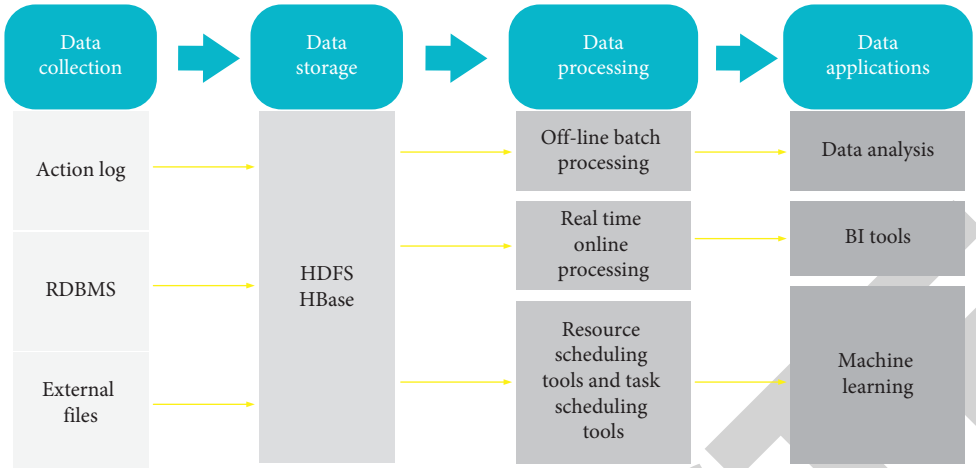

Figure 1: The basic architecture of Big Data.

(b) Data storage: massive data, which need to be stored in the system to facilitate the next use of the query.

(c) Data processing: the original data should be filtered, spliced, and converted at different levels before they can be finally applied. Data processing is a general term of these processes. Generally, there are two types of data processing: off-line batch processing and real-time online analysis.

(d) Data application: the processed data can provide external services, such as visual reports, interactive analysis, and training models for recommendation systems.

Here, the training set and test set are constructed for the model through Big Data technology.

3.2. BPNN Technology

3.2.1. Deep Learning. The year 2006 has seen the appearance of a new research direction, DL, in the research field of ML (machine learning), which has been studied by academia and gradually applied by industry [18]. In 2012, Stanford University first builds a training model called DNN (deep neural networks) with a 16,000 CPU core parallel computing platform, which has made a great breakthrough in the application field of speech and image recognition [19]. In 2016, alpha dog, an artificial go software developed based on DL, defeats Li Shishi, the world's top go, master. After that, many well-known high-tech companies in the world begin to invest in DL technology, establish research institutes, and usher technical and R&D personnel into the field of DL.

ML technology studies how the computer simulates or realizes the learning behavior of animals, then learns new knowledge or skills, rewrites the existing data structure, and improves the program performance. Statistically, it is to predict the distribution of data, learn a model from the data, and then predict new data using this model. This requires that the test data and training data must be the same distribution. Its basic feature is trying to imitate the mode of information transmission and processing between neurons in the brain. The most significant applications are in the field of computer vision and NLP (natural language processing). Noticeably, DL is strongly related to NN in ML, and NN is also its main algorithm and means. In other words, DL is an improved NN algorithm. DL is divided into CNNs (convolutional neural networks) and DBNs (deep belief networks) [20]. Its main idea is to simulate human neurons. Each neuron receives information and transmits it to all adjacent neurons after processing.

3.2.2. Artificial Neuron. An artificial neuron is a mathematical model created by imitating the basic operation function of a biological neuron, which has specific functions of a biological neuron [21]. The artificial neuron receives the given signal from the front neuron, and each given signal will be attached with a weight. Under the joint action of all the weight states, the neuron will show a corresponding activation state [22], which can be represented by equation (1).

$$f(x) = \sum_{i=1}^{n} x_i w_i. \tag{1}$$

In equation (1), $f(x)$ represents the final output state, x_i denotes the input signal, and w_i stands for the corresponding weight of the input signal, totaling n groups.

When the neuron receives a specific input signal, a specific signal will be output, and each neuron has a corresponding threshold. If the sum of the inputs received by the neuron is greater than the threshold, its state changes into the active state, and when it is less than the threshold, it is in the inhibitory state. The transfer functions of the artificial neuron are as follows:

(a) The expression of the linear function is shown in equation (2).

$$f(x) = kx. \tag{2}$$

(b) The slope function is expressed as in equations (3) to (5).

$$f(x) = \alpha(x \geq \theta), \tag{3}$$

$$f(x) = kx(-\theta < x < \theta), \tag{4}$$

$$f(x) = -\alpha(x \leq \theta). \tag{5}$$

The expression of transition function is shown in equations (6) and (7).

$$f(x) = \alpha(x \geq \theta), \tag{6}$$

$$f(x) = \beta(x \leq \theta). \tag{7}$$

The Sigmoid function is expressed as in equation (8).

$$f(x) = a + \frac{b}{1 + e^{-\mathrm{d}x}}. \tag{8}$$

The transfer function should be selected according to the specific application range. The linear function will amplify the output signal. The nonlinear ramp function can prevent the impact of network performance degradation. The S-type function is used in the hidden layer.

3.2.3. BP Neuron. Similar to artificial neuron, BP neuron also contains weight and summation. Specifically, x_i represents the input value of the ith neuron, w_{ji} stands for the weight value of the connection between the ith neuron and the jth neuron, b_j indicates the threshold, y_j denotes the output of the neuron j, and $f(x)$ is the transfer function [23].

The net output S_j of the neuron j is shown in equation (9).

$$S_j = \sum_{i=1}^{n} w_{ji} \cdot x_i + b_j. \tag{9}$$

When the threshold value is 0, the net output S_j of neuron j is shown in equation (10).

$$S_j = \sum_{i=1}^{n} w_{ji} \cdot x_i. \tag{10}$$

3.2.4. BPNN. BPNN is a multilayer feed-forward NN, featured by signal forward transmission and error BP. In forward transmission, the input signal is processed layer by layer from the input layer through the hidden layer to the output layer. The state of neurons in each layer only affects the state of neurons in the next layer. If the output layer cannot get the expected output, it will turn to BP and adjust the network weight and threshold according to the prediction error, so that the BPNN prediction output will continue to approach the expected output. BPNN must be trained before prediction to have associative memory and prediction ability. The training steps are as follows: (a) network initialization, (b) hidden-layer output calculation, (c) output-layer output calculation, (d) input-layer output calculation, (e) error calculation, (f) weight update, and (g) algorithm iteration is checked, and if the iteration is completed, the iteration continues, if not, steps (b) to (g) are repeated.

The BPNN algorithm is divided into two stages: the forward-propagation process and the BP process. In the process of forwarding propagation, the signal first comes from the input layer, passes through the hidden layer, arrives at the output layer, and then comes out from the output layer. Each layer of neurons can only affect the next state. When the output layer cannot receive the desired output correctly, it will use the BP process. Through the alternating operation of the two processes, the minimum value of the network error function will be found, and the operation of the NN memory will be completed [24].

The expression of the propagation process is shown in equations (11) and (12), in which equations (11) and (12) represent the outputs of the hidden layer and the output layer node, respectively.

$$z_k = f_1\left(\sum_{i=0}^{n} v_{ki} x_i\right), \quad (k = 1, 2, \ldots, q), \tag{11}$$

$$y_j = f_2\left(\sum_{i=0}^{n} w_{jk} z_k\right), \quad (j = 1, 2, \ldots, m). \tag{12}$$

In equations (11) and (12), n is the number of nodes in the output layer, q represents the number of hidden nodes, and m stands for the number of output layer nodes. v_{ki} indicates the weight of the connection between the input layer and hidden layer, w_{jk} represents the weight of the connection between output layer and hidden layer, $f_1(x)$ represents the transmission function of the hidden layer, and $f_2(x)$ stands for the transmission function of the output layer.

3.3. The Feature Extraction of Piano Music. The audio feature can show the MFCC feature of the jth music with the application M_j, and the application C_j shows the Chroma feature of this work. Then, the notes can be quantified through the embedded technology, and then they are pretrained with FastText, so the word vector v is generated. Then, the vector of a single note in the song is multiplied by its own TF-IDF (term frequency-inverse document frequency) value, and the sum is averaged. Consequently, the lyrics feature vector is extracted for a music work [25].

TF-IDF value can indicate the importance of a phrase to its document. The importance of this phrase is directly proportional to its TF (term frequency) but inversely proportional to its IDF (inverse document frequency). The number of phrases is normalized using equation (13).

$$tf_{ij} = \frac{n_{ij}}{\sum_k nk_j}. \tag{13}$$

In equation (13), t_i represents the phrase, d_j stands for the file, tf_{ij} denotes the above-IDF, n_{ij} indicates the number of times phrase t_i used in the data file d_j, and $\sum_k nk_j$ represents the total number of phrases used in the file d_j.

The IDF represents the importance of a note idf_i and is calculated through equation (14).

$$idf_i = \log \frac{|D|}{|D: i| + 1}, \tag{14}$$

$|D|$ represents the total number of data files in the database, and $|D: i|$ denotes the number of files with this note.

Equation (15) shows the value $tf_i df_{ij}$ of the phrase t_j in the file d_j, and the important notes to the file can be obtained through filtering.

$$tf_i df_{ij} = tf_{ij} \times idf_{ij}. \tag{15}$$

The eigenvector of the note is expressed as in equation (16).

$$L_j = \frac{\sum_i tf_i df_{ij} \times v_i}{|d_j|}. \tag{16}$$

In equation (16), $|d_j|$ represents the number of notes in the phrase.

Figure 2 illustrates that the item side automatic encoder is used as the scoring model. MFCC feature M_j, chroma feature C_j, and lyrics feature L_j are applied to the input of the convolutional coding layer. The first layer is the convolution layer, the input is the two-dimensional feature M and C. Here, X denotes the input, and the input is equivalent to the feature map with two channels. $*$ represents the two-dimensional convolution operation that acts on the activation function and compresses the convolution input through a 2×2 pooling layer using an input of $K1$ convolution kernels and the weight of the first layer and outputs A^2, with $K1$ channels. A^2 is input into the second convolution layer, and $K2$ convolution kernels act on the activation function and outputs A^3, with $K2$ channels. A^2 and A^3 are specifically expressed as in equations (17) and (18).

$$A^2 = \text{pooling}\left(\sigma\left(\sum_i^2 X_i * W_i^1 + b^1\right)\right), \tag{17}$$

$$A^3 = \text{pooling}\left(\sigma\left(\sum_i^{K1} A_i^2 * W_i^2 + b^2\right)\right). \tag{18}$$

The next part is the fully connected part of the automatic encoder, which is composed of a coding fully connected layer and a decoding fully connected layer. At the coding end, an additional connection layer is added, which makes the lyrics vector and the item side score vector in the scope network. The final coding vector U is represented as in equation (19).

$$U = \sigma\left(W^3 A^3 + V^3 L + b^3\right). \tag{19}$$

The later decoding end of the automatic encoder is opposite to this process, and the fully connected decoding end is expressed as in equations (20) and (21).

$$\overline{A}^3 = \sigma\left(\overline{W}^3 U + \overline{b}^3 1\right), \tag{20}$$

$$\overline{L} = \sigma\left(\overline{V}^1 U + \overline{b}^3 2\right). \tag{21}$$

In equations (20) and (21), $\overline{A}_3$ and $\overline{L}$ corresponds to A^3 and L in the encoder, respectively.

Then, the reverse of the convolutional coding layer is constructed, as shown in Figure 3, which is opposite to the convolutional coding layer and is represented by equations (22) and (23). The first is the upsampling layer, opposite to the pooling layer, which uses the nearest neighbor interpolation to double the dimension of $\overline{A}^3$. The second is the convolution layer with $K1$ convolution kernels, $*$ represents the two-dimensional convolution operation, and the output is $\overline{A}^2$. The third is the second upsampling layer, which doubles the input $\overline{A}^2$, uses two convolution kernels, and the outputs $\overline{X}$. Finally, the convolution layer with two convolution kernels, which convolutes the output $\overline{A}^1$ to the output $\overline{X}$. $\overline{X}$ represents two feature maps with the same dimension of two channels, corresponding to the reconstructed MFCC feature and Chroma feature, respectively.

$$\overline{A}^2 = \sigma\left(\sum_i^{K1} \text{upsampling}\left(\overline{A}^3\right) * \overline{W}_i^{\,2} + \overline{b}^2\right), \tag{22}$$

$$\overline{X}^2 = \sigma\left(\sum_i^2 \text{upsampling}\left(\overline{A}^2\right) * \overline{W}_i^{\,1} + \overline{b}^1\right). \tag{23}$$

The stacked autoencoders are used for training, and the training process is as follows. After each pretraining, an additional layer is trained, and equation (24) is used as the overall loss function of the encoder.

$$L = (1-\alpha)(\overline{X} - X)^2 + \alpha(\overline{L} - L)^2 + \lambda\left(\|W\|^2 + \|M\|^2 + \|N\|^2\right). \tag{24}$$

In equation (24), $(\overline{X} - X)^2$ represents the loss function of audio data, $(\overline{X} - X)^2$ denotes the loss function of music feature data, and $\|W\|^2 + \|M\|^2 + \|N\|^2$ stands for the regularization term. The parameter α indicates the weight represented by the item side score vector.

The degree of similarity influencing the results can be adjusted through $f(w)$. Here, the exponential function $f(w)$ is used for the experiment and is calculated as in equation (25).

$$f(w) = w^q. \tag{25}$$

When the value q is higher in $f(w)$, this model will focus on the impact most similar to the original musical works. When $q = 0$, this model will become a simple combination of scores.

3.4. Performance Scoring Function. The final scoring function is expressed as in equation (26).

$$h_{ui}^U = \sum_{v \in U} f(w_{uv}) r_{vi} = \sum_{v \in U(i)} f(w_{uv}). \tag{26}$$

In equation (26), $h_{u_i}^U$ represents the score of the system for work i at the uth time, w_{uv} denotes the similarity between the original work and the music uv performed by the performer, r_{vi} stands for the score of

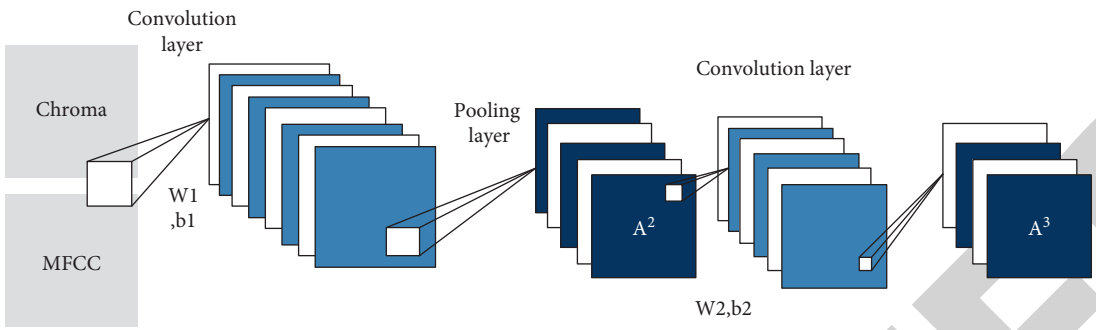

Figure 2: Convolutional coding layer.

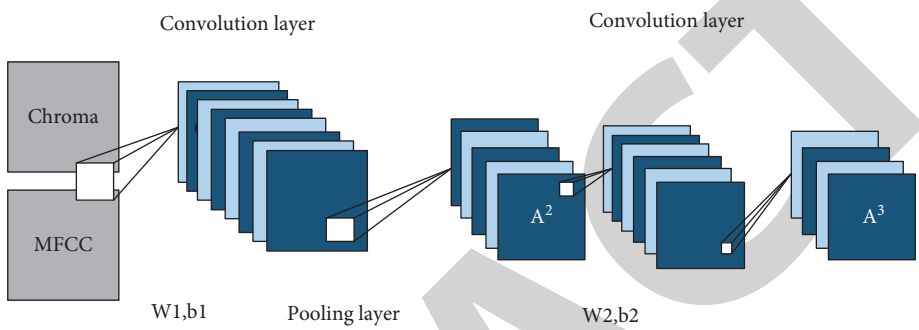

Figure 3: Convolutional decoding layer.

the system for the ith work at the vth time, and $U(i)$ is the overall data set. Hence, the user's score of the work is directly proportional to the similarity of the same track that the user has heard.

Combined with the calculation performance and its data, the item-based scoring function is improved, and equation (27) is obtained

$$h_{ui}^{S} = \sum_{j \in L} f(w_{ij}) r_{uj} = \sum_{j \in L(u)} f(w_{ij}). \tag{27}$$

In equation (27), $h_{u_i}^{U}$ represents the system scoring of the work i for the uth time, and w_{ij} denotes the degree of similarity between works ij. In this scoring system, the similarity between music work i and the other work j recognized by the systems is proportional. $f(w)$ is a monotone increasing function, which can strengthen or weaken the influence of similarity on the recommendation. The implied feature of a musical work is represented as $V = (V_1, \ldots, V_t)$, and V_j represents the implied feature vectors of the jth work, which express the characteristics of the work from different angles. After the results of V are obtained, w_{ij} is calculated as in equation (28).

$$w_{ij} = \frac{V_i \cdot V_j}{|V_i||V_j|}. \tag{28}$$

The international standard for evaluating the correctness of multipitch detection is the F-measure index of note level. The larger the value is, the more effective the detection is. The calculation method is shown as in equations (29)–(31).

$$\text{Recall} = \frac{n\text{Core}}{n\text{Re}f}, \tag{29}$$

$$\text{Precision} = \frac{n\text{Core}}{n\text{Tot}}, \tag{30}$$

$$F - \text{measure} = \frac{2\text{Recall} \cdot \text{Precision}}{\text{Recall} + \text{Precision}}. \tag{31}$$

In equations (29)–(31), nCore stands for the number of detected notes, nRef denotes the total number of standard audio notes, nTot represents the total number of detected notes, Recall indicates the relative detection accuracy of the score, and Precision is the relative detection accuracy of received notes.

3.5. Parameter Setting of BPNN. Here, a single-input neuron is used for the final comprehensive evaluation of the performance effect. In addition, to evaluate piano performance, two evaluation indexes: rhythm and expressiveness are needed. These two indexes also need two output neurons. Therefore, the output layer of the basic network structure needs three neurons. The previous output parameters need 60 neurons corresponding to the input layer, while the output layer needs three neurons. For the hidden-layer neurons, generally, only one hidden feed-forward NN is needed to approximate application functions in all cases. The structure and weight coefficient of BPNN should be determined through the learning method, thereby forming a correct mapping. The learning process of NN is to solve a group of weight coefficients with which the error function

can reach the minimum under a specific network structure. Therefore, multiple groups of experiments are needed until a satisfactory model is obtained. Finally, 67 hidden layer nodes are determined.

The mean square error in the training process of the classical BPNN algorithm is expressed as in equation (32), the global error of the cumulative error BPNN algorithm is expressed as in equation (33), and the mean square error is expressed as in equation (34).

$$E_p = \frac{1}{2}\sum_{j=1}^{m}\left(t_j^P - y_j^P\right)^2, \tag{32}$$

$$E_p = \frac{1}{2}\sum_{p=1}^{P}\sum_{j=1}^{m}\left(t_j^P - y_j^P\right)^2, \tag{33}$$

$$\mathrm{MSB} = \frac{1}{mp}\sum_{p=1}^{P}\sum_{j=1}^{m}\overline{\left(y_{kj} - y_{kj}\right)^2}. \tag{34}$$

In equations (32) to (34), E_p represents the error, t_j^p denotes the actual output of the jth time, and y_j^P stands for the expected output of the jth time. m indicates the number of output nodes, P represents the number of training samples, y_{kj} denotes the actual output of BPNN, and $\overline{y_{kj}}$ stands for the expected output of BPNN.

4. Performance Test of the Scoring System

Sound can be regarded as waves in air, water, and other media. When we record sound, we record the pressure of the medium on the microphone, more precisely the wave amplitude. Digital recording goes further because it must discrete the recording process. The microphone is sampled at a very high frequency. The higher the frequency, the better the recording quality. This frequency is also called the sampling rate. The standard CD audio sampling rate is 44,100 Hz (Hertz). This means that we get 44,100 microphone amplitude measurements per second. In this case, the measurement is usually called sampling, and each sampling step returns us a so-called sample. The sample represents the amplitude measured by the microphone at a given time. The value of the sample must be stored in some way.

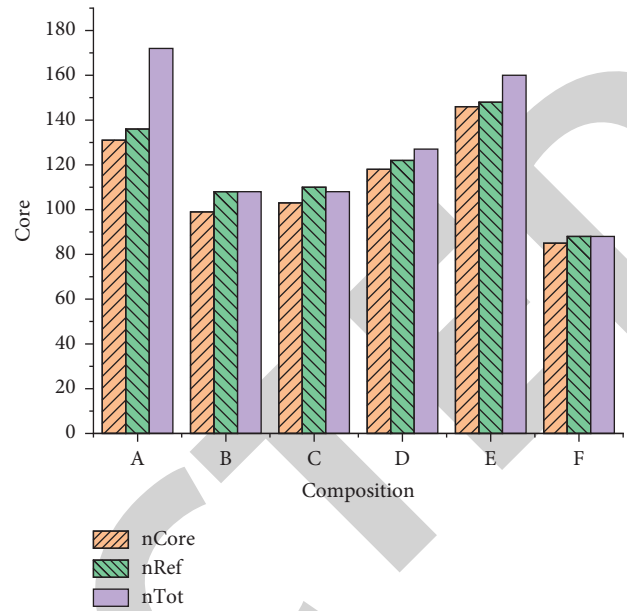

Figure 4: Test index results of note-level evaluation.

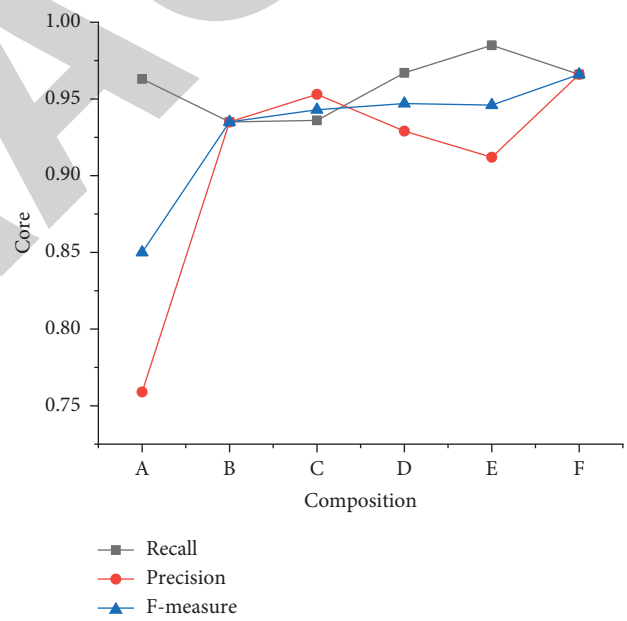

Figure 5: Final scores of note-level evaluation.

4.1. Detection of Musical Notes. Here, six pieces of music are tested by note-level test, bar score test, and whole score test. A, B, C, D, E, and F refer to each composition, respectively. A represents Blue Danube, B denotes Etude, C indicates Coming in February, D stands for Fugue, E is Nocturne, and F is Goddess Dance.

Figures 4 and 5 show the test index results and the final score of the note level evaluation of the six songs.

Figure 5 illustrates that the score index of composition F is the lowest, and the score index of composition A is the highest. Except for composition A, the final scores of other songs are all above 0.93, precision is above 0.91, and F-measure is above 0.93. This is because composition A is a world-class famous music, and its complexity is much larger than the other five pieces. Therefore, the note-level evaluation is good for the judgment of non-top music performance, which is much higher than 0.89 of the mainstream judgment methods.

4.2. Detection of Music Bar Score. This study tested the performance of six compositions by bar score. A, B, C, D, E, and F refer to each composition, respectively. The accuracy of bar performance in the test set is divided into four segments: less than 60%, 60% to 70%, 70% to 80%, and more than 80%. The actual, correct, and multidetection numbers

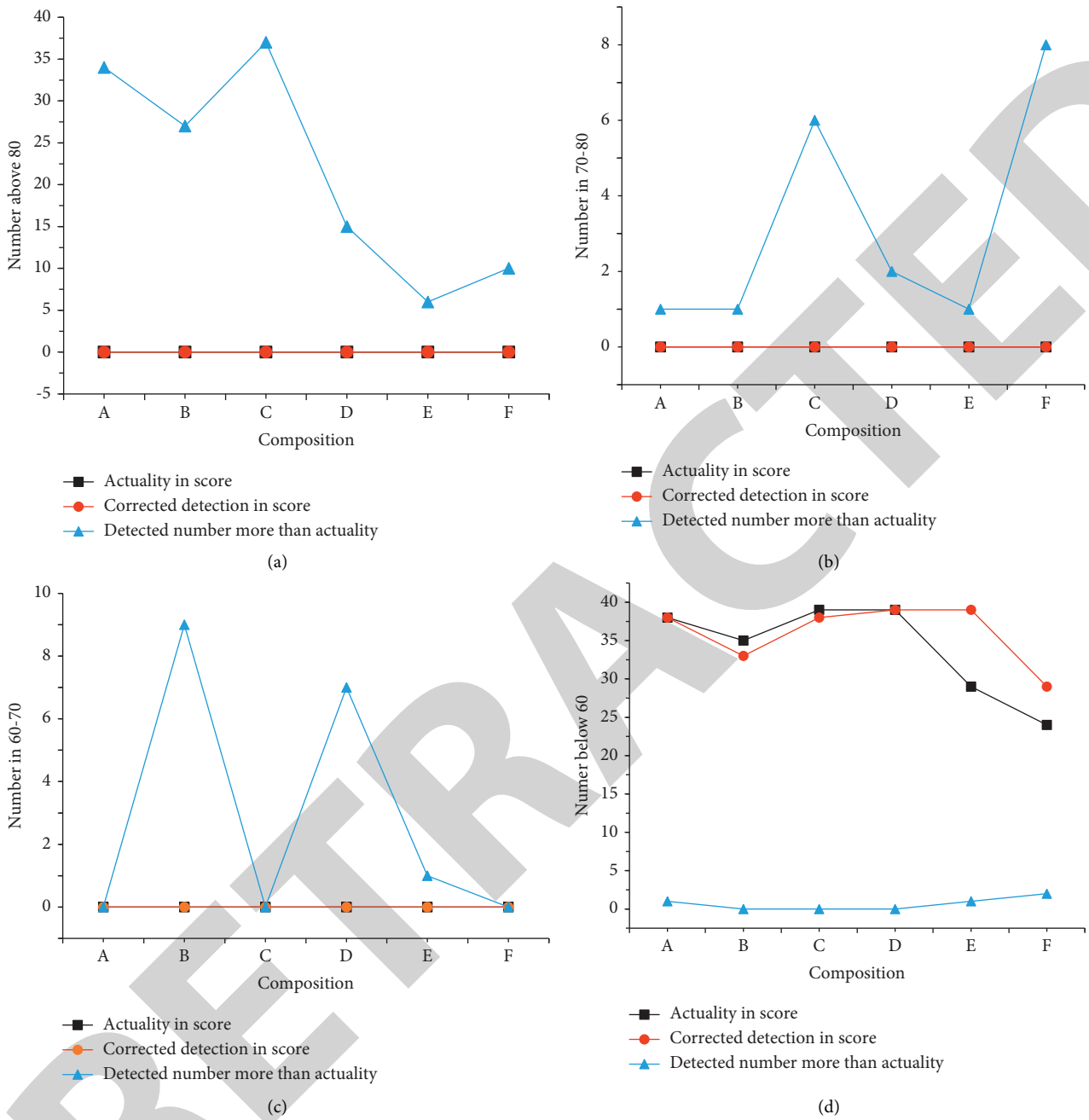

Figure 6: Bar score test result (a) above 80, (b) 70–80, (c) 60–70, (d) below 60.

are recorded. The detection rate is equal to the ratio of the number of correct detection and the actual number.

Figures 6 and 7 display the bar score test results and the final detection rate of the six compositions.

Figures 6 and 7 demonstrate that the detection rate of each composition is more than 93%, and the average detection rate of six compositions is 96.79%. After the scoring area is divided, most of the detection accuracy is between 82% and 93% because the accurately detected notes may not all be accurately converted into vector features, and inaccurate conversion leads to the decline of the subsequent detection rate.

4.3. Detection of the Score of the Whole Music. The performance of six pieces of music is tested by a whole score test. A, B, C, D, E, and F refer to each composition, respectively. Ten samples are selected for the comparison between the overall detection accuracy and the actual detection accuracy. The accuracy is equal to the ratio of the number of correct

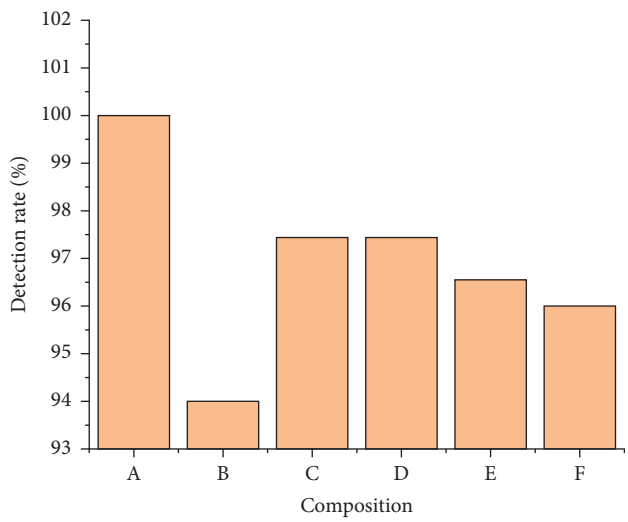

Figure 7: Final detection rate.

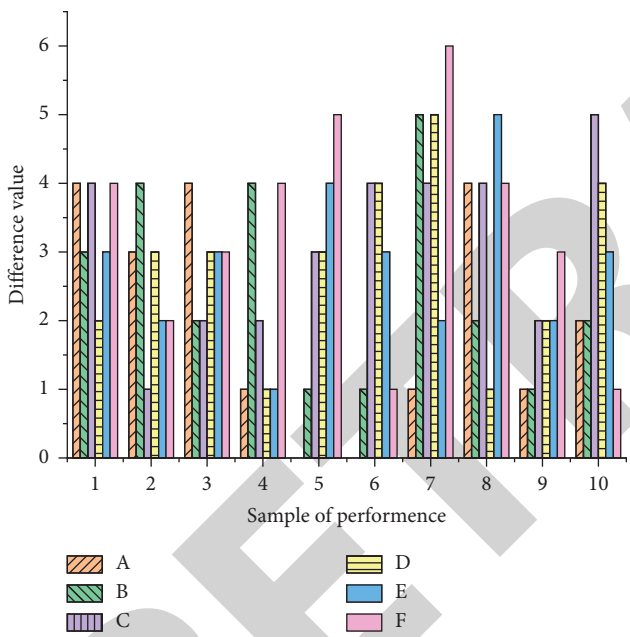

Figure 8: Score test results of music.

detection and the actual number. Figure 8 shows the score test results of the six compositions, and Figure 9 illustrates the total deviation and average deviation of the score test.

Figure 9 implies that the average deviation of the whole score test of each sample is less than 5. The average deviation of the whole score test of composition A is the smallest, only 2, and the total deviation is only 20. The average deviation of composition C is the largest, reaching 3.5, and the total deviation is 35, which is 1.75 times that of music A. The performance test result of composition C is 98%, and the accuracy is 100%. The score deviation of composition A is not big, so the actual performance accuracy is 100%, and the score deviation of other compositions is also within 5%. Overall, the performance detection accuracy is more than 93%, so it is within a reasonable error range.

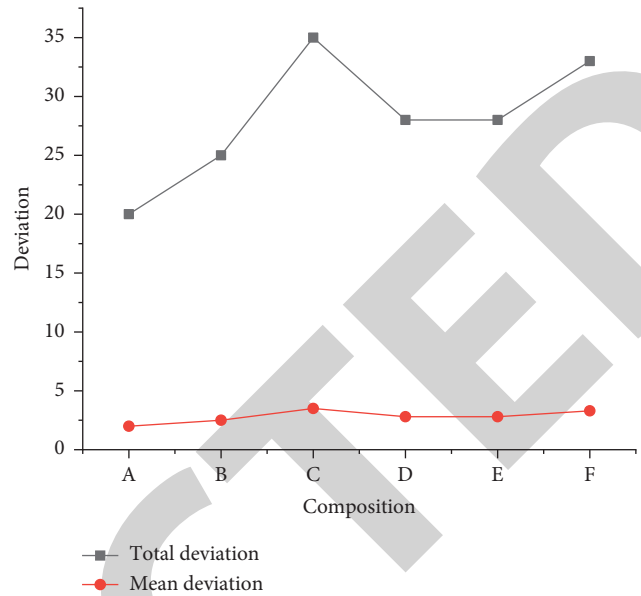

Figure 9: Total deviation and average deviation in score test of the whole composition.

5. Conclusion

Here, a piano performance scoring system model is studied based on Big Data and BPNN technologies to replace music teachers and alleviate the short supply for music teachers in the market. First, Big Data technology is introduced and used to search the data training set and test set for piano performance scores. Then, the performance score system is constructed by BPNN technology, and all notes are transformed into corresponding feature vectors. Consequently, the performance score system is trained and the model is obtained. Finally, the experiment shows that the application of Big Data technology and BPNN in the optimization of the piano performance scoring system is effective and can accurately score piano music.

However, there are still some deficiencies in this paper. Although this study has achieved the expected research objectives and reached some valuable research conclusions, the compatibility of the model is insufficient. Owing to the inability to seek the help of first-class musicians, the model may not be able to accurately identify piano music. This also points out the direction for our future research. In the future, we will focus on the following two aspects: further improving the compatibility of the model and optimizing the code. Contact first-class pianists to understand the actual situation of piano performance and optimize the model.

Data Availability

The data used to support the findings of this study are available from the corresponding author upon request.

Conflicts of Interest

The authors declare that they have no conflicts of interest.

Hindawi
Computational Intelligence and Neuroscience
Volume 2022, Article ID 3784756, 14 pages
https://doi.org/10.1155/2022/3784756

Research Article

Smart Home Control and Management Based on Big Data Analysis

Hao Chi[1] and Yuyan Chi[2]

[1]*College of Information Engineering Press, Shandong Vocational and Technical University of International Studies, Rizhao, Shandong 276800, China*
[2]*Huilin Training, Shandong Vocational and Technical University of International Studies, Rizhao, Shandong 276800, China*

Correspondence should be addressed to Yuyan Chi; 202071572@yangtzeu.edu.cn

Received 23 December 2021; Revised 13 January 2022; Accepted 18 January 2022; Published 10 February 2022

Academic Editor: Yang Gu

In order to improve the effect of smart home control and management, a new smart home control and management method based on big data analysis is designed. The basic hardware of smart home control and management is designed, including smoke sensor hardware, temperature and humidity sensor hardware, and infrared sensor hardware, so as to collect smart home data and realize data visualization and buzzer alarm. The collected data are transmitted through the indoor wireless network of smart home gateway equipment, and the data distributed cache architecture based on big data analysis is used to store smart home data. Based on the relevant data, the hybrid particle swarm optimization algorithm is used to schedule the control and management tasks of smart home to complete the control and management of smart home. The experimental results show that the device control and scenario management effect of this method is better, and the communication performance is superior and has high practical application value.

1. Introduction

The increasing development of information technology and control technology has gradually accelerated the pace of social informatization and also promoted the informatization of people's way of life, work, and communication [1, 2]. The high development of information technology, liberalization, and high level of communication have not only changed people's daily living habits, but also posed a challenge to traditional housing. The expanding material demand makes people's requirements for home no longer a simple material space, but pay more attention to a beautiful, convenient, comfortable, and safe living environment and advanced communication facilities, efficient and simple terminal control equipment, and automatic and intelligent network management of household appliances and resources [3]. Due to the trend of high informatization in modern society, people eagerly hope that all household equipment in the residential environment can be added to the Internet. With the deep integration of hardware and software, the smart home control system has fully met people's needs, because it networks all household appliances and building intelligence, which not only meets the exchange of internal environment and external information, but also realizes a safe, comfortable, and convenient lifestyle [4–6].

Smart home is a popular topic in today's era. It is one of the specific manifestations of the Internet of Things [7]. It is to deeply integrate Internet of Things technology, wiring technology, network security technology, intelligent control technology, wireless communication technology, and other technologies; connect various hardware facilities in the house; and then control household appliances, lighting equipment, security and antitheft, and environmental detection, so as to establish an intelligent management system and to facilitate people's daily life [8]. The use of a smart home system in the environment with residence as the platform not only optimizes and facilitates people's lifestyle, but also increases the beauty of life and the safety performance of people's life. After entering the new era, with the great development of information technology, people's traditional ideas have also changed greatly, so their understanding of housing is becoming deeper and deeper [9, 10].

In the future information-based life of mankind, the formation of a smart home environment has become an inevitable trend. In the future of smart home development, relevant national functional institutions and departments should also provide a lot of support and encouragement, so that the application prospect and market of smart home will be clear [11, 12]. According to the current situation, the development of smart home in China is still in the primary stage, whether at the technical level or theoretical level. For example, the unified specification of smart home technology has not been formed, so that many different products cannot be compatible, and the availability is still relatively low, which brings a lot of inconvenience to the user experience and manufacturers' production. However, due to its high design cost, many ordinary people are deterred. At the same time, the traditional smart home has complex wiring. The function of the collection is relatively single, and the traditional smart home control and management scheme are incomplete, which are urgent problems to be solved [13].

Therefore, this article designs a new smart home control and management method based on big data analysis.

2. Smart Home Control and Management

2.1. Basic Hardware Design of Smart Home

2.1.1. Smoke Sensor Hardware Circuit. The smoke concentration sensor is specially used to observe whether the smoke concentration in the kitchen exceeds the safe range. Therefore, this article designs to use the smoke sensor MQ2 to detect the smoke concentration. The gas sensor has high sensitivity and adjustable sensitivity, and can respond to most smoke [14], especially for methane (CH4), the main component of natural gas used in the family. Table 1 shows the detection range of some smoke by MQ2.

The smoke sensor module MQ2 selects digital output. That is, when the indoor smoke concentration exceeds the threshold, MQ2 module will output low level, and then, the buzzer will give an alarm. If the smoke concentration does not exceed the threshold, the MQ2 module will output high level [15, 16]. The MQ2 pin of the module is connected with pin P0.5 of CC2530 chip, so the mechanism of detecting high and low levels is used to detect whether the concentration of harmful gas smoke in the environment exceeds the standard value. The MQ2 circuit connection diagram is shown in Figure 1.

Table 1: MQ2 detection range.

Name of detected substance	Detection concentration range
Liquefied gas and propane	100 ppm~10000 ppm
Butane	300 ppm~5000 ppm
Methane	5000 ppm~20000 ppm
Hydrogen	300 ppm~5000 ppm
Alcohol	100 ppm~2000 ppm

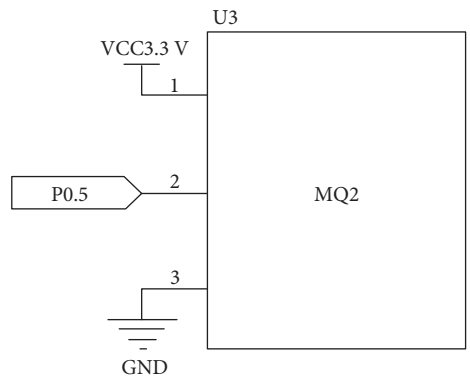

Figure 1: MQ2 circuit connection diagram.

2.1.2. Hardware Circuit of Temperature and Humidity Sensor. In this article, DHT11 temperature and humidity sensor is used to collect the temperature and humidity in the house. It is a composite sensor that can collect both temperature and humidity [17]. The pin description of DHT11 is shown in Table 2.

The connection circuit diagram according to Table 2 is shown in Figure 2.

Table 2: DHT11 pin description.

Pin	Name	Notes
1	VDD	The supply voltage is 3~5.5 V DC
2	DATA	Single bus, serial data
3	NC	The empty pin should be suspended
4	GND	Grounding terminal or negative terminal of power supply

2.1.3. Infrared Sensor Hardware Circuit. The infrared sensor module HC-SR501 is used to detect whether there are people close to the house. It can detect the infrared radiation from the human body. The high and low levels are the digital signals [18–20]. If someone steps into the sensing range of the infrared sensor, the output terminal will send a high level, and the output terminal will output a low level after the person leaves. Figure 3 shows the circuit connection diagram of the module.

The characteristic parameters of the infrared sensor are shown in Table 3.

2.1.4. Buzzer Alarm Circuit. The buzzer alarm circuit module is driven by S8550 triode, and the working voltage is 3.3 V–5 V. When the temperature and humidity exceed the preset value, the IO port P0.6 of the ZigBee module will output low level, and the buzzer will sound. At the same time, when toxic gas appears in the environment and someone approaches the house, the buzzer will also sound. Figure 4 is the connection circuit diagram of the buzzer.

2.1.5. LCD Module. This article adopts Shenzhen Qinchuangjia 12864 display screen. The controller used in the display screen is ST7920, which supports two driving modes of serial port and parallel port. Due to the limited STM32 pins used in the method design in this article and the large number of IO ports in the parallel port mode, the requirements for the screen refresh rate, that is, speed, are not

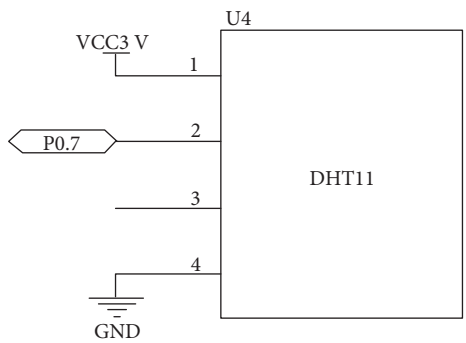

Figure 2: DHT11 circuit connection diagram.

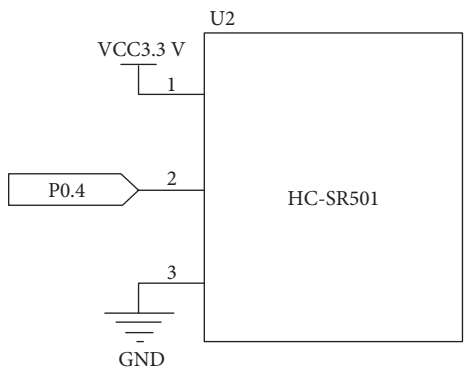

Figure 3: Circuit connection diagram of HC-SR501.

Table 3: Characteristic parameters of the infrared sensor.

Property name	Characteristic parameter
Working current	The range is 4.4 V~20 V
Quiescent current	<50 μA
Level output	High level 3.3 V, low level 0 V
Trigger mode	Repeat trigger/nonrepeat trigger
Delay time	5~200 s, adjustable
Blocking time	The default is 2.5 s, and the adjustable range is several to tens of seconds
Overall dimension	32 mm ∗ 24 mm
Induction angle	Cone angle less than 100 degrees
Working temperature	−15°C~+70°C
Sensing lens size	The default diameter is 23 mm

high. Therefore, the serial port driving mode (PSB pin connected to GND) is adopted in this article, and the schematic diagram is shown in Figure 5.

2.2. Indoor Wireless Networking Design of Smart Home Gateway Equipment. The most basic function of smart home gateway equipment is indoor networking, which enables home terminal equipment to connect to gateway equipment through home intranet. Users use client equipment to control home terminal equipment through gateway equipment. This article mainly puts forward and analyzes the hardware structure of the designed home gateway device [21–23], specifies the format of data packet, and develops and designs the intranet part of the gateway combined with Bluetooth, ZigBee, and WiFi communication modules.

The hardware part of smart home gateway device is mainly composed of embedded unit based on ARM architecture, serial port expansion board, Bluetooth, ZigBee [24, 25], and WiFi wireless communication module. The hardware structure of smart home gateway device is shown in Figure 6.

As can be seen from Figure 6, the embedded unit is first connected with the serial port expansion board, and the serial port expansion board is then connected with Bluetooth and ZigBee modules. The embedded unit is directly connected with the WiFi communication module [26].

As one of the wireless communication modules, the Bluetooth module is mainly aimed at Bluetooth devices in smart home, such as Bluetooth audio, Bluetooth headset, and smart bracelet; these kinds of smart home devices are generally configured flexibly and can be increased or decreased according to needs at any time [27, 28].

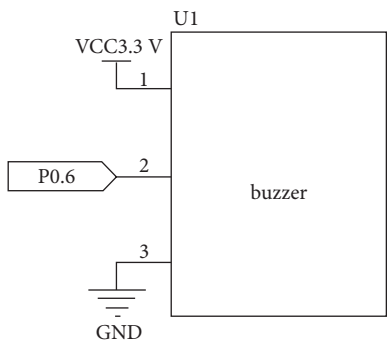

Figure 4: Circuit diagram of buzzer connection.

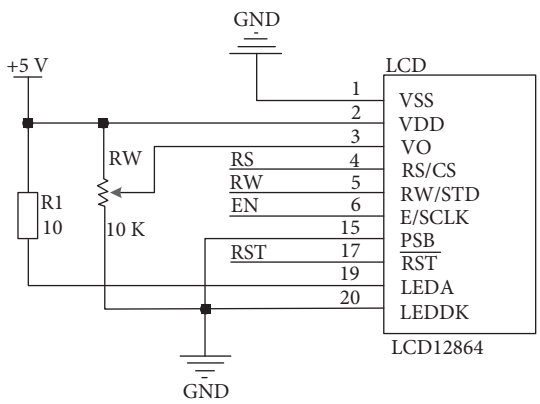

Figure 5: Circuit diagram of liquid crystal display.

ZigBee module is mainly used as coordinator equipment at the gateway of the smart home network and is the central part of the whole ZigBee network [29, 30]. ZigBee's devices are mainly relatively fixed devices with low transmission speed requirements, such as smart home devices such as lighting and environmental detection.

WiFi communication module is also one of the wireless communication modules. WiFi is the most widely used wireless communication mode at this stage. With the popularity of mobile phones, tablets, and other devices, using such devices as client devices of the smart home system can easily control home terminal devices. At the same time, the fast transmission speed of WiFi is very suitable for data transmission on multimedia smart home devices such as video.

The serial port expansion board is mainly used to connect various wireless communication device modules, preliminarily sort out the information collected by the wireless device, and transmit it to the embedded unit through the serial port. At the same time, the control instructions transmitted from the embedded unit are transmitted to the corresponding wireless communication module according to different kinds of wireless communication requirements, and then transmitted to the home intelligent terminal device to complete the communication.

The embedded unit is the core of the whole smart home gateway equipment. It is responsible for gateway authentication, data analysis, processing, storage, and data exchange between internal and external networks. It is developed based on OpenWrt embedded system [31].

The operation process of the smart home system mainly includes two parts: data transmission and data processing. Data processing can only be completed after receiving data normally, so the stability of data transmission process is particularly important. Only normal data transmission can ensure the stable operation of the whole smart home system. The design of data transmission protocol includes two points: the first point is the process design of data transmission, mainly including the direction of data transmission and the transceiver of data transmission; The second point is the data packet communication format used in the data transmission process. A reasonable data packet communication format can ensure the target of data transmission and the correctness of communication data, and ensure the stable operation of relevant equipment.

2.2.1. Data Stream Transmission. The data information flow generated in the operation of smart home mainly includes two types: control data information flow and state data information flow. The control data information flow refers to the control instructions sent by the smart client device to the home terminal device [32, 33]; Status data information flow refers to the data information that the home terminal device transmits its own status information and collected environmental information to the smart client device, and then feeds back to the user through the interactive interface. Smart home data stream transmission is shown in Figure 7.

2.2.2. Packet Format Definition. Packet format is one of the key factors affecting the normal transmission of data. The data packet with perfect format can ensure the integrity of data in the transmission process, reduce the operation load, and improve the stability and security of related equipment. The data packet includes five parts: packet header, data segment length, data segment, CRC check, and packet tail. The data packet designed in this article is shown in Figure 8.

When errors are found in the data transmission process, the data packet can be tracked by combining the data packet type, source device type, target device type, data packet number, and device unique identification to find out the causes of data abnormalities and realize the self-inspection function of transmission status in the transmission process [34]. At the same time, defining traceable data packets also facilitates function development and improves the intelligence of smart home control and management.

2.3. Data Distributed Cache Architecture Based on Big Data Analysis. File storage system is the cornerstone of the whole smart home, which is very important for the efficient and smooth operation of related devices. This chapter mainly studies the data generated in the operation of smart home and analyzes the data to be stored, such as images and videos. Among them, video data are relatively large and can be directly stored in HDFS, and structured data such as video can be stored in distributed database HBase [35, 36]. At

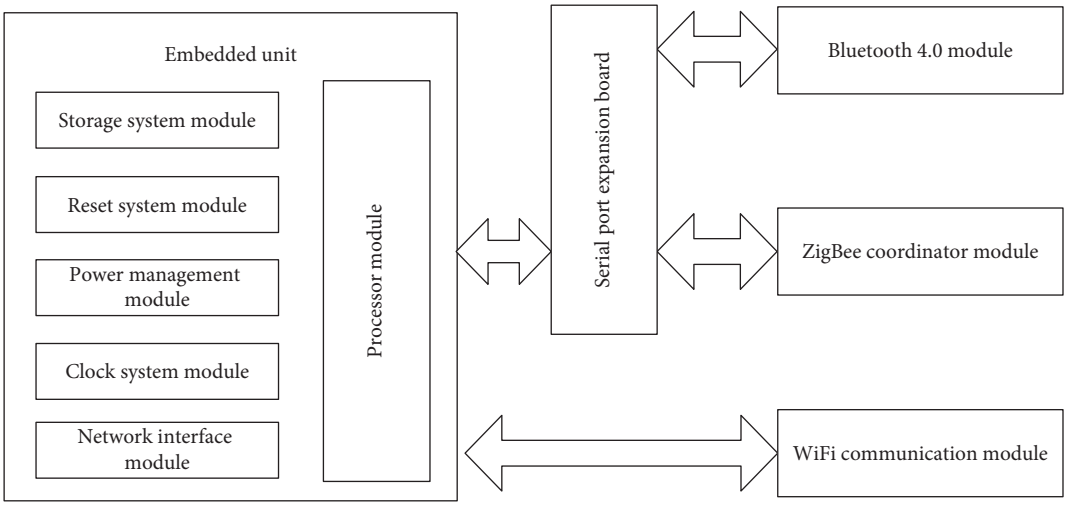

Figure 6: Hardware structure of smart home gateway.

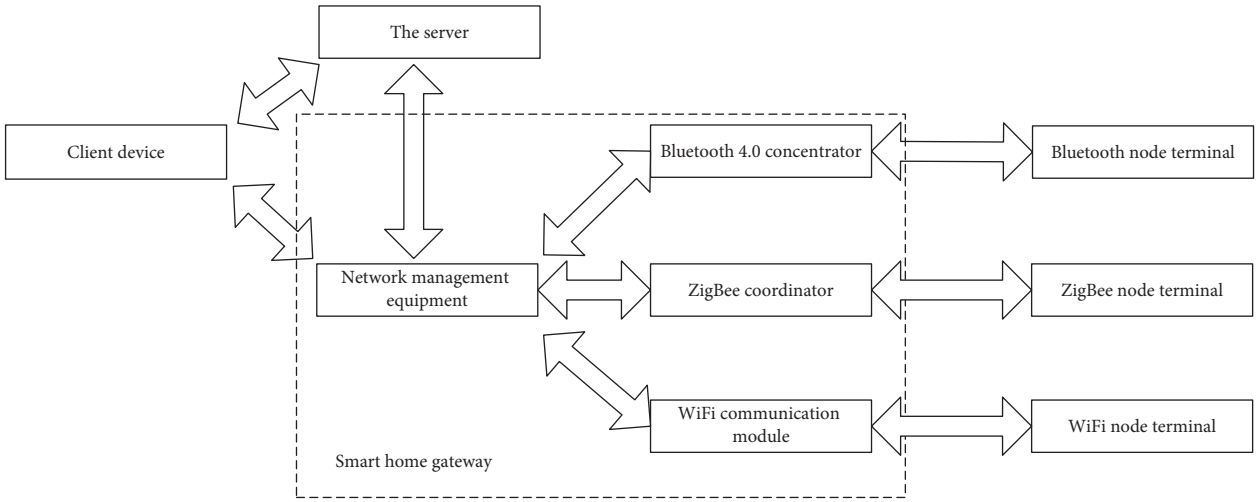

Figure 7: Data stream transmission diagram of smart home.

present, there are some problems in the distributed cache system and massive small file storage. This chapter designs a distributed cache system for caching hot data and a small file storage system for storing massive pictures.

The schematic diagram of file enclosure is shown in Figure 9.

(1) HDFS is suitable for storing large files and can ensure high reading and writing speed, so video data are stored directly in HDFS. At the same time, HBase components are arranged on the HDFS cluster to store structured data.

(2) Distributed cache. In order to improve the speed of applications accessing hotspot data, a cache needs to be built. Due to the limitation of single machine cache capacity, a distributed cache system is built to meet the high-capacity cache requirements of applications.

(3) Massive small files. A large number of small files will be generated in the process of video processing, such as image data. The loss system is designed to store a large number of small files. It merges the small files, records the index information corresponding to each small file, and stores the merged files in HDFS.

Due to the processing performance and memory capacity limitations of a single machine, the cache system built with a single machine cannot meet the needs of high-capacity cache. At the same time, if a single machine is used to cache data, once the machine fails, the whole cache will fail, which will have an extremely adverse impact on the application. Therefore, it is necessary to use multiple machines to build a distributed cache system, and each machine is responsible for the storage and processing of some cached data, so that the cache system has large storage capacity and strong processing ability. Redis is widely used to build the

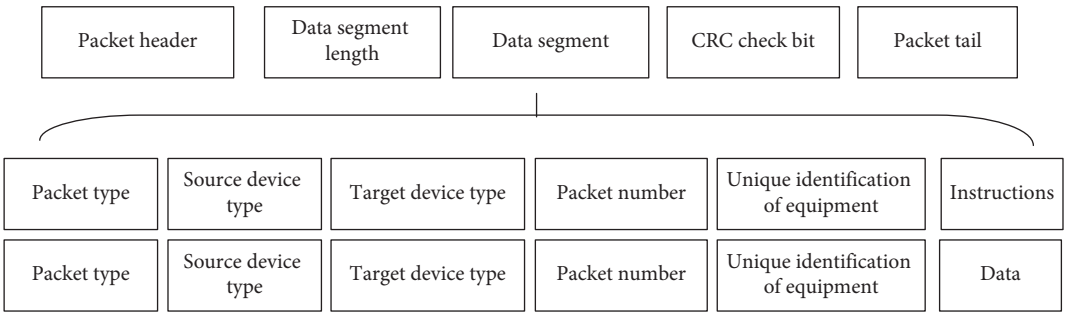

Figure 8: Communication packet structure.

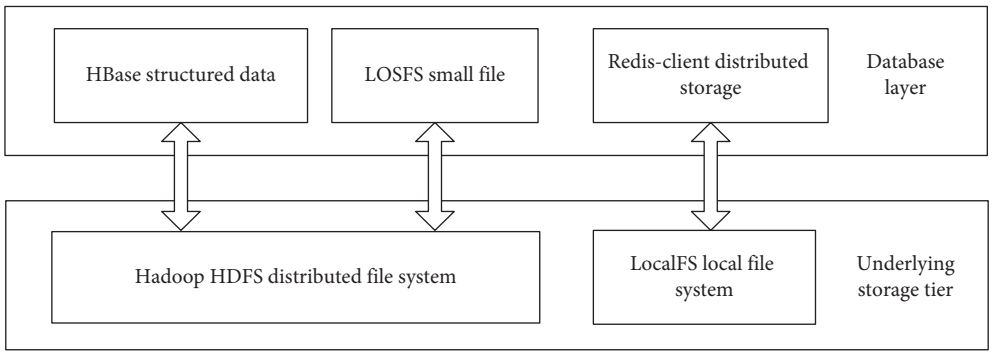

Figure 9: Module diagram of the file storage system.

cache system. Redis is an efficient key-value pair data storage system based on memory, which is written in C language. It supports the construction of a distributed cache system. The official Redis cluster is designed based on centerless and intelligent end. Redis-client must send the request directly to the corresponding node of the cluster according to the hash of the key, which means that it must be responsible for handling complex jump logic, which makes it difficult to write programs, and different Redis nodes in the cluster are highly coupled, which makes it difficult to upgrade Redis.

Based on the above analysis, this article takes Redis as the basis, and before Redis-proxy, Redis-client operates the cached data by connecting Redis-proxy. Redis-proxy will distribute the request to the corresponding node according to the key in Redis command and forward the processing results to Redis-client. At the same time, the use method of Redis-proxy is the same as that of single Redis, which solves the problem of complex Redis-client processing logic in the official Redis cluster. Figure 10 is the schematic diagram of distributed cache architecture.

The specific scheme is to add a Redis-proxy in front of Redis, which will receive the request as an agent. When the agent receives the request, Redis-proxy calculates the data storage node according to the key in the command, forwards the request to the corresponding service node, summarizes the results after processing, and forwards the results to Redis-client. Redis-proxy has no status and is easy to expand. At the same time, the underlying storage engine is still Redis itself, which uses zookeeper to store the distribution status of cached data in the cache system. For the upper application, there is no difference between connecting to Redis-proxy and connecting to the native Redis server. Request forwarding will be carried out at the bottom, but it is transparent to Redis-client.

The distributed cache system uses prepartitioning to manage cached data. By default, the cache is divided into 1024 slots. The slot numbers corresponding to data keys are determined based on formula (1). Formula (1) uses CRC32 to calculate the CRC32 check code corresponding to the crC32 key. Compared with MD5, CRC has the advantages of simple implementation and fast calculation. Therefore, CRC is selected for data hashing. The slot number is determined as follows:

$$\mathrm{ID} = \mathrm{scr32}\,(\mathrm{key})\%1024. \tag{1}$$

After receiving the migration instruction, the Redis service node establishes a TCP connection with the destination Redis service node for the transmission of migration data and migrates all data under the slot specified in the migration instruction to the destination Redis service node. After the migration is completed, the data stored by itself will be deleted. The process is shown in Figure 11.

2.4. Task Scheduling Based on Hybrid Particle Swarm Optimization Algorithm. Smart home control and management task scheduling is very important for users. Task scheduling is a reasonable scheduling between different processing nodes and tasks to reduce task completion time and improve efficiency. However, task scheduling is a NP-complete combinatorial optimization problem, and the optimal solution cannot be obtained in polynomial time. Considering the superiority of particle swarm optimization (PSO) in scheduling optimization

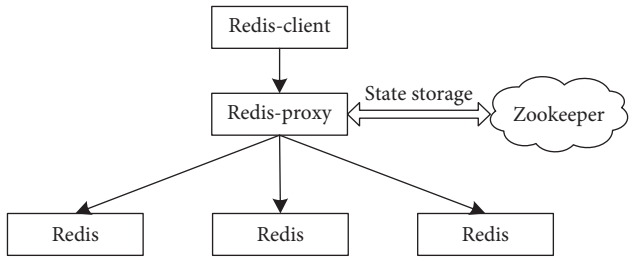

Figure 10: Schematic diagram of distributed cache architecture.

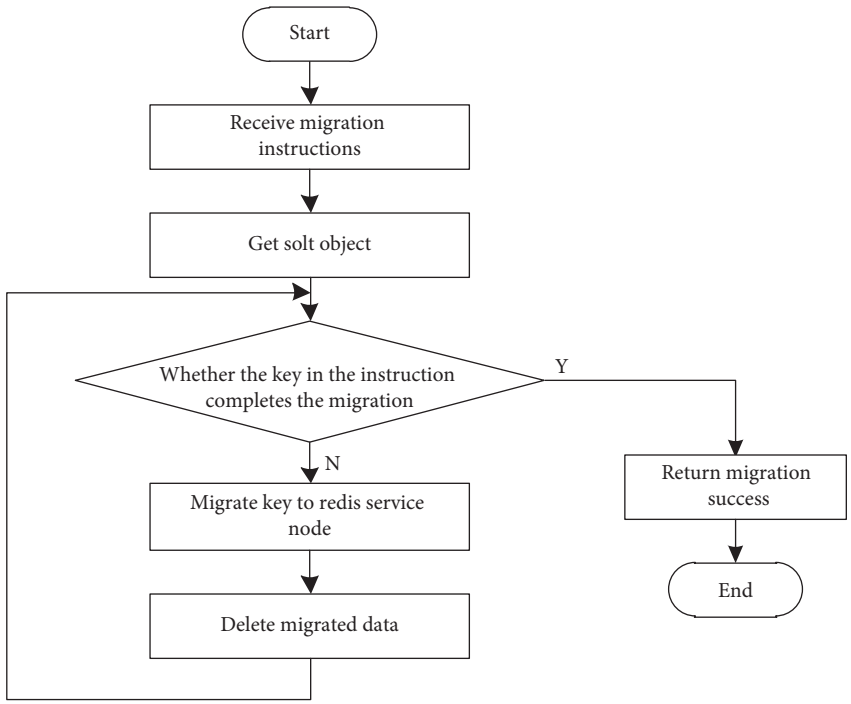

Figure 11: Migration process.

problem, the PSO algorithm is selected to find the relative optimal solution of task scheduling. Aiming at the problem that PSO is easy to fall into local optimization and convergence is too slow, a hybrid particle swarm optimization algorithm is designed and applied to smart home control and management task scheduling.

PSO algorithm is a random optimization algorithm, which is inspired by the social behavior of birds and fish. In the PSO algorithm, a group of individuals called particles fly in the search space, and each particle represents the candidate solution of the optimization problem. The current position of a particle is affected by the best position accessed by itself and the best position accessed by the whole population. The best position accessed by itself is called the historical best particle, and the best position accessed by the whole population is called the global best particle. According to different optimization problems, the position of each particle is evaluated by using the fitness function, and the particles are updated by using the following formulas until the result meets the set termination conditions or reaches the set maximum number of iterations.

$$v_{id}^{k+1} = \omega v_{id}^{k} + c_1 R_1 \left(p_{id}^{k} - x_{id}^{k}\right) + c_2 R_2 \left(p_{gd}^{k} - x_{id}^{k}\right), \quad (2)$$

$$x_{id}^{k+1} = x_{id}^{k} + v_{id}^{k+1}, \quad (3)$$

where v_{id}^{k+1} and x_{id}^{k+1} represent the current velocity and position of the particle when the number of population iterations is k, respectively; p_{id}^{k} and p_{gd}^{k} represent the historical best position of particles and the best position of particles in the whole population when the number of population iterations is k, respectively; c_1 and c_2 are weight factors, which are called cognitive learning factor and social learning factor, respectively; R_1 and R_2 are two random numbers with values between 0 and 1; and ω is the inertia weight coefficient, which is not only to avoid the infinite increase of particle velocity, but also a key parameter affecting the search results and convergence speed. During the iteration of the algorithm, ω will be dynamically adjusted. At the beginning of the iteration, a larger value of ω can make the algorithm have better global search ability. In the later stage of iteration, a smaller value of ω can improve the local exploration ability of the algorithm and carry out detailed

search in a smaller local range. The following formular is an updated formula of ω:

$$\omega = \frac{\omega_b + (\omega_e - \omega_b) * k}{K_{\max}}. \tag{4}$$

Among them, ω_b and ω_e are the initial value and end value of the iteration of the inertia weight coefficient, respectively, k is the current iteration times of the algorithm, and $K_{\max}$ is the maximum iteration times set by the algorithm.

In PSO, the size of ω, c_1, and c_2 is very important to the performance of the algorithm. Some relevant literature points out that when the three meet a certain relationship, the algorithm has convergence, but it cannot guarantee the convergence to the global optimal value. Using a random method to initialize particles may lead to particles gathering in a local area, which reduces the diversity of the population and is not conducive to the initial iteration of the population. With the increase in the number of population iterations, the particles will gradually tend to the global optimal position, and the population diversity will become worse, which may lead to the local optimization of the algorithm.

A new initialization method is designed, which uses the opposition-based learning method and chaotic system to generate the initial population of HPSO. The following is the calculation method of chaotic mapping:

$$\begin{aligned} ch_{g+1} &= \sin(\pi ch_g), \\ ck_g &\in (0, 1), \\ g &< G_{\max}, \end{aligned} \tag{5}$$

where g represents the iteration counter and $G_{\max}$ is the preset maximum chaotic iteration times. Since the value generated by chaotic mapping is between 0 and 1, it needs to be mapped to the solution space of the algorithm. The mapping method is shown in the following formula:

$$x_j = x_{\min,j} + ch_j(x_{\max,j} - x_{\min,j}). \tag{6}$$

where j represents the dimension corresponding to the particle generated by chaotic mapping, ch_j is the mapping variable generated after $G_{\max}$ iterations of the chaotic system, $x_{\max,j}$ and $x_{\min,j}$ represent the lower and upper bounds of the j-th dimension of the particle, respectively, and and x_j is the value corresponding to the third dimension of the particle generated by chaotic mapping. After an initial particle is obtained through chaotic mapping, its opposite particle is obtained by using the opposite learning method. The calculation method is shown in the following formula:

$$\begin{aligned} x_j^* &= x_{\min,j} + x_{\max,j} - x_j, \\ x_j &\in [x_{\min,j}, x_{\max,j}]. \end{aligned} \tag{7}$$

In the HPSO algorithm, the learning method based on chaotic mapping and opposition is used to initialize the population, which ensures that the initial particles are evenly distributed in the search space, improves the diversity of the initial population, speeds up the convergence speed of the algorithm, and is conducive to the algorithm searching for the optimal solution.

Inertia weight is an important control parameter of the PSO algorithm. It can effectively control the global and local search ability. Therefore, it is necessary to design an appropriate inertia weight strategy to make the HPSO algorithm achieve the best balance between global search and local search. The inertia weight adjustment function used in HPSO is shown in the following formula:

$$\omega(k+1) = \omega_{\max} e^{-(k/K\max)^2}, \tag{8}$$

where $\omega_{\max}$ is the initial inertia weight, which is generally set to 0.9, 2 represents the current iteration times of the algorithm, and k is the maximum iteration times set by the algorithm. It can be seen that in the early stage of the HPSO algorithm, the inertia weight is large and the downward trend is slow, which makes the algorithm have better global search ability. In the later stage of the HPSO algorithm, the inertia weight is small and decreases rapidly, which makes the algorithm have better local search ability.

In the PSO algorithm, each particle adjusts its self-learning behavior by approaching the best particle experienced by the population, that is, part $c_2R_2(p_{gd}^k - x_{id}^k)$ in formula (2). Therefore, the update speed and efficiency of the best particle directly affect the whole population. In the process of evolution, we should not only consider the historical best position and global best position of particles, but also consider the evolution of the overall trend of particles:

$$\mathrm{PSC}(k) = \sum_{i=1}^{S} R_i(k) * X_i^k. \tag{9}$$

where k represents the current number of iterations, X_i^k represents the i-th particle of the population, S represents the number of particles in the population, and $R_i(k)$ represents the ratio of the fitness of the i-th particle to the total fitness of all particles, which is given as

$$R_i(k) = \frac{f(X_i^k)}{\sum_{r=1}^{S} f(X_i^k)}. \tag{10}$$

where $f(X_i^k)$ represents the fitness of particle i. The larger its value, the closer the particle is to the optimal solution, and the larger $R_i(k)$, so the larger the proportion of its corresponding particles in PSC. PSC is introduced into the particle velocity update of the HPSO algorithm, and formula (2) is modified as shown in the following formula:

$$v_{id}^{k+1} = \omega v_{id}^k + c_1R_1(p_{id}^k - x_{id}^k) + c_2R_2(p_{gd}^k - x_{id}^k) + c_3R_3\alpha(PSC_d - x_{id}^k). \tag{11}$$

The PSO algorithm loses diversity quickly at the initial stage of iteration, which makes the algorithm easy to fall into local optimization. Therefore, the HPSO algorithm uses formula (11) to update particle velocity as much as possible at the initial stage of iteration, so as to maintain population diversity. In the later stage of iteration, in order to reduce the amount of calculation, improve the calculation speed, and accelerate the convergence speed of the algorithm, formula (2) is used to update the particle speed. In order to achieve the above purpose, a function whose value decreases linearly with the increase in the number of iterations of the algorithm is designed, as shown in the following formula:

$$N_k = 1 - \frac{k}{K_{\max}}. \tag{12}$$

At the later stage of the algorithm iteration, all particles in the particle swarm are guided by the global optimal particles and will gradually tend to the global optimal position. If the algorithm has found the optimal solution, all particles will gather near the optimal solution position, so that their fitness values tend to be equal. Therefore, the similarity of fitness values of all particles can be used to judge whether the algorithm finds the optimal solution. Specifically, it can be judged by the fitness variance of the population, as shown in the following formula:

$$\sigma^2 = \frac{\sum_{i=1}^{S}\left(f\left(X_i^k\right) - \overline{f}\right)}{S}, \tag{13}$$

where $\overline{f}$ represents the average fitness of all particles, and its calculation formula is as follows:

$$\overline{f} = \sum_{s=1}^{S} \frac{f\left(X_i^k\right)}{S}. \tag{14}$$

σ^2 is the fitness variance of the population, which represents the aggregation degree of particles in the population. The smaller its value is, the more aggregated the particles in the population are. When its value is close to 0, it means that the fitness values of all particles in the population are close to the same, which indicates that the algorithm converges globally and finds the optimal solution. Therefore, a threshold T is set to determine the convergence of the algorithm when the fitness variance of the population is less than the set threshold. To sum up, the termination condition of the HPSO algorithm is that the variance of fitness of all particles in the population is less than the set threshold or reaches the maximum number of iterations set by the algorithm.

Task scheduling refers to allocating the most appropriate resources to the tasks to be executed under the consideration of different factors such as time, cost, and resource utilization, which can reduce the task completion time and improve the utilization of system resources.

HPSO-based smart home control management task scheduling mainly includes the following steps:

(1) Set parameters in the HPSO algorithm, including maximum iteration times, population size, initial inertia weight value, learning factor, and other parameters.

(2) Randomly generate a specified number of tasks, set the hardware configuration parameters of the virtual machine, and generate the ETC matrix:

$$\text{ETC} = \begin{bmatrix} 0 & 0 & 0 & 0 & 1 & 0 & 0 & 0 & 1 & 0 \\ 0 & 0 & 1 & 0 & 0 & 0 & 1 & 0 & 0 & 1 \\ 1 & 0 & 0 & 1 & 0 & 1 & 0 & 0 & 0 & 0 \\ 0 & 1 & 0 & 0 & 0 & 0 & 0 & 1 & 0 & 0 \end{bmatrix}. \tag{15}$$

(3) The task scheduling scheme is encoded into particles in the HPSO algorithm, and the population is initialized by a chaotic system and opposition learning method to generate a specified number of particles, and the fitness of each particle is calculated. The calculation method is shown in the following formula:

$$\text{Fit} = \frac{1}{\text{complete Time}}, \tag{16}$$

where complete time indicates the longest running time of all virtual machines.

(4) Dynamically update the inertia weight according to the number of iterations, update the speed and position of each particle, and record the best historical position of each particle and the global best position of the population.

(5) Calculate the fitness value variance corresponding to all particles in the population. If the variance is less than the threshold set by the HPSO algorithm or the number of iterations is greater than the maximum number of iterations set by the algorithm, the algorithm stops the iteration and outputs the smart home control and management task scheduling scheme. Otherwise, the algorithm returns to step 4 to continue searching for the optimal solution.

3. Experimental Design

3.1. Function Test. The smart home control management client is developed in Java and runs under an Android system. Therefore, the functional test of this method mainly focuses on Android devices. The running environment table of APP client is shown in Table 4.

In the equipment control, the control functions of different equipment are different and limited to space. Taking the lighting control as an example, the test process of equipment control is shown in Table 5:

Scenario management is mainly set to facilitate user operation. By operating scenario management, users can operate multiple devices at the same time, facilitate user operation, and liberate the user operation process, so that users do not have to operate multiple devices at the same time. The test process of scenario management is shown in Table 6.

Table 4: Client running environment.

Client	Android model	Operating system
Host 1	Millet	Android 4.0
Host 2	Huawei	Android 4.3
Host 3	Samsung	Android 5.0

Table 5: Equipment control test process.

Test function	APP test process	APP test results	Backstage
Equipment control	(1) Enter the electrical management interface (2) Select intelligent lighting function (3) Select general opening	All lights on	The background receives the general opening instruction and sends the instruction to the equipment
Equipment control	(1) Enter the electrical management interface (2) Select intelligent lighting function (3) Select general off	All lights are off	The background receives the general closing instruction and sends the instruction to the equipment
Equipment control	(1) Enter the electrical management interface (2) Select intelligent lighting function (3) Select TV wall off	TV wall lights off	The background receives the TV wall closing instruction and sends the instruction to the equipment
Equipment control	(1) Enter the electrical management interface (2) Select intelligent lighting function (3) Select the atrium light	Atrium lights on	The background receives the atrium light on command and sends the command to the equipment

Through the test of main functional device control and scenario management, its functions can operate normally on all Android devices and meet the expected objectives. At the same time, the relevant smart home management control interface can be displayed normally and meet the requirements on all mainstream models and mainstream systems.

3.2. Communication Performance Test. Two ZigBee communication modules are selected. Both modules do not add power amplifier. One node is used as coordinator, the other is used as terminal node, the coordinator is used as sender, and the terminal node is connected to the serial port of PC as receiver. Test in the open without other interference, make the coordinator send 1000 data packets each time through the serial port assistant, test 10 times at each distance point, and finally take the average value as the result. The test results are shown in Table 7.

Through the analysis of the test results, it can be seen that the maximum distance of normal communication between the two nodes is 100 m. At this time, the communication situation is very good, and the packet loss rate is 0. When the distance exceeds 100 m, packet loss begins. At the same time, during the test, it is found that the communication situation will be affected by the surrounding environment. When a vehicle or tester calls, the communication situation will be affected, and the antenna must be placed vertically during the test.

Through the previous communication distance test, it is known that when the communication distance between two nodes exceeds 100 m, packet loss begins to occur. If a node is added between the two nodes, the packet loss rate can be reduced by relaying and transmitting information through this node. Three nodes are selected, one of which is used as the coordinator to send data, and the other two are used as routers.

Firstly, the coordinator and one of the routing nodes are placed at a distance of 200 m. It can be seen from the sending packet test that the communication between the two nodes cannot be realized at this time. Then, the second routing node is added to the two nodes, and the meaning is repeated. Delete one of "about" and "about" for 5 tests. The coordinator sends 1000 packets each time, The test results are shown in Table 8.

Through the analysis of the test results, we can know that when the communication distance between two nodes exceeds the normal communication distance, the communication between nodes can be realized by adding routing nodes. Affected by the surrounding test environment, very few packets will be lost.

3.3. Application Effect Test. In order to verify the superiority of the smart home control management task scheduling method based on the hybrid particle swarm optimization algorithm designed in this article, the convergence of the

Table 6: Scenario management test process.

Test function	APP test process	APP test results	Backstage
Scenario management	(1) Enter the main menu (2) Select scenario function (3) Choose to go home	All preset home scene functions are turned on, such as air-conditioning, and curtain	The background receives the general opening instruction and sends the instruction to the equipment
Scenario management	(1) Enter the main menu (2) Select scenario function (3) Select home mode	All preset home mode functions are turned on, such as turning off lights, and curtains	The background receives the general closing instruction and sends the instruction to the equipment
Scenario management	(1) Enter the main menu (2) Select scenario function (3) Select one key deployment	The preset one key deployment function is all turned on, the camera is turned on, the camera content can be viewed anytime and anywhere, and the user will be prompted if there is a warning during the operation of the camera	The background receives the TV wall closing instruction and sends the instruction to the equipment
Scenario management	(1) Enter the main menu (2) Select scenario function (3) Select one click disarm	The preset one button disarm function is turned on, and the camera is turned off	The background receives the atrium light on command and sends the command to the equipment

Table 7: Communication distance test.

Serial number	Test distance	Packet loss number	Packet loss rate
1	30	0	0
2	70	0	0
3	100	0	0
4	110	8	0.8%
5	120	10	1.0%
6	150	132	13.2%

Table 8: Routing test.

Serial number	Packet loss number	Packet loss rate
1	0	0
2	0	0
3	1	0.1%
4	0	0
5	2	0.2%

hybrid particle swarm optimization algorithm and the particle swarm optimization algorithm is compared, and the comparison results are shown in Figure 12.

Analysis of the results in Figure 12 shows that with the increase in iteration times, particle swarm optimization achieves convergence only at 70 times, whereas hybrid particle swarm optimization achieves convergence only at 25 times, with faster convergence speed and better comprehensive performance.

On the basis of the above, use the method to control the audio and video equipment, lighting, curtain control, air-conditioning control, security systems, digital cinema, video server, shadow cabinet system, network home appliances and other equipment, and number of the equipment processing, with 1~9, said of the equipment control management task scheduling, scheduling time consuming as shown in Figure 13.

According to the analysis of Figure 13, the control and management task scheduling method of smart home based on hybrid particle swarm optimization algorithm takes different time for the control and management task scheduling of different devices. Among them, the management task scheduling time for equipment 6 is the highest, which is 59 ms, while the control and management task scheduling time for equipment 2 is the lowest, which is 36 ms. The overall task scheduling time of smart home management and control task is always less than 59 ms, which shows that the task scheduling time of this method is shorter and more efficient

On this basis, the accuracy of the proposed method for smart home control is verified. The control accuracy refers to the ratio between the number of controlled events and the control password after executing the control password many times. The results are shown in Figure 14.

Analysis of the data in Figure 14 shows that the accuracy rate of the smart home control management method based on big data analysis is always above 93% for smart home control, among which the control accuracy rate of equipment 2, namely, lighting system, is the lowest at 93%. For equipment 5, that is, the control accuracy of security system is the highest, 98%, indicating that using this method can achieve control and management of smart home.

Comprehensively verify the method in this article for smart home control and management time, and the comparison results are shown in Figure 15.

According to the analysis of Figure 15, the smart home control management method based on big data analysis has

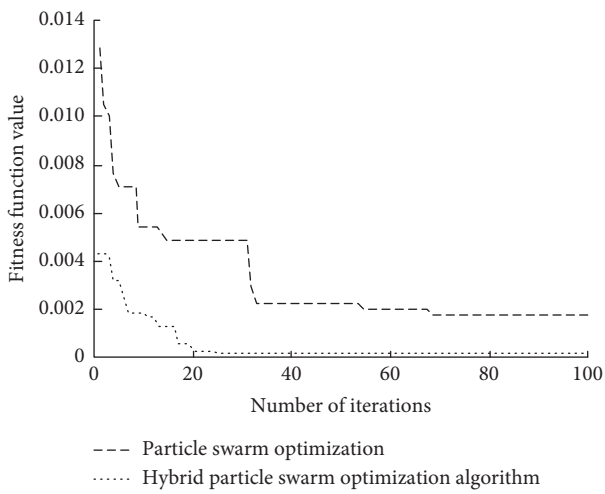

Figure 12: Algorithm convergence comparison.

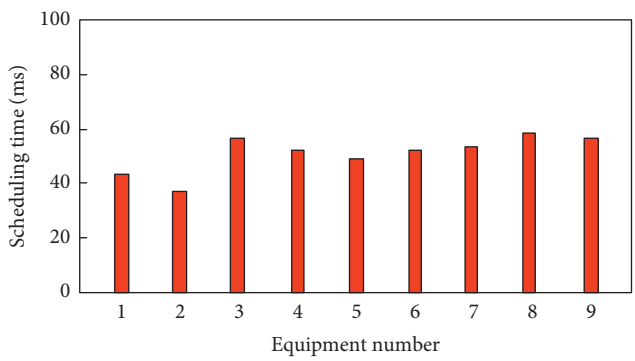

Figure 13: Task scheduling time.

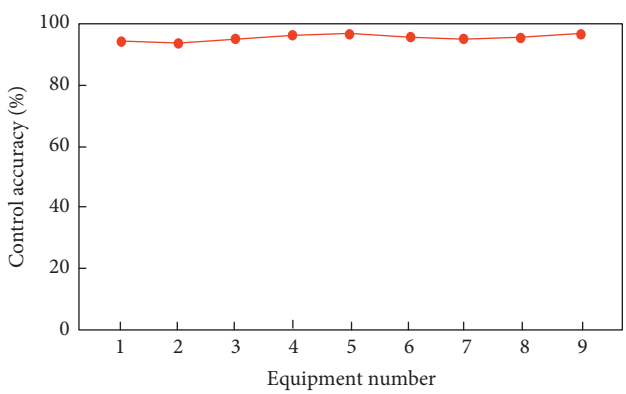

Figure 14: Control accuracy rate.

certain differences in the management and control time of different devices. The maximum value of the smart home control time of this method is 1.4 s and the minimum value of the smart home control time of this method is 0.8 s; the maximum value of smart home management time of this method is 1.3 s and the minimum value of smart home management time of this method is 0.8 s, which shows that

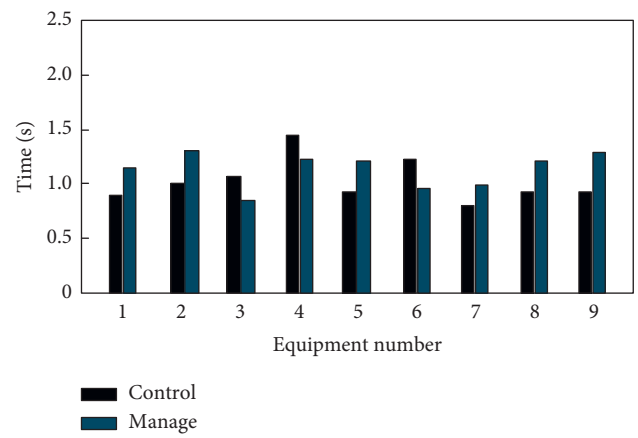

Figure 15: Controlling and managing time.

the smart home control management time of this method is shorter and more efficient

4. Conclusion

In today's society with the continuous development of science and technology and the material life-level unceasing enhancement, people has higher requirement to the household life environment. The experimental results show that the method can improve the equipment control and management situation and communication performance; the algorithm has a better convergence; smart home control task scheduling time is always under 59 ms, smart home control accuracy always stay above 93%, smart home control time shorter, to explain the practical application of this method is better. It can lay a solid foundation for the further development of smart home field.

Data Availability

The raw data supporting the conclusions of this article will be made available by the authors, without undue reservation.

Conflicts of Interest

The authors declare that they have no conflicts of interest regarding this work.

References

[1] S. Bahramara, "Robust optimization of the flexibility-constrained energy management problem for a smart home with rooftop photovoltaic and an energy storage," *Journal of Energy Storage*, vol. 36, no. 3, pp. 102358–102369, 2021.

[2] E. Anthi, L. Williams, A. Javed, and P. Burnap, "Hardening machine learning denial of service (DoS) defences against adversarial attacks in IoT smart home networks," *Computers & Security*, vol. 108, no. 7, pp. 102352–102362, 2021.

[3] Y. U. Hao, Q. Wang, and Z. Wang, "Smart home remote control system based on Internet of Things," *Henan Science and Technology*, vol. 23, no. 14, pp. 27–35, 2020.

[4] X. He, "Design of smart home system based on ZigBee wireless communication technology," *Electrical Technology of Intelligent Buildings*, vol. 14, no. 2, pp. 31–34, 2020.

[5] I. Cviti, M. Periša, D. Perakovic, and B. B. Gupta, "Ensemble machine learning approach for classification of IoT devices in smart home," *International Journal of Machine Learning and Cybernetics*, vol. 12, no. 3, pp. 3179–3202, 2021.

[6] H. Rui and C. Gao, "Neural network-based urban green vegetation coverage detection and smart home system optimization," *Arabian Journal of Geosciences*, vol. 14, no. 13, pp. 1–17, 2021.

[7] C. Gavrila, V. Popescu, M. Fadda, M. Anedda, and M. Murroni, "On the suitability of HbbTV for unified smart home experience," *IEEE Transactions on Broadcasting*, vol. 67, no. 1, pp. 253–262, 2020.

[8] S. Rana, M. T. Rahman, M. Salauddin et al., "Electrospun PVDF-TrFE/MXene nanofiber mat-based triboelectric nanogenerator for smart home appliances," *ACS Applied Materials & Interfaces*, vol. 13, no. 4, pp. 4955–4967, 2021.

[9] S. Arthanat, C. Hong, and J. Wilcox, "Determinants of information communication and smart home automation technology adoption for aging-in-place," *Journal of Enabling Technologies*, vol. 14, no. 2, pp. 73–86, 2020.

[10] V. Hayashi and W. Ruggeiro, "Non-invasive challenge response authentication for voice transactions with smart home behavior," *Sensors*, vol. 20, no. 22, pp. 6563–2579, 2020.

[11] L. Yang, H. Deng, R. P. Liu et al., "Smart home privacy protection based on the improved LSB information hiding," *International Journal of Pattern Recognition and Artificial Intelligence*, vol. 35, no. 12, pp. 1–12, 2021.

[12] T. V. Dang, S. T. Dinh, and X. T. Bui, "Investigation and optimization of power based smart home module integrated with automatic solar tracking system and MPPT techniqu," *Applied Mechanics and Materials*, vol. 889, no. 1, pp. 526–532, 2019.

[13] X. A. Dong, B. Shusong, and A. Ali, "Non–intrusive load disaggregation of smart home appliances using the IPPO algorithm and FHM model," *Sustainable Cities and Society*, vol. 67, no. 1, pp. 102731–102742, 2021.

[14] U. Bermejo, A. Almeida, A. Bilbao-Jayo, and G. Azkune, "Embedding-based real-time change point detection with application to activity segmentation in smart home time series data - ScienceDirect," *Expert Systems with Applications*, vol. 185, no. 15, Article ID 115641, 2021.

[15] Y. Zhang, G. Tian, and H. Chen, "Exploring the cognitive process for service task in smart home: a robot service mechanis," *Future Generation Computer Systems*, vol. 102, no. 1, pp. 588–602, 2020.

[16] H. Yang, R. M. Wong, P. O. Adeso, and M. E. Taylor, "Effects of a computer-based learning environment that teaches older adults how to install a smart home system," *Computers & Education*, vol. 149, no. 2, Article ID 103816, 2020.

[17] Y. H. Lin, "Trainingless multi-objective evolutionary computing-based nonintrusive load monitoring: Part of smart-home energy management for demand-side management," *Journal of Building Engineering*, vol. 33, no. 1, Article ID 101601, 2020.

[18] E. Vrain and C. Wilson, "Social networks and communication behaviour underlying smart home adoption in the UK," *Environmental Innovation and Societal Transitions*, vol. 38, no. 1, pp. 82–97, 2020.

[19] A. Gawanmeh, N. Mohammadi-Koushki, W. Mansoor, H. Al-Ahmad, and A. Alomari, "Evaluation of MAC protocols for vital sign monitoring within smart home environment," *Arabian Journal for Science and Engineering*, vol. 45, no. 12, Article ID 11007, 2020.

[20] S. Sharda, K. Sharma, and M. Singh, "A real-time automated scheduling algorithm with PV integration for smart home prosumers," *Journal of Building Engineering*, vol. 44, no. 1, Article ID 102828, 2021.

[21] B. D. Davis, J. C. Mason, and M. Anwar, "Vulnerability studies and security postures of IoT devices: a smart home case study," *IEEE Internet of Things Journal*, vol. 7, no. 10, pp. 10102–10110, 2020.

[22] F. Ramin, R. Rahim, and K. Theo, "An autonomic IoT gateway for smart home using fuzzy logic reasoner," *Procedia Computer Science*, vol. 177, no. 1, pp. 102–111, 2020.

[23] M. Batool, A. Jalal, and K. Kim, "Telemonitoring of daily activity using accelerometer and gyroscope in smart home environment," *Journal of Electrical Engineering and Technology*, vol. 15, no. 1, pp. 2801–2809, 2020.

[24] V.. Bianchi, P. Ciampolini, and I. De Munari, "RSSI-based indoor localization and identification for ZigBee wireless sensor networks in smart homes," *IEEE Transactions on Instrumentation and Measurement*, vol. 8, no. 2, pp. 566–575, 2019.

[25] M. Fard, J. Y. Chouinard, and B. Lebel, "Rogue device discrimination in ZigBee networks using wavelet transform and autoencoders," *annals of telecommunications-annales des télécommunications*, vol. 76, no. 1, pp. 1–16, 2020.

[26] C. Cengiz, I. E. Kilic, and E. Guler, "On the shear failure mode of granular column embedded unit cells subjected to static and cyclic shear loads," *Geotextiles and Geomembranes*, vol. 47, no. 2, pp. 193–202, 2019.

[27] J. Sun, B. Zhu, and S. O. Traffic, "Auto intelligent entry and start system based on arduino bluetooth module," *Shanxi Architecture*, vol. 45, no. 10, pp. 253–259, 2019.

[28] C. Huang, "Audio control circuit of bluetooth module based on android control," *Microcontrollers & Embedded Systems*, vol. 19, no. 5, pp. 67–71, 2019.

[29] P. P. Saraswala, S. B. Patel, and J. K. Bhalani, "Performance metric analysis of transmission range in the ZigBee network using various soft computing techniques and the hardware implementation of ZigBee network on ARM-based controller," *Wireless Networks*, vol. 27, no. 3, pp. 2251–2270, 2021.

[30] P. Li, Y. Yan, P. Yang, X.-Y. Li, and Q. Lin, "Coexist WiFi for ZigBee networks with fine-grained frequency approach," *IEEE Access*, vol. 7, no. 1, pp. 135363–135376, 2019.

[31] V. Camusy, L. Meiy, C. Enz, and M. Verhelst, "Review and benchmarking of precision-scalable multiply-accumulate unit architectures for embedded neural-network processing," *IEEE Journal on Emerging and Selected Topics in Circuits and Systems*, vol. 9, no. 4, pp. 697–711, 2019.

[32] H. K. Wang, H. C. Huang, and D. Mao, "Multi-carrier data stream transmission path calibration method based on devops," *Electronic Design Engineering*, vol. 27, no. 11, pp. 123–127, 2019.

[33] Z. Tong, W. Li, B. Zhang, F. Jiang, and G. Zhou, "Online bearing fault diagnosis based on a novel multiple data streams transmission scheme," *IEEE Access*, vol. 7, no. 1, pp. 66644–66654, 2019.

[34] F. Li, C. Cui, D. Wang et al., "Privacy-aware secure anonymous communication protocol in CPSS cloud computing," *IEEE Access*, vol. 8, no. 1, pp. 62660–62669, 2020.

[35] C. D. Yeo, M. He, J. Lee et al., "Recovering magnetic domains of nanoscale-mechanically damaged ferromagnetic thin film of information data storage," *Applied Materials Today*, vol. 21, no. 1, Article ID 100825, 2020.

[36] Z. Xu, Y. Wang, and X. Wang, "Research on Optimization of unstructured big data cloud storage combined with blockchain," *Computer Simulation*, vol. 38, no. 7, pp. 304–307, 2021.

Hindawi
Computational Intelligence and Neuroscience
Volume 2022, Article ID 3646264, 11 pages
https://doi.org/10.1155/2022/3646264

Research Article

Research on Quantitative Evaluation of Remote Sensing and Statistics Based on Wireless Sensors and Farmland Soil Nutrient Variability

Weishuai Ji[1] **and Yaqiu Liu**[2]

[1]*College of Information Science and Engineering, Shandong Agricultural and Engineering University, Jinan, Shandong 251100, China*
[2]*College of Resources and Environment, Shandong Agricultural University, Taian, Shandong 271018, China*

Correspondence should be addressed to Weishuai Ji; 2019120320@sdau.edu.cn

Received 9 November 2021; Revised 29 November 2021; Accepted 1 December 2021; Published 19 January 2022

Academic Editor: Yang Gu

The combination of wireless sensor networks and radio technology can form a new type of communication network. The emergence of wireless sensor networks has effectively solved the problems existing in radio technology, but traditional wireless sensor networks and radio technology networks cannot be directly applied to wireless sensors. On this basis, this paper studies the remote sensing of soil nutrient variability in agricultural land using wireless sensors. Due to traditional farmland management and agricultural systems, farmland soil nutrient variability has led to polarization: fertile soil has excess nutrients, reducing the use rate of chemical fertilizers and polluting high-quality farmland. Traditional farming methods can no longer meet the requirements, and modern technology must be used to comprehensively understand the spatiotemporal variability of soil nutrients during plant growth. Remote sensing technology has the advantages of accuracy, speed, economy, and regular monitoring. It provides new ideas and technical guarantees for soil quality evaluation in land development and consolidation projects. This paper also studies the use of statistical quantitative evaluation technology to carry out multidimensional statistical quantification of soil protection function evaluation at a given location. Finally, wireless sensor networks are used to analyze the relationship between several natural factors and quantitative estimation of soil protection. Based on wireless sensor technology, this paper studies the variability of farmland soil nutrients and statistical quantitative evaluation, hoping to lay a foundation for the development of agriculture and statistics.

1. Introduction

In the past few decades, wireless sensor networks have received great attention from academia and industry. Sensor nodes communicate over a short distance through a wireless network and communicate with each other to perform tasks. For soil detection, hundreds or even thousands of sensor nodes can be used to collect data [1]. Due to the low cost of sensor nodes, constant changes in availability, and limited sensor energy, the development of routing protocols suitable for soil detection, extending the life of the network, and increasing the utilization rate are of great significance to the promotion of agricultural development [2]. On this basis, this article investigates the variability of farmland soil nutrients. China still mainly adopts traditional farmland management measures; that is, the same fertilization measures are adopted instead of considering the spatial distribution of farmland soil nutrient variability, which results in fertility [3]. The oversupply of nutrients in the plots caused unnecessary waste, while also reducing fertilizer utilization and causing large-scale agricultural nonpoint source pollution [4]. On the barren land, the supply of nutrients was limited and could not meet the growth needs of crops [5]. In view of the complex soil types and extensive soil information, traditional farmland management methods can no longer meet the requirements [6]. To achieve effective fertilization and production management, it is necessary to use modern science and technology to understand the variable characteristics of farmland nutrients. The successful application of remote sensing technology in soil organic matter

monitoring, soil moisture monitoring, vegetation index, and other aspects has brought new ideas and technical guarantees for soil evaluation [7]. According to the quality of development and land consolidation and remote sensing based on the variability of soil nutrients in farmland, this paper also conducts research on statistical quantitative evaluation [8]. China continues to implement land development and consolidation projects and carries out acceptance evaluation of real estate development and consolidation projects [9]. Quantitative assessment of soil quality after completion becomes more and more important. At present, it is necessary to strengthen the research on soil quality evaluation after land consolidation. On the one hand, soil quality evaluation requires a lot of manpower, material resources, and financial resources [10]. On the other hand, the standards for soil quality evaluation are not standardized, so this work is rarely carried out [11]. At present, the evaluation of development and land consolidation mainly adopts artificial field analysis and statistical quantitative evaluation methods [12]. This kind of evaluation method cannot be comprehensively evaluated, and it is time-consuming, laborious, and costly and lacks objective comparison and the macroscopic nature of evaluation [13]. The above research can contribute to further in-depth research on quantitative science and remote sensing technology [14]. It can also enrich China's land development and consolidation theories, accelerate the development of land development theoretical systems and the adoption and evaluation of consolidation, and promote the development of precision agriculture and digital agriculture [15].

2. Related Work

The literature proposes that the application of remote sensing technology to wireless sensors creates a wireless sensor network, which overcomes the limitations of traditional wireless sensor networks. The sensor node evaluates the conditions independently or in cooperation with other nodes and uses the allowed channel to complete data transmission [16]. If nutrient activity is detected in the main user's soil, the remote sensing technology immediately leaves the current channel [17]. The literature states that agricultural land is an extremely precious natural resource, with a slow origin time, a small amount, and uneven spatial distribution [18]. From a natural point of view, its formation is affected by the five elements of parent material, biology, climate, topography, and time [19]. These five factors have their own characteristics and properties, but they collectively control the formation of soil development and characteristics from different angles [20]. The literature discusses the scheme of combining wireless sensor network technology and remote sensing technology for environmental geological monitoring of mining areas, and in view of the problems and difficulties faced by the scheme, it proposes the use of these two technologies to establish a dynamic model of vegetation net initial value productivity (NPP) in the mining area. The literature shows that the soil protection module of the remote sensing technology model conducts quantitative research on soil protection in a certain area, so that its spatial attributes are visible in three dimensions, and uses soil-based detectors to reveal the relationship between soil protection and various natural functions [21]. The literature introduces the research on the temporal and spatial variability of nutrients in the soil, which is an urgent problem to be solved in agronomy, forestry, horticulture, ecology, and other disciplines [22]. Research has also developed from qualitative research to quantitative research and expanded from the original classical statistical methods to quantitative methods. Compared with classical statistical research, variables should be purely random and statistical research should involve regional variables. The literature shows that the spatial variability of soil nutrients has a large-scale effect, and soil sampling at different scales demonstrates the corresponding spatial structure characteristics and changing laws. The spatial variability of the same trait varies greatly at different scales, and large-scale studies will examine the structural characteristics of small-scale soils. In order to accurately and systematically record soil variability, soil scholars gradually try to study the variability of soil nutrients from different perspectives.

3. Principles of Wireless Sensors and Remote Sensing Technology

3.1. Wireless Sensor. Wireless sensor networks use independent sensor nodes and wireless technology to communicate with other nodes to relay information to appropriate destinations. After the sensor node processes the data through its internal processor, it sends the integrated data to the next hop node. Research on wireless sensor networks has been conducted for more than 30 years and is rapidly expanding and improving to meet the needs of military applications.

The basic idea of WSN is that the capacity of each individual sensor node is limited, but the overall performance of the entire network is sufficient to perform the required tasks. The network topology of traditional WSN is shown in Figure 1.

Some characteristics of wireless sensor networks are as follows: First, compared with some deterministic networks, the nodes of sensor networks are used randomly. Second, wireless sensor networks are designed for specific scenarios, so the types and numbers of sensors equipped in different scenarios are also different. For example, building monitoring requires only a small number of sensors, which can be placed separately.

3.2. Remote Sensing Image Processing

3.2.1. Geometric Precision Correction of Images. The point selection technology provided by image registration, that is, geometric correction, includes "(image to image)" and "(image to reference map)." In this experiment, the ground control point coordinates are measured on the spot and the examples are the first two methods of selecting points.

The polynomial correction model is as follows:

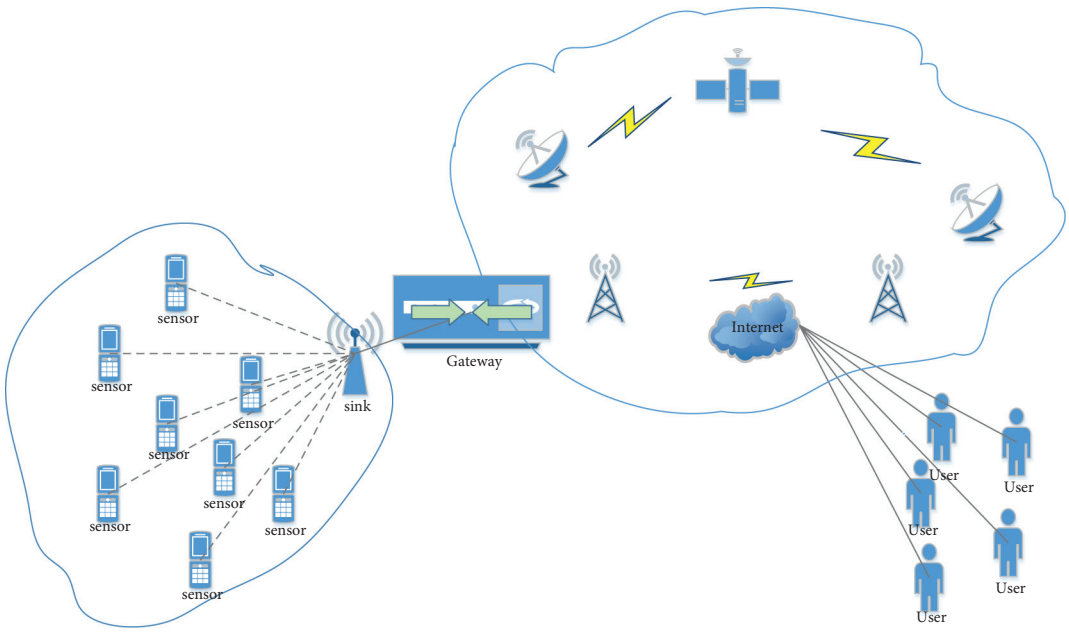

Figure 1: WSN topology.

$$x = F_x(u, v) = \sum_{i=0}^{n} \sum_{j=0}^{n-i} a_{ij} u^i v^j, \tag{1}$$

where a_{ij} and b_{ij} are undefined coefficients, n is the polynomial order, and F_x and F_y are thedistortion correction function.

3.2.2. Jurisdiction Calibration. Radiometric calibration refers to quantifying the relationship between the brightness value in the corresponding field of view of the remote sensing sensor and the digital quantitative output. Therefore, the following relationship exists between the received radiation intensity and its data value:

$$L_\lambda = \left(\frac{\mathrm{LMAX}_\lambda - \mathrm{LMIN}_\lambda}{\mathrm{Q_{cal}\,max}}\right)\mathrm{Q_{cal}} + \mathrm{LMIN}_\lambda, \tag{2}$$

where L_λ is the radiation intensity received by the sensor (W/($\mathrm{m}^2 \cdot \mu\mathrm{m} \cdot \mathrm{sr}$)), $\mathrm{Qc_{al}}$ is the gray value of the pixel, and $\mathrm{Q_{calmax}}$ is the maximum DN value.

Spectral reflectivity r outside the atmosphere at each band is as follows:

$$r = \frac{\pi \mathrm{Ld}^2}{E\cos(\theta)}. \tag{3}$$

Here, E is the average spectral irradiance outside the atmosphere of the corresponding area (unit: $\mathrm{W} \cdot \mathrm{m}^{-2} \cdot \mu\mathrm{m}^{-1} \cdot \mathrm{sr}^{-1}$), d is the astronomical unit of the distance between the sun and the Earth, and θ is the zenith angle of the sun (unit: Rad).

Atmospheric external albedo α_{toa} is as follows:

$$a_{\mathrm{toa}} = \sum c_i r_i \ (i = 1, 2, 3, 4, 5, 6, 7). \tag{4}$$

Here, c_i is the weight coefficient of the i-th band.

Ground albedo a is as follows:

$$a = \frac{a_{\mathrm{toa}} - a_{\mathrm{path}}}{\tau^2 \mathrm{sw}}. \tag{5}$$

Here, sw is the one-way transmission of the atmosphere and a_{path} is the radiation range (value between 0.025 and 0.04).

3.2.3. Correction of Radiation Errors Caused by the Sun's Altitude. Generally, the following relationship can be used to solve the radiation error correction caused by the sun's altitude:

$$f(x, y) = \frac{g(x, y)}{\sin\theta}. \tag{6}$$

In this equation, θ is the angle of the sun's height, $g(x, y)$ is the pixel coordinate of the sun's image at the elevation angle, and $f(x, y)$ is the pixel coordinate of the image obtained under direct sunlight.

3.2.4. Atmospheric Correction. The goal of atmospheric correction is to eliminate these effects caused by the atmosphere and light in remote sensing images and to obtain true reflectance data of ground objects.

$$L_\lambda = \frac{X_\lambda}{A} + B, \tag{7}$$

$$P_{\mathrm{TOA}} = \frac{\pi L_\lambda d^2}{\mathrm{ESUN}_\lambda \cos(\theta_s)}, \tag{8}$$

where X_λ is the DN value of each band, parameter A is the absolute calibration gain of the image product after radiation correction, L_λ is the brightness of each band, d is the astronomical distance between the sun and the

Earth, parameter B is the calibration offset of the image product, θ_s is the zenith angle of the sun, and ESUN is the average solar illuminance of the outer atmosphere at wavelength λ.

4. Statistical Quantitative Evaluation Analysis and Application Research on the Variability of Farmland Soil Nutrients

4.1. Principles of the Quantitative Evaluation of Soil Quality. The InVEST model is a model for evaluating ecosystem service functions. It includes three main modules and several submodules of terrestrial, freshwater, and marine ecosystems. The results of the work are visually presented in the form of a map, which helps to better understand the nature of ecosystem services. The difference between erosion and actual erosion reflects the reduction in potential erosion in each block. The latter means that the product of the amount of sand and the degree of sediment retention indicates the ability of the grid block to intercept the sediment or other sediments on the slope. The USLE equation ignores this important hydrological process. It is calculated as follows:

$$\mathrm{SEDRET}_x = \mathrm{RKLS}_x - \mathrm{USLE}\,x + \mathrm{SEDR}_x, \tag{9}$$

$$\mathrm{PKLS}x = Rx \cdot Kx \cdot \mathrm{LS}x, \tag{10}$$

$$\mathrm{USLE}\,x = Rx \cdot Kx \cdot \mathrm{LS}x \cdot Cx \cdot Px, \tag{11}$$

$$\mathrm{SDRE}x = \mathrm{SE}x \sum\nolimits_{y=0}^{x-1}, \tag{12}$$

where SEx is the sediment retention efficiency in the x grid, SEDRETx and SEDRx are the soil retention and sediment retention in the x grid, and SEz is the sediment retention efficiency in the z grid. RKLSx is the potential soil loss in grid x based on terrain and climatic conditions, and USLEx and USLEy are the actual erosion values of grid x and its upstream grid y.

Geographic detectors are divided into four types: factor, ecology, risk, and interaction. The factor detector is designed to detect the spatial differentiation of the dependent variable and the degree of interpretation of the spatial differentiation Y, expressed by the q value, and its expression is as follows:

$$q = 1 - \frac{\sum_{a=1}^{B} M_{nc_d^2}}{M_{c^2}} = 1 - \frac{\mathrm{DDE}}{\mathrm{DDR}}, \tag{13}$$

$$\mathrm{DDE} = \sum_{a=1}^{B} M_{nc_d^2}, \tag{14}$$

$$\mathrm{DDR} = M_{C^2}. \tag{15}$$

Here, $a = 1, \ldots, B$ is the division of variable Y or factor X and DDE and DDR are the sum of the intralayer variance and the total variance of the entire region, respectively.

Ecological detector: it is used to judge whether there are significant differences in the influence of two factors, b_1 and b_2, on the spatial distribution of Y attributes, which is characterized by the S statistic:

$$S = \frac{A_{x1}(A_{x2} - 1)\mathrm{DDE}_{x1}}{A_{x2}(A_{x1} - 1)\mathrm{DDE}_{x2}}, \tag{16}$$

$$\mathrm{DDE}_{x1} = \sum_{a=1}^{B1} M_{nc_d^2}, \tag{17}$$

$$\mathrm{DDE}_{x2} = \sum_{a=1}^{B2} M_{nc_d^2}, \tag{18}$$

where AXO and An represent the sample sizes of factors X_1 and X_2, respectively, and DDEn1 and DDE2 are the sum of the intralayer variances of the layer formed by X_1 and X_2, respectively. The null hypothesis H_0 is DDEn = DDE$_{X2}$. If H_0 deviates from the significance level c, this means that X_1 and X_2 are significantly different in the spatial distribution of Y.

Risk detector: it is used to determine whether there is a significant difference in the attribute mean of the two subregions and uses the t statistic to test

$$t_{\overline{T}_{g=1} - \overline{T}_{g=2}} = \frac{\overline{T}_{g=1} - \overline{T}_{g=2}}{\left[\mathrm{Csv}\left(\overline{T}_{g=1}\right)/m_{g=1} + \mathrm{Csv}\left(\overline{T}_{g=2}\right)/m_{g=2}\right]^{1/2}}, \tag{19}$$

where T_e is the average value of the attributes in the subdomain g, m is the number of samples in the subrange g, and Csv is the variance.

4.2. Soil Data Processing

4.2.1. Rainfall Erosivity R Factor. The greater the precipitation erosion coefficient, the greater the intensity of soil erosion. The methods to obtain this coefficient are listed:

(1) The classic algorithm is as follows:

$$R = E \times I_{30}, \tag{20}$$

where R is the erosion activity of rain, E is the total kinetic energy of rain, and I_{30} is the rainfall intensity within 30 minutes.

This model has extremely high requirements for data sources and must be based on a large amount of precipitation data. It has limitations in the complexity of obtaining kinetic energy and precipitation rate data, and its relatively narrow scope limits further applications.

The modified formula for the calculated R factor formula is as follows:

$$R = \sum_{i=1}^{12}\left[1.735 \times 10^{\left(1.5\lg Ti^2/T - 0.8188\right)}\right] \times 17.02, \tag{21}$$

where T is the annual average rainfall (mm) and Ti is the monthly rainfall (mm).

(2) We established a power index structure daily rainfall erosivity model:

$$\mathrm{Rds} = R\sum_{i=1}^{k}(\mathrm{Ti})^{\lambda}. \tag{22}$$

k represents the number of days, Ti represents the precipitation of the i-th day, Ti ≥ 12 mm is required; otherwise, the value is 0, Ty12 is the annual average rainfall with a daily rainfall ≥12 mm, and Td12 is the daily average rainfall with a daily rainfall ≥12 mm.

(3) We established the national daily replacement model (half-month rainfall erosivity model):

$$\mathrm{Mi} = \alpha\sum_{j=1}^{k}(\mathrm{Dj})^{\beta}. \tag{23}$$

Here, Mi is the erosion activity value in the i-th half-month period (MJ·mm·hm^{-2}·h^{-1}), α and β are the model parameters, k represents the number of days in a half-month, and Dj represents the j-th day of the first half-month. The daily precipitation requires precipitation ≥12 mm.

The numbers α and β represent model parameters reflecting the characteristics of precipitation in the area. According to the daily precipitation data, the values of α and β in the station are estimated according to

$$\beta = 0.8363 + \frac{18.144}{P(d12)} + \frac{24.455}{P(y12)}, \tag{24}$$

$$\propto = 21.586\beta^{-7.1891}. \tag{25}$$

This method uses long-term continuous daily rainfall as the main unit of data. It is generally considered to be the most accurate and most representative method of the actual rainfall erosion rate, and long-term continuous data are required.

According to the applicability of the model, combined with the existing meteorological and precipitation data, the final method of calculating the R factor is as follows:

$$R = \sum_{i=1}^{12} 73.989 \times \left(\frac{P_i^2}{P_a}\right)^{0.7387}. \tag{26}$$

Here, R is the erosion activity value (MJ·mm·hm^{-2}·h^{-1}), P_i is the precipitation of the i-th month (mm), and P_a is the average annual precipitation (mm).

The latitude and longitude of a certain area and its 6 surrounding counties and cities and the R value of precipitation erosion are shown in Table 1.

This paper uses the monthly precipitation data of a certain region and 6 counties and cities over 35 years from 1986 to 2020 to calculate the annual value of precipitation erosivity and the value of the annual average rainfall erosivity factor.

On this basis, the Kriging interpolation method was used on the GIS platform to generate an R layer based on the 6 counties from 1986 to 2020, and then, the mask was extracted to obtain the spatial distribution of the R factor of the A district and counties, as shown in Figure 2.

Figure 2 shows that the R value gradually decreases from south to north. There are high-value areas adjacent to the southwest and southeast of area A and high-precipitation areas D and E; a low value area appears in the dry hot area adjacent to the northwest of the valley.

4.2.2. Soil Erodibility K Factor. The soil erodibility K factor reflects the difficulty of separating and transporting soil with different particle sizes, and the difference in the K factor reflects the sensitivity of different types of soil to erosion. The K value can be obtained by querying data, actual measurement, and calculation. The most common method for querying data is the Vischmeier nomogram. This method requires more data on soil structure coefficients and permeability levels. At present, China's soil data are mainly based on the results of the national soil census, which is far from the data requirements. At the same time, reclamation and plowing will change the nature of the soil, so it is impractical to directly use this method. The actual measurement includes the standard battery measurement method and physical and chemical properties measurement with the highest accuracy, but time-consumption, cumbersome procedures, equipment limitations, rainfall, and other unforeseen factors are drawbacks.

The spatial distribution of the soil erosion K factor in a certain area is shown in Figure 3.

The soil erosion factor of Zone A ranges from 0.0375116 to 0.0410254, with an average of 0.0392685. From the macrodistribution of the soil erosion K value in China's water erosion area, it can be seen that the soil erosion coefficient K in a certain area is 0.0484–0.0091, with an average value of 0.0292; compared with this value, the calculation result of the soil erosion rate coefficient K in circle A is slightly higher than the provincial average. The north and northeast are bordered by the Yuanjiang River, with large dry heat evaporation and little precipitation. The conditions of erosion (precipitation) are not perfect, resulting in small and uniform K.

4.2.3. P Factor of Soil and Water Conservation Measures. Common soil and water protection measures include reducing the slope, transforming the subsoil, and building ponds and dams. These measures mainly control soil erosion by affecting speed and flow. Among them, reducing the slope can effectively reduce water flow, and the construction of ponds and dams can adjust and reduce the flow. These measures are effective in reducing soil erosion and promoting soil protection.

The calculation and verification of the soil conservation function of county A based on the InVEST model are shown in Table 2.

The current research on the P value is mainly based on different land use types; due to the different actual

Table 1: Information on latitude and longitude and rainfall erosivity R value of a certain area and its 6 surrounding counties and cities.

Area	Longitude (E)	Dimensions (N)	R factor value
Area A	102.824354	23.225596	4834
Area B	102.380196	23.367038	4094
Area C	102.823447	23.631394	3944
Area D	103.234147	22.787252	8784
Area E	102.403306	22.995532	7806
Area F	103.156728	23.377792	4987

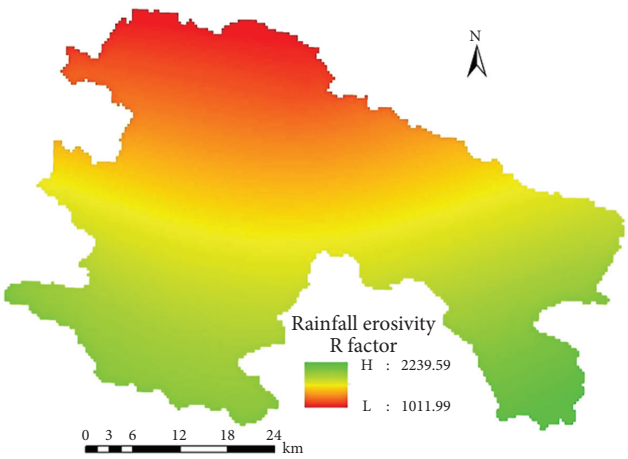

Figure 2: Spatial distribution of the R factor of rainfall erosivity.

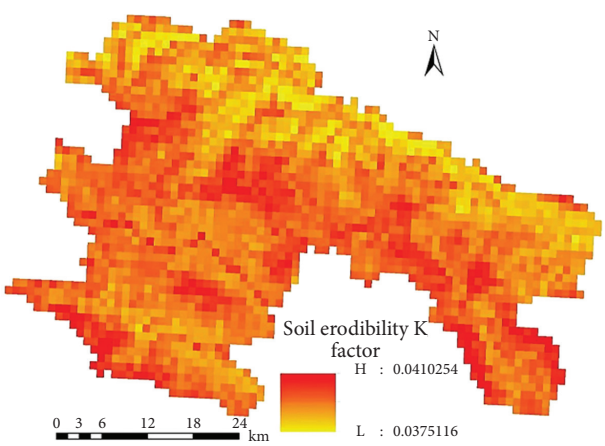

Figure 3: Spatial distribution of the soil erodibility K factor in a certain area.

conditions in the study area, the P value of the same land use type in different areas is different. When calculating the P factor, it is necessary to make extensive reference to related disciplines or similar research topics and then combine actual research to determine it. Due to its particularity, the P factor has a high degree of subjective flexibility when assigning values, so it is considered to be the most difficult to determine in the InVEST model. Area A is a mountainous area in southwest China, with a lot of deep and steep slopes, heavy rainfall, and excessive soil erosion. Soil protection measures such as afforestation, terrace construction, contour farming, and improvement of irrigation and drainage systems are adopted locally.

Table 2: Calculation and verification of the soil conservation function in a certain area and county based on the InVEST model.

Land use type	C value	P value
Paddy field	0.06	0.06
Dry land	0.05	0.31
Woodland	0.03	0.99
Bush	0.03	0.99
Other woodlands	0.02	0.99
High coverage grassland	0.05	0.99
Low coverage grassland	0.18	0.99
Canal	0.15	0.01
Reservoir pond	0.21	0.01
Beach	0.02	0.06
Urban land	0.08	0.01
Rural settlement	0.07	0.01
Other construction lands	0.06	0.01

4.3. Evaluation and Characteristics of Soil Organic Matter

4.3.1. Descriptive Statistical Characteristics of the Spatial Variability of Soil Nutrients at Different Scales. The statistical characteristics of soil available nutrients at different sampling scales are shown in Table 3.

It can be seen from Table 3 that on the sampling scale, AP has the highest change intensity, followed by AK, and AN has the lowest change intensity; on the field scale, AP shows the largest change intensity, followed by AN, and AK shows the smallest change intensity; on the plot scale, AN has the largest change intensity, followed by AP, and AK has the smallest change intensity.

4.3.2. Spatial Autocorrelation Characteristics of the Spatial Variability of Soil Nutrients at Different Scales. The model parameters of the semivariance function soil nutrient index are shown in Table 4.

At the county level, the AN, AP, and AK regions are the largest; at the field scale, the range is reduced by 118.31 m, 55.41 m, and 112.21 m, respectively; at the block scale, the range further drops to 18.61 m, 43.31 m, and 27.61 m, leading to drastic changes in small-scale soils AN, AP, and AK and significantly reducing their scope.

4.3.3. Scale Effect of Spatial Variability of Soil Nutrients. The fragmentation degree of the soil available nutrient map at different sampling scales is shown in Table 5.

The maximum effective phosphorus PD value is 1.18, and the distribution is relatively scattered. The main reason is that AP is more susceptible to random factors, which makes AP distributions disjoint, and has obvious local characteristics.

The spatial distribution of available nutrients at different sampling scales is shown in Figure 4.

It can be seen from the spatial distribution of nutrients that at the county level, except for a small part that is in a barren state, the alkali hydrolyzed nitrogen is continuously distributed in the soil, and most of the rest are at an average level.

Table 3: Statistical characteristics of soil available nutrients at different sampling scales.

Scale	Variable	Min ($mg{\cdot}kg^{-1}$)	Max ($mg{\cdot}kg^{-1}$)	Mean ($mg{\cdot}kg^{-1}$)	SD ($mg{\cdot}kg^{-1}$)	Ske	Kur	sig	Coefficient of variation (%)	Distribution type
County	AN	9.01	169.01	80.83	21.33	0.44	0.83	0.07	26.37	N
	AP	1.01	93.01	23.08	14.21	1.38	2.53	0.04	61.48	LN
	AK	24.01	553.01	177.35	81.76	1.27	2.12	0.12	46.11	LN
Field	AN	16.83	126.88	56.12	24.61	0.88	1.03	0.66	43.85	N
	AP	19.58	133.86	55.44	29.08	1 .05	0.37	0.06	52.42	N
	AK	134.08	373.17	252.85	70.59	−0.13	−1.28	0.32	27.93	N
Plot	AN	15.28	264.47	88.14	47.72	1.06	1.58	0.37	54.12	N
	AP	15.33	153.44	63.38	29.23	0.75	0.34	0.63	46.12	N
	AK	170.12	669.83	308.87	80.42	0.56	2.86	0.17	26.04	LN

Table 4: Parameters of the semivariance function model of the soil nutrient index.

Scale	Variable	Theoretical model	NuggetC_o	Sill$C_o + C$	Nugget/Sill (%)	Range (m)	Decisive factor R^2	Residual (RSS)
County	AN	Exponential	0.00235	0.01549	15.13	410.01	0.429	9.73×10^{-6}
	AP	Exponential	0.00891	0.07851	11.33	320.01	0.611	5.68×10^{-5}
	AK	Exponential	0.00582	0.03245	17.92	390.01	0.638	1.96×10^{-5}
Field	AN	Gaussian	0.00011	0.11821	0.09	118.31	0.424	6.16×10^{-4}
	AP	Exponential	0.00011	0.04061	0.26	55.41	0.958	2.41×10^{-7}
	AK	Gaussian	0.00002	0.01573	0.07	112.21	0.558	7.57×10^{-6}
Plot	AN	Exponential	0.00241	0.05861	4.11	18.61	0.26	3.75×10^{-5}
	AP	Exponential	0.00351	0.04631	7.57	43.31	0.731	1.58×10^{-5}
	AK	Exponential	0.00154	0.01107	13.84	27.61	0.362	8.15×10^{-7}

Table 5: Fragmentation degree of soil available nutrient map at different sampling scales.

Scale	Variable	Number of plaques NP (pieces)	Plaque density PD ($pcs{:}hm^{-2}$)
County	AN	75	0.16
	AP	116	0.22
	AK	89	0.17
Field	AN	13	0.23
	AP	18	0.36
	AK	14	0.25
Plot	AN	48	1.75
	AP	33	1.18
	AK	18	0.71

The corresponding curve diagram of the measured sample point of the soil organic matter content measured at the sampling point on November 2, 2020, is shown in Figure 5.

It can be seen from the obtained data that this paper adopts the method of polynomial modeling, combined with comparative experiments for research, selects one of the sample points of polynomial fitting, and uses the sample point as the control point.

The adjustment curve of soil organic matter content and reflectance at the image sampling point on November 2, 2020, is shown in Figure 6.

We select one of the sample points for polynomial fitting and check the sampling points, and the accuracy is similar, which proves that the model is very accurate and can be used to invert the soil organic matter in the entire area.

The statistical comparison table of the percentage of organic matter in a certain area in the three periods is given in Table 6.

Table 6 shows the distribution of organic matter content in the test area during the three time periods. The results show that the results of remote sensing inversion of organic matter are consistent with those of the organic matter content measured by field sampling. After land consolidation, the organic matter content in the experimental area is mainly distributed in the plains and above.

The statistical comparison table of the percentage of organic matter in a certain area in the three periods is given in Table 7.

Statistics for the distribution of organic matter over the three time periods in the study area show that the remote sensing inversion results of organic matter in the defined test area are consistent with the organic matter data obtained by field sampling. It can be seen from Table 7 that after land development and consolidation in a certain experimental area, soil fertility has been greatly improved, soil quality has been significantly improved, and the effect of land development and consolidation has been significant.

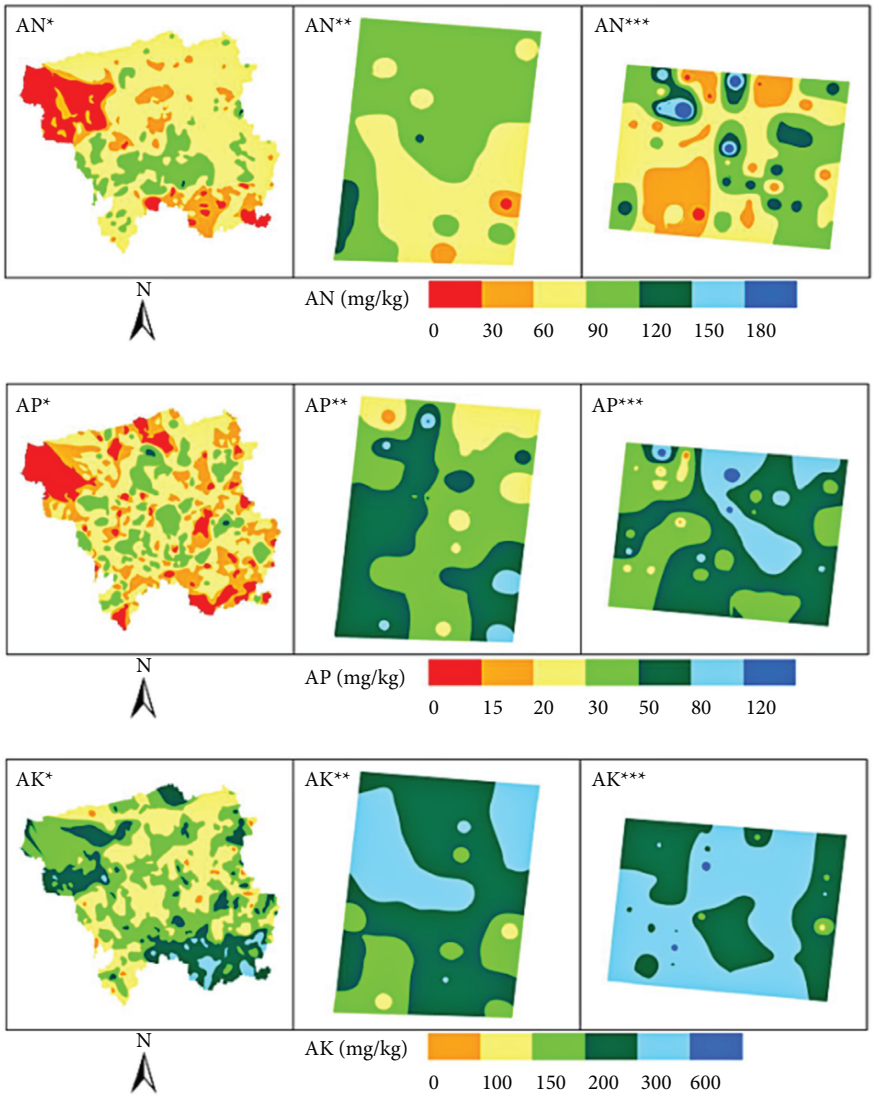

Figure 4: The spatial distribution of available nutrients at different sampling scales. (a) At the AN sampling scale of 0–180. (b) At the AP sampling scale of 0–120. (c) At the AK sampling scale of 0–600.

4.3.4. BP Neural Network Inversion Model. The BP neural network is composed of input layer, hidden layer, and output layer.

The cumulative credibility of the first six principal components is shown in Table 8.

The 26 samples in a certain experimental area are divided into a prediction set and a verification set. There are 15 sets of predictions and 9 sets of verifications. The spectral band of the sample is calculated using the full spectrum, which requires a large amount of calculation and has nothing to do with the composition of the sample. The principal component analysis method can fully reflect the information of the original multiwavelength variables and perform principal component analysis of the prediction sample and the verification set.

The statistical comparison table of organic matter content in a certain area in two periods is shown in Table 9.

The inversion results in Table 9 are approximately equal to the inversion results of the polynomial inversion model. The results showed that the content of soil organic matter in this area increased significantly after land consolidation, which significantly improved soil fertility and quality.

4.4. Research on the Analysis Method of Soil Nutrient Variability in Farmland. Research in recent years has shown that the method of combining multisource satellite images and multitemporal images with laboratory spectral analysis and ground-based in situ research is the development trend of soil organic matter measurement.

Remote sensing is obviously the preferred method for estimating the surface temperature, because the main feature of remote sensing technology is that it can provide a wide range of data and images and use satellite data to calculate the surface temperature. Sensor technology is the theory and method for detecting satellite hot air duct data. At present, the remote sensing algorithms for surface temperature mainly include single-channel and multichannel satellite sensor infrared channel methods, infrared thermometer to

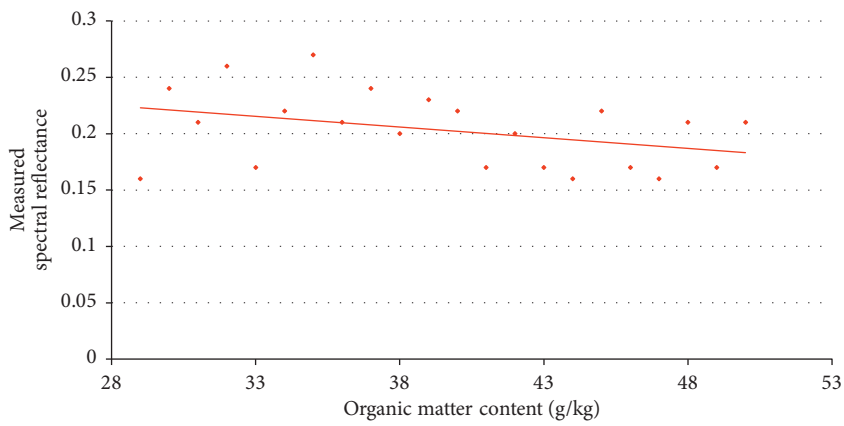

Figure 5: Fitting curve of soil organic matter content and measured sample point reflectivity on November 2, 2020. $y = -0.0002x2 + 0.0019x + 0.2098$ (fitness:0.835).

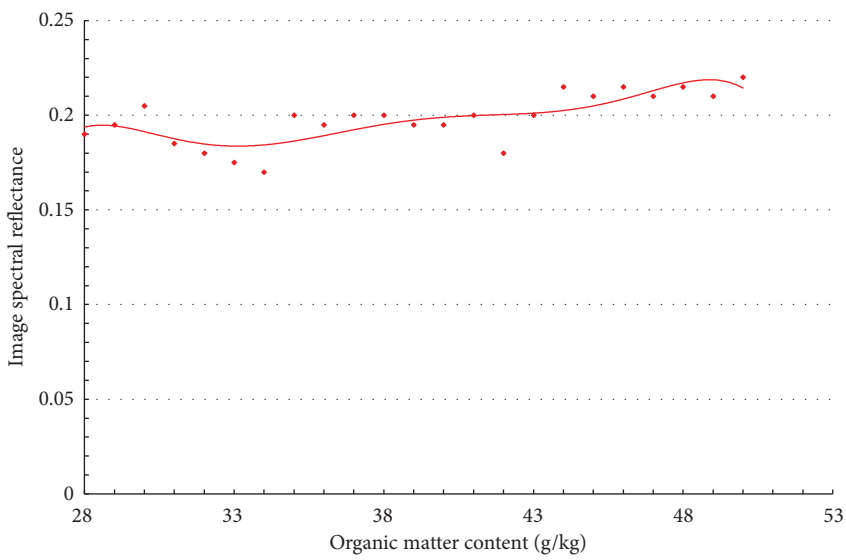

Figure 6: Fitting curve of soil organic matter content and image sample point reflectivity on November 2, 2020. $y = 5E - 0.5x^3 + 0.0017x^2 - 0.0163x + 0.2202$ (fitness:0.806).

Table 6: Comparison table of the percentage of organic matter content in a certain area in three periods.

Organic matter content (%)/time	<10	[10–20)	[20–30)	[30–40]	>40
July 17, 2014	16.523	32.592	31.087	8.958	10.841
November 2, 2019	3.407	6.554	14.056	30.072	45.912
June 16, 2020	6.666	13.304	10.011	40.262	29.756

Table 7: Comparison table of the percentage of organic matter content in a certain area in three periods.

Organic matter content (%)/time	<10	[10–20)	[20–30)	[30–40]	>40
July 2, 2003	76.527	10.592	6.82	4.924	1.123
November 27, 2019	37.407	46.552	8.967	4.715	2.356
June 7, 2020	60.666	17.334	13.011	5.911	3.075

measure surface temperature, and microwave remote sensing to monitor the surface temperature. At present, the use of infrared thermal data to monitor surface temperature is widely higher level.

Soil surface evapotranspiration is an important part of both surface heat balance and ecosystem water balance. The water balance determines the quantity and spatial distribution of water resources, and the heat balance between

Table 8: Cumulative credibility of the first six principal components.

Main ingredient	Cumulative reliability of the prediction set (%)	Cumulative credibility of the validation set (%)
P01	99.427	99.961
P02	99.576	99.937
P03	99.424	99.566
P04	99.821	99.347
P05	99.967	99.522
P06	99.978	99.431

Table 9: Statistical comparison table of organic matter content in a certain area in two periods.

Organic matter content (%)/time	<10	[10–20)	[20–30)	[30–40]	>40
July 17, 2015	16.724	32.497	30.177	9.246	11.357
November 2, 2020	3.336	6.676	13.348	30.037	46.602

water and soil is very large. It determines the weather and climate change, which in turn determines the soil quality and the formation and development of ecosystems. Remote sensing technology is currently used to monitor surface evapotranspiration. There are mainly single-layer models and double-layer models, especially the SEBAL model based on the principle of energy balance equation. Its outstanding advantage is that it has a strong physical foundation and is suitable for different climates. The vegetation index is a simple and effective indicator to characterize the vegetation coverage and plant growth status. In recent years, with the rapid development of remote sensing technology, the use of remote sensing technology to extract the vegetation index has been relatively expanded. In the field of ecology, the vegetation index examines ecosystems on a global scale, and the results of patch-level ecosystem research are extended to the global space.

5. Conclusion

A wireless sensor network consists of sensor nodes with radio functions and is a very promising solution in the era of the Internet of Things. Although remote sensing technology eliminates the drawbacks of using it, there are still energy and equipment problems. Therefore, it is necessary to find new ways to solve the problems of energy and remote sensing technology. Through the development of related algorithms, this paper mainly solves the problems of power consumption, interference, intercluster communication, and channel stability in wireless sensor networks. The soil conservation module calculates and analyzes the functional strength of soil protection in a certain area in 2020, obtains the spatial distribution of soil environmental resistance, and compares the obtained results with the coefficient of determination to test the accuracy of the research. In terms of quantitative statistics, this article uses a combination of classical statistics and geostatistics, in addition to a geostatistical analysis model of remote sensing technology to examine specific areas. Obviously, after land consolidation, the fertility of the soil in the rectified area has increased, the content of related organic matter has also increased significantly, and the fertility and quality of the soil have been improved.

Data Availability

The dataset can be accessed upon request to the corresponding author.

Conflicts of Interest

The authors declare that they have no conflicts of interest.

References

[1] A. Alsohaily and E. S. Sousa, "Dynamic spectrum management in multi-radio access technology (RAT) cellular systems," *IEEE Wireless Communications Letters*, vol. 3, no. 3, pp. 249–252, 2014.

[2] K. T. K. Cheung, S. Shaoshi Yang, and L. Hanzo, "Achieving maximum energy-efficiency in multi-relay OFDMA cellular networks: a fractional programming approach," *IEEE Transactions on Communications*, vol. 61, no. 7, pp. 2746–2757, 2013.

[3] A. Chinnasamy, B. Sivakumar, and P. Selvakumari, "Minimum connected dominating set based RSU allocation for smartCloud vehicles in VANET," *Cluster Computing*, vol. 2210 pages, 2018.

[4] J.-P. Crouzeix and J. A. Ferland, "Algorithms for generalized fractional programming," *Mathematical Programming*, vol. 52, no. 1–3, pp. 191–207, 1991.

[5] D. Das, R. Misra, and A. Raj, "Approximating geographic routing using coverage tree heuristics for wireless network," *Wireless Networks*, vol. 21, no. 4, pp. 1109–1118, 2015.

[6] T. Daxin, C. Liu, X. Duan et al., "A distributed position-based protocol for emergency messages broadcasting in vehicular ad hoc networks," *IEEE Internet of Things Journal*, vol. 5, no. 2, pp. 1218–1227, 2018.

[7] J. M. Duarte, T. Braun, and L. A. Villas, "MobiVNDN: a distributed framework to support mobility in vehicular named-data networking," *Ad Hoc Networks*, vol. 82, pp. 77–90, 2018.

[8] M. Hajiaghayi, M. Dong, and B. Liang, "Jointly optimal channel and power assignment for dual-hop multi-channel multi-user relaying," *IEEE Journal on Selected Areas in Communications*, vol. 30, no. 9, pp. 1806–1814, 2012.

[9] K. F. Hasan, Y. Feng, and Y.-C. Tian, "GNSS time synchronization in vehicular ad-hoc networks: benefits and

feasibility," *IEEE Transactions on Intelligent Transportation Systems*, vol. 99, pp. 1–10, 2018.

[10] J. Huang, V. Subramanian, R. Agrawal, and R. Berry, "Joint scheduling and resource allocation in uplink OFDM systems for broadband wireless access networks," *IEEE Journal on Selected Areas in Communications*, vol. 27, no. 2, pp. 226–234, 2009.

[11] M. Ismail, A. Abdrabou, and W. Zhuang, "Cooperative decentralized resource allocation in heterogeneous wireless access medium," *IEEE Transactions on Wireless Communications*, vol. 12, no. 2, pp. 714–724, 2012.

[12] M. Ismail, A. T. Gamage, W. Zhuang, and X. S. Shen, "Energy efficient uplink resource allocation in a heterogeneous wireless medium," in *Proceedings of the IEEE ICC*, pp. 5275–5280, Sydney, NSW, Australia, June 2014.

[13] J. Jeong, S. Guo, Y. Gu, T. He, and D. H. C. Du, "Trajectory-based data forwarding for light-traffic vehicular ad hoc networks," *IEEE Transactions on Parallel and Distributed Systems*, vol. 22, no. 5, pp. 743–757, 2011.

[14] J. Jiang, M. Peng, K. Zhang, and L. Li, "Energy-efficient resource allocation in heterogeneous network with cross-tier interference constraint," in *Proceedings of the IEEE PIMRC Workshops*, pp. 168–172, London, UK, September 2013.

[15] S. Kim, B. G. Lee, and D. Park, "Energy-per-bit minimized radio resource allocation in heterogeneous networks," *IEEE Transactions on Wireless Communications*, vol. 13, no. 4, pp. 1862–1873, 2014.

[16] S. Lakshminarayana, M. Assaad, and M. Debbah, "Transmit power minimization in small cell networks under time average QoS constraints," *IEEE Journal on Selected Areas in Communications*, vol. 33, no. 10, pp. 2087–2103, 2015.

[17] Y. Li, M. Sheng, Y. Shi, X. Ma, and W. Jiao, "Energy efficiency and delay tradeoff for time-varying and interference-free wireless networks," *IEEE Transactions on Wireless Communications*, vol. 13, no. 11, pp. 5921–5931, 2014.

[18] Y. Li, M. Sheng, Y. Zhang, X. Wang, and J. Wen, "Energy-efficient antenna selection and power allocation in downlink distributed antenna systems: a stochastic optimization approach," in *Proceedings of the IEEE ICC*, pp. 4963–4968, Sydney, NSW, Australia, June 2014.

[19] G. Lim, C. Xiong, L. J. Cimini, and G. Y. Li, "Energy-efficient resource allocation for OFDMA-based multi-RAT networks," *IEEE Transactions on Wireless Communications*, vol. 13, no. 5, pp. 2696–2705, 2014.

[20] D. Lin, J. Kang, A. Squicciarini, Y. Wu, S. Gurung, and O. Tonguz, "MoZo: a moving zone based routing protocol using pure V2V communication in VANETs," *IEEE Transactions on Mobile Computing*, vol. 16, no. 5, pp. 1357–1370, 2017.

[21] M. J. Neely, "Stochastic network optimization with application to communication and queueing systems," *Synthesis Lectures on Communication Networks*, vol. 3, no. 1, pp. 1–211, 2010.

[22] S. Parsaeefard, R. Dawadi, M. Derakhshani, and T. Le-Ngoc, "Joint user-association and resource-allocation in virtualized wireless networks," *IEEE Access*, vol. 4, pp. 2738–2750, 2016.

Hindawi
Computational Intelligence and Neuroscience
Volume 2022, Article ID 4712041, 11 pages
https://doi.org/10.1155/2022/4712041

Research Article

Study on Structural Characteristics of Composite Smart Grille Based on Principal Component Analysis

Kong Fanxiao,[1,2] Yao Huazhong,[3] and Xie Weidong[1]

[1]*College of Materials Science and Engineering, Chongqing University, Chongqing 400044, China*
[2]*School of Mechanical and Transportation Engineering of Guangxi University of Science, Guangxi, China*
[3]*Research Institute of Science and Technology of Chinalco, Beijing, China*

Correspondence should be addressed to Xie Weidong; xieweidong2019@cqu.edu.cn

Received 10 November 2021; Revised 9 December 2021; Accepted 16 December 2021; Published 5 January 2022

Academic Editor: Guobin Chen

In recent years, many scholars have conducted in-depth and extensive research on the mechanical properties, preparation methods, and structural optimization of grid structural materials. In this paper, the structural characteristics of composite intelligent grid are studied by combining theoretical analysis with experiments. According to the existing conditions in the laboratory, the equilateral triangular grid structure experimental pieces were prepared. In this paper, principal component analysis combined with nearest neighbor method was used to detect the damage of composite plates. On this basis, the multiobjective robustness optimization of the structure is carried out based on artificial intelligence algorithm, which makes the structure quality and its sensitivity to uncertain parameters lower. Particle swarm optimization (PSO) is used in neural network training. The damage characteristics of different grid structures, different impact positions, and different impact energies were studied. The results show that the structural damage types, areas, and propagation characteristics are very different when the structure is impacted at different positions, which verifies that the grid structure has a good ability to limit the damage diffusion and shows that the grid structure has a good ability to resist damage.

1. Introduction

Advanced composite materials have the characteristics of light weight, high strength, high modulus, fatigue resistance, corrosion resistance, good designability and manufacturability, etc. They are especially suitable for large-scale structures and integral structures and are ideal aviation structural materials [1]. The use of advanced composite materials in aircraft can greatly reduce the structural mass of airframe, improve aeroelasticity and enhance the comprehensive performance of aircraft. Therefore, composite materials have been widely used in civil aircraft, and composite materials will replace conventional materials such as metal and nonmetal and become the main structural materials of the new generation aircraft airframe [2, 3]. At present, the research on the static strength of composite materials has become increasingly mature after decades of development and can be used in the structural design of composite materials in the engineering field. Many scholars at home and abroad have also carried out relevant research work in the research of dynamic properties of composite structures.

In recent years, scholars at home and abroad have conducted in-depth research on the mechanical properties and damage identification of three-dimensional braided composites. In [4], the damage evolution process of composites with inclusions and microcracks is analyzed by mechanical method, and the macromechanical characteristics of composites are predicted according to the established mathematical model. Hayashi et al. use carbon nanowires embedded in three-dimensional braided composites [5], analyze the sensing characteristics of carbon nanowires in composites, and prove that carbon nanotube yarns can be used to monitor the internal damage of composite parts and then use carbon nanowires embedded in three-dimensional braided composites as tensile sensors to construct intelligent composites. Borodavchenko et al. use

statistical methods to study the structural damage of three-dimensional braided intelligent composites [6]. Liang et al. predicted the mechanical properties of lattice materials and designed and prepared a hybrid triangular grid by using the embedding and locking process [7]. According to the continuum mechanics method, the equivalent stiffness of stretch-dominated lattice grid is predicted. In-plane compression test and three-point bending test are carried out on the specimen, and the feasibility of the equivalent continuum theoretical model and the superiority of lattice materials are illustrated by comparing the test stiffness and failure mode of the specimen. Traditional materials cannot achieve the new properties of composite materials because of their unitary structure [8]. In the manufacturing process of composite materials, the properties and components of composite materials should be designed first. Only by designing composite materials can composite materials be produced.

Since the 21st century, with the gradual popularization of big data, the continuous improvement of computer computing power, and the rapid development of Artificial intelligence (AI) technologies such as deep learning and reinforcement learning, related algorithms have been applied to various disciplines. The advantage of AI method is that it no longer cares about the specific physical mechanism of the problem. AI, as a technical method, also shows a broad application prospect in the field of composite materials. In this paper, in the damage detection experiment of composite laminated plate structure, the measured frequency response function data is reduced in dimension by principal component analysis, and the damage feature information of the structure is extracted. Then, the buckling load values of these samples are calculated by the finite element model, and the neural network is trained by these sample values. In the process of training neural network, particle swarm optimization (PSO) in intelligent algorithm is used, and the final optimization process is completed by genetic algorithm (GA).

2. Related Work

The concept of grid structure was first put forward by McDonnell Douglas Company of America in 1970s. Its basic idea is that the whole structure is composed of reinforcing ribs and skin, and the reinforcing ribs are distributed in regular polygonal grid, and the structure is anisotropic. Compared with traditional structural forms (such as shell structure and truss skin structure), the reinforcing ribs of grid structure are relatively independent, and under the impact load, one rib is damaged, cracks are not easy to propagate, and the overall performance is good [9, 10]. Fukuhara et al. simulate the skin and ribs of the grid structure based on the laminated plate and laminated beam elements under Mindlin's first-order shear deformation theory [11]. Through the spatial coordinate transformation and using the geometric continuity conditions of the skin and ribs, the element tangent stiffness matrix of the composite smart grid structure is obtained, and the buckling finite element numerical simulation method of the composite smart grid structure is given. In [12], the matrix hybrid method, which is a combination of transfer matrix method and matrix displacement method, is applied to the internal force calculation of continuous grid structure, and its calculation results are compared with those of finite element method, thus verifying the correctness and practicability of this method. Jennings et al. [13] comprehensively consider the structural cost and mechanical properties and put forward the pultrusion-interlocking grid technology, which greatly reduces the manufacturing cost of the flat grid structure. Based on the production demonstration of pultrusion-interlocking flat composite intelligent grid structure, Chunxiu et al. [14] put forward several reinforcement and improvement methods and realize the manufacturing of a flat composite intelligent grid structure. Tang et al. [15] propose to use evolutionary neural network to realize the global nonlinear mapping relationship between structural design parameters (input) and structural response parameters (output), instead of the finite element calculation in the optimization process. GA is taken as the optimization solver, and the response surface of neural network buckling stability is taken as the main constraint to optimize the stiffened composite grid structure.

Grid structures are mostly composed of composite laminates. In order to apply the composite intelligent grid structure to the aerospace field to replace the existing aerospace structures, it is necessary to conduct in-depth research on the dynamic characteristics of composite materials. At present, in the research field of composite structural dynamics, the analysis and optimization of structural natural frequencies and the research on structural impact performance are mainly carried out. In [16], the natural frequency of square plates with simply supported and clamped boundary conditions was optimized by changing the laying sequence and proportion with GA, and the fundamental frequency was improved a little. Liu et al. use GA based on random constraints to optimize the fundamental frequency of laminated plates with simply supported edges [17]. Kumar et al. adopt the method of combining GA with modal experiment, aiming at maximizing the natural frequency, and realize the optimization analysis by changing the layup ratio and layup sequence [18], which improves the fundamental frequency of composite plates fixed at one end by 15%. In [19], GA was used to optimize the ply angle of composite laminates with a given number of layers under the condition of meeting the requirement of natural frequency. Li et al. [20] study the low-speed impact damage of laminated plate structures made of graphite/epoxy materials by compiling dynamic programs and analyze and predict the delamination damage and collective cracking of various laminated plate structures with various layers through self-determined failure criteria and compare with the experimental results, which has a good prediction effect. In [21], the damage of laminated plates was simulated by using elliptical elastic core with stiffness reduction, and the damage of laminated plates and stiffened panels after impact was studied. The influence of several parameters on the residual strength of

laminated plates was analyzed, and the research results proved the effectiveness of this method.

3. Research Method

3.1. Preparation of Composite Intelligent Grid Structure. In the smart grid system, many distributed generators will transmit the generated power to the power grid, and the power grid can only bear it passively. Therefore, the power quality output by distributed generators affects the power grid system to a great extent. Adding microgrid system can effectively regulate the active and reactive power in the system and play a role of regulator for the improvement of power quality in the power grid. Nanjing YanXu Electric has many years of experience in scientific research and project implementation in the power industry and has profound technical accumulation in the field of power automation and power grid dispatching automation. On this basis, it has formed the technical reserve and accumulation of microgrid system through in-depth participation in relevant demonstration projects constructed by the state and power grid companies.

Combined with the existing conditions in the laboratory, the composite intelligent grid structure specimen is prepared, and the whole preparation process includes the following processes [22].

3.1.1. Cutting of Glass Fiber Composites. According to the size of the specimen to be prepared, the glass fiber composite plate is cut into ribs with equal length and width by using a jigsaw. Glass fiber composites have different thicknesses. In order to compare with the finite element simulation results, materials with thicknesses of 4 mm and 1 mm are selected, and the corresponding rib heights are 40 mm and 20 mm, respectively.

Place the cut ribs in a row, and cut the ribs into grooves with a saw, as shown in Figure 1.

At this time, we need to consider three important parameters: slot spacing, slot depth, and slot width. Because the specimens we prepared are regular triangular grids, the slotting spacing is equal, and the slotting spacing of the two specimens is 50 mm and 70 mm. respectively. According to the particularity of preparing the specimen, we need two kinds of ribs with different slotting methods. One slotting method is as follows: 1/4 rib height notches are opened on both sides of the rib; the other is that one side of the rib is notched with a height of 1/2 rib.

After calculation, the theoretical value of slot width should be $\sqrt{3}$ times of rib thickness. In the actual process of preparing the specimen, due to some errors in the process, in order to ensure that the ribs are fully clamped, we generally choose 2 times the rib thickness.

3.1.2. Preparation of Epoxy Resin Glue Solution. The epoxy resin glue solution is reasonably prepared, so that the epoxy resin glue solution has better viscosity, actual gel time, and curing degree, thus ensuring the quality of the specimen. If the viscosity of the resin is too high, it will cause difficulties in gluing, while if the viscosity is too low, it will cause the phenomenon of glue flowing, resulting in the lack of glue in products and affecting the quality. The ratio of epoxy to coagulant in the curing agent is 1 : 2.

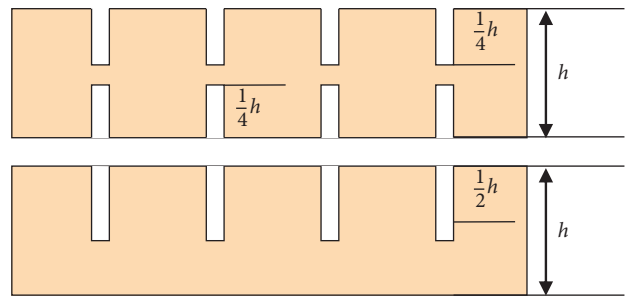

Figure 1: Schematic diagram of notch depth and width.

3.1.3. Model Pasting and Model Curing. Splicing the cut ribs, bonding the slots of the spliced triangular grid structure with epoxy adhesive, and solidifying at normal temperature, because the epoxy resin glue will flow, in order to ensure the good bonding at the slot, it is generally necessary to make up the glue several times and then curing at normal temperature.

3.1.4. Grinding and Trimming of Test Pieces. After the epoxy resin glue is solidified, the specimen is trimmed and polished according to the designed size with tools such as grinding wheel and saw, and the surface is polished smoothly, so as to prepare for the next step of pasting the skin.

3.1.5. Paste the Skin to Obtain the Test Piece. Firstly, prepare a skin with the same size as the grid plate, and the selected material of the skin should be equivalent to the grid rib, so as to ensure the material matching between the skin and the grid rib and reduce the residual stress caused by assembly. Lay the skin flat, apply epoxy resin glue evenly to the ribs and skin with a brush, and paste the prepared flat grid plate on the skin, requiring the adhesive to be filled.

This technology is easy to splice ribs, is low in cost, and does not need special fixtures. The skin can effectively compensate the stiffness by connecting with the clamping groove, and large plates can be processed and assembled.

3.2. Principal Component Analysis of Frequency Response Function. In order to facilitate the processing of frequency response function data by principal component analysis, this paper defines frequency response function spectral vector $h = [h_1, h_2, \ldots, h_p]$, where $h_i = (i = 1, 2, \ldots, p)$ is the value of frequency response function amplitude at the i-th frequency point and p is the number of frequency points of each frequency response function.

For L structures with known damage conditions, $n = (L \times K)$ frequency response function spectrum vectors h can be obtained by measuring at K different measuring points,

and they are assembled into a matrix by rows, which is called frequency response function spectrum matrix $[H]_{n\times p}$.

The original p-dimensional vector $[H]_{n\times p}$ of each row in the matrix h is transformed into a new q-dimensional vector by principal component analysis, which can be realized by the correlation matrix R of $[H]_{n\times p}$ [23].

In damage detection, the frequency response function spectrum vector h obtained from the test comes from the intact state ϕ_i and the damaged state ϕ_{d2} data categories, so the frequency response function spectrum matrix $[H]$ contains data classification information. To consider the classification information of data, we can use the generalized correlation matrix [24]:

$$R^* = P(\phi_i)R_i + P(\phi_d)R_d. \tag{1}$$

In the formula, $P(\phi_i), P(\phi_d)$ are the prior probability of intact state data and damaged state data, respectively, which is determined according to their relative numbers; R_i, R_d are the correlation matrix of intact state and damaged state, respectively.

After obtaining the generalized correlation matrix R^*, the eigenvalue $(\lambda_1 \geq \lambda_2 \geq \cdots \geq \lambda_p)$ and the corresponding eigenvector of R^* are obtained. The eigenvectors corresponding to the largest q eigenvalues are taken and assembled into a transformation matrix Φ:

$$\Phi = \left[\varphi_1, \varphi_2, \ldots, \varphi_q\right]. \tag{2}$$

Therefore, each row vector h in $[H]_{n\times p}$ can be transformed into a new vector by using the transformation matrix Φ:

$$c = h\Phi. \tag{3}$$

After the abovementioned principal component analysis method is processed, the reduced-dimensional vector c can be used as the damage feature sample of the structure for damage detection. Because of $q \leq p$, vector c is compared with the frequency response function spectrum vector h before conversion, the dimension of the data is greatly reduced, which reduces the difficulty of analysis.

3.3. Robust Optimization of Objective Function of Grid Stiffened Structure Based on AI Algorithm. The structure of a typical feedforward neural network is shown in Figure 2, where $X(x_1, x_2, \ldots, x_i)$ and $Y(y_1, y_2, \ldots, y_m)$ indicate that the network has l input nodes and m output nodes, respectively. Neurons are connected by weights, and nodes in hidden layer are lost.

$$h_j = f\left(\sum_{i=1}^{l} w_{ji}^{\text{in}} x_i + b_j^{\text{in}}\right), \quad 1 \leq j \leq q. \tag{4}$$

The output value of the output layer is

$$y_k = f\left(\sum_{j=1}^{q} w_{kj}^{\text{out}} h_j + b_k^{\text{out}}\right), \quad 1 \leq k \leq m, \tag{5}$$

in which, f is the transfer function, $w^{\text{in}}, b^{\text{in}}$ are the weight and threshold of input layer and hidden layer, respectively, and $w^{\text{out}}, b^{\text{out}}$ are the weight and threshold of hidden layer and output layer, respectively. Commonly used transfer functions include logarithmic S-shape function, hyperbolic tangent S-shape function, and linear function.

The composite grid cylinder is triangular stiffened, and the unit shape is shown in Figure 3. The cylinder has a height of 200 mm, a radius of 75 mm, and an axial compression of 1 045 kN, and the boundary condition is simply supported. The angle of skin layer is ±30°.

PSO is used to optimize the weights and thresholds of neural network; that is, in the optimization process, the weights and thresholds are taken as optimization variables to form particles, and the sum of squares of errors between the buckling load value O_i calculated by all particles and the accurate value T_i calculated by finite element is taken as fitness function. In this paper, 25 samples are selected, and the fitness function is

$$\text{fitness}(g) = \sum_{i=1}^{25} (T_i - O_i)^2. \tag{6}$$

In order to minimize the fitness function, the particle swarm optimization is carried out, and the optimal particle obtained at last constitutes a neural network for calculating buckling load.

Due to manufacturing errors, skin thickness, rib thickness, and rib height are all uncertain variables, and the actual values fluctuate around the design values. Given the tolerance, the fluctuation range is certain. In this paper, it is assumed that the fluctuation radii are $\Delta t_{\text{skin}} = 0.1$ mm, $\Delta t_{\text{rib}} = 0.1$ mm, $\Delta h_{\text{rib}} = 0.2$ mm, respectively, and now the robustness of the structure is optimized.

Firstly, the feasible robust optimization is considered; that is, the constraint problem under uncertain factors is considered. According to the parameter analysis in [7], the buckling load increases monotonously with the increase of skin thickness, rib thickness, and rib height, so the lower limit of buckling load corresponding to a set of design variables can be obtained by substituting the lower limit of interval corresponding to these three variables into neural network, so the following model can be used for optimization:

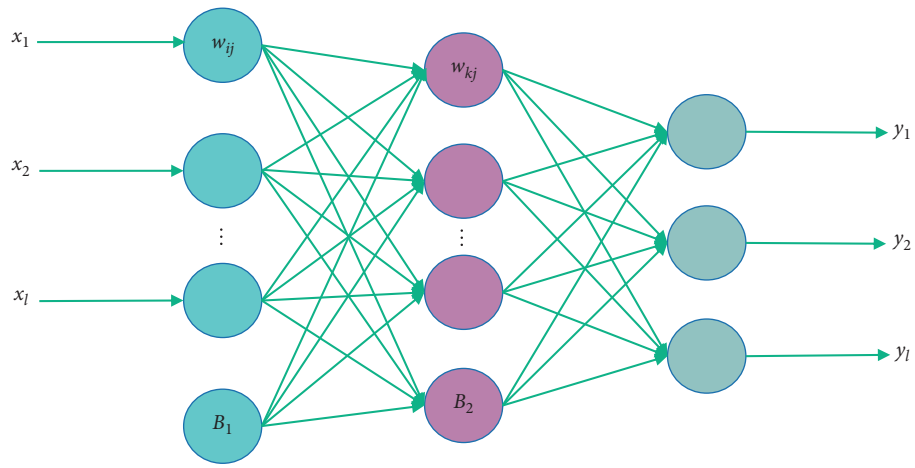

Figure 2: Typical 3-layer feedforward neural network.

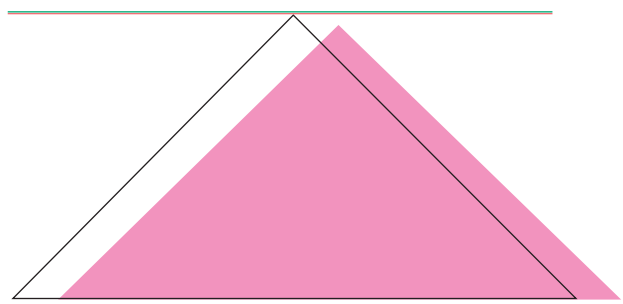

Figure 3: Triangular grid unit shape.

$$\begin{cases} \min \quad W = \rho \cdot \left[2N_a t_{\text{rib}} h_{\text{rib}} \sqrt{\left(\frac{\pi R N_b}{N_a}\right)^2 + L^2} + 2\pi R t_{\text{rib}} h_{\text{rib}} (N_b + 1) + 2\pi R L t_{\text{skin}} \right] \\ \text{s.t} \quad F_{\text{crit}} - F_{\text{buck}}^L \le 0. \end{cases} \tag{7}$$

Then, the robustness of the objective function is considered; that is, the sensitivity of the structural quality to the parameter changes is considered. Taking the lower limit of buckling load greater than the critical load as the constraint condition, the goal is to minimize the radius of mass variation interval.

Using the mass expression of triangular grid in the above formula, the partial derivative of mass to various uncertain variables can be derived:

$$\begin{aligned} \frac{\partial W(x)}{\partial t_{\text{rib}}} &= \rho \left[2N_a h_{\text{rib}} \sqrt{\left(\frac{\pi R N_b}{N_a}\right)^2 + L^2} + 2\pi R h_{\text{rib}} (N_b + 1) \right], \\ \frac{\partial W(x)}{\partial h_{\text{rib}}} &= \rho \left[2N_a t_{\text{rib}} \sqrt{\left(\frac{\pi R N_b}{N_a}\right)^2 + L^2} + 2\pi R t_{\text{rib}} (N_b + 1) \right], \\ \frac{\partial W(x)}{\partial t_{\text{skin}}} &= \rho (2\pi R L). \end{aligned} \tag{8}$$

The interval radius of available mass is

$$\Delta W(x) = \left| \frac{\partial W(x_0)}{\partial t_{\text{rib}}} \right| \Delta h_{\text{rib}} + \left| \frac{\partial W(x_0)}{\partial h_{\text{rib}}} \right| \Delta h_{\text{rib}} + \left| \frac{\partial W(x_0)}{\partial t_{\text{skin}}} \right| \Delta t_{\text{skin}}. \tag{9}$$

Therefore, the robustness optimization model is as follows:

$$\begin{cases} \min \quad \Delta W(x) = \left| \frac{\partial W(x_0)}{\partial t_{\text{rib}}} \right| \Delta h_{rib} + \left| \frac{\partial W(x_0)}{\partial h_{\text{rib}}} \right| \Delta h_{rib} + \left| \frac{\partial W(x_0)}{\partial t_{\text{skin}}} \right| \Delta t_{\text{skin}} \\ \text{s.t} \quad F_{\text{crit}} - F_{\text{buck}}^L \le 0. \end{cases} \tag{10}$$

The models expressed by test (7) and formula (10) are optimized with improved GA, and the results are shown in Table 1.

3.4. Three-Dimensional Hashin Damage Failure Criterion. Since the stress distribution of the damaged parts changes dramatically after the damage occurs in composite

Table 1: Results obtained by optimizing mass and mass change radius, respectively.

Project	Optimize W	Optimize ΔW
N_a	13	9
N_b	5	5
t_{skin}/mm	2.014	2.4471
t_{rib}/mm	3.317	2.8631
h_{rib}/mm	3.011	6.0172
F^L_{buck}/kN	1286.1	1228.7
W^*/kg	0.4133	—
ΔW^*/kg	—	0.017

laminates, and the damage caused by the damage makes the bearing capacity of the damaged units decrease significantly, it is difficult to use the failure criterion based on stress to judge the damage. By using the expression of stress-strain relationship in one dimension, the Hashin failure criterion can be transformed into a strain-based description:

$$\left.\begin{aligned}
&\sigma_{xx} = E_{11}\varepsilon_{xx}, \sigma_{yy} = E_{22}\varepsilon_{yy}, \sigma_{zz} = E_{33}\varepsilon_{zz},\\
&\sigma_{xy} = G_{12}\varepsilon_{xy}, \sigma_{xz} = G_{13}\varepsilon_{xz}, \sigma_{yz} = G_{23}\varepsilon_{yz},\\
&X_T = E_{11}\varepsilon^T_{11}, X_C = E_{11}\varepsilon^C_{11}, Y_T = E_{22}\varepsilon^T_{22},\\
&Y_C = E_{22}\varepsilon^C_{22}, Z_T = E_{33}\varepsilon^T_{33},\\
&S_{12} = G_{12}\gamma_{12}, S_{13} = G_{13}\gamma_{13}, S_{23} = G_{23}\gamma_{23}
\end{aligned}\right\}. \tag{11}$$

Among them, $\varepsilon^T_{11}, \varepsilon^C_{11}$ are the ultimate strain of each single-layer plate in the direction of 1, which reaches the tensile and compressive strength, respectively; $\varepsilon^T_{22}, \varepsilon^C_{22}$ are the ultimate strain in two directions of each single-layer board that reaches the tensile and compressive strength, respectively; ε^T_{33} is the allowable strain in the thickness direction of the single-layer plate; $\gamma_{ij}\,(i \neq j)$ is the shear strain value when the laminated plate reaches the shear strength limit.

The strain form of Hashin failure criterion is expressed as follows:

Tensile break of fiber:

$$d^2_f = \left(\frac{\varepsilon_{xx}}{\varepsilon^T_{11}}\right)^2 + \left(\frac{\varepsilon_{xy}}{\gamma_{12}}\right)^2 + \left(\frac{\varepsilon_{xz}}{\gamma_{13}}\right)^2 \geq 1, \quad \varepsilon_{xx} \geq 0. \tag{12}$$

Fiber crushing:

$$d^2_f = \left(\frac{-\varepsilon_{xx}}{\varepsilon^C_{11}}\right)^2 \geq 1, \quad \varepsilon_{xx} < 0. \tag{13}$$

Matrix cracking:

$$\begin{aligned}
d^2_m = &\left(\frac{\varepsilon_{yy} + \varepsilon_{zz}}{\varepsilon^T_{22}}\right)^2 + \left(\frac{1}{\gamma^2_{23}}\right)\left(\varepsilon^2_{yz} - \frac{E_{22}E_{33}}{G^2_{23}}\varepsilon_{yy}\varepsilon_{zz}\right)\\
&+ \left(\frac{\varepsilon_{xy}}{\gamma_{12}}\right)^2 + \left(\frac{\varepsilon_{xz}}{\gamma_{13}}\right)^2 \geq 1, \quad \varepsilon_{yy} + \varepsilon_{zz} \geq 0.
\end{aligned} \tag{14}$$

Matrix extrusion:

$$\begin{aligned}
d^2_m = &\left(\frac{E_{22}\varepsilon_{yy} + E_{33}\varepsilon_{zz}}{2G_{12}\gamma_{12}}\right)^2 + \left(\frac{\varepsilon_{yy} + \varepsilon_{zz}}{\varepsilon^C_{22}}\right)\left[\left(\frac{E_{22}\varepsilon^C_{22}}{2G_{12}\gamma_{12}}\right)^2\right] - 1\\
&+ \frac{1}{\gamma^2_{23}}\left(\varepsilon^2_{yz} - \frac{E_{22}E_{33}}{G^{23}}\varepsilon_{yy}\varepsilon_{zz}\right) + \left(\frac{\varepsilon_{xy}}{\gamma_{12}}\right)^2\\
&+ \left(\frac{\varepsilon_{xz}}{\gamma_{13}}\right)^2 \geq 1, \quad \varepsilon_{yy} + \varepsilon_{zz} < 0.
\end{aligned} \tag{15}$$

Delamination damage:

$$\begin{aligned}
d^2_l &= \left(\frac{\varepsilon_{zz}}{\varepsilon^T_{33}}\right)^2 + \left(\frac{\varepsilon_{xz}}{\gamma_{13}}\right)^2 + \left(\frac{\varepsilon_{yz}}{\gamma_{23}}\right)^2 \geq 1, \quad \varepsilon_{zz} \geq 0,\\
d^2_l &= \left(\frac{\varepsilon_{xz}}{\gamma_{13}}\right)^2 + \left(\frac{\varepsilon_{yz}}{\gamma_{23}}\right)^2 \geq 1, \quad \varepsilon_{zz} < 0.
\end{aligned} \tag{16}$$

4. Result Analysis and Discussion

4.1. Mechanical Property Test of Grid Structure. In this paper, six groups of strain sensors are attached to the structural surface of the test piece with the same size as the above finite element model, and the strain sensors are attached symmetrically. Each group includes two 120 ohm strain gauges and two 120 ohm precision resistors, which together form a bridge. There are six groups of such bridges.

The experiment steps are as follows:

(1) One end of the specimen is simply supported and the other end is fixedly supported.

(2) Turn on the DC regulated power supply for the force sensor; strain bridge circuit and measuring circuit, in which the power supply of the force sensor is adjusted to 12 V, the power supply of the bridge circuit is adjusted to 2.4 V, and the power supply of the measuring circuit is adjusted to 8 V.

(3) Rotate the handle to adjust the output of the force sensor to 2.5 V; that is, the force acting on the structure at this time is 0 N. Turn the handle counterclockwise until the output of the transmitter is 0.5 v, and the corresponding pressure value is 100 N. Start the data acquisition software program and save the data of six measuring points.

(4) Change the magnitude of the loading force and repeat the third step. To eliminate the error caused by residual strain, the handle should be rotated clockwise before changing the load every time, and the output of the force sensor should be adjusted to 2.5 V.

Figure 4 shows the load-displacement curves of the structure under different loads.

It can be concluded from Figure 4 that the load-strain curves of measuring point 2 and measuring point 5 basically coincide; the load-strain curves of measuring points 1, 3, 4, and 6 also basically coincide. The load-displacement curves

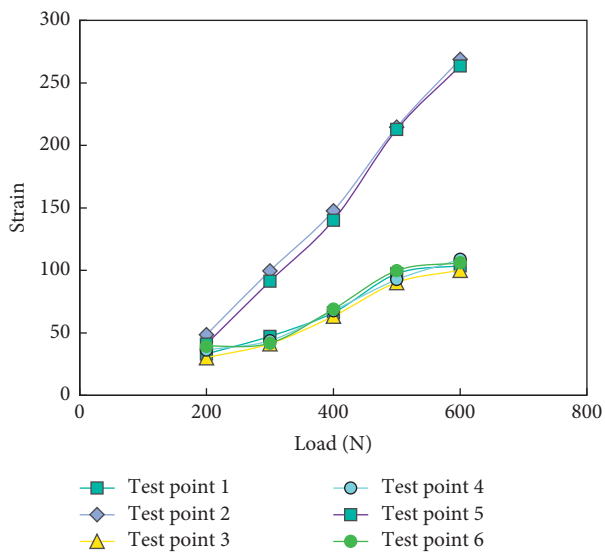

Figure 4: Experimental study on load-strain curve of grid structure.

of all measuring points show a good linear relationship. It is proved that the whole structure of the grid structure test piece is evenly distributed, the skin and structure are well bonded, and the grooves of ribs are well bonded, and the preparation process is mature and stable.

4.2. Impact Damage Characteristics. Composite structures, as load-bearing members such as skin, are often impacted by external loads. Impact and vibration are the two main mechanical environments that packages are often subjected to in the process of circulation, which cause great damage to packages. In order to reduce the damage rate of packages in the process of transportation, as far as the packaging products themselves are concerned, studying the damage mode under the action of impact and vibration is conducive to the design of cushioning packaging. In this chapter, based on the stiffness reduction law of materials under various failure conditions, a three-dimensional asymptotic damage research model of composite laminates under low-speed impact is established. By compiling stiffness reduction subroutine and finite element transient calculation, the simulation and analysis of progressive damage of laminated plate and composite smart grid structure during impact process are completed.

Three-dimensional asymptotic damage analysis method of composite laminates under low-speed impact includes three parts: stress analysis, failure analysis, and material performance degradation model. In the part of stress analysis, the governing equations of stitched laminates under impact load are derived based on the principle of virtual displacement. In the failure analysis, it is necessary to consider the fiber extrusion damage caused by the compressive stress on the impact front of the structure and the fiber tensile break on the back of the impact specimen. At the same time, after the structure is damaged, the stiffness of the damaged part drops sharply, which causes the stress concentration around the damaged part and causes the damage to be transmitted and spread around.

When the impact energy is huge, it will cause depression in the impact area, fracture of nearby fibers, and collective destruction and at the same time produce larger transverse shear. The impact energy cannot be continuously transmitted in the fiber, and the damage area caused by this damage is difficult to determine, sometimes smaller than the damage area without penetration impact under the same conditions.

4.2.1. Impact Damage Characteristics of Different Wing Grid Models at the Same Position. Figure 5 is a schematic diagram of impact positions of punches on three grid structure models. It can be seen that the impact positions are all on one side of the grille skin. The impact position of the model 1 is the center of a single rib closest to the center of the structure (Figure 5(a)). The impact position of the models 2 and 3 is the center of the model (the center of the rib plate) (Figure 5(b)).

Figures 6 and 7 show the fitting curves of punch contact force and displacement for 200 time steps in 0.005 s with the impact energy of 4 J. It can be seen that, in the punch working stage, the time of models 1, 2, and 3 is 0.0032 s, 0.0028 s, and 0.0031 s, respectively. The model punch has the shortest function, the maximum contact force, the minimum limit displacement, and the minimum elastic deformation of the grid structure.

The frequency response functions of several damage cases are selected to form the sample set of the nearest neighbor method. And the cumulative contribution rate curves are shown in Figure 8.

The contribution rate represents the proportion of the g-order principal components in the original data information, and the cumulative contribution rate represents the ability of the former k-order principal components to synthesize the original data information.

It can be seen from Figure 8 that when the order increases, the contribution rate drops rapidly, and the contribution rate after the 15th order approaches zero. At the same time, it can be seen that the cumulative contribution rate of the first 13-order principal components has exceeded 99%. Therefore, only analyzing the first 13-order principal components can reflect the change characteristics of the whole original data, greatly reducing the amount of calculation.

4.2.2. Influence of Different Impact Energy of the Same Structure on Structural Damage. In this paper, the relationship between structural damage and impact energy is observed by directly using different impact energy without using the speed of punch as a variable. Select the center point of structure 3 (i.e., the position of a single rib) and calculate the impact damage under the impact energy of 3 j, 4 j, and 5 j, respectively. Observe the sensitivity of impact damage to impact energy at a single rib position.

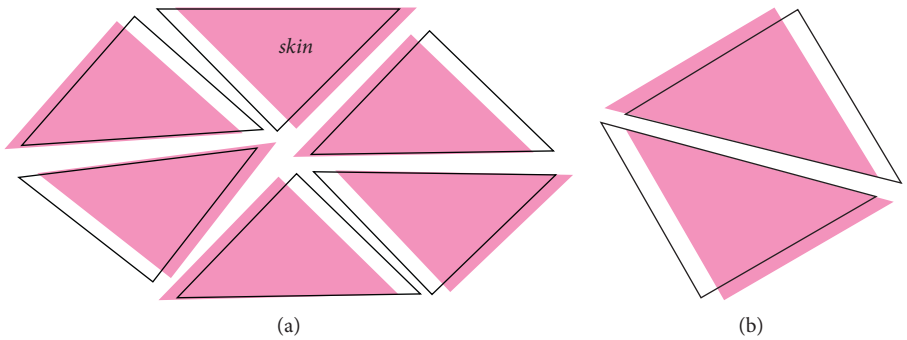

Figure 5: Schematic diagram of impact position of punch on three grid structure models. (a) Model 1. (b) Model 2 and Model 3.

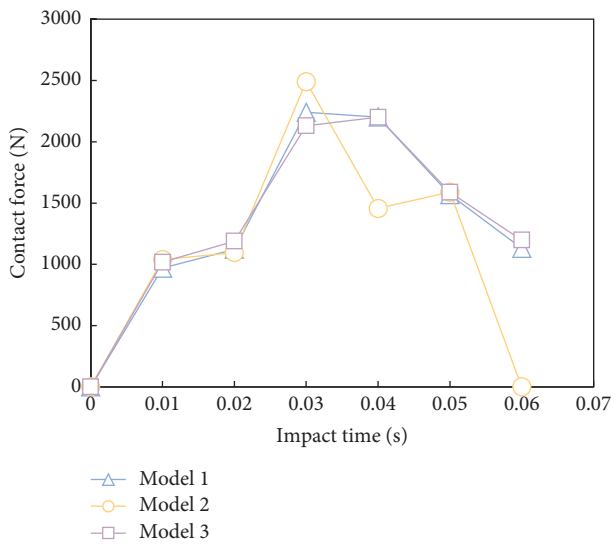

Figure 6: Curve of contact force of impact punch with time.

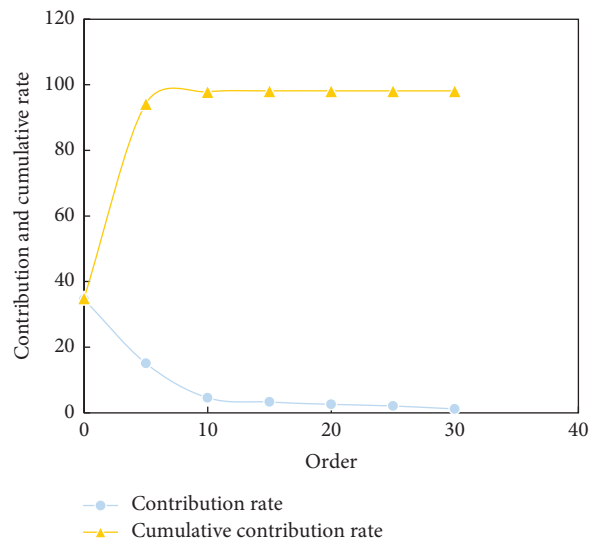

Figure 8: The contribution rate and cumulative contribution rate vary with the order of principal components.

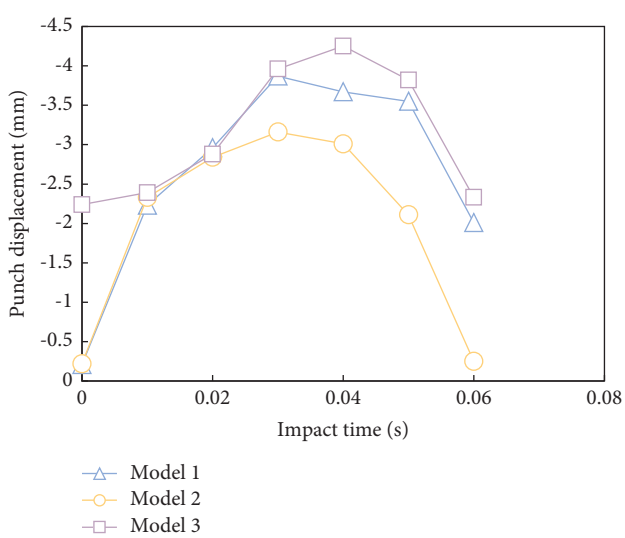

Figure 7: Impact versus time curve.

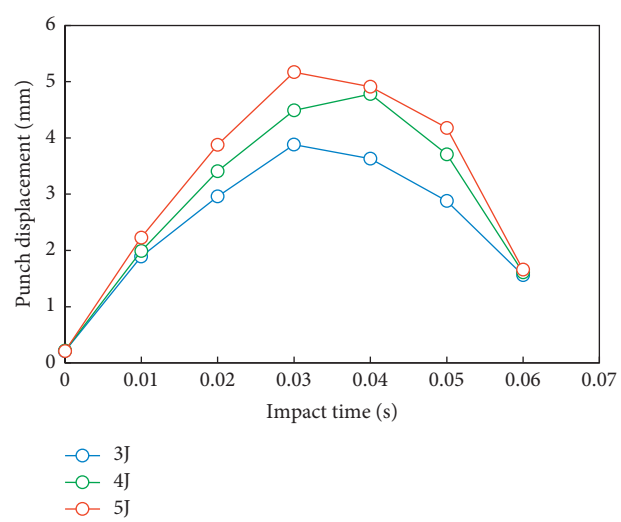

Figure 9: Punch displacement/time curve.

The 200 time steps of punch displacement and punch contact force output during the whole impact process are fitted into curves, as shown in Figures 9 and 10.

It can be seen from Figures 9 and 10 that when different energies are used to impact the skin supported by a single rib, the impact process and time are basically the same, and

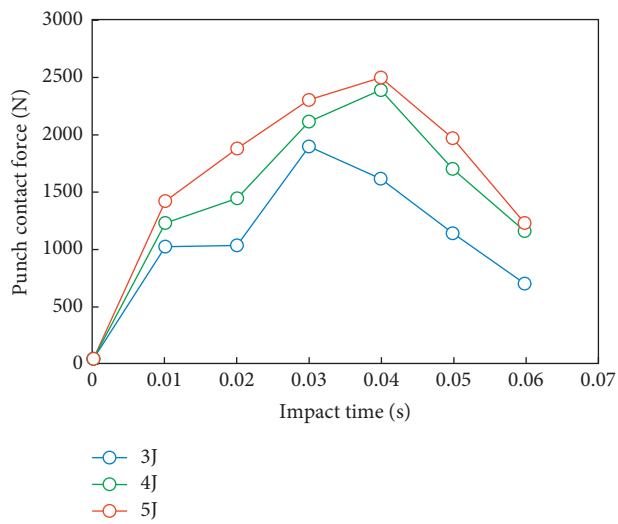

Figure 10: Contact force/time curve of punch.

the punch finishes working in about 0.0035 s. The peak contact force of punch under three kinds of energy is 1601.3 N, 2389.7 N, and 2499.8, respectively. The limit displacements of the punch are 3.63 mm, 4.25 mm, and 4.57 mm, respectively. It can be seen that, with the increase of impact energy, the contact force and displacement of the punch increase smoothly and do not change greatly.

4.3. Optimization Results of Composite Laminates. The natural frequency of composite laminates has always been a concern in the field of composite dynamics. Many scholars have given a variety of research methods to improve the natural frequency of composite materials. The research method of the natural frequency of composite materials designed in this paper is to continuously change the laying angle of each single layer of composite laminates from −180° to 180° and to improve the fundamental frequency of the whole structure by changing the stiffness and frequency of each single layer.

Firstly, the finite element model of the laminated plate structure is established in Patran, and the natural frequencies of the two boundary conditions are solved. The fundamental frequencies of the two structures are 89.24 Hz under the simply supported boundary and 169.14 Hz under the fixed boundary.

Then, the optimization problem model is established in Patran. Optimized contents are as follows.

The laying angles of eight single-layer boards symmetrically laid with laminated boards under two boundary conditions are respectively associated as optimization design variables. The response is designed as the natural frequency of the structure; the constraint is that the natural frequencies of the second- to sixth-order structures are not less than 95% of the natural frequencies of the second- to sixth-order structures before optimization. The objective function is to maximize the first natural frequency of the structure.

Taking the bdf card for optimization research of simply supported plates on four sides as an example, the bdf card fragments of design variables that need to be modified are shown in Table 2.

Table 2: Layout angle design variable card format.

DESVAR	1	com_ply_O1	−45	−180	180	0.6
DESVAR	2	com_ply_O2	90	−180	180	0.6
DESVAR	3	com_ply_O3	45	−180	180	0.6
DESVAR	4	com_ply_O4	0	−180	180	0.6
DESVAR	5	com_ply_O5	−45	−180	180	0.6
DESVAR	6	com_ply_O6	90	−180	180	0.6
DESVAR	7	com_ply_O7	45	−180	180	0.6
DESVAR	8	com_ply_O8	0	−180	180	0.6

The above card defines the names of 8 single-layer design variables, the initial value of the paving angle, the upper and lower limit variation interval of the design variables, and the maximum optimized moving step.

The optimization process curves of ply angle under two boundary conditions are shown in Figures 11 and 12 (because the structure is laid with angular symmetry, the design variable curves of symmetrical single-layer slabs coincide). Therefore, for the two boundary conditions, only the iterative curves of design variables of the first- to fourth-layer slabs are given here.

After 7 steps and 15 steps of iteration, the optimization process of the fundamental frequency of the four-sided simply supported plate and the four-sided clamped laminated plate converged, and the fundamental frequency increased by 4.96% and 16.8%, respectively. After optimization, the ply angles are different, which indicates that the ply angle when the fundamental frequency of the laminate is maximum is related to the boundary conditions of the structure. Compared with the results in [25, 26] that the optimization effect of fundamental frequency of laminated plate structure is improved by 1–2% by using optimization methods such as GA, it has better optimization effect and faster convergence speed.

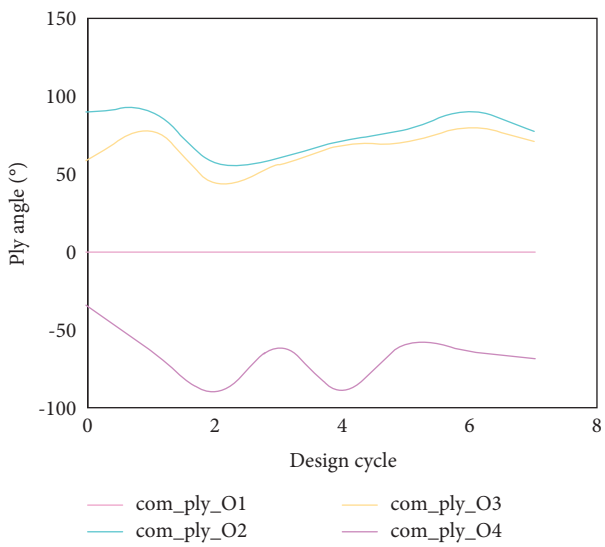

Figure 11: Iterative curve of angle optimization process of simply supported slab with four edges.

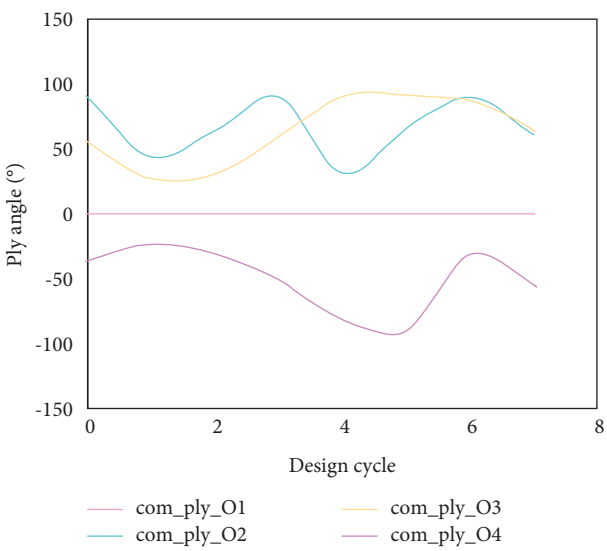

Figure 12: Iterative curve of optimization process of ply angle of four-edge fixed plate.

5. Conclusion

At present, composite structures have been widely used in the aerospace field. Intelligent grid structure is a new type of lightweight and high-strength composite material structure. After more than ten years' development, it has been preliminarily applied in practical aerospace structures. In this paper, the mechanical properties of composite laminates and composite intelligent grid structures are studied in depth. The results show the following.

(1) Principal component analysis can reduce the dimension of the test data, and at the same time, it can effectively retain the feature information of the original data.

(2) Impact damage forms, damage areas, and damage propagation forms at different positions of the grid are quite different. Under the same impact condition, the damage area of single rib support is the largest, and it also has the greatest influence on the structural strength and stiffness. Therefore, it should be regarded as the main monitoring object in structural health monitoring, and appropriate monitoring strategies and methods should be selected according to the damage types and energy transmission paths.

(3) A three-dimensional Hashin failure criterion based on strain parameters is adopted, and it is integrated into the subprograms written by users in the secondary development interface of Abaqus finite element software. The progressive damage of composite laminates during impact was simulated and studied and compared with the experimental results in the literature, which verified the reliability of the research method.

The manufacturing process of composite laminates is complex and the manufacturing cost is high. Therefore, the research work of this paper is lacking practical application experimental research. It is hoped that subsequent researchers will verify the experimental work of this paper and get more and more accurate conclusions.

Data Availability

The experimental data used to support the findings of this study are available from the corresponding author upon request.

Conflicts of Interest

The authors declare that they have no conflicts of interest regarding this work.

Acknowledgments

This work was supported by the Research Funds for the Central Universities (NO. 2021CDJXDJH003); the Chongqing Research Program of Basic Research and Frontier Technology (Project No. cstc2019jcjy-msxmX0539); the Natural Science Foundation of Guangxi, China (NO.2018GXNSFAA281273); and the Middle-aged and Young Teachers' Basic Ability Promotion Project of Guangxi (NO.2019KY0370).

References

[1] P. K. Raushan, S. K. Singh, and K. Debnath, "Turbulence characteristics of oscillating flow through passive grid," *Ocean Engineering*, vol. 224, no. 3, Article ID 108727, 2021.

[2] J. Chen, N. Hao, L. Pan, L. Hu, S. Du, and Y. Fu, "Characteristics of compressive mechanical properties and strengthening mechanism of 3D-printed grid beetle elytron plates," *Journal of Materials Science*, vol. 55, no. 20, pp. 8541–8552, 2020.

[3] Z. Liu, H. Peng, and C. Wen, "Multi-objective optimization analysis of harmonic characteristics of wind turbines in

independent microgrid," *Renewable Energy*, vol. 037, no. 007, pp. 1021–1027, 2019.

[4] Y. Du, Z. Guo, X. Li, Q. Chen, and F. Zhang, "Metallographic characteristics of Pb-Ca alloy grid and its effect on battery performance," *Storage Battery*, vol. 056, no. 004, pp. 172–174, 2019.

[5] T. Hayashi, H. Iwanaga, D. Iwasa, and Y. Ohsawa, "Analysis of structural characteristics and networks of cross-disciplinary data using data jackets," *Journal of Japan Society for Fuzzy Theory and Intelligent Informatics*, vol. 31, no. 1, pp. 534–545, 2019.

[6] O. M. Borodavchenko, V. D. Zhivulko, A. V. Mudryi, I. A. Mogilnkov, and M. V. Yakushev, "Structural characteristics and photoluminescence of thin films of Cu (In1-xgax)(Syse1-y)2 solid solutions," *Journal of Applied Spectroscopy*, vol. 88, no. 1, pp. 27–32, 2021.

[7] H. Liang, Y. Liu, L. Wan, G. Sheng, and X. Jiang, "Penetrating power characteristics of half-wavelength AC transmission in point-to-grid system," *Journal of Modern Power Systems & Clean Energy*, vol. 7, no. 1, pp. 125–132, 2019.

[8] C. Wen, M. Hu, C. Hu, Z. Piao, and J. Zhou, "Research on characteristics of bidirectional CLLC DC–DC transformer used in DC microgrid," *Journal of Engineering*, vol. 2019, no. 18, pp. 5351–5354, 2019.

[9] J. Rencoret, A. Gutierrez, E. Castro, and R. Jose, "Structural characteristics of lignin in pruning residues of olive tree (*Olea europaea* L.)," *Holzforschung*, vol. 73, no. 1, pp. 25–34, 2019.

[10] F. Xie, H. Zhang, C. Nie, T. Zhao, Y. Xia, and L. Ai, "Structural characteristics of tamarind seed polysaccharides treated by high-pressure homogenization and their effects on physicochemical properties of corn starch," *Carbohydrate Polymers*, vol. 262, no. 6, Article ID 117661, 2021.

[11] H. Fukuhara, M. H. Mwaba, and K. Maenaka, "Structural characteristics of measles virus entry," *Current Opinion in Virology*, vol. 41, pp. 52–58, 2020.

[12] S. Z. Shmurak, V. V. Kedrov, A. P. Kiselev, T. N. Fursova, I. I. Zver'kova, and S. S. Khasanov, "Spectral and structural characteristics of (Lu1-xEux)2(WO4)3 tungstates," *Physics of the Solid State*, vol. 61, no. 11, pp. 2117–2129, 2019.

[13] V. Jennings, R. S. Gragg, C. P. Brown et al., "Structural characteristics of tree cover and the association with cardiovascular and respiratory health in tampa, FL," *Journal of Urban Health*, vol. 96, no. 5, pp. 669–681, 2019.

[14] C. X Guo, L. Wang, F. He et al., "Structural characteristics of lycium ruthenicum community & soil properties on different types of desert rangeland in the lower reaches of Shiyang river," *Medicinal Plants: English Version*, vol. 010, no. 002, pp. 58–65, 2019.

[15] W. Tang, D. Liu, Y. Li et al., "Structural characteristics of a highly branched and acetylated pectin from *Portulaca oleracea* L," *Food Hydrocolloids*, vol. 116, no. 8, Article ID 106659, 2021.

[16] Liudun, "Engineering practice of intelligent grid distribution," *Integrated Circuit Applications*, vol. 036, no. 006, pp. 56-57, 2019.

[17] Y. Liu, Q. Fan, Y. Huo, M. Li, H. Liu, and B. Li, "Construction of nanocellulose-based composite hydrogel with a double packing structure as an intelligent drug carrier," *Cellulose*, vol. 28, no. 11, pp. 6953–6966, 2021.

[18] P. Kumar, M. Mahanty, A. Chattopadhyay, and A. K. Singh, "Effect of interfacial imperfection on shear wave propagation in a piezoelectric composite structure: Wentzel-Kramers-Brillouin asymptotic approach," *Journal of Intelligent Material Systems and Structures*, vol. 30, no. 18/19, pp. 2789–2807, 2019.

[19] P. Zhang, Z. Han, J. Gu, S. Sun, and H. Fu, "A strategy of parallel winding of circumferential ribs and helical ribs for composite cylindrical grid structures," *Composite Structures*, vol. 275, no. 3, Article ID 114351, 2021.

[20] J. X. Li and P. F. Liu, "Finite element analysis of adhesive failure of solid composite propellant multi-material structure for underwater intelligent equipment," *Journal of Failure Analysis and Prevention*, vol. 21, pp. 1–9, 2020.

[21] X. P. Xie, F. Q. Wei, X. J. Wang, and H. J. Yang, "Determination of optimal grid opening width for herringbone water-sediment separation structures based on sediment separation efficiency," *Journal of Mountain Science*, vol. 16, no. 03, pp. 136–146, 2019.

[22] G.-D. Sun, Y.-R. Wang, C.-F. Sun, and Q. Jin, "Intelligent detection of a planetary gearbox composite fault based on adaptive separation and deep learning," *Sensors*, vol. 19, no. 23, p. 5222, 2019.

[23] T. Zhang, K. Zhang, and W. Liu, "Exact impact response of multi-layered cement-based piezoelectric composite considering electrode effect," *Journal of Intelligent Material Systems and Structures*, vol. 30, no. 3, pp. 400–415, 2019.

[24] M. Kermani, B. Adelmanesh, E. Shirdare, C. A. Sima, D. L. Carmi, and L. Martirano, "Intelligent energy management based on SCADA system in a real microgrid for smart building applications," *Renewable Energy*, vol. 171, no. 1, 2021.

[25] Z. Jiang, J. Zhu, Y. Li, J. Wang, Z. Li, and H. Lu, "Simultaneous merging multiple grid maps using the robust motion averaging," *Journal of Intelligent & Robotic Systems*, vol. 94, no. 3, pp. 655–668, 2019.

[26] X. Wang and M. Fan, "Interaction behaviors and structural characteristics of zein/NaTC nanoparticles," *RSC Advances*, vol. 9, no. 10, pp. 5748–5755, 2019.

Hindawi
Computational Intelligence and Neuroscience
Volume 2022, Article ID 9946128, 10 pages
https://doi.org/10.1155/2022/9946128

Research Article

Based on Optimization Research on the Evaluation System of English Teaching Quality Based on GA-BPNN Algorithm

Yafei Chen, Zhenbang Yu, and Weihong Zhao

Qingdao Huanghai University, Qingdao, Shandong 266555, China

Correspondence should be addressed to Yafei Chen; chenyf02@qdhhc.edu.cn

Received 8 November 2021; Accepted 15 December 2021; Published 5 January 2022

Academic Editor: Guobin Chen

English teaching is an important part of basic teaching in our country, which has been deeply concerned by all aspects. Its teaching quality not only is related to the purpose of English teaching, but also has a far-reaching impact on students' English learning. Therefore, the construction of English teaching quality evaluation system has become the focus of research. However, the traditional English teaching quality evaluation method has some problems; for example, the subjectivity of teaching evaluation is strong, the evaluation index is not comprehensive, and the evaluation results are distorted. Therefore, this paper studies the English teaching quality evaluation system based on optimized GA-BP neural network algorithm. On the basis of BP neural network algorithm evaluation simulation, GA algorithm is introduced for optimizing, and GA-BP neural network algorithm model is further optimized by GA adaptive degree variation and entropy method. The experimental results show that the optimized GA-BP neural network algorithm has faster convergence speed and smaller error. At the same time, the optimized GA-BP neural network algorithm evaluation model has better adaptability and stability, and its expected results are more in line with the ideal value. The results of English teaching quality evaluation are more scientific, showing higher value in the application of English teaching quality evaluation.

1. Introduction

With the improvement of China's comprehensive strength, more and more people will choose to travel, work, and study, and more and more overseas people are willing to come to China for development. This not only promotes the economic exchanges between countries, but also makes the cultures of different countries constantly collide and exchange. Therefore, English teaching has been concerned by all walks of life. At present, English teaching in China has become one of the contents of basic education. There are different degrees of English teaching courses from primary school to university. Therefore, the quality of English teaching not only is related to the development of education, but also has a long-term impact on students' learning [1]. With the reform and deepening of China's teaching system, teachers' evaluation methods and contents are becoming more and more perfect. English teaching quality is constantly changing according to the teaching needs. Teaching quality evaluation system can help teachers understand students' learning situation and obtain students' real reflection information on teaching content, so as to improve teaching methods and teaching content and improve English teaching effect [2]. In addition, schools can analyze and train teachers' teaching according to the results of teaching quality evaluation, help English teachers improve teaching quality and professional quality more scientifically and reasonably, improve teaching management level, and provide new ways for schools to improve teaching quality and development and reform [3, 4].

In the past, the evaluation of English teaching quality was usually directly established by mathematical model, such as analytic hierarchy process, index weighted average method, and fuzzy comprehensive evaluation [5, 6]. These teaching quality evaluation models need a linear relationship between the evaluation index and the influencing factors, but the English teaching quality evaluation belongs to a nonlinear relationship, which cannot reduce the randomness and

subjectivity of the influencing factors, so that the final evaluation results and the actual situation show deviation or even distortion [7]. The first problem is that the traditional subject of English teaching quality evaluation is relatively single. In the traditional evaluation system, the evaluation subject is often the expert group, the teacher group, or the student group. The composition of the evaluation subject is single, and it cannot be used to evaluate the quality of English teaching [8, 9]. The second problem is that the indicators of English teaching quality evaluation system are not comprehensive; that is, the content of evaluation indicators of various schools is similar, and the content is relatively simple and more inclined to the theoretical evaluation of teaching, ignoring the characteristics of different disciplines of teaching and making the evaluation content not objective and comprehensive [10, 11]. The third problem is the distortion of the evaluation results of English teaching quality; that is, although the students, as one of the evaluation subjects, feel the most intuitive, profound, and detailed English teaching content, their evaluation objectivity needs to be determined [12]. On the one hand, because of the teacher's strictness, students have resistance emotion, which is too subjective in the evaluation. On the other hand, students' evaluation may mislead teachers, make teachers' requirements for students lower or cater to students' needs too much, and eventually lead to adverse effects on teaching effect [13].

In view of the problems existing in the traditional English teaching quality evaluation method, BP neural network algorithm can give a better solution where neural network algorithm is a kind of network information data processing system with high nonlinear dynamic processing ability. Different from linear relation algorithm, when the variable relationship and distribution form of data are uncertain or when some complex systems cannot express the relationship between input and output data with general relation, BP neural network algorithm cannot express the relationship between input and output data with general relation; neural network can still easily express the highly nonlinear mapping relationship between these data [14]. At the same time, the neural network algorithm can obtain the corresponding experience through the learning of the previous data samples, skip the cumbersome operation of the query and related expression process, and express the data sample law function close to the function that can present the best data state. The characteristics of BP neural network are mainly shown in the following points. The first point is that the nonlinear characteristics of BP neural network can make it infinitely close to any continuous nonlinear function under any given precision condition [15]. The second point is that BP neural network adopts parallel distributed processing method for information storage and processing, which means that BP neural network has strong performance and fast processing speed in information processing, and it shows strong fault tolerance for information [16]. The third point is that the ability of BP neural network to process data can be obtained through learning performance, and it has strong adaptability. It can express different regular data through weight and realize weight Generalization Application [17]. The fourth point is that BP neural network also shows strong data fusion in information processing, which shows that BP neural network can not only use traditional numerical operation skills, but also use artificial intelligence technology to process information quantitatively and qualitatively [18]. The fifth point is that BP neural network is not a single variable system; the number of output and input variables is not fixed, which provides a new general description method for the decoupling problem between subsystems [19]. Therefore, in the evaluation of English teaching quality, the nonlinear characteristics of BP neural network can build the corresponding model in the case of unclear data generation reasons and then through the learning and training of sample data to achieve the desired effect and can effectively reduce the impact of human subjective factors on the final evaluation results, so as to get more comprehensive, reasonable, and scientific results [20, 21].

Although BP neural network has been widely used in many fields and has achieved good results, it still shows some shortcomings in the application process and needs to be improved. Therefore, this paper uses genetic algorithm (GA) to improve the BP neural network algorithm; at the same time, further adaptive mutation optimization is carried out on the GA algorithm, combined with entropy method to screen the optimized GA-BP neural network algorithm data, so as to reduce the error of the optimized GA-BP neural network algorithm and reduce the influence of special individuals and randomness, so as to improve the accuracy and rationality of English teaching quality evaluation system based on GA-BP neural network algorithm.

2. Optimize GA-BP Neural Network Algorithm to Build English Teaching Quality Evaluation Model

2.1. Construction of English Teaching Quality Evaluation Model Based on 2.1 BP Neural Network Algorithm. BP neural network algorithm is a feedforward artificial neural network based on biological brain neurons, which is a parallel and distributed network structure composed of multiple neurons and can process information [22]. The structure of a single neuron in BP neural network is relatively simple, as shown in Figure 1. At the same time, the function it can achieve is also very simple. However, after different numbers of neurons are connected, its overall performance is not a simple result of one plus one, but a highly complex nonlinear relationship [23].

Each neuron has a single output, but it can be connected with other neurons. It has multiple input paths, and each connection path has a corresponding weight. When the weight value is greater than 0, it means excitation, and when it is less than 0, it means inhibition. As shown in formulas (1)–(3), there is no difference between the two methods.

$$u_k = \sum_{j=1}^{p} w_{kj} x_j, \tag{1}$$

$$v_k = u_k - \theta_k, \tag{2}$$

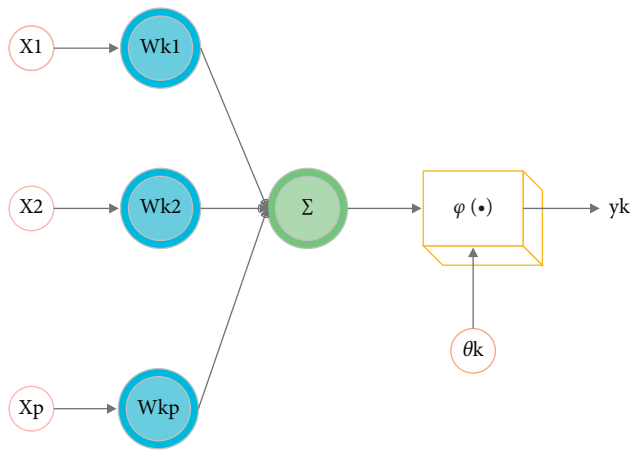

Figure 1: Simple model of the neuron.

$$y_k = \varphi(v_k). \tag{3}$$

The input signal is expressed as $X = (x_1, x_2, \ldots, x_p)^T$, the weight of neuron k is expressed as $w_{k1}, w_{k2}, \ldots, w_{kp}$, the linear combination result is expressed as u_k, the threshold value is expressed as θ_k, the excitation function is expressed as $\varphi(v_k)$, and the output of neuron is expressed as y_k. There are threshold function, piecewise linear function, and S-type function in incentive function. According to the requirements of this paper and the performance of different incentive functions, this paper selects S-type function as incentive function, as shown in the following formula:

$$\varphi(v) = \frac{1}{1 + \exp(-v)}. \tag{4}$$

BP neural network can be divided into three layers, namely, input layer, hidden layer, and output layer, and each layer contains a number of neurons that do not have any connection with each other. Neurons of each layer are only connected with neurons of adjacent levels, and the information transmission is unidirectional without feedback [24]. The topological structure of BP neural network is shown in Figure 2.

Before the sample training of BP neural network, it is necessary to initialize the network and the corresponding learning parameters and determine the fixed parameters. BP neural network training samples mainly include input vector $X = [x_1, x_2, \ldots, x_{n1}]^T$ and expected output vector $T = [t_1, t_2, \ldots, t_{N3}]^T$. The output formula of the nodes in the hidden layer is shown as follows:

$$y_h^k = f\left(\sum_{i=1}^{N1} w_{ih} \cdot x_i^k + \theta_h\right), \tag{5}$$

where k is the number of corresponding samples and $k = 1, 2, \ldots, N$, θ_h is the threshold, and f is the transfer function. The node output formula of the output layer is shown as follows:

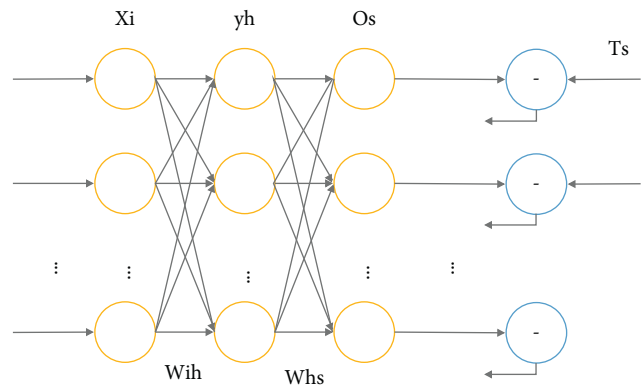

Figure 2: BP neural network topology.

$$o_s^k = g\left(\sum_{h=1}^{N2} w_{hs} \cdot y_h^k + \theta_s\right), \tag{6}$$

where k is the k-th sample and $k = 1, 2, \ldots, N$, θ_s is the threshold, and g is the transfer function.

The error function of BP neural network is shown as follows:

$$E_s = \frac{1}{2}\sum_{S=1}^{N3}\left(T_s^k - O_S^K\right). \tag{7}$$

The error function of global sum of squares error E is given by

$$E = \frac{1}{2}\sum_{k=1}^{N}\sum_{S=1}^{N3}\left(T_s^k - O_S^K\right). \tag{8}$$

When there is a gap between the output value of the output layer and the expected value, it is necessary to calculate the correction error, as follows:

$$d_s^k = \left(t_s^k - o_s^k\right) o_s^k \left(1 - o_s^k\right), \tag{9}$$

where $s = (1, 2, \ldots, N_3)$. Thus, the correction error of the hidden layer can be obtained as follows:

$$e_h^k = \left[\sum_{s=1}^{n3} d_s^k w_{hs}^k\right] y_h^k \left(1 - y_h^k\right). \tag{10}$$

The weight and threshold of BP neural network algorithm are calculated by gradient descent algorithm, and its iteration period is shown as follows:

$$w^{k+1} = w^k + \Delta w = w^k - \eta^k \frac{\partial e^k}{\partial w^k}, \tag{11}$$

where w^k is the weight vector or threshold vector of k times, η^k is the learning rate of corresponding times, and $\partial e^k / \partial w^k$ is the error gradient. It can be seen that the BP neural network algorithm has a flat error area; that is, the error is still in a slow decline state when the weight is maximum, which greatly increases the number of trainings and affects the

convergence speed. In addition, the BP neural network algorithm has a greater probability of falling into the local minimum problem, so that there is a certain gap between the training convergence result and the expected error. Because of falling into the concave point of the error surface, the activation function of neural network is s function. Both ends of this function are flat, and the algorithm runs very slowly. As long as it is a random search algorithm, this will happen, but the possibility is different. It can use the advance search with strong global optimization ability and then use the algorithm with strong local search ability to continue the search.

2.2. Optimization of GA-BP Algorithm English Teaching Quality Evaluation Model. According to the above problems of BP neural network algorithm, this paper uses GA algorithm to optimize BP neural network algorithm. When the structure of BP neural network is $x - y - 1$, the number of weights is $(x * y + y)$. The number of thresholds is $(y + 1)$. Then the total length is shown as follows:

$$\mathrm{LEN} = (x * y + y) + (y + 1). \tag{12}$$

Then, the sum of the absolute error of the BP neural network algorithm after training is taken as the individual fitness value, as shown in the following formula:

$$F = k \sum_{i=1}^{n} (y_i - o_i), \tag{13}$$

where n indicates the number of output nodes, y_i represents the ideal output, o_i represents the predicted output, and k represents the coefficient. The selection, crossover, and mutation of GA algorithm are shown in formulas (14)–(16):

$$\mathrm{pselect} = \frac{f_i}{\sum_{j=1}^{N} f_i}. \tag{14}$$

Among them, pselect represents the selection probability of individuals in a population, $f = k/F_i$ and F_i represents the individual fitness value, k is the coefficient, and N represents the number of individuals in a population.

$$\begin{aligned} a_{mj} &= a_{mj}(1 - b) + a_{nj} b, \\ a_{nj} &= a_{nj}(1 - b) + a_{mj} b. \end{aligned} \tag{15}$$

In the above formula, the coding method is real number coding; that is, chromosomes a_m and a_n are mutated at j position, b is a random number, and the range is [0, 1].

$$\begin{cases} a_{ij} = a_{ij} + \left(a_{ij} - a_{\max}\right) * f(\mathrm{ga}), & \mathrm{rand} > 0.5, \\ a_{ij} = a_{ij} + \left(a_{\min} - a_{ij}\right) * f(\mathrm{ga}), & \mathrm{rand} < 0.5, \end{cases} \tag{16}$$

where a_{ij} is the i gene of the j-th individual, $a_{\max}$ is the upper limit of a_{ij}, $a_{\min}$ is the lower limit of a_{ij}, $f(\mathrm{ga}) = r(1 - \mathrm{ga}/\mathrm{ga\_index})^2$, and r is a random number, ga is the current number of iterations, ga_index is the maximum number of iterations, and rand is a random number with the range of [0, 1].

In the GA algorithm, the adaptability of the population has a great influence on its search for the global optimal solution. When the fitness is good, that is, when the global optimal solution is nearest, the GA algorithm can be further optimized by adaptive mutation. As shown in formula (17), the adaptive mutation probability calculation formula is as follows:

$$Q = \frac{Q_1 + Q_2}{2} = \frac{\left\{Q_0 - (Q_0 - Q_{\min}) \times (\mathrm{ga}/\mathrm{ga\_index}) + Q_0 \times \left(\overline{F}/\max_{X_k \in \Omega} F(X_k)\right)\right\}}{2}. \tag{17}$$

Among them, ga represents the current number of iterations, ga_index represents the maximum number of iterations, $Q_{\min}$ represents the minimum value in the variation range, $\overline{F}$ represents the average fitness value of the population, and $\max_{X_k \in \Omega} F(X_k)$ represents the maximum fitness value of the population.

The index information of the evaluation system of English teaching quality is relatively large, and there are many influencing factors in the comprehensive evaluation. If the data is directly input into the GA-BP neural network algorithm, some special data will increase the error of the algorithm and slow down the convergence speed, so the data should be processed before the training and learning. In this paper, the entropy method is used to process the data, that is, to avoid the randomness and subjectivity of the data on the basis of the given index weight of the data, and then the GA-BP neural network algorithm is used for learning and training, as shown in the following formula:

$$x'_{pq} = \frac{x_{pq} - \overline{x}}{s_q} \tag{18}$$

Among them, x_{pq} represents the score of the p sample on the q-index, x'_{pq} represents the standardized value, $\overline{x}$ represents the average value, and s_q represents the standard deviation. The average value shift after standardization is shown in the following formula:

$$Z_{pq} = x'_{pq} + A, \tag{19}$$

where A is the translation length.

The proportion of the p sample in q index is shown in the following formula:

$$P_{pq} = \frac{Z_{pq}}{\sum_{i=1}^{n} Z_{pq}}. \tag{20}$$

The entropy value of the q index is shown as follows:

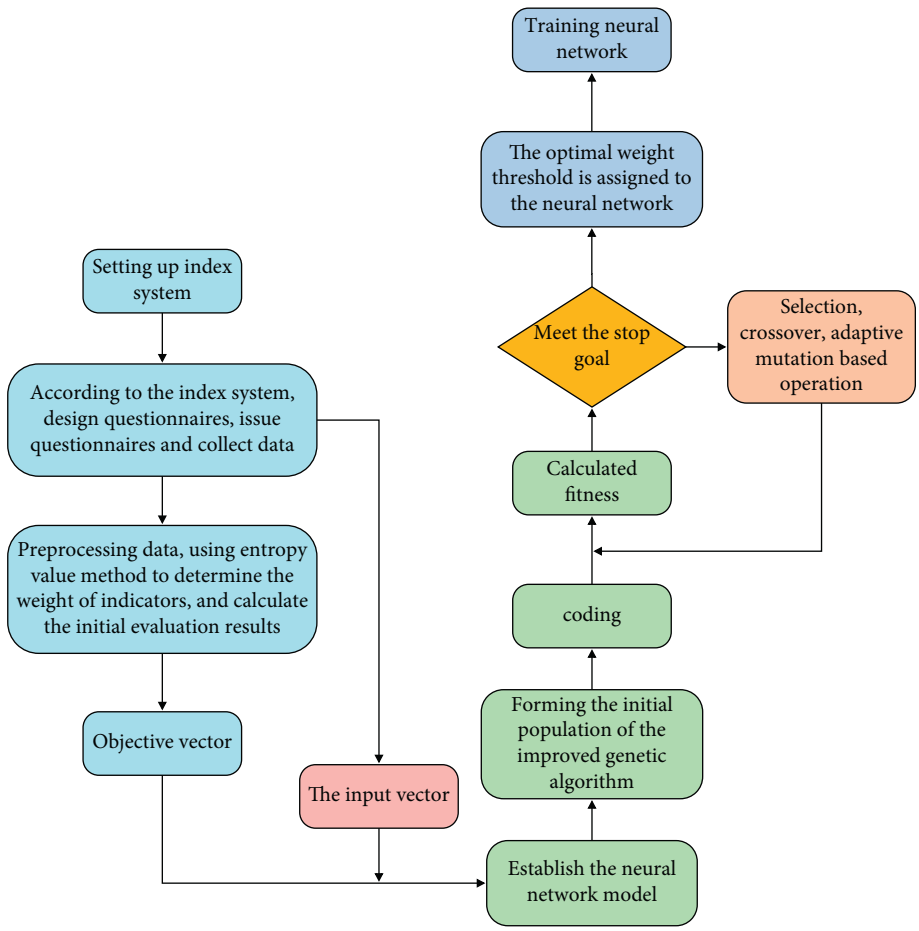

Figure 3: English teaching quality evaluation flowchart based on the optimized GA-BP neural network algorithm.

$$E_j = -k \sum_{i=1}^{n} P_{pq} \ln\left(P_{pq}\right). \tag{21}$$

The difference value of the q index is shown as follows:

$$G_j = 1 - E_j. \tag{22}$$

After normalizing the difference value, the weight of the q indicator is shown as follows:

$$w_j = \frac{G_j}{\sum_{j=1}^{m} G_j}. \tag{23}$$

Then the teaching quality of the p sample is shown as follows:

$$H_i = \sum_{j=1}^{m} w_j P_{pq}. \tag{24}$$

Figure 3 shows the flowchart of English teaching quality evaluation based on optimized GA-BP neural network algorithm.

2.3. Construction of Structural Model and Evaluation Index of English Teaching Quality Evaluation System. The evaluation of English teaching quality involves English teaching leaders, namely, teachers, English teaching audiences, namely, students, English teaching experts, and other English teachers. Therefore, the objects of English teaching quality evaluation need to be composed of different groups. As shown in Figure 4, it is the structural model of English teaching quality evaluation system.

It can be seen from the figure that the system is divided into two levels. The input information starts from the level 2 indicators, and the output of each level 2 indicator is the corresponding level 1 indicator information. The final result of English teaching quality is divided into excellent, good, general, pass, and fail. The output value range of GA-BP neural network corresponding to each level is shown in Table 1.

There are many influencing factors in the process of English teaching and learning, such as English teaching methods, teaching content difficulty level, teachers' professional quality, students' English foundation, students' interest in English learning, and so on. Therefore, according

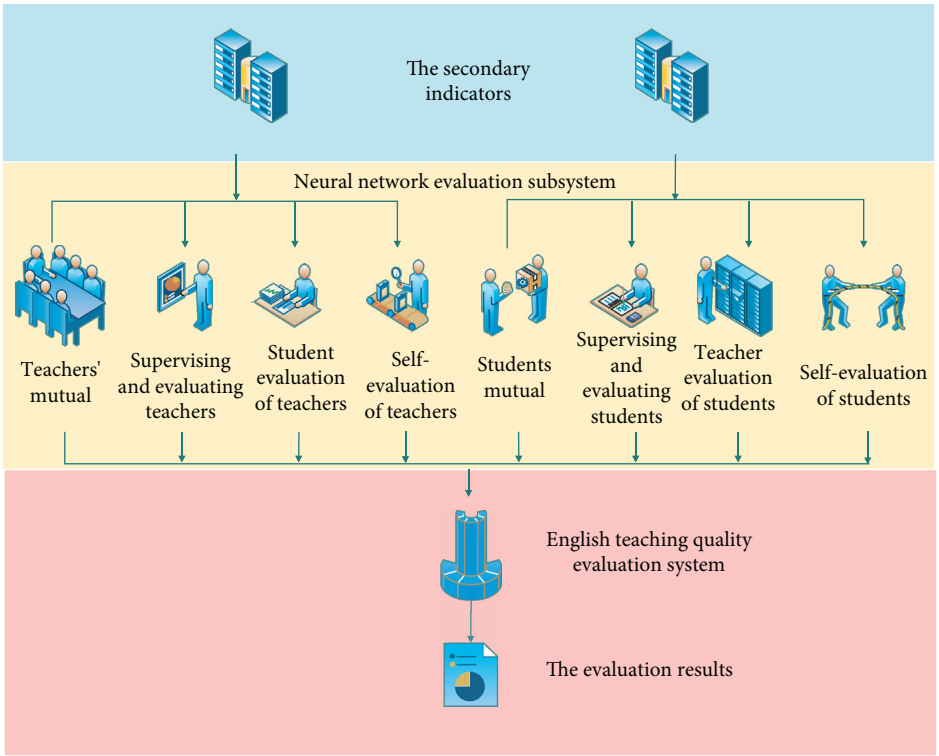

Figure 4: The structural model of English teaching quality evaluation system.

Table 1: The corresponding table of grading standards and GA-BPNN output values.

Level	GA-BPNN output values
Excellent	1.00–0.90
Good	0.89–0.80
Fair	0.79–0.70
Pass	0.69–0.60
Fail	<0.59

to the characteristics of English teaching and the needs of students, the evaluation index of English teaching quality is constructed, as shown in Figure 5.

3. Simulation Results of English Teaching Quality Evaluation System Based on Optimized GA-BP Algorithm

3.1. Algorithm System Training Results. According to Figure 5, we can see that there are 17 secondary indexes of English teaching quality evaluation index, then the corresponding optimized GA-BP neural network algorithm has 17 input layer nodes, 1 output layer node, and 5 hidden layer nodes, the maximum number of iterations is 120 and the accuracy is 10–8, the real coding length of GA algorithm is 80, the initial scale is 22, and the cross probability is 0.7. As shown in Figures 6 and 7, the mean square errors of GA-BP neural network and optimized GA-BP neural network are shown, respectively.

It can be seen from Figure 6 that the mean square error of GA-BP neural network algorithm decreased greatly in the first five iterations. From the fifth to the twenty-seventh iterations, the mean square error of GA-BP neural network algorithm decreased slightly, gradually tended to a gentle decline state, and reached convergence in the thirty-fifth iteration. In the first five iterations, the mean square error of the optimized GA-BP neural network algorithm decreases rapidly and then decreases slowly until the 20th iteration and reaches the convergence state in the 25th iteration. This shows that the optimized GA-BP neural network algorithm has a faster mean square error reduction rate than GA-BP neural network algorithm, improves the convergence speed of the algorithm, and can achieve the convergence effect in fewer iterations.

As shown in Figures 8 and 9, the fitness diagrams of GA-BP neural network algorithm and optimized GA-BP neural network algorithm are shown. It can be seen from the figure that the GA-BP neural network algorithm has a faster convergence speed in the first 40 iterations and gradually

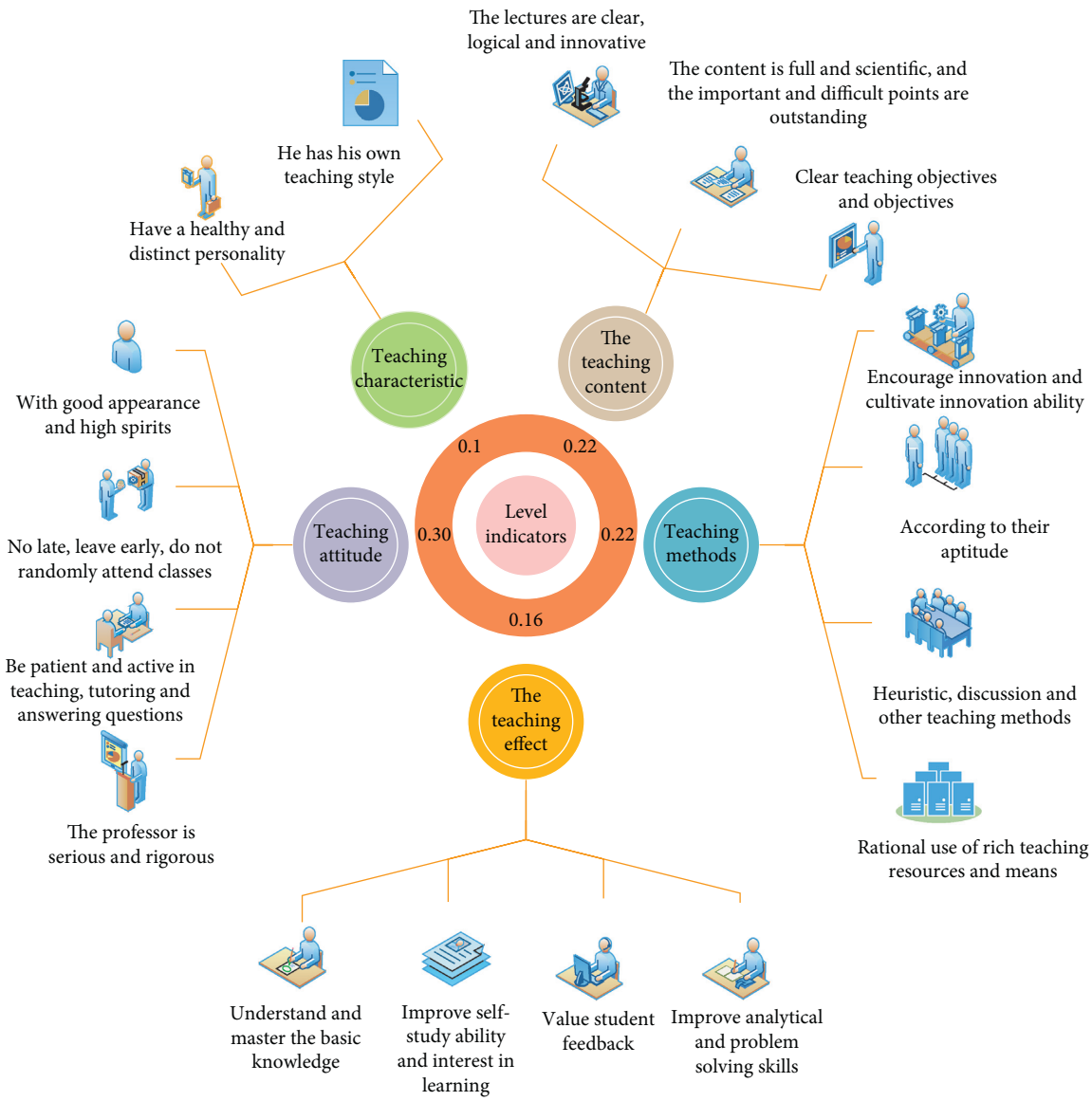

Figure 5: The evaluation index of English teaching quality.

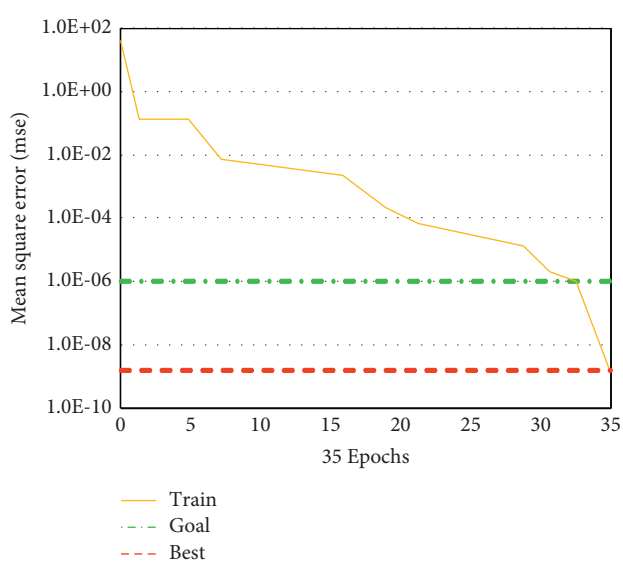

Figure 6: GA-BPNN mean square error.

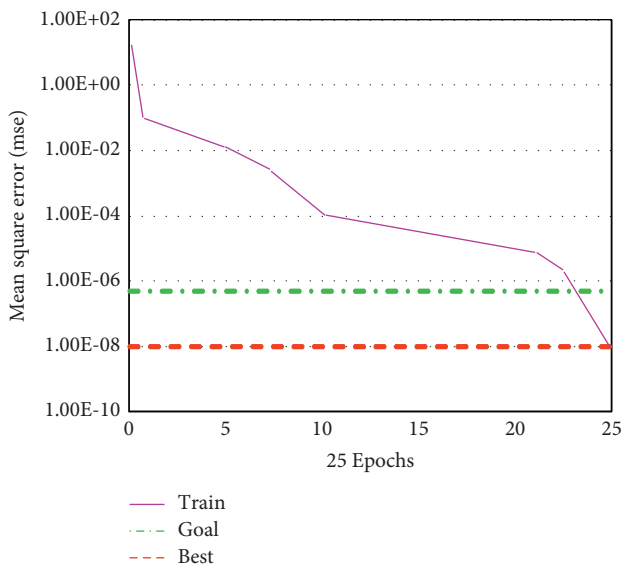

Figure 7: The mean square error of GA-BPNN was optimized.

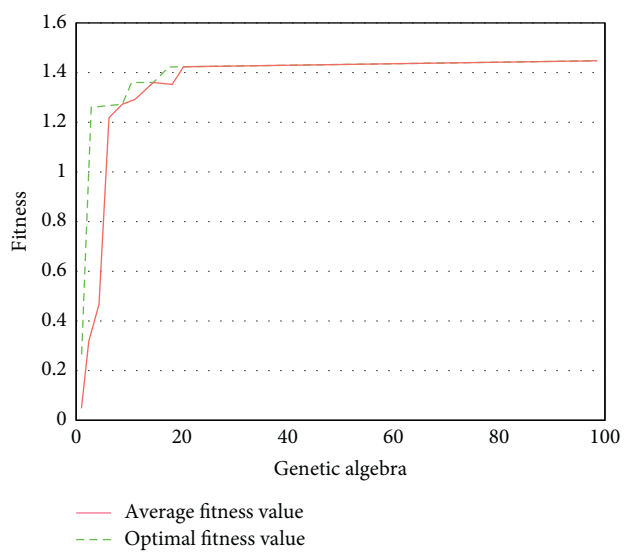

Figure 8: The fitness of GA-BPNN.

tends to be flat from 40 to 50 iterations. After 50 iterations, it is stable, and the final fitness value is 0.83. The convergence speed of the optimized GA-BP neural network algorithm is faster, reaching a stable state in the 20th iteration, and the fitness value reaches 1.43. This shows that the optimized GA-BP neural network algorithm model has faster convergence speed than GA-BP neural network algorithm model under the condition of the same genetic times, can reach a stable state in a shorter time, and has higher fitness value; that is, the optimized GA-BP neural network algorithm model has higher adaptability.

3.2. Experimental Results of English Teaching Quality Evaluation System Based on Optimized GA-BP Neural Network Algorithm. Genetic algorithm optimizes BP, including

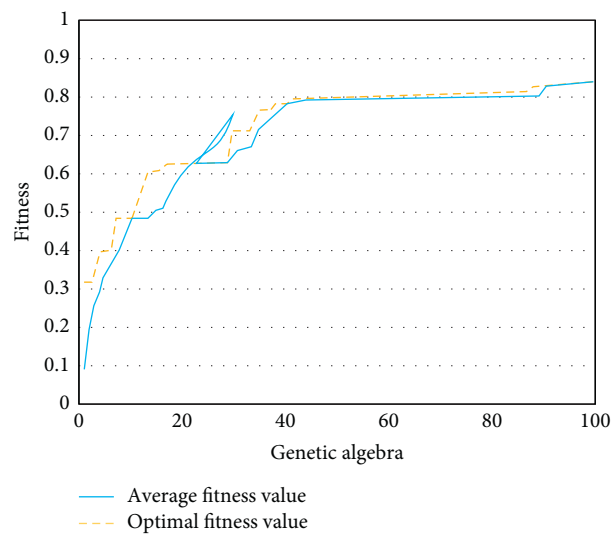

Figure 9: The fitness of GA-BPNN was optimized.

three parts: neural network structure determination, genetic algorithm optimization, and BP neural network prediction. Among them, genetic algorithm is used to optimize the initial weight and threshold of BP neural network, so that the optimized BP neural network can better predict the function output. The purpose of optimizing BP neural network by genetic algorithm is to obtain better network initial weight and threshold through genetic algorithm. Its basic idea is to use the initial weight and threshold of individual representative network and the prediction error of BP neural network initialized by individual value as the fitness value of the individual and find the optimal individual through selection, crossover, and mutation operations, that is, the optimal initial weight of BP neural network.

In order to effectively verify the effect of the English teaching quality evaluation system based on the optimized GA-BP neural network algorithm, this paper selects 15 sample data for learning and training and another 8 groups of data for simulation experiments. As shown in Figure 10, it is the result of GA-BP neural network algorithm and optimized GA-BP neural network algorithm after learning and training 15 groups of sample data.

It can be seen from the figure that the prediction results of GA-BP neural network algorithm after sample learning and training are similar to the ideal results as a whole, but the error of individual prediction results is large; in particular the data error of samples 6 to 10 is the largest, which indicates that GA-BP neural network algorithm is greatly affected by individual factors. The prediction result of optimized GA-BP neural network algorithm is closer to the ideal result, both the overall sample error and individual sample error are relatively small, and it is more stable than GA-BP neural network algorithm. Therefore, the evaluation system model of English teaching quality based on optimized GA-BP neural network has higher value in application, and the evaluation of English teaching quality is more scientific.

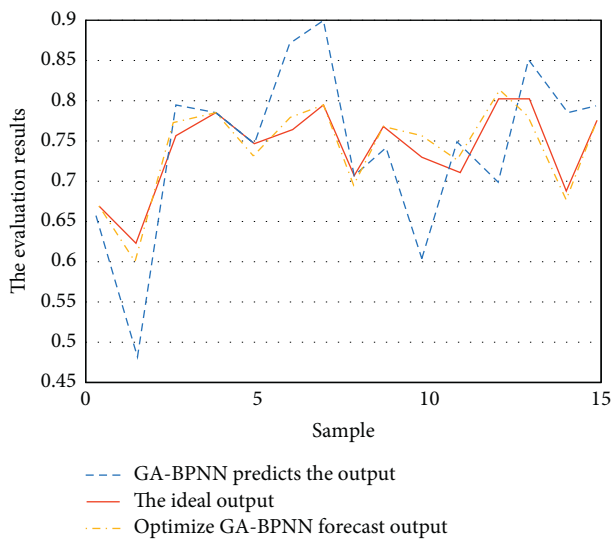

Figure 10: Comparison of prediction results between GA-BP neural network algorithm and optimized GA-BP neural network algorithm.

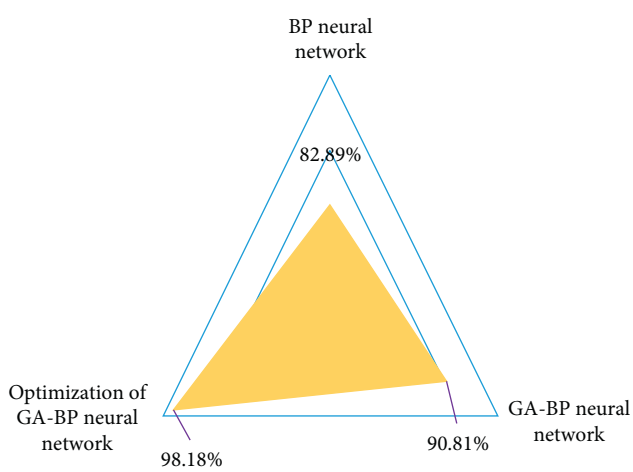

Figure 11: Performance comparison table of different English teaching quality evaluation models.

Figure 11 shows the performance comparison table of different English teaching quality evaluation models. From the data in the table, it can be seen that, in the BP neural network algorithm, GA-BP neural network algorithm, and optimized GA-BP neural network algorithm, the average evaluation accuracy of optimized GA-BP neural network algorithm is the highest, and it is 15.29% and 7.37% higher than BP neural network algorithm and GA-BP neural network algorithm, respectively. This shows that the optimized GA-BP neural network has better evaluation performance.

Figure 12 shows the simulation experiment results of eight groups of data by the English teaching quality evaluation system based on the optimized GA-BP neural network algorithm. It can be seen from the figure that the error of the test sample is very close to the training error, and the prediction accuracy of both the training and the test results is

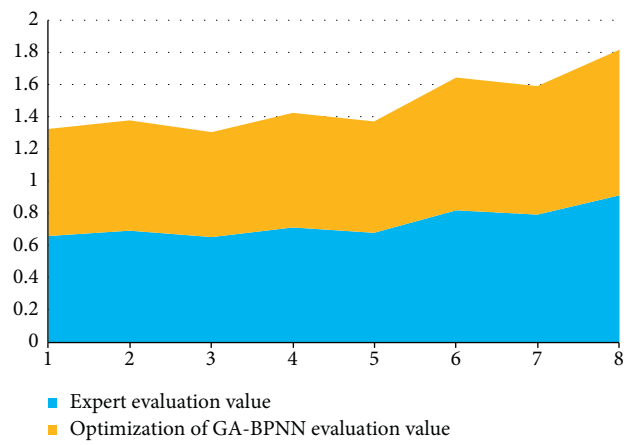

Figure 12: The simulation results of English teaching quality evaluation system based on the optimized GA-BP neural network algorithm.

within the allowable range, and there is no individual error increase. This shows that the English teaching quality evaluation system based on optimized GA-BP neural network algorithm is reasonable, scientific, and feasible.

4. Conclusion

With the continuous improvement of China's economic level and international status, people have more and more opportunities to choose to communicate in their study, work and life, study, tourism, etc. The importance of English is becoming more and more prominent. As one of the important contents of basic education in China, English teaching quality level and teaching content are related to the ultimate goal of English teaching, so the construction of English teaching quality evaluation system has been widely concerned. The traditional English teaching quality evaluation system mainly analyzes and evaluates the data by constructing linear mathematical model, but this way cannot reduce the influence of subjective factors in the data to the minimum and cannot comprehensively analyze and consider the nonlinear factors, which makes the evaluation results of English teaching quality not comprehensive and does not conform to the characteristics of English teaching. Even the result of English teaching quality evaluation is distorted. Therefore, in view of the above problems, this paper studies the English teaching quality evaluation system based on the optimized GA-BP neural network algorithm. The nonlinear characteristics of BP neural network can well reflect the nonlinear relationship between the evaluation index and the result of English teaching quality and reduce the randomness and subjectivity of influencing factors. At the same time, in order to solve and improve the convergence speed and global optimal solution of BP neural network, this paper optimizes BP neural network by GA algorithm. In addition, combined with GA adaptive mutation optimization and entropy method, the prediction effect of GA-BP neural network is further improved to achieve the purpose of optimization. The experimental results show that, compared with GA-BP neural network

algorithm, the optimized GA-BP neural network has better performance in both convergence speed and mean square error. At the same time, under the condition of the same number of iterations, the optimized GA-BP neural network algorithm fitness value can achieve stable effect faster and has higher fitness value; that is, it has better adaptive ability. After training, the sample test results show that the prediction value of the optimized GA-BP neural network algorithm is closer to the ideal value, with higher accuracy and better stability. It shows greater application value in the English teaching quality evaluation system, and the evaluation results are more scientific and reasonable. However, the probability of BP neural network algorithm falling into the local minimum problem is large, so there is a certain gap between the training convergence result and the expected error, a concave point that falls into the error surface. The activation function of neural network is *s* function. Both ends of the function are flat, and the algorithm runs very slowly. As long as it is a random search algorithm, this will happen, but the possibility is different. Use the advanced search with strong global optimization ability and then continue the search with the algorithm with strong local search ability. This needs to be improved in future research.

Data Availability

The data used to support the findings of this study are available from the corresponding author upon request.

Conflicts of Interest

The authors declare that they have no conflicts of interest.

Acknowledgments

This work was supported by Qingdao Huanghai University.

References

[1] S. Natek and M. Zwilling, "Student data mining solution-knowledge management system related to higher education institutions," *Expert Systems with Applications*, vol. 41, no. 14, pp. 6400–6407, 2014.

[2] O. K. Oyedotun and A. Khashman, "Deep learning in vision-based static hand gesture recognition," *Neural Computing & Applications*, vol. 28, no. 12, pp. 1–11, 2017.

[3] K. Simonyan and A. Zisserman, "Very deep convolutional networks for large-scale image recognition," in *Proceedings of the 3rd International Conference on Learning Representations, ICLR 2015*, San Diego, CA, USA, May 2015.

[4] H. Zhang, "A neural network based method for student achievement prediction," *Journal of Liaoning Normal College (Natural Science Edition)*, vol. 21, no. 3, pp. 94–96, 2019.

[5] B. Zhou and H. Zhao, X. Puig, T. Xiao, S. Fidler, A. Baniuso, and A. Torralba, Semantic understanding of scenes through the ade20k dataset," *International Journal of Computer Vision*, vol. 127, pp. 302–321, 2016.

[6] S. Li, Z.-Q. Liu and A. B. Chan, Heterogeneous multi-tasklearning for human pose estimation with deep convolutional neural network," *International Journal of Computer Vision*, vol. 113, no. 1, pp. 19–36, 2015.

[7] G. Chun, H. Wang, and S. X.-L. Wu, "Research of classroom teaching quality evaluation model based on improved BP neural network," *Journal of Radio Engineering*, vol. 6, pp. 5–17, 2016.

[8] Y. Zhang, "Prediction of college sports performance based on improved grey neural network," *Electronic Measurement Technology*, vol. 11, no. 42, pp. 86–90, 2019.

[9] J. Feldman, A. Monteserin, and A. Amandi, "Detecting students' perception style by using games," *Computers & Education*, vol. 71, no. 1, pp. 14–22, 2014.

[10] L. Li, W. Xiulan, and L. Yixue, "Target recognition method based on GA-BP neural network," *Transducer and Microsystem*, vol. 38, no. 10, pp. 47–50, 2019.

[11] Z. Cao, G. Hidalgo, T. Simon, S.-E. Wei, and Y. Sheikh, "Realtime multi-person 2D pose estimation using part affinity fields," *IEEE Transactions on Pattern Analysis and Machine Intelligence*, vol. 43, no. 1, 2019.

[12] H. Shuai, G. Yan, J. Hua, and Q. Weiwei, "Study of student score prediction model based on PCA-BPnetwork," *The key magazine of China technology*, vol. 12, no. 9, pp. 35–38, 2015.

[13] F. Wang, "Prediction of 2020 Olympic games medal performance based on neural network," *Statistics & Decisions*, vol. 35, no. 5, pp. 89–91, 2019.

[14] A. Sadollah, H. Sayyaadi, and A. Yadav, "A dynamic metaheuristic optimization model inspired by biological nervous systems: neural network algorithm," *Applied Soft Computing*, vol. 71, pp. 747–782, 2018.

[15] I. Jugo, B. Kovačić, and V. Slavuj, "Increasing the adaptivity of an intelligent tutoring system with educational data mining: a system overview," *International Journal of Emerging Technologies in Learning*, vol. 11, no. 3, pp. 423–425, 2016.

[16] Y. Qi and X. Wen, "Research on teaching quality evaluation model based on GA and BP neural network," *Journal of Inner Mongolia University (Natural Science Edition)*, vol. 49, no. 2, pp. 204–211, 2018.

[17] Z. Zhao and H. Huang, "New discussion on classroom teaching quality and evaluation criteria in colleges and universities," *Chinese Journal of Higher Education*, vol. 8, pp. 45–47, 2019.

[18] X. Jie and Z. Tao, "Multi-objective particle swarm inversion algorithm for two-dimensional magnetic data," *Applied Geophysics*, vol. 12, no. 2, pp. 127–136, 2015.

[19] Z. Zhou, L. Liu, and P. Cheng, "Discharge fault diagnosis of GIS equipment based on genetic algorithm optimization BP neural network," *Electrical switch*, vol. 54, no. 3, pp. 37–40, 2016.

[20] X. Yan, H. Li, A. R. Li, and H. Zhang, "Wearable IMU-based real-time motion warning system for construction workers' musculoskeletal disorders prevention," *Automation in Construction*, vol. 74, pp. 2–11, 2017.

[21] Y. Zhang, "Study on the construction of English performance prediction model based on naive bayes," *Automation Technology and Application*, vol. 38, no. 10, pp. 67–69, 2019.

[22] W. Yan-xin, "Analysis of the factors influencing the quality of junior high school English teaching based on analytic hierarchy process," *Educational Modernization*, vol. 49, pp. 388–390, 2017.

[23] D. Mehta, S. Sridhar, O. Sotnychenko et al., "VNect: real-time 3D human pose estimation with a single RGB camera," *ACM Transactions on Graphics*, vol. 36, no. 4, 2017.

[24] Y. Yang and J. Li, "Research on employment quality evaluation of college graduates based on AHP and BP neural network," *Journal of Chinese Education*, vol. 11, pp. 148-149, 2015.